PAXVE, INC.
JULY, 1971

FINAL REPORT

EVALUATION OF A LOW NO_x BURNER

BY

E. B. ZWICK
T. R. MILLS
R. FIO RITO

PREPARED FOR

DIVISION OF ADVANCED AUTOMOTIVE POWER
SYSTEMS DEVELOPMENT,
OFFICE OF AIR PROGRAMS

ENVIRONMENTAL PROTECTION AGENCY

PAXVE REPORT USG–1
CONTRACT EHS 70 - 125

PAXVE, INC.

840 PRODUCTION PLACE • NEWPORT BEACH, CALIFORNIA 92660

PAXVE, INC.
840 PRODUCTION PLACE • NEWPORT BEACH, CALIFORNIA 92660

EVALUATION OF A LOW NO_x BURNER

FINAL REPORT

For the period of June 29, 1970 thru July 28, 1971

By

E. B. Zwick

T. R. Mills

R. FioRito

PAXVE REPORT USG-1

The work upon which this publication is based was performed pursuant to Contract No. EHS 70-125 with the Division of Advanced Automotive Power Systems Development, Office of Air Programs, Environmental Protection Agency.

TABLE OF CONTENTS

ILLUSTRATIONS

ILLUSTRATIONS (Cont.)

SECTION V

ILLUSTRATIONS (Cont.)

ILLUSTRATIONS (Cont.)

ILLUSTRATIONS (Cont.)

SECTION VIII

TABLES

I. INTRODUCTION AND SUMMARY

A. Introduction

During the past twelve months, Paxve, Inc. of Newport Beach, has been engaged in an experimental and analytical investigation of the Paxve burner, a low emission combustion system. The Paxve Burner is a proprietary device developed by Paxve in conjunction with work on an automotive Rankine cycle engine. The burner in its present form consists of a structure embodying certain fuel injection and combustion concepts, together with a set of operating conditions which allow low emission operation.

Preliminary emission surveys conducted by Paxve during the summer and fall of 1969, showed the unusually low emission characteristics of the Paxve Burner, particularly with reference to oxides of nitrogen. Correlations of the NOx data at that time showed that the NOx emission levels could be correlated with the operating temperature of the burner. Those preliminary results also suggested that the low NOx was a benefit derived from the wide stability limits of the burner.

On June 29, 1970, Paxve entered into a contract with the Division of Advanced Automotive Power Systems Development, Office of Air Programs, Environmental Protection Agency. The purpose of that contract was to investigate the emission and stability characteristics of the Paxve burner. Experimental work on the program was completed early in May, 1971. That experimental work together with analytical investigations of the burner and correlation of the experimental data form the subject of this final report.

B. Summary

The results of the experimental and analytical investigation conducted herein may be summarized as follows:

1. Program

Measurement of emissions from the Paxve burner including oxides of nitrogen, carbon monoxide and unburned hydrocarbons were made as a function of burner operating conditions. Variables investigated during the program included burner air flow rate, fuel/air ratio, air and fuel inlet temperature, and burner volume. Stability characteristics of the burner were investigated using both propane and vaporized kerosene as fuel. Emission characteristics of the burner were determined for both of these fuels over a range of mixture ratios ranging from lean blowout to rich blowout. (Rich operation at high flow rates was limited by the fuel handling capability of the facility.) Emission measurements were made directly from the burner exhaust. Additional measurements were also made downstream of a vapor generator operating in conjunction with the burner. The vapor generation loop was one in which an organic working fluid was circulated through a helical coil over which the burner exhaust passed. An approximation of the influence of vapor

generator quenching on burner emissions was thus determined.

A theoretical analysis was conducted of burner operation which provided predictions of burner stability limits and the efficiency of the burner operation under stable operating conditions. That analysis was used as an aid in correlating the experimental data.

2. Burner Stability

Stability of the burner was found to be closely within the limits predicted by the theoretical analysis. Figure 1 shows a typical set of burner stability data with the corresponding theoretical lean blowout limit. The influence of air flow rate, air temperature, and burner volume showed good agreement with the theoretical blowout limits predicted by the theory for lean operation. Some rich blowout data was obtained, the theoretical analysis did not treat this case and therefore, no comparsion with theory here is possible.

The theoretical analysis predicted somewhat wider blowout limits at very low flow rates than were experimentally observed. This has been attributed to the failure of the theory to account for heat loss from the burner which can be significant at low flow rates. The Paxve burner is a very low heat loss device and hence the deviations from theory in this regard were not large.

3. NOx Emissions From the Burner

Figure 2 shows the influence of fuel/air ratio and air flow on the oxides of nitrogen emissions from the Paxve burner, burning vaporized kerosene with an air inlet temperature of 400°F. This data is typical of the experimental NOx data taken from the burner after run 282 when a fuel injector problem was solved. The oxides of nitrogen emissions fall below the 1975 EPA goal* of 1.38 gr/Kg for fuel/air ratios less than 80% of stoichiometric (f/a = 0.051). The influence of the air flow rate on the NOx emissions is minor and tends to be obscured by scatter in the data. The influence of air inlet temperature is rather strong. When the data is plotted against combustion temperature, however, the effect of the inlet air temperature is greatly reduced.

Oxides of nitrogen levels increase with increasing fuel/air ratio, approaching the theoretical equilibrium values at about an equivalence ratio of 1.2 (f/a = 0.08). At low fuel/air ratios, the levels are orders of magnitude below the equilibrium values.

Normal operation of the Paxve burner lies in a combustion temperature range of 2400° to 2700°F. The corresponding fuel/air range of operation the burner generally has emission levels of less than 0.2 gm/Kg. This is seven times better than the EPA goals.

* See paragraph 10 below

4. CO Emissions From the Burner

Figure 3 shows the influence of fuel/air ratio and air flow on the carbon monoxide emissions from the Paxve burner, burning kerosene. The data in this curve are typical of the experimental CO values reported here. At low fuel/air ratios carbon monoxide emissions are determined primarily by burner efficiency considerations. These in turn are quite sensitive to air flow per unit volume, fuel air ratio, and air inlet temperature. Carbon monoxide emissions at high fuel air ratios parallel the curve of theoretical equilibrium concentration of CO in the burner exhaust.

CO emission levels can be kept below the 1975 goal* of 16.2 gr/Kg of fuel by providing the proper combination of fuel/air ratio, volume, air flow and air inlet temperature. In the normal operating range of the burner (between f/a = 0.033 and f/a = 0.038) carbon monoxide emissions are within acceptable range below air flow rates of 180#/hr.

5. Hydrocarbon Emissions From the Paxve Burner

Figure 4 shows hydrocarbon emissions from the burner operating with vaporized kerosene and heated inlet air. It is typical of the HC data from the burner. In the very low fuel/air range near the burner stability limit hydrocarbon emissions from the burner with kerosene as the fuel show a very strong dependence on fuel/air ratio. In this region the HC emissions with kerosene are somewhat influenced by burner efficiency considerations. A similar increase of HC emissions near the lean stability limits is observed with propane, but the hydrocarbon levels are much lower and the appearance of any hydrocarbon is generally an indication of incipient flame out.

At high fuel/air ratios hydrocarbon emissions climb to relatively high values particularly beyond stoichiometric. Between these two extremes there is a broad range of operating conditions for which hydrocarbon emissions from the Paxve burner are essentially zero. In this range of operation the emission levels were so low that they could not be accurately measured with a flame ionization detector.

Emission levels for hydrocarbons can be kept below the 1975 EPA goal* of 0.48 gr/Kg by the proper selection of fuel/air ratio operating range. Within the desired operating range, of f/a = 0.032 - 0.038, the burner HC emission levels were less than 1975 goal over the entire range of air flow per unit volume tested.

6. Influence of the Vapor Generator on Emission Level

Figures 2, 3, and 4 also show the comparsions between the emissions from the vapor generator exhaust and the burner. There was some reduction in the oxides of nitrogen emissions between samples drawn from the burner (bottom of the

* See paragraph 10 below

stack) and samples drawn from the vapor generator exhaust (top of the stack). CO emission levels and hydrocarbon emission levels were strongly influenced by the vapor generator. The low values of hydrocarbon and CO emissions which occur in the mid-range of fuel/air ratios continued to occur with the vapor generator exhaust. The increase in carbon monoxide and hydrocarbons which characterize the burner exhaust at very low fuel/air ratios disappeared when samples were taken downstream of the vapor generator exhaust. In examining the CO curves, it should be noted that the limit of resolution of the gas chromatograph was 5 ppm. Almost all of the vapor generator CO data actually failed to show any measurable CO. These data points were then recorded as 5 ppm. It appears that the net influence of the vapor generator is to quench the NOx formation reaction while permitting continued oxidation of the hydrocarbons and carbon monoxide into carbon dioxide and water vapor.

The emissions measured in the vapor generator exhaust fall below the EPA goals over a much wider range of operating conditions than the emissions from the burner. The upper limit on the allowable fuel/air ratio range in both cases is set by the oxides of nitrogen levels. Fuel/air ratios below f/a = 0.05 are necessary to keep the NOx emissions below 1.38 gm/Kg. The low fuel/air ratio limit for the burner is set primarily by the CO and HC emissions since the NOx emissions continue to fall as the fuel/air ratio is dropped. This lower limit is reduced considerably by the presence of the vapor generator. If this result persists in combination with a vapor generator designed for an automobile, the Paxve burner will be capable of providing very low emission levels over an extremely wide range of operating conditions.

7. Effect of Non-Uniform Fuel Distribution

The Paxve burner described here used propane or vaporized kerosene as its fuel. The fuel and the air were premixed in the inlet pipe before entering the burner. Most of the information described in this summary is based on the behavior of the burner with well mixed homogeneous inlet flow which was achieved after run 282. Earlier experiments with the burner included some in which there was an unsuspected maldistribution of the fuel/air mixture in the inlet pipe. With severe maldistribution of the fuel, burner emission levels of all types were found to increase significantly. Most startling in this regard were the very high levels of hydrocarbons (on the order of 30 ppm) measured downstream of the vapor generator exhaust. The oxides of nitrogen and carbon monoxide emissions from both the burner and vapor generator exhaust were also higher when the improper fuel air distribution existed. All of these problems disappeared as soon as the fuel injection problem was discovered and corrected.

8. Theoretical Analysis

A simplified well stirred reactor model of burner operation was used to provide estimates of burner stability limits and efficiency as a function of the operating conditions. Variables in the analysis included the volume of the burner, the air flow rate, the equivalence ratio, and the air inlet temperature.

The anlaysis followed well established lines of theoretical burner analysis.

It was found that the burner stability data correlated very well with the blowout limits predicted by the burner theory. It was further found that the carbon monoxide and hydrocarbon emission levels were considerably below those predicted by the theoretical analysis, but they followed the same trends and were influenced by the expected variables.

Oxides of nitrogen emission show a strong correlation with temperature, and are less influenced by air flow levels than had been expected. Efforts to provide a theoretical model for correlating the oxides of nitrogen data have been only partially successful.

9. Problems of Emissions Measurement

Problem areas were encountered in all of the emission measurements, including oxides of nitrogen, carbon monoxide, and hydrocarbons. All of these problems were resolved and satisfactory data obtained which is reported herein. Some of the problems encountered deserve special recognition and more investigation.

Oxides of nitrogen data include both NO_2 and NO. The NO_2 is highly soluable in water. The NO is unstable and readily oxidizes to NO_2. At very low NOx emission levels, it is important not to lose the NO_2. This in turn requires special care in handling the water vapor which is produced by the combustion process. Many of the presently accepted standard techniques involve separation of the water in a fashion which can trap the NO_2 before it is measured. This may mean a loss of as much as 50% of the total NOx in a lean operating, low emission mode.

Carbon monoxide data from the Paxve burner was frequently below 5 ppm, this was the lower limit of resolution of the gas chromatograph which was used for this purpose. There are instruments available which will read to lower levels, but these are not common in the automotive research field.

The measurement of hydrocarbons with a flame ionization detector proved generally satisfactory after a heated sample line and heated sampling pump were installed. Two problems remained. The first of these is the so called oxygen synergism effect. The change in sensitivity of the instrument with varying oxygen content in the exhaust stream was not only a nuisance in data reduction, but is a potential source of error. The magnitude of the effect is a function of the compositon of the stream, and hence the appropriate correction can only be made if an accurate hydrocarbon analysis is available. Most of those using these instruments are unable to make such an anlaysis, or to use it properly since the magnitude of the effect is not readily available for all of the combinations of hydrocarbons which one might expect to encounter.

The most severe problem found in hydrocarbon emission

measurement was closely related to the unusually low levels of hydrocarbons which are found in the Paxve burner exhaust. We frequently observed negative output from the recorder which was monitoring the signal from the FID. The negative values were on the order of -0.5 ppm expressed as hexane. These were not spurious readings caused by drift in the instrument or recorder zero setting. An extensive investigation of this problem showed that it might be caused by the presence of water vapor in the burner exhaust gas stream. Addition of 10% water vapor to a stream of "zero" air caused a similar negative zero shift. This of course represents the lower limit of resolution of the hydrocarbon measurement capability of the FID used in this program. This zero shift deserves further investigation. We have not seen it reported elsewhere.

Combustion of hydrocarbon fuels with air can be achieved with emission levels substantially below the goals set by the EPA for 1975 automotive standards. Experiments with the Paxve burner indicate that this burner is a device which is capable of achieving these low emission levels.

10. 1975 EPA Emission Goals

The Division of Advanced Automotive Power Systems Development, EPA, has established certain vehicle emission goals to be met for hydrocarbons, carbon monoxide, and oxides of nitrogen. These goals expressed in grams per mile are: 0.14 g/mi of HC, 4.7 g/mi of CO and 0.4 g/mi of NOx expressed as NO_2. Using an assumed average fuel economy of 10 mi/gal over the Federal Driving Cycle, we can derive emission goals based on grams of pollutant per kilogram of fuel. The resulting values are: 0.48 g/Kg of HC, 16.2 g/Kg of CO and 1.38 g/Kg of NOx. While these values of grams of pollutant per kilogram of fuel are only approximations to what is needed for an automobile, they provide a convenient means of comparing burner emission performance with the 1975 vehicle standards. The phrases "EPA Goals" and "1975 standards" which are used extensively in this report refers to these derived g/Kg values.

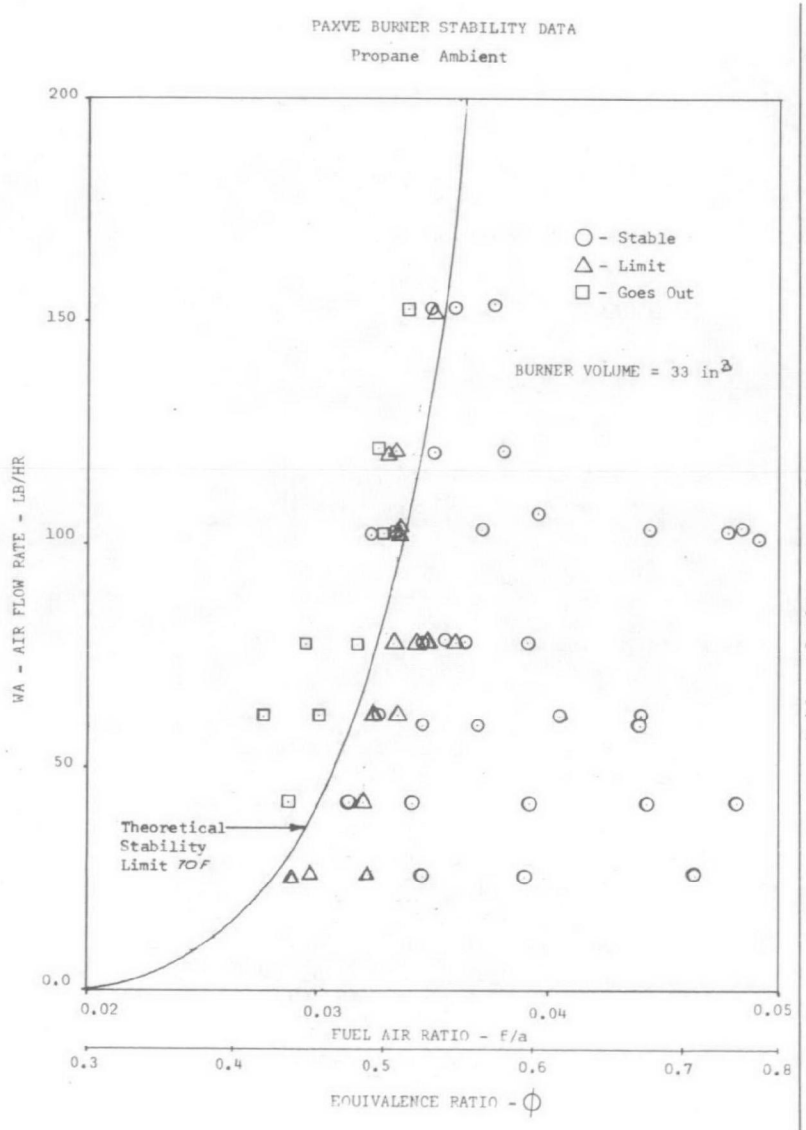

Figure I-1

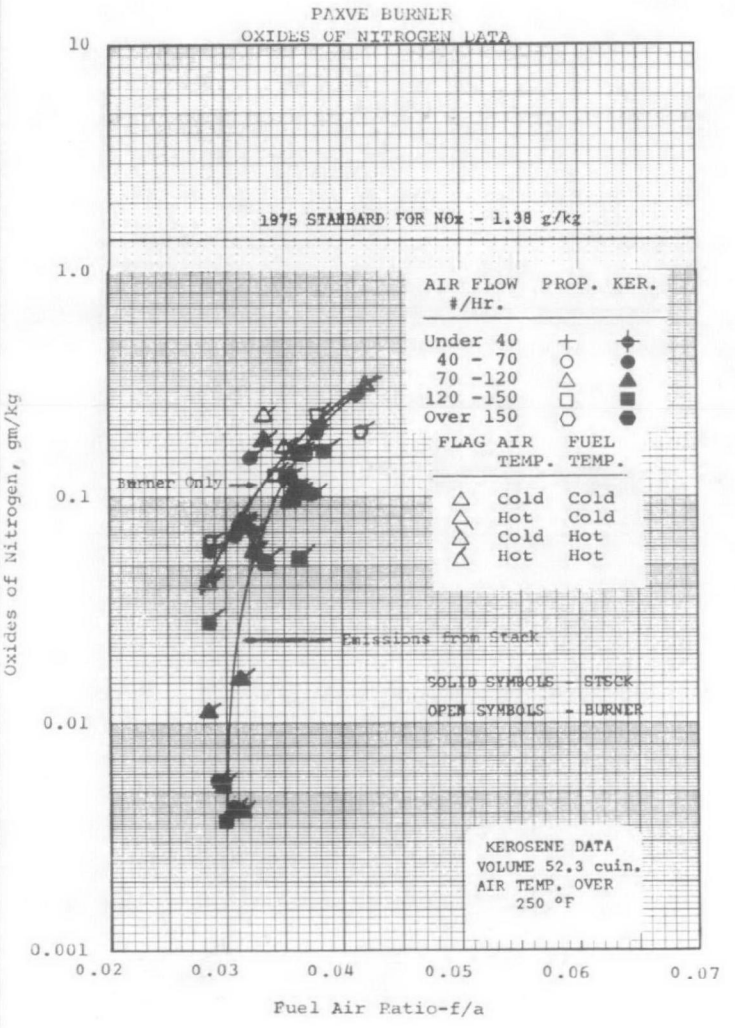

Figure I-2

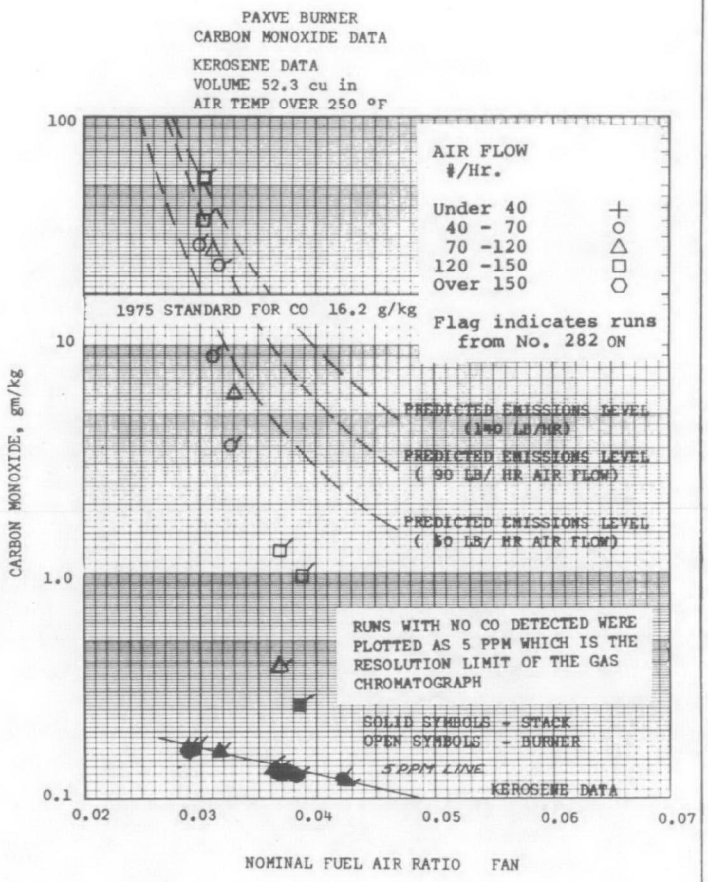

Figure I-3

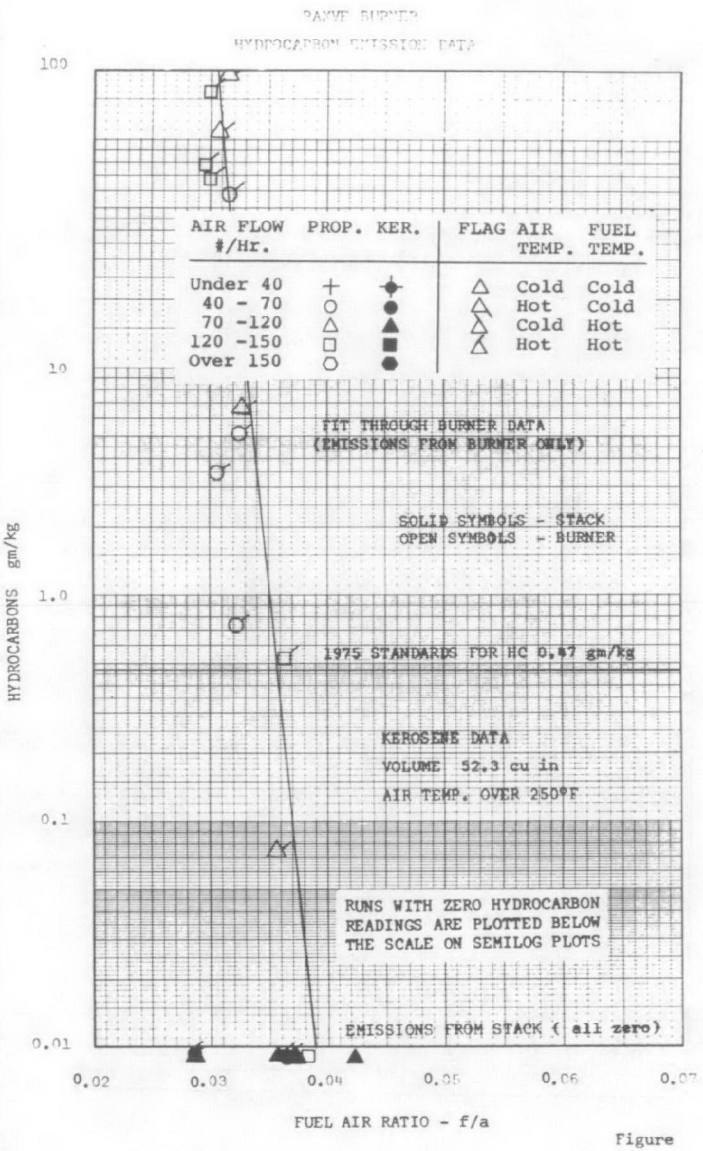

Figure I-4

II. OBJECTIVES OF THE PROGRAM

The objectives of the research program described in this report were to obtain data on the characteristics of the Paxve burner, a low emissions burner. The characteristics to be evaluated were the exhaust emissions and the stability limits of the burner. These data were to be combined with a theoretical analysis of burner stability and operating characteristics in order to provide a thorough evaluation of this burner concept.

A. Experimental Investigation

The experimental investigation was designed to determine (1) the lean and rich blowout limits (stability limits) of the burner, and (2) the emissions characteristics of the burner over a wide range of operating conditions.

1. Stability Limits

The lean and rich blowout limits for the burner were determined for a wide variety of operating conditions. The variables tested included fuel and air temperatures, fuel and air flow rates, and fuel types.

a. Fuel Type

The stability limits were determined for propane and kerosene.

b. Air Temperature

The air temperature was varied from ambient to 400°F.

c. Fuel Temperature

The fuel temperature was varied from ambient to 800°F.

d. Air Flow Rate

The air flow rate was varied from 15 to 150 lbs/hr.

Sufficient data were taken near each blowout limit so that gross extrapolations were avoided.

2. Emissions Characteristics

Burner emission measurements were made over the range of operating conditions used in the stability limits study. Measurements on the burner exhaust were made over a fuel/air ratio range from the lean blowout limit to the rich blowout limit. Exhaust gas measurements included (1) total unburned

hydrocarbons, (2) oxides of nitrogen, (3) carbon monoxide, (4) carbon dioxide, and (5) oxygen.

A closed circulating working fluid loop was constructed to permit burner operation in combination with a vapor generator. The effect of the vapor generator quenching on emissions was determined by sampling the burner gases as they were exhausted from the vapor generator stack.

B. Analytical Effort

1. Literature Survey

A literature survey was made of burner performance and stability analyses. Background data was gathered to assist in making an analysis of stability and emission characteristics of burners.

2. Analytical Study

The literature survey provided the basis for an analysis of the stability and emissions characteristics of the burner under study. The analysis investigated the effects of various parameters on the stability limits and performance characteristics of the burner. The burner was modeled using a simplified stirred reactor concept.

3. Data Analysis

The experimental data on stability limits and emissions were correlated with the results of the analytical study. Additional semi-empirical correlation of data not treated by the burner analysis, was conducted.

III. CONCLUSIONS AND RECOMMENDATIONS

A. Conclusions

The results of the experimental and analytical program discussed in this report show that for the size burner tested (approximately 100,000 BTU/HR), the Paxve burner is capable of low emission operation. If these favorable emission characteristics can be retained as the size is increased to a value of heat release rate and turn down ratio that would be required by a practical automotive propulsion system (approximately 2,500,000 BTU/HR, and at least 20:1), then the Paxve burner should be capable of substantially bettering the goals for pollutants expressed in grams/kilogram established for burners by the Division of Advanced Automotive Propulsion System Development, EPA. The results of the analytical investigation and the correlation of that analysis with the experimental data permit a fairly accurate prediction of burner stability and emission levels. Some correlation has been achieved for emission levels of oxides of nitrogen which are not treated directly by the burner theory.

In addition to these conclusions with regard to the characteristics of the Paxve burner, we must also make some observations about the problem of emission measurements. It was clear that emission measurement is a difficult task and that much remains to be done in order to establish emission measurement procedures which give reliable and consistent data. During the course of this program Paxve uncovered problem areas in emission measurement which we have not seen treated in the literature.

Conclusions from the program are presented below. The subdivisions are as follows:

1. Characteristics of the Paxve Burner
2. Influence of the Vapor Generator on Burner Emissions
3. Influence of Non-uniform Flow Distribution on Emissions
4. Theoretical Analysis
5. Data Correlation
6. Emission Measurement Problems
7. Summary

1. Characteristics of the Paxve Burner

The characteristics of the Paxve burner as investigated in the experimental program described here fall into two general categories; the stability characteristics of the burner, and the emission characteristics of the burner.

a. Burner Stability Characteristics

The experimentally determined stability characteristics of the Paxve burner are presented in Section VI of this report. The burner exhibits more or less

conventional lean blowout and rich blowout behavior. Lean blowout occurs at a fuel air ratio which depends on air flow rate and air inlet temperature. At an air flow rate of 100 lbs/hr and ambient inlet temperatures lean blowout occurs at approximately 50% of stoichiometric mixture ratio (f/a = 0.032 for propane). With increasing inlet temperature the blowout inlet decreases. At 400°F inlet temperature the stability limit for propane at 100 lbs/hr of air flow is approximately 43% of stoichiometric (f/a = 0.028). In both cases, lean blowout occurs at a combustion temperaure of approximately 2150°F.

Rich blowout was more difficult to determine because of the limited fuel flow capabilities of the Paxve test facility. At 50 lb/hr of air flow rich blowout occurs at approximately 0.17 fuel/air ratio which corresponds to about 2.7 times stoichiometric. Stability data with kerosene shows blowout occuring at slightly higher fuel/air ratios then with propane, but at about the same equivalence ratio.

The emission behavior of the burner near the stability limit is different from the two fuels. With propane, lean blowout is characterized by relativly high carbon monoxide emissions, but almost no unburned hydrocarbons are detectable. When the blowout limit is finally reached, the hydrocarbon emissions start to appear and begin to climb. Eventually the burner goes out without a change in the operating conditions. Burning flame out under these conditions can take as long as ten to twelve minutes to occur.

With kerosene, hydrocarbon emission begins to appear before the lean limit is reached. There are essentiallly no hydrocarbon emissions from the burner down to about f/a = 0.038 with hot air and kerosene. As the fuel/air ratios are reduced further, hydrocarbon emissions start to appear, but reach steady values which remain constant while the burner continues to operate stably. A further reduction in fuel/air ratio causes another climb in the emissions which again stabilize at some value. Finally as the blowout condition is reached hydrocarbon emissions climb without leveling off and gradually the burner temperature falls, the oxygen content in the exhaust increases, and the burner goes out.

The presence of a significant amount of hydrocarbon emissions at lean operating points close to the lean blowout limit is a major difference between the behavior of the burner with kerosene near the lean limit and the behavior of the burner with propane under similar conditions.

Near rich blowout the burner emits considerable hydrocarbons both with propane and with kerosene, although the kerosene emissions seem to be generally higher at the rich operating conditions.

b. Oxides of Nitrogen Emissions Characteristics

Oxides of nitrogen emissions from the

Paxve burner show a very distinct correlation with fuel/air ratio. This can of course, be interpreted as being a strong correlation with burner combustion temperature. The influence of inlet temperature is very nearly what one might expect if a true correlation with burner temperature were to apply. In the data which is plotted in the ppm mode it is difficult to see any pattern showing an influence of flow rate on the burner emissions because of the data scatter. In general it appears that lower flow ratios give somewhat higher emissions at a given fuel/air ratio.

For both kerosene and propane with ambient fuel and air we can keep the emissions of oxides of nitrogen below 10 ppm by maintaining the fuel/air ratio of the burner below 0.045 (approximately 70% of stoichiometric). At 400°F inlet temperature, the 10 ppm value is reached at about f/a = 0.04 (0.625 equivalence ratio).

The oxides of nitrogen data from the burner in lean combustion fall far below the equilibrium NO concentrations which would exist in equilibrium at the burner operating conditions. At rich operating conditions of approximately 1.3 equivalence ratio and higher (fuel/air ratio of = 0.08) the burner emissions are approximately equal to the equilibrium values. In terms of the emissions goals of 0.4 grams of NO_2 per Kg of fuel, we find that the burner shows emission characteristics below this level up to mixture ratios of approximately 70% of stoichiometric.

Maximum oxides of nitrogen measurements from the Paxve burner were on the order of 110 ppm or 2.6 grams per Kg of fuel. Under these conditions, the burner was operating at or near stoichiometric mixture ratio, an operating point which the burner is not designed for and at which only very limited burner life could be achieved. At its nominal operating condition of 2500°F flame temperature the Paxve burner shows emissions levels on the order of 0.1 gm/Kg of oxides of nitrogen. This is a significant improvement over the stated emissions goals of EPA.

c. Carbon Monoxides Emissions Data

Emissions of carbon monoxide from the Paxve burner show two distinct trends. For mixture ratios above f/a = 0.05 the carbon monoxide emissions are characterized by a line of rapidly increasing emissions with increasing mixture ratio which follows the equilibrium carbon monoxide concentration in the burner exhaust. At mixture ratios below f/a = 0.035 the carbon monoxide concentration in the exhaust follows a characteristic of increasing CO emissions with decreasing mixture ratio. The nature of these curves suggest a falling burner efficiency with decreasing mixture ratio. Both families of curves show some dependence on flow rate and a strong correlation with fuel/air ratio. Increasing flow velocity increases the CO emissions in both cases.

We can maintain carbon monoxide emissions in the burner exhaust below 16 gr/Kg of fuel, by providing an appropriate combination of fuel/air ratio, air flow rate, and air inlet temperature.

At ambient inlet temperature, a flow rate of 50 lb/hr will give less than 16 gr/Kg of CO at a fuel/air ratio above 0.036. Increasing the inlet temperature to 400°F decreases the fuel/air requirement to 0.030 and 0.032 at 50 lbs/hr and 100 lb/hr respectively.

d. Hydrocarbon Emissions From the Paxve Burner

Hydrocarbon emissions from the Paxve burner exhibit some of the same characteristics as the carbon monoxide emissions. At mixture ratios above about f/a = 0.050 hydrocarbon emissions increase with increasing mixture ratio, increasing rapidly above stoichiometric. There is a wide range of operating conditions for the burner between approximately 0.032 mixture ratio up to approximately 0.050 mixture ratio within which the hydrocarbon emissions from the burner are zero to within the limits of our measurement capability. At mixture ratios below approximately 50% stoichiometric, hydrocarbon emissions again appear at ambient inlet temperatures. With elevated temperatures, the mixture ratio at which hydrocarbon emissions begin to appear from the burner is somewhat lower.

The marked increase in hydrocarbon emissions at very lean mixtures approaching lean blowout is characteristic of the kerosene combustion data. With propane only minor hydrocarbon emissions were observed as lean limit was approached until a limit point had actually been reached. For propane combustion the first significant appearance of hydrocarbons in the exhaust was a sensitive indication of incipient lean blowout.

Hydrocarbon emissions can be kept within the nominal limits assigned by EPA (0.48 gm/Kg) by an appropriate choice of operating fuel/air range, at a given flow rate and inlet temperature. At ambient inlet temperature and 50 lb/hr, hydrocarbon emissions from the burner will be below 0.048 gm/Kg above f/a = 0.035 with kerosene as the fuel. At 100 lb/hr a slightly higher f/a value is required. When the inlet temperature is increased to 400°F, the required minimum f/a for satisfactory HC levels is about f/a = 0.032 at 50 lb/hr and 0.035 at 100 lb/hr. The fuel/air limits necessary to meet the EPA hydrocarbon limitations are wider than the f/a limits for satisfactory CO levels.

2. Influence of the Vapor Generator on Burner Emissions

The vapor generator appears to have a major effect on the CO and HC emission levels in the exhaust stream. Oxides of nitrogen measurements downstream of the vapor generator were in substantial agreement with the oxides of nitrogen measurements upstream of the vapor generator. The influence of the vapor generator on the CO and HC emissions is inferred primarily from the plots of emissions versus fuel/air ratio. Simultaneous measurements of CO were taken on only a few runs. No simultaneous measurements of hydrocarbon emissions from the vapor generator and burner were taken.

a. Effect on NOx Emissions

NOx was measured in both locations for a wide variety of runs.

On some runs there appeared to be a slight increase in the NOx at the top of the stack compared to the burner, while on other runs there appeared to be a slight decrease. The decrease was frequently associated with conditions where the vapor generator had not yet warmed up and some of the water vapor in the burner exhaust was condensing on the vapor generator coils. Previous experience with NOx measurements showed that NO_2 dissolves in condensed water from the exhaust, leading to a reduction in the NOx level in the exhaust stream. The increased residence time of the gases as they flow through the vapor generator does not appear to significantly alter the NOx exhaust concentration.

b. Effect on CO Emissions

Carbon monoxide emissions in the exhaust from the vapor generator are generally much lower than the emissions measured from the burner. We did not in general make simultaneous measurements of these parameters hence it is difficult to establish one to one correspondence between the levels. An examination of the CO emissions as a function of mixture ratio, however, and specific point by point comparisons indicate the extent of this reduction. At the lean operating points where the CO emissions tend to become excessive, the measurements in the vapor generator exhaust were generally below the limit of the measuring instrument.

Part of the difficulty in assessing the influence of the vapor generator on the carbon monoxide emissions lies in the very low levels of CO which are found in the Paxve burner exhaust under normal operating conditions. These normal operating conditions correspond to mixture ratios which give combustion temperatures in the range of 2400°F to 2700°F. Testing outside this range was limited to the burner alone. The structural capabilities of the burner made it possible to do this. Testing with the vapor generator loop in place, however, required limitation of the combustion temperature range to avoid damage to the working fluid passing the vapor generator loop. Within this somewhat narrower temperature range, the CO emissions were usually quite low, frequently below the ability of the chromatograph to read, which was about 5 ppm. We have generally identified the low levels of CO in our data which were otherwise unreadable as being 5 ppm. Many of the CO values undoubtedly were below this level. It would require sensitive instrumentation to accurately establish the influence of the vapor generator on the OC emission levels. It is reasonable to suppose, however, that the reduction in temperature of the gases as they pass through the burner is gradual enough to permit some recombination of the CO with the available oxygen.

c. Effect on HC Emissions

The influence of the vapor generator on hydrocarbon emissions was more difficult to determine than its influence on carbon monoxide. The restricted operating range of the burner when the vapor generator was in place resulted almost entirely in zero or negative hydrocarbon readings, from the top of the stack. Negative readings were obtained at conditions which gave positive readings from the burner alone.

The negative readings, as explained elsewhere, are probably due to the presence of water vapor in the exhaust which causes a zero shift in the flame ionization detector. With zero or negative readings, one has no reliable values that he can use as a basis for an exact comparsion. We can say, however, that the effect of the vapor generator loop was to eliminate hydrocarbon emissions under conditions where there were some measurable emissions. This effect is undoubtedly attributable to increased residence time and gradual quenching.

3. Influence of Non-Uniform Flow Distribution on Emissions

During the course of the experimental work performed here, a number of modifications were made in the test set up and instrumentation as it became evident that a problem existed in one or the other of these. The problems involved in the measurements of emissions are discussed elsewhere. There was, however, a problem involved in the hydrocarbon emissions which sheds some interesting light on the problems of emission control.

The early vapor generator exhaust data showed large quantities of hydrocarbons in the vapor generator exhaust which were not found in measurements made directly from the burner. This peculiar behavior suggesting that a source of hydrocarbons existed between the burner and the top of the exhaust stack was investigated extensively.

An examination of the flame from the burner inlet showed that there was a substantial maldistribution of fuel in the inlet stream, causing rich mixtures to occur in some portions of the burner with lean mixtures in the other portions. When the improper fuel injection pattern was modified to provide a uniform mixture, the anamolous hydrocarbon reading in the vapor generator exhaust immediately disappeared. Correction of the fuel injection pattern was made between runs 279 and 282.

The maldistribution of flow from the fuel injector influenced all of the emission levels, not just that of hydrocarbon data. Examination of NOx data from the burner after the fuel injector was corrected show a reduction in NOx as a function of mixture ratio. This suggests that the local mixture ratio and local temperature are the principal factors in the formation of oxides of nitrogen, and that the uniform mixture which yields the lowest maximum temperature in the burner also provides the lowest overall emission levels.

4. Theoretical Analyses

Theoretical analysis of the burner performance has been conducted using the heat balance theory described by Vulis, Longwell and others. The theory permits an analysis of several interesting parameters in the burner operation. These include burner stability limits, and the prediction of burner emissions in the form of unburnt material as a function of burner design and operating conditions. The theoretical analysis was conducted to determine the influence of the burner volume, air flow rate, ambient pressure and inlet temperature on burner stability, burner efficiency and combustion temperature. Only lean burning cases were treated. Prediction of lean blowout limits and burner emissions due to incomplete combustion were made for each lean operating point for comparsion with the experimental data.

An interesting feature of the analysis is the prediction that at elevated inlet temperatures, on the order of 1600°F and higher, the burner will no longer show critical burner characteristics at very lean mixture ratios. Thus at high inlet temperature and low combustion temperature it appears that the burner will ignite and burn independently of the air flow. Under these conditions the burner will not exhibit blowout characteristics, but the efficiency of combustion will still be strongly dependent on the flow rate and other factors.

5. Data Correlation

The theoretical analyses conducted as a part of this program were used to assist in the correlation of experimental data from the Paxve burner.

a. Correlation of Stability Data

Stability data from the Paxve Burner shows very good correlation with the blowout predictions based on the burner theory. At very low flow rates, the burner seems to be somewhat less stable than the theory would predict. This lessened stability has not been examined in detail but is probably attributable to heat loss from the burner. The theory appears to account properly for the influence of air flow, inlet temperature and burner volume.

b. Correlation of Carbon Monoxide and Hydrocarbons Emissions Data

The carbon monoxides emission data has been examined in the light of the combustion theory outlined in this report. What we expect is that as we approach the lean stability limit, the efficiency will decrease, and this inefficiency will show up as either unburned hydrocarbons, carbon monoxide, or both. Experimentally, we find that with propane combusiton there are virtually no unburned hydrocarbons in the exhaust as the lean limit is approached, but there is a relatively large amount of carbon monoxide.

The shape of the carbon monoxide emission curves is

substantially the same as that predicted by the theoretical analysis. The influence of the flow rate and temperature on the carbon monoxide emissions is also in the direction we would expect based on the experimental data and the theoretical analysis. This is probably due to the simplifications used in the burner analysis. Heat release associated with partial combustion of the fuel to water vapor and carbon monoxide was ignored. This tends to underestimate the efficiency as lean blowout is approached, and to overestimate the emissions. A more exact expression for the heat release could probably yield still closer agreement with experimental data. The present analysis is useful, however, for obtaining a conservative estimate of burner CO emissions.

The influence of flow rate, inlet temperature and mixture ratio on the hydrocarbon emissions near lean blowout with kerosene, shows similar characteristics to those obtained for the carbon monoxide. The effect of fuel/air ratio, flow rate, and inlet temperature are along the lines predicted by the theory.

The emissions of both CO and HC are greatly diminished by passage through the vapor generator. This is probably due in part to continued oxidation as gases cool off. The lower CO values at fuel/air ratios approaching stoichiometric is also attributable in part to shifting equilibrium in the flow through the heat exchanger.

We have not attempted to correlate the reductions in CO arising from passage through the vapor generator. By using the predicted unreactedness to estimate the CO, we thus have an even more conservative estimate for a burner/heat exchanger installation.

c. Correlation of the NOx Data

We do not have a theoretical basis for correlating the oxides of nitrogen data which is totally in agreement with the experimentally determined values. It appears that the oxides of nitrogen data can be correlated as a function of the combustion temperature. If one writes an equation of the form:

$$[NO] = Ke^{-E/RT}$$

and use this as a basis for correlation of the experimental data we find that:

$$K = 4.38 \times 10^5 \text{ ppm}$$

$$E = 36.8 \text{ K cal/mole}$$

seems to give a fair fit to the data.

The empirical correlation produced here is of value since it permits a relatively accurate prediction of the oxides of nitrogen content in the burner exhaust as a function of operating conditions.

6. Emission Measurement Problems

A number of emission measurement problems were covered during the course of the experimental investigation reported here. The most important of these dealt with erroneous measurements which can be made in the measurement of oxides of nitrogen due to improper technique. It appears that some of these improper techniques are widespread. Additional discoveries deal with the problems of measuring hydrocarbons at very low levels.

a. Oxides of Nitrogen Measurement Problems

Difficulties experienced in measurement of oxides of nitrogen by the Griess-Saltzman method during the course of this program are discussed in some detail in this report. These problems included saturation of the dye caused by using too small a quantity of reagent for the volume of the gas being sampled, and failure to detect NO in rich mixtures due to the lack of oxygen in the flask to oxidize the NO into NO_2. Those errors on our part were avoidable. Someone who was more familiar with Saltzman's work and with the standard measurement procedures used in the automotive field would probably not have experienced those difficulties.

An additional problem was discovered, however, which to the best of our knowledge is not discussed elsewhere. At low levels of concentration in the exhaust from our burner, NO_2 appears to form a substantial portion of the total NOx. It further appears that the NO_2 which is highly soluble in water, can be readily lost prior to analysis by improper sampling. The use of a sampling procedure which permits or encourages the water formed during the combustion process to be removed from the flow before analysis, can be expected to give erroneous results at low NOx concentrations due to the loss of NO_2. It is probable that other forms of water removal equipment, such as desiccants and absorbers will also tend to trap NO_2.

Removal of water vapor from the exhaust stream prior to analysis is a common procedure in NOx emissions measurements. In the case of NDIR analyzers which have been widely used in the past, for NO measurement, water vapor must be removed because it interferes with the detection of the NO. It is our conclusion, based on the work done at Paxve, that every effort should be made to eliminate water dropout if all of the oxides of nitrogen are to be detected in a low NOx stream.

b. Problems in the Detection of Hydrocarbon Emissions

Difficulties experienced at Paxve in the detection of hydrocarbon emissions were of three types. These included the oxygen synergism effect on the flame ionization detector, the problem of inaccurate measurement due to use of a cold sampling line, and the problem of zero shift of the instrument, apparently due to water vapor in the exhaust.

Oxygen synergism is a name given to the change in sensitivity of the flame ionization detector to hydrocarbon in the presence of oxygen. The change in sensitivity depends on both the oxygen concentration and on the hydrocarbon being detected. For hydrocarbons of interest to the analysis being conducted by Paxve this effect was on the order of 25% reduction in sensitivity at 10% oxygen concentration. The oxygen synergism effect could have been minimized by the use of a nitrogen hydrogen mixture as the combustible gas in the flame. The manufacturer who supplied the flame ionization detector which was used did not advise us in this regard. We discovered the problem during instrument calibrations.

Heating of the hydrocarbon sampling line and pumping equipment is necessary to obtain accurate measurement of hydrocarbon emissions. There seems to be some misconception as to why this heating is desirable. It was suggested to us that heating of the lines was an effective means for preventing condensation of higher hydrocarbons. While this is true, the concentration of hydrocarbons necessary to actually permit condensation even at ambient temperatures is quite high. That concentration is unlikely to occur in the exhaust from a clean burner such as the Paxve burner. The problem which does arise in this regard is not one of true condensation, but rather psuedo-condensation caused by the adsorption of the hydrocarbons in the surface of the sampling line. Heating of the sampling line and pump undoubtedly serves to eliminate adsorption of higher hydrocarbon in the same fashion.

Perhaps the most vexing problem which arose in the measurement of hydrocarbons during the course of this program, was the repeated observation of negative values of hydrocarbon emissions from the burner and the vapor generator exhaust. Negative readings of as much as 0.5 ppm expressed as hexane were common place. Efforts to attribute this to a drift in the instrument were in vain. Preliminary experiments with zero air into which 10% water vapor was evaporated showed a zero shift of about 0.5 ppm. This was a zero shift as opposed to a change in sensitivity of the sort associated with oxygen synergism.

Thiz zero shift presents somewhat of a dilemma. On the one hand, we would like to remove the water vapor from the flow so as to avoid the zero shift. On the other hand, all methods for eliminating the water vapor from the flow that we have been able to think of would simultaneously influence the measurement of the hydrocarbon content. It appears that the only practical method for taking this into account is to measure the water vapor content and use this together with known calibrations of zero shift to correct the data.

We used pure hydrogen in our FID. We do not know whether the zero shift would be as pronounced with some other gas mixture. A 40/60 hydrogen-helium mixture is commonly used in FIDs to minimize the oxygen synergism effect. This might also influence the zero shift.

c. Carbon Monoxide Measurement Problems

Most of the CO data from the vapor generator exhaust showed levels which were well below the detection limit of our equipment. We were delighted and somewhat surprised with the low CO emission levels from our burner. It would have been nice to be able to measure them more accurately. The equipment which we used permitted us to make carbon monoxide measurements down to about 5 ppm. Obtaining lower readings through ordinary gas chromatography is quite difficult since the carbon monoxide separation from nitrogen on the molecular sieve is not as complete as one might like. More sensitive techniques for measurement of carbon monoxide have been devised. These include a method for converting carbon monoxide into methane and then measuring the methane in a flame ionization detector, and highly sensitive NDIR instruments.

7. Summary

In its normal mode of operation, the Paxve combustion process is capable of very low emission operation. Oxides of nitrogen on the order of 0.1 gm/Kg are achieved simultaneously with carbon monoxide levels of less than 1.0 gm/Kg and hydrocarbon readings which are so low as to be undetectable.

The Paxve combustion process appears to be one which requires more sophisticated measurement devices than those currently available for testing vehicle emissions.

B. Recommendations

1. Prototype Burner Development

A program should be funded to support the development of the Paxve burner into a prototype unit suitable for incorporation into a Rankine Cycle Engine.

a. Burner

A prototype burner vapor generator assembly would be a desirable line of approach.

b. Fuel Vaporizer

In conjunction with this type of prototype development, a fuel vaporizer development program should also be funded. The fuel vaporizer which was used in conjunction with the kerosene burner data reported here, should serve as the basis for development of a practical prototype.

2. Liquid Injection Investigation

Further reasearch should be conducted into the factors affecting the emissions characteristics of the Paxve burner. Limited data on liquid kerosene injection shows that under some conditions the burner seemed to operate with low emissions

using very poorly atomizing liquid injection. This should be explored further to determine whether fuel vaporization is a necessary feature in the development of this burner. This program should not take precedence however, over the prototype development suggested as recommendation 1 above. It is important that practical application of this promising low emission technology be made, with product improvement of somewhat less priority.

3. Transient Effects on the Paxve Burner

Further research on the Paxve burner is desirable to investigate the effect of transient operation on burner emissions. Transient changes in flow rate through the burner were not examined during the course of the program discussed here. Such measurements would be highly desirable. This work might proceed in parallel with the prototype development suggested above.

4. Influence of Vapor Generator

Additional research on the influence of the vapor generator on the Paxve burner emissions, particularly on the carbon monoxide and hydrocarbon emissions would be desirable. Continuous measurement equipment is mandatory if this type of development supporting research is to be conducted in an efficient manner. The grab sample techniques utilized by Paxve during the course of the program described here were selected because of their availability and accuracy. The advent of the chemiluminescent NOx technique and high sensitivity NDIR for carbon monoxide should permit continuous flow instrumentation for these parameters. Continuous flow instrumentation for the hydrocarbons is already available and was found to be quite adequate for the program.

Carbon monoxide and hydrocarbon emissions improve greatly in passage through the vapor generator under lean operating conditions. It would be desirable to determine the extent to which this is the case, since it is the balance between the carbon monoxide and the oxides of nitrogen emissions which limit the operating range of the burner otherwise.

5. Elevated Pressure and Temperature Effects

Further research into the influence of pressure and temperature on the Paxve burner should be funded. The Paxve burner may be applicable not only to Rankine cycle engines, but also other forms of combustion equipment, including gas turbine engines. If a Paxve burner is to be used as an element in an automotive or stationary gas turbine, it will have to operate under conditions of elevated inlet pressure and temperature which are considerably outside the range of the testing accomplished to date.

The influence of elevated pressure and temperature are to some extent predicted by the theoretical analysis conducted here. Only experimental investigation of these phenomena will verify the validity of that analysis. A preliminary examination of this

problem suggests that full scale testing of burners of a size suitable for gas turbine application would be the most feasible approach to conducting research in this area.

6. Extended Burner Analysis Including Heat Loss and NOx Correlation

Additional analysis should be funded to extend the theoretical investigations discussed here and to improve the experimental correlation with theory.

a. Burner Theory

The burner theory discussed here showed excellent agreement with the experimental blowout data at high flow rates. At lower flows there was some deviation. Improvement in the theory to account for heat loss from the burner would undoubtedly resolve this discrepancy. It would also show whether or not other types of burners which are more susceptible to heat loss can be expected to achieve the same excellent results that we have achieved with the Paxve burner.

The burner heat release equations should also be modified to account for some heat release when partial oxidation of the fuel to water vapor and carbon monoxide takes place. This should improve the accuracy of the CO emission predictions.

b. NOx Correlation

Additional correlation of the oxides of nitrogen data obtained during this program would be highly desirable. The fact that the oxides of nitrogen do not appear to be strongly influenced by the air flow rate suggests that combustion related atomic oxygen may be a significant factor. This should be investigated analytically.

IV. EXPERIMENTAL METHODS

This section covers a description of the experimental apparatus, critical instrumentation, and test procedures used in obtaining the experimental data. Special test facilities were designed and fabricated to permit testing the Paxve burner under controlled conditions of inlet fuel and air temperature and pressure for the evaluation of emissions and stability.

A. Experimental Installations

1. General Description

All of the burner emission and stability testing reported here was accomplished in the Paxve combustion laboratories. These include two primary combustion test facilities: Stand 1 and Stand 2 ("The Blockhouse"). A schematic diagram of the overall burner test facilities incorporating burner test stands No. 1 and 2 as well as the auxiliary instrumentation and gas analysis facilities is shown in Figure 1. The two burner test stands are nearly equivalent in terms of burner testing capacity, instrumentation, and test fuels. The major difference is that test stand 2 contains a working fluid vapor generator loop. This allows study of the effect of burner gas quenching on emissions.

As indicated in the diagram of Figure 1, the two test stands are self contained for individual burner testing. They consist of a burner control console, an enclosure in which the burner is installed, an air system which supplies combustion air to the burner, a fuel system supplying the particular fuel under test, an instrumentation system which provides direct readout for control of burner operating conditions, and instrumentation for measurement of the burner exhaust gas emissions. External view photographs of burner test stand No. 1 and control console for test stand 2 are shown in Figure 2.

Test stand No. 2 is constructed to perform the same functions as burner test stand No. 1 with the additional feature that a vapor generator system has been added to the burner. The burner and vapor generator systems are totally enclosed in a well ventilated blockhouse for safety reasons. Photographs of burner test stand No. 2 showing the interior view of the blockhouse are shown in Figure 3.

The two burner test facilities are served by a common gas sampling instrumentation center. This instrumentation center contains the instrumentation for the measurement of exhaust gas emissions which include CO, CO_2, unburned hydrocarbons, and oxygen. In addition, gas analysis equipment is provided for the colorimetric evaluation of oxides of nitrogen in the exhaust. The instrumentation and emissions measurement techniques are described in detail later in this report. Photographs of the emissions instrumentation center are presented in Figure 4.

2. Air Flow Subsystems

A schematic diagram of the air and fuel system for burner stand No. 1 is shown in Figure No. 5. The schematic diagram for Stand No. 2, is shown in Figure 6. The air system consists of two variable speed air blowers connected in parallel, capable of providing up to 250 lb/hr of air. The blowers are controlled by a variac to set blower speed and consequently air mass flow. Air flow is measured through a rotameter. The air temperature is varied by means of a nichrome wire air heater immersed in the air flow. Air temperatures of up to 500°F can be obtained. Current flow in the nichrome wire is regulated by a variac auto transformer. The thermally conditioned air flow is discharged coaxially with the injected fuel flow into the burner for ignition and combustion.

3. Fuel Flow Subsystems

The fuel systems consist of two parallel storage and control systems, one to handle propane, the other for diesel/ kerosene fuels. A major element of the fuel system is the fuel heater vaporizer. The heater/vaporizer for Stand 2 is shown in the photograph of Figure 7. Figure 8 shows a drawing of the unit which was designed and fabricated to meet the specific requirements of this burner evaluation program. It consists of a high thermal conductivity core section containing an encapsulated electrical heating element. Helical grooves are machined on the outside of the core which provide a vaporization passage for the fuel flow. The encapsulation of the electrical heating element in a high thermal conductivity aluminum core mass provides isothermal heat transfer at the helical fuel heating passages. Maintaining uniform wall temperatures through mixed phase flow eliminates "hot spots" which could lead to thermal decomposition (carburization) of the hydrocarbon fuels.

The outside case of the heater consists of a tube with a side wall inlet to the spiral fuel grooves and an outlet through a domed end piece. During operation, the fuel enters through the case and travels up the spiral path to the dome and cap. The end cap is designed so that liquid vapor separation is achieved with the vapor leaving through a centrally located port. Unvaporized droplets are retained by the dome to fall back onto the heated core for further vaporization. The unit is thermostatically controlled to achieve the desired vaporization for various fuel flow rates.

Figure 7 shows the disassembled vaporizer after operation on kerosene. More than 20 gallons of kerosene and 1000 lbs of propane have flowed through the heater unit. The core operated at approximately 900°F at a flow rate of approximately 7 lb/hr. Examination of the vaporizer shows only a thin powdery layer of black carbon covered the top of the core where the flow could stagnate. The helical flow passages discolored but were free from any carbon deposit.

As shown in Figure 6 a line heater is also installed between the fuel vaporizer and the burner fuel injector to maintain

fuel temperature at the desired value after vaporization. The line heater consists of a resistance heated length of quarter inch stainless steel tubing. Electrical control is achieved through a current transformer and control Variac. The line is insulated to minimize the convection losses.

This fuel conditioning system has demonstrated good performance. Vaporized fuel or hot propane can be delivered to the burner at any desired temperature up to 800°F over a flow range from less than 1 lb/hr to more than 12 lb/hr.

4. Vapor Generator System

The system which is unique to Stand 2 is the vapor generator system, a schematic of which is shown in Figure 9. The purpose of this installation is to study the effects of quenching by cold surfaces on burner emissions. The vapor generator itself is a counter flow heat exchanger in which the working fluid circulates through a 6 foot tall coil of 3/8 in. O.D. tubing. The coil dimensions after winding were 2 in. I.D. x 2 5/8 in. O.D. The coil is surrounded on the outside by 3 in. I.D. ceramic tubing and is bordered on the inside by a 1.5 in. O.D. air tube leading to the burner. The working fluid runs counter flow in the coil to the hot burner gases which rise in the annular area between the center air tube and the ceramic wall. Figure 3a is a photograph of the vapor generator stack. Figure 10 shows a drawing of the unit.

The working fluid is circulated by a geroter pump which is driven by an air cooled Volkswagon Automotive engine. The pump can provide outlet pressures of up to 1500 psi at flow rates of 7.8 gpm at 1200 rpm. The automotive drive engine is provided with remote control ignition, starting, throttling and clutching capability to vary pump speed and circulating flow rate.

The initial design of the vapor generator loop included a jet pump at the inlet to the gerotor pump to prevent cavitation. It was found that this did not permit the system to start flowing properly. The jet pump must have a supply of high pressure fluid in order to provide the desired characteristics. For our case a startup problem results since the pump cannot supply high pressure unless it has full flow at the inlet. In a future automotive system, this difficulty could be overcome by the slow cranking of the pump during initial system starting. It was beyond the scope of the present test facility installation to provide this necessary flexibility, and the jet pump was removed. The cavitation problem was circumvented by installing a low pressure accumulator pressurized with N_2 at the pump inlet to set the minimum pressure level in the system. This provided adequate cavitation supression and also a reserve fluid supply.

The system also includes a high pressure accumulator at the pump outlet to minimize water hammer effects. For additional flow control, a pump bypass line is provided which is manually operated and set at a given condition which is normally unchanged during testing. Provisions are made for filling the system at the low and high pressure accumulators while bleeding gas at a high

point bleed. A filter at the pump inlet is provided to protect the close tolerance of the pump rotor.

The vapor generator system has been operated in conjunction with the burner to working fluid outlet temperatures of 500°F and flow rates of 2.0 GPM through the vapor generator coil. The vapor generator system also includes a condenser coil which is cooled in a water bath and returns the working fluid temperature to approximately 212°F before entering the pump.

5. Control Consoles

Each test stand is provided with a control console which incorporates all necessary operating controls and visual monitoring instrumentation. The operating controls include: switches for the blowers, heaters, igniter, and fuel flow solenoids; Variacs (autotransformers) to control air flow rate and electrical power to the air heater and the fuel line heaters; needle valves for control of fuel flow and nitrogen pressurizing and purge flows; and a thermostatic controller for the fuel heater/vaporizer. Instrumentation includes: flow meters (rotameters) for fuel and air flow rate; pressure gages for fuel supply and delivery, burner air supply pressure, pressure at the rotameters, and pressure levels throughout the vapor generator loop; and temperatures in the burner, at the vapor generator coil exhaust, in the fuel and air streams both at the flow meters and at the burner inlet, and throughout the vapor generator loop. A table of all control and measurement functions on the two operating consoles is presented in Tables 1 and 2.

B. Instrumentation

The burner test stands are provided with pressure, temperature and flow instrumentation. These instruments permit the test operator to set and hold a desired test condition. The instruments together with the corresponding controls (described in A-5 above) are tabulated in Tables 1 and 2.

In addition to the test operation instruments, Paxve has provided emissions measuring equipment which incorporates measurements for CO, CO_2, O_2, HC, and NOx.

1. Pressure Measurements

All pressure measurements involved in the burner research program were made with conventional Bourdon tube or diaphragm (Magnehelic) pressure gages. Pressure measurements were made for several purposes:

a. The pressure level of each fuel tank was monitored to help set up repeatable test points.

b. The pressure level at the propane flow meters was used to correct propane flow rate for density.

c. Pressure drop across the fuel vaporizer

was monitored to see if the vaporizer was loading up with carbon deposits.

d. Pressure levels throughout the working fluid loop were monitored to ensure that the working fluid was above its critical pressure in the vapor generator and also to avoid cavitation problems in the gerotor pump. Pressure drop across the filter was also monitored.

e. Pressure loss through the burner was measured.

f. Pressure level at the FID input was measured to control the flow rate through that instrument.

2. Temperature Measurements

All temperature measurements were made with bare junction thermocouples and microammeter type readouts (Assembly Products, Inc. "Simplytrol" Meters). Iron-constantan and chromel-alumel couples were used for low temperatures. Platinum vs platinum-13% rhodium couples were used to measure the burner temperature.

Temperature measurements were made for the following purposes:

a. The air temperature was measured at the air flow meter to permit correction of flow rate for air density. Although the air flow was measured before the air was heated, there was significant heating of the air by the air blowers.

b. The fuel temperature at the flow meter was measured to permit density correction.

c. Air temperature was measured downstream of the air heater.

d. Fuel temperature was measured downstream of the fuel/vaporizer and also downstream of the heated fuel line.

e. The temperature of the fuel heater/vaporizer was measured by a thermocouple buried in the aluminum core. The thermocouple was connected to an automatic controller which kept the core temperature within a few degrees of a set point.

f. The temperature in the burner was measured by a ceramic encased Pt-Pt 13% Rh thermocouple inserted through the walls of the burner. Early tests in Stand No. 1 used a movable probe which could be inserted into the burner through the air intake pipe. It was found that this sometimes interfered with the normal combustion process and was discontinued. Measurements of the gas temperature in the burner exhaust was substantially the same as the measurement made inside the burner. Burner temperature measurements were made primarily to tell if the burner was lit and/or operating stably. Flame out could be detected

almost immediately, but incipient flame out was difficult to detect. Because the burner temperature probe was not shielded, it suffered from inaccuracy due to radiant heat loss. This generally resulted in a 200°F to 300°F difference between the burner temperature reading and the theoretical flame temperature.

g. The temperature of the burner exhaust gases was measured downstream of the vapor generator stack.

h. The temperature of the fluid within the vapor generator loop was measured at several points including upstream and downstream of the "condenser".

i. The temperature of the pump and line used for hydrocarbon sampling were monitored to be sure that these components were above 300°F.

3. Flow Measurements

Flow measurements for the experimental program reported here were made with the variable area flow meters commonly referred to as"rotameters". All flow meters were calibrated throughout their range at ambient pressure and temperature, with appropriate corrections for gas density as necessary. The propane flow meters were also calibrated at elevated pressures to verify the density correction technique.

Flow measurements included:

a. Air flow to the burner, increased upstream of the air heater. Air temperature at the flow meter was measured for density correction.

b. Fuel flow into the burner, measured upstream of the fuel heater/vaporizer. Both high and low range rotameters were used for propane flow. Pressure and temperature at the flow meter exit were measured for density correction. One wide range flow meter was sufficient for kerosene flow measurements on Stand 2. Kerosene flow on Stand 1 was measured with a low flow rotameter and one of the propane meters, recalibrated for the liquid fuel.

c. Flow of working fluid through the vapor generator loop, measured upstream of the pump inlet. The temperature of the liquid at the flowmeter was measured to allow density correction.

d. Flow of sample gas through the Flame Ionization Detector Hydrocarbon Analyzer. This was not measured directly, but was maintained at a constant value by heating any gas flow through the instrument to the temperature of the sample line, and by holding a fixed pressure ahead of the capillary line restriction at the instrument inlet.

e. Flow of helium through the thermal conductivity, detector gas chromatograph. This was measured by using a "soap

bubble flow meter". The helium flow rate was set to 15 cc/min each time the instrument was used.

4. Emissions Measurements

Measurements of the burner exhaust gas were made for oxides of nitrogen (NOx), carbon monoxide (CO), unburned hydrocarbons (HC), carbon dioxide (CO_2) and oxygen (O_2). The instruments and techniques used are described in detail in section V of this report. Briefly they were:

a. Griess-Saltzman method for NOx. This is a wet chemistry method that requires drawing a sample into a container that contains a chemical solution which turns a reddish purple color in the presence of NO_2.

b. Thermal conductivity detector gas chromatograph for CO and CO_2. This instrument permitted analysis of discrete samples of burner exhaust which were supplied by a sampling pump.

c. Flame Ionization for hydrocarbons. This instrument permitted continuous analysis for total hydrocarbons. It required a heated sampling line and heated sample pump. The FID is part of a chromatograph which can be used for hydrocarbon separations and analysis.

d. Bailey Heat Prover for O_2 and combustibles (CO and H_2). This instrument draws a sample from the burner flow providing continuous analysis. This instrument was the principal means used for setting the burner fuel/air mixture ratio. It provides an oxygen reading which was in close agreement with the more accurate values obtained by volumetric analysis.

3. Volumetric gas analyzer for CO_2, O_2, and CO. This instrument, commonly referred to as an "Orsat" apparatus was in fact manufactured by the Burrell Corporation. It provides an accurate analysis of a gas sample drawn into the instrument. Volumetric analysis is obtained for CO_2, O_2, and CO to an accuracy of about 0.1%.

C. Test Procedures and Techniques

Testing was conducted for the general purpose of investigating and documenting the emissions characteristics and the stability characteristics (rich and lean blowout limits), of the Paxve burner. Testing was conducted in burner test stands 1 and 2. Test stand 1 was used primarily for stability testing and burner emissions with propane. Stand 2 was utilized for the detailed investigation of the influence of the vapor generator system on burner emissions and for kerosene stability testing.

1. Burner Operation

The general burner test procedure was to ignite the burner and bring it to the desired combination of air mass flow,

air and fuel inlet temperature and fuel/air ratio. Ignition of the burner with propane was accomplished by setting a low airflow, turning on the igniter and bringing in the fuel so as to approach ignition from the lean ignition limit. Ignition in this case was always smooth and continuous. Once the burner was ignited, air flow and fuel flow were increased simultaneously to the desired total mass flow and fuel/air ratio setting. In the case of kerosene combustion a burner warmup period was usually allowed during which the burner was ignited and operated with propane. Then after the burner and lines were hot the kerosene was brought in and propane flow reduced until kerosene combustion was self sustaining.

The burner test condition was established by visual readout of the console pressure, temperature, and flow meters, and the Bailey Heat Prover. The latter instrument gives continuous reading of the percent oxygen and percent combustibles in the exhaust gas. The combustion data of Figure 11 shows the variation of the percent oxygen and combustibles with fuel/air ratio for operation with propane and octane. It should be noted that the combustibles reading on the Bailey is a combination of the CO and H_2 content in the gas.

Once a stablized operation test point is established readings are taken of all the operational instruments. Chromatograph records are taken and identified on the strip chart. In the case of the 9000 instrument (FID), the continuous level of total hydrocarbons is identified with a run number. The recorder is then switched to the left channel of 8004 instrument to measure carbon monoxide and oxygen using the left hand column. The right channel and column are then used to measure carbon dioxide. Burner gas samples are collected in flasks for Greiss-Saltzman analysis of NO_2. Concurrently, a gas sample is drawn into the Burell volumetric analyzer and is then analyzed for CO_2, oxygen, and CO. After all data has been recorded and spot checks made to establish consistency, a new operational test point is established by adjusting the air flow, or an inlet temperature.

Testing of the burner was conducted over a wide range of fuel/air ratios, ranging from the lean limit to the rich limit of burner operation. At times these tests were destructive to the burner or portions of test apparatus. This was particularly true at stoichiometric and rich burning operation. Stoichiometric combustion of propane or kerosene with air leads to combustion temperatures on the order of 3500°F to 4000°F. Such temperatures are well in excess of the structural capabilities of any of the materials used for the fabrication of the Paxve burner.

Fortunately, the burner materials do not reach the theoretical flame temperature, and therefore the burner is capable of surviving periods of stoichiometric operation. The ceramic portions of the Paxve burner can withstand temperatures on the order of 3300°F, but the metallic portions of the structure do not have these capabilities and hence destruction of various metallic sections such as inlet pipes or external supports sometimes occurred.

When rich combustion was being investigated, there were in general two combustion processes going on. Combustion within the burner was taking place using the burner air supplied through the inlet pipe. This internal combustion during rich operation might involve combustion temperatures on the order of 2500°F to 3000°F, well within the burner capabilities. Simultaneously, however, after-burning was taking place outside the burner where the burner exhaust mixed with ambient air. That external combustion process impinged directly on some portions of the test stand or inlet tubing. Protection of these elements was therefore necessary. Potential destruction of the test stand sometimes limited the capability for extensive stoichiometric or rich testing.

Attempts were made early in the program to make measurements of the combustion air and burner temperatures by means of probes extending through the air inlet pipe. It was found that these probes sometime interfered with the operation of the burner causing flash back or flame holding on the probe. This was in general accompanied by rapid deterioration of the inlet pipe. Inlet pipe probing was discontinued in order to avoid this type of problem.

During some tests near stoichiometric operating conditions, combustion within the burner inlet pipe would occur, particularly at low flows with high inlet temperatures. Data were gathered under these difficult conditions to the fullest extent possible. This type of phenomenon did, however, restrict the range of burner operating conditions we could conveniently explore.

2. Vapor Loop Operation

For those tests in which measurements were made downstream of the working fluid vapor generator, it was necessary to start the working fluid system before igniting the burner. This avoided problems of overheating the fluid in the coils which could otherwise have taken place.

Once the vapor loop system was circulating working fluid at an acceptable rate, the burner was ignited and the usual procedures previously described for burner operation and data measurement were followed.

Start up of the vapor generating loop was initiated by pressurizing the low pressure reservoir to about 30 psi. This eliminated problems of pump cavitation during start up and operation of the system. The pump drive was then started and the loop brought up to an acceptable operating condition. Early in the program, a remotely actuated clutch between the engine and the working fluid pump was disengaged when starting the motor. The clutch was then engaged in order to drive the pump. It was found that this disengagement and re-engagement of the clutch was unnecessary and in later stages of the program the clutch was left permanently engaged.

Operation of the vapor loop was generally uneventful unless the nitrogen gas bubble at the top of the high pressure

accumulator had been lost. When there was no gas bubble in the high pressure accumulator, the pump pulsations were fed to the pressure gauges resulting in physical damage to those gauges.

All of the operating parameters of the vapor generator system were monitored including the working fluid flow rate and the liquid and burner exhaust inlet and exit temperatures. No funds were provided in the contract to investigate the performance of the vapor generator from an efficiency point of view and therefore this data has not been reduced.

Exposure of the working fluid to excessively high temperatures in the presence of even small amounts of oxygen causes thermal degradation of the working fluid. The nitrogen utilized for the low pressure reservoir pressurization system and the high pressure accumulator contained small but nevertheless significant quantities of oxygen. Care was taken, therefore, to avoid excessive vapor generator tube wall temperatures. Vapor outlet temperatures as high as 600°F were occasionally permitted, but in general the vapor loop exit temperature was kept below 400°F. Since the purpose of the vapor loop was to quench reactions in the burner exhaust it was not felt necessary to permit higher working fluid temperatures.

Operation of the burner in connection with the vapor generator loop was restricted to a fairly narrow range of burner operating conditions as a further step towards avoiding problems with the working fluid. The burner itself will operate from an oxygen concentration near the lean limit of about 12% through stoichiometric to a combustible concentration at the rich limit of over 20%. Unfortunately the operation of the burner at oxygen concentrations of less than about 6% to 8% yields gas temperatures which are too hot for safe operation of the vapor generator loop.

The policy, therefore, was to operate the burner in connection with the vapor generator from its lean limit up to a maximum combustion temperature of about 2700°F. This corresponds with ambient inlet temperature to about 6% oxygen concentration. With an elevated inlet temperature (T air 400°F), the oxygen concentration in the burner exhaust was not allowed to fall below 8%.

Operation of the vapor generator in connection with the burner required special system shut down procedures. The burner was shut off by cutting the fuel flow with the air blower still operating, the blower was then continued in operation until the gas temperature level leaving the burner was below 500°F. Working fluid circulation was maintained during this time. This precaution during shutdown was necessary to avoid overheating the working fluid in the coils.

Instrumentation for monitoring the burner operating point, specifically the Bailey Heat Prover and the volumetric gas analysis equipment, were set up to draw their gas samples from the exit to the burner, ahead of the vapor generator loop. This permitted rapid

response of the system to changes in burner input variables. It also avoided questions of inadvertent dilution of the burner exhaust with ambient air which occasionally arose when the system was improperly set up.

The exit temperature of the gases from the vapor generator exhaust were monitored as well as the temperature of the gases in the burner. Vapor generator air exhaust temperature was frequently in the range of 200°F or less. During start up it was common to see water condensing on the vapor generator coils. This condition persisted until the working fluid became hot enough to cause evaporation. It was found that the presence of water on the vapor generator coil and air intake tube surfaces influenced the oxides of nitrogen readings from the top of the vapor generator stack. This influence was duly noted during the course of the program.

3. Blowout Test Procedure

Lean and rich blowout limits are defined as the demarcation between the burner's ability to burn or not burn due to a change in fuel or air flow. It is not actually possible to operate at the blowout limit. The blowout limits are found by showing that a burner will stay lit at a particular set of conditions (a specific fuel/air ratio) but not stay lit at another set of conditions (another fuel/air ration) not far removed from the first set of conditions. Further, it is not sufficient that the burner merely operate for a short period of time at a set of conditions, but is required that sustained (steady state) operation be evident so that an equilibrium condition exists within the burner.

Determining blowout conditions, then, requires that the burner operate for a sustained period of time while being observed to see whether the operation is steady or if the burner is going out. Determining blowout limits with propane or kerosene involves substantially the same operation, so that a description of one will characterize the other. The determination of lean limits is somewhat different than determining rich limits. Both methods will be described.

The emission measurement equipment needed for the tests are (1) the Bailey Heat Prover, (2) the FID hydrocarbon detector, and (3) the volumetric gas analyzer. The gas chromatograph (thermal conductivity detector) may be used, but it was not essential for these tests.

a. Lean Blowout Using Propane

A burner is set up and ignited, as previously described in the burner operation procedure. The air flow rate is set at the desired value. The fuel flow rate is set to obtain a reasonably hot burner (f/a ≈ 0.04 to 0.05) to heat up the burner and system. After a period of warm up, the fuel flow rate is reduced substantially (f/a ≈ 0.03). The continuous emissions measuring equipment (Bailey and FID) are continuously monitored to determine when steady state is reached. The

thermocouple reading inside the burner is also helpful in this regard. It generally takes several minutes for most traces of burner variation to disappear.

Steady state is characterized by a relatively unchanging reading on the aforementioned instruments (Bailey, FID and burner thermocouple). The most sensitive instrument for this purpose is usually the FID. It will detect small changes in burner operation near blowout well in advance of the other instruments.

When a steady state burning condition has been reached, the fuel flow rate is decreased in increasingly smaller increments with allowances made between each change for the burner to come to a steady state condition. As lean blowout is approached, it will be noticed that unburned hydrocarbon output begins to increase as a result of incomplete burning in the burner. However, as long as the blowout limit is not exceeded the unburned hydrocarbon output will attain a steady value when steady state conditions exist.

After the unburned hydrocarbon output first indicates that lean blowout is being approached, the Bailey Heat Prover begins to show an increase in oxygen content and a measurable reading of combustibles. This indicates an increase in hydrogen and carbon monoxide output due to inefficient combustion. The thermocouple for burner temperature starts to drop.

When the Bailey first begins to show a combustibles output, a volumetric analysis is taken at each fuel flow setting (or the gas chromatograph may be used) to determine the composition of the exhaust stream.

As fuel flow is gradually reduced, a point will be reached when the burner will eventually go out. This condition is characterized by a gradually accelerating increase in unburned hydrocarbon output, which never steadies out. When this condition is noted, a volumetric analysis is rapidly made. The fuel/air ratio previous to the blowout point is termed incipient blowout and represents the last steady state burning condition on the rich side of lean blowout. The lean blowout condition is now straddled by two points, one on either side of the lean blowout limit.

The air flow rate or inlet temperature is now changed and the process repeated until the lean blowout limit has been characterized as a function of the burner inlet condition.

b. Rich Blowout Using Propane

Rich blowout limits are somewhat more difficult to determine since burning will continue to occur outside the burner even though the blowout limit has been exceeded within the burner. The Bailey Heat Power is not used for these tests since the combustible output is beyond the range of the meter. Some of the combustibles produced have carbon chains longer than 2 which gives erroneous results on the Bailey and can coat the detector with carbon. The FID's use is also limited by the high unburned hydrocarbon output under these test conditions.

Rich operation is characterized by stable but incomplete combustion within the burner and a large flame outside the burner. Combustion with insufficient air within the burner produces large amounts of hydrogen, and carbon monoxide (see Figure 11). There is usually some hydrocarbon content to the rich exhaust stream in addition to the H_2 and CO.

The products of incomplete combustion burn outside the burner as they mix with the ambient air, producing a large yellowish luminous flame.

Detecting rich blowout limits requires some art. It involves (1) watching combustible temperature in the burner via the burner thermocouple, and (2) determining whether the burner responds to reignition at a leaner condition than a suspected rich blowout condition.

The burner is set up similar to determining lean limits. When the system is hot the fuel is increased until rich burning occurs outside the burner as described above. The fuel flow rate is gradually increased. At each fuel setting, a fuel/air ratio is determined by taking a volumetric analysis. Instead of increasing the fuel flow in a straightforward manner, after each fuel setting the fuel flow is first decreased to the previous setting then increased to another setting. If the burner has not gone out at a particular setting decreasing the fuel flow should show an increase in the burner temperature when the burner is leaned out. If the burner has gone out at a particular condition, leaning the burner should show no effect on the indicated burner temperature. Also if the igniter is initiated at the leaner condition the burner will reignite (as evidenced by the burner thermocouple output). The rich blowout limit is thus spanned by a condition where it is shown that the burner is still lit and a condition where it has gone out.

Visual observations of burning in the burner and audible sounds of burner operation are also helpful for absolute assurance of blowout.

D. Emission Data Collection and Data Reduction

The procedures used to obtain and reduce emission data will be discussed here. Familiarity with Section V is helpful in understanding the operation of the equipment discussed. Reference will be made to Section V when a specific point must be made.

Numerical determination of emission concentration is either in parts per million (ppm) or grams per kilogram (gm/Kg or mg/g). PPM data refers to the concentration of pollutants in the exhaust gas expressed as volume of pollutant per volume of total flow. This data is most useful in considering emissions from stationary sources. Gm/Kg data refers to grams of pollutant per kilogram of fuel. This data is the most significant for mobile emission sources. Emission data in gm/Kg is necessary to determine grams of emission per mile.

1. Oxides of Nitrogen

a. Collection Procedure

The oxides of nitrogen concentration was determined by the Greiss-Saltzman method which is explained in Section V and Appendix A. Data collection involves evacuating a flask and then drawing the gas to be analyzed into the evacuated flask. For the tests, a quartz tube, close coupled to the flask was inserted directly into the point being sampled; the stack and/or the burner exhaust. The flask is then sealed.

When a sample is being taken during rich operation, the evacuated flask is first 1/2 filled with air by connecting it to a flask of equal size at atmospheric pressure. The sample is then drawn into the half empty flask.

To analyze the gas in the flask for NOx, Saltzman reagent is added, the flask is resealed and shaken for 1 hour to ensure contact of the gas sample with solution. The solution is then poured into a cuvette and its optical density at 5500 Angstrom units is determined, using a colorimeter.

Early in the program, the Saltzman solution was placed in the flasks before they were evacuated. The sample was then drawn and the flask resealed and shaken. This procedure produced identical results to the method previously described.

When a NOx sample after being shaken in the flask for 1 hour produces a very intense color which is known to be saturated, an additional amount of Saltzman solution is added to the flask and the shaking period is extended to provide additional dilution and produce a readable transmission value.

b. Data Reduction

Calibration of the absorbing solution, explained in Section V and Appendix A, produces calibration curves shown in Figures V3 and V4. The best fit through the experimental calibration data is a family of straight lines on semi-log paper. The data reduction has usually been done by hand using the curves. When the computer has been used to reduce the Saltzman data, the following formula is used.

$$NO_2 = 5(1+D)\,\frac{\ln(C_x R_x)}{\ln(R_5)}$$

$$NO_x = 5(1+D)\,\frac{\ln(I/I_o)}{\ln(I_5/I_o)}$$

Where:

D = dilution ratio

I = reading obtained after spanning with distilled water

I_5 = reading at 5 ppm

I_o = reading with pure Saltzman reagent

The data obtained by the data reduction procedures outlined above is ppm by volume.

2. Hydrocarbons

a. Collection Procedure

Gas was pumped through a heated pump and sample line to a flame ionization detector used to detect total hydrocarbons. The sample gas passes directly through the detector without going through a packed column, as explained in Section V.

b. Reference Gases

The instrument was calibrated with zero air and span gas. The zero is adjusted while zero air is flowing through the instrument. "Zero air" is not truly free from hydrocarbons, although every effort is made by the company which distributes the gas to achieve this result. The degree of impurity is evident to some extent when the flow rate through the instrument is changed. Very pure "zero air" shows almost no response on the FID to a change in flow rate. Zero gases are generally guaranteed to have less than 0.5 ppm of methane which is equivalent to 0.08 ppm of hexane.

It is conceivable that a really pure gas flowing through the FID will read less than zero. During the course of the tests conducted here, zero or slightly negative values were obtained frequently for hydrocarbon emissions. The zero to the instrument was then checked for drift by immediately running a "zero air" sample before the next test point. Whenever drift occurred, an appropriate correction was made in the data. There were, nevertheless, a number of points which gave zeros that could not be distinguished from the "zero air" setting and this "zero air" was usually pure.

c. Sensitivity and Data Reduction

The sensitivity is adjusted while the span gas is flowing through the instrument. The current practice is to adjust the instrument flow rates so that a full scale reading at the most sensitive position corresponds to 10 ppm of hydrocarbon expressed as hexane. The span gas used normally contains about 200 - 250 ppm hexane equivalent. With this adjustment, the scale factor for the FID becomes S(FID) = 0.1 ppm/division.

The response of the FID is sensitive to the amount of oxygen present in the gas stream. This is called the oxygen synergism effect. With the FID used by Paxve, oxygen decreases the sensitivity of the instrument to the propane-butane mixture used for span gas. Figure 12 shows the reduction in sensitivity of the FID. The attenuation factor is fitted very closely by

$$\text{Att} = 1 - 0.32 \tanh \left(\frac{O_2}{9.6}\right)$$

where

O_2 = oxygen concentration in percent

Final data reducton was accomplished by taking into account the presence of oxygen in the sampled mixture. This problem is discussed further in Section V.

3. Carbon Monoxide and Carbon Dioxide

a. Collection Procedure

Carbon monoxide and carbon dioxide were measured by a gas chromatograph using a thermal conductivity detector, as explained in Section V. Carbon dioxide was measured by volumetric analysis, also described in Section V. Since the use of the volumetric analysis is straightforward and was adequately covered in Section V it will not be discussed here.

Gas samples were pumped from the burner exhaust to a common manifold and valved from the manifold to each side of the chromatograph. The sample pump supplies a maximum pressure of 14 psig. During burner operation, sample gas is continuously being pumped from the burner through the sample manifold, through the gas sample valve, through the sample loop (see Section V, Fig. 6a) and is finally vented to atmosphere. During sampling the gas sample valve is switched so that the sample loop is now ported on one side to the carrier gas and on the other side to the column inlet. The carrier gas now flows through the sample loop, pushing the gas sample into the instrument.

Due to the common manifolding in the instrument to the column inlets for carrier gas, it is necessary that the sample gas not enter the instrument at a higher pressure than the carrier gas pressure. If the pressure in the sample loop is much higher than ambient, when the gas sample value is switched some of the sample gas can enter the instrument and travel to the wrong column inlet (see Figure V-6a). This condition will give erroneous results. To eliminate this condition the valve on the sample manifold leading to the sample valve is first closed, so that the gas in the sample loop returns to atmospheric pressure. Then the sample valve is switched.

b. Reference Gases and Data Reduction

Calibrations and zero conditions are obtained similar to those obtained when detecting hydrocarbons. No correction must be applied to the data since both sides of the instrument are linear within the range of interest.

4. Conversion of Volumetric Data to Gravimetric Data (ppm to gm/Kg)

It is desirable particularly in the case of pollutants to express the emission levels in terms of the grams of pollutant per Kg of fuel. In order to do this we must account

for the difference between the molecular weight of the pollutant and the molecular weight of the exhaust gas. We must also correct for the water vapor which is formed during the combustion process but then condenses in the sampling line before the gas sample is analyzed. An analysis of this problem has been conducted. The result can be expressed as:

$$W_p = K\phi X_p M_p$$

Where

$$K\phi = \left(1 + \frac{(a/f)s}{\phi}\right) \left(\frac{1-X_w}{M_{ow}}\right)$$

Wp = weight fraction of the pollutant gm/gm

Xp = Mole fraction of the pollutant in the sample

Mp = Molecular weight of the pollutant

$K\phi$ = A constant which depends on fuel and the equivalence ratio

ϕ = Equivalence ratio - $\frac{(a/f)s}{(a/f)}$

$(a/f)_s$ = Stoichiometric air/fuel ratio

X_w = Mole fraction of water in the exhaust

M_{ow} = Molecular weight of the wet exhaust gas

Values of X_p are first determined expressed in the ppm. To obtain the weight fraction of the pollutant in the sample, it is necessary to multiply X_p by $K_p = K\phi\ M_p$ to obtain W_p in grams/kilogram of fuel. Plots of $K_p = K\phi M_p$ versus f/a ratio for the various pollutants produced by propane and kerosene are seen in Figure 13 and 14. These curves are used to obtain the pollutant emissions in grams/kilograms fuel.

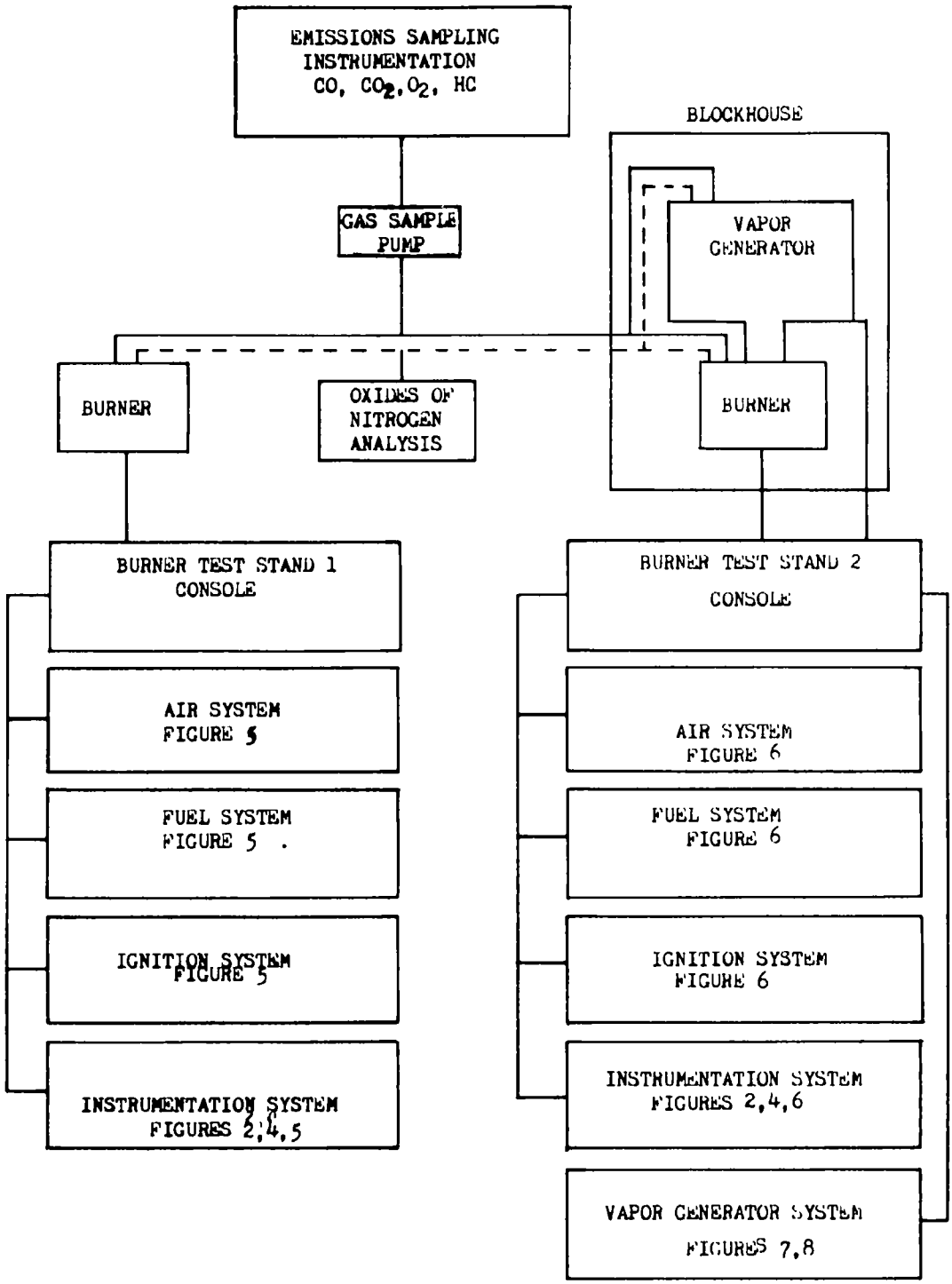

FIGURE IV - 1 BURNER EVALUATION FACILITIES

A. Console for Burner and Component Test Facility
(Test Stand Two)

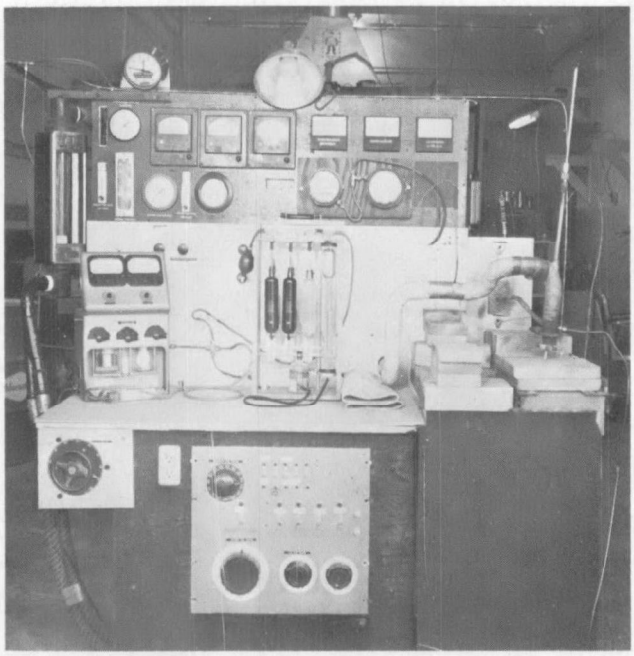

B. Console for Subscale Burner Test Facility
(Test Stand One)

TEST FACILITIES

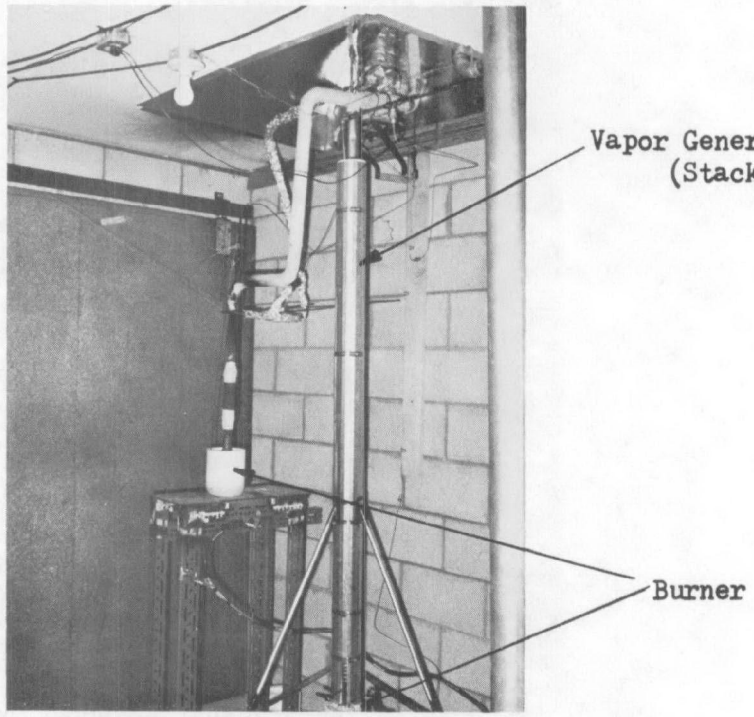

a. Burner/Vapor Generator Installation
In Stand No 2

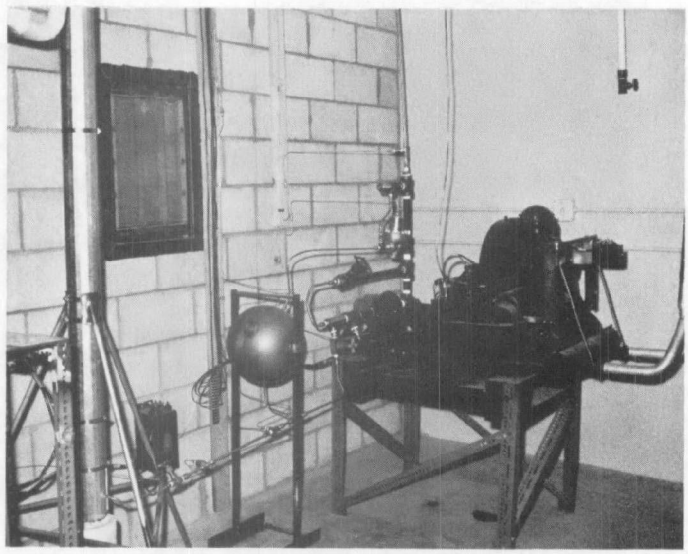

b. Burner and Vapor Generator System Assembled in Blockhouse
Burner Test Stand No. 2

BURNER TEST FACILITIES

Figure IV - 3

A. Overall View of Facility

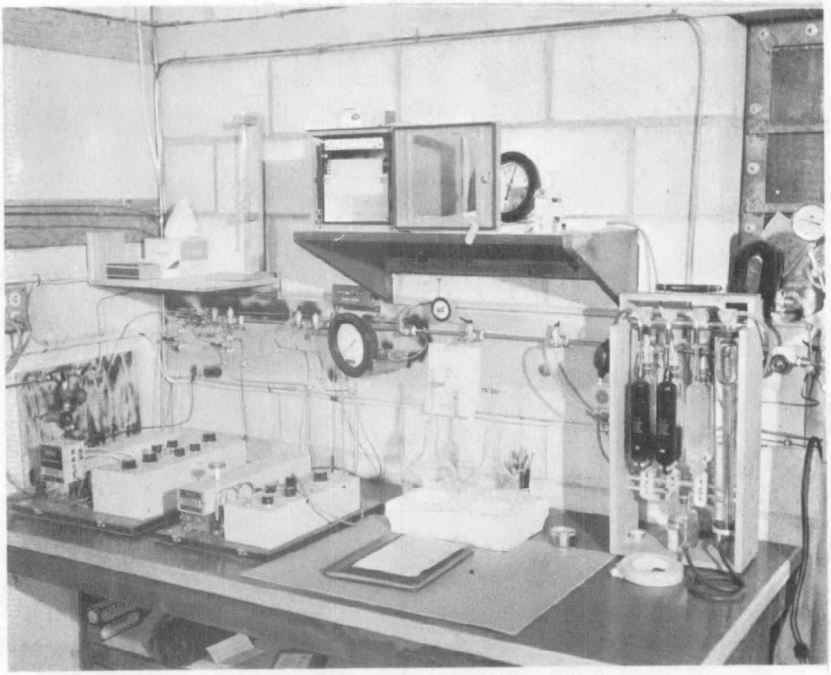

B. View of Emission's Sampling and Analysis Equipment

TEST FACILITY FOR GAS EMISSIONS ANALYSIS

Figure
IV-4

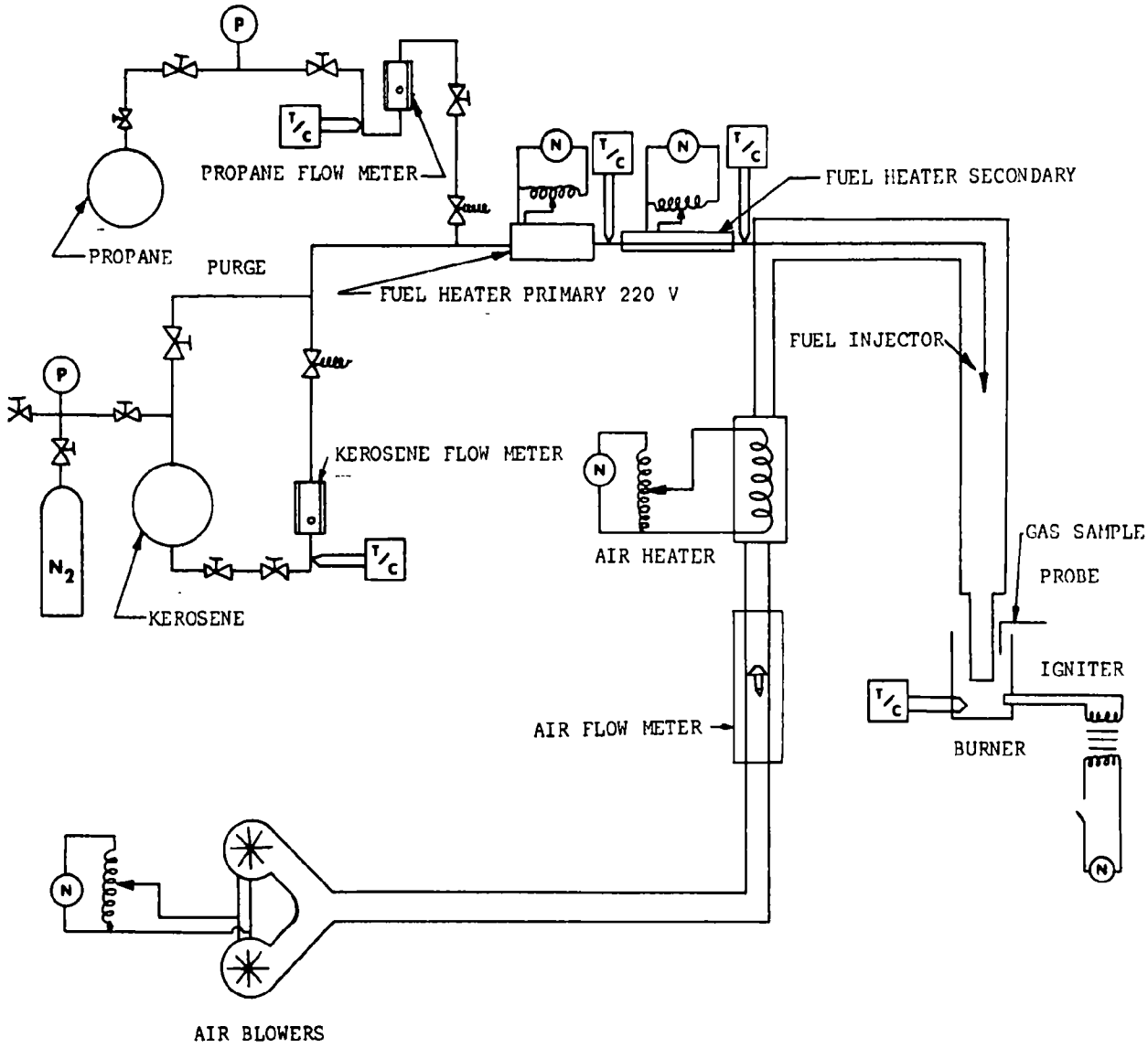

TEST STAND 1 BURNER SCHEMATIC

FIGURE IV-5

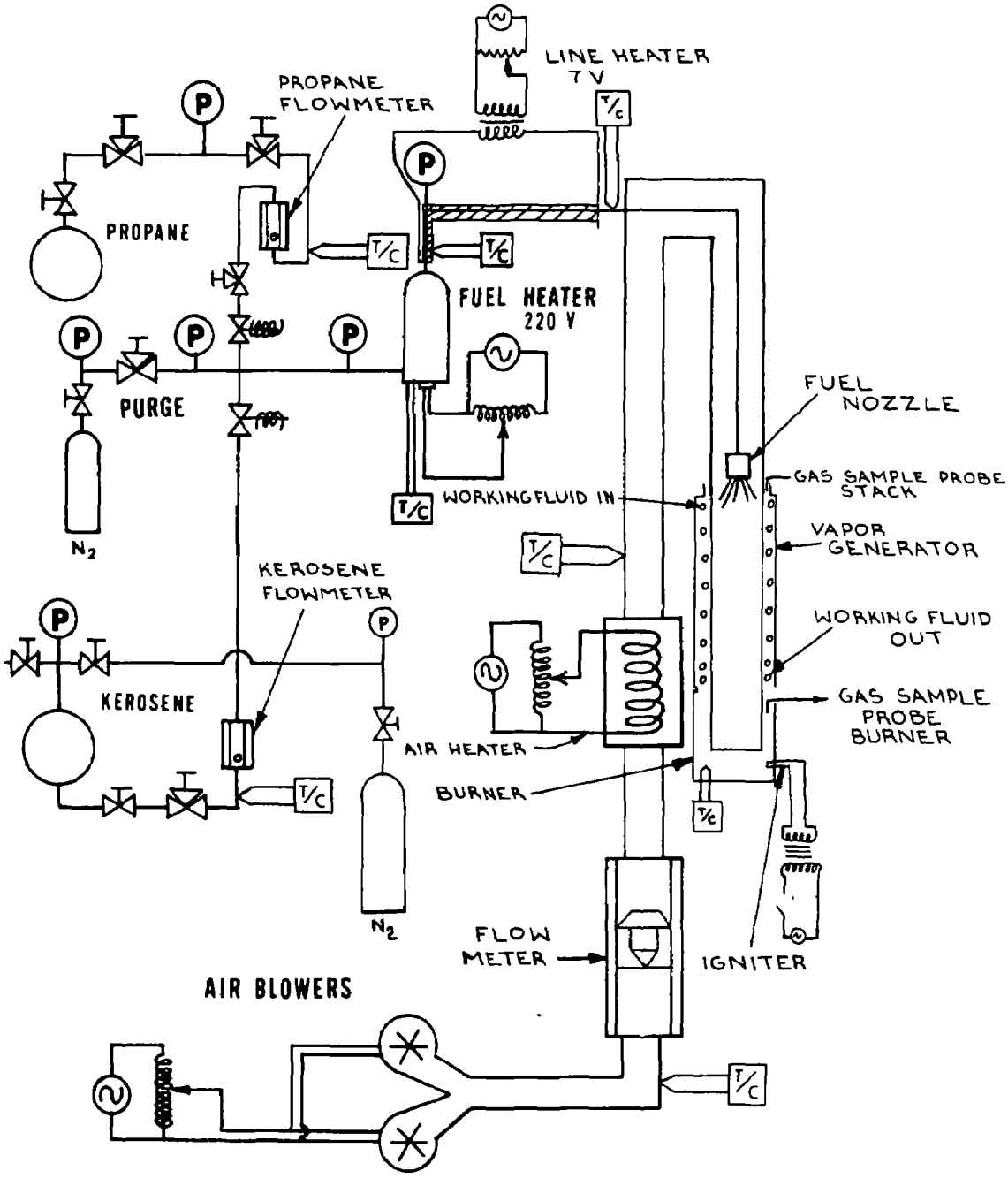

Schematic Diagram of Fuel & Air Systems

Figure
IV-6

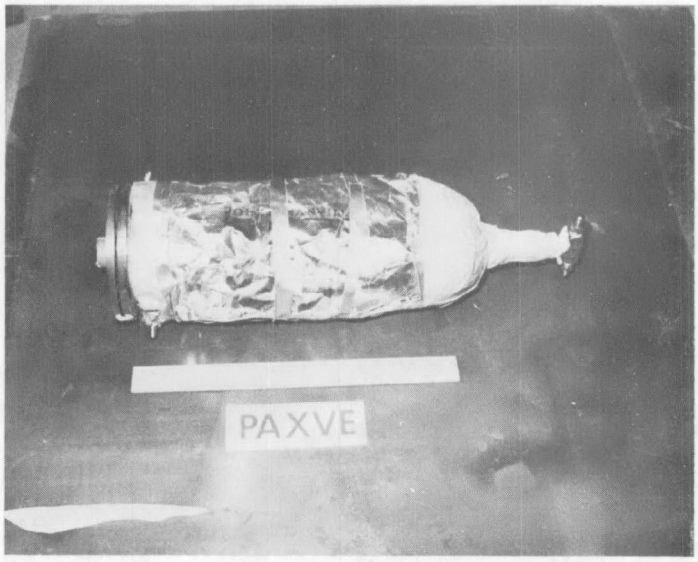

A. Assembled and Insulated Fuel Heater - Vaporizer

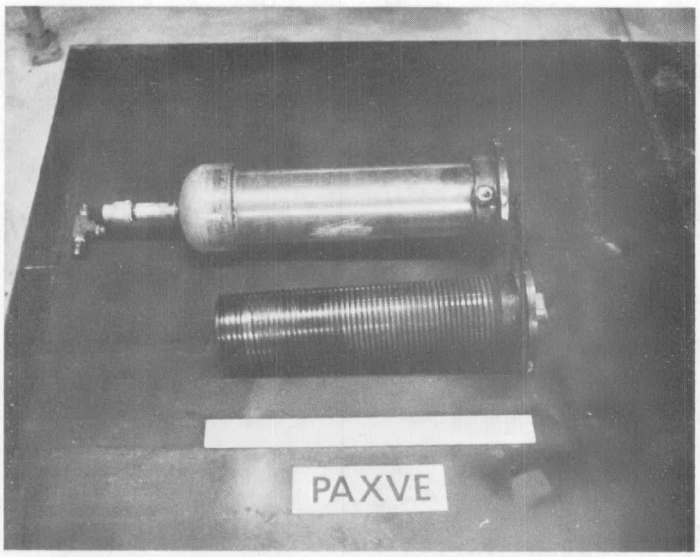

B. Disassembled Fuel Heater Vaporizer After Testing

FUEL HEATER - VAPORIZER

BURNER FUEL SYSTEM

Figure IV -7

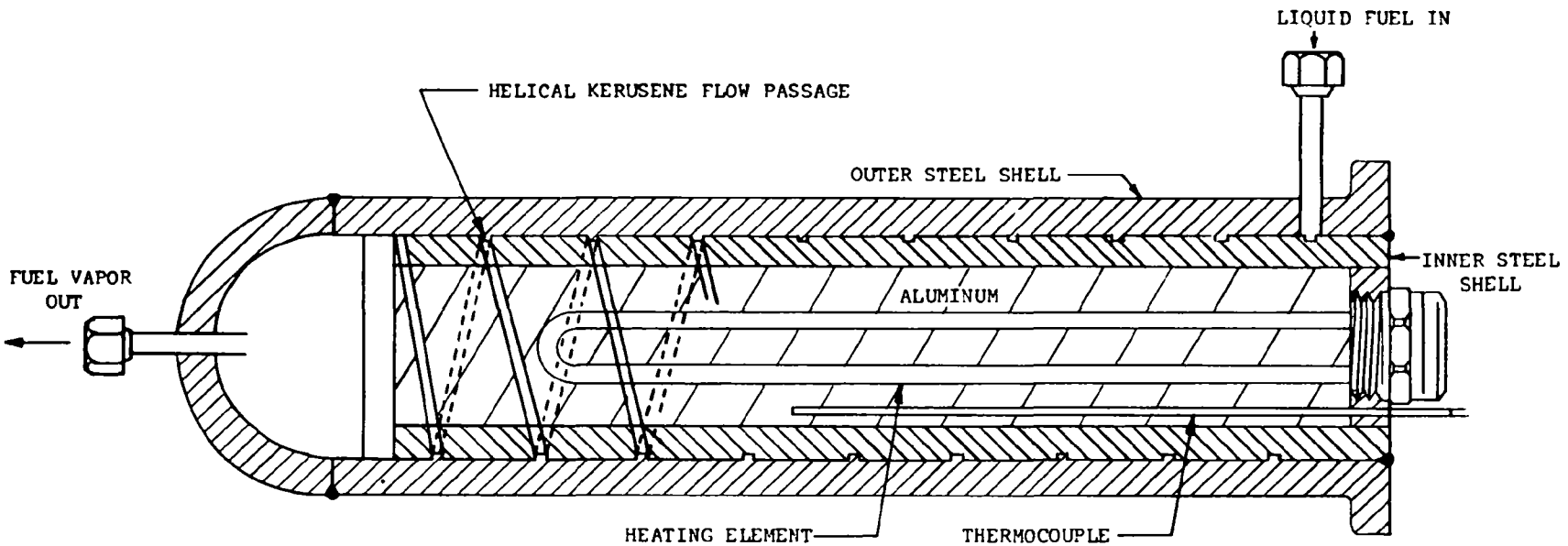

ELECTRICAL FUEL VAPORIZER

FIG. IV 8

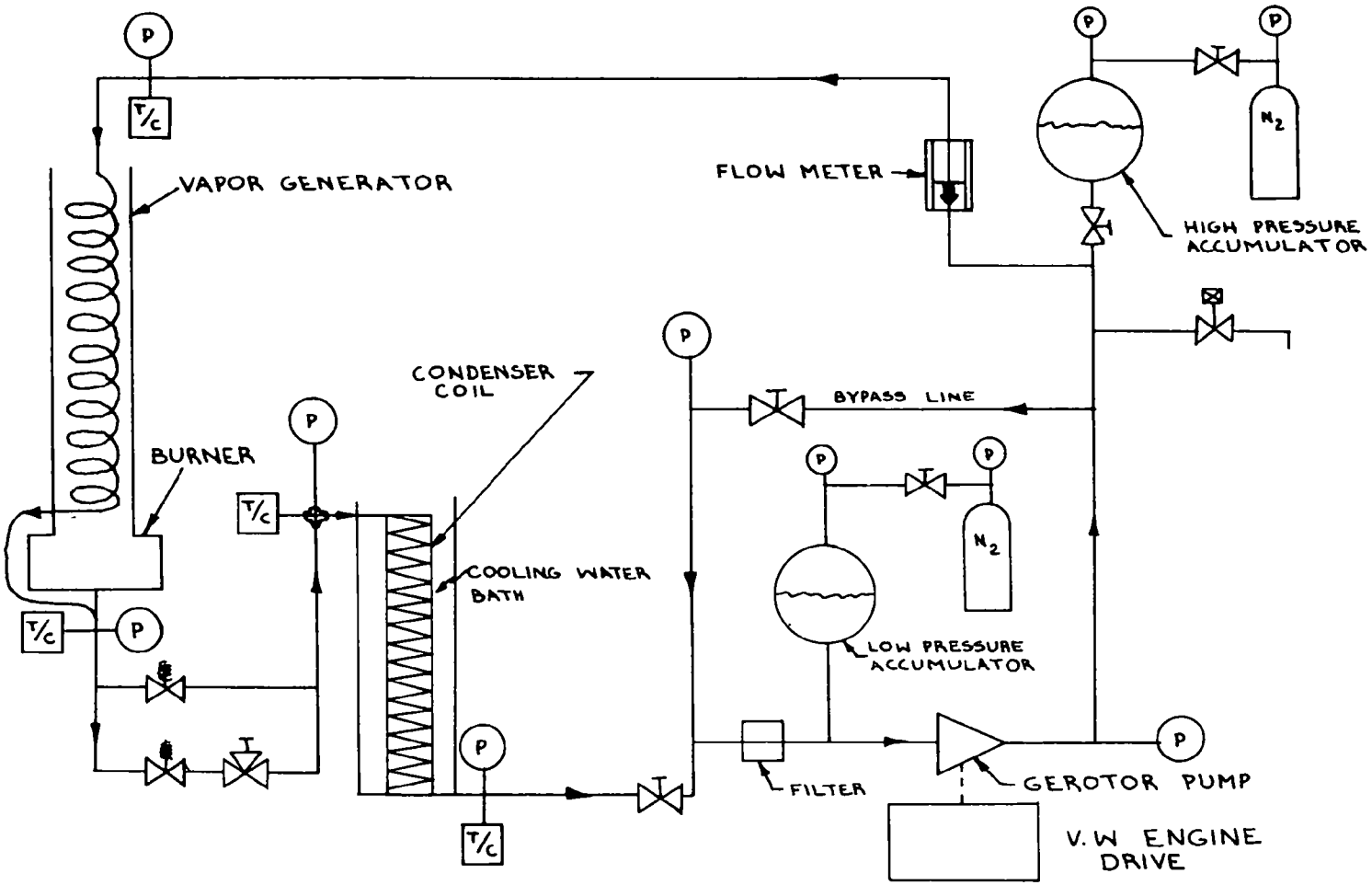

Figure IV-9

BURNER TEST STAND 2

SCHEMATIC DIAGRAM OF VAPOR GENERATOR SYSTEM

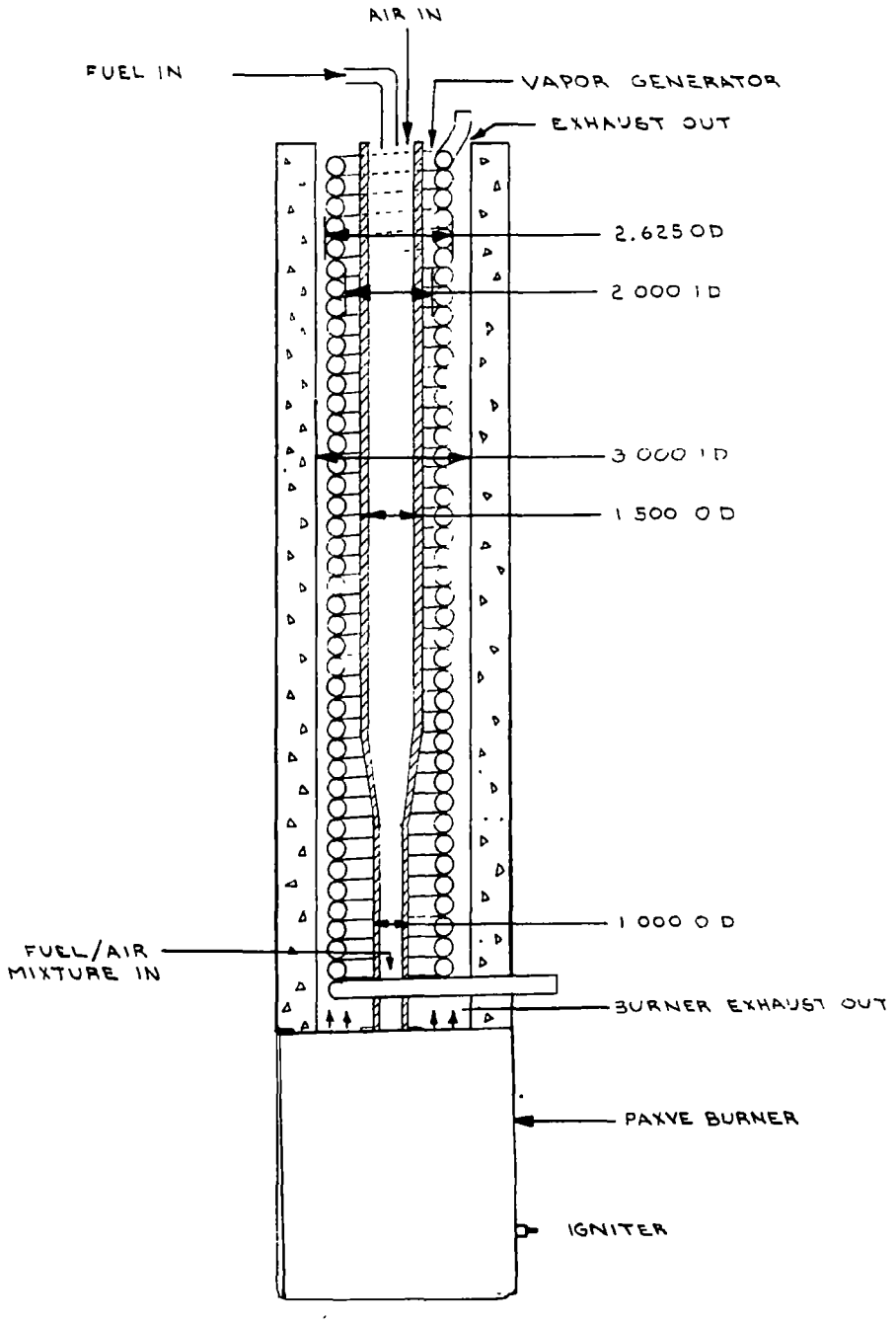

BURNER VAPOR GENERATOR ASSEMBLY

FIGURE IV-10

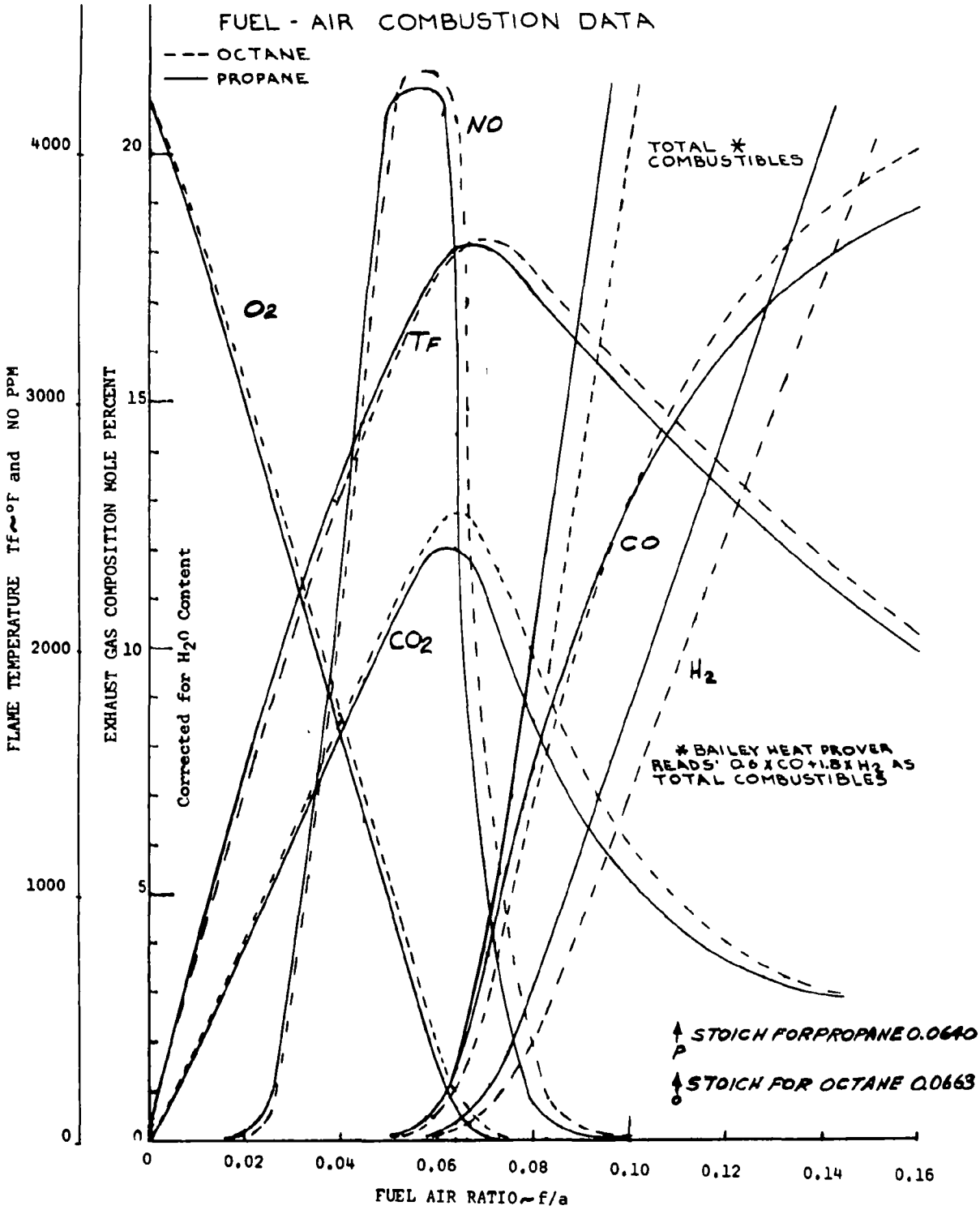

Reference: Combustion of Hydrocarbons-- Property Tables
Purdue University, Eng. Ext. Ser #122, May 66

Figure IV-11

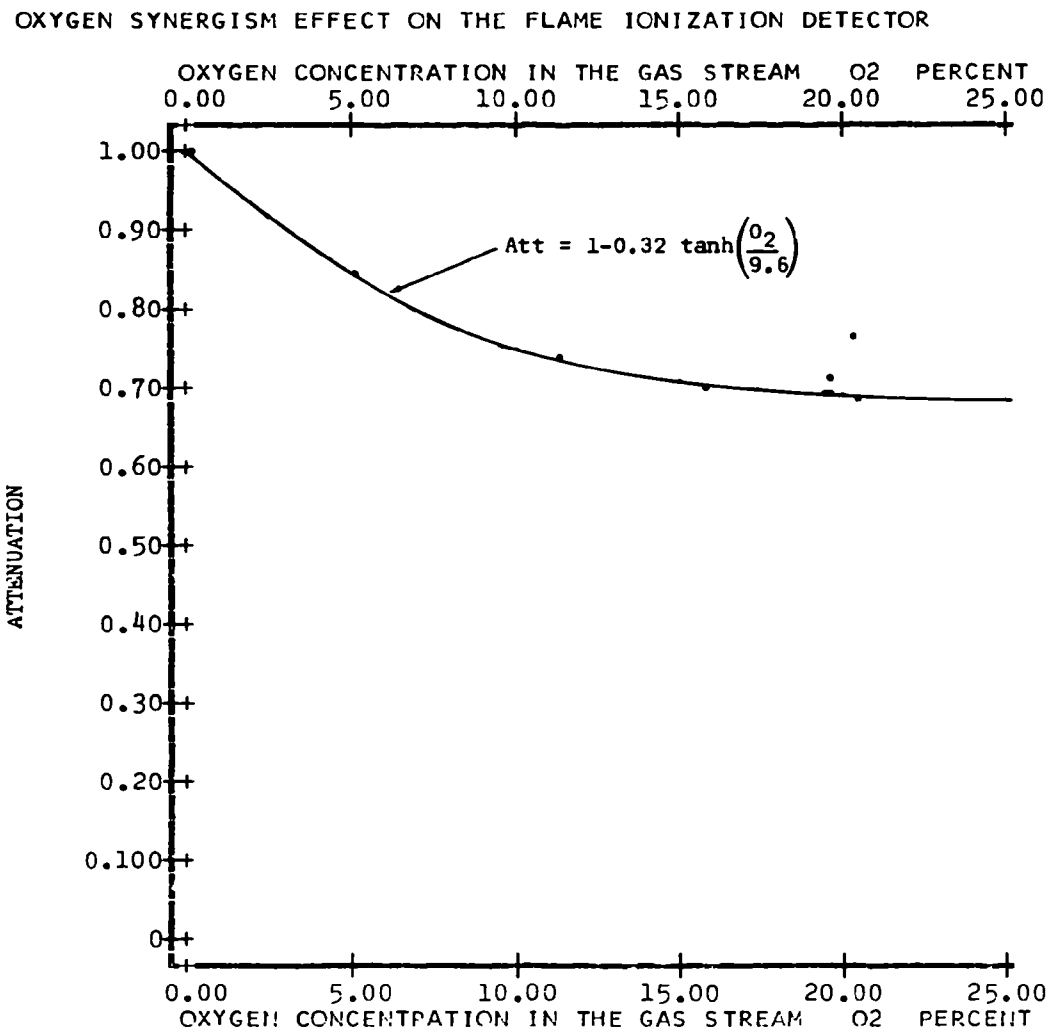
OXYGEN SYNERGISM EFFECT ON THE FLAME IONIZATION DETECTOR
OXYGEN CONCENTRATION IN THE GAS STREAM O2 PERCENT
0.00
5.00
10.00
15.00
20.00
25.00
1.00
0.90
0.80
0.70
0.60
0.50
0.40
0.30
0.20
0.100
0
ATTENUATION
Att = 1-0.32 tanh(O2/9.6)
OXYGEN CONCENTRATION IN THE GAS STREAM O2 PERCENT

Figure IV-12

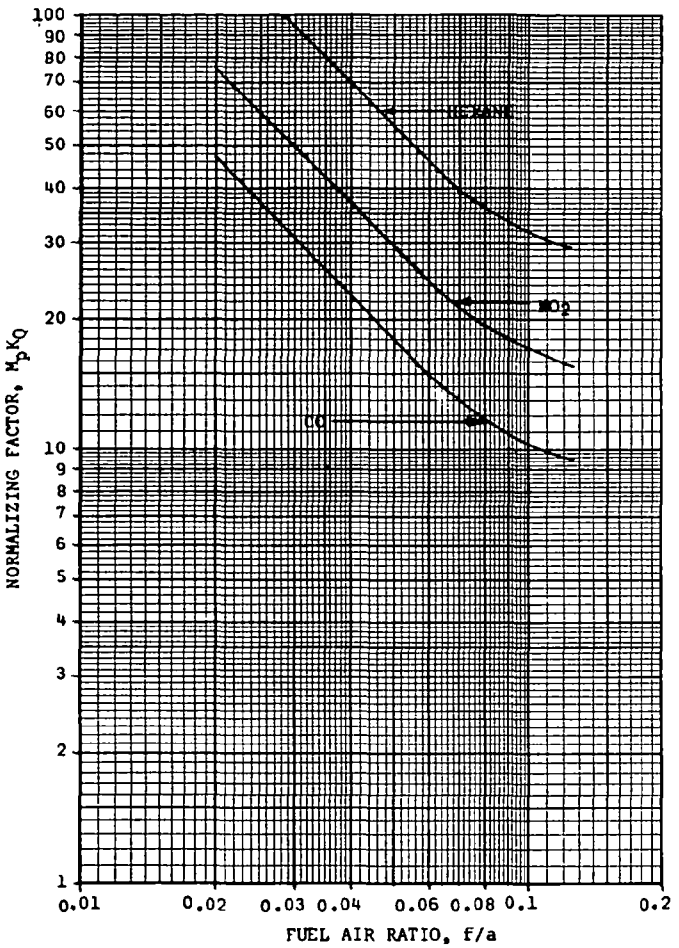

EMISSIONS NORMALIZING FACTORS FOR PROPANE-AIR

Figure IV-13

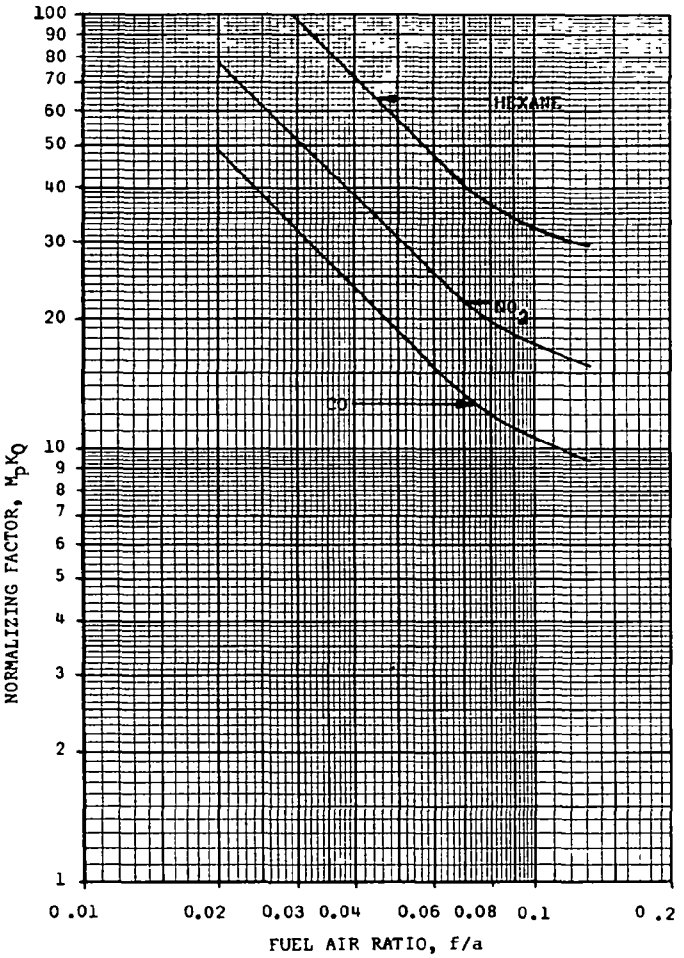

EMISSIONS NORMALIZING FACTORS FOR OCTANE-AIR

Figure IV-14

TABLE I

BURNER STAND NO. 1

TABULATION OF SUBSYSTEMS AND CONTROLS

SUBSYSTEM	PRIME MOVER	CONTROL	VISUAL MEASUREMENTS
Air supply system	(2) Electrically driven centrifugal blowers in parallel	1. On-off switch to variac 2. Indicator Lamp 3. Variac-variable voltage to air blower motors	1. Flowmeter 0-250 pph 2. Flowmeter inlet temperature -75° to +225°F 3. Air temperature to burner 0 to 1000°F
Propane supply system	Self pressurized propane tank and electrical heater	1. Propane tank pressure regulator 2. Remote solenoid valve on-off switch 3. Indicator lamp 4. Flow control needle valve	1. Propane Regulated pressure 0-6 psig 2. Propane flowmeter 0-8 pph 3. Propane pressure at injector 0-30 psig
Kerosene supply system	1. Kerosene tank 2. Nitrogen supply pressure cylinder	1. N_2 pressure regulator 2. Remote solenoid valve on-off switch 3. Indicator lamp 4. Flow control needle valve 5. Kerosene tank N_2 pressurization valve 6. Kerosene tank N_2 pressure vent valve	1. Kerosene tank regulator pressure 0-60 psig. 2. Kerosene flowmeter 0-8 pph
Fuel thermal conditioning	1. Primary heater-electric immersion heating element 2. Secondary heater external resistance heated tubing	1. Primary heater a. On-off switch b. Indicator Lamp c. Temperature adjusting variac 2. Secondary heater a. On-off switch b. Indicator lamp c. Temperature adjusting variac	1. Temperature at primary heater outlet 0-1000°F 2. Temperature at secondary heater outlet 0-1000°F

Table 1 (cont)
BURNER STAND NO. 1

TABULATION OF SUBSYSTEMS AND CONTROLS (CON'T)

SUBSYSTEM	PRIME MOVER	CONTROL	VISUAL MEASUREMENTS
Air thermal conditioning	Electrical immersion heating element (Paxve) in line	1. Heater on-off switch 2. Heater indicator lamp 3. Temperature control variac	1. Air temperature at inlet to flowmeter -75 to 225°F 2. Air temperature at inlet to burner 0 to 1000°F
Burner igniter	High voltage transformer 20 KV/30ma.	1. Power switch 2. Indicator lamp	
Burner	Fuel/air/igniter subsystems	1. Power switch 2. Indicator lamp	1. Combustion chamber temp. 0-3000°F

TABLE 2
BURNER STAND NO. 2

TABULATION OF SUBSYSTEMS AND CONTROLS

SUBSYSTEM	PRIME MOVER	CONTROL	VISUAL MEASUREMENTS
Air supply system	2. Electrically driven centrifugal blowers in parallel	1. On-off switch to variac 2. Indicator lamp 3. Variac-variable voltage to air blower motors	1. Flow meter 0-250 PPH 2. Flow meter inlet temperature 0-300° F
Propane supply	Self pressurized propane tank and electrical heater	1. Propane tank pressure regulator 2. Remote solenoid valve on-off switch 3. Indicator lamp 4. Flow control needle valve	1. Propane regulated pressure 0-100 PSIG 2. Propane flow meter 0-8 PPH
Kerosene supply system	1. Kerosene tank 2. Nitrogen supply pressurized cylinder	1. N_2 pressure regulator 2. Remote solenoid valve on-off switch 3. Indicator lamp 4. Flow control needle valve 5. Kerosene tank N_2 pressurization valve 6. Kerosene tank N_2 pressure vent valve	1. Kerosene tank regulator pressure 0-200 PSIG 2. Kerosene flow meter 0-8 PPH
Air thermal conditioning	Air heater unit 220 V/AD-20 AMP Immersion heating	1. Remote power contactor 2. Variac (220 V/AC 2AMP variable voltage control to heater 3. Indicator lamp	1. Temperature at heater outlet 0-500° F
Fuel thermal conditioning	1. Fuel vaporizer unit (Paxve isothermal heater unit 220 V/AC 40 AMP 2 Line heater unit (Paxve resistance heating flow element	1a Power switch and remote contactor b Indicator lamp c Wheelco pyrometric temperature controller 2a Multiple coil current transformer 7.5 V/AC 70AMP b On-off power switch c Indicator lamp d Variac voltage control to transformer 0-12 V/AC	1. Surface temperature Paxve vaporizer heating unit 0-1000°F 2. Fuel temperature at burner inlet 0-1000°F

Table 2 (cont)
BURNER STAND NO. 2

TABULATION OF SUBSYSTEMS AND CONTROLS (CONTINUED)

SUBSYSTEM	PRIME MOVER	CONTROL	VISUAL MEASUREMENTS
Burner igniter	High voltage transformer 20 KV/30 ma.	1. Power switch 2. Indicator lamp	
Burner	Fuel, air, igniter subsystems	Fuel, air, igniter subsystems	1. Combustion chamber temperature 0-3000°F 2. Exhaust gas (stack) temperature 0-1400°F
Vapor generator system	1. Working fluid pump	Valve pump bypass Valve drain or vent upper Valve drain lower Filter total flow working fluid	1. Pump outlet pressure - side 0-3000 PSIG 2. Pump bypass pressure 0-400 PSIG (pump side of valve) 3. Working fluid flow meter 0-3.5 GPM
	2. Pump driven 34 HP VW air cooled engine	2a IGN switch and lamp b Cranking switch and lamp c Electrical control to throttle (incr.-decr.) with lamp d Pneumatic valve to engage clutch e Pneumatic valve to disengage clutch	
	3. Fuel condenser		1. Condenser inlet pressure 0 - 3000 PSIG 2. Condenser outlet pressure -15 + 60 PSIG 3. Condenser outlet temp. 0° - 300° F
	4. Hydraulic surge suppressors a. Accumulator pump inlet b. Reservoir pump outlet	Valve nitrogen supply to reservoir Valve reservoir pressure vent Valve reservoir isolation Valve surge chamber isolation	1. Reservoir pressure -15 + 60 PSIG 2. Surge chamber pressure 0 - 3000
	5. Vapor generator heat exchanger	Valve flow limiting	1. Vapor generator inlet pressure 2. Vapor generator outlet pressure 0-200 PSIG 3. Vapor generator inlet temperature 0-300°F 4. Vapor generator outlet temperature 0-1000°F

V. EMISSIONS MEASURING TECHNIQUES

A. Description and Operation of Instruments Used

During the testing phase of this contract, emission measurements were made on the burner to determine: (1) the unburned hydrocarbons, (2) the oxides of nitrogen, (3) the carbon monoxide, (4) the carbon dioxide, and (5) the oxygen content of the burner exhaust. The instruments used to determine these emissions are as follows:

1. Bailey Heat Prover detected oxygen (O_2) and combustibles (a combination of CO and H_2).

2. Volumetric gas absorption analysis detected oxygen (O_2), carbon dioxide (CO_2), and on some occasions carbon monoxide (CO).

3. Griess-Saltzman method detected oxides of nitrogen (NO and NO_2) as equivalent nitrogen dioxide (NO_2).

4. Gas Chromatography using a thermal conductivity detector with thermistor elements detected oxygen (O_2), carbon dioxide (CO_2) and carbon monoxide (CO).

5. A flame ionization detector detected total unburned hydrocarbons.

The description, operation, and use of these instruments will be discussed in this section along with the need and use of auxiliary equipment and calibration techniques.

1. Bailey Heat Prover

The Bailey Heat Prover (Figure 1) is a portable gas analysis instrument requiring only a source of 105-130 volt ac, 50-60 cycle power. It is otherwise self contained. It is a continuous reading device which measures oxygen and combustibles. The instrument is 8.25" deep, 11" wide and 11.25' tall when closed and 16.5" tall when open and operating. During operation the instrument must be level, in an area free from drafts and sudden temperature changes, and provided with an auxiliary filter to eliminate water and particulate matter which could harm the instrument.

The instrument has two operating ranges for both the oxygen and combustibles side: 4% and 20%. When properly calibrated, the instrument should be accurate to within $\pm$0.5% of the oxygen or combustibles content when on the 20% range and $\pm$0.1% when on the 4% range. These accuracies should not be expected in the upper or lower 10% of either range.

Gas analysis is performed within the instrument as follows (see Figure 1-b): A rotary pump having multiple pumping

chambers draws in air and sample gas at a rate of approximately 100 in^3/min. A large portion of the sample gas is discharged to atmosphere through a blowoff port. Hydrogen is generated in a hydrogen cell by the electrolysis of a 10% sodium hydroxide solution. Hydrogen from the cell passes through the valve block where it is mixed with a portion of the sample gas and then passes to the oxygen analysis cell. Another portion of the sample gas is mixed with air in the pump and then flows to the combustibles analysis cell.

Analysis in each cell is done having the gas mixture pass over a noble-metal catalyst which is one leg of a Wheatstone bridge circuit. The reaction which occurs on the catalyst causes the temperature to change which in turn unbalances the bridge circuit. The output of each bridge is proportional to the heat released on the catalyst and is read out on meters in terms of oxygen and combustibles.

When properly calibrated, the instrument measures combustibles directly only when measuring one part hydrogen to two parts carbon monoxide in nitrogen. Other combustible mixtures may be determined using the correction curves provided by Bailey. Large quantities of hydrocarbons with carbon chains longer than C_2 do not give accurate readings and will deposit carbon on the detector which requires a few minutes of lean operation to burn off and return the instrument to accurate operation.

During operation, the instrument is plugged into the appropriate power, the hydrogen generator checked for liquid level and tightness, the sample jar checked for air tightness, and the filter checked for cleanliness and dryness.

The instrument is turned on approximately 30 minutes ahead of analysis by turning the center lever to "check zeros" to allow for warm-up and to fill the appropriate manifolds with hydrogen. Before making a test each meter is zeroed and the center lever turned to "check cell" to determine if the instrument is reacting properly. At "check cell" the oxygen meter should swing past the red portion of the meter and then fall back into the red space. Correct operation is achieved with and the cell adjuster. After the instrument is operating correctly the center lever is turned to read the desired analysis position.

During operation, care should be taken to prevent the meters from remaining in a "pegged" full scale position since this may overheat and burn out the detectors. Extended continuous operation should be avoided due to heat build up in some components.

2. Volumetric Gas Analysis

The volumetric gas analysis apparatus shown in Figure 2 is a cabinet model manufactured by Burrell for flue gas analysis. The cabinet measures 10.5" wide, 5.75" deep, by 21.25" high. It is completely portable and self-contained. This model is set up to detect and absorb, in the following sequence, carbon dioxide (CO_2) in the contact pipette, oxygen (O_2) in the first

bubbler pipette, and carbon monoxide (CO) in the second bubbler pipette. The liquids contained in each pipette are specifically compounded to completely absorb only the gas for which it was designed, i.e. oxygen, carbon dioxide, or carbon monoxide. They all have low vapor pressures, form stable compounds with the absorbed gas, and do not outgas other gases.

Operation of this instrument is straight forward. It requires some manual dexterity and only a little practice to become proficient with its use. It is necessary to run the analysis in the proper sequence since the oxygen absorber slowly removes carbon dioxide and the carbon monoxide absorber slowly absorbs oxygen. The flushing manifold is provided in the event any of the solution should enter the manifold. Flushing is achieved by turning the stopcocks to a through position on the manifold and flushing it with a %5 sulfuric acid solution. The stopcocks should be periodically cleaned and greased to prevent gas flowby through dry or solid build up areas which may develop on the sealing surfaces.

3. Griess-Saltzman Method

The Griess-Saltzman method is a wet chemistry technique for detecting the oxides of nitrogen. Paxve followed the preparation and analytical procedures, described in Appendix A which are recommended by the Air Pollution Control District, County of Los Angeles. The gas sample collection procedure was somewhat modified as directed by Truesdail Laboratories and will be described in this section.

The essential equipment necessary for this method is listed below:

1. Spectrophotometer (used as a colorimeter)
2. Vacuum pump
3. Wrist Action Shaker
4. Analytical balance
5. Glassware
    a. Brown ground glass bottles (500 and 250 ml)
    b. 1000 ml graduated cylinder
    c. 100 ml graduated cylinder
    d. 1 liter volumetric flask
    e. 50 ml volumetric flask
    f. 25 ml volumetric flasks (4 or 5)
    g. 10 ml volumetric pipettes
    h. 10 ml measuring pipettes
    i. 1 ml measuring pipette
    j. cuvettes for spectrophotometer
    k. collection bottles
        (1) 1000 - ml
        (2) 300 - ml
        (3) 100 - ml

6. Chemicals

    a. N - (1-naphthyl) ethylenediamine dihydrochloride
    b. Sulfanilic Acid
    c. Glacial acetic acid
    d. Sodium nitrite

7. Tubing for collection bottles
8. Screw clamps for collection bottles

The sample flasks used are ordinary round bottom flasks with the neck tapered and attached to a glass tube over which a tygon tube and screw clamp may be attached. Gas sampling procedure for NOx varied somewhat during the test program. A discussion of the problems of NOx measurement is presented in Section V B below. The final procedure adopted is as follows: A short L shaped length of quartz tube is inserted into the flask's tygon tube and then the quartz tube in inserted into an appropriate location of the burner. The gas sample is obtained by opening the screw clamp and allowing the gas to enter the evacuated flask. The screw clamp is then retightened and the quartz tube removed. When the analysis is to be made, an appropriate amount of Saltzman reagent is added to the flask and the flask is shaken for an hour to absorb the gas and develop the color in the dye. After an hour the now colored absorbing reagent is poured into a cuvette and read on the spectrophotometer at a wavelength of 550 mμ. The spectrophotometer instrument is first spanned by setting 100% transmission with a cuvette of distilled water. The oxides of nitrogen is read directly from either Figure 3 or 4 by entering the appropriate curve (volume of flask and volume of absorbing reagent used) at the transmission read. If it is found that the colored absorbing reagent is too dark to get an accurate reading on the spectrophotometer (transmission below 10%) and the reagent is not color saturated, then it may be diluted with distilled water and then read. The oxides of nitrogen concentration resulting from this light transmission reading must be multiplied by a suitable factor to correct for the dilution.

4. Gas Chromatograph Using a Thermal Conductivity Detector

a. The Instruments

Carbon dioxide and carbon monxide were separated and detected by using a gas chromatograph using a thermal conductivity detector. This instrument is manufactured by Carle Instruments and is designated as Model 8004, Figure 5. It measures 18.5" deep by 13" wide by 4.75" high with the lid on and 16" deep by 13" wide by 6.5" high with the lid removed and with a thermometer installed in the column oven block. Power requirements are 115 volts ac, 60 H_z. For maximum stability the line voltage to the instrument should be steady, between 100 volts and 125 volts, and not subject to fluctuation. If the voltage exceeds 125 volts, a regulating transformer should be used. In use, the instrument requires, in addition to power, a carrier gas for sweeping the gas

sample through the columns. Helium is normally used as the carrier gas due to the large difference between its thermal conductivity and that of most other gases or liquid vapors. Any cylinder of convenient size having a regulator capable of delivering gas at a pressure between 0 and 60 psig is suitable.

The Model 8004 Gas Chromatograph is a dual column, dual inlet instrument. There are septum covered inlets which allow samples to be deposited directly at the head of each chromatographic column. There are also two sample loops which permit a 2 ml gas sample to be injected into each column by turning a valve. The left column is a 6 foot long molecular sieve column which is used to separate O_2, N_2, and CO. The right column is a 3 foot long silica gel column which is used to separate carbon dioxide.

Under optimum operating conditions of column temperature and carrier gas flow rate, this instrument is capable of resolving 5 parts per million of CO_2. To obtain the optimum separation, it is necessary to systematically vary the operating conditions (column temperature and carrier gas flow rate) and examine the output signal from the instrument.

The columns are packed 1/8" stainless steel tubes mounted in contact on either side of an aluminum heater plate which serves as the column oven and is designed to minimize thermal gradients. The column oven temperature is adjustable up to 200°C. It is heated independently of the detector oven. The detector oven is maintained at a fixed elevated temperature by a constant voltage supply. The inlet block temperature is controlled by the column temperature adjustment but is maintained a few degrees above the column temperature.

The detector is a matched pair of glass coated thermistors having 100 K impedance that serve as two legs of a Wheatstone bridge circuit. The thermistors are mounted in 100µ liter chambers to maintain high resolution and response, in keeping with the small diameter, low-loaded columns. (Figure 6a).

The output from the instrument is usually fed to a pen recorder, in this case a Westronics Model S5E recorder having 6" wide chart paper traveling at one inch per minute. The response time is 0.5 seconds full scale. 0.1% full scale resolution is provided.

Helium carrier gas enters the instrument through a Nupro metering valve, which is used for fine flow adjustments, and then flows into the heated inlet block. The column inlets (see Figure 6a) are designed so that the carrier gases flush the annular space surrounding the column head eliminating unswept dead spaces. The helium then flows through the gas sampling valve, and then flows through the packed column, through the detector, and then exhausts through 1/8" tubes on either side of the instrument name-plate.

Two position, six port sample valves are located ahead of each column. They are designed with minimum valve body volume and have an optically flat ported stainless steel fixed body that

seals against a rotating Teflon coated body. The fixed body connects to the chromatograph and the sample loop by means of 1/16" stainless steel tubes.

When the valve is in the "load" position (Figure 6c):

a. Gas to be analyzed flows into the valve from the sample pump and is ported through a 2 ml sample loop. The exit flow from the sample loop returns to another valve port and is vented to the atmosphere.

b. Helium flows into the valve from a regulated source and is ported into the inlet to the column. It passes through the column and then to the detector. After flowing through the detector, the helium carrier gas is vented to the atmosphere.

When the sample valve is switched to the "inject" position (Figure 6d):

a. The gas from the sample pump flows into the valve and is immediately vented to the atmosphere. There is thus no interruption in sample gas flow through the sampling pump.

b. Helium flows into the valve and is ported into the sample loop. The return from the sample loop is ported to the inlet to the column. The sample of gas which was trapped in the sample loop is thus swept into the column by the helium flow. Flow through the column is not interrupted, but the 2 ml plug of gas to be anlayzed is carried in a "sandwich" of helium into the column inlet.

b. Principle of Operation

Separation of gases in a chromatograph column is a result of the distribution of the gas between two phases. One of these phases is a stationary bed of large surface area (the packed column) and the other phase is a gas (carrier gas) which percolates through the bed. Gas-solid chromatography, the technique employed here, involves a solid column packing which separates the gaseous constituents based on their differential absorption on the column packing. Common packings are silica gel, molecular sieve, and charcoal.

As gases pass through the column the sample gas mixture is partitioned between the carrier gas and the solid stationary phase. The solid phase selectivity retards the sample components according to their distribution coefficient until they form separate bands in the carrier gas. These component bands leave the column in the gas stream and produce an output signal from the detector based on each components thermal conductivity. The fluctuation in the output signal produces a series of peaks on the recorder paper according to component bands of gases leaving the column.

The record of the output signal is termed a chromatogram, and the time from the start of the analysis to the time any gas component is eluted is called the retention time. The area under each peak on the chromatogram is proportional to the concentration

of the corresponding gas in the sample mixture. The area may be determined by any number of methods. The peak height gives a good indication of the area when the peak is symmetrical, tall, and thin and produces good results when the instrument has been calibrated in terms of peak height. The majority of chromatographers use peak height methods in preference to any other integration technique (Reference 1) even though it is not the most basic method.

To maximize the peak height for a particular gaseous component, a gas mixture having the component in the concentration desired is run through the instrument while the column temperature and carrier gas flow rate is systematically varied. The carrier gas flow rate is accurately determined by attaching a soap bubble flow meter to the tube leading from the detector. The meter consists of a vertical tube with etched marks 10 ml apart and a reservoir of soap at the bottom. The carrier gas is bubbled through the soap and the flow rate of the gas is measured by timing the passage of the bubble between the two marks. Figure 7 shows the results of such an optimization procedure. From this figure the instrument was operated with a column temperature of 100°C and a carrier gas flow rate of 15 cc/minute.

c. Operating Procedure

Emissions measurements procedures with the thermal conductivity gas chromatograph for carbon dioxide and for carbon monoxide are substantially the same. To put the instrument into operation, the Helium carrier gas flow is first started to prevent oxidization of the column material. The electrical power to the instrument is then turned on and the column oven temperature control adjusted to obtain 100°C. The instrument is allowed to warm up for at least one half hour before further adjustments are made.

The instrument is operated at 100°C because, when combined with an appropriate carrier gas flow this produces an optimum carbon monoxide separation and peak height. A thermocouple is fitted into the column head to monitor its temperature.

After the instrument is up to temperature, the chromatograph attenuation switch is put on "test" and the recorder is zeroed. The attenuation switch is then put on "1" and the recorder is zeroed by adjusting the coarse and fine zero adjustment potentiometers on the instrument body. The instrument is now ready for use.

During use, samples are pumped to a common manifold and are valved from the manifold to each side of the chromatograph. The sample pump supplies a maximum pressure of 14 psig. During burner operation, sample gas is continuously being pumped from the burner through the sample manifold, through the gas sample valves, through the chromatograph sample loops. In order to take a reading, the sample flow from the manifold is shut off, and the gas in the sample loop of the chromatograph is allowed to blow down to atmospheric pressure.

The gas sample valve then is switched so that sample loop is ported on one side to the carrier gas and on the other side to the column inlets. The carrier gas now flows through the sample loop, pushing the gas sample into the instrument.

The blow down of pressure in the sample loop is required in part by the design of the dual column chromatograph. Due to the common manifolding in the instrument column inlets for carrier gas, it is necessary that the sample gas not enter the instrument at a higher pressure than the carrier gas pressure. If the pressure in the sample loop is higher than the carrier gas pressure when the gas sample valve is switched, some of the sample gas will blow back through the carrier gas line to the wrong column inlet (see Figure V6a). This condition gives erroneous results. To eliminate this condition the valve on the manifold leading to the sample valve is first closed, so that the gas in the sample loop returns to atmospheric pressure. Then the sample valve is switched.

5. Hydrocarbon Analysis Using a Flame Ionization Detector

a. The Instrument

Total hydrocarbon emissions were determined using a flame ionization detector. The instrument used for this purpose was a gas chromatograph manufactured by Carle Instruments designated the Model 9000. The instrument measures 9" high by 19.875" deep by 16" wide with the lid on, and 6.5" high by 18.75" deep by 16" wide with the lid removed and the instrument in use. Power requirements are similar to those of the thermal conductivity gas chromatograph. In addition, however, two polarizing batteries, each 300 volts must be used. These need to be replaced approximately once a year.

This chromatograph is normally used as a dual flame, dual column FID gas chromatograph instrument with the dual-inlets extending into the columns. The columns are heated by a central, aluminum plate, sandwich-type heater designed to minimize gradients in the column. The column temperature can be varied between ambient and 200°C. The detector oven is heated separately by a small cartridge heater maintained a few degrees above the column temperature by a common variable transformer setting.

The instrument used by Paxve used only one column. It is set up to measure total hydrocarbons in the left hand detector and to separate and identify hydrocarbons in the right hand detector. Gas samples entering the total hydrocarbon side of the instrument pass continuously through a flow restrictor (needed to balance the restriction due to the column on the other side of the instrument) and then to the detector. When using the instrument as a total hydrocarbon analyzer, emission data is obtained continuously, as opposed to the sampling techniques needed for CO, CO_2 and hydrocarbon separation.

Gas samples entering the separation side of the instrument pass through a gas sample valve where the gas is continuously

flushed through a sample loop. For a gas analysis, the valve is switched so that carrier gas is flushed through the loop and the sample gas is sent through the column for separation and finally to the detector for readout. The column used in this instrument is a 24 foot, 1/8" OD stainless steel tube packed with DC 200, a material chosen for separating saturated hydrocarbons (although equally efficient for aromatic and olefinic hydrocarbons).

The Model 9000 FID chromatograph requires three gases for operation; a carrier gas for flushing the sample gas through the column, and hydrogen and air for the flame ionization detector. When the instrument is used as a total hydrocarbon detector, the carrier gas is only needed to prevent air from entering the separation column and oxidizing its surface.

b. Principle of Operation

The detector consists of dual hydrogen flames enclosed in a teflon and metal walled chamber (Figure 6b). Sample gases continuously pass through the hydrogen flame, and produce ions. The electrical conductivity of a hydrocarbon free hydrogen flame is very small. When hydrocarbons in the sample gas pass through the flame the conductivity of the flame rises due to the creation of charged particles (electrons and negative and positive ions) with the result that a current will flow from the charged plates to the input electrodes. To achieve a low background level, it is necessary to supply the instrument with so called 'zero gases" which are virtually free of hydrocarbons.

The current which flows across the charged plates produces a voltage drop across a resistor in an electrometer (a portion of the electronic circuitry) which is amplified and then fed into a recorder. The detector operates in the same way regardless of whether the instrument is being used to record continuous data or sampling data.

c. Operating Procedure

During hydrocarbon emissions testing the instrument was operated at 200°C in keeping with the heated sampling line leading to the instrument. A thermometer fitted into the column head is used to determine the instrument temperature.

To operate the total hydrocarbon side of the instrument, carrier gas flow is started to prevent oxidization of the column. The instrument is turned on and the temperature adjusted until the thermometer reads 200°C. Air flow is turned on and adjusted to about 800 ml/min (excess air flow). The hydrogen is now turned on and adjusted to about 20 ml/min with the bubbler flow meter. The hydrogen is now lit and the detector housing returned in place and allowed to come to temperature equilibrium.

Optimum hydrogen flow is related to flow of gas to be analyzed. Optimum conditions exist when hydrogen flow rate = 1.1 x sample flow rate. Since the flow restrictors are located in the oven, all gaseous flow rates are temperature dependent. Figure 8

shows the calibration curves which were determined for this instrument and were used to determine the appropriate flow rates.

The instrument is adjusted by first balancing the amplifier for zero output. The instrument is then zeroed by running "zero air" through the instrument at the same rate as the sampling rate. The instrument is then spanned by passing a hydrocarbon mixture of known concentration through the instrument. The sample flow rate was set at this point by adjusting the flow rate of span gas mixture (containing 239 ppm of HC expressed as hexane), so that the output of the recorder is 2390 scale divisions. The recorder now will register 10 scale divisions for every ppm of hexane in the sample gas. The sampling pump bypass is then adjusted so that it delivers the same flow rate as the span gas.

B. Instrument Calibration

1. Bailey Heat Prover

The Bailey Heat Prover reads both oxygen and combustibles. The oxygen calibration is built into the instrument. Adjustments for both the 4% and 20% full scale settings are provided together with a built in zero adjustment.

The Bailey Heat Prover combustibles meter is factory calibrated. A calibration may be made using a Heat Prover Checker. In essence, the calibration consists of flowing a gas of known composition through the instrument and adjusting calibration resistors so that the instrument reads the given gas composition. The calibration technique results in producing a one to one relationship between the indicated combustibles and the actual combustibles when the ratio of carbon monoxide to hydrogen is 2 to 1. Other carbon monoxide to hydrogen ratios and other combustibles will not produce a one to one ratio of indicated to actual combustibles. Curves giving correction for other combustibles are given by Bailey for various gases and mixtures. These curves were used when the theoretical total indicated combustibles data shown in Figure IV-11 was plotted.

Periodic factory calibrations for combustibles were performed during the testing period. Frequent checks for proper oxygen calibration were made during each day.

Daily minor adjustments as indicated in Secion V-A-1 are necessary to keep the instrument in factory calibration. Other adjustments may be needed as the instrument is used. The procedure for the many other adjustments may be found in the operation manual E65-15.

2. Volumetric Gas Analysis

The volumetric gas analysis equipment requires no calibration. Periodic checks are sometimes run when it is suspected that one of the fluids has reached its saturation. To obtain complete absorption of a particular gas component, it

is usually necessary to make two or three passes through a gas absorption pipette. If more than three passes are required for complete absorption, the reagent is becoming saturated. Once a particular reagent becomes saturated, it is necessary to replace it.

3. Oxides of Nitrogen

The absorbing reagent is prepared per the procedure outlined in Appendix A. According to Saltzman (Appendix A) and the ASTM procedure D 1607 "Nitric Dioxide of the Atmosphere", the absorbing reagent is stable for several months if kept refrigerated and well stoppered in brown bottles. The absorbing reagent is calibrated with a standard sodium nitrite solution.

Sodium nitrite solution is added to the absorbing reagent so as to make a total mixture of 25 ml. This is then shaken and allowed to stand for 15 minutes. The NO_2 in the $NaNO_2$ reacts with the chemicals in the solution to produce a dye which is reddish purple in color. The dye has a strong light absorption peak at 550 mμ. Increasing the amount of sodium nitrite added caused increasing dye intensity until a maximum is reached when all of the dye has been used up. This condition is known as 'saturation' of the Saltzman absorbing reagent. Further addition of $NaNO_2$ causes the light absorption to decrease due to dilution.

A curve of light transmission versus equivalent concentration of nitrogen dioxide in micrograms per 10 ml of absorbing reagent is obtained from the $NaNO_2$ data. This curve is then used to draw curves for determining the concentration of NO_2 in the gas samples. It is also used to determine the point at which the absorbing reagent becomes saturated with regard to the maximum amount of nitrogen dioxide it can detect.

The $NaNO_2$ light transmission curve and formula (1) from Appendix A, are used to draw families of curves for various flask sizes and reagent quantities from which the nitrogen oxides concentration in ppm may be read directly as a function of light transmission (Figures 3 and 4). Flask sizes were chosen so that it was possible to detect nitrogen oxides from 0.1 ppm up to 200 ppm, with a reasonable range of sample flask size and volume of absorbing reagent required.

4. Gas Chromatograph Using a Thermal Conductivity Detector

This instrument is used to separate and measure carbon dioxide (on the right side of the instrument) and carbon monoxide (on the left side of the instrument). Since both sides of the instrument are similar in operation, only the calibration of the carbon monoxide side of the instrument will be described in detail.

a. Zero and Span Gas Calibration

After the instrument is set up

according to the directions in Section V-A-4, it is zeroed by setting the attenuation to 1 and zeroing the recorder pen with the zero controls. A span value is now obtained by introducing into the instrument through the sample loop, a span gas mixture having a known concentration of carbon monoxide.

The span gas is a mixture of gases designed to permit calibration of all of the chromatographic equipment with the same gas. The span gas mixture used for this purpose by Paxve has the following nominal compostion

200 ppm-propane
200 ppm-n-butane
300 ppm-carbon monoxide
5% -carbon dioxide
balance-nitrogen

The span gas produces a scale reading on the chromatograph recorder when the gas in question is eluted from the column. Dividing the known carbon monoxide concentration by the recorder deflection produces a scale factor. This scale factor is then used to multiply all subsequent scale deflections to obtain carbon monoxide concentration of any unknown sample gas being analyzed. The scale factor may change due to internal changes in the chromatograph during testing. For this reason, span calibrations are made frequently during the course of testing and the scale factor noted.

b. Linearity of the Instrument

The use of a scale factor as described above assumes that the instrument is linear over the operating range of interest. This question, the linearity of the thermal conductivity gas chromatographs, was investigated by means of a dilution test procedure which is described in Section 6 below. That test procedure allowed us to put known concentrations of gases to be anlayzed through the chromoatograph and to observe the resulting output signal as read on the recorder. We were able to explore the entire range from a pure gas down to the lowest concentration that could be distinguished on the chromatogram.

Figures 9 thru 11 show the results of the dilution tests for carbon monoxide, carbon dioxide, and oxygen. It was found that both the carbon monoxide and carbon dioxide peak heights were in fact linear with concentration over most of the range, to within the accuracy of the experiment. Oxygen concentration was not linear with peak height, showing an increasing sensitivity as the concentration was reduced. Since the chromatograph was not used to analyze for oxygen, this nonlinearity was not significant for the work reported here.

5. Hydrocarbon Analyzer Using Flame Ionization Detector

The Carle Model 9000 gas chromatograph is used to detect and measure total hydrocarbons by passing the sample gas

directly into the detector, without going through a packed column, as explained in Section V-A. Calibration of this instrument is virtually the same as calibrating the thermal conductivity gas chromatograph with the following exceptions:

(1) The FID gas chromatograph is a continuous reading instrument so that gas samples are not injected directly into a column with a valve, and
(2) The response of the instrument's output to a particular gas concentration can be varied by adjusting the delivery pressure and hence the flow rate of the unknown gas into the detector.

a. Zero and Span Gas Calibration

After the instrument is set up, zero air is flowed through the detector with the attenuator settings both on 1. The recorder pen is zeroed by adjusting the coarse and fine suppression controls. It may be necessary to adjust the polarity of the suppression controls to obtain a zero. The instrument was then spanned by running a span gas mixture through the instrument and adjusting the delivery pressure so that 1 scale division was equivalent to 0.1 ppm hydrocarbon expressed as hexane. The zero and span are now re-adjusted if necessary to obtain consistent values.

"Zero air" is not truly free from hydrocarbons, although every effort is made by the company which distributes the gas to achieve this result. The degree of impurity is evident to some extent when the flow rate of zero air through the instrument is changed. Very pure "zero air" shows almost no response on the FID to a change in flow rate. The gas is generally guaranteed to have less than 0.5 ppm of methane which is equivalent to 0.08 ppm of hexane. It is conceivable therefore that a really pure gas flowing through the FID will read slightly less than zero.

During the course of the tests conducted by Paxve, zero or slightly negative values were obtained frequently for hydrocarbon emissions. The zero of the instrument was then checked for drift by immediately running a "zero air" sample before the next test point. If drift had occurred, an appropriate correction was made in the data. There were, nevertheless, a number of points which gave zeros that could not be distinguished from the "zero air" setting. There were also many readings which were definitely negative.

b. Linearity of the Instrument

Dilution calibrations described in Section 6 were run for the FID gas chromatograph. These were run for both the left hand and the right hand sides of the Model 9000. Dilution by both air and nitrogen were used.

It was found from the data for the right hand side of the Model 9000 (which separates the gases with a column) that the

detector itself is linear with concentration for both propane and butane over the entire range of the instrument. This is shown in Figure 12.

Flow through the left hand side of the Model 9000 FID showed that the detector was sensitive to the presence of oxygen. When N_2 was used to dilute the span gas, the response of the totals side of the instrument was linear with the span gas content. When zero air was used as the diluent, the response of the instrument was not linear. There is a reduction in sensitivity of the instrument with increasing oxygen concentration.

The apparent nonlinearity of the FID with O_2 present is in fact not a nonlinear response to hydrocarbons. Rather, it is a suppression of FID sensitivity to hydrocarbons in the presence of oxygen. This suppression is called oxygen synergism. It is discussed in more detail in Secion V-C-2-c of this report.

Of particular interest here is the magnitude of the suppression as a function of oxygen content. Figure IV-12 shows the ratio of the FID response with air dilution versus its response with N_2 dilution, plotted against O_2 concentration We see that for O_2 of approximately 10%, the ratio is 0.76.

c. Zero Shift

The negative readings of the hydrocarbons emissions from the burner was a continual problem area during burner emissions testing. After the fuel injector problems on Stand 2 were cleared up (Runs 282 and later), almost all normal runs showed hydrocarbon emissions which were in the range from +0.5 ppm to -0.5 ppm HC (5 scale divisions on the recorder) expressed as hexane.

The possibility that water vapor was the cause of this problem was investigated. It was found that water vapor at about 10% concentration in air did not influence the span gas reading of the instrument. It was also found that 10% water vapor did produce about a -5 scale division shift in the recorder output, equivalent to -0.5 ppm of hexane.

Paxve has not made a systematic investigation of the influence of water vapor on the FID. We believe that the zero shift which we observed is the probable explanation for the negative readings which were obtained during burner operation. We did not devise or employ any calibration technique in this regard, but we feel that this is an important area for further work. This becomes increasingly desirable with the development of unusually low emission burners such as the Paxve burner being reported on here.

6. Dilution Calibrations

In using a scale factor we have assumed that the response of the chromatograph is linear with concentration. Thus we assume that a CO concentration of 300 ppm will give twice the recorder deflection as a CO concentration of 150 ppm. In order

to investigate the linearity of the instrument, a range of known mixtures must be analyzed. Two dilution techniques were used to achieve this information:

(1) a dynamic dilution technique using an "exponential dilution flask".
(2) A static dilution technique where a gas mixture of known concentration was repeatedly diluted in a determinable fashion.

In each case the resulting mixtures were then fed to the instrument whose linearity was being examined.

a. Dynamic Dilution

The dynamic dilution tests were conducted using an "exponential dilution flask" of known volume in which a gas of known composition was diluted continuosly by a measured flow of a diluting gas. The exponentially varying concentration of the resulting mixture was then analyzed measured by the instrument at measured time intervals.

The change in concentration of the calibrating gas being drawn from the dilution flask with time is given by

$$C = C_o \, e^{\frac{-tw}{v}}$$

where

t = time from start of run - sec
C = concentration at time t - ppm
C_o = concentration at time $t = 0$ - ppm
v = volume of the mixing flask - cc
w = flow rate of diluent - $\frac{cc}{sec.}$

A schematic diagram of the exponential dilution test apparatus is shown in Figure 13. As shown in this schematic diagram the typical calibrating gas storage bottles consisting of span gas, zero air, pure nitrogen, carbon monoxide, and carbon dioxide are connected by appropriate valving to a supply manifold which can be individually valved to the exponential dilution flask. A given calibrating gas can be locked into the flask through an appropriate set of valves. The diluting gas flow may then be set and the apparatus connected to the particular chromatrograph channel under evaluation.

At the start of the test, the diluting gas is switched into the flask at a known flow rate and an exponential dilution of the calibrating gas in the flask then takes place which is analyzed at timed intervals by the chromatograph. In this manner a continuously decreasing concentration of the original gas in the flask can be evaluated over the full range of the instrument. It was found that heat must be added to the flask as the dilution process proceeded in order to maintain a constant stirring of the

gas molecules and to prevent surface adsorption of the gas molecules on flask walls.

Results of the dilution sensitivity test of the Carle 9000 FID gas chromatograph are shown in Figure 14. This test was conducted with span gas diluted with zero air using a heated flask. The effect of an unheated flask is shown in Figure 15. It is evident from Figure 15 that deviations in linearity were appreciable at both the extreme limits of the span when no heating was provided. This was not the case, as shown in Figure 14, when the flask was heated.

b. Static Dilution

The static dilution technique involved filling a sample cylinder with span gas or with pure gas (carbon monoxide or carbon dioxide), depending on which instrument is to be calibrated, repeatedly diluting the sample, and then analyzing the cylinder contents. The procedure was initially started with the flame ionization chromatograph. Flasks were filled with samples of span gas and accurately diluted with nitrogen or zero air to obtain several different known span gas mixtures. These mixtures were then run through both the totals (left side) side and the separation (right side) of the Model 9000 FID chromatograph.

The resulting curves Figures 16 and 17, show that when nitrogen is used as a diluent, both sides of the instrument are linear with concentration. When air is used as a dilutent, the right hand side of the instrument (separations side) remains linear (Figure 12), while the left side of the instrument shows a nonlinearity. Since the right side sees the constituents separately, it is clear that the nonlinearity on the left hand side is due to the simultaneous presence of O_2 and hydrocarbons. This is the oxygen synergism effect discussed in Section V-C-2.

A similar dilution procedure was followed to obtain gas mixtures for the thermal conductivity gas chromatograph. The proven linearity of the FID right side was used to assist in the analysis. Gas compositions having concentrations less than 300 ppm for carbon monoxide and 5% for carbon dioxide were obtained by diluting span gas with zero air or nitrogen. Gas compositions having higher concentrations of CO and CO_2 were obtained by diluting pure carbon monoxide or carbon dioxide with span gas. In either case, the concentration of the diluted gas mixture was determined from the concentration of the hydrocarbon in the mixture. This was in turn obtained from the FID.

An oxygen calibration for the left side of the thermal conductivity gas chromatograph was accomplished using the static dilution technique. Zero air diluted with span gas was found to be unsatisfactory for this purpose because the high concentrations of nitrogen caused the leading edge of the nitrogen peak to overlap the oxygen peak in the chromatogram. This in turn gave rise to an apparent nonlinearity in the oxygen calibration. To avoid this problem, a 50/50 mixture of air and span gas was diluted with carbon dioxide. The hydrocarbons in the span gas were used to

establish the composition of the mixture. This technique yielded satisfactory separation of the oxygen and nitrogen peaks.

Figures 9, 10 and 11, show the results of the Model 8004 gas chromatograph linearity investigations. The CO and CO_2 responses are seen to be linear. The oxygen response shows nonlinearity of peak height at high concentrations.

C. Emission Measuring Problems

During the course of this program many unforeseen problems arose in connection with the emission measuring equipment and the sampling techniques used in conjunction with that equipment. Some of these problem areas are treated in the technical literature, but they were unknown to us at the beginning of the program and were not brought to our attention by the manufacturers of the emission equipment we purchased. Other problem areas are either unknown to workers in this field or are merely considered part of the "art". They are not discussed in any available literature. These problems and our solutions to them are reported here in the hope that others may profit from the work.

In addition, data reduction techniques not discussed elsewhere have been included here as an aid in understanding the reduced data presented in Section VI.

1. Oxides of Nitrogen

The oxides of nitrogen are determined by a wet chemistry method known as the Griess-Saltzman method. This method is described in Section V, A3, B3 and Appendix A. During the course of the program the testing procedures were modified as new knowledge was gained.

Initial NOx data was gathered by sampling from a manifold (Figure IV-4 B) used to feed the TC gas chromatograph. This manifold was the terminal end of a 52 foot sample line carrying gases from the burner on stand 1 to the chromatograph (see Figure 19). The initial NOx results using gas from this sampling point collected in 1000 ml sampling flasks with 10 ml of absorbing reagent are shown in Figure 18 labeled "Initial Data". The highest NOx values obtained during these tests were 17 ppm.

Suspicion was raised about the flat top and overall shape of the curve of NOx compared to the equilibrium NO values shown. As a result, some studies were initiated which revealed three problem areas in NOx measurement. These problems are indicated by a, b, and c in Figure 18. They are discussed below.

a. Absorption of NOx by Condensed Water

As explained earlier, NOx data gathered from a remote sampling point was considered suspicious. It was initially thought that the hot tip of the metal sample line might be catalyzing a reaction which the NO_2 or NO was breaking

down to form compounds which were undetectable by the absorbing reagent. A test was run where gas samples for NOx analysis were taken from several points (labeled #1, 2, 3, and 4 in Figure 19) using 2 sample probe materials.

Gas samples were taken from the burner directly (point 1) using a 1 foot length of stainless steel line for a sample probe and a 1 foot quartz tube sample probe. For the same set of burner operating conditions, samples were taken from the sample line at points, #2, #3, and #4. This last location was the sample point at the manifold which was used to gather the NOx data in the earlier test runs. Table 1 shows the results of these tests.

It is seen that there is virtually no difference in the NOx for the two sampling materials when sampled at point #1. The idea that stainless steel destroys or otherwise alters the NO or NO_2 to produce low readings is clearly not supported by this data.

As the sampling point was moved away from the burner the measured NOx concentration decreased. This reduction in detectable NO_2 can be attributed to the absorption of NO_2 in the condensed water vapor which drops out in the sample line.

Nitrogen dioxide (NO_2) dissociates in water according to

$$2\ NO_2 + H_2O \rightarrow HNO_3 + HNO_2 \quad \text{(cold)}$$

$$3\ NO_2 + H_2O \rightarrow 2HNO_3 + NO \quad \text{(warm)}$$

Nitric acid is infinitely soluble in water and therefore remains in solution. Nitric oxide (NO) is only slightly soluble in water (.0059 gms NO dissolve in 1 gm water at 23°C and 760 mm Hg) so that some of it will become dissolved in the water and some of it will come out of solution and enter the flowing gas stream. In the gas stream nitric oxide (NO) is slowly oxidized by the available oxygen to nitrogen dioxide which is further trapped in the water as explained above. Except for being slowly oxidized to nitrogen dioxide, as explained above, nitric oxide is recovered in the sample gas and detected by the Griess-Saltzman method.

The loss of NO_2 as opposed to NO in the long sample line could be readily observed when the sample flasks were developed on the shaker. When samples were taken from the long stainless steel line a considerable period of time (about 15-30 minutes) was required before any color developed in the absorbing reagent. This time period was a result of the NO being slowly oxidized to NO_2. When samples were taken with the short quartz tube, color began to develop almost immediately due to the presence of NO_2.

As further substantiation of the absorption of NOx by condensed water, a sample of the condensed water was analyzed by the Griess-Saltzman method and was found to contain 18μ grams of equivalent NO_2/10 ml of absorbing reagent. Although nitric acid is not supposed to produce a positive response with the absorbing reagent (See Saltzman, Appendix A), nitric acid is unstable and breaks down under sunlight and also heat according to:

$$4\ HNO_3 \rightarrow 2\ H_2O + 4\ NO_2 + O_2\uparrow$$

Nitric acid is a powerful oxidizing agent and decomposes in the presence of a reducing material according to:

$$2\ HNO_3 \rightarrow H_2O + 2\ NO\uparrow + \frac{3}{2}O_2\uparrow$$

In any event a compound which is detected by the absorbing reagent (NO_2) or readily converted to such a compound (NO) is formed.

A simple analysis was also performed to show the equilibrium concentrations of the various species of nitrogen oxides with water.

let α = solubility of NO in water gm/gm Atm

$[NO]_l$ = concentration of NO in water gm/gm

$[NO]_g$ = concentration of NO in gas gm/gm

P_{NOG} = Partial pressure of NO in gas Atm

MWW = Molecular weight of water

MW_{NO} = Molecular weight of NO

MW_{EX} = The molecular weight of exhaust gas

W_l = Weight of NO in liguid per pound of exhaust

W_G = Weight of NO in gas per pound of exhaust gas

XW = The mole fraction of the exhaust gas which is water

XNO = The mole fraction of the exhaust gas which is NO

Then if most of the NO is in the gas

$$P_{NO} = XNO$$

$$[NO]_l = PNO\ \alpha$$

$$[NO]_G = PNO\ \frac{MWNO}{MW_{EX}}$$

The weight of No in the water per pound of exhaust will be

$$W_L = [NO]_l\ X\ W\ \frac{MWW}{MW_{EX}}$$

The weight of NO in the gaseous phase per pound of exhaust will be

$$W_g = [NO]_g$$

The fraction of the NO in the liquid phase is then

$$\frac{W_L}{W_g} = \frac{\alpha \, X_W \, MW}{MWNO}$$

Substituting

$$\alpha = 5.6 \times 10^{-5} \text{ gm/gm}$$

$$X_W = 0.10$$

$$MWW = 18$$

$$MWNO = 28$$

we obtain

$$\frac{W_L}{W_g} \simeq 3.6 \times 10^{-6}$$

thus the amount of NO which is lost to the water which condenses in the line is negligible.

Our interpretation of the experiments and the analysis was that we were losing the NO_2 in the line, but not the NO. This of course did not consider the possiblity that some of the NO was converting to NO_2 in the line. The residence time in the line, however, did not seem sufficient for that reaction to proceed.

As a result of the tests described above, the sampling procedure for oxides of nitrogen was modified. All test data for oxides of nitrogen taken after run 103 used a short quartz tube which drew the sample to be analyzed directly into an evacuated flask. Some of the early data gathered using this procedure was plotted in Figure 18. The comparsion between the new data and the old data is clear. The new data still shows the flat top exhibited by the old data (peak values of NO always less than or equal to 17 ppm). It did, however, show larger values of NOx at low fuel air values.

Superimposed on Fig. 18 is a curve of the theoretical NO_2 which exists in equilibrium in the exhaust as a function of the fuel air ratio. We see that the difference between the new NOx values and the old NOx values is approximately the same as the theoretical NO_2. From this we might infer that the NO_2 in the burner is approximately in equilibrium, and that when we lost it in the lines, we were losing NOx of at most 3 ppm. For most burners, a combustion exhaust gas analyses which failed to find a 3 ppm of NOx would not be considered a serious problem. In the case of the Paxve burner at low fuel air ratios, however, this may represent 50% or more of the entire NOx in the exhaust.

b. Saturation of the Absorbing Reagent

It was apparent from the flat top of

the NOx data curve that some type of saturation phenomenon might be occurring. Another possibility that was considered was that the Saltzman solution responds differently to NO or NO_2 gas than it does to the $NaNO_2$ calibrating solution. This latter idea was not considered too seriously, since it was precisely this problem which Saltzman investigated. Nevertheless, we decided to attempt a direct NO or NO_2 calibration of the Saltzman reagent, in spite of the considerable difficulties involved.

Mixtures of NO (which contained some NO_2) in dry N_2 were prepared which should have been about 100 ppm. The Saltzman reagent only indicated 23 ppm. When a similar mixture was prepared by collecting the gases over water, the Saltzman reagent showed almost no color.

Finally mixtures of NO_2 in air were prepared. A mixture which contained approximately 5 ppm indicated 5 ppm in the Saltzman reagent, but a 100 ppm mixture only indicated 19 ppm.

It was clear that saturation of the reagent was occurring. It was also clear that the reagent was sensitive to NO_2, but did not respond to NO. The saturation phenomena was further investigated by means of the $NaNO_2$ solution.

The standard procedure for calibrating the Saltzman solution involves making up a mixture of Saltzman reagent and $NaNO_2$ standard solution of total volume 25 ml. We normally use from 0.2 ml to 6 ml of the $NaNO_2$ with the balance made up of Saltzman reagent. The optical transmission of the resulting solution plots as a straight line on semi-log graph paper, indicating that the transmissibility is given by

$$\ln \frac{I}{I_o} = K_1 P$$

$$= K_2 [NO_2]$$

Where:

I = light transmission at 550 m

I_o = transmission through clear reagent

α = the concentration of the dye in the liquid mixture

$[NO_2]$ = the concentration of NO_2 in the mixture

K_1 K_2 = appropriate constants

As long as there is enough dye to indicate all of the NO_2 that is present, we should expect

$$\ln \left(\frac{I}{I_o}\right) = K_3[NO_2]$$

$$= -K_4 \frac{V_N}{V_N+V_S} = \frac{K_4}{25} V_N$$

Where

V_N = volume of $NaNO_2$ solution

V_S = volume of Saltzman reagent

If however, we continue to increase the proportion of $NaNO_2$ solution until there is an excess of NO_2 and insufficient dye available, we would then expect the transmission to be given by:

$$\ln \frac{I}{I_o} = K_1 P_D$$

$$= K_4 \frac{V_S}{V_S+V_N}$$

$$= -\left(\frac{K_4}{25}\right) V_S$$

$$= -\left(\frac{K_4}{25}\right) \left(25-V_N\right)$$

Figure 20 shows the light transmission data obtained by varying the amount of $NaNO_2$ solution from .2 ml to 20 ml. The data is well fitted by two straight lines on semi-log paper. The left hand line represents the usual calibration curve for the Saltzman solution. In this region, there is an excess of dye and all of the NO_2 present is indicated. The right hand line represents the saturation region. In this region, there is a deficiency of dye and only the amount of dye present is indicated. This behavior is exactly that predicted by the above analysis.

By finding the slope of the saturation line in the graph, the maximum dye concentration at saturation can be found. From this we can deduce what concentration of NO_2 will yield saturation. In the case shown here, the dye saturates if it is exposed to 21µg per 10 ml of NO_2. This is equivalent to approximately 19 ppm of NO_2 in a 1 liter flask containing 10 ml of reagent.

Much of our early data showed values which were between 12 ppm and 17 ppm at conditions where higher values were expected. We therefore decided to disregard any early data over 10 ppm as possibly saturated. We also decided to change our procedure to avoid saturation.

From Figure 20 it was found that the absorbing reagent saturates at approximately 21µ gms of NO_2/10 ml of absorbing reagent. If this number is substituted into formula (1) of the procedure for preparing the absorbing reagent (Oxides of Nitrogen, Appendix A) the following results:

$$\text{Concentration (in ppm)} = \frac{(0.532)(21 \text{ gm}/10\text{ml})}{Vc} .$$

This is rearranged to give: $Vc = \frac{11.2}{\text{concentration}}$

Thus to detect 100 ppm of NO_2 with 10 ml of absorbing reagent without saturating the reagent, a gas sample having a volume of approximately 112 ml as needed, or $Vc = \frac{11.2}{100} = .112$ liters. The sample flask must allow an additional 10 ml for the volume occupied by the absorbing reagent.

The effective range of this method can also be extended by increasing the volume of absorbing reagent used in a sample flask. For example, if 20 ml of the absorbing reagent is saturated, 42 gms of NO_2 will have reacted with the absorbing reagent. If 112 ml of sample gas resulted in saturating these 20 ml of reagent, the NO_2 concentration would be:

$$\text{Concentration (in ppm)} = \frac{(.532)(42 \text{ gm}/20 \text{ ml})}{.112} = 200 \text{ ppm.}$$

By varying the sample flask size (100 ml, 300ml, and 1000 ml flasks were used) and the amount of absorbing reagent used (10 ml, 20 ml, and 30 ml were used) we were able to extend the effective range of this method without approaching absorbing reagent saturation. Families of calibration curves were generated for the various flask sizes and various amounts of absorbing reagents used (See Figures 3 and 4).

To verify the validity of this approach, several tests were run with the burner. In test No. 218 and again in test No. 219, three NO_2 samples were collected in 1000 ml flasks containing 10, 20, and 50 ml of Saltzman reagent. The results are shown in the following table

Indicated NOx ppm

Test No.	f/a	10/1000	20/1000	50/1000
218	.0311	2.5	1.9	2.6
219	.046	19.2	32.6	33.2

It is clear that, except for some scatter in the data, the first run, #218, was not saturated, and gave substantially the same result in all three flasks. Run #219, on the other hand, saturated the 10/1000 flask, but gave comparable results for both the 20/1000 and the 50/1000 flasks.

All testing from run 218 on used adequate amounts of Saltzman solution to avoid saturation effects.

c. Detection of NO in Gases Which are Low in Oxygen

As mentioned in the previous section, when the nitrogen oxides were mixed with nitrogen by collecting over water and then analyzed for NOx virtually no color was obtained in the Saltzman reagent. Nitric oxide is apparently not detected by the Griess-Saltzman method but NO_2 is. This agrees

with Saltzman's observations (App. A). Therefore if NO cannot be oxidized to NO_2 in the flask, it will not be detected. The lack of oxygen and the presence of water in the experiment cited previously virtually eliminated any NO_2 from the NO-NO_2 mixture.

For detection of nitric oxide, Truesdail Laboratories recommends that the gas sample and reagent be shaken in the sampling flask for at least an hour before the dye intensity is measured. This allows the NO to be oxidized to NO_2. If there is not sufficient oxygen in the flask, it must be added. Figure 16 shows the region where there is insufficent oxygen in an equilibrium propane/air combustion mixture to adequately oxidize NO to NO_2. In this region oxygen must be introduced into the sample to detect nitric oxide. The procedure used here to achieve this was to partially evacuate the flask. This was done by evacuating a flask fully and connecting it to another unevacuated flask of equal size and allowing the two to equilibrate. The sample was then drawn in this partially evacuated flask. The oxides of nitrogen concentration level read from Figures 3 or 4 must be doubled to account for the flask being half evacuated (in effect only half of the flask volume was used to take the gas sample).

When these two final procedures were adopted: (1) using smaller size sampling flasks and/or larger amounts of absorbing reagent, and (2) introducing air (oxygen) into samples when there is insufficient air to oxidize the NO to NO_2 the final data curve seen in Figure 18 resulted.

d. Effect of Absorbing Reagent Temperature on Sensitivity

During the course of testing, a question was raised regarding the storage and use of the absorbing reagent. ASTM procedures (Nitrogen Dioxide Content of the Atmosphere, (D 1607) pg 455 personnel at Truesdail Laboratories, and Saltzman (Appendix A) all contend that the absorbing reagent will remain stable for several months if refrigerated in well stoppered brown bottles. The ASTM procedure further contends that the absorbing reagent should be allowed to warm to room temperature before use. Other workers in the field, however, feel that the absorbing reagent should be made fresh (as close to the time of use as possible) and should be kept cold until immediately before use. To investigate the effect of age and temperature of the absorbing reagent on its reactivity, a series of tests were conducted.

Newly prepared absorbing reagent (less than 5 days old) and older reagent (approximately one month old) were compared at room temperature (approximately 70°F) and also at refrigerated temperatures (approximately 35°F). Some of the older reagent had, in fact, been stored at room temperature for approximately one month before the test. The cold sample of older reagent had been previously stored in a refrigerator for the same period of time. The cold new

reagent had been kept refrigerated since it had been made. The warmed new reagent was removed from the refrigerator just long enough to come to room temperature before being tested.

Each batch of reagent was tested with the standard calibrating solution and by introducing it into previously sampled flasks containing the same concentration of oxides of nitrogen. Table 2 shows the results of these tests. It is seen that there are no significant differences between the results from these variable conditions.

e. Effect of Evacuating Procedure on Sampling Results

Saltzman (Appendix A), the APCD procedure (Appendix A) and the ASTM procedure referred to on the previous page, all indicate that an appropriate sampling procedure is to put the absorbing reagent in the sample flask, evacuate the sample flask to the vapor pressure of the reagent and then obtain the gas sample. Other workers in this field believe that the sample flask should be evacuated first, the gas sample obtained, and then the absorbing reagent added to the flask. This procedure is in keeping with the idea of using only fresh cold absorbing reagent.

A test was made to investigate the effect of evacuating the sample flask before or after the addition of the absorbing reagent. In this case a gas sample was used to test this effect. Table 3 shows the results of this test. Again no significant differences are seen between these two procedures. Addition after sampling was adopted as a standard procedure, however, because it was generally more convenient.

2. Hydrocarbon

a. Heated Sample Line

In obtaining valid emissions data, the FID sample line has come under close scrutiny in two respects. First, there has been some difficulty in maintaining a clean line. This has been a result of the unexpected introduction of hydrocarbons into the line from valves and other component fittings. It can also be caused by hydrocarbons brought in from a burner during blowout testing. The second consideration has been the problem of avoiding condensation of hydrocarbons from the sample in the line.

It has been suggested that a heated line with a temperature on the order of 300°F would avoid this problem. The diesel and kerosene fuel which were used in this program have a final boiling point on the order of 550°F to 625°F as shown in the chart of Table 4. It has an approximate molecular weight of 170 corresponding to dodecane ($C_{12}H_{26}$). To avoid condensation of the pure vapor in the line it would be necesssary to maintain the line above this temperature. When a gas sample consisting of several constituents is under consideration, however, only the partial pressure of the hydrocarbon

concerns us. This in turn depends on its volumetric concentration.

The dew point characteristic of a gas mixture containing dodecane is shown in Figure 21. The ordinate of Figure 21 is concentration of hydrocarbons in ppm by volume. The abcissa is temperature in degrees F. Since the Paxve FID chromatograph is calibrated for hydrocarbons expressed as hexane, it will read twice the true concentrations of dodecane. This FID reading is shown by the middle line in Figure 21.

It is seen that a sampling line at ambient temperature 70°F will not have condensation if the indicated hydrocarbon concentration is less than approximately 1000 ppm. All of the measurements to date on the Paxve burner in normal operation indicate hydrocarbon readings of much less than this value. Therefore it would not appear that condensation will contribute emission measurement errors unless there are higher hydrocarbons present. The third line on Figure 21 was added to indicate the relationship between the dew point and the fuel/air ratio for diesel fuel/air mixtures. In this case the ordinate is fuel/air ratio by weight. The top of the graph corresponds to a fuel/air ratio equal to 1 and the next lower decade corresponds to a fuel/air ratio 0.1 etc. For the fuel/air range of interest (f/a ≈ 0.04) the dew point is 265°F. Thus a sample line heated to 300°F should permit passage of even an unburnt mixture through the instrument without condensation.

Although we did not expect true condensation to be a problem with our exhaust samples, there are other phenomena to be considered. In the curve of our FID calibration work, we have often noted the strong tendency for hydrocarbon gases to adhere to the walls of containers and lines. This adsorbtion phenomenon is not unlike condensation, except that no truly liquid film need be involved. We have found that heating the walls and lines minimizes any adsorbtion problems. Based upon these considerations, the sample line has been heated for all of the burner testing data presented in this report.

b. Heated Pump

The necessity for maintaining temperature control of the sample gas has been discussed. In order to accomplish continuous sampling of the burner exhaust gas at elevated temperature, a sampling pump was designed and fabricated by Paxve. No commercially available pumps were found capable of meeting the requirements. A photograph of the pump is shown in Figure 22. It utilizes two metal bellows driven by a rotary eccentric mechanism. The eccentric mechanism is in turn driven by an electric motor through a long shaft. The valves in the pump are two steel balls retained by a steel shim stock in a valve hole with a lap seat. All parts of the pump can be operated to over 500°F. In operation the pump is situated in a small oven with the heated sample line coupled into the pump. The outlet side of the pump is a heated 1/4" line which leads from the pump through a small receiver to the flame ionization detector. A bypass bleed is provided at the end of the FID to adjust

sample line pressure. The small receiver smooths out the pump pressure pulsations. The receiver is contained in the oven.

The FID chromatograph body is maintained at temperature of 200°C (392°F) with the detector head about 50° hotter. Initial operation of the Paxve sample gas pump in connection with the FID chromatograph produced erratic results. The chromatograph traces showed erratic fluctuations combined with random drifting of the instrument. The erratic signals from the line were traced to a cold spot (where calibration gases were introduced). Condensation at this spot with subsequent dripping of condensed water into the line was eliminated with an immediate and permanent improvement in signal quality. During subsequent operation of the system the line was found to be "dirty" (high unburned hydrocarbon readings) on one occasion. This condition was corrected by running hot exhaust products through the line till this spurious signal was cleared.

d. Oxygen Synergism

As was previously explained in the discussion on calibration of the FID, the addition of oxygen to the span gas altered the linear response of the FID to hydrocarbons. This altering of the response due to oxygen is known as oxygen synergism. The effect of various pure hydrocarbon-oxygen mixtures sampled in a Beckman FID using pure hydrogen is seen in Figure 23.

It is seen that the presence of oxygen, in most but not all cases, shows a suppression of the response from the instrument. This effect may be reduced using a hydrogen mixture with either nitrogen or helium for the FID flame. Figures 24 and 25 show the result. The mechanism which produces these results is not known.

Paxve used pure H_2 for our FID because we were unaware of the synergism problem until after we had taken the bulk of our data. A correction factor was applied to the data to account for the reduced sensitivity of the instrument in the lean combustion (high O_2) mode. Figure IV-12 shows the oxygen synergism effect for our FID, with our span gas.

D. References

1. Littlewood, A.B., "Gas Chromatography - Principles, Techniques and Applications" Academic Press, 1970.

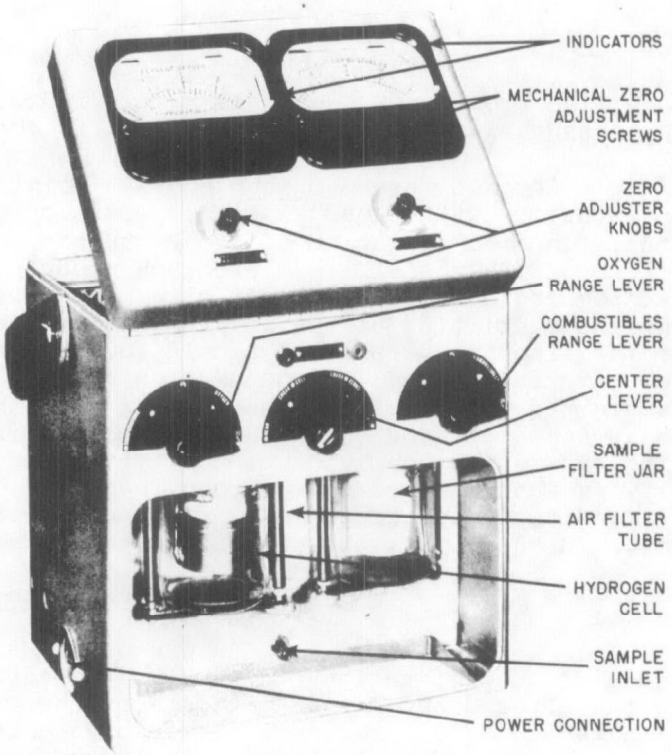

a. BAILEY HEAT PROVER

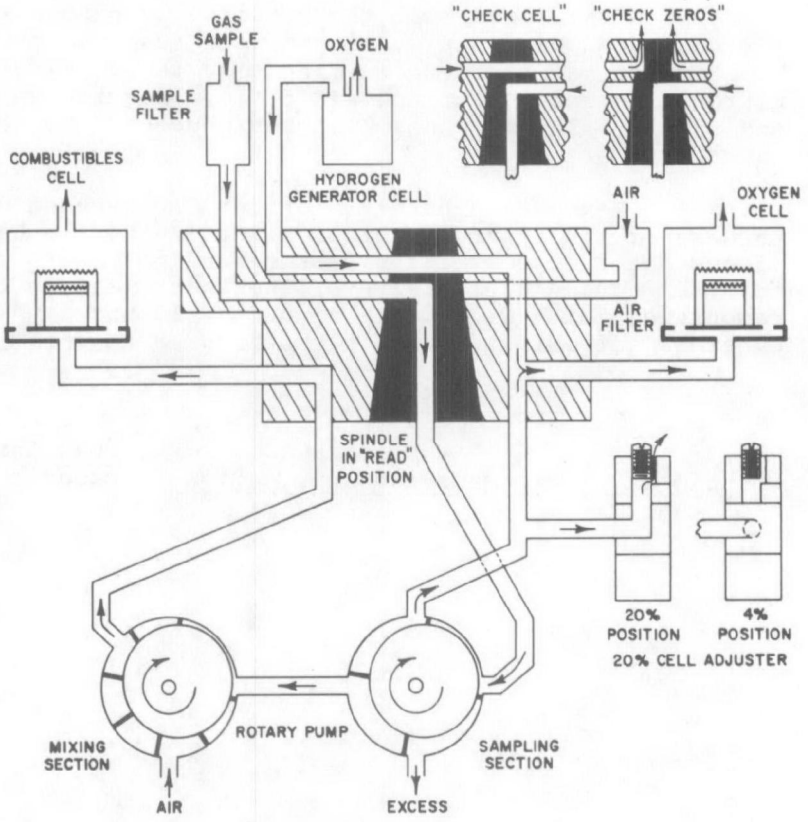

b. OPERATING SCHEMATIC

FIG. 1 BAILEY HEAT PROVER WITH OPERATING SCHEMATIC

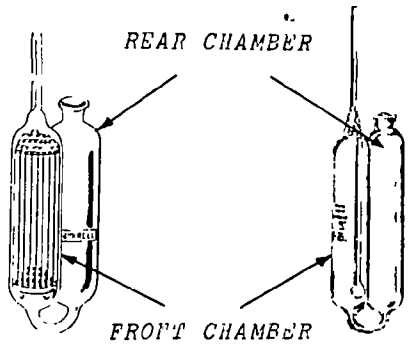

CONTACT PIPETTE BUBBLER PIPETTE

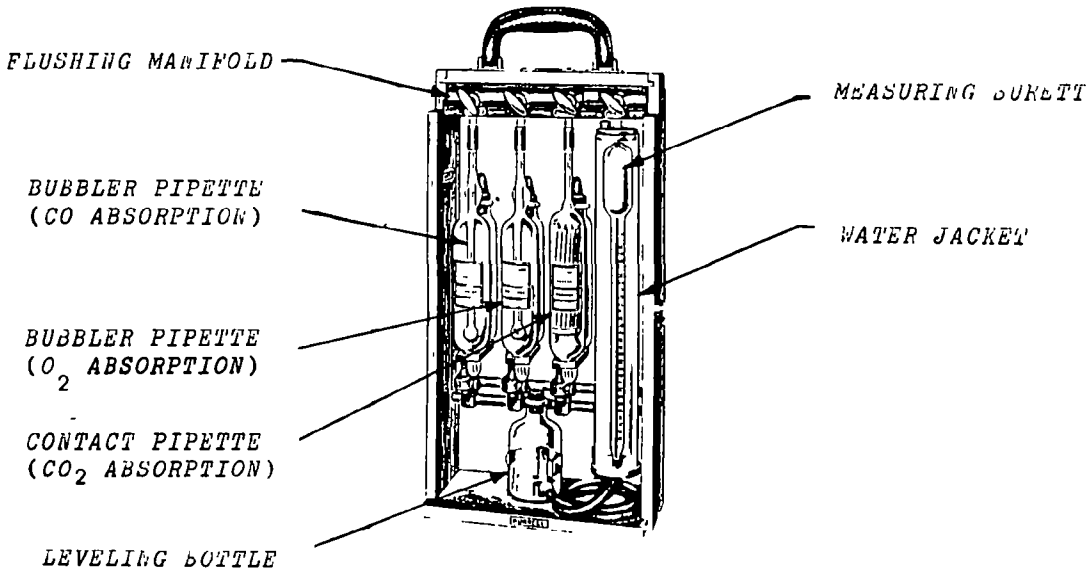

FIG.V-2 VOLUMETRIC GAS ANALYSIS APPARATUS

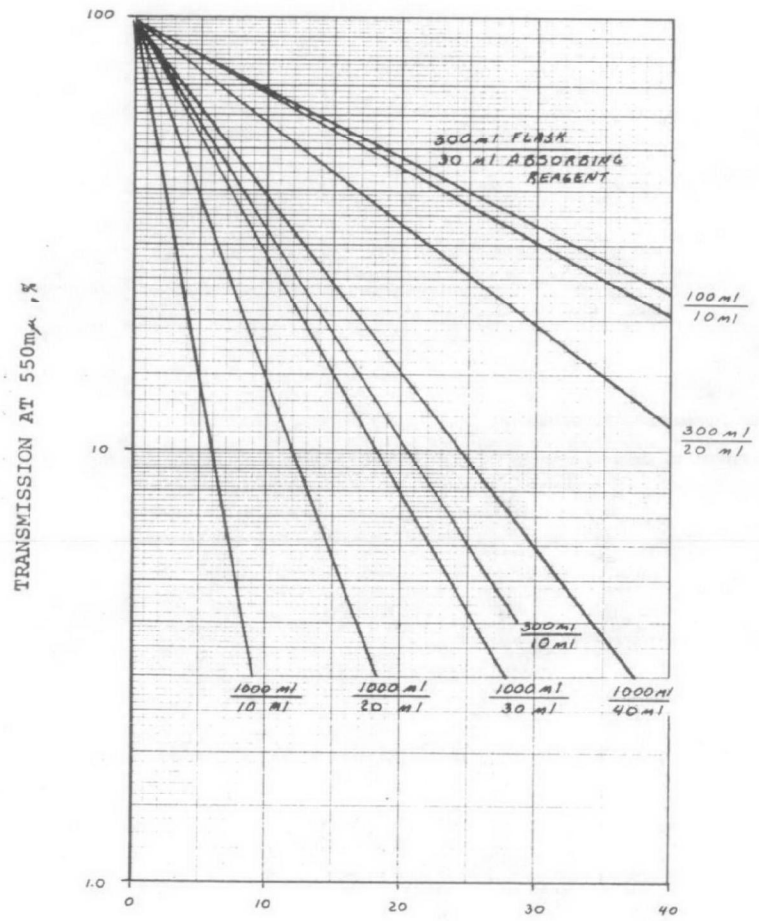

CALIBRATION CURVE FOR DETERMINING OXIDES OF NITROGEN CONCENTRATION BY GRIESS SALTZMAN METHOD, LOW RANGE

Figure V - 3

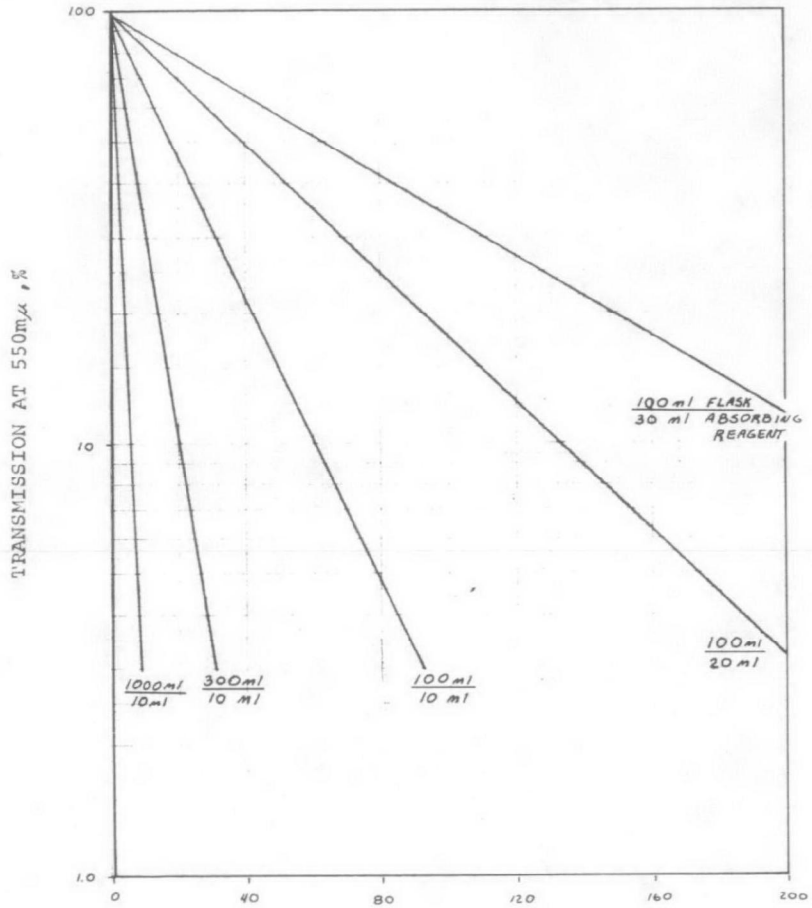

CALIBRATION CURVE FOR DETERMINING OXIDES OF NITROGEN CONCENTRATION BY GRIESS SALTZMAN METHOD, HIGH RANGE

Fig. V 4

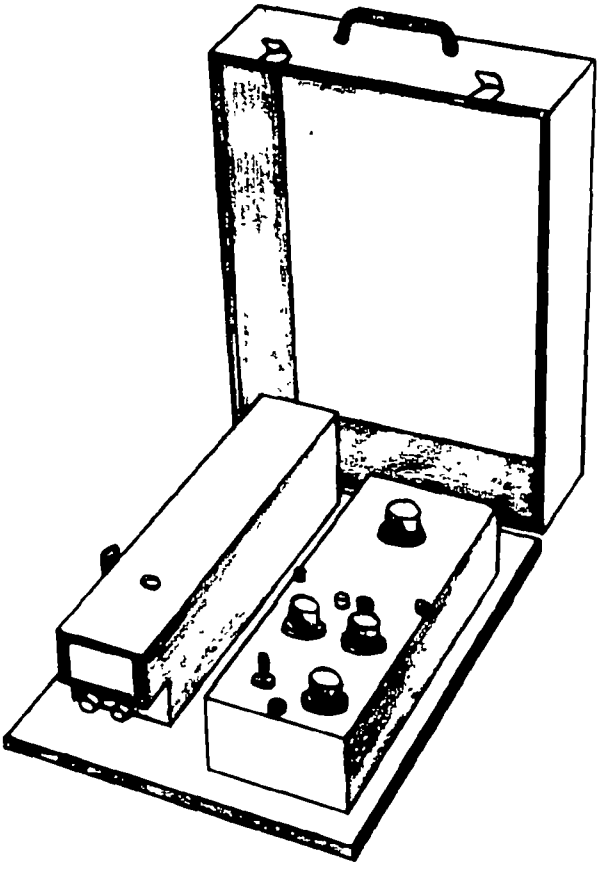

MODEL 8004 GAS CHROMATOGRAPH
USING THERMAL CONDUCTIVITY DETECTOR
FOR DETECTING CARBON DIOXIDE (CO_2)
AND CARBON MONOXIDE (CO)

FIGURE V 5

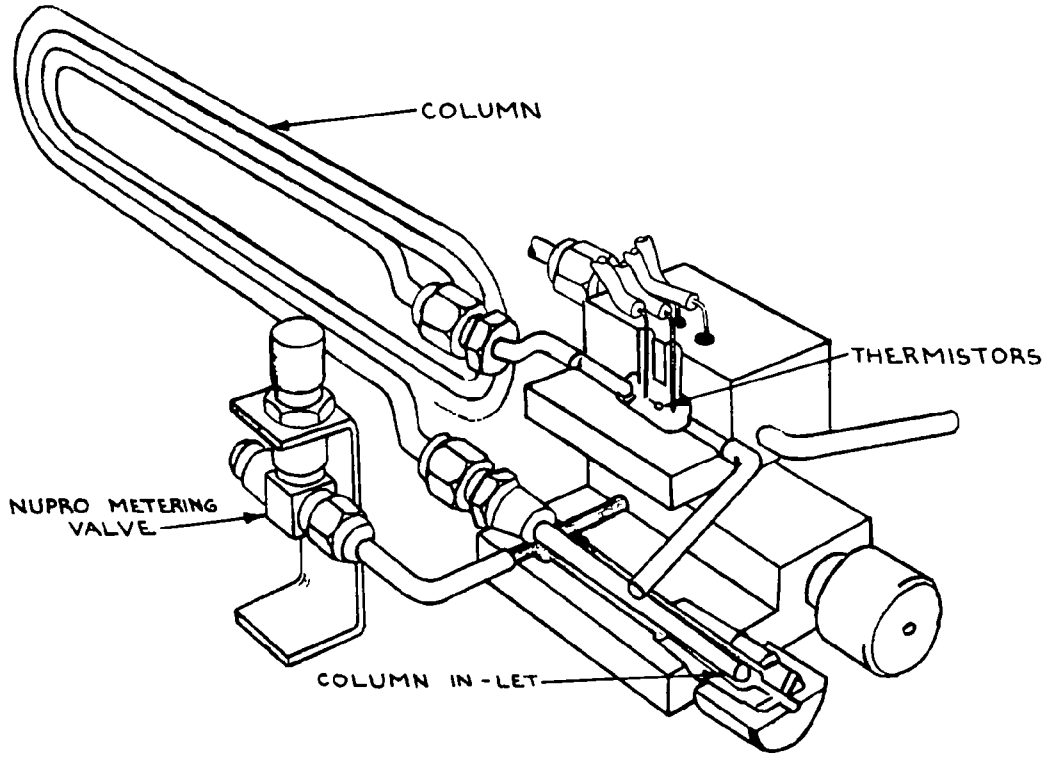

a. THERMAL CONDUCTIVITY DETECTOR

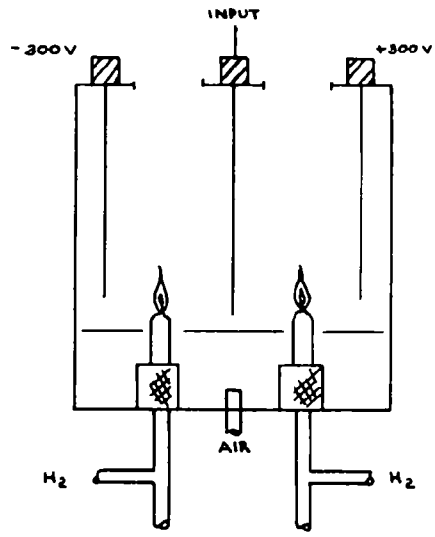

b. FLAME IONIZATION DETECTOR

INTERNAL CONFIGURATIONS OF GAS CHROMATOGRAPH DETECTORS

Figure
V- 6

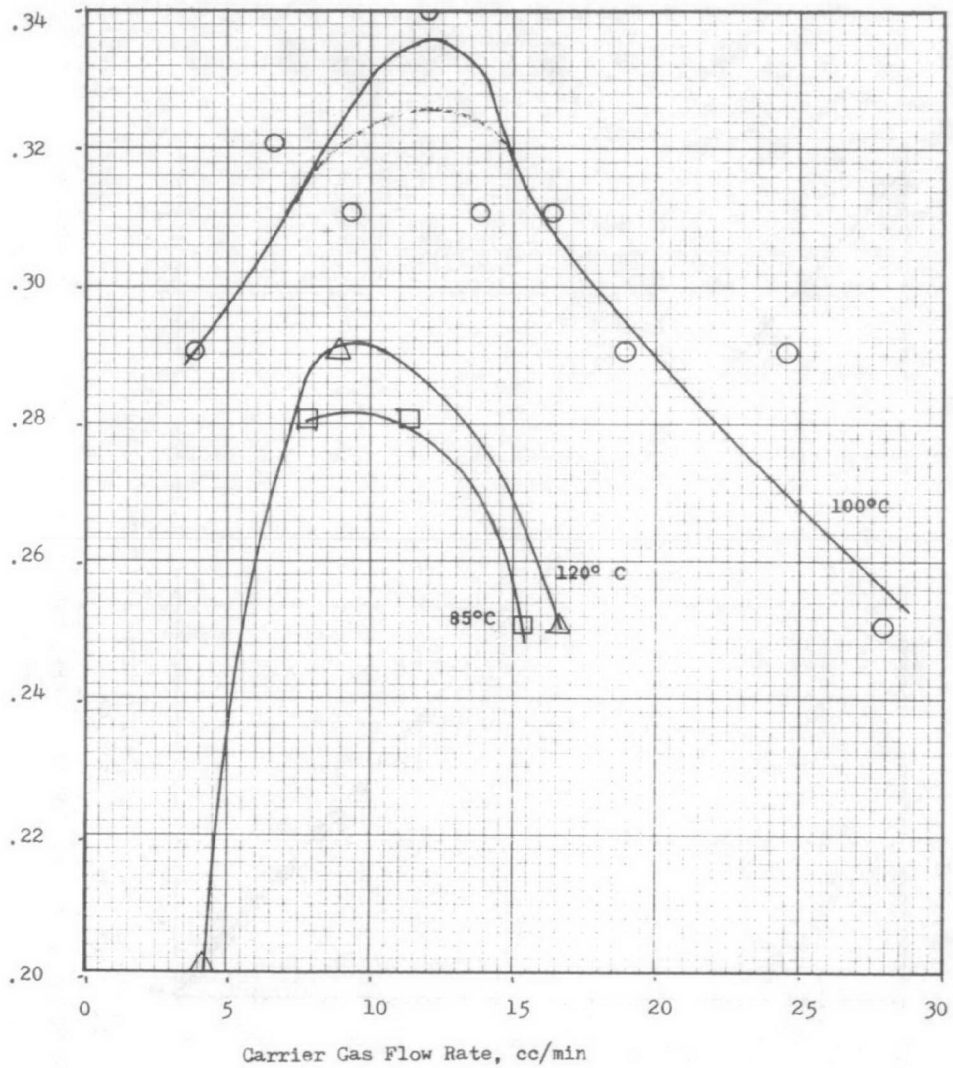

PEAK HEIGHT OPTIMIZATION FOR CO ELUTION FROM GAS CHROMATOGRAPH

Figure V-7

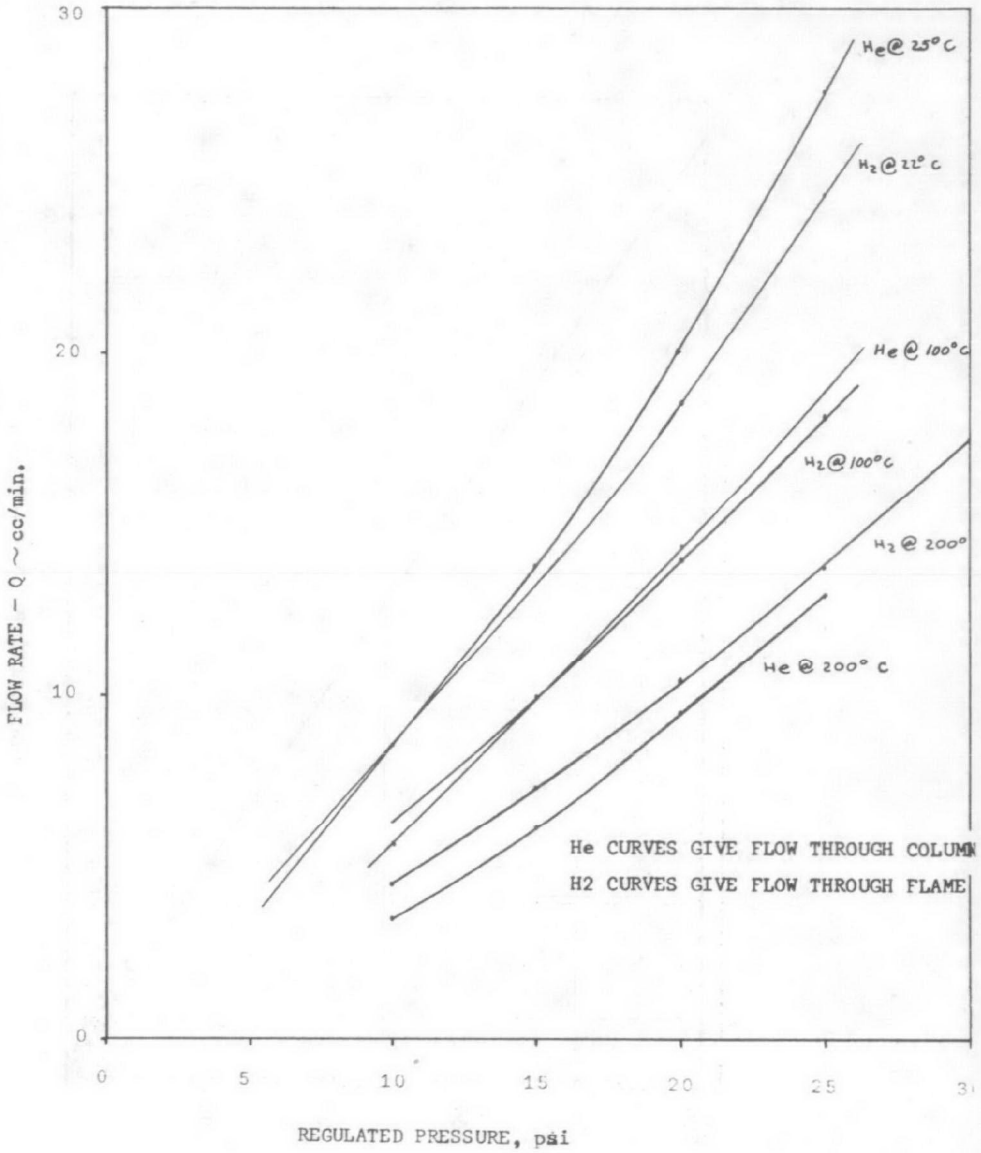

CALIBRATION CURVES FOR GASES USED WITH THE FLAME IONIZATION DETECTOR

FIGURE V 8

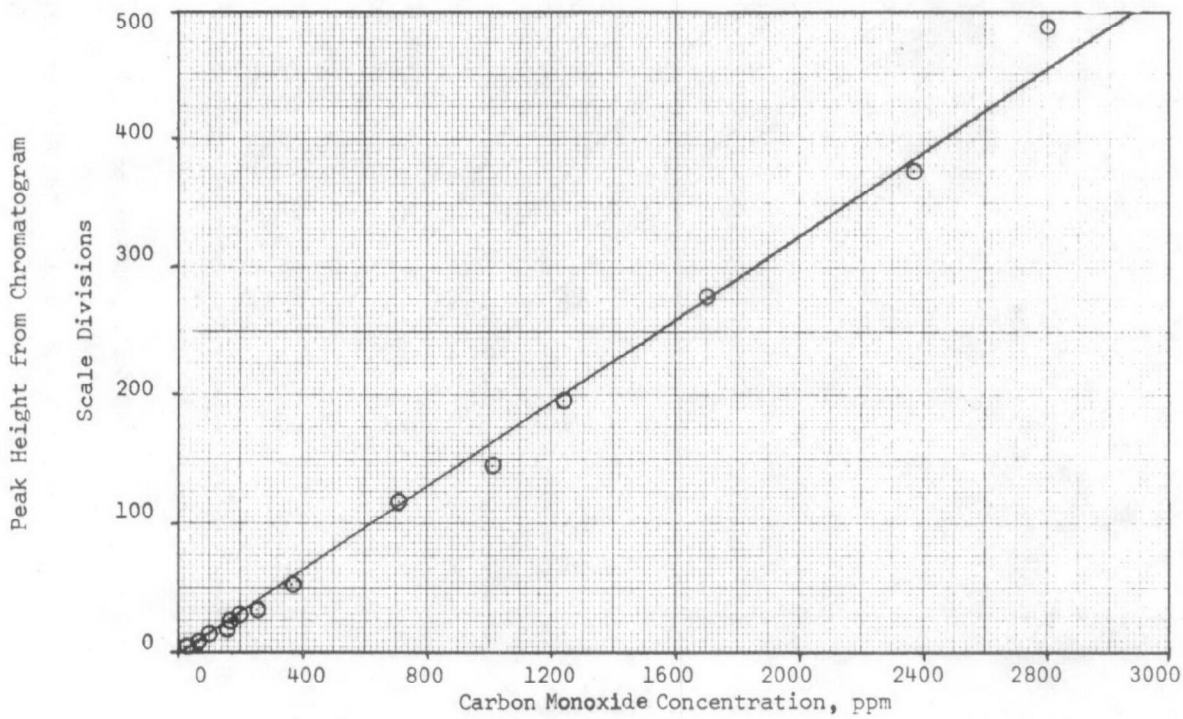

a. Low Range Calibration

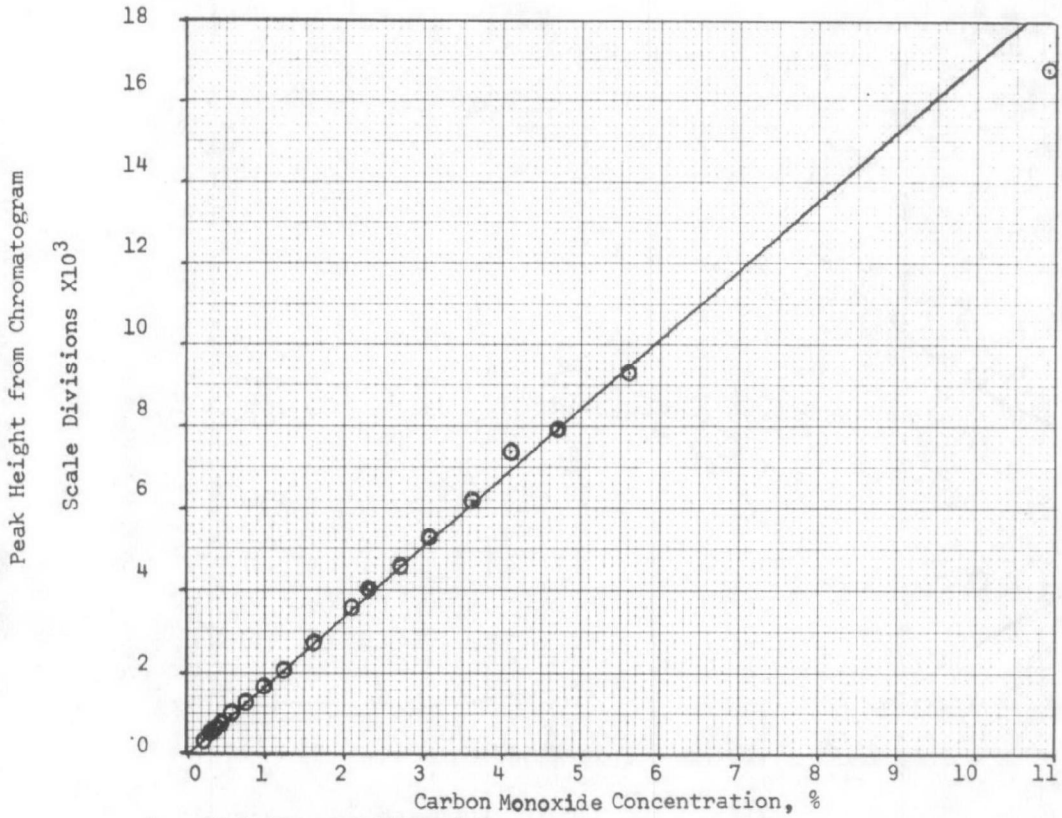

b. High Range Calibration

CARBON MONOXIDE CALIBRATION ON THERMAL CONDUCTIVITY DETECTOR GAS CHROMATOGRAPH

Figure V - 9

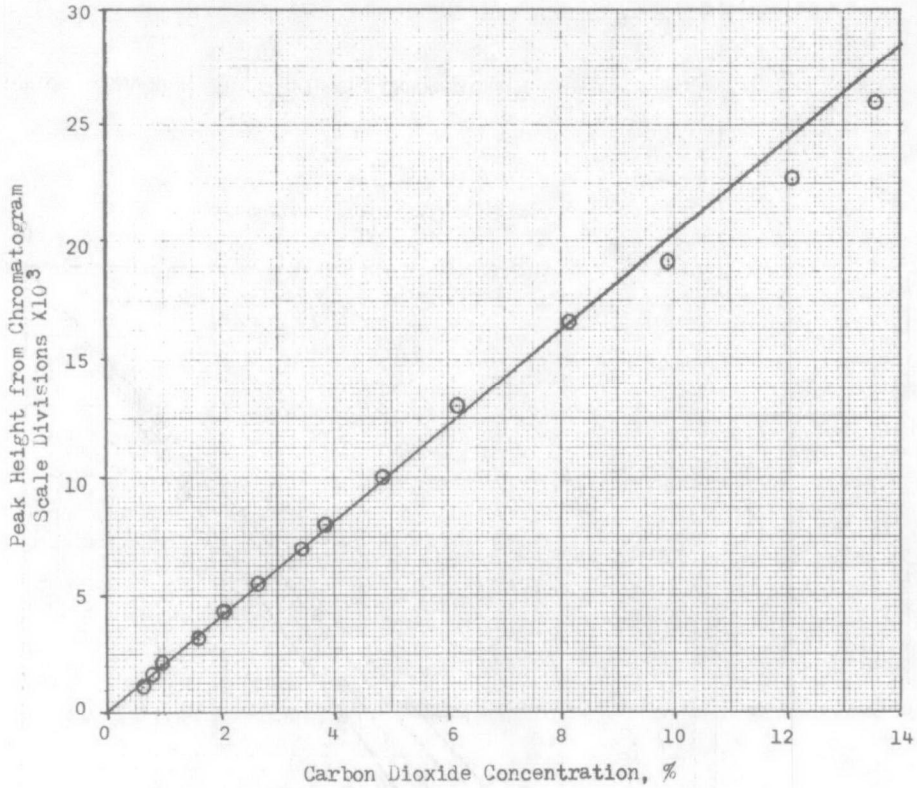

CARBON DIOXIDE CALIBRATION ON THERMAL CONDUCTIVITY DETECTOR GAS CHROMATOGRAPH

Figure V - 10

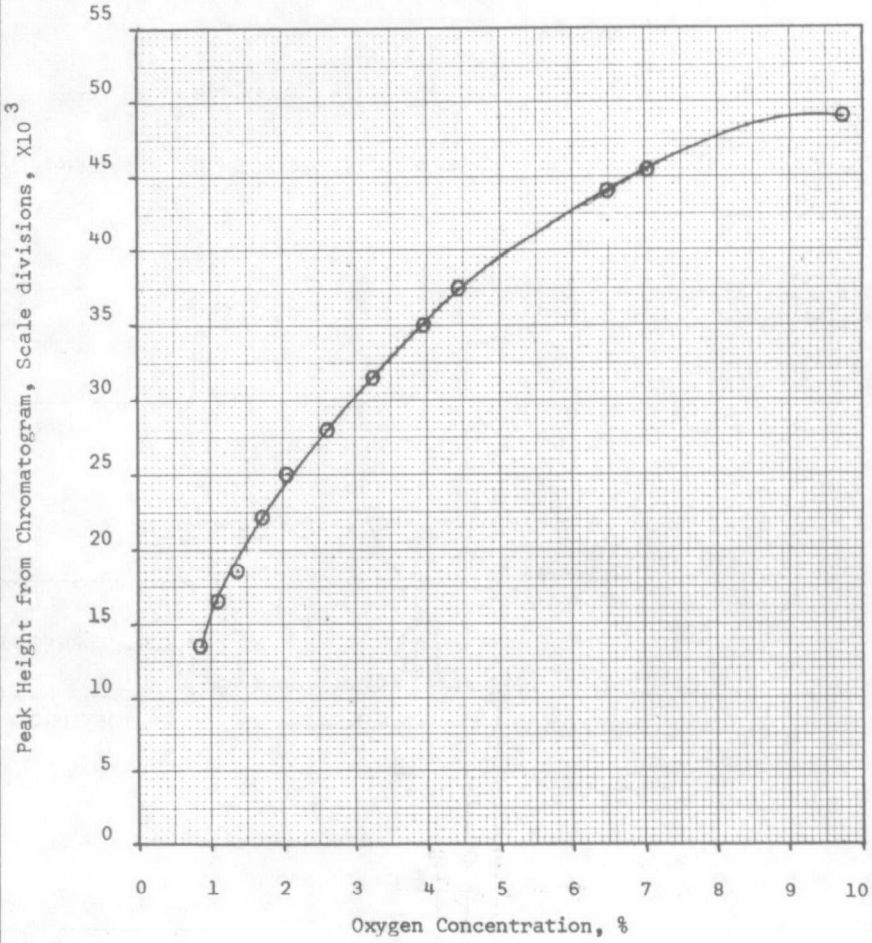

OXYGEN CALIBRATION ON THERMAL CONDUCTIVITY DETECTOR

GAS CHROMATOGRAPH

Figure V - 11

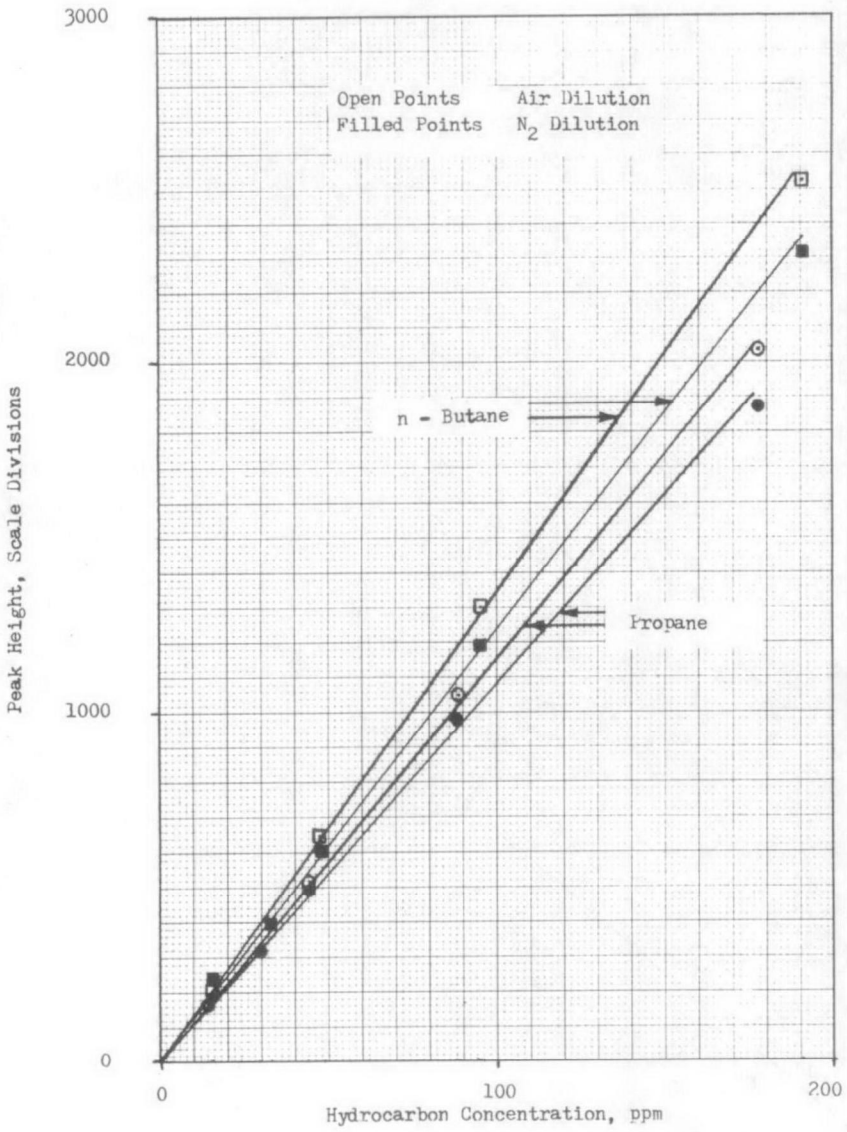

CALIBRATION OF SEPARATION SIDE OF FID GAS CHROMATOGRAPH

Figure V-12

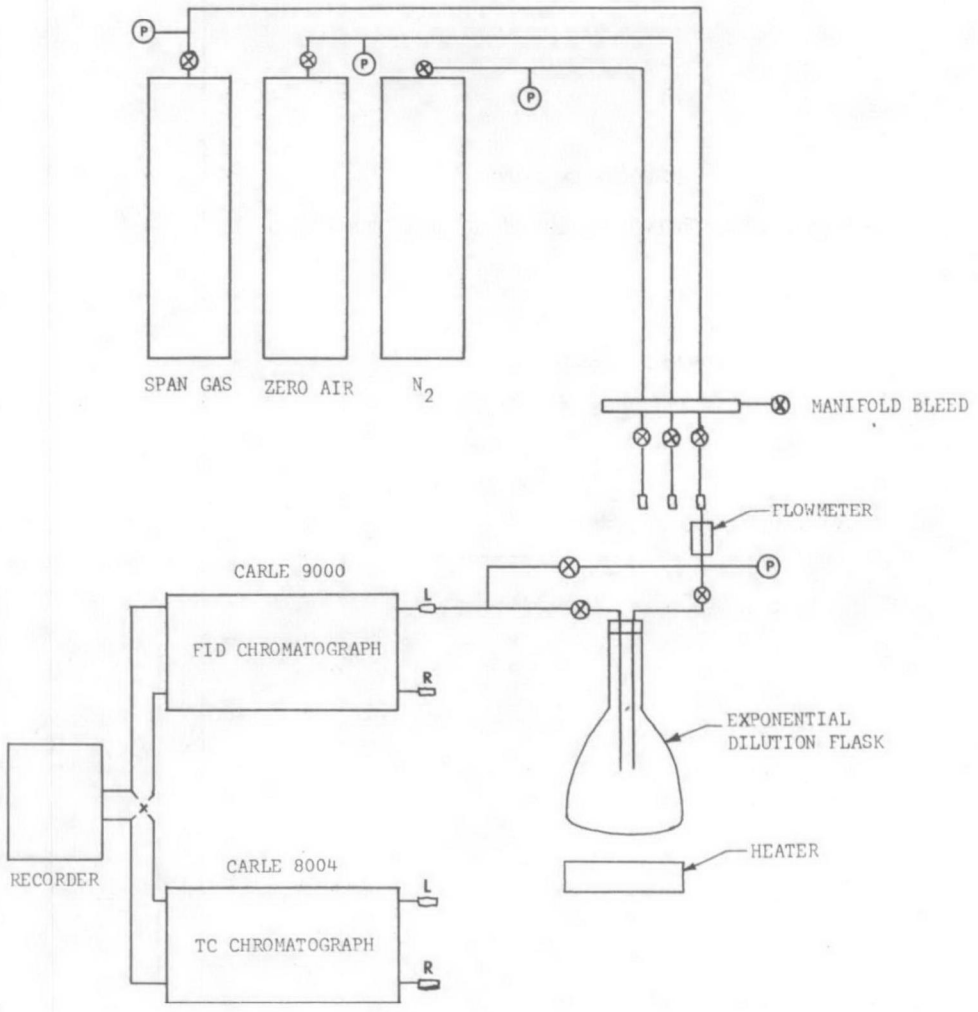

SCHEMATIC DIAGRAM OF EXPONENTIAL DILUTION APPARATUS

Figure V - 13

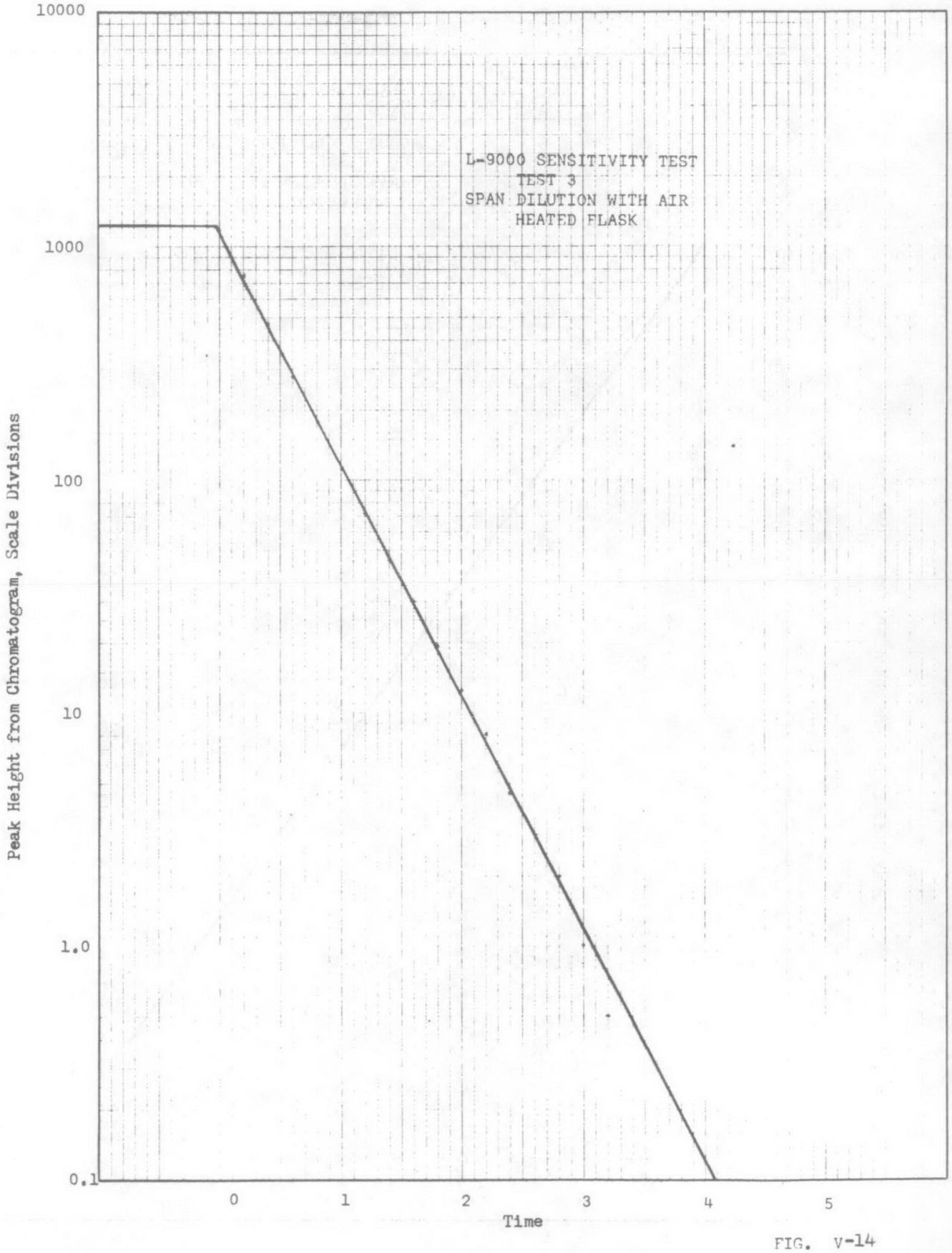
L-9000 SENSITIVITY TEST
TEST 3
SPAN DILUTION WITH AIR
HEATED FLASK
10000
1000
100
10
1.0
0.1
Peak Height from Chromatogram, Scale Divisions
0
1
2
3
4
5
Time

FIG. V-14

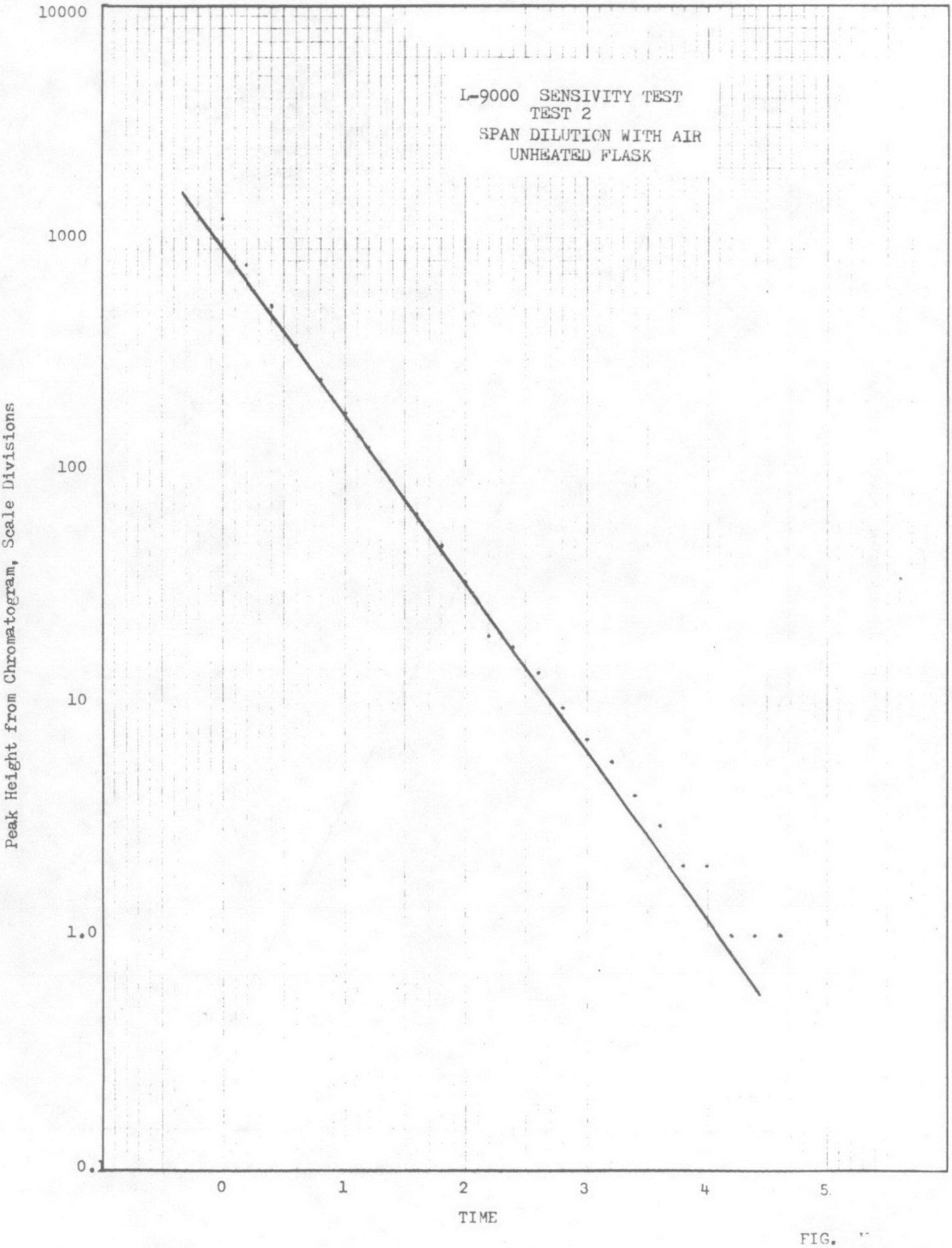
L-9000 SENSIVITY TEST
TEST 2
SPAN DILUTION WITH AIR
UNHEATED FLASK
10000
1000
100
10
1.0
0.1
Peak Height from Chromatogram, Scale Divisions
0
1
2
3
4
5
TIME

FIG.

Calibration of Flame Ionization Detector

Span Gas Diluted with Nitrogen

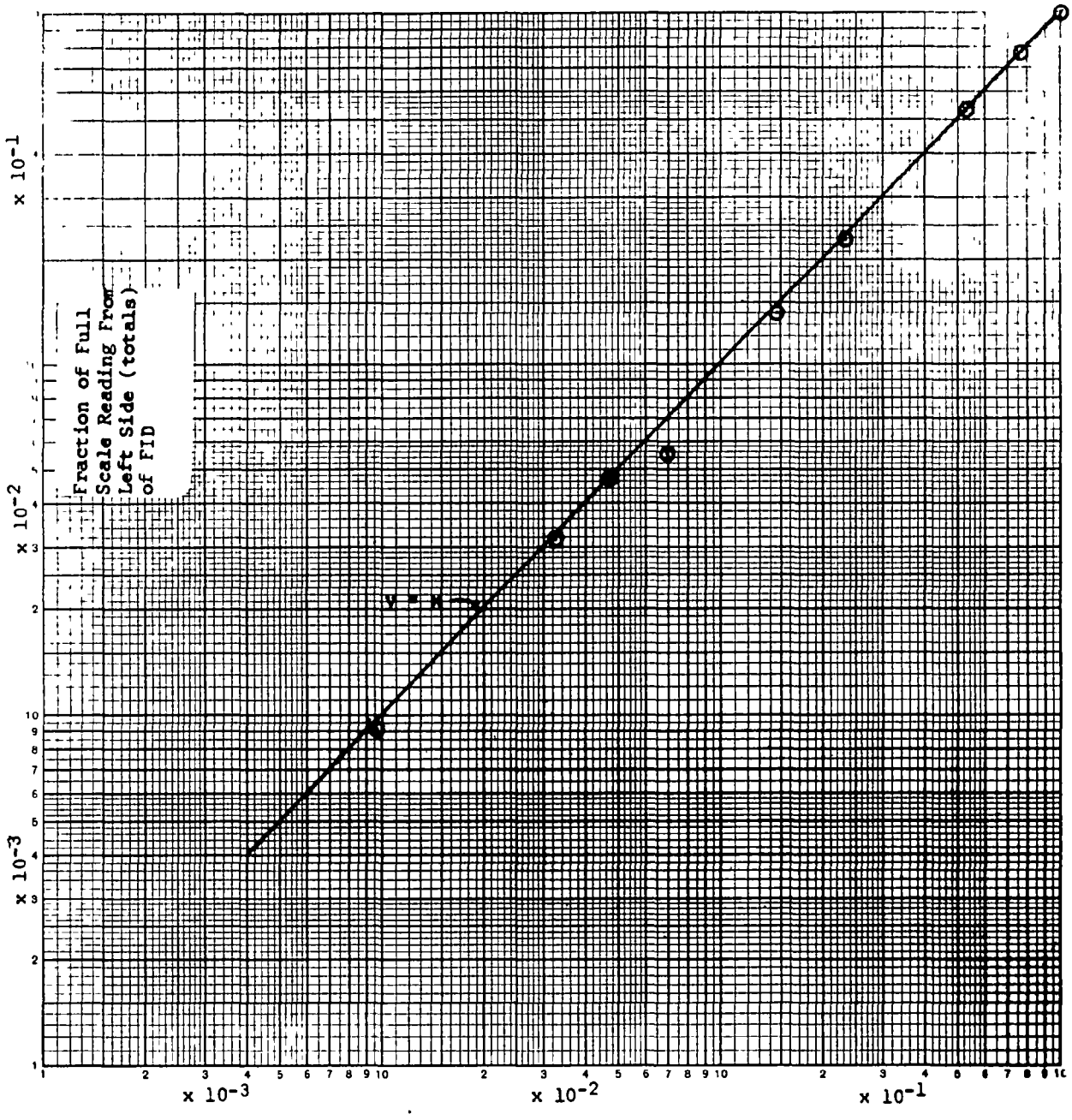

Figure V-16

Calibration of Flame Ionization Detector
Showing Oxygen Synergism Effect
Span Gas Diluted with Zero Air

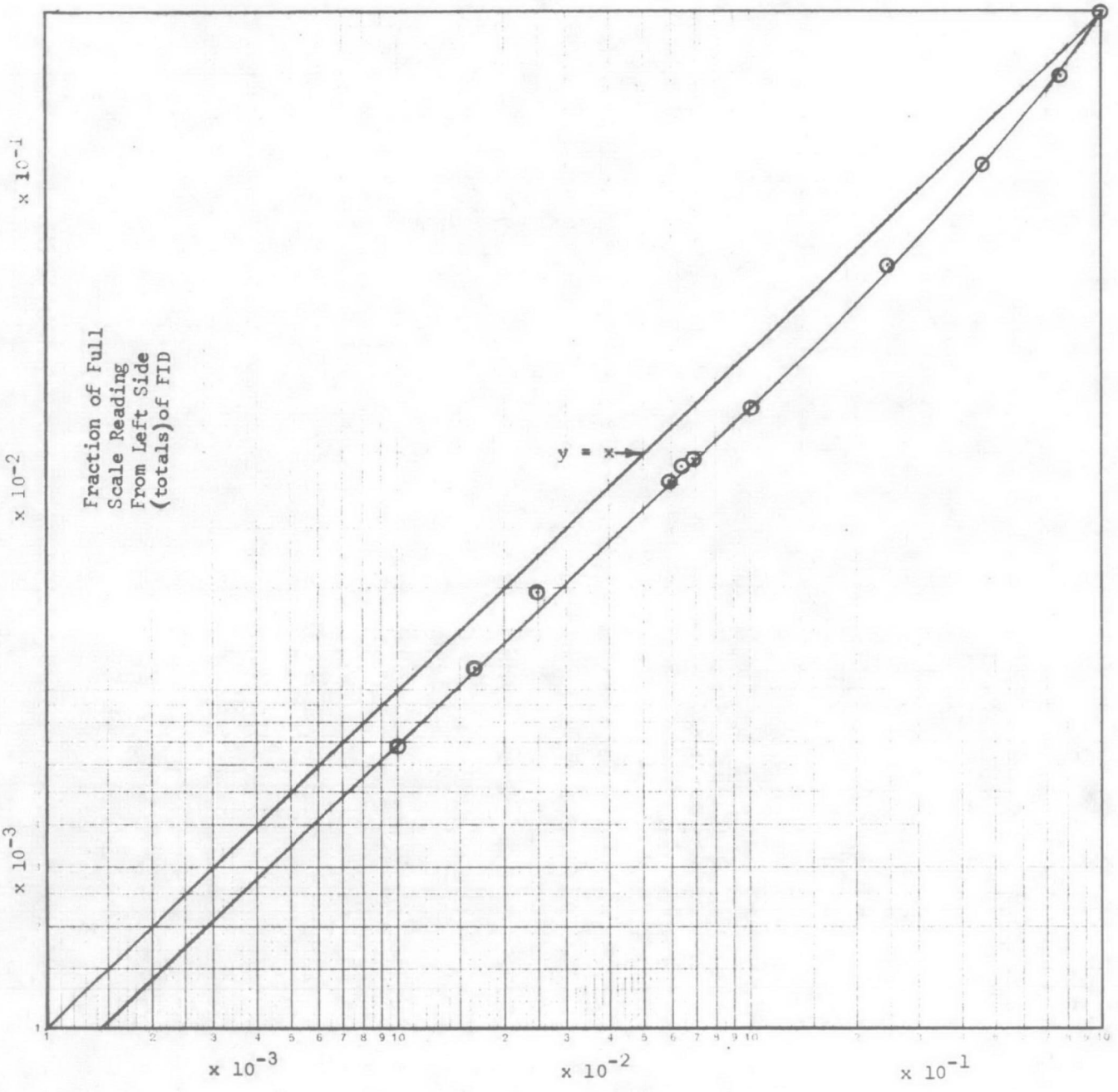

Figure
V-17

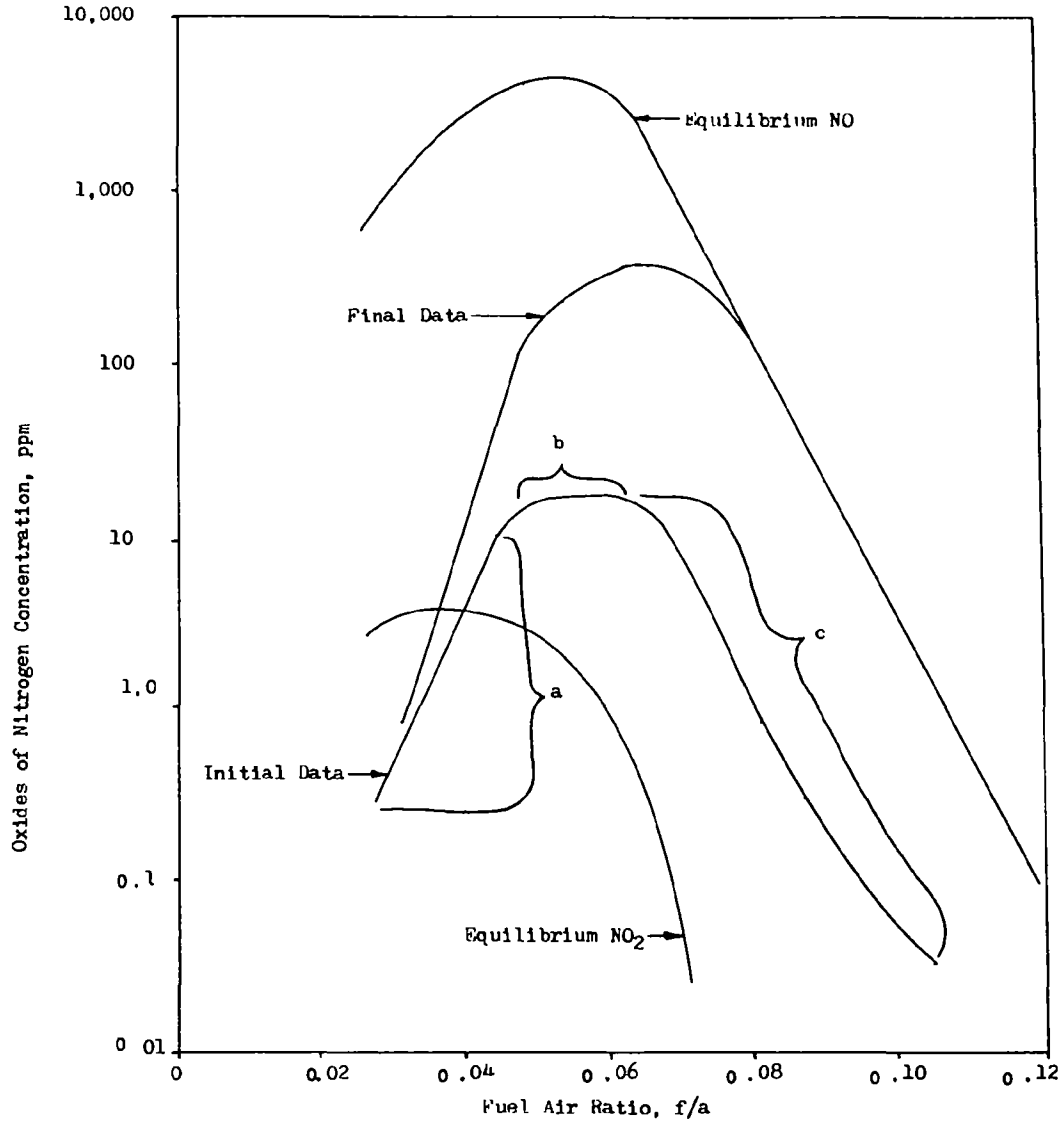

COMPARISON OF INITIAL AND FINAL DATA

Figure V-18

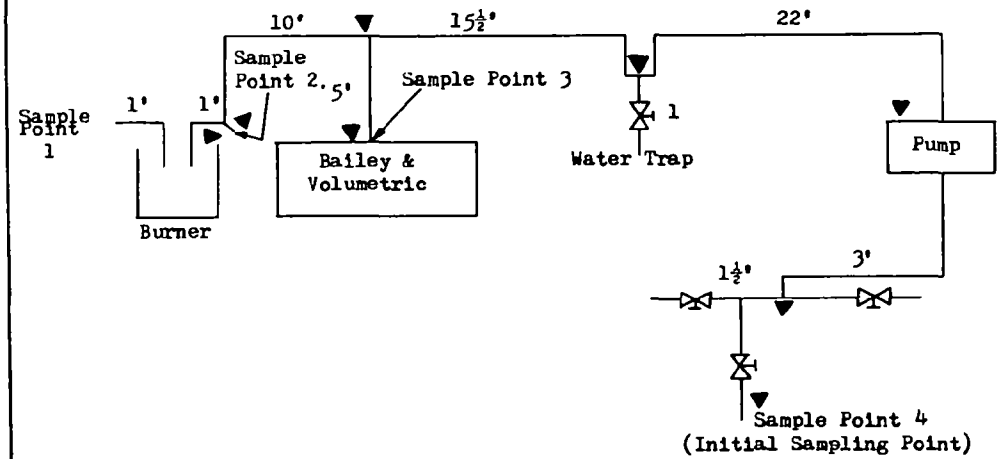

Distance Between are indicated

Distance Between Burner and Sample Point #1 - 1 ft.
#2 - 1 ft.
#3 - 15 ft.
#4 - 52 ft.

NO_x SAMPLING POSITIONS

Figure V-19

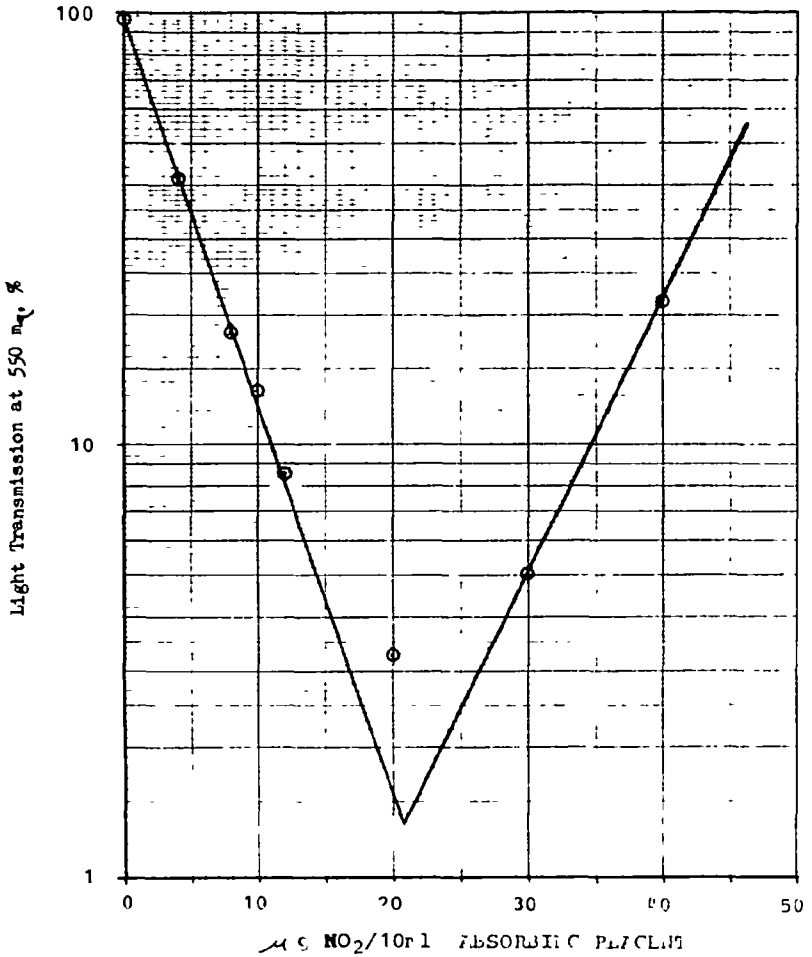

CALIBRATION OF GRIESS-SALTZMAN ABSORBING REAGENT

Figure V-20

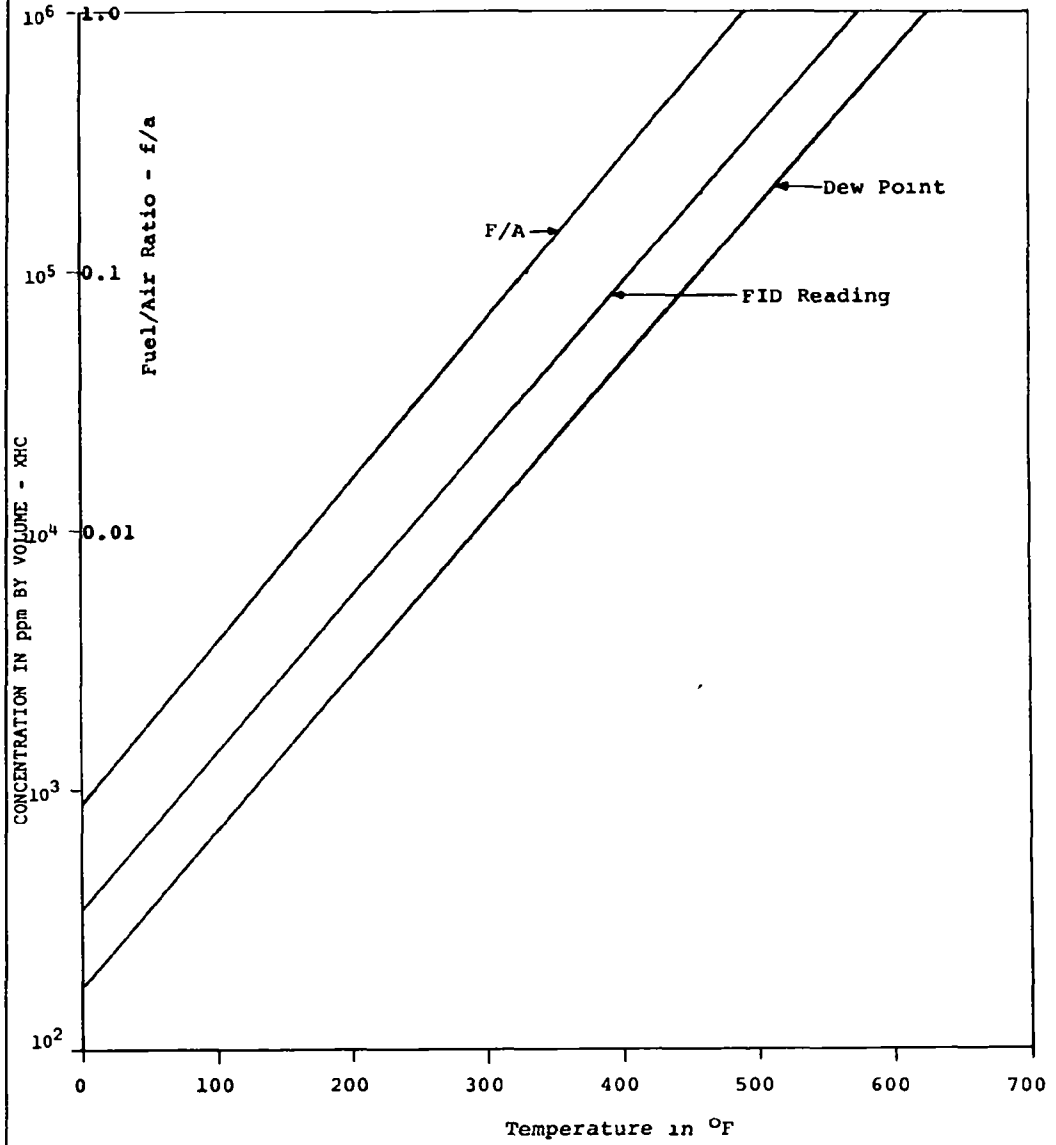

Kerosene Dew Point Data

Figure V-21

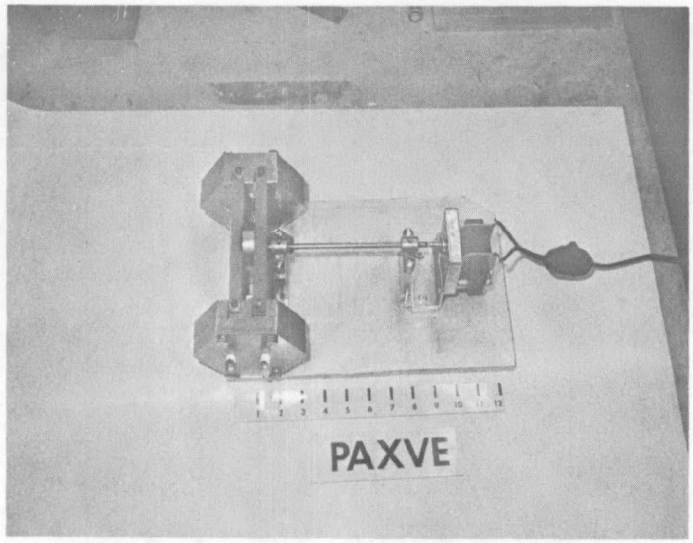

a. Top View of Pump

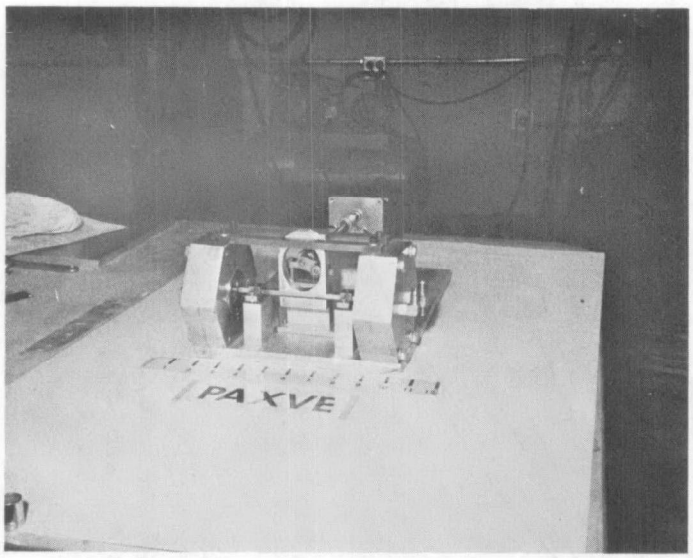

b. Side View of Pump

DIAPHRAGM PUMP USED TO OBTAIN HYDROCARBON DATA

BURNER EXHAUST SAMPLING SYSTEM

Figure V-22

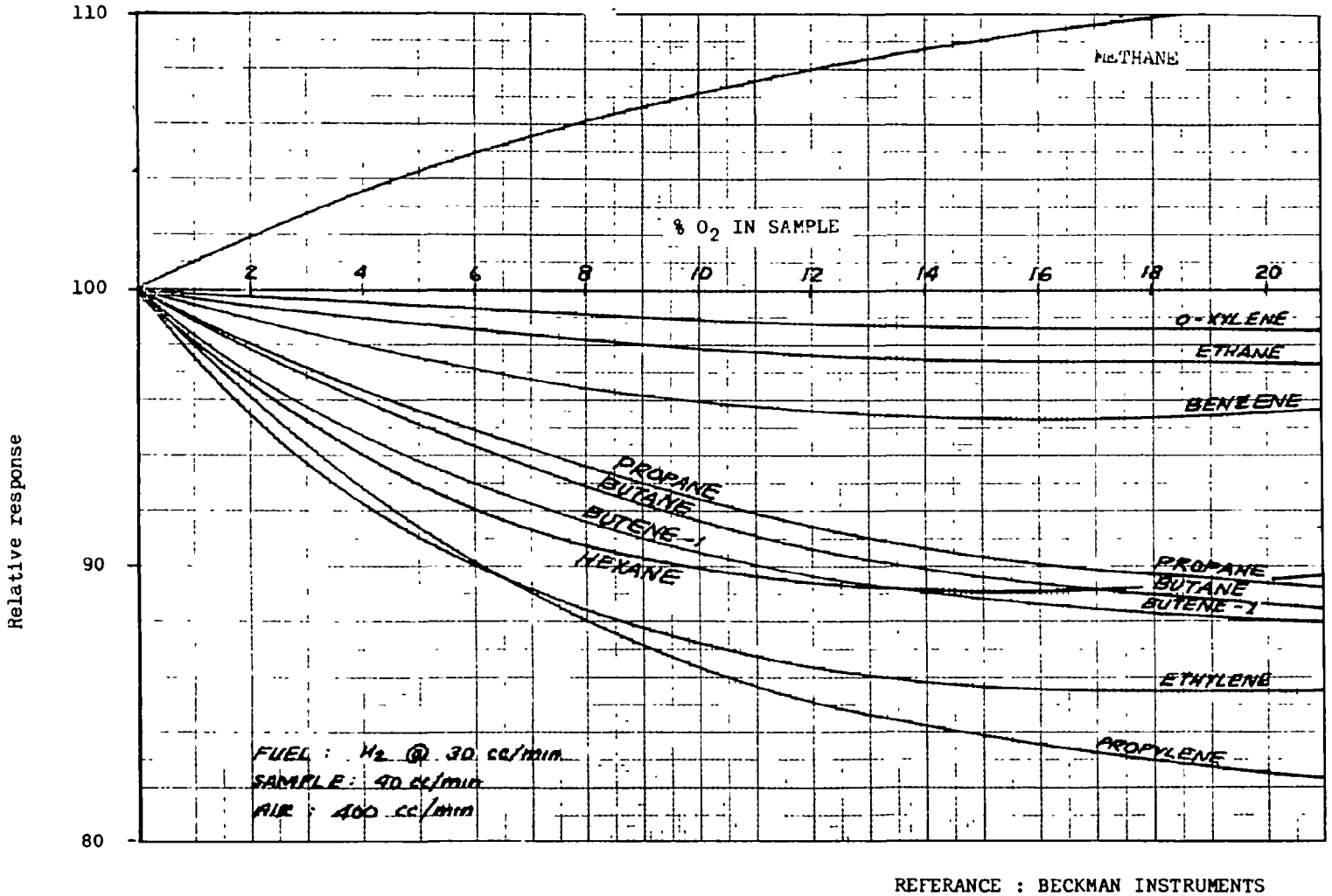

REFERANCE : BECKMAN INSTRUMENTS

Figure V-23

OXYGEN SYNERGISM EFFECT ON VARIOUS HYDROCARBONS USING PURE HYDROGEN AND AIR

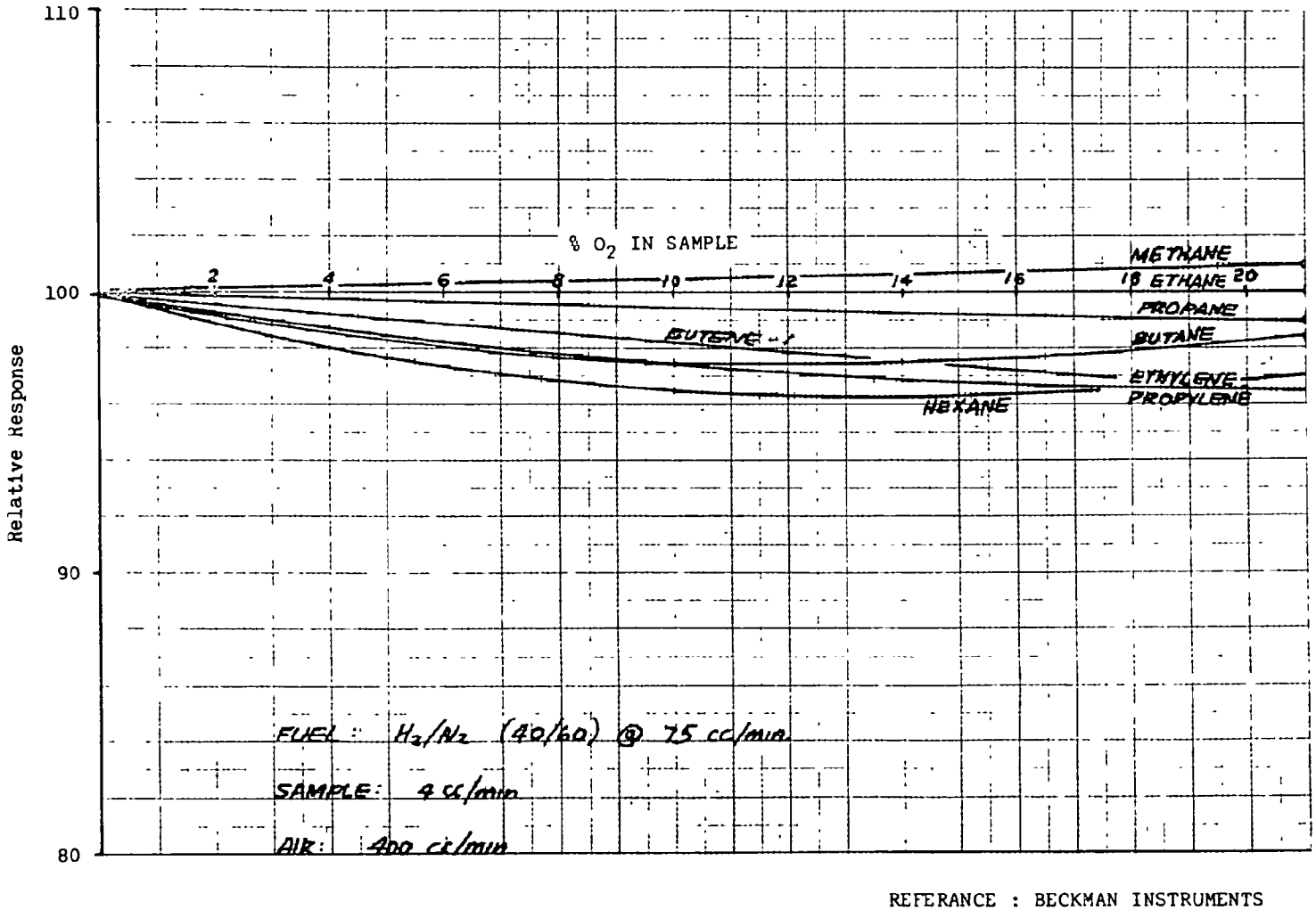

REFERANCE : BECKMAN INSTRUMENTS

Figure V-24

OXYGEN SYNERGISM EFFECT ON VARIOUS HYDROCARBONS USING A NITROGEN-HYDROGEN BLEND AND AIR

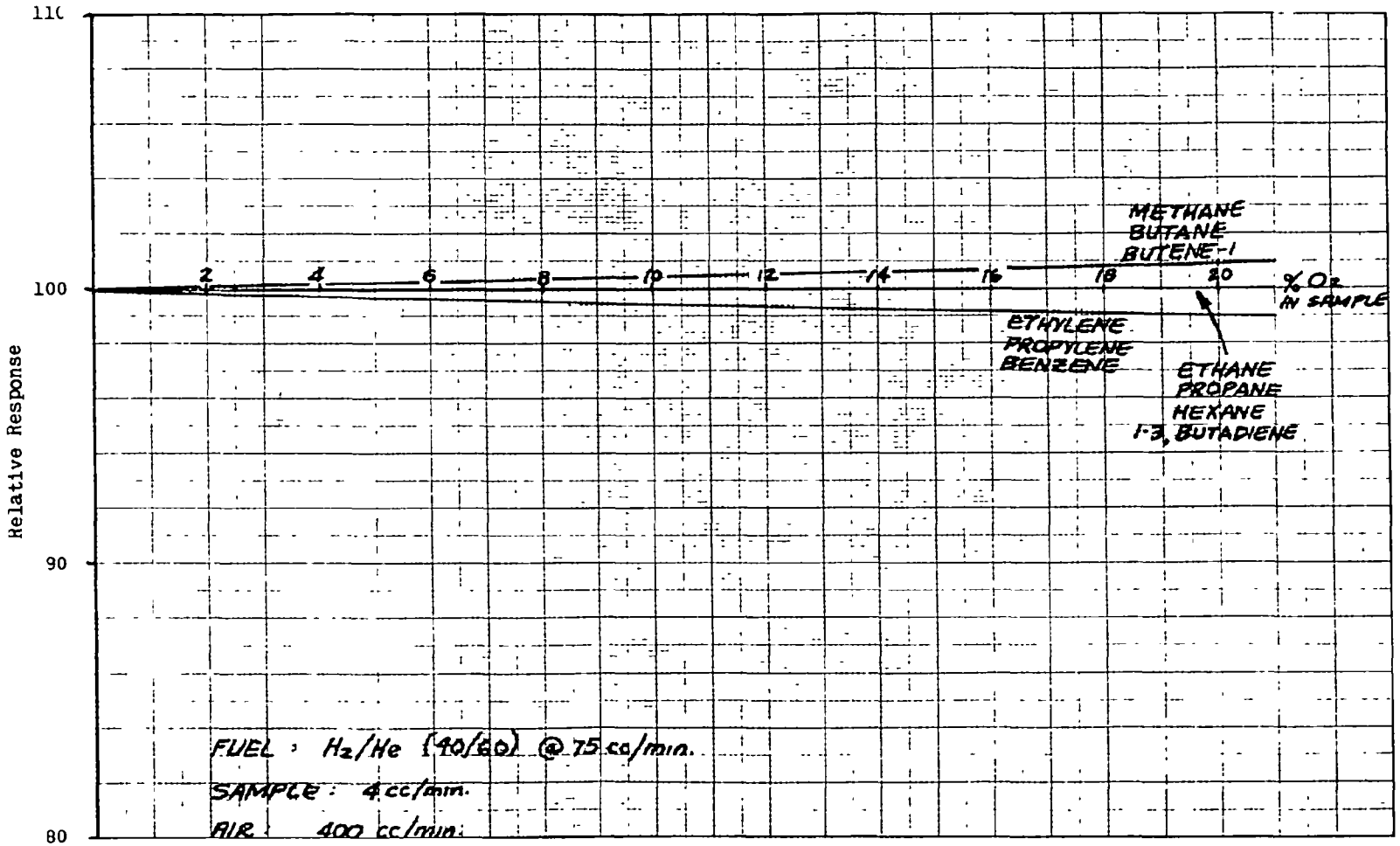

REFERANCE : BECKMAN INSTRUMENTS

OXYGEN SYNERGISM EFFECT ON VARIOUS HYDROCARBONS USING A HELIUM-HYDROGEN BLEND AND AIR

SAMPLE	POINT	PROBE MATERIAL	NO_x CONCENTRATION (EQUIVALENT NO_2, ppm)	
			Test 1	Test 2
#1	(At Burner)	Quartz	9.5	9.5
#1	(At Burner)	Stainless Steel	9.8	10.2
#3	(15' from Burner)	Stainless Steel	5.15	8.8
#4	(52' from Burner)	Stainless Steel	0.1	2.8

COMPARISON OF NO_x SAMPLING POSITIONS Table V -1

	Standard Solution Transmission at 550 mμ (%)
New Reagent, Cold	42.0
New Reagent, Warmed	42.0
Old Reagent, Cold	42.5
Old Reagent, Warmed	42.5

TEMPERATURE AND AGING EFFECTS ON GRIESS-SALTZMAN ABSORBING REAGENT Table V-2

	Transmission At 550 mμ (%)	Equivalent Oxides of Nitrogen (ppm)
Reagent added before evacuation	62.3	2.3
Reagent added after evacuation	64.0	2.2

EFFECT OF EVACUATING PROCEDURE ON SAMPLING RESULTS Table V-3

FUEL SPECIFICATION - KEROSENE

PROPERTIES

Gravity, °API	39.8 (0.826)
Color, Saybolt	30+
Flash, Tag c.c., °F	136
Pour Point, °F	B-60
Viscosity, cs at 30°F	10.24
Copper Strip at 122°F	1
Copper Strip at 212°F	1
Corrosion, Silver Strip	0
Mercaptan Sulfur, % wt	0.0001
Odor	ok
Smoke Point, mm	20
Aromatics, % vol	14.1
Freezing Point, ASTM °F	B-58
Water Reaction, Inc. or Dec., ml	0.5
Interface Rating	1
ASTM Distillation, °F - I.B.P.	344
10% Evaporated	365
50% Evaporated	419
90% Evaporated	478
95% Evaporated	491
End Point	504
Recovery, % vol	98
Residue, % vol	1.0
Loss, % vol	1.0
Aniline Gravity Constant	5532
BTU/lb (Calc)	18,500
Gum, Existent, Steam Jet Mgs.	1
Gum, Potential, Steam Jet, Mgs.	1
TAN-C	Neutral
SAN-C	Nil
Olefine, % vol	0.7
Naphthalenes, (Diaromatics)	0.31
Water Separometer Index Mod	98
Luminometer Number	47.3
Thermal Stability, ACTM-CFR Coker	
Pressure Drop, In. Hg	.05
Preheater Deposit Rating	0

Table V-4

VI. EXPERIMENTAL RESULTS

A. Experimental Data Listings

A complete listing of all emission and stability data for the Paxve burner obtained during this program is given in Tables 1 through 13. This listing consists of all the basic raw data obtained from burner testing which was conducted intermittently over a period from October 1970 to May 1971. The run numbers were assigned in chronological order and are listed consecutively with deletions of runs 173, 187, 204, 208 thru 216, 276, 277 and 278. These runs were either misnumbered or did not apply to this program. The data tables were compiled by inputting the test data sheets into the APL IBM/360 computer. Data sorting, checking, editing and final printout were greatly facilitated through the use of the computer.

All pertinent burner data that was taken is listed and the test parameter symbols are defined in the table of nomenclature, Table 14. Each run is categorized under test type according to the fuel used, test objective, the burner system configuration and the test stand in which the test was conducted. The minus one (-1) notation given in the various columns of the data is an IBM 360 computer expedient to indicate data elements which are blank. The data voids will occur as a function of the particular run objective. Where applicable, run comments are given to describe or indicate runs which were made for procedural checks such as stability testing techniques or emission testing techniques to improve the quality of data. Also, in the course of the program, as elements of the test facility were added, such as the vapor generator loop, some runs were allocated for providing a check of the system additions. Comments are also made to indicate data which through the sorting technique has been indicated to be obviously bad. Improvements were made to the burner in the course of testing. These improvements consisted primarily of better fuel/air mixing to eliminate fuel/air stratification. The injector improvements were applied to the burners in both stands 1 and 2. The comment column of the data listing indicates when the finalized burner improvements were instituted by the designation N which stands for new burner, in contrast to O for the old burner. As a further clarification of the major events affecting the test program and relating to the data listings, a table of significant test program events is given in Table 15. The notes indicate by run number when significant changes in test operation or data evaluation techniques took place during the burner evaluation program.

1. Explanation of Data Tabulation Column Headings

A table of nomenclature for the symbols given in the column headings of the Experimental Data Tables 1 thru 13 is given in Table 14. The table of nomenclature is self explanatory and further amplification is not necessary. The data given in

the experimental data tabulation is all basic raw data with the exception of the nominal fuel/air ratio (FAN). The detailed explanation for the derivation of FAN is presented in Section VI-B. The chromatographic and FID data (CO_2C, NOT, NOB, CO and HC) is given in either percent concentration or in parts per million. These values were obtained from the measured strip chart recorder deflections and applying the appropriate spanning factor. Span was obtained by calibrating the instrument with a gas of known concentration as discussed in detail elsewhere in this report.

For those runs for which the CO emissions were not detectable, the CO values were reported as 5 ppm which was the lower limit of resolution for the chromatograph. Those runs for which the FID readings were below zero were reported as zero ppm.

The air flow data (WA) was taken from the meter as a volumetric reading from Stand 1, in percent of full scale (SCM). The meter reading was then converted to a mass flow rate by using the meter calibration curve and correcting for temperature and pressure in the following manner:

$$(WA)_{CORR.} = P_{STD.}\ (VA_{CFM})\ IND. \sqrt{\frac{T_{IND}°R}{T_{STD}°R}}$$

$$P_{STD} = \frac{P_{STD}(PSIA)}{RT(°R)}$$

The temperature and pressure corrections were required for Stand 1 air flow meter since it is calibrated for volumetric flow at standard conditions. Corrections are required when the test temperature and pressure varied from the values for which it was calibrated. Stand 1 operates at ATM pressure so pressure corrections are not necessary.

Stand 2 air flow meter reads in standard pounds per minute and the equation for correcting the indicated flow readings as a function of the temperature and pressure is shown below:

$$(WA)_{CORR.} = (WA)_{IND.} \sqrt{\frac{T_{IND}(°R)}{T_{STD}(°R)} \cdot \frac{P_{STD}(PSIA)}{P_{STD}(PSIA)}}$$

Stand 2 operated slightly above 1 ATM and both pressure and temperature corrections were applied to the data.

The fuel flow readings (WF) for propane were read in standard cubic feet per hour for both Stands 1 and 2. These meter readings were converted to mass flow in pounds per hour as a function of the propane supply pressure by calibration curves. Temperature variations at the meter were negligible and corrections were not necessary. The kerosene liquid flow meter was nearly linear over the required flow range and the meter readings were converted to mass flow rate in pounds per hour by referring to the calibration curve. Corrections for pressure and temperature were unnecessary since liquid flow at the flow meter was maintained at essentially ambient temperature conditions.

As described elsewhere in this report, it was found that the FID chromatograph was sensitive to oxygen concentration. A correction factor has been applied to all the hydrocarbon emission measurements given in Tables 1 through 13 in accordance with the calibration factor given in Figure IV-12 when oxygen was present in the gas sample.

2. Explanation of Significant Test Program Events

In the course of the burner evaluation program, significant events occurred which influenced the quality of the data. Facility improvements were added and procedural methods were developed which aimed at obtaining data of the best quality. The more important events in this regard have been listed to provide the reader with a better understanding of the progression in testing and instrumentation technology achieved during the course of the program.

a. Stability Test Procedure

The test program began with an evaluation of burner stability lean limit with propane on Stand 1. Runs 1 through 7 were devoted to exploring the best indicators for a true indication of the lean blowout limit. These tests established a procedure which was utilized in subsequent runs and this group of runs in themselves did not produce valid stability data. The initial difficulty in establishing the lean blowout limit was associated with the fact that the residual heat capacity of the burner appeared to sustain burning beyond the lean limit fuel/air ratio. It was found necessary to make a number of runs on and near the lean limit point for extended time duration to establish that the burner remained at a steady state burning condition.

b. NOx Line Loss Check Out

During initial testing the gas samples for NOx analysis were drawn from the long sample line which provided the gas samples for all other emission data. The readings became suspect from this testing configuration when only very low values were consistently obtained. Beginning with run 95, a series of tests were conducted in both test stands 1 and 2 to evaluate the effects of drawing the NOx sample from various line lengths and from sample lines of different materials. It was found that NO_2 was being absorbed by the condensed water vapor in the long sample line and a procedure was established for drawing NOx sample through short quartz tubes which gave satisfactory results and was followed for the remaining runs.

c. Propane Accumulator Installed Stand 2

It was noted during testing that propane flow oscillations were occurring in test stand 2. Due to low propane supply pressure, pressure coupling with the burner

chamber pressure oscillations occurred which caused oscillations in flow and interferred with the propane flow measurements. This difficulty was eliminated by installing a propane accumulator downstream of the propane supply tank. This change was made during run 108 and served for the balance of the Stand 2 testing in the program.

d. Air Flow Straightener Stand 2

During initial testing in Stand 2 it was noted that unsymmetrical air flow profiles existed at the burner inlet. The air flow plumbing in stand 2 for which the vapor generator loop is utilized, requires that a 90° bend be installed upstream of the burner inlet. To eliminate the effects of the flow discontinuity, a flow straightener consisting of a bundle of small diameter tubes was installed at a secion downstream of the 90° bend which eliminated the problem.

e. Hot Sample Line Installation

During initial emissions testing, long unheated sample lines were used to draw the sample to the chromatograph instruments. It was suspected that condensation of some of the exhaust gas constituents could occur in the sample line. This is particularly true of the unburned hydrocarbon fuels or decomposition products which might exist in the exhaust gas sample. Difficulty was also encountered in hydrocarbons or impurities being retained in the long sample line from previous running modes and obscuring the data for following runs. This problem was resolved by installing a line heater over the entire length of the sample line and maintaining the line temperature at 300°F or above. This temperature was sufficient to vaporize any of the heavier fuel fractions occurring in kerosene. The hot sample line was installed and checked out during run 128 for Stand 2.

It was necessary to complete the sample line heating system by installing a specially designed and fabricated electrically heated diaphram pump in the sample line. A pump was required to maintain the necessary pressure for accurate chromatograph data. The pump installation was completed and checked out at run 138 with completely satisfactory results. From this point on the heated system was used in all burner testing.

f. No Data Runs

Run Nos. 173, 187, and 204 are runs during which no data was collected due to misnumbering of the run sequence or due to transient variations which did not permit collecting steady state data. Run groups 208 through 216 and 276 through 278 were made as special runs using special burner equipment for other purposes and are not pertinent to this program.

g. Liquid Kerosene Runs

Runs 203, 342, and 348 through 350 were made with liquid kerosene instead of vaporized kerosene. The liquid kerosene was atomized by injecting a small amount of nitrogen into the fuel line. These runs are identified to differentiate the normal kerosne runs which were conducted with vaporized fuel.

h. Vapor Generator Loop Check Out

A vapor generator system was installed in Stand 2 to operate in conjunction with the burner. The purpose of this configuration was to study the effect on emissions of exhaust gas quenching over the vapor generator heat exchanger. This system consisted of a complex arrangement of mechanical, hydraulic and pneumatic components as well as an engine driven pump. It was necessary to run the burner in conjunction with the vapor generator loop to establish th effect of thermal conditions on the operation of the loop. This was accomplished during runs 205 through 207.

i. Vapor Generator Stack Clean-Out

During the early emissions testing it was found that higher hydrocarbon concentrations were being emitted from the top of the vapor generator stack than from the burner at the bottom of the stack. In the course of investigating the possibility of hydrocarbon emissions being generated from accumulations on the vapor generator coil, a special test was run in which the vapor generator coil was exposed to the burner exhaust gas while flowing nitrogen through the loop instead of the normal working fluid. This procedure was done in order to raise the coil temperature sufficiently to vaporize any absorbed hydrocarbons.

j. NOx Saturation Evaluation

Further doubt was cast upon the NOx gas analysis procedures which were being used by the fact that limiting values for NOx were being obtained which never seemed to be exceeded for the various runs. It was suspected that the proportions of Saltzman solution per sample which was being used for colormetric analysis might be insufficent to avoid saturating the solution. To investigate this possibility further three one liter flasks were prepared containing 10, 20, and 50 ml of Saltzman solution respectively.

During test No. 218, burner exhaust samples were collected in each of the three flasks while the run condition was maintained constant. It was found that the 10 ml flask indicated a maximum NOx value of 19.7 ppm, the 20 ml flask indicated 33.2 ppm, and the 50 ml flask indicated 32.6 ppm. These data indicate that saturation of the Saltzman solution was indeed occurring. The NOx analysis technique was modified as described in detail elsewhere and checked out fully

during runs 219 and 220. This technique was then utilized for all subsequent runs and gave satisfactory results.

k. Fuel Injector Improvements

During runs 220 - 237 it was found that hydrocarbon readings from the top of the vapor generator stack were much higher than those obtained from the burner. A series of investigations were conducted to determine the cause of this phenomenon. Oil deposits on the vapor generator coils and leakage of organic working fluid from the vapor generator tubing were both investigated and ruled out as possible explanations for the high HC readings. The fuel distribution patterns in the burner were then examined. The oxygen, carbon dioxide and hydrocarbon levels were determined at various locations in the plane of the burner exhaust. It was found that the exhaust flow was highly non-uniform. Disassembly of the burner revealed a damaged fuel injector which was flowing most of the fuel into one side of the burner. To remedy this situation and promote even better mixing, new fuel injectors were introduced into both the Stand 1 and Stand 2 test installations. This work was partially documented in runs 279 - 281. During this time, the joint between the inlet pipe and the burner was also modified to prevent raw fuel from being carried up the stack without passing through the burner.

After the modifications noted above had been made to the test installations, it was found that hydrocarbons data from the burner and the top of the vapor generator stack were in substantial agreement. It was also found in later examination of the data, that the NOx readings from the burner were improved as compared to data taken before the modifications. Data taken during and subsequent to run 282 reflect these improved results.

B. Fuel Air Ratio Analysis and Correlation

1. Introduction

The ratio of fuel mass flow to air mass flow is a very important and basic correlation parameter in burner performance evaluation. All emission and stability characteristics of the burner are established on the basis of operation at a given fuel/air ratio. To provide the most accurate definition of burner emission and stability performance and to reduce data scatter, considerable effort was made to establish a reliable fuel/air ratio for each test run. Various sources of measurement were employed to establish a true value of fuel/air ratio for each run. The following discussion will describe the various methods used and the rationale in selecting the value of fuel/air ratio which was assigned to the particular run.

2. Methods of Fuel/Air Ratio Measurement

Values for fuel/air ratio were obtained for each run from various instrumentation sources using two methods of determination. The first method employed the direct flowmeter

measurement of fuel flow and air flow. The appropriate calibration factors to the flow meters were then applied and corrections were made for temperature and pressure to the fluid flows in arriving at a test fuel/air ratio. The second method employed an indirect means of determining the fuel/air ratio by measurements and analysis of the exhaust gas. The indirect method employed two instruments to measure the exhaust gas oxygen concentration and carbon dioxide concentration as well as the unburned combustible constituent concentration. These measured constituent concentrations were then compared with the theoretical equilibrium composition for the combustion of hydrocarbons as given in Figure 1 for the given fuel/air ratio. The exhaust gas carbon dioxide and oxygen composition was measured by the volumetric (Orsat) apparatus during steady state combustion operation. In addition, the Bailey meter gave continuous readings of oxygen composition and combustible gas composition of the exhaust gas sample. The Bailey Heat Prover was used during the burner testing to estimate the burner operating point. The Heat Prover has two meters, one which reads oxygen, and the other, labeled combustibles, which reads a mixture of the hydrogen and carbon monoxide present. For lean runs, the oxygen meter was used in conjunction with theoretical exhaust composition curves to find the approximate fuel/air ratio at which the burner was operating. For rich operation the Bailey combustibles meter was used in conjunction with an especially prepared curve (see Fig. 1) for the same purpose. Figure 2 shows the comparsion of the Bailey oxygen data with the volumetric oxygen information. Although there is fair agreement, it is clear that the Bailey reads low at the higher oxygen values. As a further check, the chromatograph (TC) was used to also measure CO_2 and CO for a comparative examination of the operation fuel/air ratio. The specific instruments used in both methods of fuel/air ratio determination are discussed in extensive detail in other secions of the report and will not be discussed further here.

3. Assessment of the Methods of Fuel/Air Measurement

In the analysis of fuel/air ratio measurement accuracy the fuel/air ratios indicated by the various instruments were tabulated for all the runs as shown in tables 16 thru 23. The basic measurements which are given in the tables are:

a. FA, which is the fuel/air ratio as measured by the flow meters.

b. FAO, the fuel/air ratio determined by the oxygen reading from the Orsat apparatus.

c. FAC, the fuel/air ratio as determined by the carbon dioxide readings of the Orsat.

d. FAB, the fuel/air ratio determined by the Bailey apparatus.

Of the three basic measurements the greatest weight was given to

the volumetric Orsat analysis. This instrument has the best inherent accuracy (approximately 0.1% of reading) and further provides a self contained check in the balance between the oxygen and the carbon dioxide measurements. The Bailey meter is convenient as a continuous recording device but is less accurate than the Orsat and was used primarily for a check of the Orsat readings in the lean combustion mode. As will be noted from the data of Table 24, the flow meter fuel/air ratio values during the early phases of testing in Stand 1 and in Stand 2 fall below the Orsat readings. This fact is attributed to air leaks tht existed in the facility plumbing downstream from the flowmeter which gave erroneously high air flow readings. This would result in an indicated lower fuel/air ratio at the burner than true value. The lower fuel/air ratio readings from the flow meters as compared to the volumetric were noted in particular while testng in Stand 1 during rhe early test runs. During a later test period an overhaul was made of the Stand 1 air plumbing to eliminate all possible leakage points by welding all joints and it is noted that the correlation with volumetric data improved markedly. The consistency of the Orsat volumetric readings of fuel/air ratio derived from carbon dioxide and oxygen exhaust gas concentration measurements are shown in Figure 3. The general consistency of the volumetric measurements and the greater inherent accuracy of the apparatus makes it a first choice or primary standard in establishing the true value of fuel/air ratio. It is further noted that the volumetric measurements of fuel/air ratio are applicable with the greatest degree of confidence in the regimes of combustion where the equilibrium composition can be reasonably established as given in Figure 1. The Orsat fuel/air ratio determination therefore is not applied at the lean limit or rich limit points.

In the early phases of testing, Orsat data was taken periodically and is not available for every run. This was done to expedite testing since the Orsat analysis requires that a grab sample be taken and a rather time consuming process is required in performing the gas constituent analysis during the test run. Since the Orsat data is not available for every run, it was necessary to arrive at an adjusted composite of fuel/air data which could be applied for every run to arrive at the true fuel/air ratio. In order to arrive at cross-correlation of fuel/air ratio from the various instrumentation sources the method described below was employed.

4. Description of Fuel/Air Ratio Correction Procedure

A tabulation of all the fuel/air ratios derived from the various measurements is given in Table 16-23. The FA column is a listing of the fuel/air ratios obtained from the flow meters and is uncorrected. The column headed FA COR is the flow meter fuel/air ratio determination as corrected by factors which will be described. Correction factors for the flow meter data were determined on the following basis.

a. Propane, Stand 1 - early tests
b. Propane, Stand 2 - later tests (after air plumbing leak repair)
c. Propane, Stand 2
d. Kerosene, Stand 2

The correction to the fuel flow meter readings is derived from the Orsat data using selected runs for which the Orsat data was available. The above correction factors were determined for lean combustion, maximum burner efficiency operation for which the theoretical equilibrium combustion criiteria given in Fig. 1 is closely applicable.

The flow meter fuel/air value was divided by the value obtained from the average of the Orsat CO_2 and O_2 fuel/air determination. The ratio thus determined for each of the selected runs was averaged by the computer for all the particular selected run group and a standard deviation was determined. Obviously bad data points which deviated in excess of three standard deviations were excluded. A final correction factor was then obtained by re-averaging all of the ratios. In this manner, correction factors were obtained for the propane Stand 1 early testing and later testing, the propane Stand 2 testing, and the kerosene Stand 2 testing. A tabulation of the flow meter correction factors is shown in Table 24. These correction factors are to be applied to the appropriate values of FA to arrive at the values listed under FA COR. Referring again to Tables 16 thru 23, the column heading given by FAO is made up of fuel/air values obtained from the Orsat volumetric oxygen measurements. The fuel/air values under FAC are the corresponding Orsat values derived from the CO_2 measurement. The values for FAB are the fuel/air ratios obtained from the Bailey Heat Prover. The column headed FAN gives nominal fuel/air ratios upon which the reported burner performance is based. As a result of the previous discussion and general rationale, the FAN values are based primarily on the Orsat measurements. The corrected flow meter data (FACOR) was used for test runs in which the volumetric data was not available and at lean or rich limit stability test points where combustion efficiency is reduced and non-equilibrium values of CO_2 and O_2 are generated. The Bailey Heat Prover fuel/air measurements (FAB), as derived from the measured concentration of combustible consitituents, are also applied for rich mode operation when the Orsat data was not available.

5. Cross Correlation of Fuel/Air Measurements

Further cross correlation among the various fuel/air instrumentation sources are shown in the following plots. Figure 3 shows a comparison of the fuel/air ratios derived from the measured Orsat oxygen concentration versus the corresponding Orsat CO_2 concentration. It is seen that excellent correlation is obtained on an $x = y$ theoretical line. Figure 4 shows a comparsion of the nominal fuel/ air ratio (FAN) versus the CO_2 concentration as measured by the Orsat. The theoretical equilibrium CO_2 concentration is also shown superimposed on the data and it is seen that very good correlation is obtained with minimal data scatter over the

entire range of fuel/air ratio values from lean to rich operation. Figure 5 is a similar comparsion of the nominal fuel air ratio (FAN) versus the O_2 concentration as measured by the Orsat. This curve also shows the theoretical equilibrium oxygen line. Here again, it is seen that the nominal fuel/air ratio (FAN) provides a good basic correlation between the measured O_2 concentration and the theoretical for combustion of propane and kerosene. When the corrected fuel/air ratio from the flow meters (FACOR) is used as a reference to plot CO_2 concentration (from Orsat) as shown in Figure 6, it is seen that the data scatter increases. When the uncorrected values of fuel/air ratios from the flowmeters are examined in a similar manner, as shown in Figure 7, it is again apparent that much wider data scatter is in evidence. A comparsion of the fuel/air ratio derived from the Bailey Heat Prover versus the Orsat fuel/air ratio from the oxygen measurements is shown in Figure 2. It is seen here that reasonable correlation is obtained. It appears that the Bailey has a systematic error and reads O_2 concentrations which are slightly lower than the Orsat values. The Bailey combustibles, however, gave values of fuel/air which were in good agreement with Orsat CO_2 values for rich operation.

On the basis of the above comparsions of fuel/air ratio measurements, it has been shown that the selection of the nominal fuel/air ratio (FAN) gives the closest correlation of hydrocarbon combustion characteristics with the theoretical values. This selection of a nominal fuel/air ratio will best serve as a correleating parameter in the documentation of the Paxve burner emissions and stability characteristics.

C. Experimental Emissions Data

1. Carbon Dioxide Data

Carbon dioxide is not an objectionable emission resulting from hydrocarbon combustion. Its measurement during this test program serves primarily to provide an index of the completeness of combustion and to establish a basis for the determination of fuel/air ratio.

Figure 4 shows all of the volumetric data for carbon dioxide plotted against the nominal fuel/air ratio (FAN). The good agreement is of course a result of the method by which the nominal fuel/air ratio was selected, which is discussed in detail in a preceding paragraph. In general, the averaged CO_2 and O_2 volumetric data was used when possible for the nominal fuel/air ratio. When this could not be done the next choice was the CO_2 data, then the Bailey combustibles data, and finally the corrected fuel/air ratio from the flow meters. The fuel/air ratio as measured from the flow meters was corrected to give the best average agreement with the volumetric data.

Figure 4 shows the CO_2 data as measured from the burner by the volumetric apparatus. Figure 8 shows the CO_2 data as determined by the chromatograph measured from the top of the vapor generator loop. The comparsion of these two values is shown in Figure 9. Computer evaluation of the ratio of CO_2C to CO_2V was

conducted. It was determined that the average ratio of these two values was 0.993 $\pm$0.120.

2. O_2 Data

The measurements of oxygen in the burner exhaust gas products were taken, in general for the same purpose as those for carbon dioxide mentioned above.

Figure 5 shows the volumetric oxygen data from the burner plotted against the nominal fuel/air ratio (FAN). As discussed previously the method of selecting FAN causes this curve to lie close to the theoretical oxygen curves shown in the figure. Chromatograph data for the oxygen concentration was not reduced since data from various other sources were available.

As noted previously the volumetric oxygen data is in close agreement with the expected values based on the volumetric carbon dioxide data. Figure 3 shows the fuel/air based on the volumetric oxygen compared to the fuel/air based on the volumetric CO_2. A computer evaluation of the average ratio shows the value to be 1.0174 $\pm$0.0374.

3. Carbon Monoxide Data

Figure 10 shows all of the carbon monoxide data obtained from the burner plotted versus the nominal fuel/air ratio. The interpretation of this data will be discussed in more detail in Section VII. It will be noticed however, that for fuel/air ratios above approximately 0.04, carbon monoxide data agrees generally with the theoretical prediction based on the information presented in Purdue University Bulletin (Ref. 1). The higher values of carbon monoxide obtained at low fuel/air ratios near the lean stability limit has been attributed to inefficient combustion. Correlation of this data is discussed in Section VII.

Figure 11 shows the carbon monoxide data measured from the top of the vapor generator stack. A comparison of this data with the values obtained from the burner shows that there is substantial agreement for the high fuel/air ratios. Figure 12 shows a comparison of carbon monoxide data taken from the bottom of the stack (the burner) and the top of the stack on the same run. Examination of this Figure indicates that the top of the stack values of CO are lower than those at the bottom of the stack. This is attributed to the oxidation of carbon monoxide in the gas flowing through the stack. In general, the maximum values obtained at the top of the stack are lower for the same fuel/air ratio than those obtained at the bottom of the stack.

4. Hydrocarbon Data

Figure 13 shows all of the hydrocarbon data obtained from the burner. The hydrocarbon data is generally characterized by low readings over a wide range of fuel/air ratios near the so-called operating point of the Paxve burner. As lean blow out is approached hydrocarbon values increase for

kerosene becoming rather large near lean blowout. This phenomena is not observed in general for propane operation. As lean blowout is approached the hydrocarbon values remain substantially zero until the burner is actually at the lean limit. This fact was useful in establishing the lean limit during burner stability investigations. As the lean blowout limit was approached, the flame ionization detector measuring the hydrocarbon output was always the first instrument to register incipient lean blowout. When the FID first showed an increase in signal, the operator would stabilize the burner at that point and wait. In general, in a matter of 10 to 15 minutes, the other burner operation indicators such as the temperature and the oxygen indication on the Bailey would have begun to rise and if allowed to continue, burner blow out would ensue. The operator could always prevent this lean blowout condition from occurring by a slight increase in fuel/air ratio which would cause the FID to once again drop to the low value characteristic of normal burner operation.

The use of the FID as a blowout indicator was not found to be effective for kerosene runs. Kerosene operation as with propane operation generally showed zero or slightly negative readings on the FID during normal burner operation. However, as the lean limit was approached with kerosene positive readings of hydrocarbon, content began to appear and would stabilize at some measurable value. This was in contrast to operation with propane where either the hydrocarbon reading was essentially zero or it would not stabilize but would continue to increase with time and the burner went out. A further decrease in fuel/air ratio for the kerosene operation caused a further increase in the hydrocarbon output. This continued until incipient blowout was reached at which point the hydrocarbon signal would no longer stabilize but would continue to climb as the burner flamed out.

An examination of the hydrocarbon data near stoichiometric or rich operation of the burner shows that as with the carbon monoxide there is a gradual increase in hydrocarbon content in the exhaust with increasing fuel/air ratio. The increase in hydrocarbons starts as approximately 90% of stoichiometric for propane and slightly lower values for kerosene. We see again that the kerosene provides higher hydrocarbon readings for a given equivalence ratio than propane during rich operation.

Figure 14 shows hydrocarbon data measured from the top of the vapor generator stack. We see here that almost all of the runs are plotted as zero hydrocarbons. In fact, most of these runs indicate negative readings but as discussed previously the negative values must be interpreted as being a result of zero shift of the flame ionization detector due to the presence of water vapor.

The low hydrocarbon readings evidenced by the plot of the top of the stack data should not be interpreted as a difference between the top and bottom of the stack. In fact, lower values were obtained at the bottom of the stack than the top. The main reason for the great accumulation of zero and very low

hydrocarbon readings in this Figure is that the fuel/air range of operation was fairly narrow. When the burner was being operated in conjunction with the vapor generator it was not desirable to use a high value of fuel/air ratio since this would create high flame temperatures which in turn would lead to degradation of the working fluid and difficulty in operating the vapor generator loop over extended time periods. Low values of fuel/air ratio approaching lean blowout were avoided as much as possible during loop operation, particularly when we were operating with kerosene. The reason for this is that the vapor generator coils tend to act like a trap for hydrocarbons and lean operation with significant quantities of hydrocarbon emissions would deposit some hydrocarbon materials on the coils which then continue to flow into the flame ionization detector on a subsequent run. On one or two occasions an inadvertant lean blowout occurred due to operator error. When this situation arose during kerosene testing, it was necessary to conduct sustained operation of the vapor generator loop with clean burner exhaust to remove all traces of hydrocarbon from the loop coils and the FID output.

One of the notes referring to the run data tabulated in Tables 1 thru 13 referes to the use of a new injector. Prior to run 282 we found high levels of hydrocarbons in the vapor generator exhaust although the burner exhaust showed low or even negative hydrocarbon readings. We were prepared to believe that the hydrocarbons might disappear on the way up the stack but we found it difficult to accept the idea that they would be generated in the stack and hence we conducted a series of investigations designed to explain this anamolous behavior.

Several causes for spurious hydrocarbon signals were considered. The first of these was the acutal emission of some hydrocarbon material that had existed in the fuel and air intake pipe but failed to move into the burner. Such a situation could arise due to improper seating of the fuel and air intake pipe at the burner mouth. It was found that, in fact, there was leakage of raw fuel/air mixture up the vapor generator stack and this situation was corrected by providing an adequate seal at the joint between the burner inlet pipe and the burner. This problem is one which is peculiar to the test installation under study here and not a problem which should be considered a factor in burner development for automotive application.

Another factor which was considered a possible source of hydrocarbons in the stack was leakage of the organic working fluid from the loop. Extensive investigation of possible sources of leakage in the loop were conducted and none were located. This included pressure checking and helium leak testing. All welds were found to be sound and fittings were tight.

The third possible source of hydrocarbons in the loop was oil deposited on the walls of the vapor generator stack or the coils of the loop. The stack was cleaned out by operating the burner with the coil removed so that the exhaust gas exiting from the burner was still at high temperature. This did in fact reduce some of the

hydrocarbon levels during subsequent tests. The coil was cleaned by passing dry nitrogen through the inside of it while it was held in place and subjected on the outside to the exhaust gas from the burner. This further reduced some of the spurious hydrocarbon signals. Nevertheless hydrocarbon readings continued to show on the order of 30 to 40 ppm from the top of the stack while no comparable values could be found from the burner. The fuel injector assembly was then disassembled and its flow pattern observed. It was found that a serious maldistribution of flow existed in the fuel injector. This caused a non-uniform fuel/air distribution to the burner with locally excessively rich zones. Subsequent modification of the injector succeeded in eliminating the maldistribution of fuel. Tests after run 282 were conducted with a new fuel injector configuration which assured adequate mixing of the fuel and air in a homogeneous fashion prior to entrance of fuel/air mixture into the burner.

Although the burner is successful in eliminating hydrocarbon emissions over a range of fuel/air operating conditions, it nevertheless emits hydrocarbon under two sets of conditions:

a. operation near lean blowout with kerosene
b. extremely rich operation near blowout with both kerosene and propane.

When a poorly mixed fuel/air mixture passes through the burner, local regions of the flow can be near rich or lean blowout while other portions have normal good operating fuel/air values. If the probe which is sampling the burner is in the portion of the burner exhaust which is at the nominal fuel/air ratio no emissions will be seen here. However, the averaged values finally exhausting from the top of the stack after traversing the long mixing length may contain properly burnt and improperly burnt material which issued from the burner. Thus if a portion of the burner is very rich, while the rest of it, including the probe location, is at a normal fuel/air ratio, we can expect to see apparently clean operation of the burner accompanied by excessive hydrocarbons from the top of the stack. Improvement in the fuel injection pattern eliminated this problem and provided a wide range of hydrocarbon free operation on top of the stack comparable to that previously measured from the bottom of the stack.

5. Oxides of Nitrogen

Oxides of nitrogen (NO_2 and NO) formed during combustion of hydrocarbon fuels with air are among the more objectionable atmospheric pollutants. One of the primary objectives of this test program was to document over a wide range of conditions, the oxides of nitrogen emissions from the Paxve burner. This data is given in the curves shown in Figures 15 through 19 representing the complete nitrogen oxides emissions documentation of the burner during the test program. Figure 15 shows the NOx emissions measured from the burner alone while Figure 16 shows the NOx emissions from the burner with the vapor generator installed. Both of these plots show NOx emissions as a function of

nominal fuel/air ratio. These data show no appreciable difference beyond the normal data scatter. Figure 17, shows the oxides of nitrogen measured at the top of the vapor generator stack as as function of nominal fuel/air ratio. Here again there is no distinguishable difference in the NOx emissions between the burner and the top of the vapor generator stack. Figure 18 presents a comparison of emissions data between the top and the bottom of the vapor generator stack. This comparison shows that the emissions from the top of the vapor generator stack are essentially unchanged from those measured at the burner. It is also noted that there is no distinguishable influence on NOx emissions by the inlet temperature conditions or the air mass flow. Referring again to Figure 15, we wish to point out that the bulk of the emission data was taken on the lean side of stoichiometric. In observing the variation of the composite data with fuel/air ratio as shown in Figure 15, it can be seen that the NOx emissions increase with increasing fuel/air ratio to a maximum occuring at or near stoichiometric. This is consistent with the data shown in Figure 19 which shows NOx as a function of combustion gas temperature. It is seen that NOx emissions increase directly with gas temperature. Since the combustion gas temperature reaches a maximum near the stoichiometric point one would expect that the highest emission rate of oxides of nitrogen would occur as shown in the data of Figure 15. Over the normal operating range of the Paxve burner which is nominally at a fuel/air ratio of 0.034 the NOx emissions are maintained within a range of 10 to 20 ppm. All of the data in Figures 15 thru 19 was obtained using the finalized oxides of nitrogen analysis collection and gas analysis techniques as described during previous sections.

D. Experimental Stability Data

Figures 20 through 26 show experimental stability data measured on the Paxve burner. Early stability data was taken in Stand 1 using propane together with a burner of relatively small internal volume (33 cu. in.). Later data on a considerably larger burner was obtained in Stand 1. This larger burner had a volume of approximately 66.5 cu. in. All of the kerosene experimental data was obtained in test stand 2 on a burner having an internal volume of 52.3 cu. in. Tests were conducted with kerosene for lean blowout only due to limitations in the test equipment. The parameters varied during the stability testing included the flow rate, the mixture ratio, and both the air and fuel temperatures independently.

Figure 20 shows the stability data obtained with propane on test stand 1 using ambient air and fuel. The circles represent runs for which stable operation of the burner was obtained. The triangles represent runs which were considered to be lean limit operations. Lean limit points are those in which either (1) combustion was sustained but was erratic in operation with incipient local flameout due to minor fluctuations in air flow, or (2) the burner did go out after a long period of time (on the order of 10 minutes or more). Squares represent runs for which the burner was below the lean limit. In this mode it continued to operate for a short period of time while decreasing in temperature. Flame

out would then occur unless the fuel/air was adjusted to a condition of stable operation.

Superimposed on Figure 20 is the prediction of stability limit at ambient operating conditions. That prediction was made using the burner theory discussed in Section VII. Examination of Figure 20 shows that the theory and the experimental correlation agree remarkable well at high flow rates. At low flow rates the theory predicts stable operation will be possible under leaner conditions than those for which stable operation was actually achieved. This disparity between the theory and the experiment at low flows is attributable to the fact that the theory does not take into account heat loss from the burner. At low flows this heat loss can be a significant factor and can be altered by appropriate thermal design of the burner. For the Paxve burner tested, there was no attempt made to reduce radiation heat losses from the burner. The heat rejection by radiation constitutes the major thermal loss influencing lean limit operation.

The lean stability analysis given in Section VII required the calculation of adiabatic flame temperature for each run condition or fuel air ratio and burner inlet air temperature. This calculation was accomplished by writing a computer program designated CAL for use with the APL IBM 360 computer. The results of the calculations are given in Tables 25 thru 32. Theoretical flame temperatures are given for each run of the test program. The temperature calculation considers air inlet temperature and fuel characteristics.

E. Detailed Emissions Investigation

As a means of examining in further detail the influence of air flow, inlet temperature, and vapor generator loop on critical burner emissions, expanded plots of the data were made. Data segregation took into account the various burner volumes which were tested and improvements in data quality derived from improvements to the experimental techniques relating to the measurement of oxides of nitrogen and hydrocarbons. In addition, the data plots show the influence of the injector modifications which were made to improve fuel/air mixing and distribution. The data taken from run 282 on was obtained using the modified injector configuration and includes all of the latest experimental measurement techniques for NO and HC. This data is considered to be the most representative of the emissions characteristics of the Paxve burner. The emissions data is given in parts per million as well as grams/kilogram of fuel.

1. Carbon Monoxide Emissions

Figures 27 through 37 show carbon monoxide emissions in ppm correlated against nominal fuel/air ratio. Figures 38 thru 48 are the corresponding plots converted to carbon monoxide concentration in grams per kilogram of fuel. The points are identified for air flow rate, run data from run 282 on, and inlet air temperature.

2. Unburned Hydrocarbon Emissions

The unburned hydrocarbons plotted against nominal fuel/air ratio in ppm are shown in Figure 49 thru 55. These data indicate the effects of lean operation down to the blowout limit on unburned fuel emissions. The effect on rich operation is also shown. Corresponding plots of hydrocarbon emission concentration in grams/kilogram of fuel are shown in Figures 56 thru 64. The hydrocarbon data shown was all taken after the heated sample lines and heated sample line pump were installed. In addition, the runs after modification of the fuel injector (from run 282 on) are identified. The hydrocarbon data shown includes both the measurements taken at the burner and those taken from the top of the vapor generator loop.

3. Oxides of Nitrogen From the Burner

NOx emissions from the burner plotted against nominal fuel/air ratio for concentrations in both ppm and gr/Kg of fuel are shown in Figures 65 thru 74. This data was all taken after the initiation of the short quartz tube sampling line technique and the non-saturation precautions for the Saltzman reagent. The influence of nonstratified fuel injection and optimal mixing of fuel is shown in the data from run 282 on.

4. Oxides of Nitrogen from the Vapor Generator Stack

Similiar plots to the preceding for NOx taken from the top of the vapor generator stack are shown in Figures 75 thru 82. These data, are of course limited to runs taken with the vapor generator installed and all these data were taken in test stand 2. The comments relative to the sampling and gas analysis techniques applied to the burner NOx emissions also apply for the vapor generator NOx emissions measurements.

RUN NO.	TEST TYPE	TA °F	TF °F	WA LB/HR	WF LB/HR	CO2V PCT	CO2C PCT	O2V PCT	O2B PCT	NOT PPM	NOB PPM	CO PPM	HC PPM	FAN	COMMENTS RUN	PRO	DAT	BUP
1	PSB1	75	71	22.3	0.54	-1.0	-1.0	-1.0	18.7	-1.0	-1.0	-1.0	-1.0	0.0299	LO	PS	B	O
2	PSB1	80	71	22.2	0.61	-1.0	-1.0	-1.0	11.0	-1.0	-1.0	-1.0	-1.0	0.0340	LO	PS		O
3	PSB1	85	72	45.3	1.13	-1.0	-1.0	-1.0	9.5	-1.0	-1.0	-1.0	-1.0	0.0309	LO	PS		O
4	PSB1	85	73	45.3	1.06	-1.0	-1.0	-1.0	10.0	-1.0	-1.0	-1.0	-1.0	0.0290	LO	PS		O
5	PSB1	85	73	47.0	1.13	-1.0	-1.0	-1.0	-1.0	-1.0	-1.0	-1.0	-1.0	0.0298	LO	PS		O
6	PSB1	88	74	61.8	1.44	-1.0	-1.0	-1.0	10.5	-1.0	-1.0	-1.0	-1.0	0.0288	LO	PS		O
7	PSB1	90	75	61.7	1.58	3.8	-1.0	14.0	8.5	-1.0	-1.0	-1.0	-1.0	0.0317	LO	PS	B	O
8	PSB1	90	73	61.7	2.02	-1.0	-1.0	-1.0	-1.0	-1.0	-1.0	-1.0	-1.0	0.0405	LB			O
9	PSB1	90	74	61.7	1.62	-1.0	-1.0	-1.0	-1.0	-1.0	-1.0	-1.0	-1.0	0.0325	LL			O
10	PSB1	90	74	61.7	1.50	-1.0	-1.0	-1.0	-1.0	-1.0	-1.0	-1.0	-1.0	0.0301	LO			O
11	PSB1	90	74	61.7	1.67	-1.0	-1.0	-1.0	-1.0	-1.0	-1.0	-1.0	-1.0	0.0335	LL			O
12	PSB1	90	74	61.7	1.38	-1.0	-1.0	-1.0	-1.0	-1.0	-1.0	-1.0	-1.0	0.0277	LO			O
13	PSB1	90	74	61.7	1.72	-1.0	-1.0	-1.0	-1.0	-1.0	-1.0	-1.0	-1.0	0.0345	LO			O
14	PSB1	90	75	61.7	1.62	-1.0	-1.0	-1.0	-1.0	-1.0	-1.0	-1.0	-1.0	0.0325	LL			O
15	PSB1	90	74	61.7	1.67	6.5	-1.0	10.5	8.0	-1.0	-1.0	-1.0	-1.0	0.0326	LB			O
16	PSB1	90	75	78.1	2.30	-1.0	-1.0	-1.0	-1.0	-1.0	-1.0	-1.0	-1.0	0.0364	LB			O
17	PSB1	90	75	78.1	2.19	-1.0	-1.0	-1.0	-1.0	-1.0	-1.0	-1.0	-1.0	0.0347	LL			O
18	PSB1	90	73	78.1	2.24	-1.0	-1.0	-1.0	-1.0	-1.0	-1.0	-1.0	-1.0	0.0355	LB			O
19	PSB1	91	73	78.0	2.47	-1.0	-1.0	-1.0	-1.0	-1.0	-1.0	-1.0	-1.0	0.0391	LB			O
20	PSB1	92	74	78.0	2.17	-1.0	-1.0	-1.0	-1.0	-1.0	-1.0	-1.0	-1.0	0.0344	LB			O
21	PSB1	92	74	78.0	1.86	-1.0	-1.0	-1.0	-1.0	-1.0	-1.0	-1.0	-1.0	0.0295	LO			O
22	PSB1	93	72	77.9	2.00	-1.0	-1.0	-1.0	-1.0	-1.0	-1.0	-1.0	-1.0	0.0317	LO			O
23	PSB1	93	72	77.9	2.10	-1.0	-1.0	-1.0	-1.0	-1.0	-1.0	-1.0	-1.0	0.0333	LL			O
24	PSB1	93	74	77.9	2.17	-1.0	-1.0	-1.0	-1.0	-1.0	-1.0	-1.0	-1.0	0.0344	LL			O
25	PSB1	93	75	77.9	2.24	7.4	-1.0	9.5	9.0	-1.0	-1.0	-1.0	-1.0	0.0360	LL			O
26	PSB1	90	72	103.3	3.71	-1.0	-1.0	-1.0	-1.0	-1.0	-1.0	-1.0	-1.0	0.0444	LB			O
27	PSB1	93	73	103.1	3.09	-1.0	-1.0	-1.0	-1.0	-1.0	-1.0	-1.0	-1.0	0.0371	LB			O
28	PSB1	96	73	102.8	2.78	-1.0	-1.0	-1.0	-1.0	-1.0	-1.0	-1.0	-1.0	0.0334	LO			O
29	PSB1	97	73	102.7	2.72	-1.0	-1.0	-1.0	-1.0	-1.0	-1.0	-1.0	-1.0	0.0328	LO			O
30	PSB1	97	74	102.7	2.78	1.9	-1.0	17.6	17.0	-1.0	-1.0	-1.0	-1.0	0.0335	LL			O

CODES

TEST TYPE

P-PROPANE
K-KEROSENE
E-EMISSIONS
S-STABILITY
B-BURNER
L-LOOP
1-STAND 1
2-STAND 2

RUN COMMENTS

NL-NORMAL LEAN
NR-NORMAL RICH
LB-LEAN BURNING
LL-LEAN LIMIT
LO-LEAN GOES OUT
RB-RICH BURNING
RL-RICH LIMIT
RO-RICH GOES OUT

PROCEDURAL COMMENTS

PS-STABILITY PROCED. CK.
PN-NOX EMISS. PROCED. CK.
FH-HOT SAMPLE LINE CK.
FV-VAPOR GENER. OPER. CK.

DATA COMMENTS

B-BAILEY N.G.
H-HC N.G.
N-NOX N.G.
V-VOLUMETRIC N.G.
T-TRANSIENT OPER.

BURNER COMMENTS

O-OLD INJECT. CONFIG.
N-NEW INJECT. CONFIG.

Table VI-1

RUN NO.	TEST TYPE	TA °F	TF °F	WA LB/HR	WF LB/HR	CO2V PCT	CO2C PCT	O2V PCT	O2B PCT	NOT PPM	NOB PPM	CO PPM	HC PPM	FAN	COMMENTS RUN	PRO	DAT	BUR
31	PSB1	102	75	120.9	3.71	-1.0	-1.0	-1.0	-1.0	-1.0	-1.0	-1.0	-1.0	0.0380	LB			O
32	PSB1	105	75	120.6	3.41	-1.0	-1.0	-1.0	-1.0	-1.0	-1.0	-1.0	-1.0	0.0350	LB			O
33	PSB1	108	77	120.2	3.21	-1.0	-1.0	-1.0	-1.0	-1.0	-1.0	-1.0	-1.0	0.0330	LL			O
34	PSB1	95	75	121.6	3.21	-1.0	-1.0	-1.0	-1.0	-1.0	-1.0	-1.0	-1.0	0.0326	LO			O
35	PSB1	102	73	120.9	3.33	6.7	-1.0	10.4	9.6	-1.0	-1.0	-1.0	-1.0	0.0332	LL			O
36	PSB1	112	74	153.8	4.68	-1.0	-1.0	-1.0	-1.0	-1.0	-1.0	-1.0	-1.0	0.0376	LB			O
37	PSB1	117	74	153.2	4.45	-1.0	-1.0	-1.0	-1.0	-1.0	-1.0	-1.0	-1.0	0.0359	LB			O
38	PSB1	120	74	152.8	4.31	-1.0	-1.0	-1.0	-1.0	-1.0	-1.0	-1.0	-1.0	0.0349	LB			O
39	PSB1	120	75	152.8	4.19	-1.0	-1.0	-1.0	-1.0	-1.0	-1.0	-1.0	-1.0	0.0339	LO			O
40	PSB1	120	75	152.8	4.06	-1.0	-1.0	-1.0	-1.0	-1.0	-1.0	-1.0	-1.0	0.0329	LO			O
41	PSB1	124	75	152.3	4.31	6.5	-1.0	10.5	9.6	-1.0	-1.0	-1.0	-1.0	0.0350	LL			O
42	PSB1	91	75	103.2	3.71	10.1	9.4	5.5	4.9	-1.0	-1.0	124.0	-1.0	0.0484	LB			O
43	PSB1	93	75	103.1	2.78	6.9	-1.0	10.6	10.0	-1.0	-1.0	-1.0	-1.0	0.0334	LL			O
44	PSB1	87	73	41.8	1.63	-1.0	-1.0	-1.0	-1.0	-1.0	-1.0	-1.0	-1.0	0.0482	LB			O
45	PSB1	85	75	41.9	1.50	-1.0	-1.0	-1.0	-1.0	-1.0	-1.0	-1.0	-1.0	0.0443	LB			O
46	PSB1	84	75	41.9	1.33	-1.0	-1.0	-1.0	-1.0	-1.0	-1.0	-1.0	-1.0	0.0392	LB			O
47	PSB1	82	75	42.0	1.16	-1.0	-1.0	-1.0	-1.0	-1.0	-1.0	-1.0	-1.0	0.0341	LB			O
48	PSB1	82	74	42.1	1.07	-1.0	6.9	-1.0	-1.0	-1.0	-1.0	8.0	-1.0	0.0314	LB			O
49	PSB1	80	72	42.1	0.98	-1.0	5.8	-1.0	-1.0	-1.0	-1.0	688.0	-1.0	0.0288	LO			O
50	PSB1	80	73	42.1	1.03	6.5	6.6	10.9	10.5	-1.0	-1.0	350.0	-1.0	0.0320	LL			O
51	PSB1	83	73	25.4	0.80	-1.0	-1.0	-1.0	-1.0	-1.0	-1.0	-1.0	-1.0	0.0390	LB			O
52	PSB1	82	73	25.4	0.71	-1.0	-1.0	-1.0	-1.0	-1.0	-1.0	-1.0	-1.0	0.0346	LB			O
53	PSB1	82	73	25.4	0.61	-1.0	-1.0	-1.0	-1.0	-1.0	-1.0	-1.0	-1.0	0.0297	LL			O
54	PSB1	83	73	25.4	0.66	5.9	-1.0	12.0	10.9	-1.0	-1.0	-1.0	-1.0	0.0289	LL			O
55	PSB1	83	73	42.0	6.90	-1.0	-1.0	-1.0	-1.0	-1.0	-1.0	-1.0	-1.0	0.2032	RL			O
56	PSB1	81	73	42.1	5.75	-1.0	-1.0	-1.0	-1.0	-1.0	-1.0	-1.0	-1.0	0.1690	RB			O
57	PSB1	82	73	42.0	6.30	0.8	0.4	17.3	-1.0	-1.0	-1.0	713.0	-1.0	0.1854	RO		V	O
58	PSB1	85	75	41.9	5.75	0.6	0.7	19.3	-1.0	-1.0	-1.0	12200.0	-1.0	0.1697	RO		V	O
59	PSB1	85	75	41.9	6.90	0.1	0.5	20.3	-1.0	-1.0	-1.0	5530.0	-1.0	0.2036	RO		V	O
60	PSB1	90	75	41.7	4.20	0.0	0.3	20.9	-1.0	-1.0	-1.0	5560.0	-1.0	0.1245	RB		V	O

CODES

TEST_TYPE

P-PROPANE
K-KEROSENE
E-EMISSIONS
S-STABILITY
B-BURNER
L-LOOP
1-STAND 1
2-STAND 2

RUN_COMMENTS

NL-NORMAL LEAN
NR-NORMAL RICH
LB-LEAN BURNING
LL-LEAN LIMIT
LO-LEAN GOES OUT
RB-RICH BURNING
RL-RICH LIMIT
RO-RICH GOES OUT

PROCEDURAL_COMMENTS

PS-STABILITY PROCED. CK.
PN-NOX EMISS. PROCED. CK.
FH-HOT SAMPLE LINE CK.
FV-VAPOR GENER. OPER. CK.

DATA_COMMENTS

B-BAILEY N.G.
H-HC N.G.
N-NOX N.G.
V-VOLUMETRIC N.G.
T-TRANSIENT OPER.

BURNER_COMMENTS

O-OLD INJECT. CONFIG.
N-NEW INJECT. CONFIG.

Table VI-2

RUN NO.	TEST TYPE	TA °F	TF °F	WA LB/HR	WF LB/HR	CO2V PCT	CO2C PCT	O2V PCT	O2R PCT	NOT PPM	NOB PPM	CO PPM	HC PPM	FAN	COMMENTS RUN	PRO	DAT	BUR
61	PSB1	90	75	41.7	4.20	5.3	5.3	0.1	-1.0	-1.0	-1.0	131000.0	-1.0	0.1245	RB			O
62	PSB1	85	72	41.9	5.75	3.7	3.8	0.4	-1.0	-1.0	0.1	126000.0	-1.0	0.1697	RB		N	O
63	PSB1	87	72	41.8	6.90	1.0	0.5	16.3	-1.0	-1.0	0.1	382.0	-1.0	0.2040	RO		N	O
64	PSB1	85	72	41.9	5.75	5.1	5.3	0.1	-1.0	-1.0	0.0	101000.0	-1.0	0.1697	RB		N	O
65	PSB1	88	75	41.8	5.99	5.8	-1.0	0.0	-1.0	-1.0	-1.0	-1.0	-1.0	0.1772	RB			O
66	PSB1	85	75	41.9	6.20	-1.0	-1.0	-1.0	-1.0	-1.0	-1.0	-1.0	-1.0	0.1829	RL			O
67	PSB1	85	75	41.9	5.99	5.5	2.6	4.7	-1.0	-1.0	0.1	31500.0	-1.0	0.1767	RB		N	O
68	PSB1	78	75	25.5	3.33	0.5	-1.0	17.9	-1.0	-1.0	-1.0	-1.0	-1.0	0.1617	RB		V	O
69	PSB1	82	75	24.7	3.07	3.4	4.3	6.8	-1.0	-1.0	0.1	140000.0	4385.5	0.1535	RB		NH	O
70	PSB1	85	78	25.3	3.82	4.5	5.1	5.1	-1.0	-1.0	0.1	115000.0	16971.2	0.1867	RL		NH	O
71	PSB1	86	78	25.3	4.01	-1.0	-1.0	-1.0	-1.0	-1.0	-1.0	-1.0	-1.0	0.1961	RO			O
72	PSB1	90	78	61.7	7.62	4.7	4.3	0.0	-1.0	-1.0	0.0	132000.0	5420.0	0.1527	RO		NH	O
73	PSB1	93	78	61.5	7.80	-1.0	-1.0	-1.0	-1.0	-1.0	-1.0	-1.0	-1.0	0.1568	RO			O
74	PEB1	86	73	25.3	0.66	-1.0	6.7	-1.0	-1.0	-1.0	0.0	42.0	108.3	0.0323	LL		NH	O
75	PEB1	85	73	25.3	0.95	8.2	9.0	8.3	7.0	-1.0	2.7	8.4	-1.0	0.0398	NL		N	O
76	PEB1	85	75	25.3	1.00	11.2	8.4	3.9	4.5	-1.0	14.5	18.8	95.8	0.0534	NL		NH	O
77	PEB1	85	75	25.3	1.32	13.3	12.1	0.8	1.0	-1.0	17.0	471.0	53.4	0.0637	NL		NH	O
78	PEB1	90	75	61.7	1.78	5.3	5.6	12.5	11.1	-1.0	0.3	3920.0	719.5	0.0357	LL		NH	O
79	PEB1	92	79	61.6	2.34	9.3	9.2	7.1	5.5	-1.0	7.3	46.0	23.3	0.0440	NL		NH	O
80	PEB1	90	79	61.7	3.11	13.1	12.5	0.9	1.0	-1.0	15.5	1510.0	-1.0	0.0635	NR		N	O
81	PEB1	92	80	61.6	4.60	7.6	7.8	1.4	0.2	-1.0	0.0	62800.0	-1.0	0.0924	NR		N	O
82	PEB1	103	75	102.1	2.78	6.6	6.9	10.7	10.0	-1.0	0.0	3660.0	87.6	0.0323	NL		NH	O
83	PEB1	105	78	101.9	3.88	10.3	2.1	5.3	4.5	-1.0	11.0	149.0	60.8	0.0491	NL		NH	O
84	PEB1	100	72	102.4	3.95	10.0	10.5	5.6	3.4	-1.0	14.4	186.0	67.3	0.0478	NL		NH	O
85	PEB1	103	77	102.1	4.62	12.5	12.1	2.0	1.9	-1.0	16.2	822.0	28.9	0.0587	NL		NH	O
86	PEB1	105	77	101.9	6.76	9.2	9.0	0.0	0.2	-1.0	1.4	73900.0	27.0	0.0820	NR		NH	O
87	PEB1	300	600	59.3	1.71	7.1	6.4	10.1	9.0	-1.0	0.9	5.0	18.7	0.0345	NL		NH	O
88	PEB1	300	600	59.3	2.28	9.2	6.8	7.0	4.5	-1.0	9.4	58.0	3.5	0.0440	NL		NH	O
89	PEB1	300	600	59.3	3.40	10.1	6.2	0.4	0.6	-1.0	1.7	36800.0	21.6	0.0709	NR		NH	O
90	PEB1	300	720	59.6	1.71	7.6	6.5	9.3	8.0	-1.0	5.4	16.3	7.4	0.0369	NL		NH	O

CODES

TEST_TYPE

P-PROPANE
K-KEROSENE
E-EMISSIONS
S-STABILITY
B-BURNER
L-LOOP
1-STAND 1
2-STAND 2

RUN_COMMENTS

NL-NORMAL LEAN
NR-NORMAL RICH
LB-LEAN BURNING
LL-LEAN LIMIT
LO-LEAN GOES OUT
RB-RICH BURNING
RL-RICH LIMIT
RO-RICH GOES OUT

PROCEDURAL_COMMENTS

PS-STABILITY PROCED. CK.
PN-NOX EMISS. PROCED. CK.
FH-HOT SAMPLE LINE CK.
FV-VAPOR GENER. OPER. CK.

DATA_COMMENTS

B-BAILEY N.G.
H-HC N.G.
N-NOX N.G.
V-VOLUMETRIC N.G.
T-TRANSIENT OPER.

BURNER_COMMENTS

O-OLD INJECT. CONFIG.
N-NEW INJECT. CONFIG.

Table VI-3

RUN NO.	TEST TYPE	TA °F	TF °F	WA LB/HR	WF LB/HR	CO2V PCT	CO2C PCT	O2V PCT	O2B PCT	NOT PPM	NOB PPM	CO PPM	HC PPM	FAN	COMMENTS RUN	PRO	DAT	BUP
91	PEB1	310	720	59.3	2.28	11.0	8.9	4.1	3.0	-1.0	13.4	104.0	1.6	0.0526	NL		NH	O
92	PEB1	300	720	59.3	3.40	7.7	7.5	3.0	0.1	-1.0	4.3	54000.0	3.1	0.0709	NR		NH	O
93	KEB2	250	440	165.3	5.86	6.8	5.5	11.0	9.5	-1.0	0.3	1770.0	-1.0	0.0324	NL		N	O
94	KEB2	250	485	165.3	7.24	9.3	7.7	7.9	5.8	-1.0	3.2	186.0	-1.0	0.0432	NL		N	O
95	KEB2	250	510	165.3	7.98	11.9	8.7	4.2	3.2	-1.0	18.0	561.0	-1.0	0.0553	NL		N	O
95.1	PEB1	95	78	107.0	3.57	8.1	-1.0	8.2	8.0	-1.0	9.5	-1.0	-1.0	0.0397	NL	PN		O
96	KEB2	250	520	132.9	7.98	13.6	9.5	0.3	0.6	-1.0	17.0	14900.0	-1.0	0.0658	NR	PN	N	O
97	KEB2	95	77	55.9	1.66	-1.0	-1.0	-1.0	-1.0	-1.0	7.7	-1.0	-1.0	0.0325	NL	PN		O
98	KEB2	95	77	55.9	2.10	-1.0	-1.0	-1.0	-1.0	-1.0	12.1	-1.0	-1.0	0.0412	NL	PN	N	O
99	KEB2	95	77	55.9	2.75	-1.0	-1.0	-1.0	-1.0	-1.0	16.5	-1.0	-1.0	0.0539	NR	PN	N	O
100	KEB2	100	77	55.6	3.38	-1.0	-1.0	-1.0	-1.0	-1.0	15.6	-1.0	-1.0	0.0666	NR	PN	N	O
101	PEB2	102	77	55.5	4.03	-1.0	-1.0	-1.0	-1.0	-1.0	17.6	-1.0	-1.0	0.0795	NR	PN	N	O
102	PEB2	102	77	89.0	3.62	-1.0	-1.0	-1.0	-1.0	-1.0	14.3	-1.0	-1.0	0.0481	NL	PN	N	O
103	PEB2	400	770	50.0	2.00	-1.0	-1.0	-1.0	3.6	-1.0	-1.0	-1.0	-1.0	0.0535	NL			O
104	PSB2	400	800	50.0	1.30	-1.0	-1.0	-1.0	10.0	-1.0	-1.0	-1.0	-1.0	0.0346	NL			O
105	PSB2	84	88	49.9	1.73	11.9	-1.0	1.9	3.2	-1.0	-1.0	-1.0	-1.0	0.0592	NL			O
106	PSB2	85	95	49.9	1.32	-4.8	-3.5	13.6	10.5	-1.0	0.1	132.0	-1.0	0.0313	NL		VC	O
107	PSB2	85	89	49.9	1.06	-1.0	-1.0	-1.0	-1.0	-1.0	-1.0	-1.0	-1.0	0.0251	LO			O
108	PSB2	85	92	49.9	1.20	5.6	-1.0	12.0	12.5	-1.0	-1.0	-1.0	-1.0	0.0285	NL	FC		O
109	PSB2	85	98	49.9	1.32	7.4	-1.0	9.8	9.5	-1.0	-1.0	-1.0	-1.0	0.0356	NL			O
110	PSB2	400	730	50.0	1.06	5.1	3.2	12.8	12.1	-1.0	0.1	450.0	-1.0	0.0258	LB			O
111	PSB2	400	730	50.0	1.06	4.1	2.6	14.0	13.0	-1.0	1.4	1260.0	-1.0	0.0251	LL			O
112	PSB2	400	720	33.2	0.75	6.0	3.3	11.4	11.2	-1.0	14.4	0.0	-1.0	0.0300	LB		N	O
113	PSB2	400	725	33.2	0.66	5.1	2.8	13.5	12.2	-1.0	1.8	465.0	-1.0	0.0249	LB			O
114	PSB2	400	730	33.2	0.66	4.7	2.9	13.2	12.6	-1.0	3.9	300.0	-1.0	0.0243	LB			O
115	PSB2	400	720	33.1	0.59	4.9	-1.0	13.2	13.0	-1.0	0.3	-1.0	-1.0	0.0248	LL			O
116	PSB2	400	710	82.7	2.27	7.1	-1.0	10.3	9.9	-1.0	-1.0	-1.0	-1.0	0.0344	LB			O
117	PSB2	400	710	82.8	1.87	5.6	-1.0	12.4	12.0	-1.0	-1.0	-1.0	-1.0	0.0276	LB			O
118	PSB2	400	730	82.8	1.73	4.6	-2.6	13.5	13.1	-1.0	0.2	1800.0	-1.0	0.0247	LO			O
119	PSB2	400	720	126.8	2.94	6.1	-1.0	11.6	11.5	-1.0	0.6	-1.0	-1.0	0.0299	LB			O

CODES

TEST_TYPE

P-PROPANE
K-KEROSENE
E-EMISSIONS
S-STABILITY
B-BURNER
L-LOOP
1-STAND 1
2-STAND 2

RUN_COMMENTS

NL-NORMAL LEAN
NR-NORMAL RICH
LB-LEAN BURNING
LL-LEAN LIMIT
LO-LEAN GOES OUT
RB-RICH BURNING
RL-RICH LIMIT
RO-RICH GOES OUT

PROCEDURAL_COMMENTS

PS-STABILITY PROCED. CK.
PN-NOX EMISS. PROCED. CK.
FH-HOT SAMPLE LINE CK.
FV-VAPOR GENER. OPER. CK.

DATA_COMMENTS

B-BAILEY N.G.
H-HC N.G.
N-NOX N.G.
V-VOLUMETRIC N.G.
T-TRANSIENT OPER.

BURNER_COMMENTS

O-OLD INJECT. CONFIG.
N-NEW INJECT. CONFIG.

Table VI-4

RUN NO.	TEST TYPE	TA °F	TF °F	WA LB/HR	WF LB/HR	CO2V PCT	CO2C PCT	O2V PCT	O2B PCT	NOT PPM	NOB PPM	CO PPM	HC PPM	FAN	COMMENTS RUN	PRO	DAT	BUR
120	PSB2	400	475	127.0	2.94	5.1	-1.0	12.6	12.2	-1.0	-1.0	-1.0	-1.0	0.0274	LB			O
121	PSB2	400	450	126.8	2.87	5.7	-1.0	11.8	11.6	-1.0	-1.0	-1.0	-1.0	0.0286	LB			O
122	PEB2	400	450	126.8	2.75	4.0	-1.0	13.8	-1.0	-1.0	-1.0	-1.0	-1.0	0.0257	LO			O
123	PEB2	74	70	50.5	2.20	10.6	8.7	4.5	4.1	-1.0	14.6	18.0	-1.0	0.0509	NR	FC	N	O
124	PEB2	80	78	49.5	1.27	1.9	7.3	17.0	8.0	-1.0	1.5	450.0	-1.0	0.0304	LL		V	O
125	PEB2	85	78	47.6	1.27	4.5	3.3	13.0	-1.0	-1.0	1.2	585.0	-1.0	0.0316	NL			O
126	PEB2	95	78	127.3	3.68	6.4	5.5	10.4	7.5	-1.0	5.2	430.0	-1.0	0.0323	LO			O
127	PEB2	95	78	119.6	3.68	-1.0	5.3	-1.0	-1.0	-1.0	5.0	630.0	-1.0	0.0364	LL			O
128	PEB2	90	100	67.8	1.99	-1.0	-1.0	-1.0	1.8	-1.0	-1.0	-1.0	-1.0	0.0346	LB	FH	T	O
129	PEB2	80	80	86.2	2.36	-1.0	-1.0	-1.0	-1.0	-1.0	-1.0	-1.0	-1.0	0.0324	LB		T	O
130	PEB2	80	80	82.8	2.61	-1.0	-1.0	-1.0	-1.0	-1.0	-1.0	-1.0	-1.0	0.0373	LB		T	O
131	PEB2	80	80	66.7	2.48	-1.0	-1.0	-1.0	-1.0	-1.0	-1.0	-1.0	-1.0	0.0440	LB		T	O
132	PEB2	80	80	44.5	2.54	-1.0	-1.0	-1.0	1.2	-1.0	-1.0	-1.0	-1.0	0.0675	LB		T	O
133	PEB2	80	80	83.4	2.54	-1.0	-1.0	-1.0	6.8	-1.0	-1.0	-1.0	-1.0	0.0360	LB		T	O
134	PEB2	80	80	66.7	2.54	-1.0	-1.0	-1.0	2.5	-1.0	-1.0	-1.0	-1.0	0.0450	LB		T	O
135	PEB2	80	80	72.3	1.70	-1.0	-1.0	-1.0	9.5	-1.0	-1.0	-1.0	369.5	0.0278	LB		TH	O
136	PEB2	88	90	72.3	2.08	-1.0	-1.0	-1.0	7.5	-1.0	-1.0	-1.0	1137.9	0.0340	LB		TH	O
137	PEB2	90	90	66.7	2.54	-1.0	-1.0	-1.0	2.6	-1.0	-1.0	-1.0	14.7	0.0450	LB		TH	O
138	PEB2	95	95	96.6	2.95	8.5	-1.0	7.9	7.6	-1.0	9.8	-1.0	-1.0	0.0410	NL			O
139	PEB2	95	100	95.0	3.73	-1.0	-1.0	-1.0	3.8	-1.0	-1.0	-1.0	-1.0	0.0465	NL			O
140	PEB2	95	100	91.1	5.06	-1.0	-1.0	-1.0	-1.0	-1.0	-1.0	-1.0	-1.0	0.0657	NL			O
141	PEB2	95	100	77.3	5.06	-1.0	-1.0	-1.0	-1.0	-1.0	-1.0	-1.0	-1.0	0.0774	NR			O
142	PEB2	95	100	77.8	2.27	-1.0	-1.0	-1.0	-1.0	-1.0	-1.0	-1.0	-1.0	0.0345	NL			O
143	PEB2	95	100	77.8	5.06	-1.0	-1.0	-1.0	-1.0	-1.0	-1.0	-1.0	-1.0	0.0769	NL			O
144	PEB2	95	100	91.1	5.06	-1.0	-1.0	-1.0	-1.0	-1.0	-1.0	-1.0	-1.0	0.0657	NL			O
145	PEB2	95	100	94.4	3.73	-1.0	-1.0	-1.0	-1.0	-1.0	-1.0	-1.0	-1.0	0.0467	NL			O
146	PEB2	95	100	96.6	2.84	-1.0	-1.0	-1.0	9.5	-1.0	-1.0	-1.0	-1.0	0.0348	NL			O
147	PEB2	95	100	98.3	2.50	-1.0	-1.0	-1.0	10.8	-1.0	-1.0	-1.0	-1.0	0.0301	LL			O
148	PEB2	95	100	90.5	3.73	-1.0	-1.0	-1.0	5.0	-1.0	-1.0	-1.0	-1.0	0.0487	NL			O
149	PEB2	95	100	53.6	3.73	7.4	-1.0	-1.0	0.0	-1.0	0.0	-1.0	-1.0	0.0824	NR			O

CODES

TEST TYPE

P-PROPANE
K-KEROSENE
E-EMISSIONS
S-STABILITY
B-BURNER
L-LOOP
1-STAND 1
2-STAND 2

RUN COMMENTS

NL-NORMAL LEAN
NR-NORMAL RICH
LB-LEAN BURNING
LL-LEAN LIMIT
LO-LEAN GOES OUT
RB-RICH BURNING
RL-RICH LIMIT
RO-RICH GOES OUT

PROCEDURAL COMMENTS

PS-STABILITY PROCED. CK.
PN-NOX EMISS. PROCED. CK.
FH-HOT SAMPLE LINE CK.
FV-VAPOR GENER. OPER. CK.
FC-FACILITY CK.

DATA COMMENTS

B-BAILEY N.G.
H-HC N.G.
N-NOX N.G.
V-VOLUMETRIC N.G.
T-TRANSIENT OPER.

BURNER COMMENTS

O-OLD INJECT. CONFIC.
N-NEW INJECT. CONFIC.

Table VI-5

RUN NO.	TEST TYPE	TA °F	TF °F	WA LB/HR	WF LB/HR	CO2V PCT	CO2C PCT	O2V PCT	O2B PCT	NOT PPM	NOB PPM	CO PPM	HC PPM	FAN	COMMENTS RUN	PRO	DAT	BUR
150	PEB2	95	100	56.9	1.35	-1.0	-1.0	-1.0	10.8	-1.0	-1.0	-1.0	-1.0	0.0281	NL			O
151	PEB2	400	160	84.0	3.21	-1.0	-1.0	-1.0	5.8	-1.0	-1.0	-1.0	-1.0	0.0452	NL		T	O
152	PEB2	400	330	79.5	3.21	-1.0	-1.0	-1.0	4.7	-1.0	-1.0	-1.0	1.9	0.0478	NL			O
153	PEB2	360	300	111.2	2.83	-1.0	-1.0	-1.0	11.5	-1.0	-1.0	-1.0	0.0	0.0301	LL			O
154	PEB2	355	200	55.6	2.11	-1.0	-1.0	-1.0	6.0	-1.0	-1.0	-1.0	-1.0	0.0449	NL			O
155	PEB2	270	275	98.9	2.70	-1.0	-1.0	-1.0	10.0	-1.0	-1.0	-1.0	1.3	0.0323	NL			O
156	PEB2	260	255	103.3	2.40	-1.0	-1.0	-1.0	12.8	-1.0	-1.0	-1.0	-1.0	0.0275	LO			O
157	PEB2	260	290	100.0	3.17	0.1	-1.0	-1.0	8.8	-1.0	-1.0	-1.0	0.1	0.0375	LL			O
158	PEB2	260	317	100.6	3.47	-1.0	-1.0	-1.0	7.5	-1.0	-1.0	-1.0	1.0	0.0408	NL			O
159	PEB2	265	350	97.3	4.00	-1.0	-1.0	-1.0	3.8	-1.0	-1.0	-1.0	1.1	0.0486	NL			O
160	PEB2	270	410	90.7	6.00	-1.0	-1.0	-1.0	0.0	-1.0	-1.0	-1.0	-1.0	0.0782	NR			O
161	PEB2	275	392	89.6	6.02	-1.0	-1.0	-1.0	0.0	-1.0	-1.0	-1.0	2.1	0.0795	NR			O
162	PEB2	275	480	87.9	7.42	-1.0	-1.0	-1.0	0.0	-1.0	-1.0	-1.0	200.0	0.0998	NR			O
163	PEB2	360	110	22.0	0.65	-1.0	-1.0	-1.0	8.5	-1.0	-1.0	-1.0	776.1	0.0350	LL			O
164	PEB2	370	120	22.0	0.90	-1.0	-1.0	-1.0	1.6	-1.0	-1.0	-1.0	496.2	0.0484	NL		B	O
165	PEB2	375	120	30.8	1.32	-1.0	-1.0	-1.0	5.3	-1.0	-1.0	-1.0	1.3	0.0507	NR			O
166	PEB2	365	140	44.5	1.60	-1.0	-1.0	-1.0	7.7	-1.0	-1.0	-1.0	0.5	0.0425	NL			O
167	PEB2	370	150	44.0	2.00	-1.0	-1.0	-1.0	5.0	-1.0	-1.0	-1.0	0.6	0.0538	NR			O
168	PEB2	370	170	41.2	2.17	-1.0	-1.0	-1.0	2.2	-1.0	-1.0	-1.0	1.5	0.0623	NR			O
169	PEB2	345	180	55.0	2.17	-1.0	-1.0	-1.0	6.7	-1.0	-1.0	-1.0	0.4	0.0467	NL			O
170	PEB2	325	190	69.8	2.18	-1.0	-1.0	-1.0	9.6	-1.0	-1.0	-1.0	0.1	0.0369	NL			O
171	PEB2	305	195	78.1	2.18	-1.0	-1.0	-1.0	10.8	-1.0	-1.0	-1.0	0.0	0.0330	NL			O
172	PEB2	275	195	97.8	2.18	-1.0	-1.0	-1.0	13.0	-1.0	-1.0	-1.0	9.7	0.0264	LO			O
174	PEB2	400	250	96.6	3.40	-1.0	-1.0	-1.0	8.2	-1.0	-1.0	-1.0	0.4	0.0416	NL			O
175	PEB2	405	275	93.3	4.00	-1.0	-1.0	-1.0	4.8	-1.0	-1.0	-1.0	0.5	0.0507	NL			O
176	PEB2	405	280	93.1	4.40	-1.0	-1.0	-1.0	3.5	-1.0	-1.0	-1.0	0.6	0.0559	NR			O
177	PEB2	405	200	98.6	2.40	5.4	-1.0	12.5	12.2	-1.0	3.6	-1.0	0.0	0.0271	NL			O
178	PEB2	405	195	95.9	2.81	-1.0	-1.0	-1.0	10.1	-1.0	-1.0	-1.0	0.0	0.0346	NL			O
179	PEB2	350	300	133.7	6.07	-1.0	-1.0	-1.0	3.5	-1.0	-1.0	-1.0	0.2	0.0537	NR			O
180	PEB2	345	310	134.6	5.20	-1.0	-1.0	-1.0	6.3	-1.0	-1.0	-1.0	0.2	0.0457	NL			O

CODES

TEST TYPE

P-PROPANE
K-KEROSENE
E-EMISSIONS
S-STABILITY
B-BURNER
L-LOOP
1-STAND 1
2-STAND 2

RUN COMMENTS

NL-NORMAL LEAN
NR-NORMAL RICH
LB-LEAN BURNING
LL-LEAN LIMIT
LO-LEAN GOES OUT
RB-RICH BURNING
RL-RICH LIMIT
RO-RICH GOES OUT

PROCEDURAL COMMENTS

PS-STABILITY PROCED. CK.
PN-NOX EMISS. PROCED. CK.
FH-HOT SAMPLE LINE CK.
FV-VAPOR GENER. OPER. CK.

DATA COMMENTS

B-BAILEY N.G.
H-HC N.G.
N-NOX N.G.
V-VOLUMETRIC N.G.
T-TRANSIENT OPER.

BURNER COMMENTS

O-OLD INJECT. CONFIG.
N-NEW INJECT. CONFIG.

Table VI-6

RUN NO.	TEST TYPE	TA °F	TF °F	WA LB/HR	WF LB/HR	CO2V PCT	CO2C PCT	O2V PCT	O2R PCT	NOT PPM	NOB PPM	CO PPM	HC PPM	FAN	COMMENTS RUN	PRO	DAT	BUR
181	PEB2	340	305	136.1	4.57	1.0	1.0	1.0	8.2	1.0	1.0	1.0	0.2	0.0397	NL			O
182	PEB2	340	303	138.8	4.10	1.0	1.0	1.0	9.6	1.0	1.0	1.0	0.1	0.0349	NL			O
183	PEB2	335	295	139.0	3.68	1.0	1.0	1.0	11.0	1.0	1.0	1.0	0.1	0.0313	NL			O
184	PEB2	334	280	141.7	3.40	1.0	1.0	1.0	11.8	1.0	2.0	1.0	0.1	0.0284	LL			O
185	PEB2	335	320	139.0	3.77	1.0	1.0	1.0	10.7	1.0	1.0	1.0	0.3	0.0321	NL			O
186	PEB2	335	340	139.0	4.22	7.4	1.0	9.5	9.1	1.0	9.8	1.0	0.0	0.0360	NL			O
188	KSB2	430	340	77.9	3.30	9.6	1.0	6.7	5.0	1.0	1.0	1.0	0.1	0.0455	NL			O
189	KSB2	430	320	79.0	2.77	7.7	1.0	9.4	9.0	1.0	1.0	1.0	0.0	0.0369	NL			O
190	KSB2	430	300	79.0	2.35	1.0	1.0	1.0	11.2	1.0	1.0	1.0	0.0	0.0326	LL			O
191	KSB2	400	295	66.9	2.35	1.0	1.0	1.0	9.5	1.0	1.0	1.0	0.2	0.0384	NL			O
192	KSB2	405	295	56.0	2.35	1.0	1.0	1.0	7.1	1.0	1.0	1.0	0.1	0.0460	NL			O
193	KSB2	410	360	51.6	3.95	1.0	1.0	1.0	1.0	1.0	1.0	1.0	670.0	0.0839	NR			O
194	KSB2	410	420	113.0	3.77	7.6	1.0	9.7	8.5	1.0	1.0	1.0	0.4	0.0364	NL			O
195	KSB2	410	410	113.6	3.36	1.0	1.0	1.0	9.5	1.0	1.0	1.0	0.4	0.0324	NL			O
196	KSB2	410	390	115.2	3.07	1.0	1.0	1.0	11.0	1.0	1.0	1.0	101.5	0.0328	LC			O
197	KSB2	430	340	101.4	3.07	7.3	1.0	9.9	9.8	1.0	1.0	1.0	11.3	0.0354	NL			O
198	KSB2	360	260	41.2	1.65	1.0	1.0	1.0	8.5	1.0	1.0	1.0	0.1	0.0439	NL		F	O
199	KSB2	340	320	38.5	2.30	1.0	1.0	1.0	1.1	1.0	1.0	1.0	0.9	0.0655	NR		F	O
200	KSB2	410	270	38.5	1.55	6.4	1.0	9.2	8.2	1.0	1.0	1.0	7.9	0.0441	NL		VF	O
201	PEB2	86	82	83.2	3.70	1.0	1.0	1.0	4.0	1.0	1.0	1.0	1.0	0.0526	NR			O
202	PEB2	82	82	102.9	4.00	1.0	1.0	1.0	7.7	1.0	1.0	1.0	1.0	0.0460	NL			O
203	KEB2	110	100	148.0	5.60	1.0	6.7	1.0	10.5	1.0	9.8	81.0	0.4	0.0414	NL	LK		O
205	PEL2	313	77	76.8	2.90	1.0	1.0	1.0	6.0	1.0	1.0	1.0	1.0	0.0447	NL	FV		O
206	PEL2	253	77	167.8	5.90	1.0	1.0	1.0	7.0	1.0	1.0	1.0	1.0	0.0416	NL	FV		O
207	PEL2	245	77	181.5	5.50	1.0	1.0	1.0	10.0	3.6	6.1	1.0	1.0	0.0358	NL	FV		O
217	PEB2	80	1	83.8	2.74	1.0	1.0	1.0	11.0	1.0	1.0	1.0	1.0	0.0387	NL	FV		O
218	PEB1	100	70	91.5	2.30	7.0	6.1	9.8	9.5	1.0	1.9	7.0	1.0	0.0396	NL	PN		O
219	PEB1	110	70	95.3	3.55	10.7	8.1	5.3	4.0	1.0	32.6	307.0	1.0	0.0502	NL	PN		O
220	PEL2	100	100	86.2	2.73	1.0	1.0	1.0	8.0	6.0	7.1	1.0	4.5	0.0375	NL			O
221	PEL2	100	100	116.8	3.64	1.0	1.0	1.0	9.0	1.0	1.0	1.0	4.6	0.0369	NL			O

CODES

TEST TYPE

P-PROPANE
K-KEROSENE
E-EMISSIONS
S-STABILITY
B-BURNER
L-LOOP
1-STAND 1
2-STAND 2

RUN COMMENTS

NL-NORMAL LEAN
NR-NORMAL RICH
LB-LEAN BURNING
LL-LEAN LIMIT
LO-LEAN GOES OUT
RB-RICH BURNING
RL-RICH LIMIT
RO-RICH GOES OUT

PROCEDURAL COMMENTS

PS-STABILITY PROCED. CK.
PN-NOX EMISS. PROCED. CK.
FH-HOT SAMPLE LINE CK.
FV-VAPOR GENER. OPER. CK.
LK-LIQUID KEROSENE

DATA COMMENTS

B-BAILEY N.G.
H-HC N.G.
N-NOX N.G.
V-VOLUMETRIC N.G.
T-TRANSIENT OPER.

BURNER COMMENTS

O-OLD INJECT. CONFIG.
N-NEW INJECT. CONFIG.

Table VI-7

RUN NO.	TEST TYPE	TA °F	TF °F	WA LB/HR	WF LB/HR	CO2V PCT	CO2C PCT	O2V PCT	O2B PCT	NOT PPM	NOB PPM	CO PPM	HC PPM	FAN	COMMENTS RUN	PRO	DAT	BUP
222	PEL2	100	100	131.8	3.64	-1.0	-1.0	-0.1	10.0	-1.0	-1.0	-1.0	24.0	0.0327	NL			O
223	PEL2	100	100	108.4	3.64	-1.0	-1.0	-0.1	8.0	-1.0	-1.0	-1.0	7.9	0.0397	NL			O
224	PEL2	100	100	168.5	5.07	-1.0	-1.0	-0.1	9.0	-1.0	-1.0	-1.0	4.3	0.0356	NL			O
225	PEL2	100	100	151.8	5.07	-1.0	-1.0	-0.1	8.2	-1.0	-1.0	-1.0	12.9	0.0395	NL			O
226	PEL2	100	100	177.9	5.07	-1.0	-1.0	-0.1	10.0	-1.0	-1.0	-1.0	-1.0	0.0337	LL			O
227	PEL2	76	82	55.8	1.75	-1.0	8.5	-0.1	7.5	-1.0	17.2	7.0	12.6	0.0371	NL			O
228	PEL2	82	90	58.4	1.82	-1.0	7.4	-0.1	11.0	-1.0	2.4	7.0	5.4	0.0369	NL		F	O
229	PEL2	85	95	57.6	1.80	-1.0	8.5	-0.1	9.0	-1.0	7.6	7.0	8.5	0.0369	NL		F	O
230	PEL2	433	98	57.6	1.80	-1.0	-1.0	-0.1	9.5	-1.0	5.0	-1.0	5.9	0.0370	NL		F	O
231	PEL2	420	100	60.8	1.80	-1.0	-1.0	-0.1	11.2	-1.0	2.7	-1.0	4.1	0.0350	NL		F	O
232	PEL2	410	100	90.9	1.70	-1.0	-1.0	-0.1	10.5	-1.0	4.1	-1.0	3.4	0.0333	NL		F	O
233	PEL2	407	100	90.2	1.25	-1.0	-1.0	-0.1	8.3	-1.0	13.8	-1.0	6.4	0.0395	NL		F	O
234	PEL2	90	82	76.9	2.80	-1.0	-1.0	-0.1	4.0	-1.0	36.6	-1.0	24.0	0.0430	NL			O
235	PEL2	92	89	77.3	2.48	-1.0	-1.0	-0.1	6.2	-1.0	22.4	-1.0	35.5	0.0380	NL			O
236	PEL2	89	89	77.7	2.05	-7.0	-1.0	10.6	8.8	-1.0	15.0	-1.0	40.4	0.0384	NL			O
237	PEL2	82	82	38.4	1.32	-1.0	-1.0	-0.1	4.0	53.8	42.6	-1.0	42.3	0.0407	NL			O
238	PEB1	79	70	49.1	1.55	5.4	-1.0	12.4	10.0	-1.0	1.3	-1.0	-1.0	0.0312	NL			O
239	PEB1	80	71	48.9	1.90	7.4	-1.0	10.2	8.0	-1.0	4.2	-1.0	-1.0	0.0345	NL			O
240	PEB1	82	71	48.9	2.04	8.7	-1.0	7.5	6.0	-1.0	12.6	-1.0	-1.0	0.0420	NL			O
241	PEB1	82	72	48.8	2.50	9.7	-1.0	6.0	4.0	-1.0	60.0	-1.0	-1.0	0.0465	NL			O
242	PEB1	78	68	49.2	2.45	9.9	-1.0	4.8	4.0	-1.0	58.7	-1.0	-1.0	0.0488	NL			O
243	PEB1	80	72	48.8	2.62	11.7	-1.0	2.4	2.0	-1.0	104.0	-1.0	-1.0	0.0573	NL			O
244	PEB1	79	68	98.1	3.36	6.5	-1.0	10.7	10.0	-1.0	2.5	-1.0	-1.0	0.0323	NL			O
245	PEB1	80	70	97.6	3.88	7.8	-1.0	8.6	8.0	-1.0	6.6	-1.0	-1.0	0.0384	NL			O
246	PEB1	80	70	60.5	2.50	7.2	-1.0	9.5	12.0	-1.0	-1.0	-1.0	-1.0	0.0409	NOT	VALID	DATA	
247	PEB1	75	70	-1.0	-1.00	-1.0	-1.0	-0.1	11.8	-1.0	-1.0	-1.0	-1.0	0.0295	NOT	VALID	DATA	
248	PEB1	85	70	47.2	-1.00	-1.0	-1.0	-0.1	9.5	-1.0	-1.0	-1.0	-1.0	0.0360	NOT	VALID	DATA	
249	PEB1	75	70	49.2	2.70	7.3	-1.0	9.6	9.5	-1.0	4.1	-1.0	-1.0	0.0542	NOT	VALID	DATA	
250	PEB1	85	70	48.8	2.70	10.0	-1.0	-0.1	5.1	-1.0	46.5	-1.0	-1.0	0.0548	NOT	VALID	DATA	
251	PEB1	85	70	100.8	3.25	5.6	-1.0	14.3	10.0	-1.0	1.6	-1.0	-1.0	0.0319	NOT	VALID	DATA	

CODES

TEST_TYPE

P-PROPANE
K-KEROSENE
E-EMISSIONS
S-STABILITY
B-BURNER
L-LOOP
1-STAND 1
2-STAND 2

RUN_COMMENTS

NL-NORMAL LEAN
NR-NORMAL RICH
LB-LEAN BURNING
LL-LEAN LIMIT
LO-LEAN GOES OUT
RB-RICH BURNING
RL-RICH LIMIT
RO-RICH GOES OUT

PROCEDURAL_COMMENTS

PS-STABILITY PROCED. CK.
PN-NOX EMISS. PROCED. CK.
FH-HOT SAMPLE LINE CK.
FV-VAPOR GENER. OPER. CK.
FC-FACILITY CK.
LK-LIQUID KEROSENE RUN

DATA_COMMENTS

B-BAILEY N.G.
H-HC N.G.
N-NOX N.G.
V-VOLUMETRIC N.G.
F-FLOW N.G.
T-TRANSIENT OPER.

BURNER_COMMENTS

O-OLD INJECT. CONFIG.
N-NEW INJECT. CONFIG.

Table VI-8

RUN NO.	TEST TYPE	TA °F	TF °F	WA LB/HR	WF LB/HR	CO2V PCT	CO2C PCT	O2V PCT	O2B PCT	NOT PPM	NOB PPM	CO PPM	HC PPM	FAN	COMMENTS RUN	PRO	DAT	BUR
252	PEB1	90	70	100.4	3.25	-1.0	-1.0	-0.1	9.5	-1.0	1.1	-1.0	-1.0	0.0320	NOT	VALID	DATA	
253	PEB1	92	70	97.0	3.62	7.0	-1.0	7.8	8.0	-1.0	3.1	-1.0	-1.0	0.0369	NOT	VALID	DATA	
254	PEB1	93	70	100.1	******	8.5	-1.0	7.8	6.3	-1.0	6.6	-1.0	-1.0	0.0410	NOT	VALID	DATA	
255	PEL2	93	70	90.0	2.18	8.0	-1.0	7.0	-1.0	-1.0	-1.0	-1.0	-1.0	0.0388	NL	FV		O
256	PEB1	85	70	97.6	-1.00	9.5	-1.0	6.3	6.0	-1.0	14.7	-1.0	-1.0	0.0460	NL			O
257	PEB1	85	70	97.6	-1.00	10.5	-1.0	4.8	4.0	-1.0	44.0	-1.0	-1.0	0.0503	NR			O
258	PEB1	85	70	97.5	5.25	12.4	-1.0	2.6	2.0	-1.0	78.5	-1.0	-1.0	0.0576	NR			O
259	PEB1	85	70	97.4	-1.00	12.9	-1.0	0.0	0.0	-1.0	113.0	-1.0	-1.0	0.0640	NR			O
260	PEB1	85	70	97.3	6.10	12.2	-1.0	0.5	1.0	-1.0	41.0	-1.0	-1.0	0.0615	NR			O
261	PEB1	89	70	97.2	-1.00	9.5	-1.0	0.9	0.2	-1.0	59.0	-1.0	-1.0	0.0760	NR			O
262	PEB1	90	70	144.4	4.83	6.7	-1.0	10.5	10.0	-1.0	5.0	-1.0	-1.0	0.0331	NL			O
263	PEB1	97	70	143.5	5.75	8.0	-1.0	9.1	8.0	-1.0	9.4	-1.0	-1.0	0.0381	NL			O
264	PEB1	85	73	48.8	1.68	6.6	6.0	11.1	11.3	-1.0	2.2	5.0	-1.0	0.0317	NL			O
265	PEB1	85	73	48.8	-1.00	7.7	7.5	9.2	9.2	-1.0	10.2	7.0	-1.0	0.0372	NL			O
266	PEB1	96	70	143.0	4.82	7.4	9.8	9.3	8.9	-1.0	-1.0	10.0	-1.0	0.0363	NL			O
267	PEB1	96	70	97.8	3.20	6.9	-1.0	11.2	11.0	-1.0	2.0	-1.0	-1.0	0.0323	NL			O
268	PEB1	96	70	97.2	3.55	7.7	-1.0	9.2	9.0	-1.0	6.6	-1.0	-1.0	0.0372	NL			O
269	PEB1	96	72	97.2	4.15	8.7	-1.0	7.4	7.0	-1.0	19.0	-1.0	-1.0	0.0421	NL			O
270	PEB1	96	72	97.1	4.30	9.0	-1.0	6.7	6.0	-1.0	56.5	-1.0	-1.0	0.0439	NL			O
271	PEB1	100	75	144.1	5.10	7.1	-1.0	9.4	9.4	-1.0	4.2	-1.0	-1.0	0.0357	NL			N
272	PEB1	100	71	141.7	5.95	8.9	-1.0	6.9	6.9	-1.0	14.1	-1.0	-1.0	0.0424	NL			N
273	PEB1	100	70	143.1	6.65	9.0	-1.0	7.2	6.0	-1.0	42.0	-1.0	-1.0	0.0432	NL			N
274	PEB1	100	70	143.5	6.60	10.2	9.7	5.5	5.4	-1.0	12.5	24.5	0.0	0.0484	NL			N
275	PEB1	95	70	143.7	7.30	11.1	10.3	4.1	3.8	-1.0	36.5	42.7	-1.0	0.0528	NL			N
279	PEL2	109	70	91.0	2.82	-7.4	7.7	-8.8	8.1	4.0	8.2	5.0	2.6	0.0371	NL			N
280	PEL2	110	70	90.9	3.35	-1.0	8.3	-1.0	5.9	20.8	22.6	10.0	14.5	0.0436	NL			N
281	PEL2	110	70	111.3	3.46	7.7	8.0	8.7	8.3	4.1	8.3	5.0	0.6	0.0380	NL			N
282	PEL2	94	70	46.4	1.35	8.0	8.5	8.6	8.0	7.7	9.4	5.0	0.0	0.0389	NL			N
283	PEL2	100	70	47.3	1.25	7.3	6.0	10.0	9.5	2.0	2.8	5.0	0.0	0.0386	NL			N
284	PEL2	105	70	46.5	1.08	5.4	5.8	12.5	11.3	0.8	1.1	5.0	0.0	0.0271	NL			N

CODES

TEST TYPE

P-PROPANE
K-KEROSENE
E-EMISSIONS
S-STABILITY
B-BURNER
L-LOOP
1-STAND 1
2-STAND 2

RUN COMMENTS

NL-NORMAL LEAN
NR-NORMAL RICH
LB-LEAN BURNING
LL-LEAN LIMIT
LO-LEAN GOES OUT
RB-RICH BURNING
RL-RICH LIMIT
RO-RICH GOES OUT

PROCEDURAL COMMENTS

PS-STABILITY PROCED. CK.
PN-NOX EMISS. PROCED. CK.
FH-HOT SAMPLE LINE CK.
FV-VAPOR GENER. OPER. CK.
FC-FACILITY CK.
LK-LIQUID KEROSENE RUN

DATA COMMENTS

B-BAILEY N.G.
H-HC N.G.
N-NOX N.G.
V-VOLUMETRIC N.G.
F-FLOW N.G.
T-TRANSIENT OPER.

BURNER COMMENTS

O-OLD INJECT. CONFIG.
N-NEW INJECT. CONFIG.

Table VI-9

RUN NO.	TEST TYPE	TA °F	TF °F	WA LB/HP	WF LB/HR	CO2V PCT	CO2C PCT	O2V PCT	O2B PCT	NOT PPM	NOB PPM	CO PPM	HC PPM	FAN	COMMENTS RUN	PRO	DAT	BUR
285	PEL2	116	70	136.5	3.30	6.4	-6.3	11.1	11.0	-1.2	-1.0	-8.2	-0.0	0.0312	NL			N
286	PEB1	82	75	58.8	1.95	6.3	-1.0	10.5	9.6	-1.0	2.3	-1.0	-1.0	0.0321	NL			N
287	PEB1	92	70	144.0	4.90	5.5	6.9	11.6	10.5	-1.0	3.5	95.0	0.0	0.0337	NL			N
288	PEB1	90	69	144.3	5.07	7.4	7.0	9.4	9.3	-1.0	4.4	-1.0	0.0	0.0362	NL			N
289	PEB1	95	69	143.6	5.48	8.0	7.5	8.9	8.5	-1.0	6.5	-1.0	0.0	0.0385	NL			N
290	PEB1	99	60	142.9	6.30	9.5	9.0	6.1	5.6	-1.0	4.0	41.0	5.9	0.0460	NL			N
291	PEB1	73	68	66.0	5.15	-1.0	-1.0	-1.0	-1.0	-1.0	35.0	-1.0	-1.0	0.0895	NR			N
292	PEB1	75	70	49.1	4.00	-1.0	0.3	-1.0	-1.0	-1.0	26.8	12.5	5000.0	0.1000	NR		V	N
293	PEB1	82	70	47.1	3.85	7.0	6.3	0.3	-1.0	-1.0	-1.0	98000.0	30.3	0.0870	NR			N
294	PEB1	90	70	51.1	3.45	8.4	9.0	2.4	-1.0	-1.0	-1.0	64500.0	76.0	0.0805	NR			N
295	PEB1	72	70	49.2	3.85	7.5	7.5	1.0	-1.0	-1.0	63.2	83500.0	25.9	0.0845	NR			N
296	PEB1	86	73	48.6	3.65	7.2	8.0	0.2	-1.0	-1.0	90.0	82800.0	17.6	0.0860	NR			N
297	PEB1	92	71	48.3	4.30	6.5	6.5	0.0	-1.0	-1.0	55.6	104000.0	17.0	0.0905	NR			N
298	PEB1	95	71	48.2	3.73	-8.1	9.0	-2.2	-1.0	-1.0	109.6	75000.0	24.2	0.0820	NP			N
299	PEB1	96	71	87.2	8.00	-1.0	7.5	-1.0	-1.0	-1.0	-1.0	87500.0	26.5	0.0880	NR		V	N
300	PEB1	85	69	49.3	4.31	-1.0	8.0	-1.0	-1.0	-1.0	40.0	81500.0	27.0	0.0750	NR		V	N
301	PEB1	88	69	48.5	3.40	9.0	10.1	2.8	-1.0	-1.0	117.0	52000.0	15.4	0.0780	NR			N
302	PEB1	92	70	96.9	8.75	6.4	6.5	0.8	-1.0	-1.0	17.8	100000.0	-1.0	0.0910	NR			N
303	PEB1	74	68	98.5	7.30	8.0	7.9	0.0	-1.0	-1.0	30.0	36200.0	65.0	0.0820	NR			N
304	PEB1	87	70	141.5	10.92	7.2	7.4	1.5	-1.0	-1.0	22.7	83400.0	28.9	0.0860	NR			N
305	PEB1	100	67	124.2	11.65	6.9	7.0	0.0	-1.0	-1.0	24.0	91600.0	25.0	0.0880	NR			N
306	PEB1	100	68	139.8	10.26	9.8	9.9	0.1	-1.0	-1.0	30.0	45900.0	157.5	0.0750	NR			N
307	PEB1	104	69	94.3	6.40	9.4	9.9	0.0	-1.0	-1.0	18.8	45500.0	-1.0	0.0765	NR			N
308	PEL2	90	320	46.6	1.60	7.2	6.9	9.5	8.6	2.3	4.8	75.0	-1.0	0.0350	NL			N
309	PEL2	98	350	47.5	1.50	6.7	5.9	11.0	10.3	1.3	1.9	75.0	0.0	0.0323	NL			N
310	PEL2	94	310	48.4	0.90	4.0	5.0	15.2	12.4	0.8	0.8	13.8	1.4	0.0220	LB			N
311	PEL2	385	350	49.4	1.75	7.7	7.4	8.9	8.5	7.6	8.4	75.0	0.0	0.0377	NL			N
312	PEL2	388	348	48.3	1.30	6.8	6.3	10.8	10.5	1.6	0.4	5.0	0.0	0.0326	NL			N
313	PEL2	395	340	47.2	1.00	5.0	-5.0	13.1	12.5	0.6	0.1	-5.0	-0.0	0.0252	NL			N
314	PEL2	340	450	88.2	2.78	7.2	-1.0	10.2	8.6	3.6	2.0	-1.0	-1.0	0.0345	NL			N

CODES

TEST TYPE

P-PROPANE
K-KEROSENE
E-EMISSIONS
S-STABILITY
B-BURNER
L-LOOP
1-STAND 1
2-STAND 2

RUN COMMENTS

NL-NORMAL LEAN
NR-NORMAL RICH
LB-LEAN BURNING
LL-LEAN LIMIT
LO-LEAN GOES OUT
PB-RICH BURNING
RL-RICH LIMIT
RO-RICH GOES OUT

PROCEDURAL COMMENTS

PS-STABILITY PROCED. CK.
PN-NOX EMISS. PROCED. CK.
PH-HOT SAMPLE LINE CK.
PV-VAPOR GENER. OPER. CK.
PC-FACILITY CK.
LK-LIQUID KEROSENE RUN

DATA COMMENTS

B-BAILEY N.G.
H-HC N.G.
N-NOX N.G.
V-VOLUMETRIC N.G.
F-FLOW N.G.
T-TRANSIENT OPER.

BURNER COMMENTS

O-OLD INJECT. CONFIG.
N-NEW INJECT. CONFIG.

Table VI-10

RUN NO.	TEST TYPE	TA °F	TF °F	WA LB/HR	WF LB/HR	CO2V PCT	CO2C PCT	O2V PCT	O2B PCT	NOT PPM	NOB PPM	CO PPM	HC PPM	FAN	COMMENTS RUN	PRO	DAT	BUR
315	PEL2	364	450	93.1	2.40	6.1	-1.0	11.4	10.4	1.0	-1.0	-1.0	-1.0	0.0302	NL			N
316	PEL2	400	460	90.5	2.16	6.5	6.1	10.7	10.3	0.7	-1.0	5.0	0.0	0.0323	NL			N
317	PEL2	435	460	90.0	1.95	5.0	5.3	12.6	12.2	0.4	0.1	5.0	0.0	0.0260	NL			N
318	PEL2	350	638	137.1	3.75	6.4	6.4	11.0	10.3	1.8	0.8	5.0	0.0	0.0316	NL			N
319	PEL2	350	620	137.2	3.08	4.8	5.3	12.8	12.3	0.6	0.0	9.2	0.0	0.0266	NL			N
320	PEL2	351	600	134.5	4.47	7.9	7.6	6.6	8.6	3.6	1.9	8.3	0.0	0.0415	NL			N
321	PEL2	140	540	89.8	2.95	7.7	7.9	8.5	8.4	3.5	2.4	15.0	0.0	0.0383	NL			N
322	PEL2	115	490	90.0	2.34	6.2	6.0	11.0	10.3	0.8	-0.1	16.7	0.0	0.0311	NL			N
323	PEL2	105	530	90.0	2.18	5.2	5.6	12.2	11.9	0.6	-1.0	158.5	2.8	0.0287	LL			N
324	PEL2	95	585	135.5	4.45	7.6	7.1	8.9	8.5	2.8	1.5	5.0	0.3	0.0374	NL			N
325	PEL2	105	550	137.3	3.85	5.7	6.3	11.1	10.2	1.0	0.4	33.5	0.1	0.0332	NL			N
326	PEL2	110	610	138.7	3.60	5.7	5.9	12.0	11.0	0.8	0.1	150.0	2.7	0.0307	LL			N
327	PEL2	412	77	48.2	1.50	7.8	8.1	8.5	8.4	6.0	3.7	16.8	0.4	0.0385	NL			N
328	PEL2	395	90	47.3	1.15	6.0	6.1	11.6	11.2	1.3	0.6	15.9	0.0	0.0297	NL			N
329	PEL2	390	95	47.1	0.87	4.8	5.0	13.3	12.6	0.4	0.0	82.4	0.0	0.0245	LB			N
330	PEL2	407	97	90.3	2.93	7.7	7.8	8.6	8.3	9.2	6.7	5.0	0.0	0.0381	NL			N
331	PEL2	400	100	92.7	2.30	6.2	6.3	11.1	10.5	1.8	1.8	5.0	0.0	0.0309	NL			N
332	PEL2	435	92	89.7	2.02	5.0	5.5	12.6	11.0	7.0	0.0	9930.0	0.0	0.0260	LL			N
333	PEL2	392	95	135.2	3.22	5.8	1.2	9.2	10.6	1.1	0.0	144.0	0.0	0.0282	NL			N
334	PEL2	395	100	140.3	2.89	4.8	-1.0	13.2	12.2	0.7	0.0	-1.0	0.0	0.0246	LL			N
335	KEL2	92	590	91.3	2.75	7.8	7.8	9.5	8.5	3.1	1.8	5.0	0.0	0.0370	NL			N
336	KEL2	90	630	92.6	2.41	6.1	6.3	11.2	10.3	1.2	0.0	300.0	0.7	0.0311	LL			N
337	KEL2	90	610	48.5	1.85	7.1	7.3	9.5	8.2	2.4	3.5	5.0	0.0	0.0362	NL			N
338	KEL2	90	660	49.6	1.78	6.0	-1.0	9.4	9.2	1.5	0.2	-5.0	0.0	0.0393	NL			N
339	KEL2	100	660	136.7	4.46	7.5	-1.0	8.9	8.4	3.9	4.4	-1.0	2.6	0.0379	NL			N
340	PEL2	395	90	138.3	3.79	6.5	6.6	10.9	8.6	2.3	0.5	5.0	0.1	0.0320	NL			N
341	PEL2	150	100	92.4	2.55	6.9	6.6	10.5	8.8	2.1	0.6	5.0	0.0	0.0336	NL			N
342	KEL2	90	85	93.3	2.88	7.2	7.1	9.5	8.4	19.8	0.0	5.0	-1.0	0.0365	NL	LK		N
343	PEL2	102	100	91.3	2.54	6.7	7.0	10.1	10.4	2.1	1.0	5.0	0.0	0.0337	NL			N
344	PEL2	100	100	91.9	2.25	6.0	6.6	11.4	11.4	1.4	0.1	5.0	6.8	0.0300	NL			N

CODES

TEST_TYPE

P-PROPANE
K-KEROSENE
E-EMISSIONS
S-STABILITY
B-BURNER
L-LOOP
1-STAND 1
2-STAND 2

RUN_COMMENTS

NL-NORMAL LEAN
NR-NORMAL RICH
LB-LEAN BURNING
LL-LEAN LIMIT
LO-LEAN GOES OUT
RB-RICH BURNING
RL-RICH LIMIT
RO-RICH GOES OUT

PROCEDURAL_COMMENTS

PS-STABILITY PROCED. CK.
PN-NOX EMISS. PROCED. CK.
FH-HOT SAMPLE LINE CK.
FV-VAPOR GENER. OPER. CK.
FC-FACILITY CK.
LK-LIQUID KEROSENE RUN

DATA_COMMENTS

B-BAILEY N.G.
H-HC N.G.
N-NOX N.G.
V-VOLUMETRIC N.G.
F-FLOW N.G.
T-TRANSIENT OPER.

BURNER_COMMENTS

O-OLD INJECT. CONFIG.
N-NEW INJECT. CONFIG.

Table VI-11

RUN NO.	TEST TYPE	TA °F	TF °F	WA LB/HR	WF LB/HR	CO2V PCT	CO2C PCT	O2V PCT	O2B PCT	NOT PPM	NOB PPM	CO PPM	HC PPM	FAN	COMMENTS RUN	COMMENTS PRO	COMMENTS DAT	COMMENTS BUR
345	PEL2	102	95	135.3	3.97	7.0	7.3	9.8	9.8	3.9	0.6	-5.0	0.0	0.0348	NL			N
346	PEL2	105	95	138.2	3.65	6.3	6.6	11.0	11.2	1.9	0.0	-1.0	2.0	0.0313	NL			N
347	PEL2	105	97	134.5	4.80	8.6	8.9	7.5	8.4	11.7	5.8	-1.0	0.0	0.0417	NL			N
348	KEL2	107	95	90.1	2.88	8.5	7.1	8.9	9.5	14.4	0.7	37.5	0.0	0.0401	NL	LK		N
349	KEL2	100	100	91.9	2.60	6.8	6.4	10.3	11.0	3.1	0.1	4680.0	30.1	0.0342	NL	LK		N
350	KEL2	101	105	136.4	4.00	7.9	1.9	9.5	10.4	8.2	1.0	555.0	1.3	0.0380	NL	LK		N
351	KEL2	105	810	92.4	3.00	8.7	7.2	8.3	8.4	4.7	2.6	5.0	0.0	0.0421	NL			N
352	KEL2	110	815	93.1	2.65	7.3	6.9	10.9	9.6	0.3	0.4	5.0	0.0	0.0336	LL			N
353	KEL2	120	790	137.7	4.45	8.7	7.1	8.3	8.4	5.7	4.0	5.0	19.3	0.0421	NL			N
354	KEL2	430	630	81.4	2.62	7.6	6.8	9.9	9.2	3.7	2.3	5.0	0.0	0.0359	NL			N
355	KEL2	438	610	82.0	2.15	5.9	5.5	12.1	11.2	0.8	0.2	5.0	0.0	0.0287	NL			N
356	KEL2	450	625	43.8	1.70	7.7	7.0	9.4	8.4	3.7	2.4	5.0	0.0	0.0371	NL			N
357	KEL2	140	690	180.5	4.97	7.0	6.5	10.5	9.7	1.7	0.6	5.0	0.0	0.0337	NL			N
358	KEL2	110	690	46.8	1.64	6.4	6.2	11.5	8.3	1.6	2.0	5.0	0.0	0.0312	NL			N
359	KEL2	120	730	138.2	4.18	7.1	6.9	10.8	8.2	2.2	1.4	5.0	0.0	0.0335	NL			N
360	KEL2	380	570	92.6	3.00	7.5	6.8	-1.0	8.7	3.8	2.5	5.0	0.0	0.0355	NL			N
361	KEL2	400	620	90.9	2.65	6.5	6.1	11.5	10.4	1.6	0.3	5.0	0.0	0.0312	NL			N
362	KEL2	405	670	89.8	3.30	9.0	9.2	8.0	7.6	8.9	5.3	5.0	0.0	0.0420	NL			N
363	KEL2	405	645	90.8	3.05	6.9	7.0	10.8	10.5	5.0	3.7	5.0	0.7	0.0332	NL			N
364	KEL2	405	670	48.7	1.90	8.0	7.0	9.2	10.5	4.8	4.4	5.0	6.6	0.0379	NL			N
365	KEL2	405	670	48.0	2.10	8.8	7.9	8.1	9.5	5.2	7.2	5.0	0.9	0.0416	NL			N
366	KEL2	410	660	47.9	1.55	5.9	5.6	12.1	13.5	1.2	1.0	-5.0	0.0	0.0287	NL			N
367	KEL2	405	670	137.0	4.00	7.0	-6.5	10.3	12.5	2.8	1.1	-1.0	0.0	0.0340	NL			N
368	KEL2	410	690	137.1	3.48	5.9	-1.0	12.1	13.6	0.8	0.5	5.0	-1.0	0.0287	NL			N
369	KEL2	400	690	136.3	4.36	8.0	-7.6	9.2	11.5	-5.6	3.6	10.0	0.0	0.0379	NL			N
370	KSB2	403	710	90.9	2.98	7.7	-1.0	9.8	9.5	-1.0	2.4	14.6	1.9	0.0365	LB			N
371	KSB2	426	720	137.1	4.36	8.1	7.5	9.1	9.5	-1.0	3.8	37.3	0.0	0.0383	LB			N
372	KSB2	425	700	138.7	4.27	7.5	6.6	9.5	10.0	-1.0	1.2	46.2	6.6	0.0362	LL			N
373	KSB2	425	720	90.9	2.72	7.5	6.6	10.1	9.8	-1.0	2.2	5.0	0.9	0.0355	LB			N
374	KSB2	430	700	90.3	2.62	6.8	6.1	10.7	10.5	-1.0	1.2	205.0	74.1	0.0327	LL			N

CODES

TEST TYPE

P-PROPANE
K-KEROSENE
E-EMISSIONS
S-STABILITY
B-BURNER
L-LOOP
1-STAND 1
2-STAND 2

RUN COMMENTS

NL-NORMAL LEAN
NR-NORMAL RICH
LB-LEAN BURNING
LL-LEAN LIMIT
LO-LEAN GOES OUT
RB-RICH BURNING
RL-RICH LIMIT
RO-RICH GOES OUT

PROCEDURAL COMMENTS

PS-STABILITY PROCED. CK.
PN-NOX EMISS. PROCED. CK.
FH-HOT SAMPLE LINE CK.
FV-VAPOR GENER. OPER. CK.
FC-FACILITY CK.
LK-LIQUID KEROSENE RUN

DATA COMMENTS

B-BAILEY N.C.
H-HC N.G.
N-NOX N.G.
V-VOLUMETRIC N.G.
F-FLOW N.G.
T-TRANSIENT OPER.

BURNER COMMENTS

O-OLD INJECT. CONFIG.
N-NEW INJECT. CONFIG.

Table VI-12

RUN NO.	TEST TYPE	TA °F	TF °F	WA LB/HR	WF LB/HR	CO2V PCT	CO2C PCT	O2V PCT	O2B PCT	NOT PPM	NOB PPM	CO PPM	HC PPM	FAN	COMMENTS RUN	PRO	DAT	BUR
375	KSB2	400	710	91.4	2.57	3.9	5.9	14.5	12.5	-1.0	0.1	825.0	1155.3	0.0308	LL			N
376	KSB2	400	710	90.3	2.59	4.5	5.1	13.6	13.0	-1.0	0.1	2850.0	1956.5	0.0314	LL			N
377	KSB2	405	705	48.3	1.62	6.8	6.4	11.1	10.4	-1.0	2.7	-1.0	8.1	0.0322	LB			N
378	KSB2	428	730	45.5	1.55	6.8	5.7	10.8	10.5	-1.0	1.4	120.0	56.7	0.0325	LL			N
379	KSB2	375	720	47.0	1.50	6.4	5.5	11.6	10.5	-1.0	1.3	280.0	36.9	0.0310	LL			N
380	KSB2	412	715	45.7	1.38	5.4	5.1	12.6	12.0	-1.0	0.1	860.0	760.0	0.0293	LL			N
381	KSB2	411	728	138.5	3.80	5.6	5.6	12.5	11.0	-1.0	0.1	1025.0	690.5	0.0300	LL			N
382	KSB2	411	721	138.7	3.80	4.1	5.6	14.4	12.5	-1.0	0.1	1570.0	1618.9	0.0300	LL			N
383	KSB2	403	700	47.1	1.54	6.4	5.7	11.3	11.5	-1.0	1.4	695.0	625.4	0.0315	LB			N
384	KSB2	76	710	91.4	3.12	8.1	7.8	9.1	8.8	-1.0	2.0	18.3	0.7	0.0385	LL			N
385	KSB2	90	430	91.6	3.12	7.9	7.9	9.2	9.5	-1.0	3.4	-1.0	0.5	0.0375	LB			N
386	KSB2	91	470	89.8	2.89	4.3	6.1	13.9	13.0	-1.0	0.6	1210.0	105.1	0.0352	LL			N
387	KSB2	80	740	47.8	1.53	6.7	6.2	10.9	9.5	-1.0	2.2	150.0	12.2	0.0350	LL			N
388	KSB2	81	740	45.5	1.48	4.3	4.7	13.8	11.5	-1.0	0.1	2035.0	350.1	0.0356	LL			N
389	KSB2	85	390	48.2	3.62	10.4	6.0	0.2	1.6	-1.0	27.5	102400.0	503.4	0.0822	NR			N
390	KSB2	90	515	80.9	2.58	7.6	7.1	9.7	9.6	-1.0	5.8	5.0	2.6	0.0360	LL			N
391	KSB2	93	550	80.5	2.40	2.2	5.0	17.3	13.5	-1.0	0.2	2700.0	215.2	0.0327	NL			N

CODES

TEST_TYPE	RUN_COMMENTS	PROCEDURAL_COMMENTS	DATA_COMMENTS	BURNER_COMMENTS
P-PROPANE	NL-NORMAL LEAN	PS-STABILITY PROCED. CK.	B-BAILEY N.G.	O-OLD INJECT. CONFIG.
K-KEROSENE	NR-NORMAL RICH	PN-NOX EMISS. PROCED. CK.	H-HC N.G.	N-NEW INJECT. CONFIG.
E-EMISSIONS	LB-LEAN BURNING	FH-HOT SAMPLE LINE CK.	N-NOX N.G.	
S-STABILITY	LL-LEAN LIMIT	FV-VAPOR GENER. OPER. CK.	V-VOLUMETRIC N.G.	
B-BURNER	LO-LEAN GOES OUT	FC-FACILITY CK.	F-FLOW N.G.	
L-LOOP	RB-RICH BURNING	LK-LIQUID KEROSENE RUN	T-TRANSIENT OPER.	
1-STAND 1	RL-RICH LIMIT			
2-STAND 2	RO-RICH GOES OUT			

NOMENCLATURE FOR EXPERIMENTAL DATA TABLES

Item	Symbol	Description	Units
1.	Run No.	Chronological run sequence	
2.	Test type	Fuel type, test objectives, system configuration, test stand	
3.	TA	Inlet air temperature to the burner	°F
4.	TF	Inlet fuel temperature to the burner	°F
5.	WA	Air flow rate	lb/hr
6.	WF	Fuel flow rate	lb/hr
7.	CO2V	Carbon dioxide concentration as measured by the Orsat apparatus	% by volume
8.	CO2C	Carbon dioxide concentration as measured by the Chromatograph	% by volume
9.	O2V	Oxygen concentration as measured by the Orsat apparatus	% by volume
10.	O2B	Oxygen concentration as measured by the Bailey intrument	% by volume
11.	NOT	Nitrogen dioxide as measured from the top of the generator loop	PPM
12.	NOB	Nitrogen dioxide as measured from the burner	PPM
13.	CO	Carbon monoxide as measured by the chromatograph	PPM
14.	HC	Hydrocarbons as measured by the chromatograph	PPM
15.	FAN	Nominal fuel air ratio	
16.	Comments	Run comments as explained by the footing of the data tables	

SIGNIFICANT TEST PROGRAM MILESTONES

Run No.	Event
1-7	Stability test procedure investigation.
95	NOx line loss checkout on stand 1.
96-102	NOx line loss checkout on stand 2.
103	Started quartz tube sample technique for NOx.
108	Propane accumulator installed stand 2.
123	Air flow straightener installed stand 2.
128	Hot sample line installed stand 2.
138	Heated hydrocarbon pump installed. Start of good data from burner.
173	Tried to stop LBO by raising TA. Burner out. No data.
187	No data.
203	Liquid kerosene atomized by N_2 carrier flow.
204	No data.
205-207	Vapor generator loop checkout.
208-216	Not part of this program.
217	Vapor generator stack clean out.
218	Start of finalized good NOx measurement procedure.
218-220	NOx saturation evaluation.
220	NOx top of stack and burner comparison.
264-254	New employee ran tests. Data invalid.
255	Vapor generator check out.
271	New fuel injector stand 1; start of good HC data stand 1.
276-278	Not part of this program.
282	New fuel injector stand 2; start of good HC data stand 2.

Table
VI-15

COMPARISON OF FUEL AIR RATIO VALUES *PAGE* 1

RUN NO.	*FA*	*FACOR*	*FAC*	*FAO*	*FAB*	*FAN*
1	0.0242	0.0299	1.0000	1.0000	1.0000	0.0299
2	0.0275	0.0340	1.0000	1.0000	0.0320	0.0340
3	0.0250	0.0309	1.0000	1.0000	0.0360	0.0309
4	0.0234	0.0290	1.0000	1.0000	0.0345	0.0290
5	0.0241	0.0298	1.0000	1.0000	1.0000	0.0298
6	0.0233	0.0288	1.0000	1.0000	0.0330	0.0288
7	0.0256	0.0317	1.0000	1.0000	0.0390	0.0317
8	0.0327	0.0405	1.0000	1.0000	1.0000	0.0405
9	0.0263	0.0325	1.0000	1.0000	1.0000	0.0325
10	0.0243	0.0301	1.0000	1.0000	1.0000	0.0301
11	0.0271	0.0335	1.0000	1.0000	1.0000	0.0335
12	0.0224	0.0277	1.0000	1.0000	1.0000	0.0277
13	0.0279	0.0345	1.0000	1.0000	1.0000	0.0345
14	0.0263	0.0325	1.0000	1.0000	1.0000	0.0325
15	0.0271	0.0335	0.0320	0.0331	0.0410	0.0326
16	0.0294	0.0364	1.0000	1.0000	1.0000	0.0364
17	0.0280	0.0347	1.0000	1.0000	1.0000	0.0347
18	0.0287	0.0355	1.0000	1.0000	1.0000	0.0355
19	0.0316	0.0391	1.0000	1.0000	1.0000	0.0391
20	0.0278	0.0344	1.0000	1.0000	1.0000	0.0344
21	0.0239	0.0295	1.0000	1.0000	1.0000	0.0295
22	0.0257	0.0317	1.0000	1.0000	1.0000	0.0317
23	0.0270	0.0333	1.0000	1.0000	1.0000	0.0333
24	0.0279	0.0344	1.0000	1.0000	1.0000	0.0344
25	0.0288	0.0356	0.0360	0.0361	0.0380	0.0360
26	0.0359	0.0444	1.0000	1.0000	1.0000	0.0444
27	0.0300	0.0371	1.0000	1.0000	1.0000	0.0371
28	0.0271	0.0334	1.0000	1.0000	1.0000	0.0334
29	0.0265	0.0328	1.0000	1.0000	1.0000	0.0328
30	0.0271	0.0335	1.0000	1.0000	1.0000	0.0335
31	0.0307	0.0380	1.0000	1.0000	1.0000	0.0380
32	0.0283	0.0350	1.0000	1.0000	1.0000	0.0350
33	0.0267	0.0330	1.0000	1.0000	1.0000	0.0330
34	0.0264	0.0326	1.0000	1.0000	1.0000	0.0326
35	0.0275	0.0341	0.0330	0.0334	0.0360	0.0332
36	0.0304	0.0376	1.0000	1.0000	1.0000	0.0376
37	0.0291	0.0359	1.0000	1.0000	1.0000	0.0359
38	0.0282	0.0349	1.0000	1.0000	1.0000	0.0349
39	0.0274	0.0339	1.0000	1.0000	1.0000	0.0339
40	0.0266	0.0329	1.0000	1.0000	1.0000	0.0329
41	0.0283	0.0350	0.0320	0.0331	0.0360	0.0350
42	0.0359	0.0444	0.0490	0.0478	0.0500	0.0484
43	0.0270	0.0334	0.0340	0.0328	0.0350	0.0334
44	0.0390	0.0482	1.0000	1.0000	1.0000	0.0482
45	0.0358	0.0443	1.0000	1.0000	1.0000	0.0443
46	0.0317	0.0392	1.0000	1.0000	1.0000	0.0392
47	0.0276	0.0341	1.0000	1.0000	1.0000	0.0341
48	0.0254	0.0314	1.0000	1.0000	1.0000	0.0314
49	0.0233	0.0288	1.0000	1.0000	1.0000	0.0288
50	0.0245	0.0303	0.0320	0.0320	0.0330	0.0320

FA -FUEL/AIR FROM FLOW METERS *FACOR-CORRECTED VALUES OF FA*
FAC-FUEL/AIR FROM VOLUMETRIC CO2 *FAO -FUEL/AIR FROM VOLUMETRIC O2*
FAB-FUEL/AIR FROM BAILEY DATA *FAN -NOMINAL FUEL/AIR FOR ANALYSES*

Table
VI-16

RUN NO.	*FA*	*FACOR*	*FAC*	*FAO*	*FAB*	*FAN*
51	0.0316	0.0390	-1.0000	-1.0000	-1.0000	0.0390
52	0.0280	0.0346	-1.0000	-1.0000	-1.0000	0.0346
53	0.0240	0.0297	-1.0000	-1.0000	-1.0000	0.0297
54	0.0260	0.0322	0.0290	0.0287	0.0320	0.0289
55	0.1643	0.2032	-1.0000	-1.0000	-1.0000	0.2032
56	0.1367	0.1690	-1.0000	-1.0000	-1.0000	0.1690
57	0.1499	0.1854	-1.0000	-1.0000	-1.0000	0.1854
58	0.1372	0.1697	-1.0000	-1.0000	-1.0000	0.1697
59	0.1646	0.2036	-1.0000	-1.0000	-1.0000	0.2036
60	0.1007	0.1245	-1.0000	-1.0000	-1.0000	0.1245
61	0.1007	0.1245	0.0990	-1.0000	-1.0000	0.1245
62	0.1372	0.1697	0.1180	-1.0000	-1.0000	0.1697
63	0.1649	0.2040	-1.0000	-1.0000	-1.0000	0.2040
64	0.1372	0.1697	0.1010	-1.0000	-1.0000	0.1697
65	0.1433	0.1772	0.0960	-1.0000	-1.0000	0.1772
66	0.1479	0.1829	-1.0000	-1.0000	-1.0000	0.1829
67	0.1429	0.1767	0.0976	-1.0000	-1.0000	0.1767
68	0.1307	0.1617	-1.0000	-1.0000	-1.0000	0.1617
69	0.1241	0.1535	0.1250	-1.0000	-1.0000	0.1535
70	0.1510	0.1867	0.1075	-1.0000	-1.0000	0.1867
71	0.1586	0.1961	-1.0000	-1.0000	-1.0000	0.1961
72	0.1235	0.1527	0.1055	-1.0000	-1.0000	0.1527
73	0.1268	0.1568	-1.0000	-1.0000	-1.0000	0.1568
74	0.0261	0.0323	-1.0000	-1.0000	-1.0000	0.0323
75	0.0375	0.0464	0.0400	0.0396	0.0430	0.0398
76	0.0395	0.0489	0.0542	0.0525	0.0510	0.0534
77	0.0522	0.0645	0.0640	0.0635	0.0610	0.0637
78	0.0289	0.0357	0.0263	0.0273	0.0310	0.0357
79	0.0380	0.0470	0.0448	0.0431	0.0480	0.0440
80	0.0504	0.0623	0.0640	0.0631	0.0626	0.0635
81	0.0747	0.0924	0.0840	-1.0000	-1.0000	0.0924
82	0.0272	0.0337	0.0321	0.0325	0.0350	0.0323
83	0.0381	0.0471	0.0497	0.0484	0.0510	0.0491
84	0.0386	0.0477	0.0480	0.0475	0.0540	0.0478
85	0.0452	0.0559	0.0590	0.0585	0.0590	0.0587
86	0.0663	0.0820	0.0770	-1.0000	-1.0000	0.0820
87	0.0288	0.0356	0.0347	0.0343	0.0380	0.0345
88	0.0384	0.0475	0.0445	0.0434	0.0510	0.0440
89	0.0573	0.0709	0.0739	0.0660	-1.0000	0.0709
90	0.0287	0.0355	0.0372	0.0367	0.0410	0.0369
91	0.0384	0.0475	0.0533	0.0519	0.0550	0.0526
92	0.0573	0.0709	0.0839	-1.0000	-1.0000	0.0709
93	0.0354	0.0388	0.0320	0.0328	0.0380	0.0324
94	0.0438	0.0479	0.0440	0.0424	0.0485	0.0432
95	0.0483	0.0528	0.0569	0.0538	0.0560	0.0553
96	0.0601	0.0658	0.0663	0.0700	-1.0000	0.0658
97	0.0297	0.0325	-1.0000	-1.0000	-1.0000	0.0325
98	0.0376	0.0412	-1.0000	-1.0000	-1.0000	0.0412
99	0.0492	0.0539	-1.0000	-1.0000	-1.0000	0.0539
100	0.0608	0.0666	-1.0000	-1.0000	-1.0000	0.0666

FA -FUEL/AIR FROM FLOW METERS *FACOR-CORRECTED VALUES OF FA*
FAC-FUEL/AIR FROM VOLUMETRIC CO2 *FAO -FUEL/AIR FROM VOLUMETRIC O2*
FAB-FUEL/AIR FROM BAILEY DATA *FAN -NOMINAL FUEL/AIR FOR ANALYSES*

RUN NO.	FA	FACOR	FAC	FAO	FAB	FAN
101	0.0726	0.0795	-1.0000	-1.0000	1.0000	0.0795
102	0.0407	0.0481	-1.0000	-1.0000	1.0000	0.0481
103	0.0400	0.0473	0.0535	-1.0000	0.0550	0.0535
104	0.0260	0.0307	0.0346	-1.0000	0.0350	0.0346
105	0.0347	0.0410	0.0595	0.0589	0.0560	0.0592
106	0.0264	0.0313	0.0240	0.0240	0.0330	0.0313
107	0.0212	0.0251	-1.0000	-1.0000	1.0000	0.0251
108	0.0241	0.0285	0.0277	0.0289	0.0272	0.0285
109	0.0265	0.0313	0.0360	0.0352	0.0360	0.0356
110	0.0212	0.0251	0.0255	0.0262	0.0281	0.0258
111	0.0212	0.0251	0.0210	0.0228	0.0258	0.0251
112	0.0226	0.0267	0.0295	0.0305	0.0311	0.0300
113	0.0199	0.0235	0.0255	0.0243	0.0280	0.0249
114	0.0199	0.0235	0.0235	0.0252	0.0269	0.0243
115	0.0178	0.0211	0.0245	0.0252	0.0258	0.0248
116	0.0275	0.0325	0.0350	0.0338	0.0350	0.0344
117	0.0226	0.0267	0.0277	0.0275	0.0288	0.0276
118	0.0209	0.0247	0.0230	0.0242	0.0255	0.0247
119	0.0232	0.0274	0.0300	0.0298	0.0302	0.0299
120	0.0232	0.0274	0.0255	0.0269	0.0280	0.0274
121	0.0226	0.0268	0.0280	0.0292	0.0298	0.0286
122	0.0217	0.0257	0.0205	0.0235	-1.0000	0.0257
123	0.0436	0.0515	0.0510	0.0508	0.0519	0.0509
124	0.0257	0.0304	-1.0000	-1.0000	0.0405	0.0304
125	0.0267	0.0316	0.0228	0.0258	-1.0000	0.0316
126	0.0289	0.0342	0.0312	0.0334	-1.0000	0.0323
127	0.0308	0.0364	-1.0000	-1.0000	-1.0000	0.0364
128	0.0293	0.0346	-1.0000	-1.0000	0.0592	0.0346
129	0.0274	0.0324	-1.0000	-1.0000	0.0420	0.0324
130	0.0315	0.0373	-1.0000	-1.0000	0.0375	0.0373
131	0.0372	0.0440	-1.0000	-1.0000	-1.0000	0.0440
132	0.0571	0.0675	-1.0000	-1.0000	0.0615	0.0675
133	0.0305	0.0360	-1.0000	-1.0000	0.0440	0.0360
134	0.0381	0.0450	-1.0000	-1.0000	0.0568	0.0450
135	0.0235	0.0278	-1.0000	-1.0000	0.0362	0.0278
136	0.0288	0.0340	-1.0000	-1.0000	0.0420	0.0340
137	0.0381	0.0450	-1.0000	-1.0000	0.0565	0.0450
138	0.0305	0.0361	0.0412	0.0408	0.0420	0.0410
139	0.0393	0.0465	-1.0000	-1.0000	0.0528	0.0465
140	0.0555	0.0657	-1.0000	-1.0000	-1.0000	0.0657
141	0.0655	0.0774	-1.0000	-1.0000	-1.0000	0.0774
142	0.0292	0.0345	-1.0000	-1.0000	-1.0000	0.0345
143	0.0650	0.0769	-1.0000	-1.0000	-1.0000	0.0769
144	0.0555	0.0657	-1.0000	-1.0000	-1.0000	0.0657
145	0.0395	0.0467	-1.0000	-1.0000	-1.0000	0.0467
146	0.0294	0.0348	-1.0000	-1.0000	0.0362	0.0348
147	0.0254	0.0301	-1.0000	-1.0000	0.0320	0.0301
148	0.0412	0.0487	-1.0000	-1.0000	0.0492	0.0487
149	0.0696	0.0824	0.0850	-1.0000	0.0865	0.0824
150	0.0237	0.0281	-1.0000	-1.0000	0.0320	0.0281

FA -FUEL/AIR FROM FLOW METERS *FACOR-CORRECTED VALUES OF FA*
FAC-FUEL/AIR FROM VOLUMETRIC CO2 *FAO -FUEL/AIR FROM VOLUMETRIC O2*
FAB-FUEL/AIR FROM BAILEY DATA *FAN -NOMINAL FUEL/AIR FOR ANALYSES*

Table
VI-18

COMPARISON OF FUEL AIR RATIO VALUES *PAGE 4*

RUN NO.	*FA*	*FACOR*	*FAC*	*FAO*	*FAB*	*FAN*
151	0.0382	0.0452	1.0000	1.0000	0.0470	0.0452
152	0.0404	0.0478	1.0000	1.0000	0.0502	0.0478
153	0.0254	0.0301	1.0000	1.0000	0.0300	0.0301
154	0.0379	0.0449	1.0000	1.0000	0.0465	0.0449
155	0.0273	0.0323	1.0000	1.0000	0.0345	0.0323
156	0.0232	0.0275	1.0000	1.0000	0.0265	0.0275
157	0.0317	0.0375	1.0000	1.0000	0.0380	0.0375
158	0.0345	0.0408	1.0000	1.0000	0.0420	0.0408
159	0.0411	0.0486	1.0000	1.0000	0.0525	0.0486
160	0.0662	0.0782	1.0000	1.0000	0.0775	0.0782
161	0.0672	0.0795	1.0000	1.0000	0.0750	0.0795
162	0.0844	0.0998	1.0000	1.0000	0.0930	0.0998
163	0.0296	0.0350	1.0000	1.0000	0.0390	0.0350
164	0.0409	0.0484	1.0000	1.0000	0.0595	0.0484
165	0.0429	0.0507	1.0000	1.0000	0.0485	0.0507
166	0.0359	0.0425	1.0000	1.0000	0.0415	0.0425
167	0.0455	0.0538	1.0000	1.0000	0.0495	0.0538
168	0.0526	0.0623	1.0000	1.0000	0.0578	0.0623
169	0.0395	0.0467	1.0000	1.0000	0.0445	0.0467
170	0.0312	0.0369	1.0000	1.0000	0.0360	0.0369
171	0.0279	0.0330	1.0000	1.0000	0.0320	0.0330
172	0.0223	0.0264	1.0000	1.0000	0.0258	0.0264
174	0.0352	0.0416	1.0000	1.0000	0.0400	0.0416
175	0.0429	0.0507	1.0000	1.0000	0.0500	0.0507
176	0.0472	0.0559	1.0000	1.0000	0.0535	0.0559
177	0.0243	0.0288	0.0270	0.0273	0.0282	0.0271
178	0.0293	0.0346	1.0000	1.0000	0.0345	0.0346
179	0.0454	0.0537	1.0000	1.0000	0.0535	0.0537
180	0.0386	0.0457	1.0000	1.0000	0.0458	0.0457
181	0.0336	0.0397	1.0000	1.0000	0.0400	0.0397
182	0.0295	0.0349	1.0000	1.0000	0.0360	0.0349
183	0.0265	0.0313	1.0000	1.0000	0.0315	0.0313
184	0.0240	0.0284	1.0000	1.0000	0.0290	0.0284
185	0.0271	0.0321	1.0000	1.0000	0.0325	0.0321
186	0.0304	0.0359	0.0360	0.0361	0.0385	0.0360
188	0.0424	0.0464	0.0450	0.0461	0.0510	0.0455
189	0.0351	0.0384	0.0360	0.0378	0.0390	0.0369
190	0.0297	0.0326	1.0000	1.0000	0.0320	0.0326
191	0.0351	0.0384	1.0000	1.0000	0.0370	0.0384
192	0.0420	0.0460	1.0000	1.0000	0.0445	0.0460
193	0.0766	0.0839	1.0000	1.0000	0.0900	0.0839
194	0.0334	0.0365	0.0360	0.0368	0.0400	0.0364
195	0.0296	0.0324	1.0000	1.0000	0.0370	0.0324
196	0.0266	0.0292	0.0328	1.0000	0.0328	0.0328
197	0.0303	0.0331	0.0345	0.0362	0.0367	0.0354
198	0.0401	0.0439	1.0000	1.0000	0.0405	0.0439
199	0.0598	0.0655	1.0000	1.0000	0.0630	0.0655
200	0.0403	0.0441	0.0305	0.0384	0.0415	0.0441

FA -FUEL/AIR FROM FLOW METERS *FACOR-CORRECTED VALUES OF FA*
FAC-FUEL/AIR FROM VOLUMETRIC CO2 *FAO -FUEL/AIR FROM VOLUMETRIC O2*
FAB-FUEL/AIR FROM BAILEY DATA *FAN -NOMINAL FUEL/AIR FOR ANALYSES*

Table
VI-19

RUN NO.	FA	FACOR	FAC	FAO	FAB	FAN
201	0.0445	0.0526	1.0000	1.0000	1.0000	0.0525
202	0.0389	0.0460	1.0000	1.0000	1.0000	0.0460
203	0.0378	0.0414	1.0000	1.0000	1.0000	0.0414
205	0.0378	0.0447	1.0000	1.0000	0.0464	0.0447
206	0.0352	0.0416	1.0000	1.0000	0.0435	0.0416
207	0.0303	0.0358	1.0000	1.0000	0.0347	0.0358
217	0.0327	0.0387	1.0000	1.0000	0.0317	0.0387
218	0.0251	0.0249	0.0440	0.0352	1.0000	0.0396
219	0.0372	0.0368	0.0520	0.0484	1.0000	0.0502
220	0.0317	0.0375	1.0000	1.0000	0.0406	0.0375
221	0.0312	0.0369	1.0000	1.0000	0.0378	0.0369
222	0.0276	0.0327	1.0000	1.0000	0.0346	0.0327
223	0.0336	0.0397	1.0000	1.0000	0.0406	0.0397
224	0.0253	0.0300	1.0000	1.0000	0.0378	0.0356
225	0.0281	0.0333	1.0000	1.0000	0.0400	0.0395
226	0.0240	0.0284	1.0000	1.0000	0.0346	0.0337
227	0.0314	0.0371	1.0000	1.0000	0.0420	0.0371
228	0.0312	0.0369	1.0000	1.0000	0.0315	0.0369
229	0.0312	0.0369	1.0000	1.0000	0.0378	0.0369
230	0.0313	0.0370	1.0000	1.0000	0.0360	0.0370
231	0.0296	0.0350	1.0000	1.0000	0.0310	0.0350
232	0.0187	0.0221	1.0000	1.0000	0.0333	0.0333
233	0.0139	0.0164	1.0000	1.0000	0.0395	0.0395
234	0.0364	0.0430	1.0000	1.0000	0.0522	0.0430
235	0.0321	0.0380	1.0000	1.0000	0.0460	0.0380
236	0.0264	0.0312	0.0440	0.0328	0.0380	0.0384
237	0.0344	0.0407	1.0000	1.0000	0.0522	0.0407
238	0.0316	0.0312	0.0270	0.0275	0.0350	0.0312
239	0.0388	0.0384	0.0350	0.0340	0.0410	0.0345
240	0.0417	0.0413	0.0420	0.0420	0.0465	0.0420
241	0.0512	0.0507	0.0465	0.0465	0.0520	0.0465
242	0.0498	0.0492	0.0475	0.0500	0.0520	0.0488
243	0.0537	0.0531	0.0575	0.0570	0.0580	0.0573
244	0.0342	0.0339	0.0320	0.0325	0.0350	0.0323
245	0.0398	0.0393	0.0380	0.0387	0.0410	0.0384
246	0.0414	0.0409	1.0000	1.0000	0.0289	0.0409
247	1.0000	1.0000	1.0000	1.0000	0.0295	0.0295
248	1.0000	1.0000	1.0000	1.0000	0.0360	0.0360
249	0.0548	0.0542	1.0000	1.0000	0.0360	0.0542
250	0.0553	0.0548	1.0000	1.0000	0.0490	0.0548

FA -FUEL/AIR FROM FLOW METERS *FACOR-CORRECTED VALUES OF FA*
FAC-FUEL/AIR FROM VOLUMETRIC CO2 *FAO -FUEL/AIR FROM VOLUMETRIC O2*
FAB-FUEL/AIR FROM BAILEY DATA *FAN -NOMINAL FUEL/AIR FOR ANALYSES*

Table
VI-20

RUN NO.	*FA*	*FACOR*	*FAC*	*FAO*	*FAB*	*FAN*
251	0.0322	0.0319	1.0000	1.0000	0.0348	0.0319
252	0.0324	0.0320	1.0000	1.0000	0.0360	0.0320
253	0.0373	0.0369	1.0000	1.0000	0.0410	0.0369
254	1.0000	1.0000	0.0410	1.0000	0.0470	0.0410
255	0.0242	1.0000	0.0388	1.0000	1.0000	0.0388
256	1.0000	1.0000	0.0460	0.0460	0.0460	0.0460
257	1.0000	1.0000	0.0505	0.0500	0.0500	0.0503
258	0.0539	0.0533	0.0589	0.0564	0.0565	0.0576
259	1.0000	1.0000	0.0640	1.0000	1.0000	0.0640
260	0.0627	0.0620	0.0580	0.0650	0.0625	0.0615
261	1.0000	1.0000	0.0760	1.0000	1.0000	0.0760
262	0.0335	0.0331	0.0330	0.0331	0.0348	0.0331
263	0.0401	0.0397	0.0390	0.0372	0.0410	0.0381
264	0.0344	0.0341	0.0320	0.0314	0.0310	0.0317
265	1.0000	1.0000	0.0375	0.0370	0.0375	0.0372
266	0.0337	0.0334	0.0360	0.0367	0.0383	0.0363
267	0.0327	0.0324	0.0335	0.0311	0.0323	0.0323
268	0.0365	0.0361	0.0375	0.0370	0.0380	0.0372
269	0.0427	0.0422	0.0420	0.0422	0.0438	0.0421
270	0.0443	0.0438	0.0435	0.0443	0.0467	0.0439
271	0.0354	0.0350	0.0350	0.0364	0.0365	0.0357
272	0.0420	0.0415	0.0410	0.0437	0.0455	0.0424
273	0.0465	0.0460	0.0435	0.0428	0.0480	0.0432
274	0.0460	0.0455	0.0490	0.0478	0.0495	0.0484
275	0.0508	0.0503	0.0537	0.0519	0.0540	0.0528
279	0.0310	0.0366	0.0360	0.0381	0.0400	0.0371
280	0.0368	0.0436	1.0000	1.0000	1.0000	0.0436
281	0.0311	0.0368	0.0375	0.0384	0.0395	0.0380
282	0.0291	0.0344	0.0390	0.0387	0.0410	0.0389
283	0.0264	0.0313	0.0425	0.0346	0.0360	0.0386
284	0.0232	0.0275	0.0270	0.0273	0.0310	0.0271
285	0.0242	0.0286	0.0310	0.0314	0.0315	0.0312
286	0.0332	0.0328	0.0310	0.0331	0.0360	0.0321
287	0.0340	0.0337	0.0280	0.0299	0.0335	0.0337
288	0.0351	0.0348	0.0360	0.0364	0.0370	0.0362
289	0.0382	0.0378	0.0390	0.0380	0.0385	0.0385
290	0.0441	0.0436	0.0460	0.0461	0.0478	0.0460
291	0.0780	0.0772	1.0000	1.0000	0.0895	0.0895
292	0.0815	0.0806	1.0000	1.0000	0.1000	0.1000
293	0.0818	0.0809	0.0870	1.0000	0.0945	0.0870
294	0.0675	0.0668	0.0805	1.0000	0.0770	0.0805
295	0.0782	0.0774	0.0845	1.0000	0.0875	0.0845
296	0.0751	0.0743	0.0860	1.0000	0.0820	0.0860
297	0.0890	0.0880	0.0905	1.0000	0.0960	0.0905
298	0.0774	0.0766	0.0820	1.0000	0.0790	0.0820
299	0.0918	0.0908	1.0000	1.0000	0.0880	0.0880
300	0.0874	0.0865	1.0000	1.0000	0.0750	0.0750

FA -FUEL/AIR FROM FLOW METERS *FACOR-CORRECTED VALUES OF FA*
FAC-FUEL/AIR FROM VOLUMETRIC CO2 *FAO -FUEL/AIR FROM VOLUMETRIC O2*
FAB-FUEL/AIR FROM BAILEY DATA *FAN -NOMINAL FUEL/AIR FOR ANALYSES*

RUN NO.	FA	FACOR	FAC	FAO	FAB	FAN
301	0.0701	0.0694	0.0780	-1.0000	0.0730	0.0780
302	0.0903	0.0894	0.0910	-1.0000	0.0930	0.0910
303	0.0741	0.0733	0.0820	-1.0000	0.0805	0.0820
304	0.0772	0.0764	0.0860	-1.0000	0.0845	0.0860
305	0.0938	0.0928	0.0880	-1.0000	0.0895	0.0880
306	0.0734	0.0726	0.0750	-1.0000	0.0755	0.0750
307	0.0679	0.0672	0.0765	-1.0000	0.0745	0.0765
308	0.0343	0.0406	0.0340	0.0360	0.0390	0.0350
309	0.0316	0.0373	0.0330	0.0317	0.0338	0.0323
310	0.0186	0.0220	0.0205	0.0193	0.0275	0.0220
311	0.0354	0.0419	0.0375	0.0378	0.0390	0.0377
312	0.0269	0.0318	0.0330	0.0323	0.0330	0.0326
313	0.0212	0.0251	0.0250	0.0255	0.0272	0.0252
314	0.0315	0.0373	0.0350	0.0340	0.0390	0.0345
315	0.0258	0.0305	0.0300	0.0305	0.0335	0.0302
316	0.0239	0.0282	0.0320	0.0325	0.0339	0.0323
317	0.0217	0.0256	0.0250	0.0270	0.0279	0.0260
318	0.0274	0.0324	0.0315	0.0317	0.0338	0.0316
319	0.0225	0.0266	0.0240	0.0264	0.0279	0.0266
320	0.0332	0.0393	0.0384	0.0446	0.0390	0.0415
321	0.0329	0.0389	0.0375	0.0390	0.0395	0.0383
322	0.0260	0.0308	0.0305	0.0317	0.0338	0.0311
323	0.0242	0.0287	0.0260	0.0281	0.0290	0.0287
324	0.0328	0.0388	0.0370	0.0378	0.0390	0.0374
325	0.0280	0.0332	0.0280	0.0314	0.0340	0.0332
326	0.0260	0.0307	0.0280	0.0287	0.0317	0.0307
327	0.0311	0.0368	0.0380	0.0390	0.0395	0.0385
328	0.0243	0.0288	0.0295	0.0299	0.0320	0.0297
329	0.0185	0.0219	0.0240	0.0249	0.0270	0.0245
330	0.0324	0.0384	0.0375	0.0387	0.0396	0.0381
331	0.0248	0.0293	0.0305	0.0314	0.0330	0.0309
332	0.0226	0.0267	0.0250	0.0270	0.0320	0.0260
333	0.0238	0.0282	0.0285	0.0370	0.0330	0.0282
334	0.0206	0.0244	0.0240	0.0252	0.0280	0.0246
335	0.0301	0.0330	0.0380	0.0361	0.0390	0.0370
336	0.0260	0.0285	0.0300	0.0322	0.0335	0.0311
337	0.0382	0.0418	0.0350	0.0375	0.0400	0.0362
338	0.0359	0.0393	-1.0000	0.0362	0.0380	0.0393
339	0.0326	0.0357	0.0365	0.0393	0.0390	0.0379
340	0.0274	0.0324	0.0320	0.0320	0.0388	0.0320
341	0.0276	0.0326	0.0340	0.0331	0.0388	0.0336
342	0.0309	0.0338	0.0355	0.0375	0.0390	0.0365
343	0.0278	0.0329	0.0330	0.0345	0.0335	0.0337
344	0.0245	0.0289	0.0295	0.0305	0.0305	0.0300
345	0.0294	0.0347	0.0345	0.0352	0.0352	0.0348
346	0.0264	0.0312	0.0310	0.0317	0.0310	0.0313
347	0.0357	0.0422	0.0415	0.0420	0.0390	0.0417
348	0.0319	0.0350	0.0410	0.0393	0.0360	0.0401
349	0.0283	0.0310	0.0335	0.0350	0.0317	0.0342
350	0.0293	0.0321	0.0385	0.0375	0.0335	0.0380

FA -FUEL/AIR FROM FLOW METERS *FACOR-CORRECTED VALUES OF FA*
FAC-FUEL/AIR FROM VOLUMETRIC CO2 *FAO -FUEL/AIR FROM VOLUMETRIC O2*
FAB-FUEL/AIR FROM BAILEY DATA *FAN -NOMINAL FUEL/AIR FOR ANALYSES*

COMPARISON OF FUEL AIR RATIO VALUES

RUN NO.	*FA*	*FACOR*	*FAC*	*FAO*	*FAB*	*FAN*
351	0.0325	0.0355	0.0430	0.0411	0.0415	0.0421
352	0.0285	0.0312	0.0340	0.0331	0.0370	0.0336
353	0.0323	0.0354	0.0430	0.0411	0.0415	0.0421
354	0.0322	0.0352	0.0355	0.0362	0.0380	0.0359
355	0.0262	0.0287	0.0280	0.0295	0.0320	0.0287
356	0.0388	0.0425	0.0365	0.0378	0.0410	0.0371
357	0.0275	0.0302	0.0330	0.0344	0.0370	0.0337
358	0.0350	0.0383	0.0310	0.0313	0.0410	0.0312
359	0.0302	0.0331	0.0335	0.0335	0.0415	0.0335
360	0.0324	0.0355	0.0350	1.0000	0.0400	0.0355
361	0.0292	0.0319	0.0310	0.0313	0.0350	0.0312
362	0.0367	0.0402	0.0420	0.0421	0.0430	0.0420
363	0.0336	0.0368	0.0330	0.0335	0.0330	0.0332
364	0.0390	0.0427	0.0375	0.0384	0.0330	0.0379
365	0.0438	0.0479	0.0415	0.0418	0.0370	0.0416
366	0.0324	0.0355	0.0280	0.0295	0.0250	0.0287
367	0.0292	0.0320	0.0330	0.0350	0.0280	0.0340
368	0.0254	0.0278	0.0280	0.0295	0.0250	0.0287
369	0.0320	0.0350	0.0375	0.0384	0.0410	0.0379
370	0.0328	0.0359	0.0365	0.0365	0.0370	0.0365
371	0.0318	0.0348	0.0380	0.0385	0.0370	0.0383
372	0.0308	0.0337	0.0350	0.0375	0.0360	0.0362
373	0.0299	0.0328	0.0350	0.0360	0.0370	0.0355
374	0.0290	0.0318	0.0320	0.0335	0.0330	0.0327
375	0.0281	0.0308	0.0190	0.0230	0.0260	0.0308
376	0.0287	0.0314	0.0220	0.0265	0.0260	0.0314
377	0.0335	0.0367	0.0320	0.0325	0.0340	0.0322
378	0.0341	0.0373	0.0320	0.0330	0.0340	0.0325
379	0.0319	0.0350	0.0310	0.0310	0.0330	0.0310
380	0.0302	0.0330	0.0260	0.0280	0.0290	0.0330
381	0.0274	0.0300	0.0268	0.0280	0.0315	0.0300
382	0.0274	0.0300	0.0200	0.0230	0.0280	0.0300
383	0.0327	0.0358	0.0310	0.0320	0.0300	0.0315
384	0.0341	0.0374	0.0380	0.0390	0.0390	0.0385
385	0.0340	0.0373	0.0360	0.0390	0.0375	0.0375
386	0.0322	0.0352	0.0210	0.0240	0.0260	0.0352
387	0.0320	0.0350	0.0320	0.0330	0.0370	0.0350
388	0.0325	0.0356	0.0210	0.0250	0.0300	0.0356
389	0.0751	0.0822	0.0780	1.0000	0.0770	0.0822
390	0.0319	0.0349	0.0350	0.0370	0.0370	0.0360
391	0.0298	0.0327	0.0115	0.0140	0.0260	0.0327

FA -FUEL/AIR FROM FLOW METERS *FACOR-CORRECTED VALUES OF FA*
FAC-FUEL/AIR FROM VOLUMETRIC CO2 *FAO -FUEL/AIR FROM VOLUMETRIC O2*
FAB-FUEL/AIR FROM BAILEY DATA *FAN -NOMINAL FUEL/AIR FOR ANALYSES*

FUEL AIR RATIO CORRECTION FACTORS

FOR FLOWMETER DATA

RUN GROUP (From which factor obtained)	FUEL	TEST STAND	FACTOR	COMMENT
Early runs (Approx. runs 15 to 91)	Propane	1	0.8087 ± .0467	Air leaks
later runs (Approx. runs 244 to 290)	Propane	1	1.017 ± .0568	Air leaks eliminated
Approx. runs 123 to 341	Propane	2	0.8454 ± .0560	Air leaks
Approx. runs 93 to 369	Kerosene	2	0.9133 ± .1028	Air leaks

NOTE: To correct measured flowmeter fuel-air values, divide by factor.

THEORETICAL FLAME TEMPERATURES

RUN NO.	AIR TEMP °F	FUEL/AIR	FLAME TEMP °F
1	75	0.0299	2157
2	80	0.0340	2400
3	85	0.0309	2221
4	85	0.0290	2105
5	85	0.0298	2154
6	88	0.0288	2099
7	90	0.0317	2272
8	90	0.0405	2776
9	90	0.0325	2320
10	90	0.0301	2177
11	90	0.0335	2378
12	90	0.0277	2031
13	90	0.0345	2436
14	90	0.0325	2320
15	90	0.0326	2325
16	90	0.0364	2545
17	90	0.0347	2447
18	90	0.0355	2492
19	91	0.0391	2699
20	92	0.0344	2434
21	92	0.0295	2144
22	93	0.0317	2279
23	93	0.0333	2372
24	93	0.0344	2436
25	93	0.0360	2526
26	90	0.0444	2982
27	93	0.0371	2585
28	96	0.0334	2381
29	97	0.0328	2342
30	97	0.0335	2384
31	102	0.0380	2638
32	105	0.0350	2475
33	108	0.0330	2364
34	95	0.0326	2333
35	102	0.0332	2372
36	112	0.0376	2627
37	117	0.0359	2536
38	120	0.0349	2480
39	120	0.0339	2425
40	120	0.0329	2364
41	124	0.0326	2350
42	91	0.0484	3167
43	93	0.0334	2377
44	87	0.0482	3154
45	85	0.0443	2973
46	84	0.0392	2701
47	82	0.0341	2410
48	82	0.0314	2252
49	80	0.0288	2091
50	80	0.0320	2283

Table
VI-25

RUN NO.	*AIR TEMP* °F	*FUEL/AIR*	*FLAME TEMP* °F
51	83	0.0390	2688
52	82	0.0346	2437
53	82	0.0297	2150
54	83	0.0289	2098
55	83	0.2032	1492
56	81	0.1690	1798
57	82	0.1854	1639
58	85	0.1697	1794
59	85	0.2036	1490
60	90	0.1245	2447
61	90	0.1245	2447
62	85	0.1697	1794
63	87	0.2040	1488
64	85	0.1697	1794
65	88	0.1772	1717
66	85	0.1829	1661
67	85	0.1767	1720
68	78	0.1617	1875
69	82	0.1535	1978
70	85	0.1867	1629
71	86	0.1961	1549
72	90	0.1527	1993
73	93	0.1568	1942
74	86	0.0323	2306
75	85	0.0464	3075
76	85	0.0534	3356
77	85	0.0637	3554
78	90	0.0357	2504
79	92	0.0440	2962
80	90	0.0635	3555
81	92	0.0924	3143
82	103	0.0323	2321
83	105	0.0491	3203
84	100	0.0478	3143
85	103	0.0587	3502
86	105	0.0820	3371
87	300	0.0345	2587
88	300	0.0440	3080
89	300	0.0709	3658
90	300	0.0369	2717
91	310	0.0526	3446
92	300	0.0709	3658
93	250	0.0324	2362
94	250	0.0432	2926
95	250	0.0553	3431
96	250	0.0658	3634
97	95	0.0325	2251
98	95	0.0412	2724
99	95	0.0539	3305
100	100	0.0666	3563

RUN NO.	*AIR TEMP* °F	*FUEL/AIR*	*FLAME TEMP* °F
101	102	0.0795	3485
102	102	0.0481	3160
103	400	0.0473	3284
104	400	0.0307	2459
105	84	0.0410	2801
106	85	0.0313	2246
107	85	0.0251	1872
108	85	0.0285	2076
109	85	0.0313	2248
110	400	0.0251	2131
111	400	0.0251	2131
112	400	0.0267	2229
113	400	0.0235	2037
114	400	0.0235	2039
115	400	0.0211	1885
116	400	0.0325	2555
117	400	0.0267	2229
118	400	0.0247	2110
119	400	0.0274	2272
120	400	0.0274	2269
121	400	0.0268	2234
122	400	0.0257	2167
123	74	0.0509	3262
124	80	0.0304	2187
125	85	0.0316	2262
126	95	0.0342	2423
127	95	0.0364	2548
128	90	0.0346	2445
129	80	0.0324	2308
130	80	0.0373	2586
131	80	0.0440	2955
132	80	0.0675	3562
133	80	0.0360	2517
134	80	0.0450	3007
135	80	0.0278	2033
136	88	0.0340	2409
137	90	0.0450	3013
138	95	0.0410	2807
139	95	0.0465	3082
140	95	0.0657	3569
141	95	0.0774	3460
142	95	0.0345	2440
143	95	0.0769	3472
144	95	0.0657	3569
145	95	0.0467	3095
146	95	0.0348	2456
147	95	0.0301	2182
148	95	0.0487	3183
149	95	0.0824	3356
150	95	0.0281	2061

RUN NO.	*AIR TEMP* °F	*FUEL/AIR*	*FLAME TEMP* °F
151	400	0.0452	3196
152	400	0.0478	3303
153	360	0.0301	2391
154	355	0.0449	3155
155	270	0.0323	2443
156	260	0.0275	2158
157	260	0.0375	2718
158	260	0.0408	2898
159	265	0.0486	3268
160	270	0.0782	3546
161	275	0.0795	3525
162	275	0.0998	3096
163	360	0.0350	2657
164	370	0.0484	3315
165	375	0.0507	3412
166	365	0.0425	3050
167	370	0.0538	3516
168	370	0.0623	3687
169	345	0.0467	3229
170	325	0.0369	2734
171	305	0.0330	2511
172	275	0.0264	2105
173	-1	-1.0000	-1
174	400	0.0416	3030
175	405	0.0507	3429
176	405	0.0559	3595
177	405	0.0288	2354
178	405	0.0346	2675
179	350	0.0537	3502
180	345	0.0457	3185
181	340	0.0397	2891
182	340	0.0349	2639
183	335	0.0313	2439
184	334	0.0284	2271
185	335	0.0321	2481
186	335	-0.0359	2688
187	-1	-1.0000	-1
188	430	0.0455	3147
189	430	0.0369	2734
190	430	0.0326	2513
191	400	0.0384	2788
192	405	0.0460	3151
193	410	0.0839	3587
194	410	0.0364	2695
195	410	0.0324	2487
196	410	0.0292	2313
197	430	0.0354	2657
198	360	0.0439	3027
199	340	0.0655	3677
200	410	0.0441	3070

RUN NO.	*AIR TEMP* °F	*FUEL/AIR*	*FLAME TEMP* °F
201	86	0.0526	3331
202	82	0.0460	3054
203	110	0.0414	2749
204	-1	-1.0000	-1
205	313	0.0447	3120
206	253	0.0416	2935
207	245	0.0358	2621
208	-1	-1.0000	-1
209	-1	-1.0000	-1
210	-1	-1.0000	-1
211	-1	-1.0000	-1
212	-1	-1.0000	-1
213	-1	-1.0000	-1
214	-1	-1.0000	-1
215	-1	-1.0000	-1
216	-1	-1.0000	-1
217	80	0.0387	2666
218	100	0.0311	2245
219	110	0.0460	3072
220	100	0.0375	2611
221	100	0.0369	2578
222	100	0.0327	2339
223	100	0.0397	2738
224	100	0.0300	2179
225	100	0.0333	2374
226	100	0.0284	2083
227	76	0.0371	2574
228	82	0.0369	2566
229	85	0.0369	2572
230	433	0.0370	2817
231	420	0.0350	2706
232	410	0.0221	1959
233	407	0.0164	1584
234	90	0.0430	2914
235	92	0.0380	2632
236	89	0.0312	2244
237	82	0.0407	2781
238	79	0.0390	2686
239	80	0.0480	3143
240	82	0.0516	3293
241	82	0.0634	3550
242	78	0.0615	3530
243	80	0.0664	3563
244	79	0.0323	2300
245	80	0.0384	2647
246	80	0.0511	3275
247	75	0.0295	2131
248	85	0.0360	2519
249	75	0.0678	3558
250	85	0.0684	3559

RUN NO.	AIR TEMP °F	FUEL/AIR	FLAME TEMP °F
251	85	0.0399	2738
252	90	0.0400	2751
253	92	0.0462	3068
254	93	0.0410	2809
255	93	0.0388	2681
256	85	0.0460	3056
257	85	0.0503	3242
258	85	0.0576	3472
259	85	0.0640	3556
260	85	0.0775	3453
261	89	0.0760	3482
262	90	0.0331	2354
263	97	0.0381	2645
264	85	0.0317	2270
265	85	0.0372	2589
266	96	0.0363	2545
267	96	0.0323	2313
268	96	0.0372	2595
269	96	0.0421	2869
270	96	0.0439	2961
271	100	0.0357	2511
272	100	0.0424	2884
273	100	0.0432	2926
274	100	0.0484	3172
275	95	0.0528	3343
276	-1	-1.0000	-1
277	-1	-1.0000	-1
278	-1	-1.0000	-1
279	109	0.0371	2594
280	110	0.0436	2953
281	110	0.0380	2644
282	94	0.0389	2685
283	100	0.0313	2257
284	105	0.0271	2011
285	116	0.0312	2263
286	82	0.0321	2290
287	92	0.0290	2111
288	90	0.0362	2533
289	95	0.0385	2664
290	99	0.0460	3065
291	73	0.0965	3042
292	75	0.1008	2948
293	82	0.1011	2945
294	90	0.0835	3329
295	72	0.0967	3036
296	86	0.0929	3128
297	92	0.1100	2754
298	95	0.0957	3073
299	96	0.1135	2682
300	85	0.1081	2792

RUN NO.	*AIR TEMP* °F	*FUEL/AIR*	*FLAME TEMP* °F
301	88	0.0867	3261
302	92	0.1117	2718
303	74	0.0917	3147
304	87	0.0954	3074
305	100	0.1160	2631
306	100	0.0907	3183
307	104	0.0839	3329
308	90	0.0406	2782
309	98	0.0323	2317
310	94	0.0199	1554
311	385	0.0377	2816
312	388	0.0326	2553
313	395	0.0252	2138
314	340	0.0345	2616
315	364	0.0302	2402
316	400	0.0323	2544
317	435	0.0260	2215
318	350	0.0316	2465
319	350	0.0252	2097
320	351	0.0393	2878
321	140	0.0383	2680
322	115	0.0311	2257
323	105	0.0271	2008
324	95	0.0374	2605
325	105	0.0332	2371
326	110	0.0284	2090
327	412	0.0385	2878
328	395	0.0297	2397
329	390	0.0245	2086
330	407	0.0381	2854
331	400	0.0309	2470
332	435	0.0260	2215
333	392	0.0282	2307
334	395	0.0246	2099
335	92	0.0370	2499
336	90	0.0311	2165
337	90	0.0362	2453
338	90	0.0393	2620
339	100	0.0379	2550
340	395	0.0320	2524
341	150	0.0336	2427
342	90	0.0365	2467
343	102	0.0329	2353
344	100	0.0289	2117
345	102	0.0347	2458
346	105	0.0312	2259
347	105	0.0422	2880
348	107	0.0401	2675
349	100	0.0342	2351
350	101	0.0380	2555

Table
VI-31

RUN NO.	AIR TEMP °F	FUEL/AIP	FLAME TEMP °F
351	105	0.0421	2780
352	110	0.0336	2320
353	120	0.0421	2789
354	430	0.0359	2683
355	438	0.0287	2312
356	450	0.0371	2761
357	140	0.0337	2349
358	110	0.0312	2183
359	120	0.0335	2322
360	380	0.0355	2624
361	400	0.0312	2413
362	405	0.0420	2969
363	405	0.0332	2527
364	405	0.0379	2767
365	405	0.0416	2949
366	410	0.0287	2289
367	405	0.0340	2567
368	410	0.0287	2289
369	400	0.0379	2763
370	403	0.0359	2664
371	426	0.0348	2627
372	425	0.0337	2568
373	425	0.0328	2518
374	430	0.0318	2470
375	400	0.0308	2393
376	400	0.0314	2426
377	405	0.0367	2707
378	428	0.0373	2754
379	375	0.0350	2594
380	412	0.0330	2523
381	411	0.0300	2362
382	411	0.0300	2360
383	403	0.0358	2660
384	76	0.0374	2506
385	90	0.0373	2510
386	91	0.0352	2399
387	80	0.0350	2380
388	81	0.0356	2411
389	85	0.0822	3423
390	90	0.0349	2380
391	93	0.0327	2256

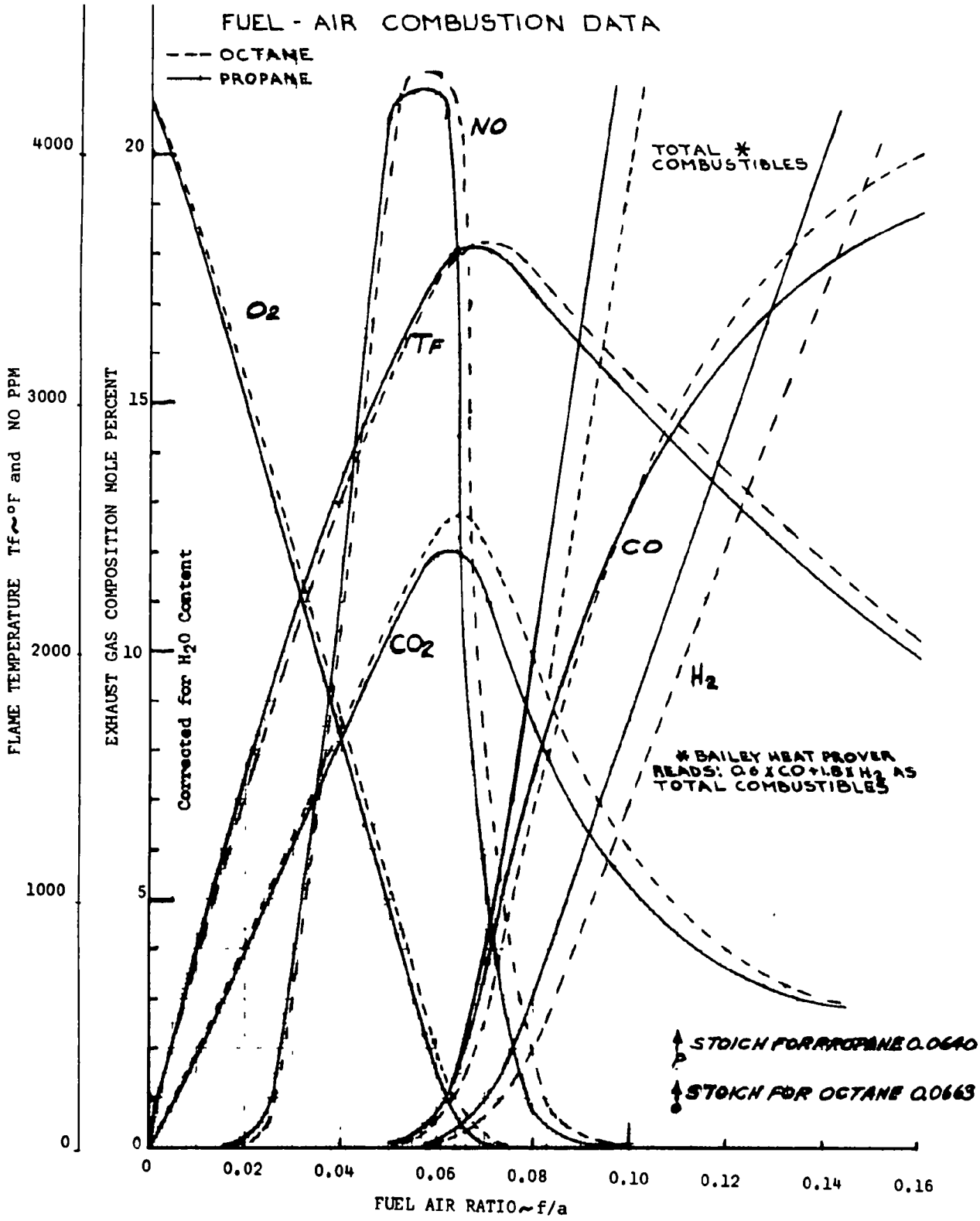

Reference: Combustion of Hydrocarbons-- Property Tables
Purdue University, Eng. Ext. Ser #122, May 66

Figure VI-1

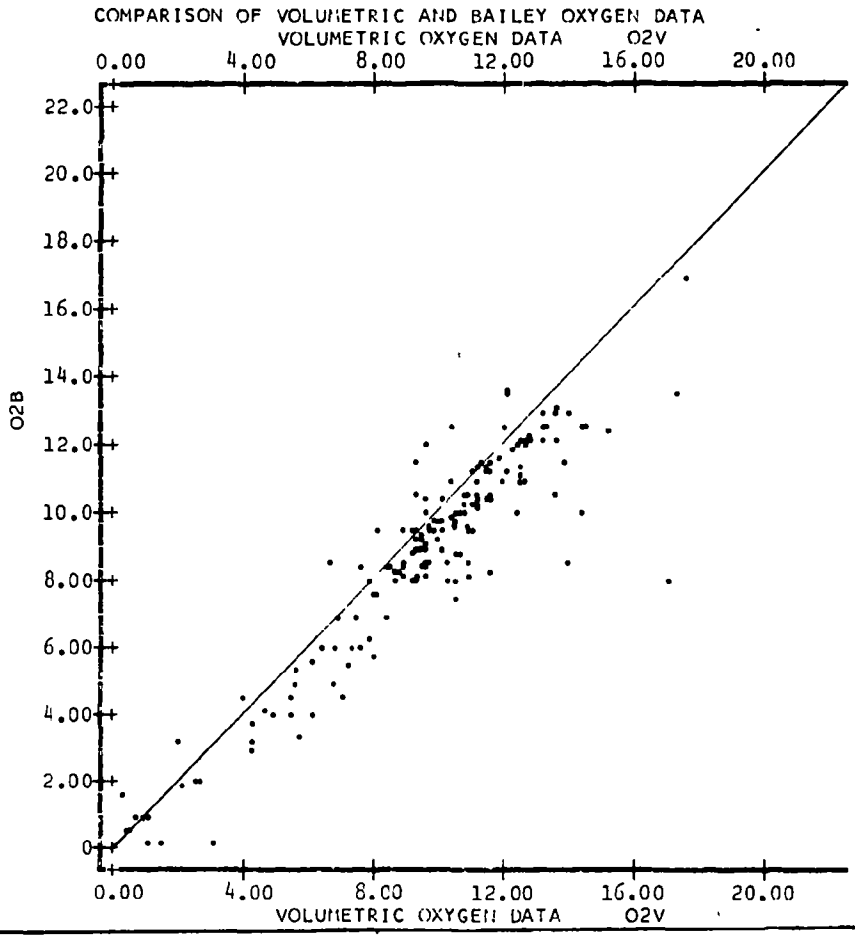

Figure VI-2

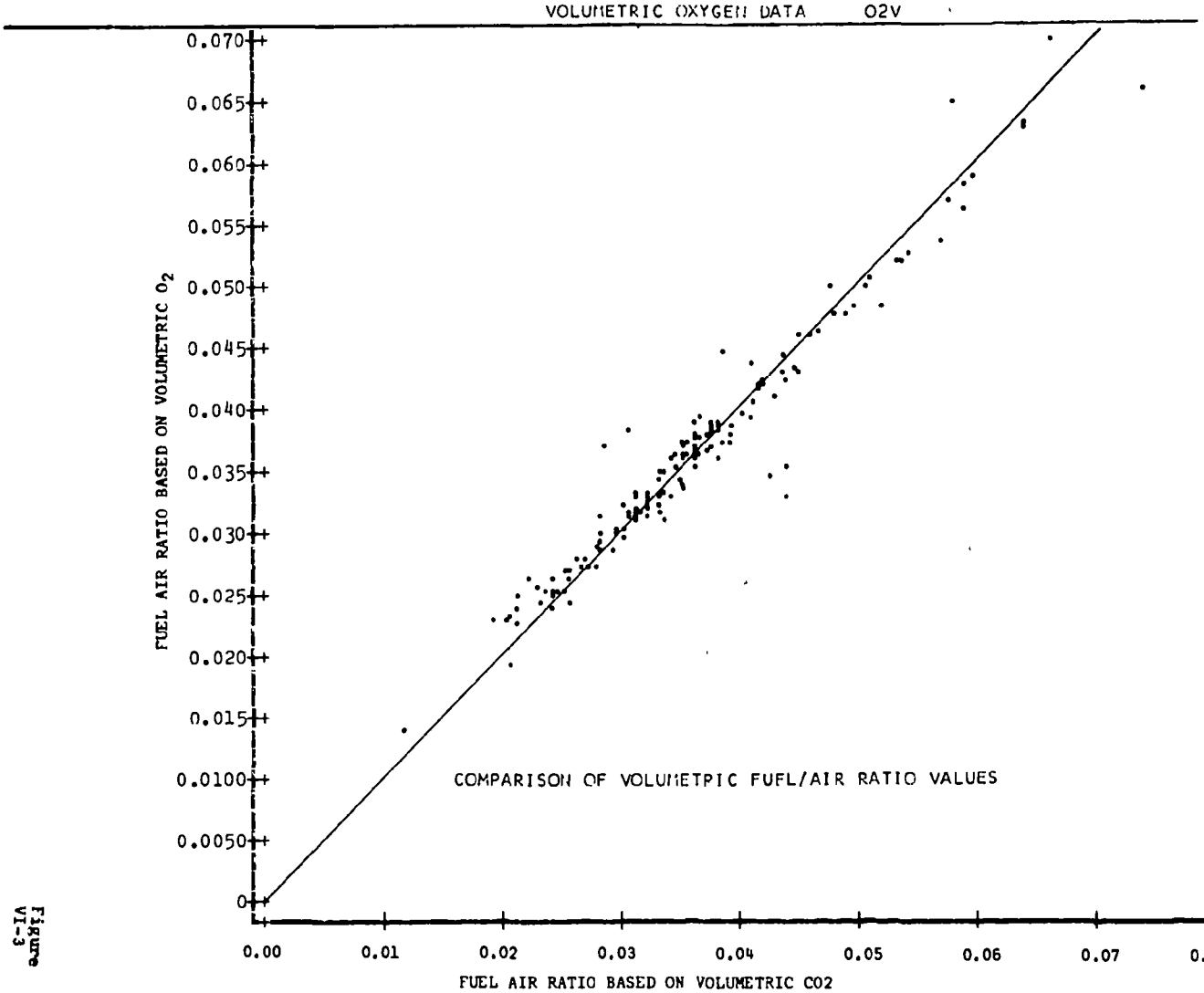

Figure VI-3

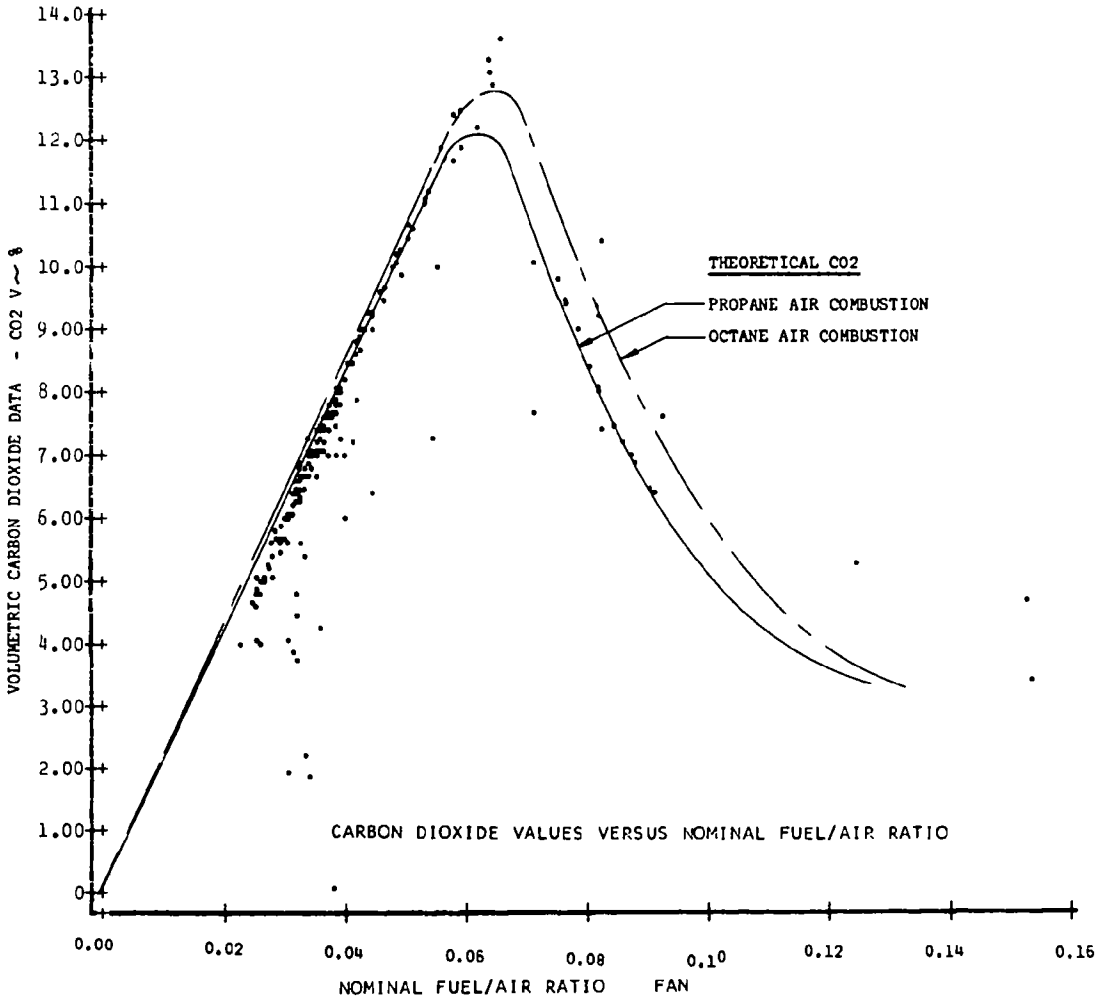

Figure VI-4

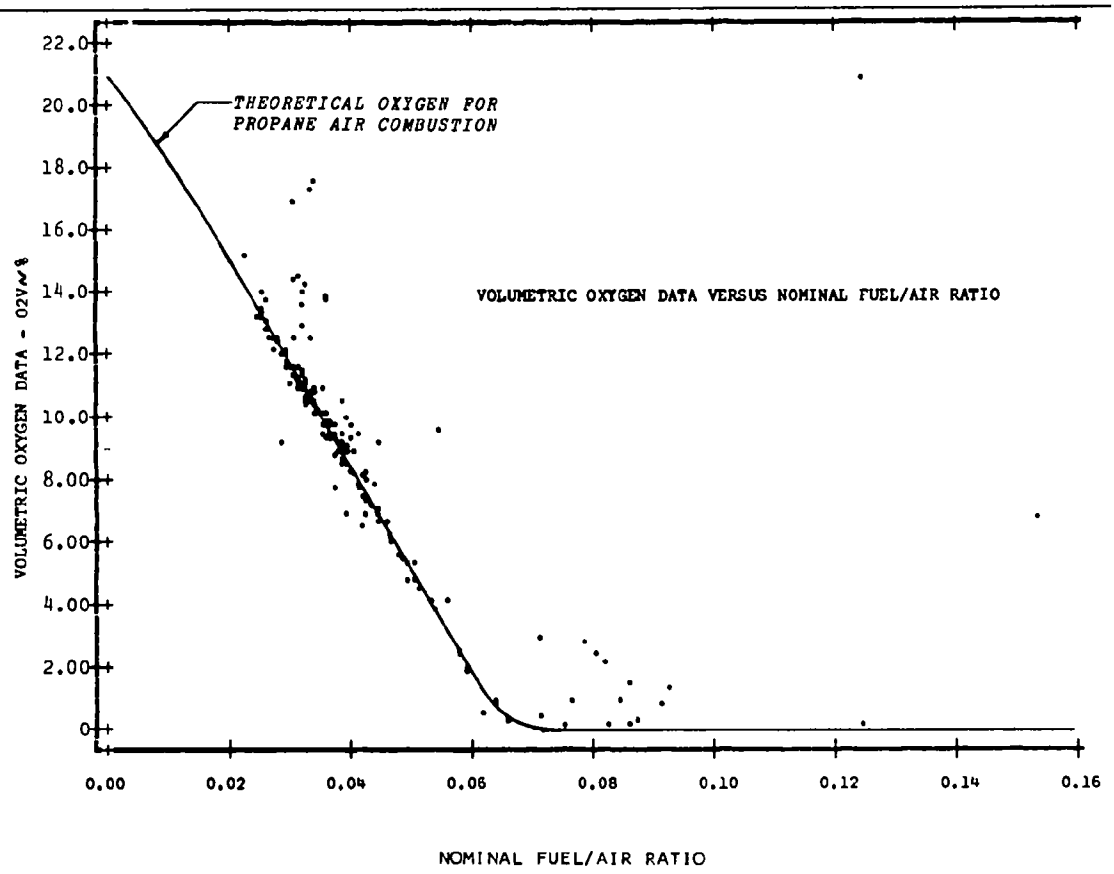

Figure VI-5

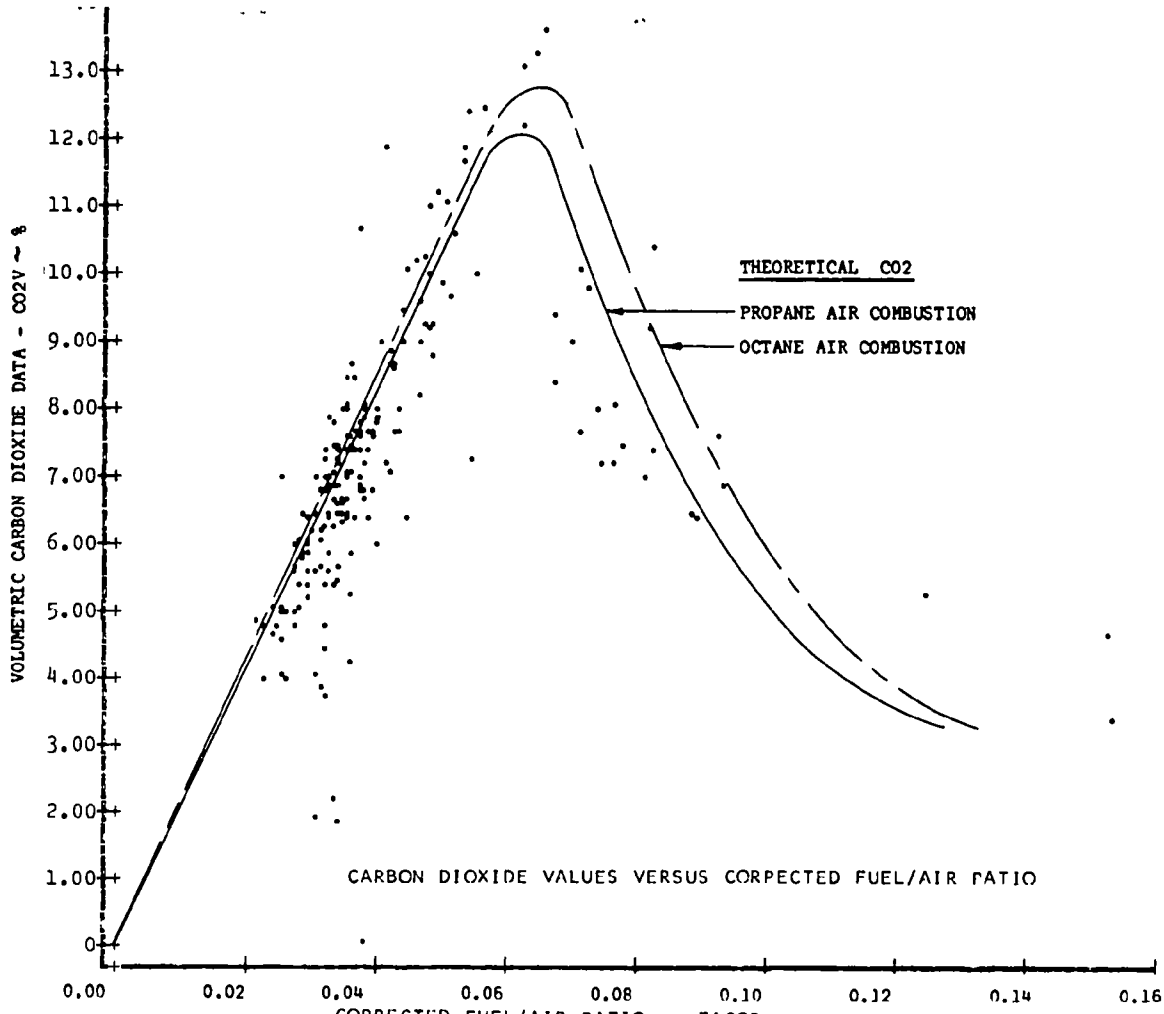

Figure VI-6

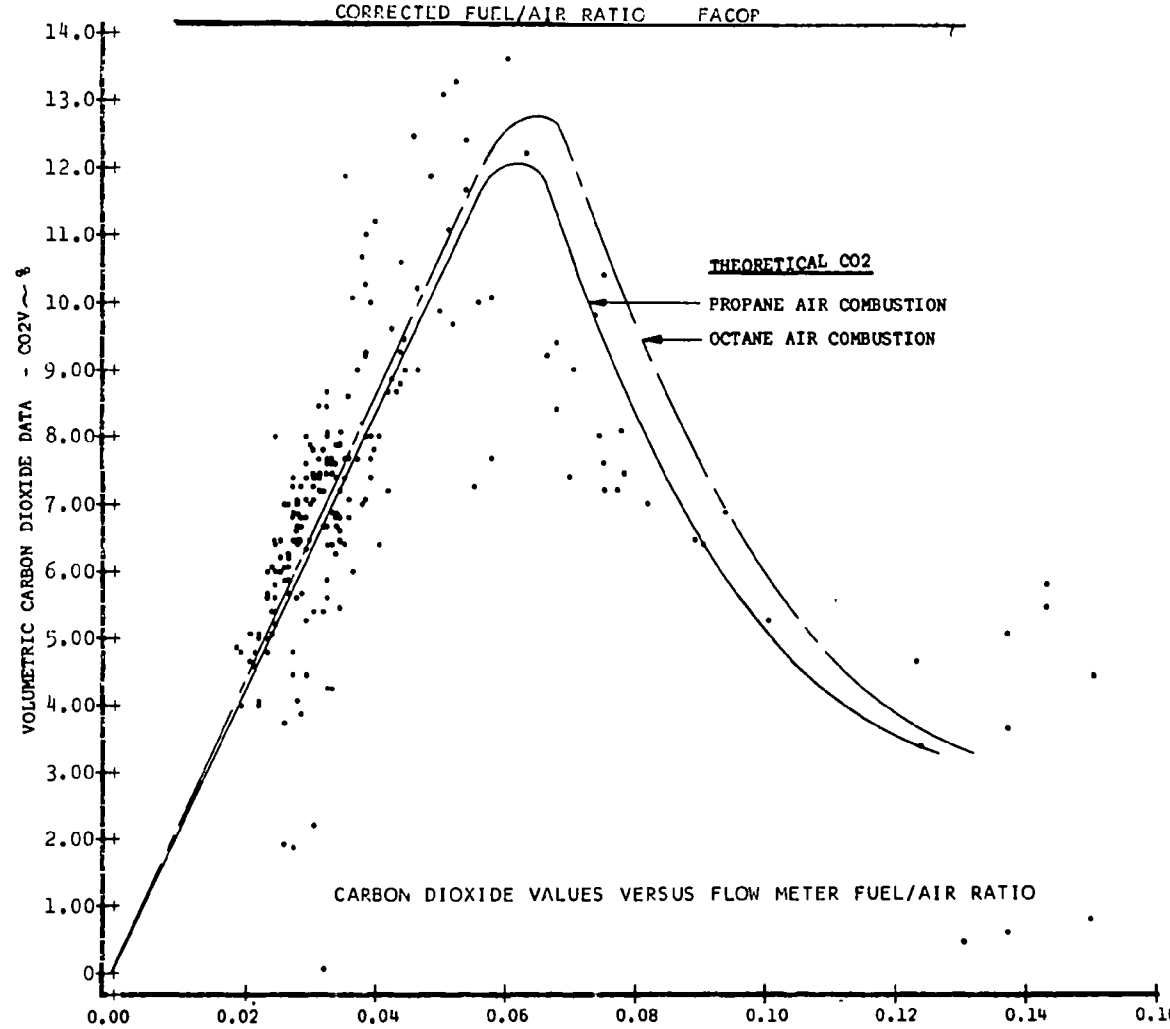

Figure VI-7

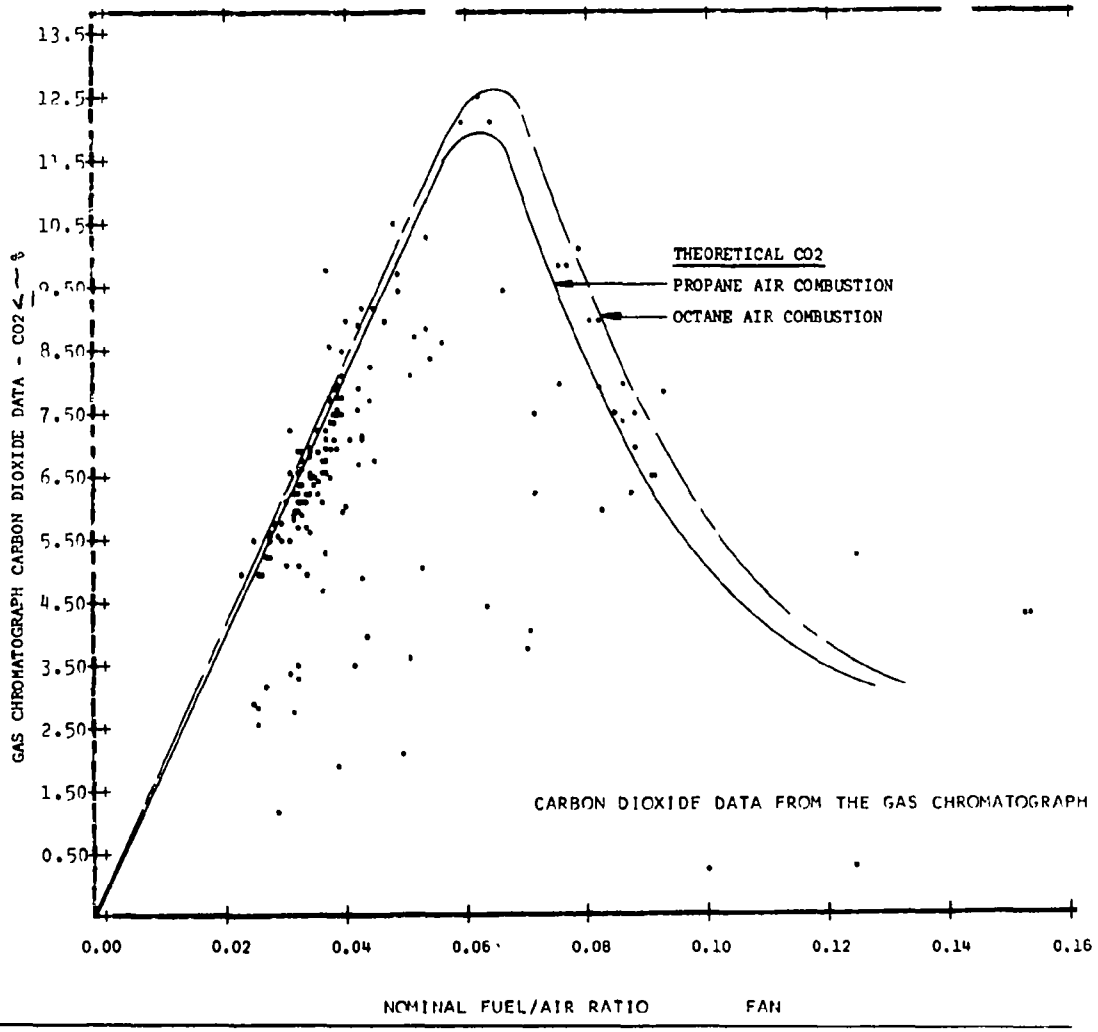

Figure VI-8

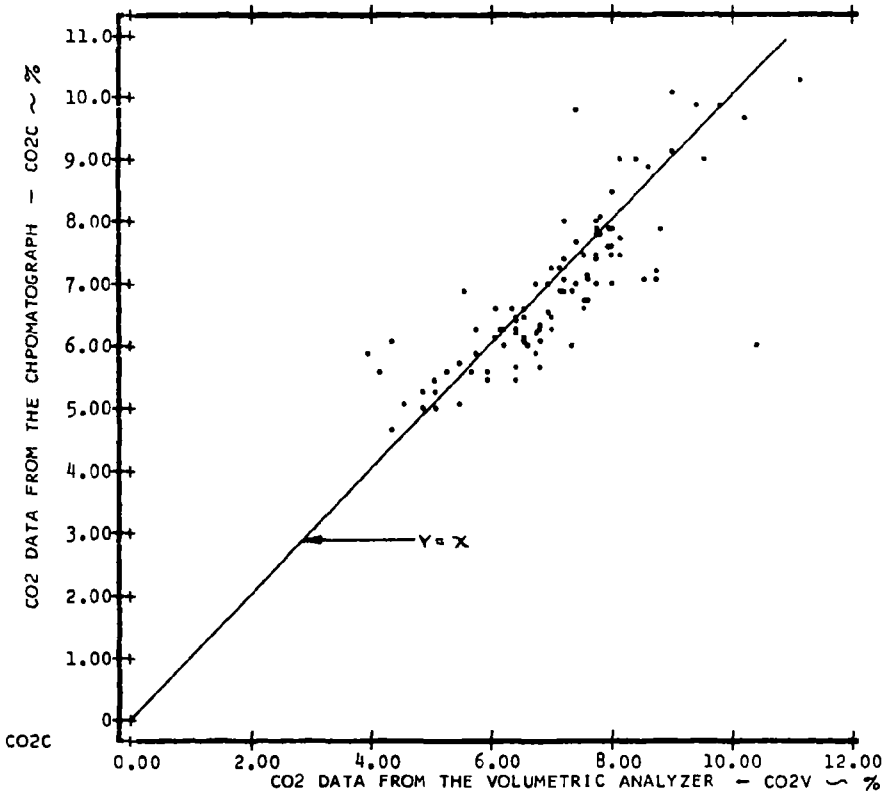

Figure VI-9

COMPARISON OF CARBON DIOXIDE CHROMATOGRAPH AND VOLUMETPIC DATA

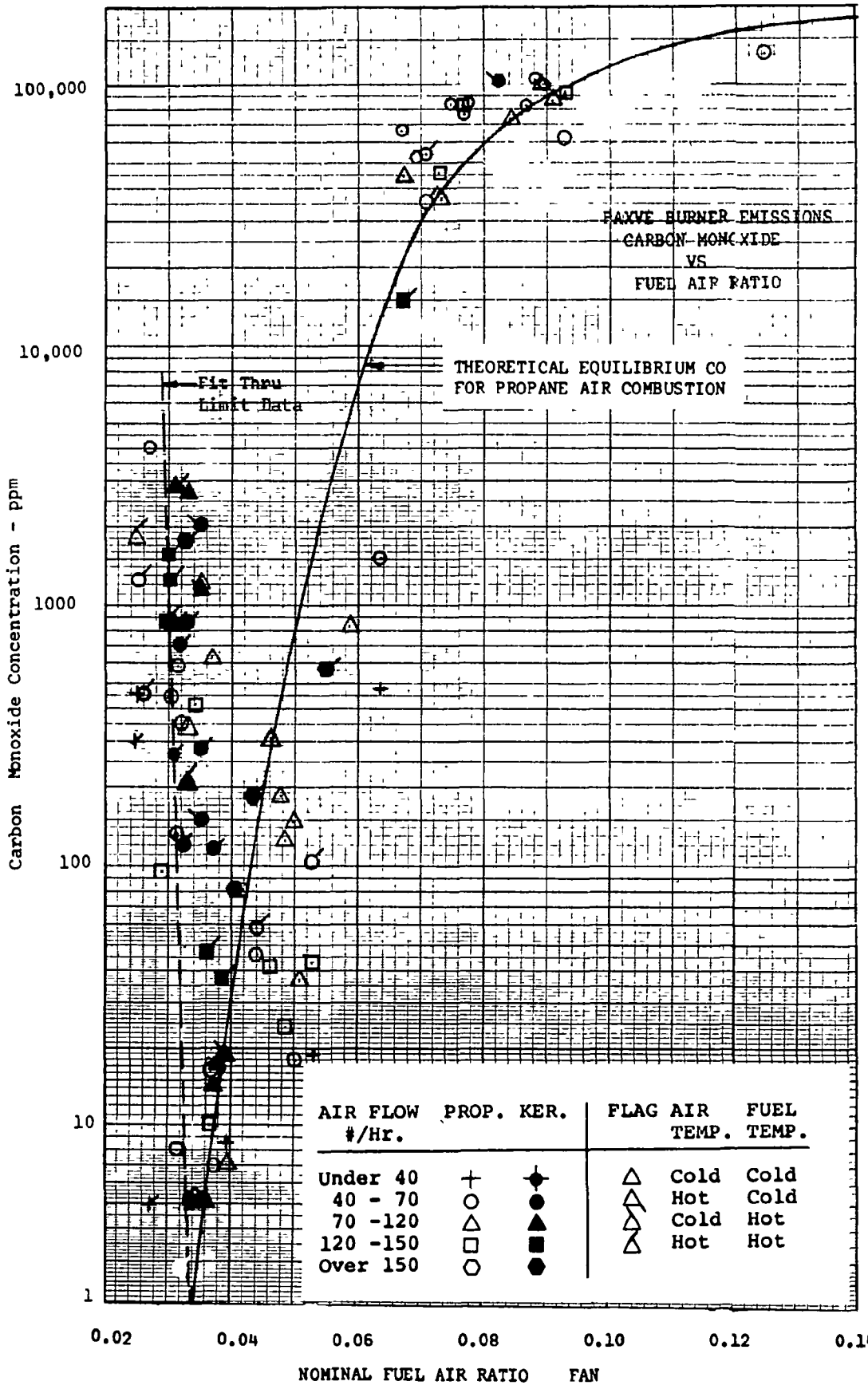
100,000
10,000
1000
100
10
1
Carbon Monoxide Concentration - ppm
0.02
0.04
0.06
0.08
0.10
0.12
0.14
NOMINAL FUEL AIR RATIO FAN
FAXVE BURNER EMISSIONS
CARBON MONOXIDE
VS
FUEL AIR RATIO
THEORETICAL EQUILIBRIUM CO
FOR PROPANE AIR COMBUSTION
Fit Thru
Limit Data
AIR FLOW #/Hr.
PROP.
KER.
Under 40
40 - 70
70 -120
120 -150
Over 150
FLAG AIR TEMP.
FUEL TEMP.
Cold Cold
Hot Cold
Cold Hot
Hot Hot

Figure VI-10

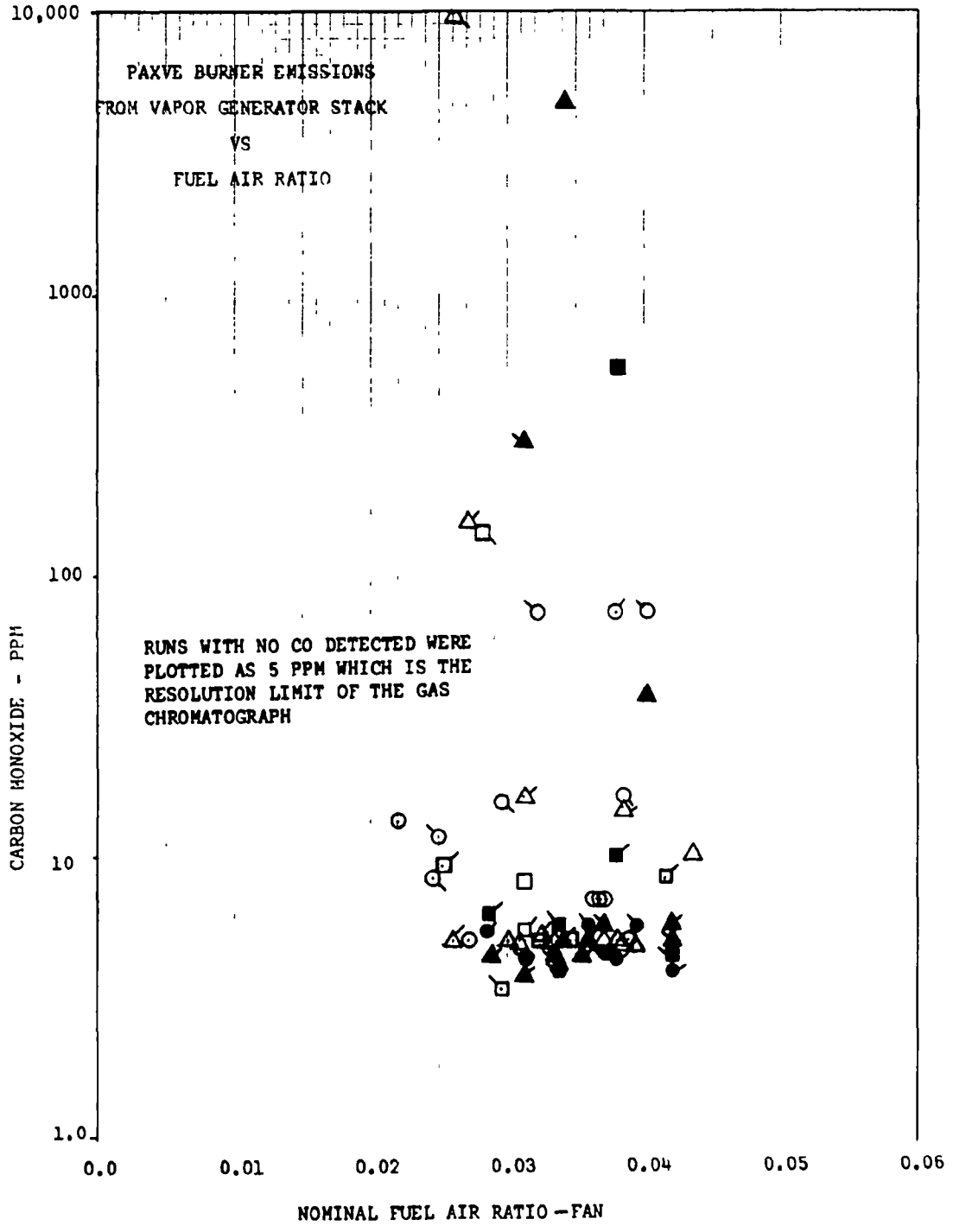

AIR FLOW #/Hr.	PROP.	KER.	FLAG	AIR TEMP.	FUEL TEMP.
Under 40	+	✦	△	Cold	Cold
40 - 70	○	●	△	Hot	Cold
70 -120	△	▲	△	Cold	Hot
120 -150	□	■	△	Hot	Hot
Over 150	⬡	⬢			

Figure VI-11

CO EMISSIONS COMPARISON

VAPOR GENERATOR VS BURNER

KEROSENE LEAN COMBUSTION

RUN NO.	CO_{top} PPM	CO_{burner} PPM
360	5	5
361	5	5
362	5	-
363	5	5
364	5	5
365	5	5
366	5	5
367	-	-
368	5	5
369	10	20
370	14.6	25.6

RUNS WITH NO CO DETECTED WERE PLOTTED AS 5 PPM WHICH IS THE RESOLUTION LIMIT OF THE GAS CHROMATOGRAPH

Figure VI-12

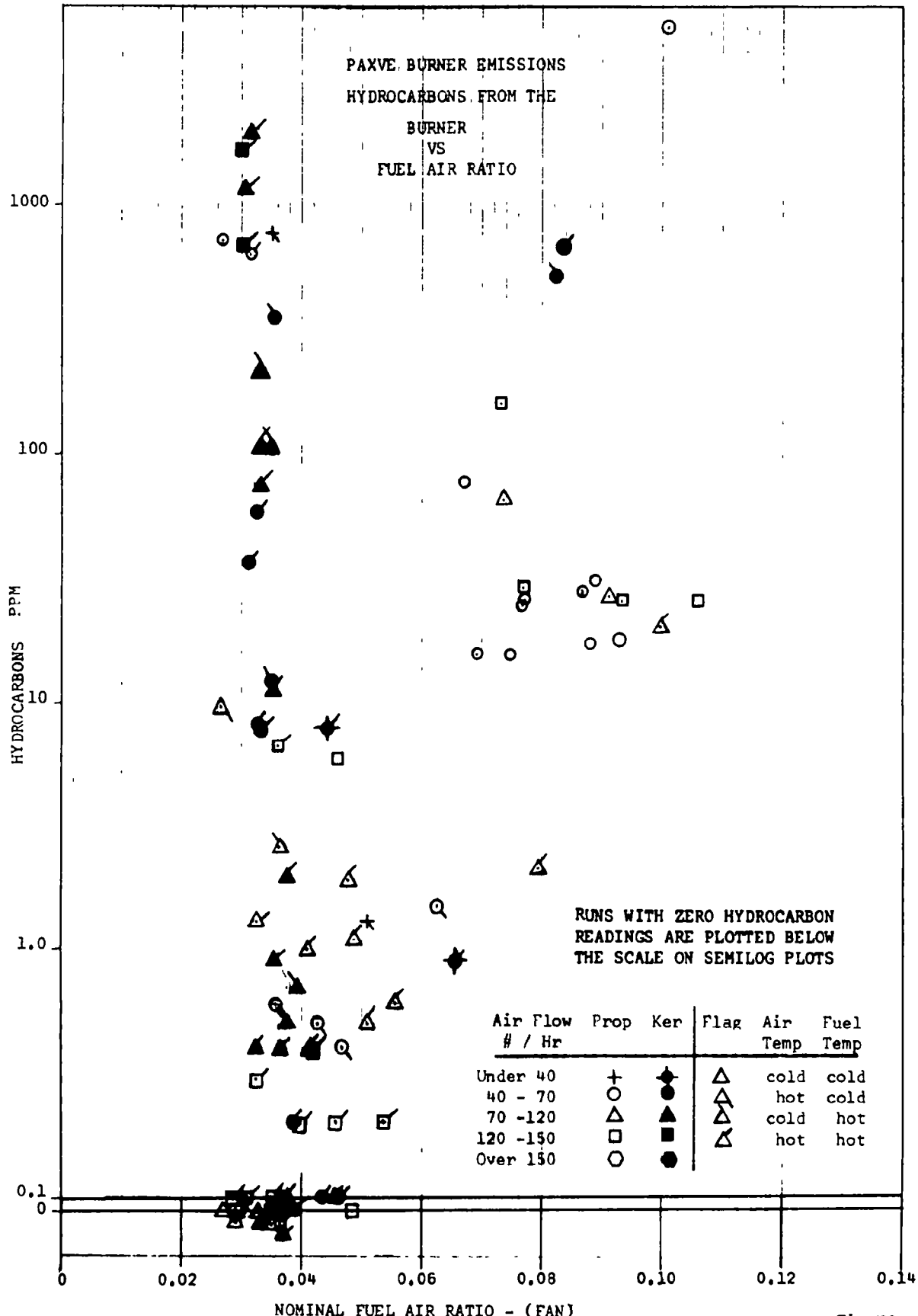
PAXVE BURNER EMISSIONS
HYDROCARBONS FROM THE
BURNER
VS
FUEL AIR RATIO
1000
100
10
1.0
0.1
0
HYDROCARBONS PPM
0
0.02
0.04
0.06
0.08
0.10
0.12
0.14
NOMINAL FUEL AIR RATIO - (FAN)
RUNS WITH ZERO HYDROCARBON
READINGS ARE PLOTTED BELOW
THE SCALE ON SEMILOG PLOTS
Air Flow # / Hr
Prop
Ker
Flag
Air Temp
Fuel Temp
Under 40
40 - 70
70 -120
120 -150
Over 150
cold cold
hot cold
cold hot
hot hot

Figure
VI-13

PAXVE BURNER EMISSIONS
HYDROCARBONS FROM
VAPOR GENERATOR STACK
VS
FUEL AIR RATIO
HC
ppm
10
5
4
3
2
1
0
0.02
0.03
0.04
0.05
NOMINAL FUEL AIR
AIR FLOW #/Hr.
PROP. KER.
Under 40
40 - 70
70 -120
120 -150
Over 150
FLAG
AIR TEMP.
FUEL TEMP.
Cold Cold
Hot Cold
Cold Hot
Hot Hot

Figure VI-14

PAXVE BURNER EMISSIONS
NITROGEN OXIDES FROM BURNER
VS
FUEL AIR RATIO

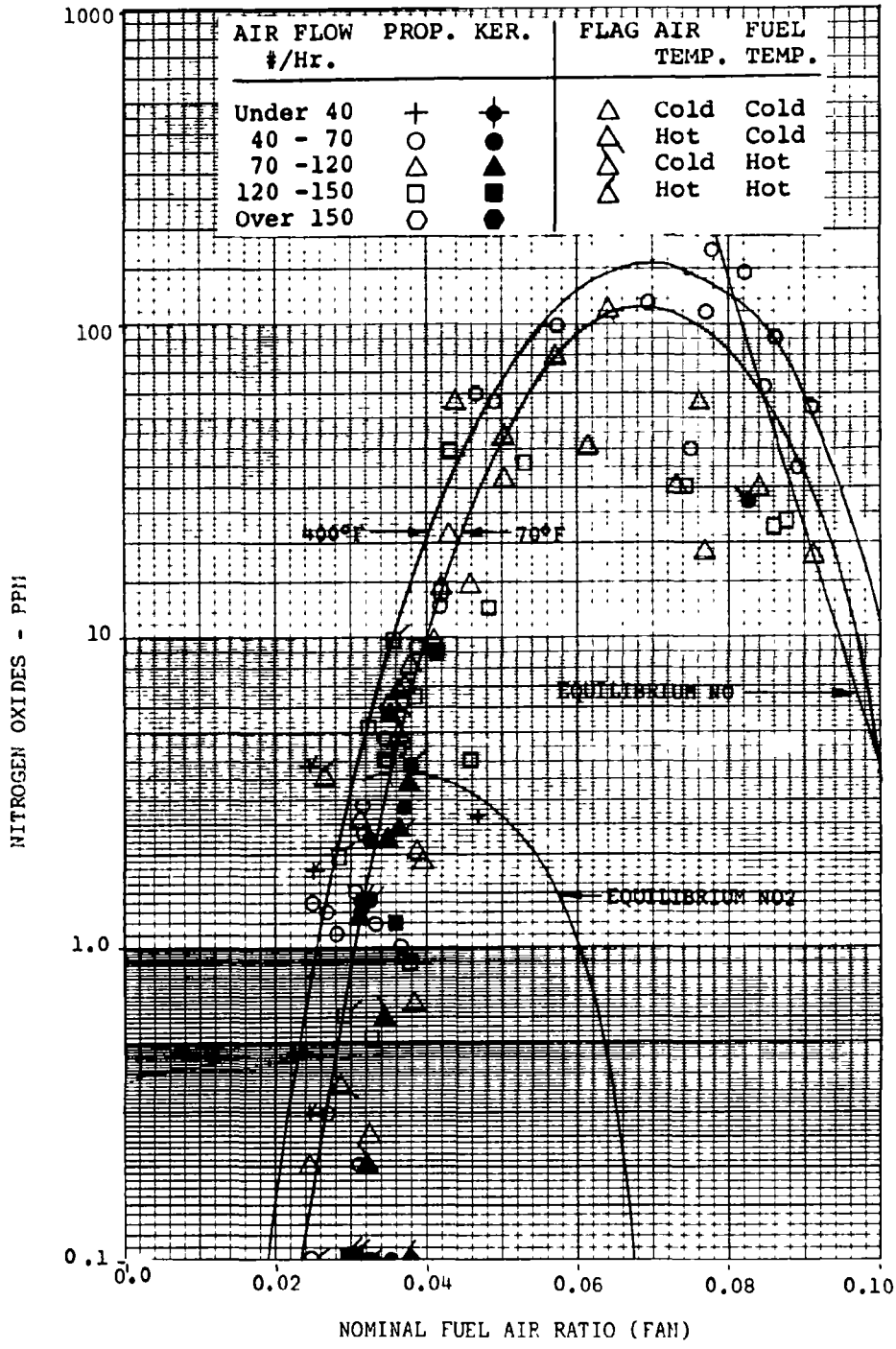

Figure
VI-15

PAXVE BURNER EMISSIONS

NITROGEN OXIDES FROM BURNER

WITH VAPOR GENERATOR OPERATION

VS FUEL AIR RATIO

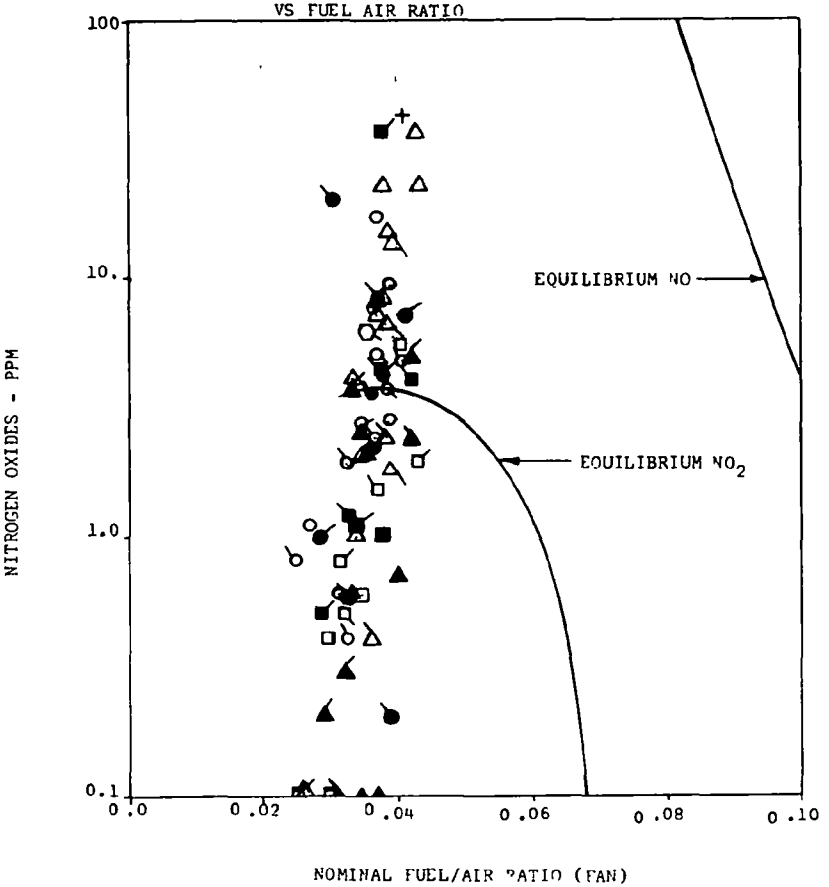

AIR FLOW #/Hr.	PROP.	KER.	FLAG	AIR TEMP.	FUEL TEMP.
Under 40	+	✦	△	Cold	Cold
40 - 70	○	●	△	Hot	Cold
70 -120	△	▲	△	Cold	Hot
120 -150	□	■	△	Hot	Hot
Over 150	○	●			

Figure VI-16

PAXVE BURNER EMISSIONS

NITROGEN OXIDES

FROM VAPOR GENERATOR STACK VS

FUEL AIR RATIO

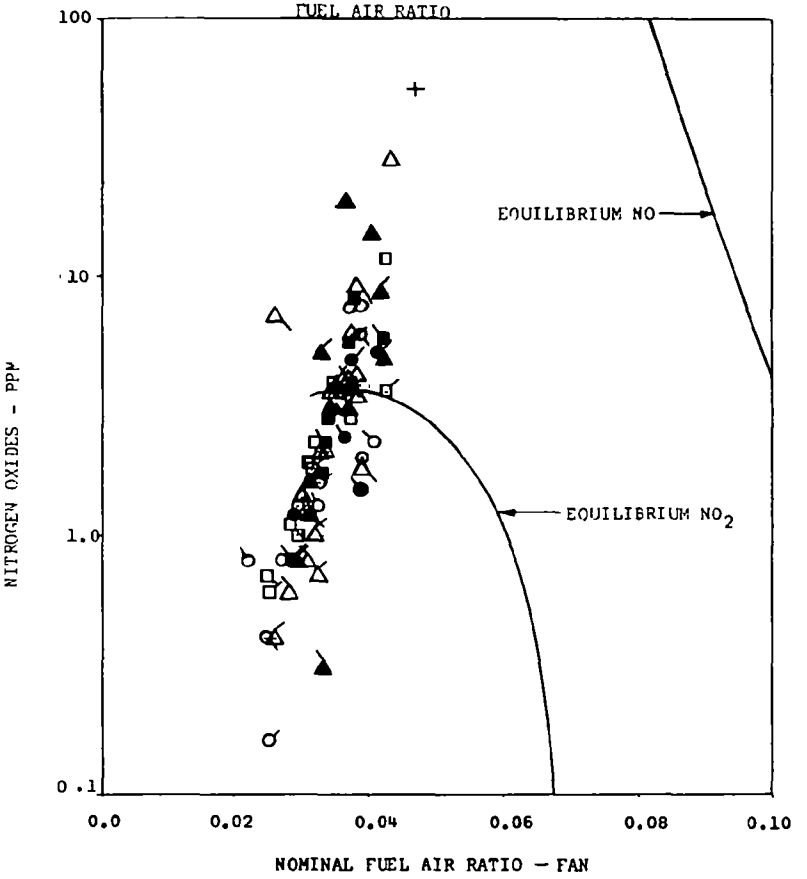

AIR FLOW #/Hr.	PROP.	KER.	FLAG	AIR TEMP.	FUEL TEMP.
Under 40	+	✦	△	Cold	Cold
40 - 70	○	●	△	Hot	Cold
70 -120	△	▲	△	Cold	Hot
120 -150	□	■	△	Hot	Hot
Over 150	○	●			

Figure VI-17

PAXVE BURNER EMISSIONS

NITROGEN OXIDES COMPARISONS

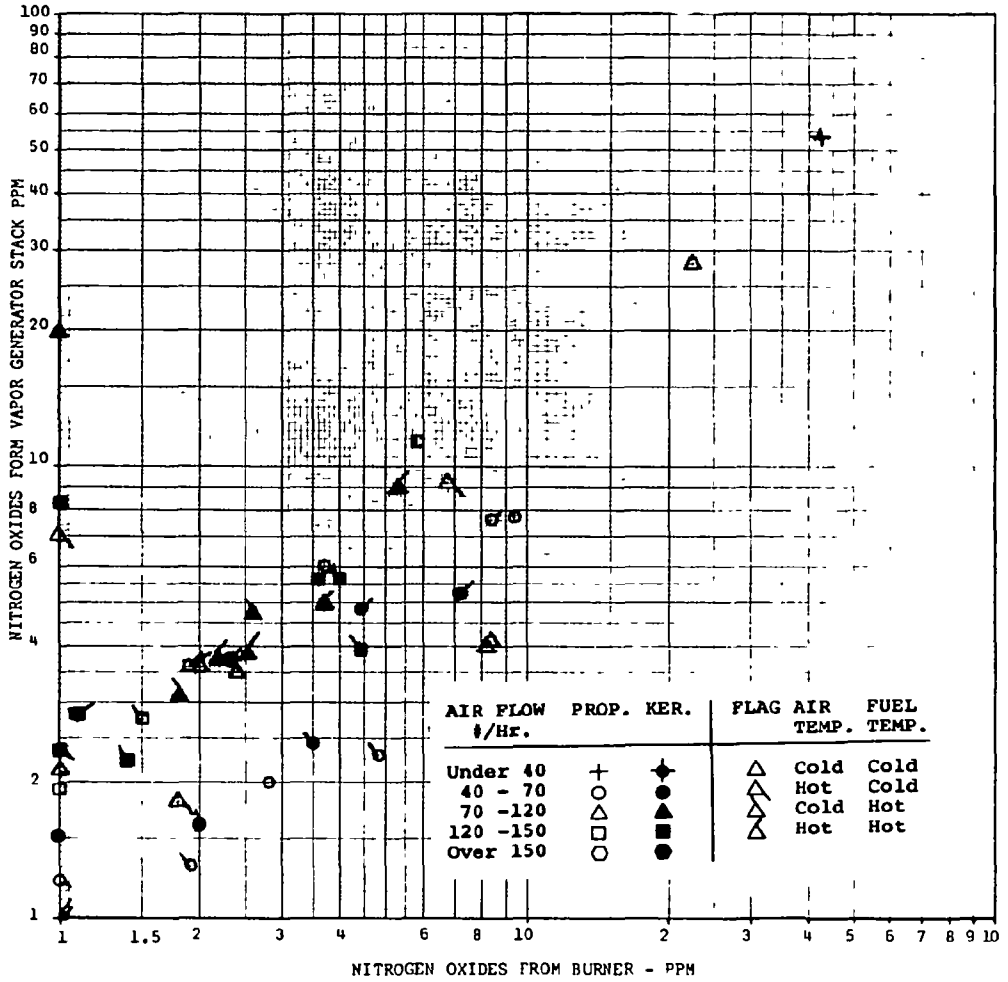

Figure VI-18

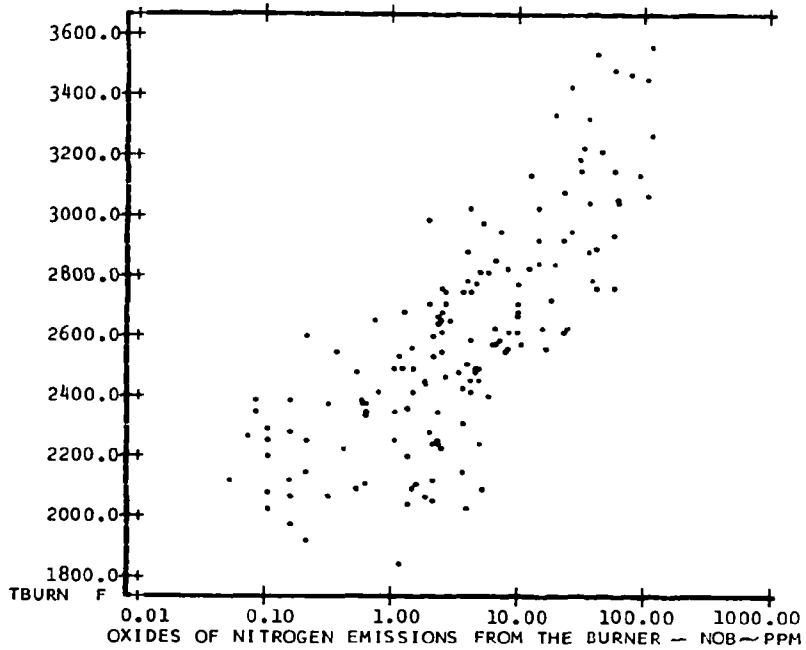

CORRELATIONS OF OXIDES OF NITROGEN DATA

Figure VI-19

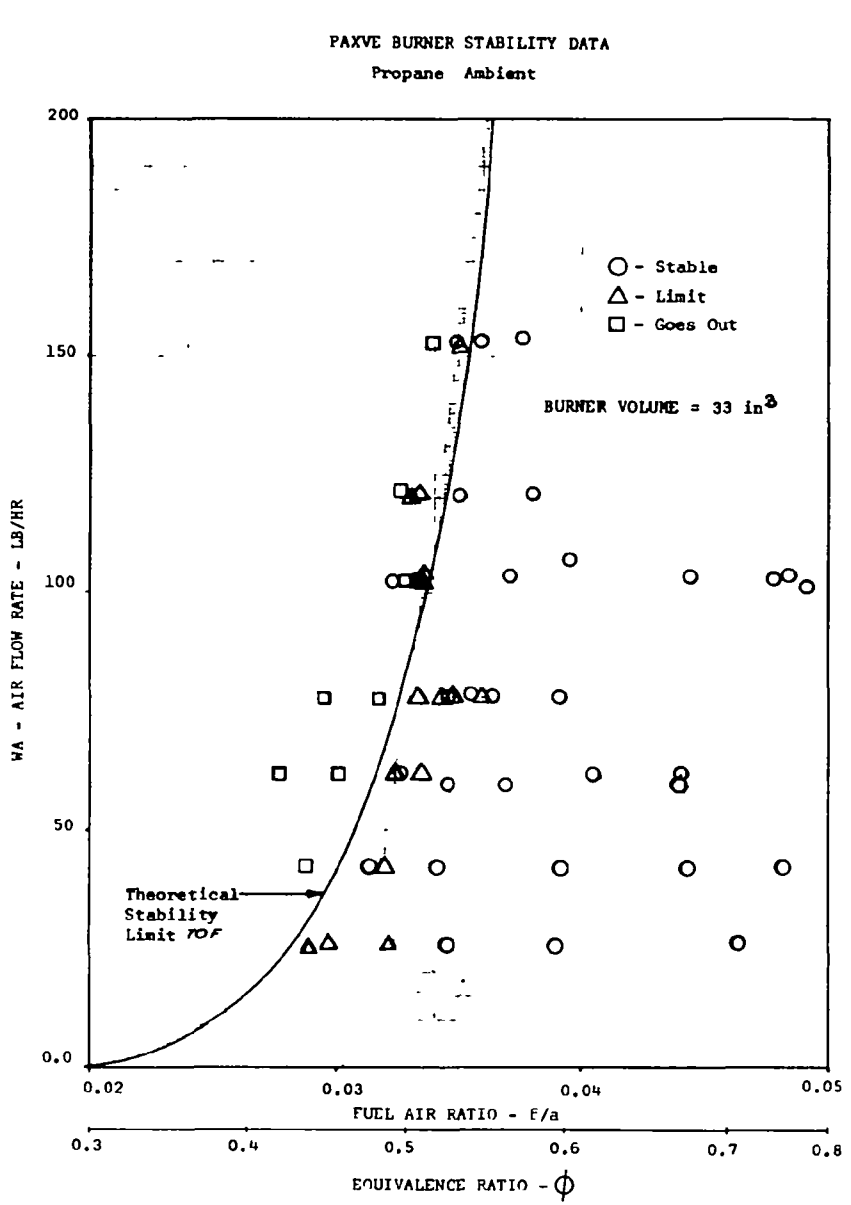

Figure VI-20

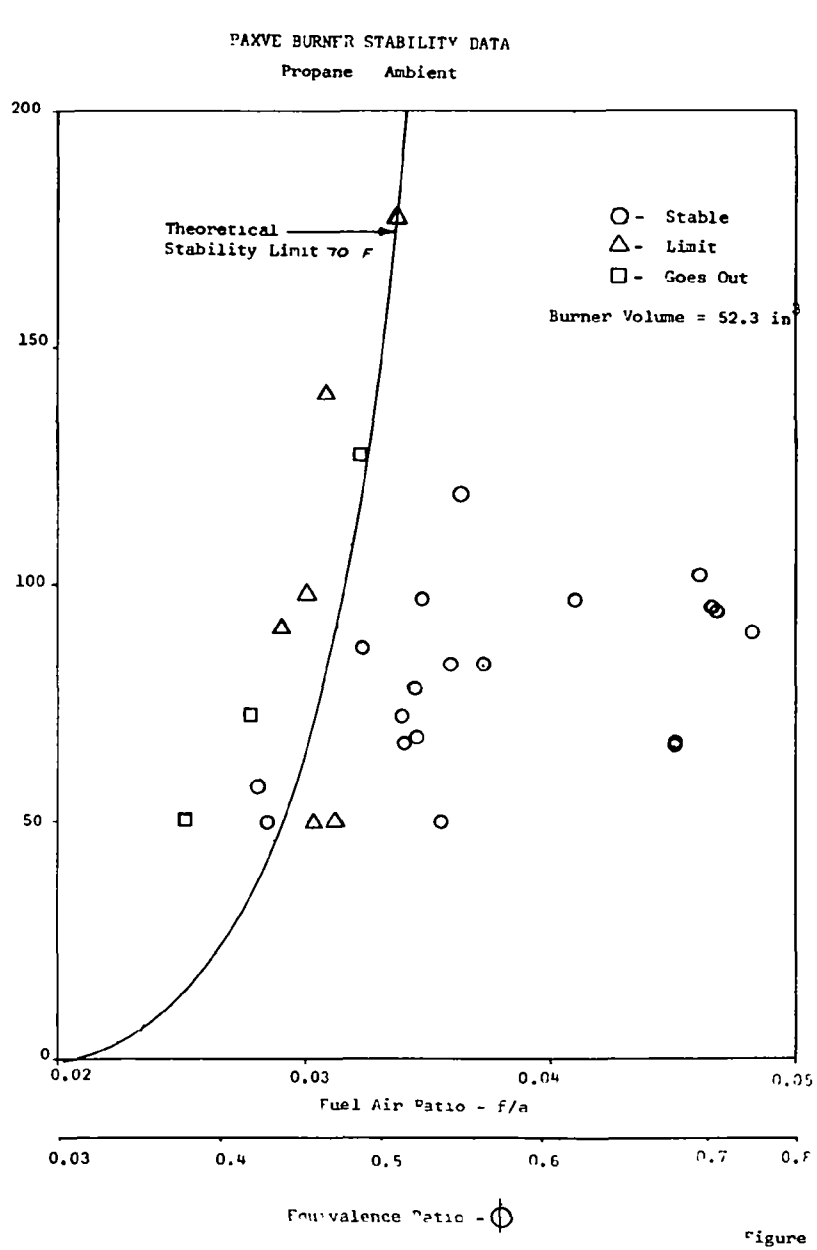

Figure VI-21

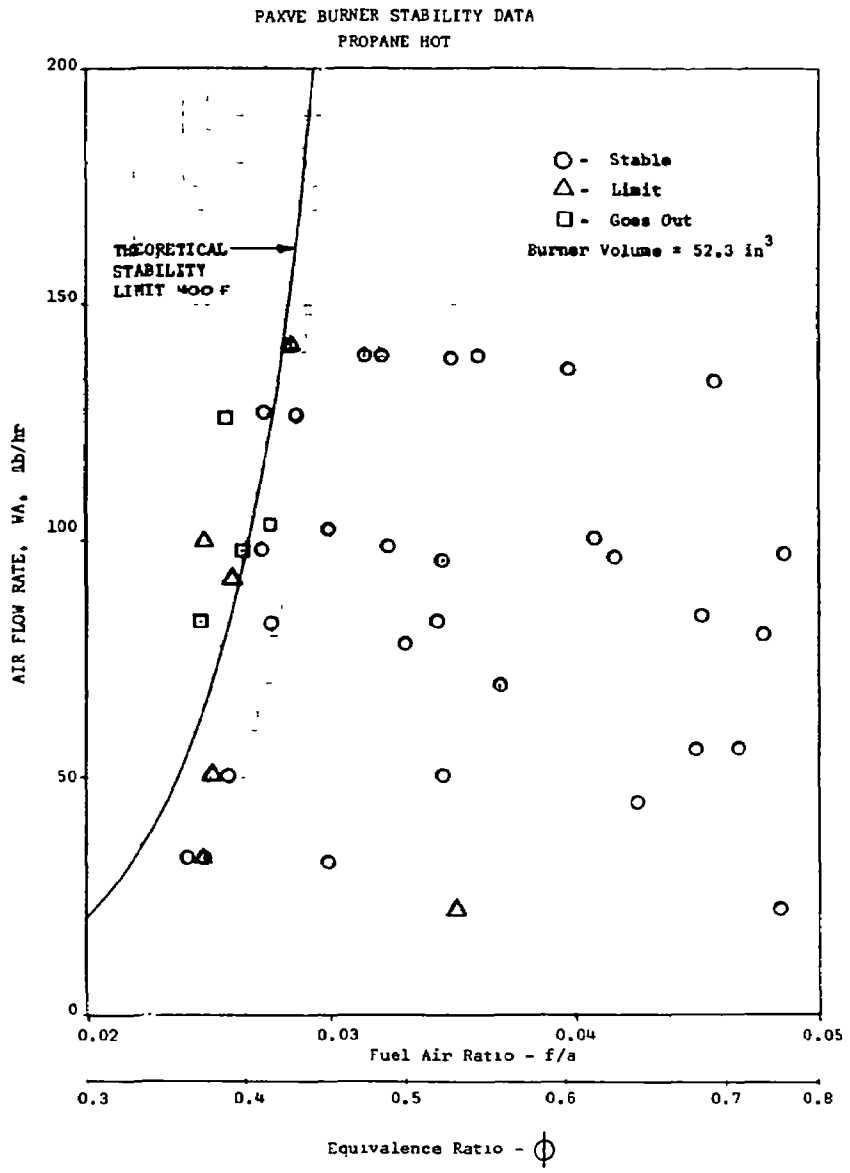
PAXVE BURNER STABILITY DATA
PROPANE HOT
200
150
100
50
0
AIR FLOW RATE, WA, Lb/hr
○ - Stable
△ - Limit
□ - Goes Out
Burner Volume = 52.3 in3
THEORETICAL
STABILITY
LIMIT 400 F
0.02
0.03
0.04
0.05
Fuel Air Ratio - f/a
0.3
0.4
0.5
0.6
0.7
0.8
Equivalence Ratio - ϕ

Fig VI
22

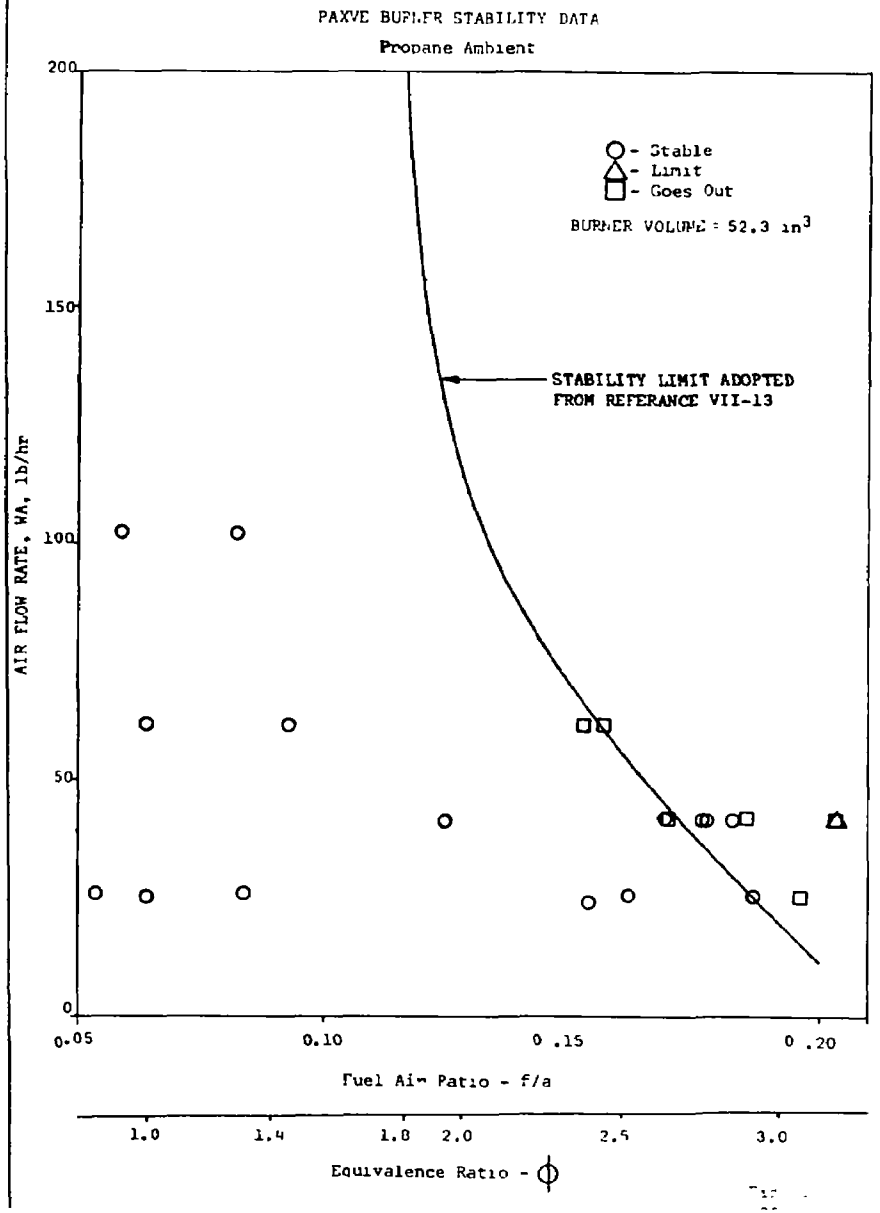
PAXVE BURNER STABILITY DATA
Propane Ambient
200
150
100
50
0
AIR FLOW RATE, WA, lb/hr
○ - Stable
△ - Limit
□ - Goes Out
BURNER VOLUME = 52.3 in3
STABILITY LIMIT ADOPTED
FROM REFERANCE VII-13
0.05
0.10
0.15
0.20
Fuel Air Ratio - f/a
1.0
1.4
1.8
2.0
2.5
3.0
Equivalence Ratio - ϕ

PAXVE BURNER STABILITY DATA
Kerosene - Ambient

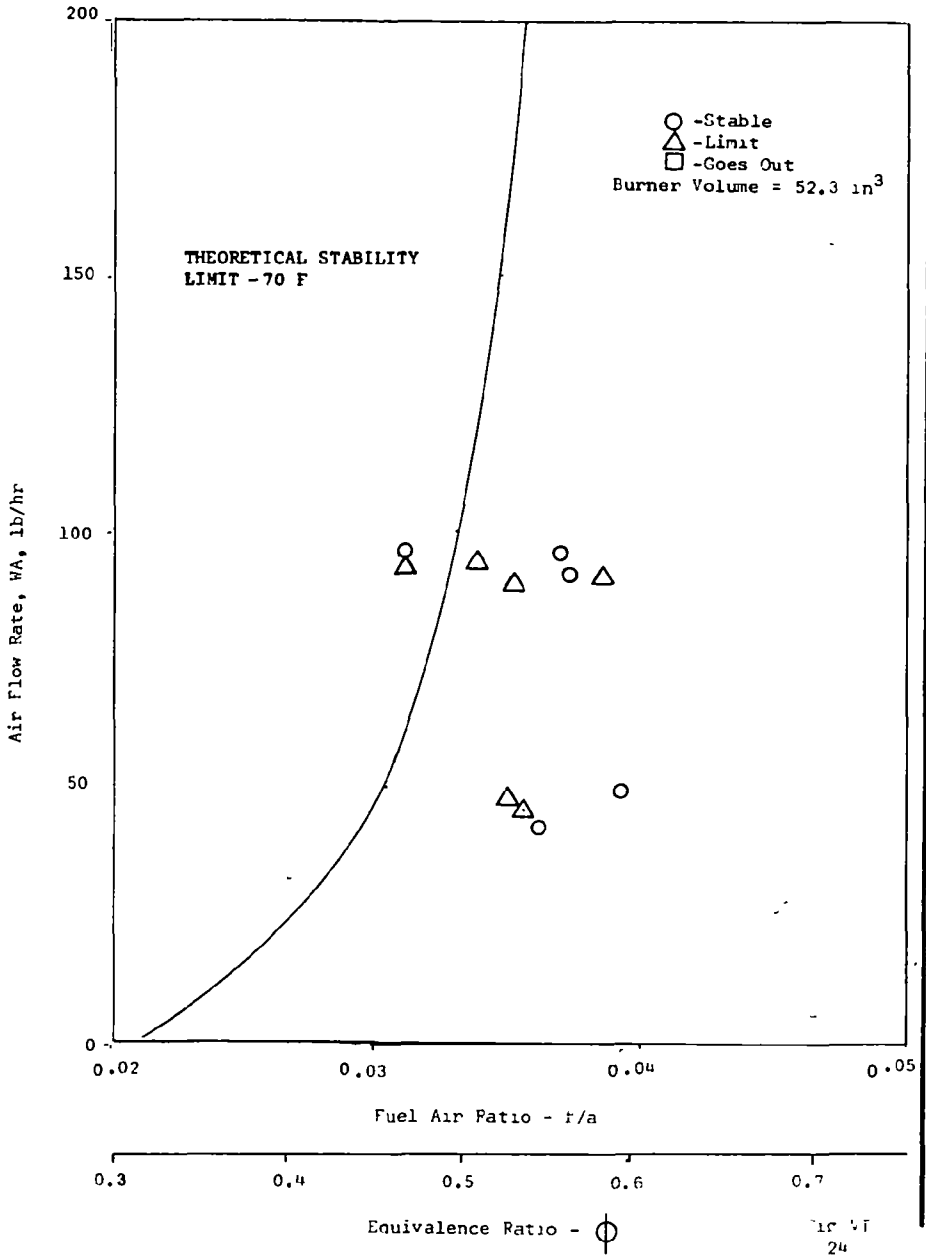

PAXVE BURNER STABILITY DATA
Kerosene - Hot

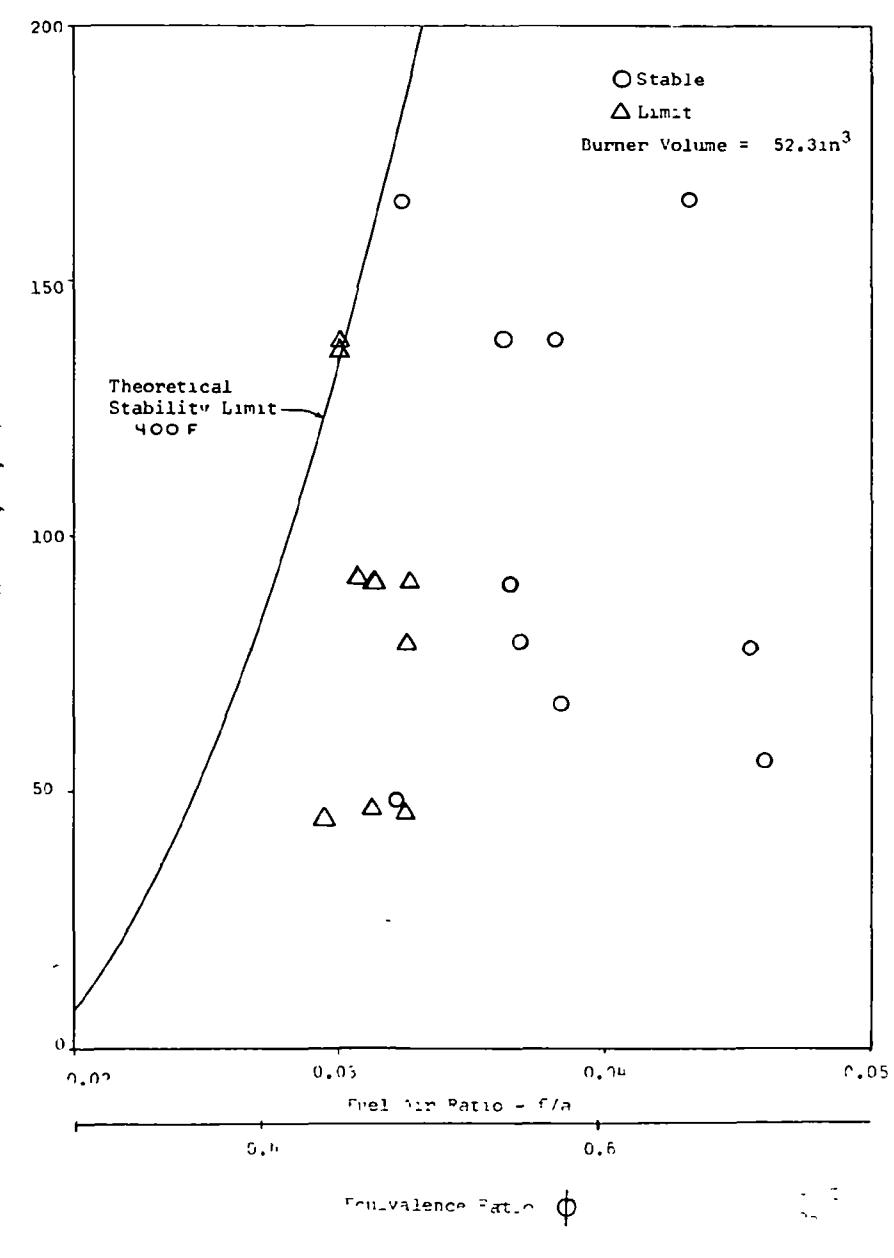

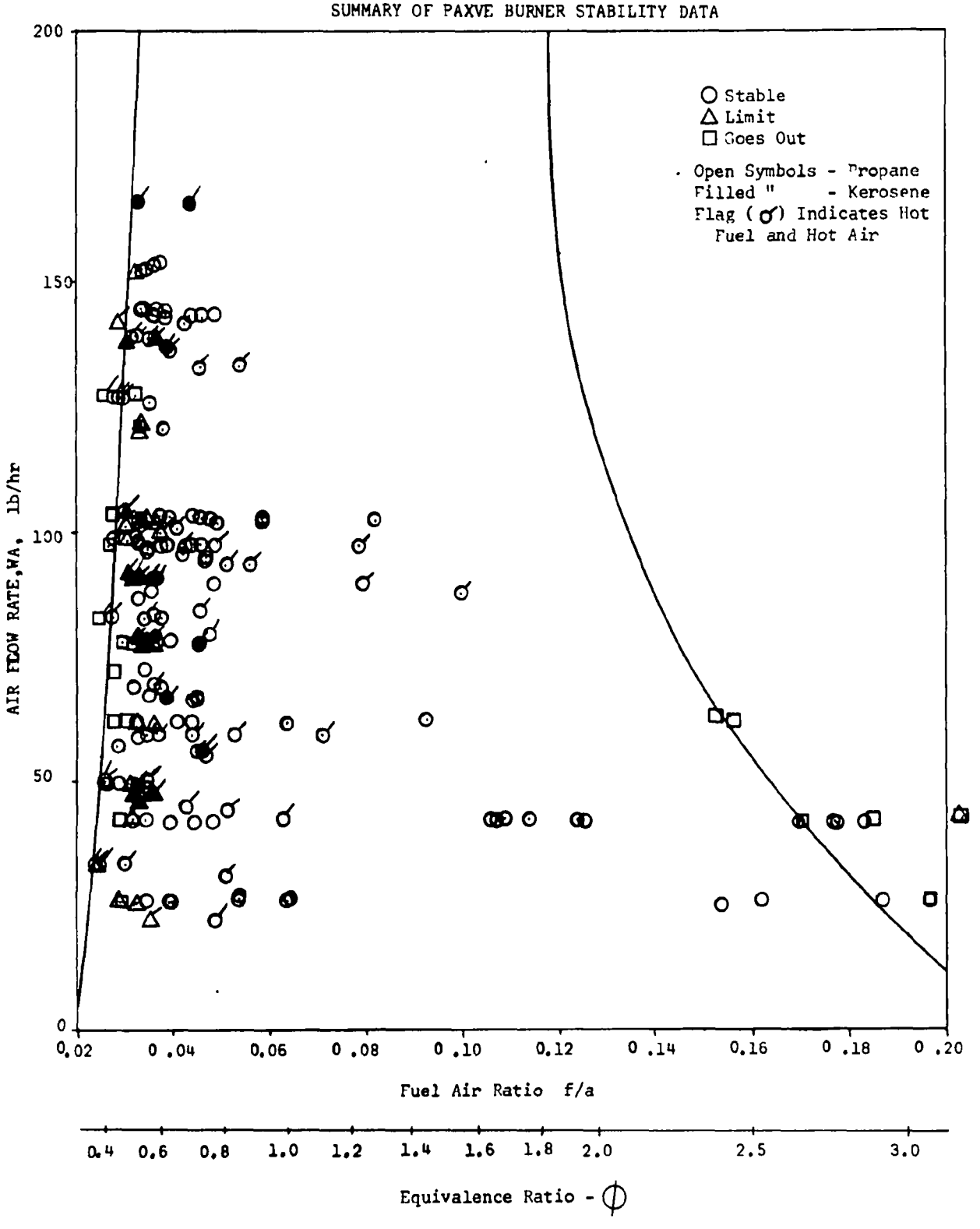
SUMMARY OF PAXVE BURNER STABILITY DATA
Stable
Limit
Goes Out
Open Symbols - Propane
Filled " - Kerosene
Flag (♂) Indicates Hot Fuel and Hot Air
AIR FLOW RATE, WA, lb/hr
200
150
100
50
0
0.02
0.04
0.06
0.08
0.10
0.12
0.14
0.16
0.18
0.20
Fuel Air Ratio f/a
0.4
0.6
0.8
1.0
1.2
1.4
1.6
1.8
2.0
2.5
3.0
Equivalence Ratio - ϕ

Fig VI
26

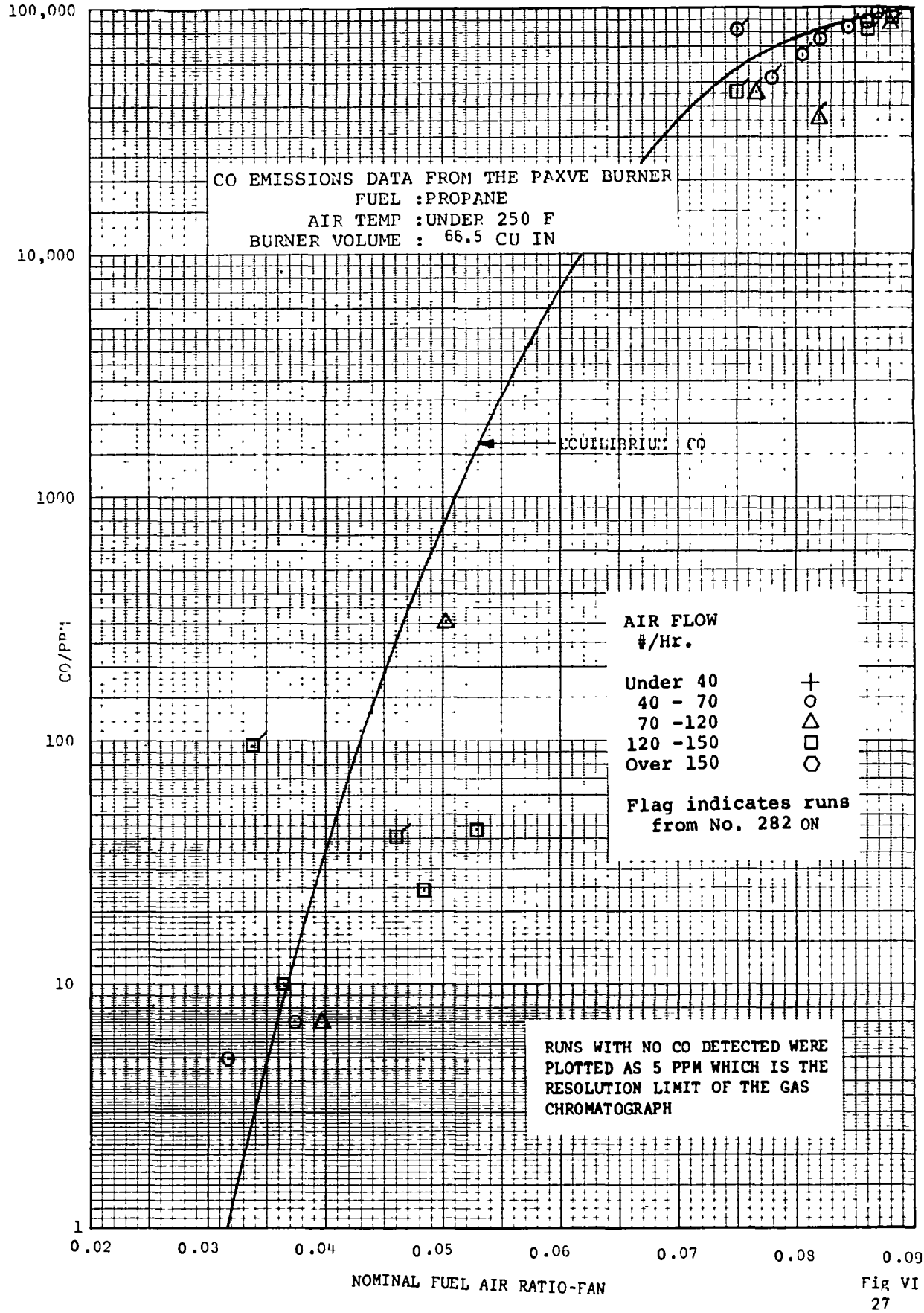
CO EMISSIONS DATA FROM THE PAXVE BURNER
FUEL :PROPANE
AIR TEMP :UNDER 250 F
BURNER VOLUME : 66.5 CU IN
EQUILIBRIUM CO
AIR FLOW #/Hr.
Under 40
40 - 70
70 -120
120 -150
Over 150
Flag indicates runs from No. 282 ON
RUNS WITH NO CO DETECTED WERE PLOTTED AS 5 PPM WHICH IS THE RESOLUTION LIMIT OF THE GAS CHROMATOGRAPH
CO/PPM
100,000
10,000
1000
100
10
1
0.02
0.03
0.04
0.05
0.06
0.07
0.08
0.09
NOMINAL FUEL AIR RATIO-FAN

Fig VI
27

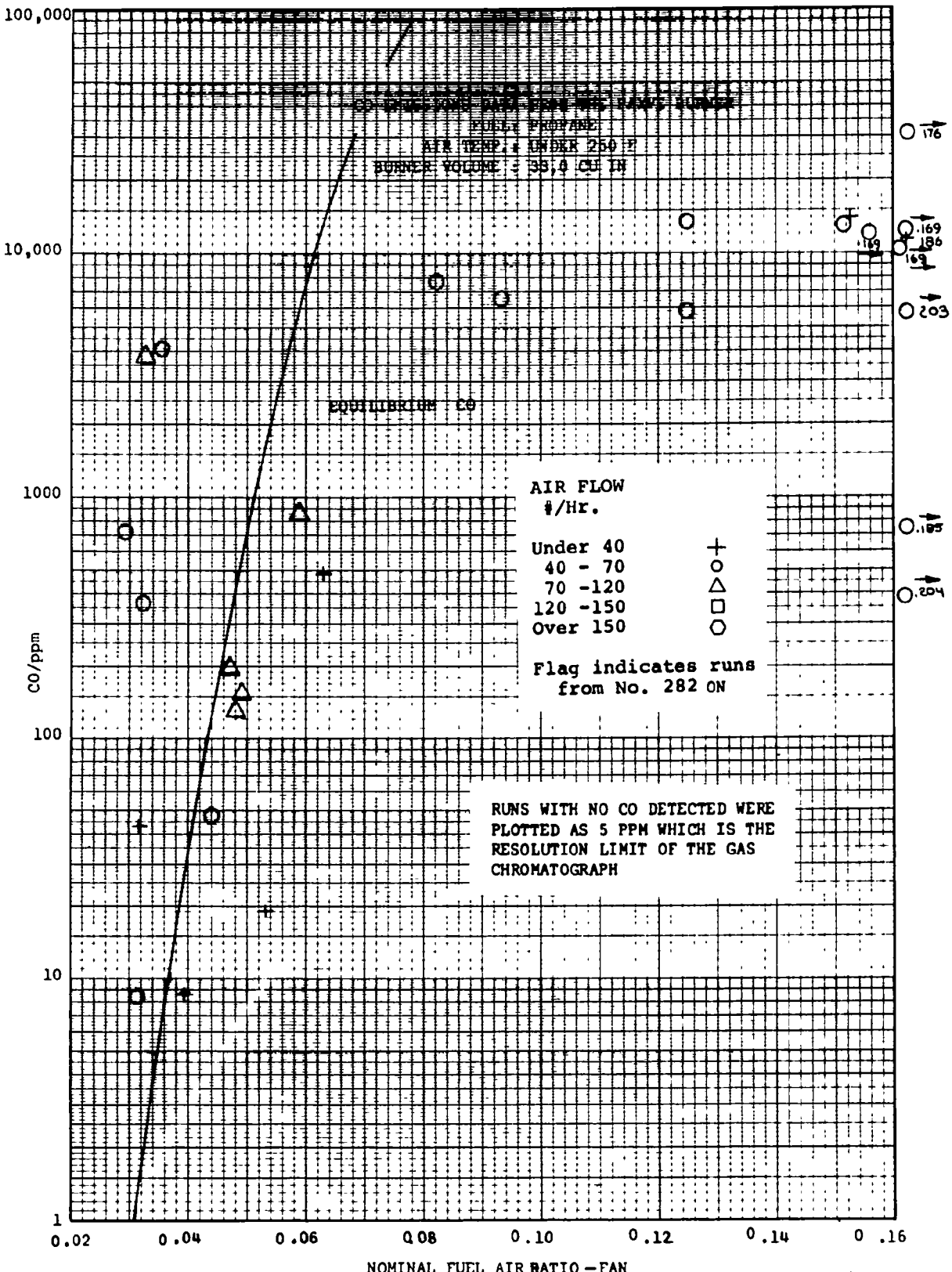
100,000
10,000
1000
100
10
1
CO/ppm
FUEL: PROPANE
AIR TEMP.: UNDER 250 F
BURNER VOLUME = 35.0 CU IN
EQUILIBRIUM CO
AIR FLOW
#/Hr.
Under 40
40 - 70
70 -120
120 -150
Over 150
Flag indicates runs
from No. 282 ON
RUNS WITH NO CO DETECTED WERE
PLOTTED AS 5 PPM WHICH IS THE
RESOLUTION LIMIT OF THE GAS
CHROMATOGRAPH
176
169
186
169
203
0.02
0.04
0.06
0.08
0.10
0.12
0.14
0.16
NOMINAL FUEL AIR RATIO — FAN

Figure
VI-28

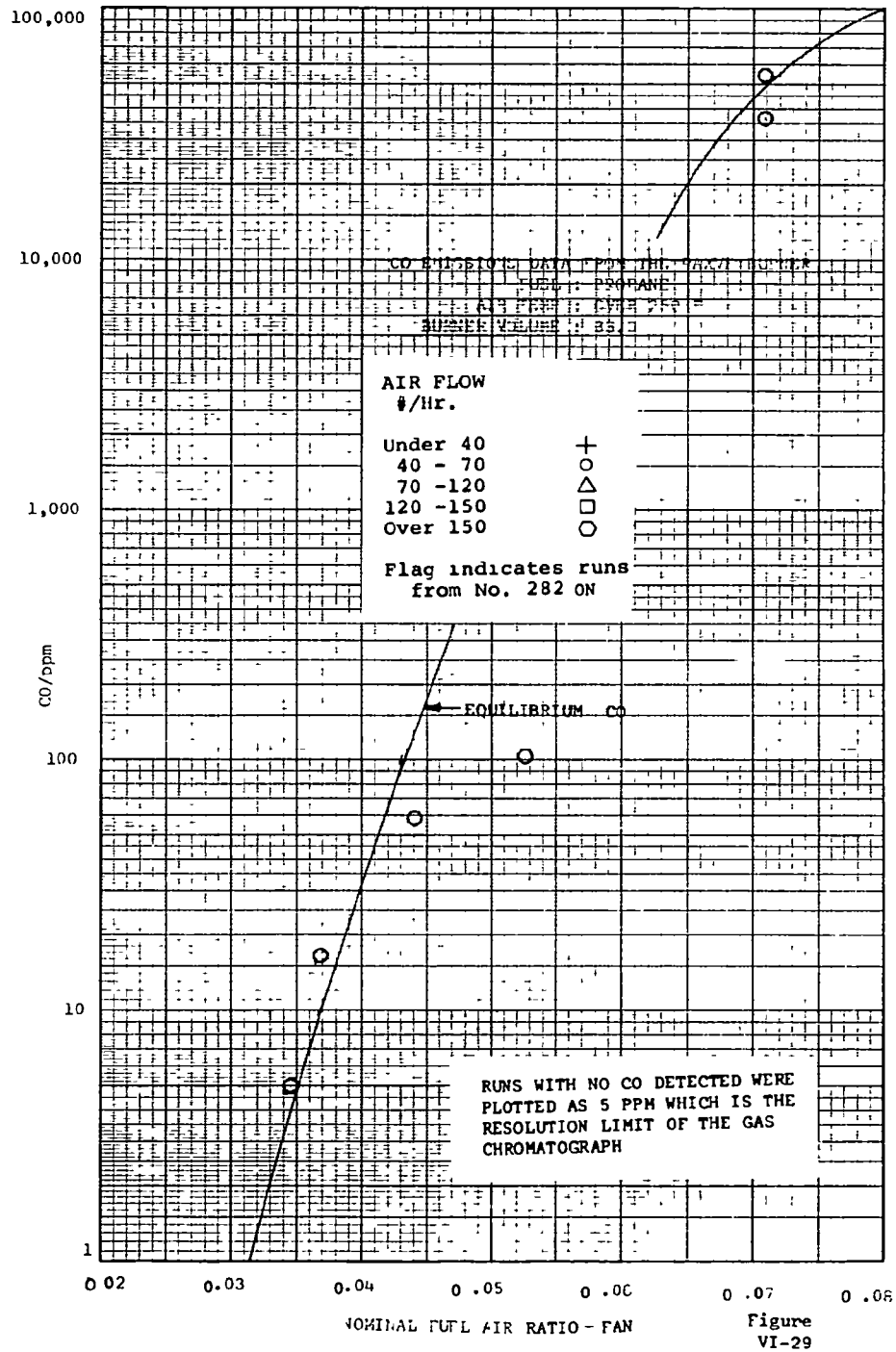

Figure VI-29

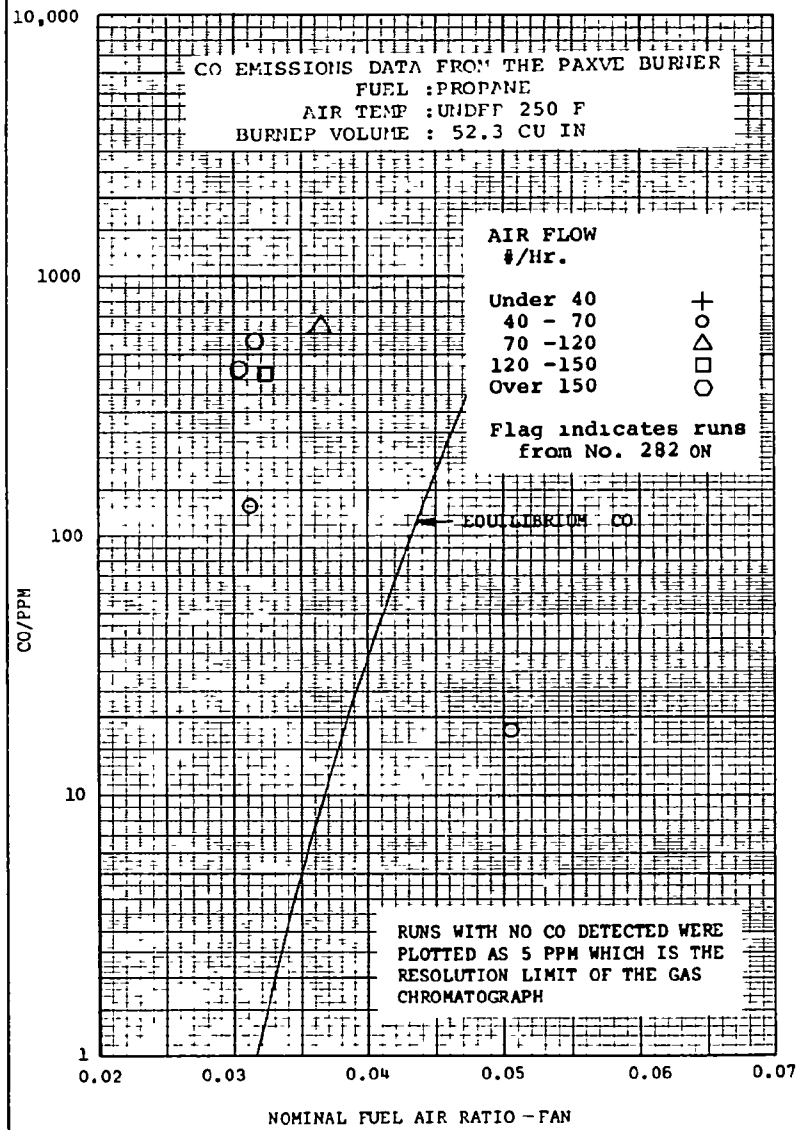

Figure VI-30

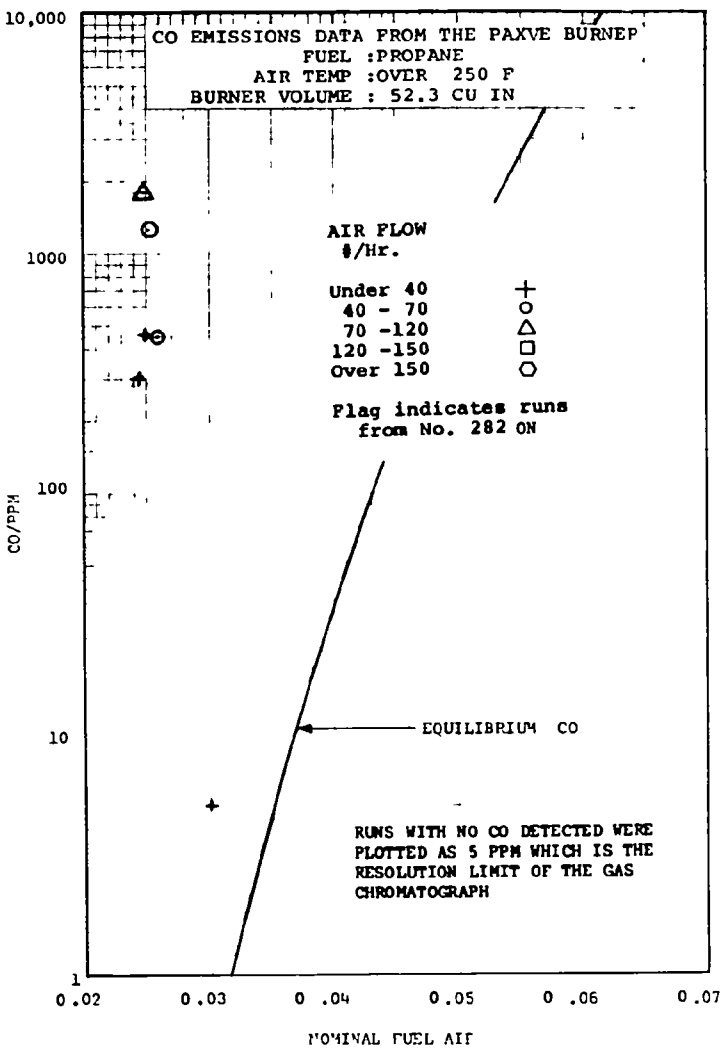

Figure VI-31

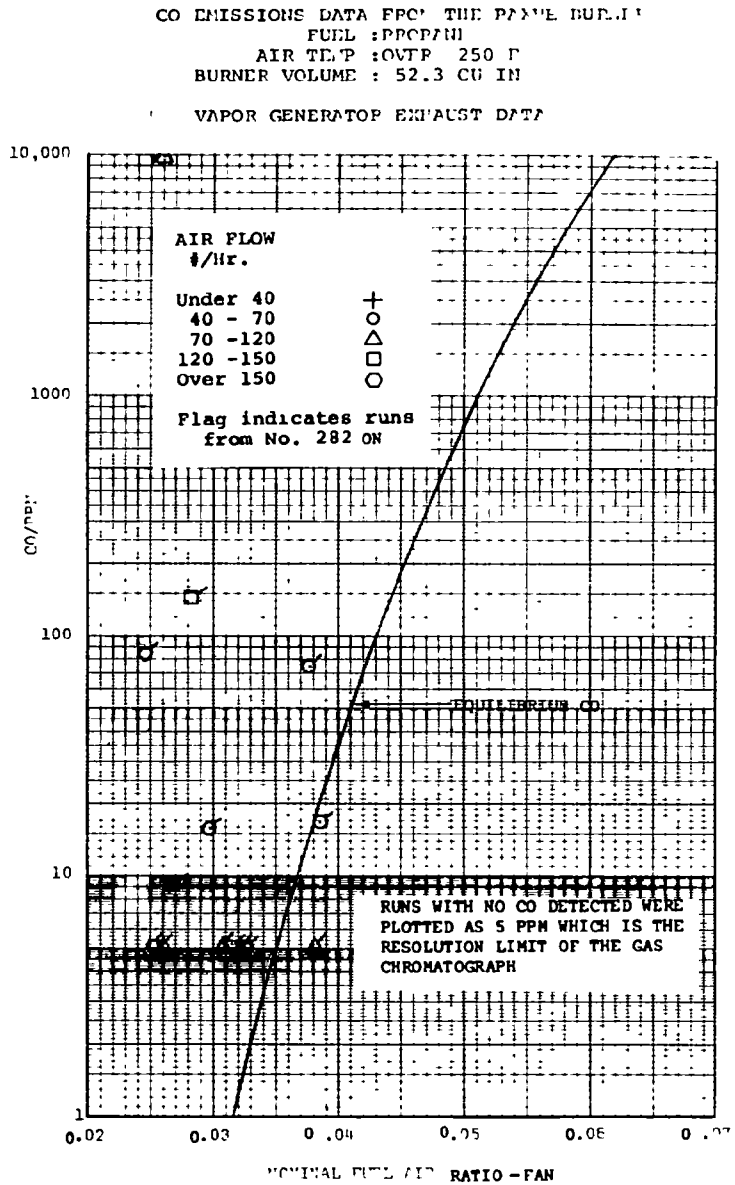

Figure VI-32

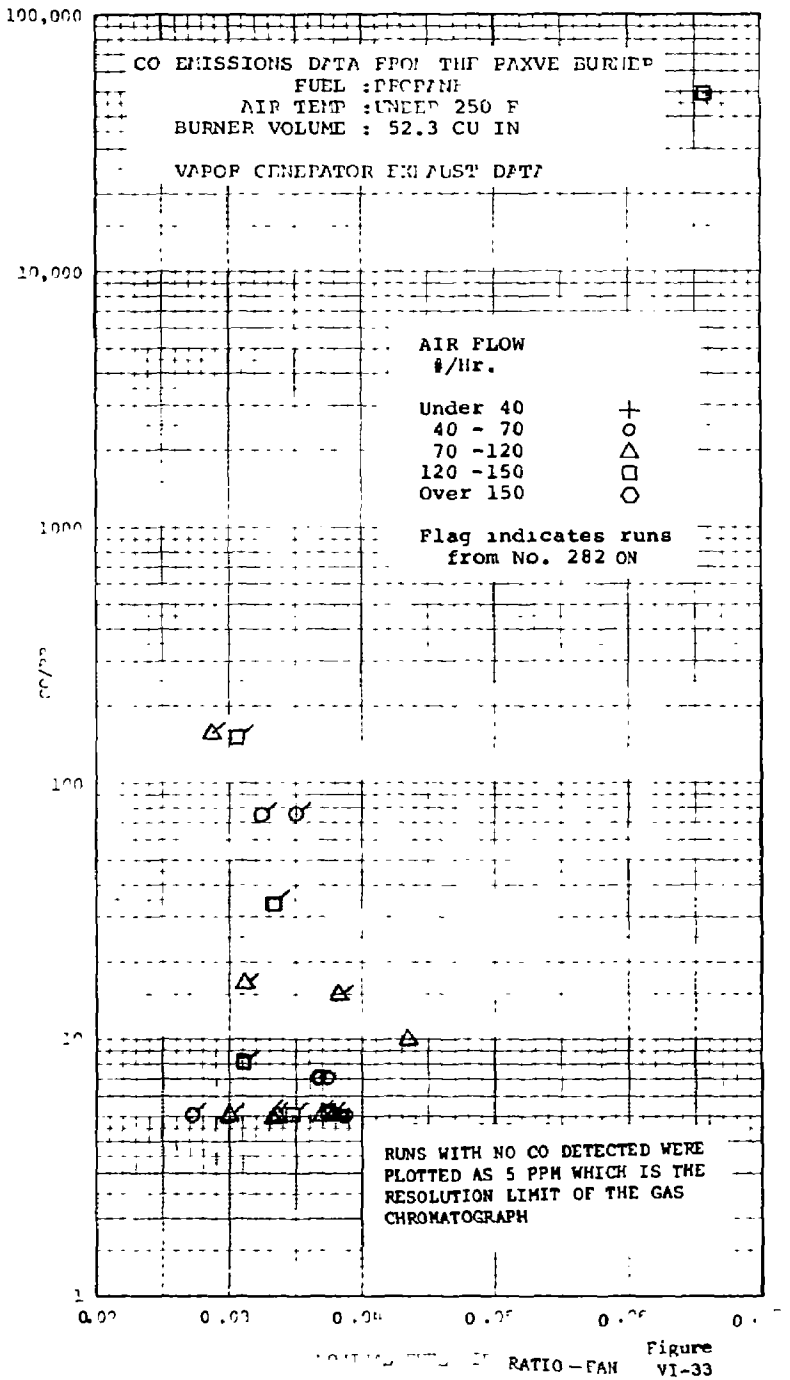

Figure VI-33

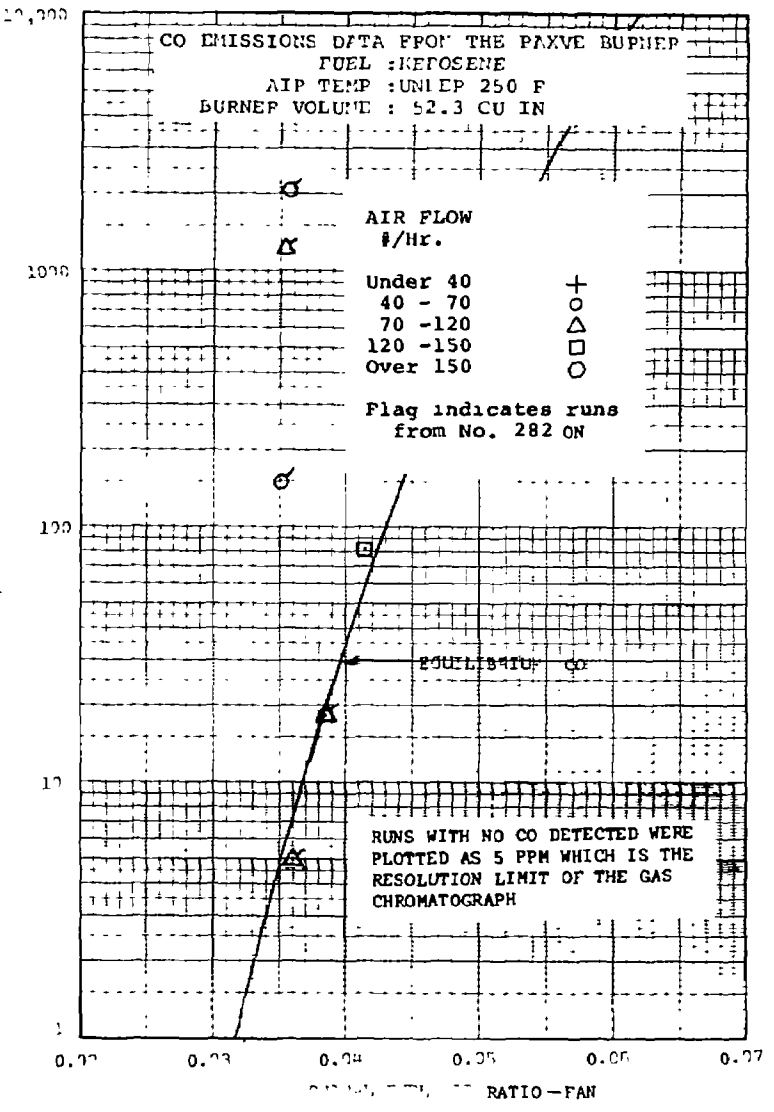

Figure VI-34

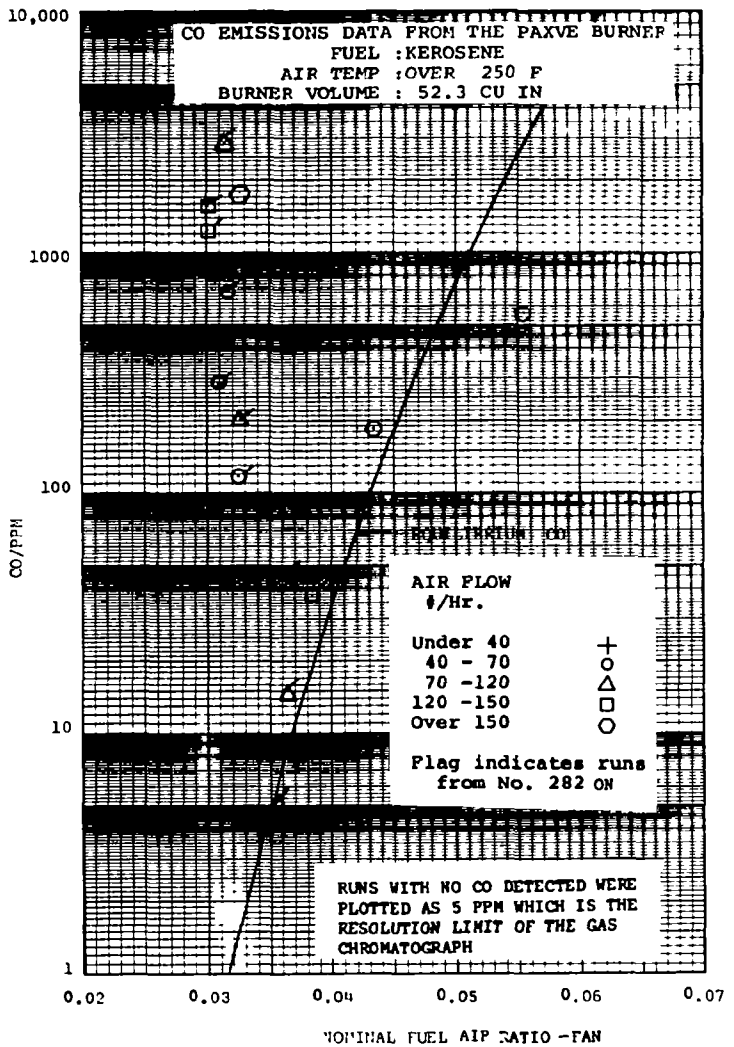

Figure
VI-35

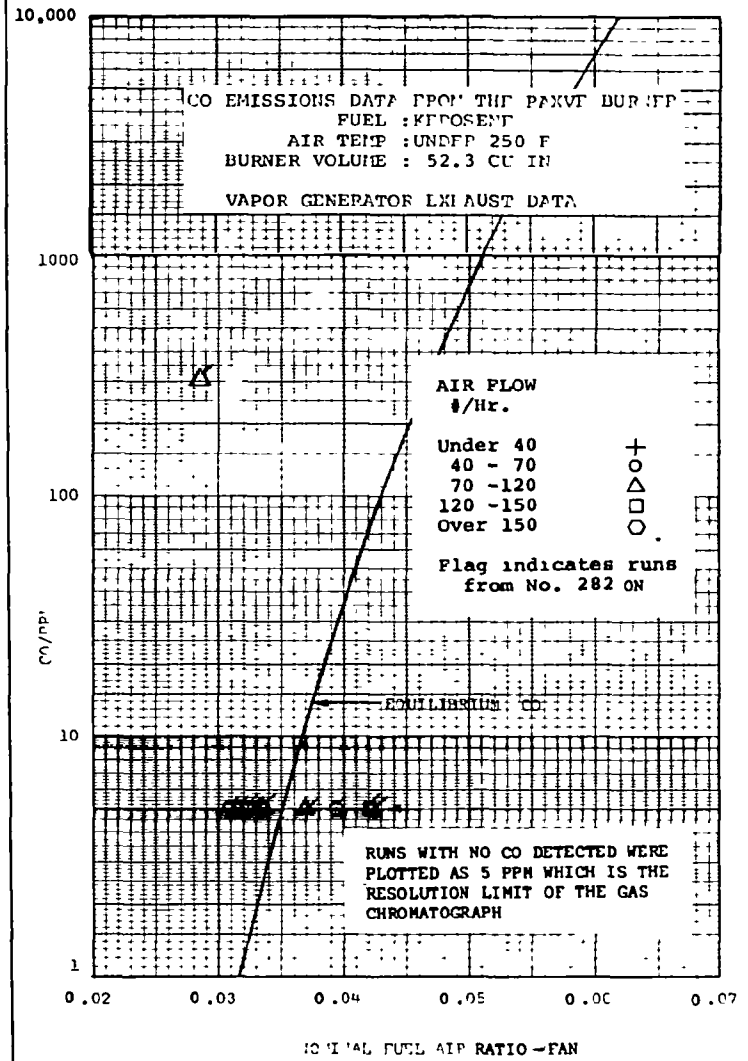

Figure
VI-36

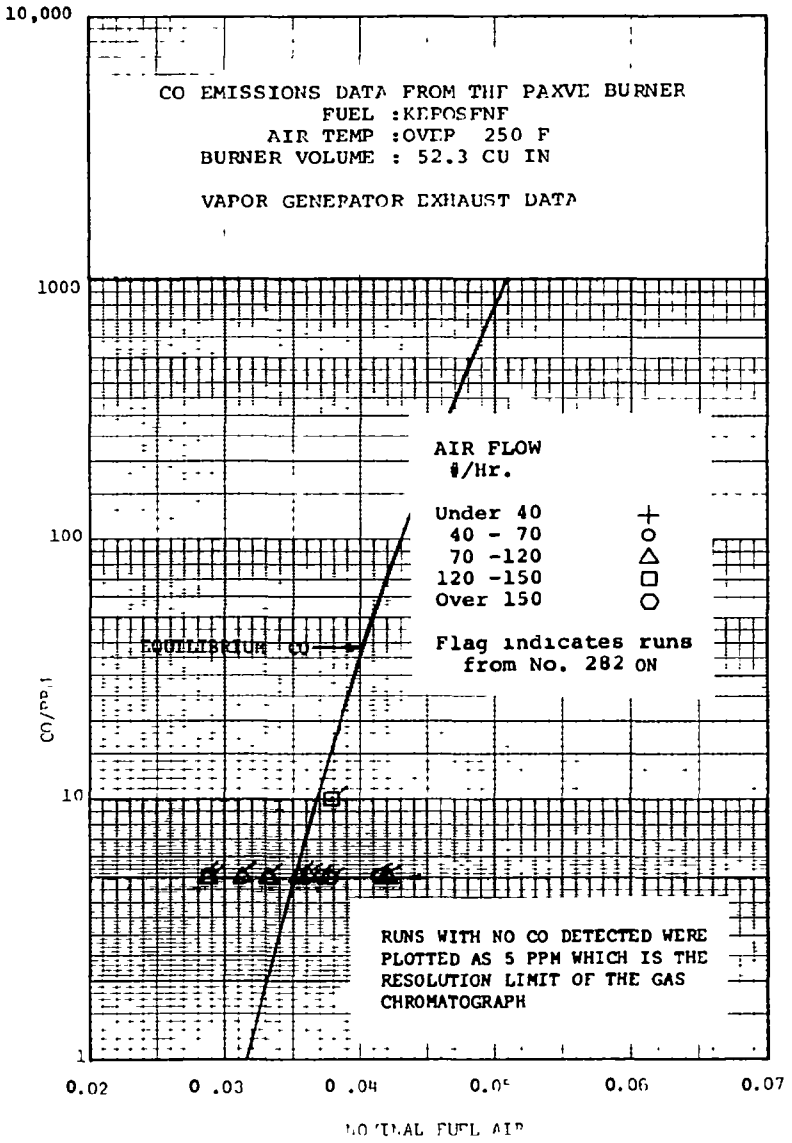

Figure VI-37

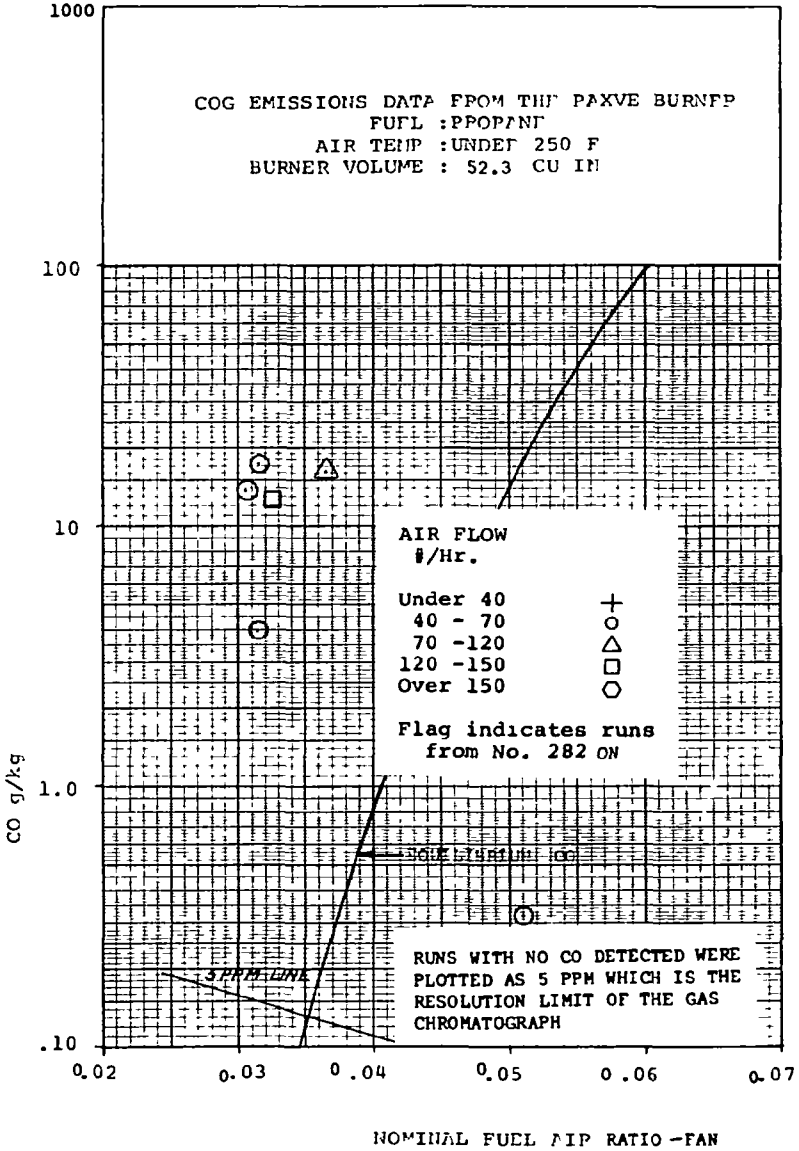

Figure VI-38

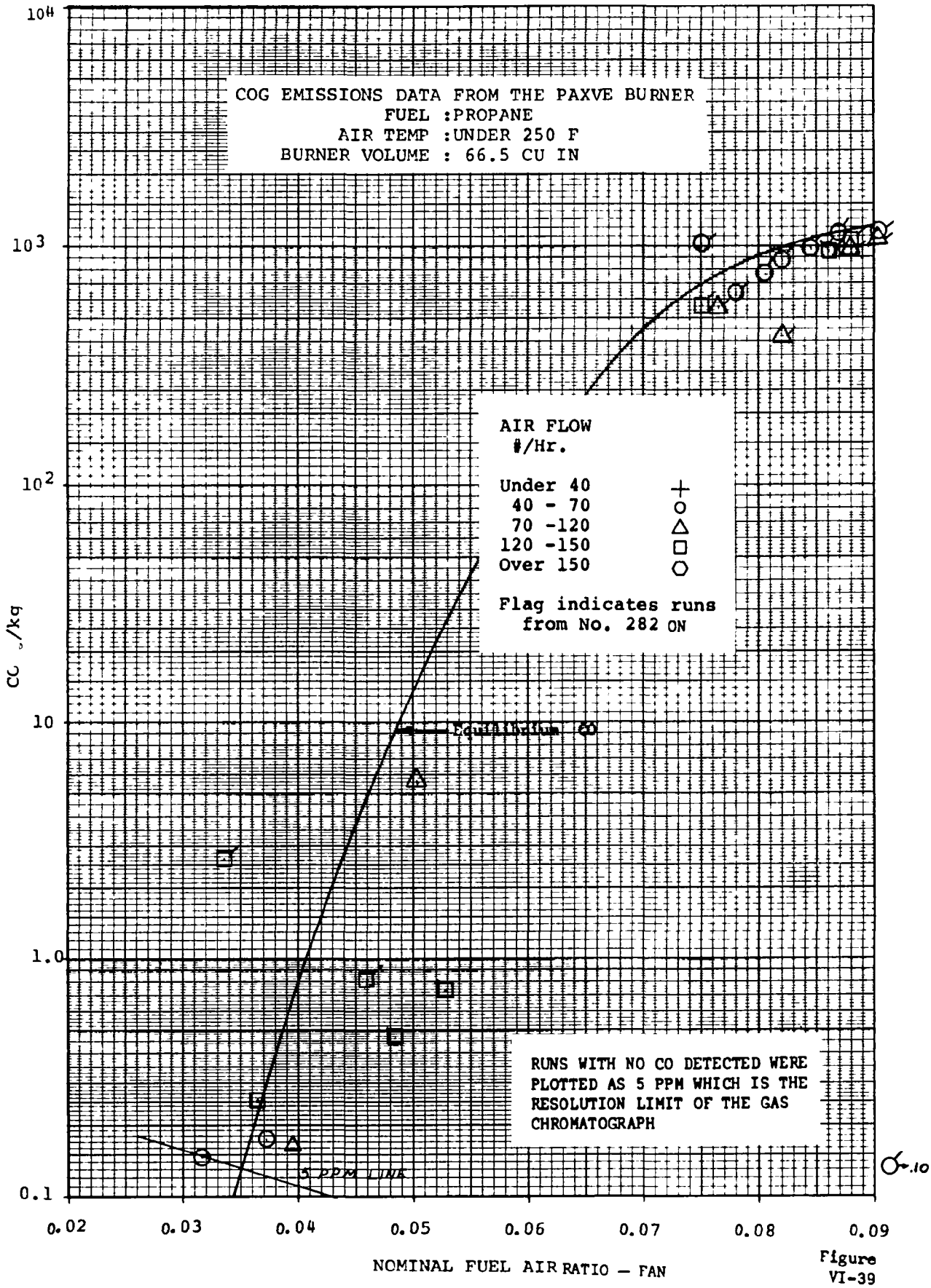
COG EMISSIONS DATA FROM THE PAXVE BURNER
FUEL :PROPANE
AIR TEMP :UNDER 250 F
BURNER VOLUME : 66.5 CU IN
AIR FLOW #/Hr.
Under 40 +
40 - 70 ○
70 -120 △
120 -150 □
Over 150 ○
Flag indicates runs from No. 282 ON
Equilibrium CO
5 PPM LINK
RUNS WITH NO CO DETECTED WERE PLOTTED AS 5 PPM WHICH IS THE RESOLUTION LIMIT OF THE GAS CHROMATOGRAPH
CO /kg
NOMINAL FUEL AIR RATIO — FAN
10⁴
10³
10²
10
1.0
0.1
0.02
0.03
0.04
0.05
0.06
0.07
0.08
0.09

Figure VI-39

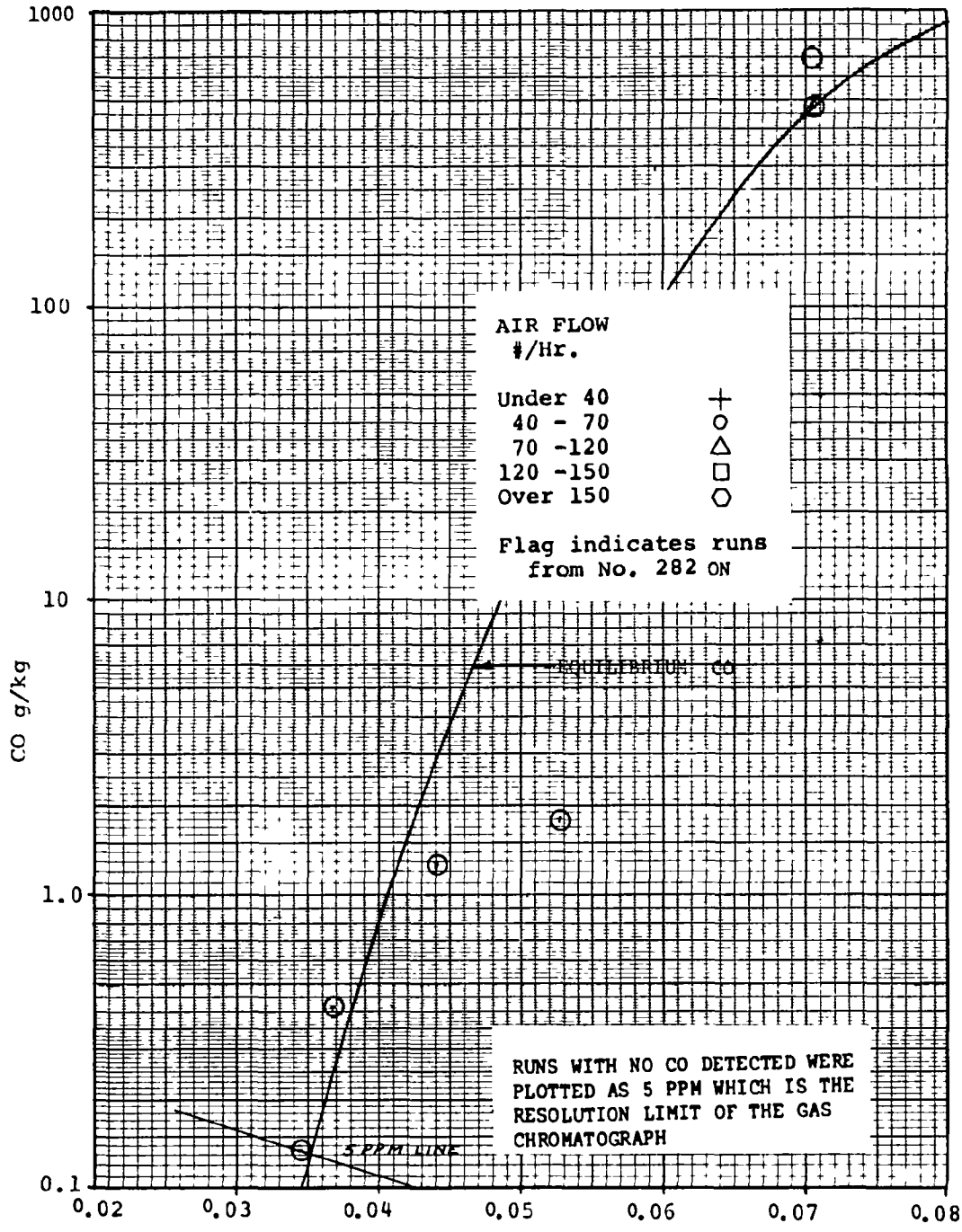

COG EMISSIONS DATA FROM THE PAXVE BURNER
FUEL :PROPANE
AIR TEMP :OVER 250 F
BURNER VOLUME : 33.0 CU IN

Figure
VI-40

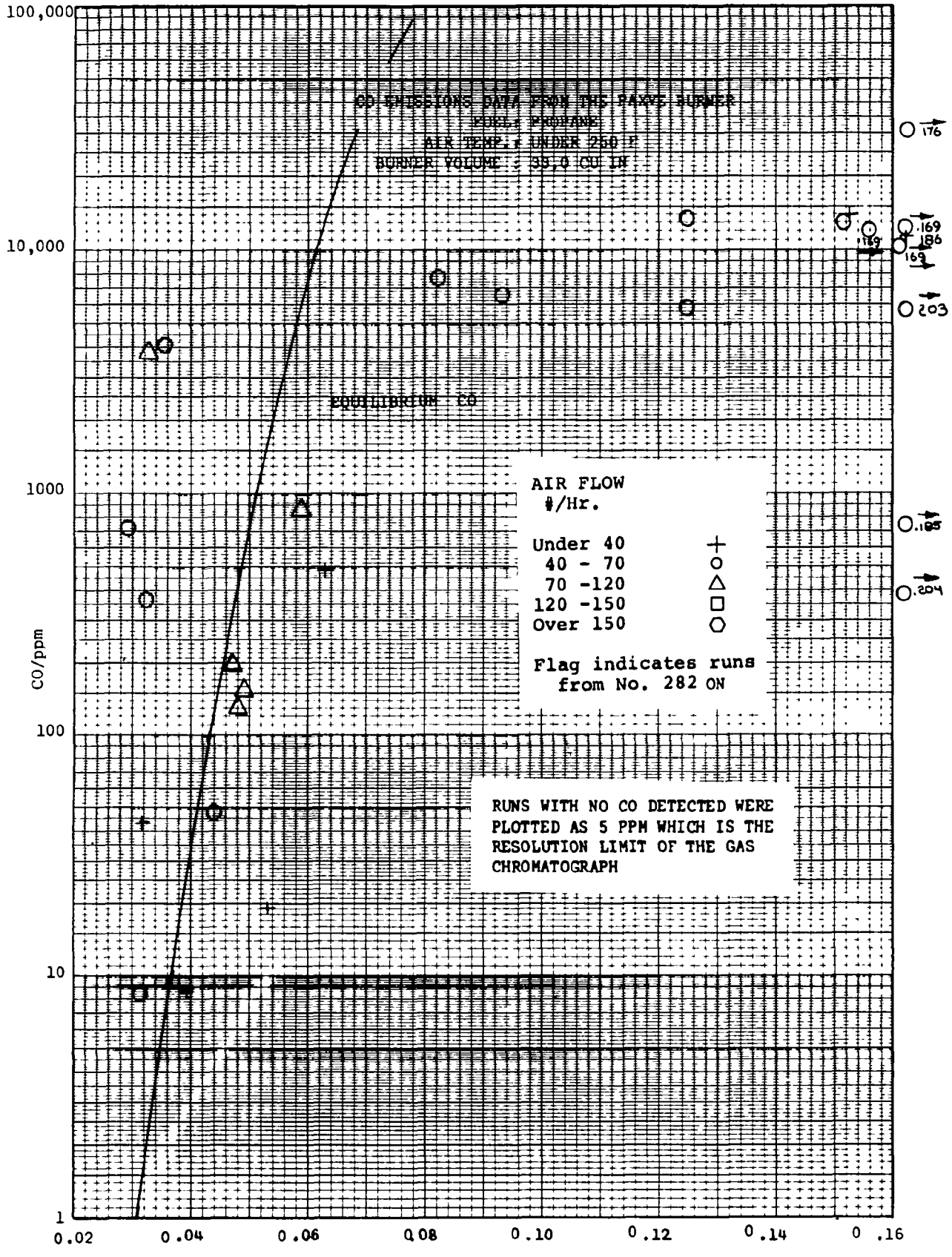
CO EMISSIONS DATA FROM THE RAYVE BURNER
FUEL: PROPANE
AIR TEMP.: UNDER 250 F
BURNER VOLUME : 35.0 CU IN
EQUILIBRIUM CO
AIR FLOW #/Hr.
Under 40
40 - 70
70 -120
120 -150
Over 150
Flag indicates runs from No. 282 ON
RUNS WITH NO CO DETECTED WERE PLOTTED AS 5 PPM WHICH IS THE RESOLUTION LIMIT OF THE GAS CHROMATOGRAPH
CO/ppm
100,000
10,000
1000
100
10
1
0.02
0.04
0.06
0.08
0.10
0.12
0.14
0.16
NOMINAL FUEL AIR RATIO — FAN
176
169
186
169
203
185
204

Figure VI-41

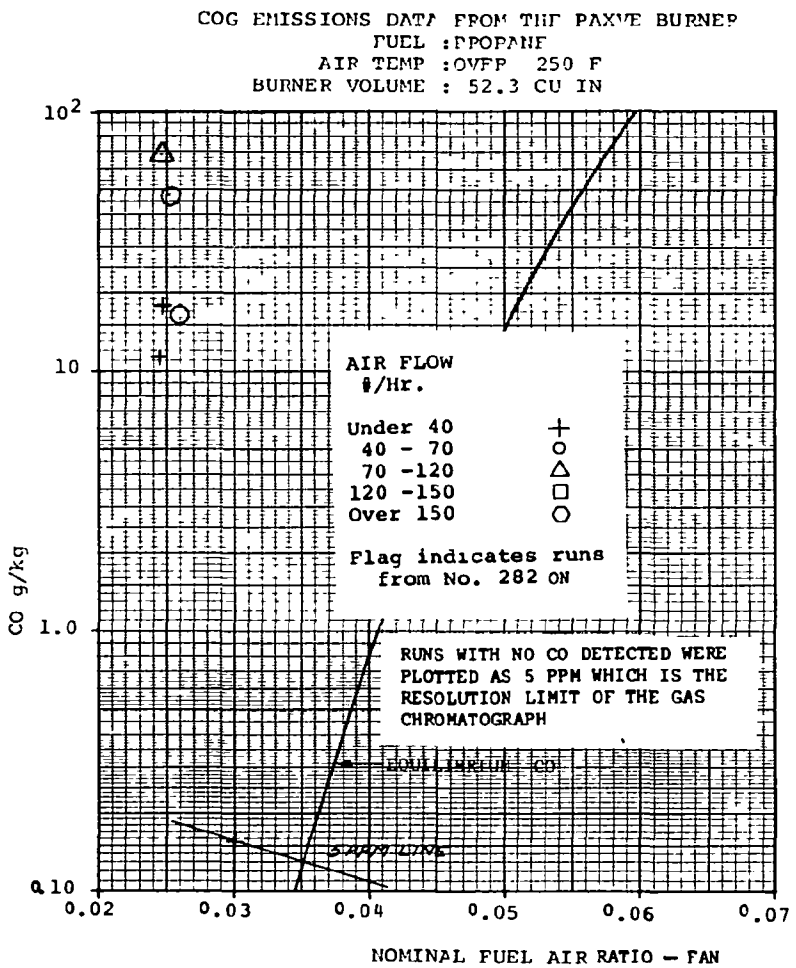

Figure VI-42

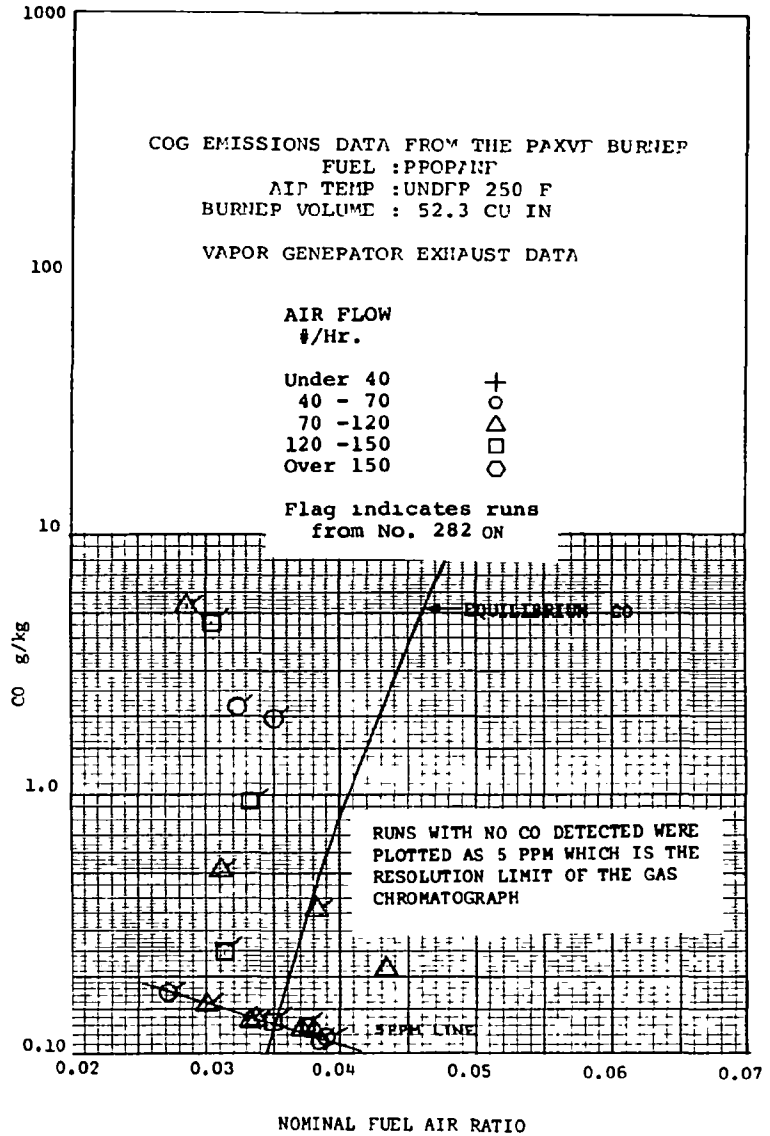

Figure VI-43

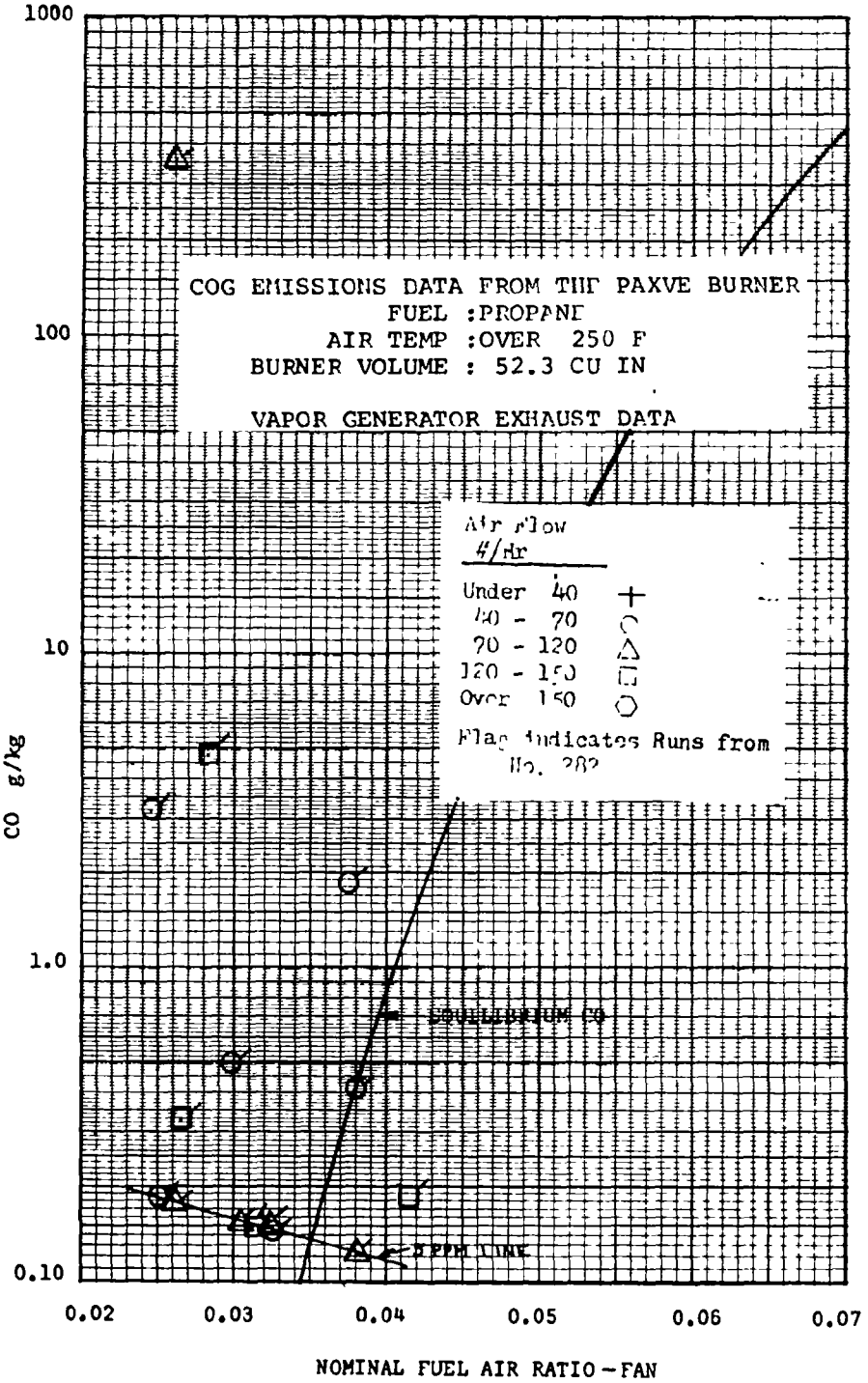
COG EMISSIONS DATA FROM THE PAXVE BURNER
FUEL :PROPANE
AIR TEMP :OVER 250 F
BURNER VOLUME : 52.3 CU IN
VAPOR GENERATOR EXHAUST DATA
Air Flow
#/Hr
Under 40
40 - 70
70 - 120
120 - 150
Over 150
Flag Indicates Runs from
No. 282
EQUILIBRIUM CO
2 PPM LINE
CO g/kg
1000
100
10
1.0
0.10
0.02
0.03
0.04
0.05
0.06
0.07
NOMINAL FUEL AIR RATIO - FAN

Figure
VI-44

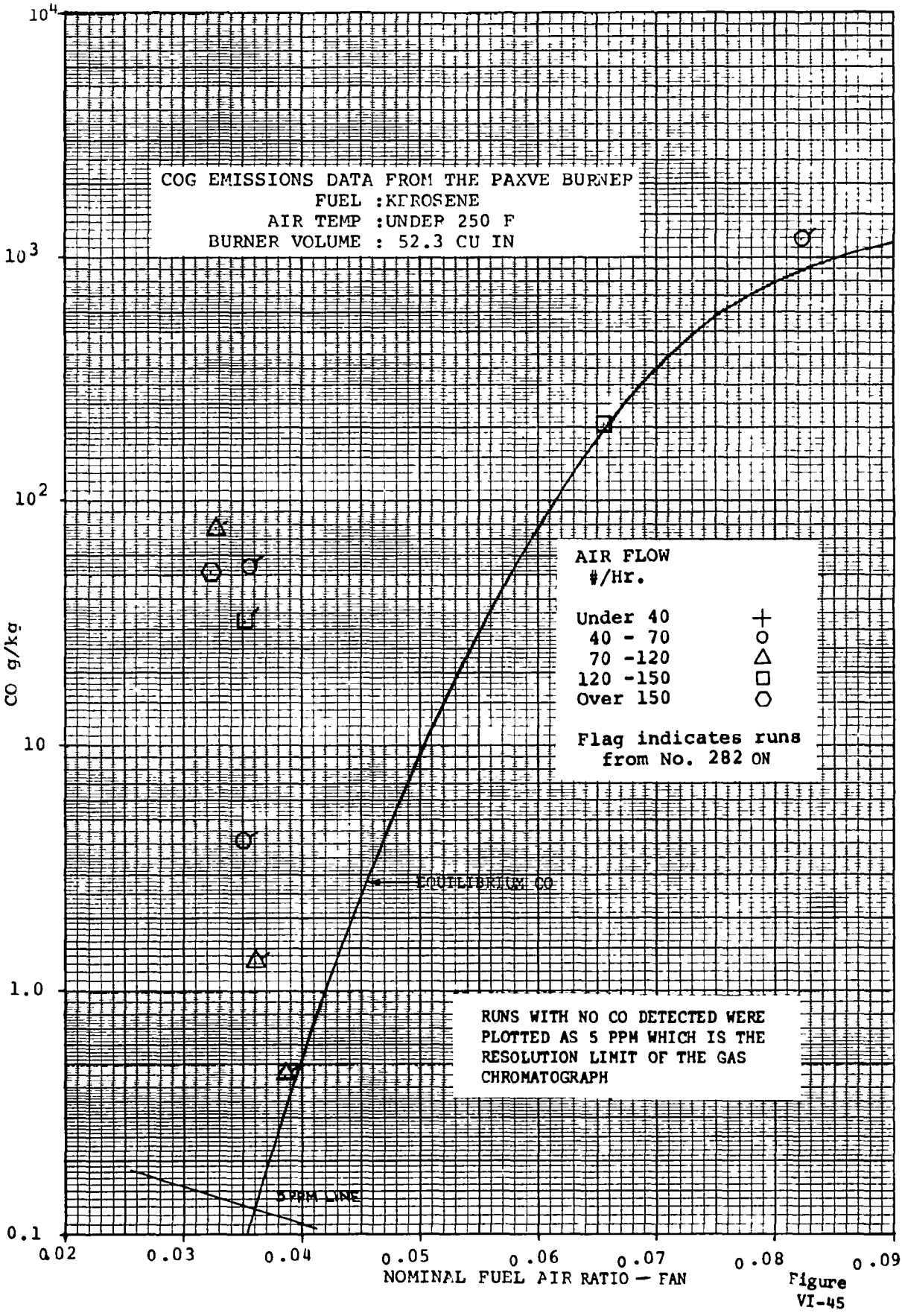
COG EMISSIONS DATA FROM THE PAXVE BURNER
FUEL :KEROSENE
AIR TEMP :UNDER 250 F
BURNER VOLUME : 52.3 CU IN
AIR FLOW #/Hr.
Under 40 +
40 - 70 o
70 -120 △
120 -150 □
Over 150 ○
Flag indicates runs from No. 282 ON
EQUILIBRIUM CO
RUNS WITH NO CO DETECTED WERE PLOTTED AS 5 PPM WHICH IS THE RESOLUTION LIMIT OF THE GAS CHROMATOGRAPH
5PPM LINE
CO g/kg
10^4
10^3
10^2
10
1.0
0.1
0.02
0.03
0.04
0.05
0.06
0.07
0.08
0.09
NOMINAL FUEL AIR RATIO — FAN

Figure VI-45

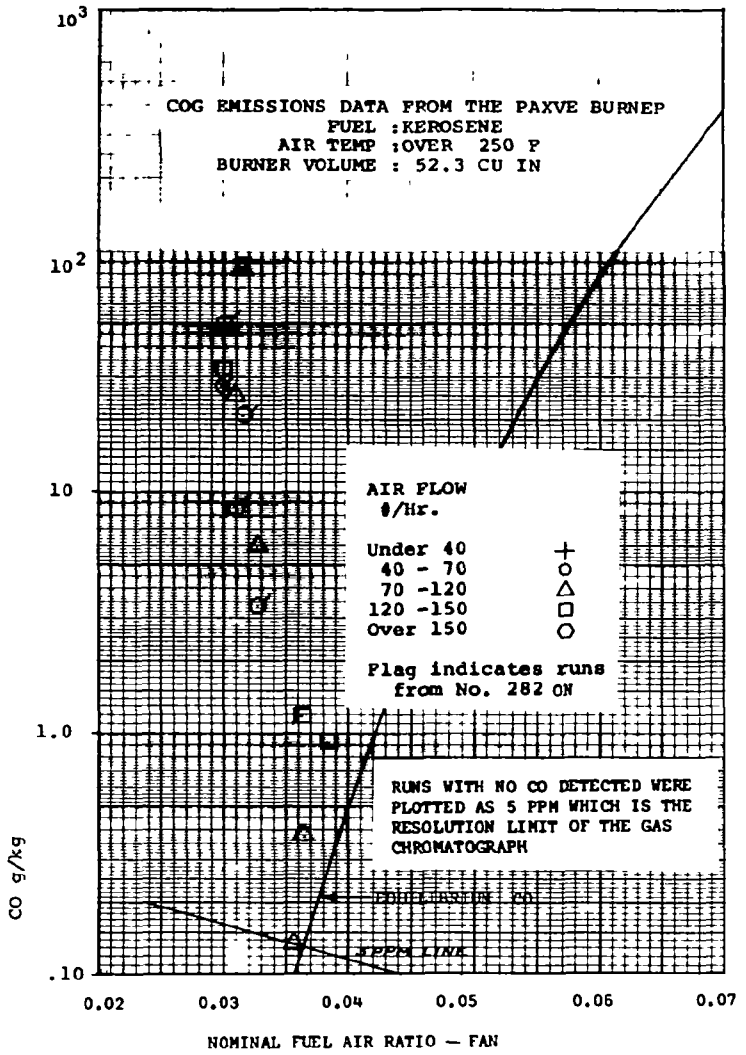

Figure VI-46

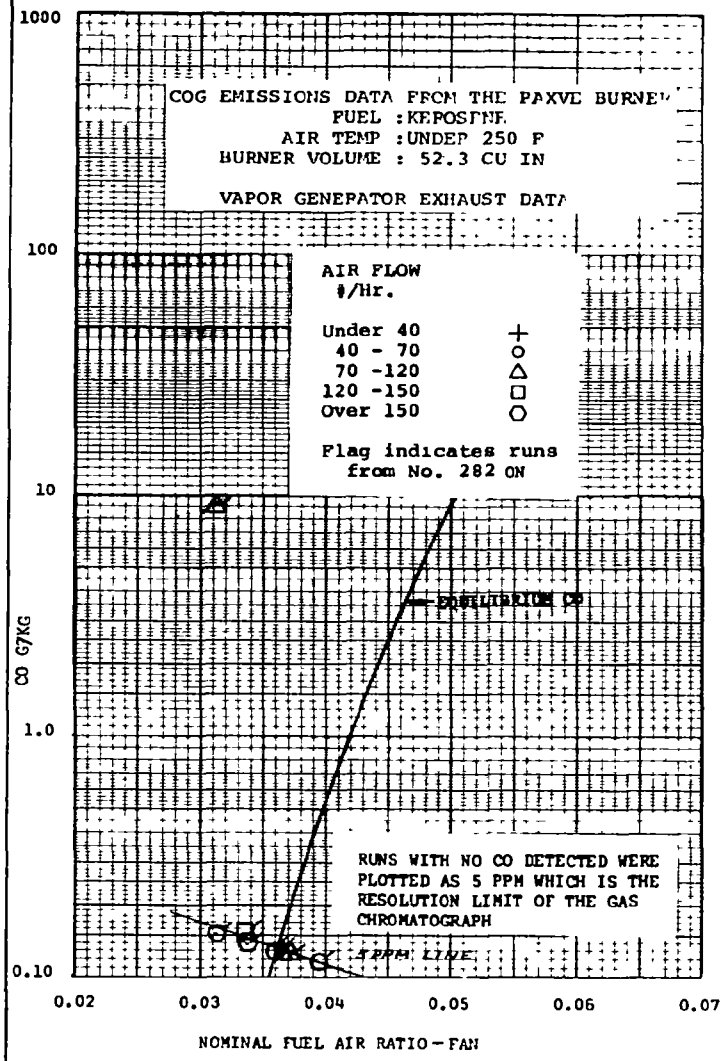

Figure VI-47

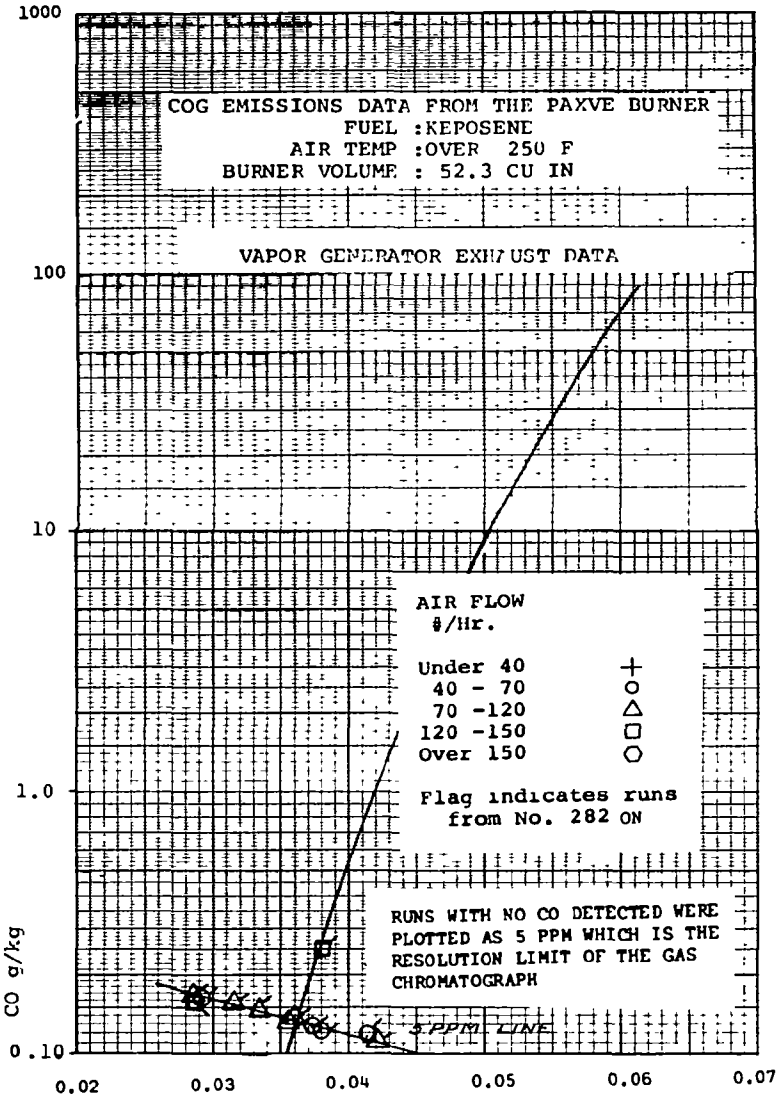

Figure VI-48

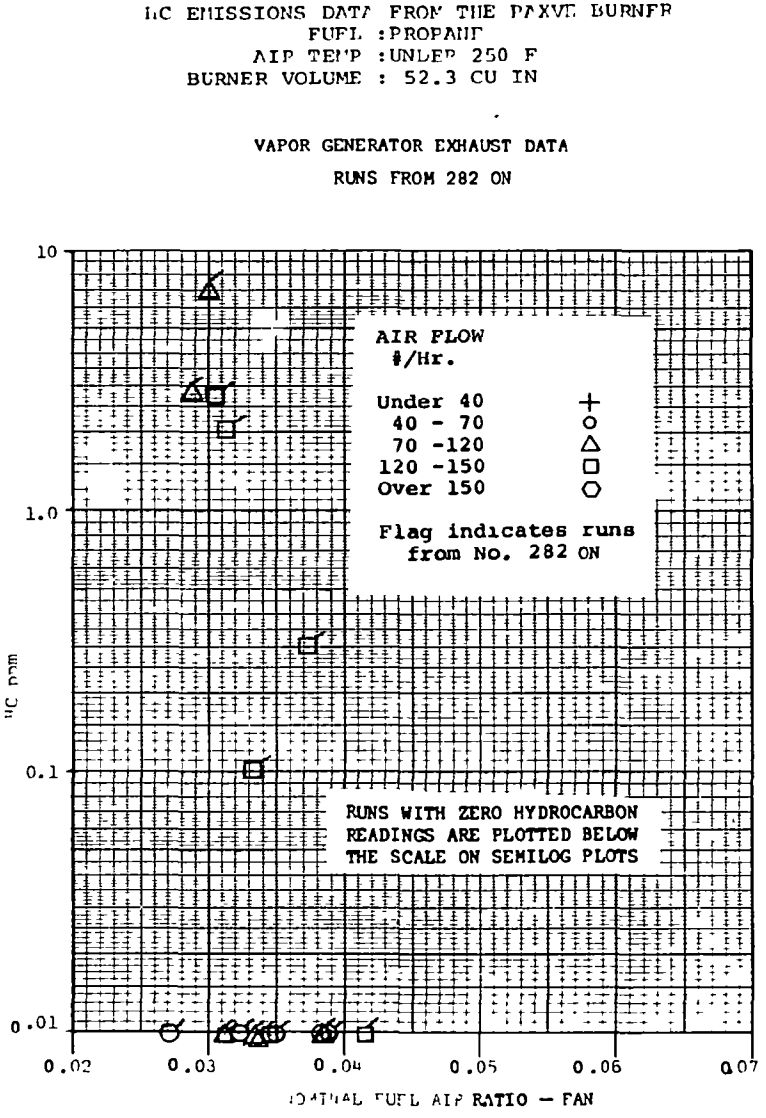

Figure VI-49

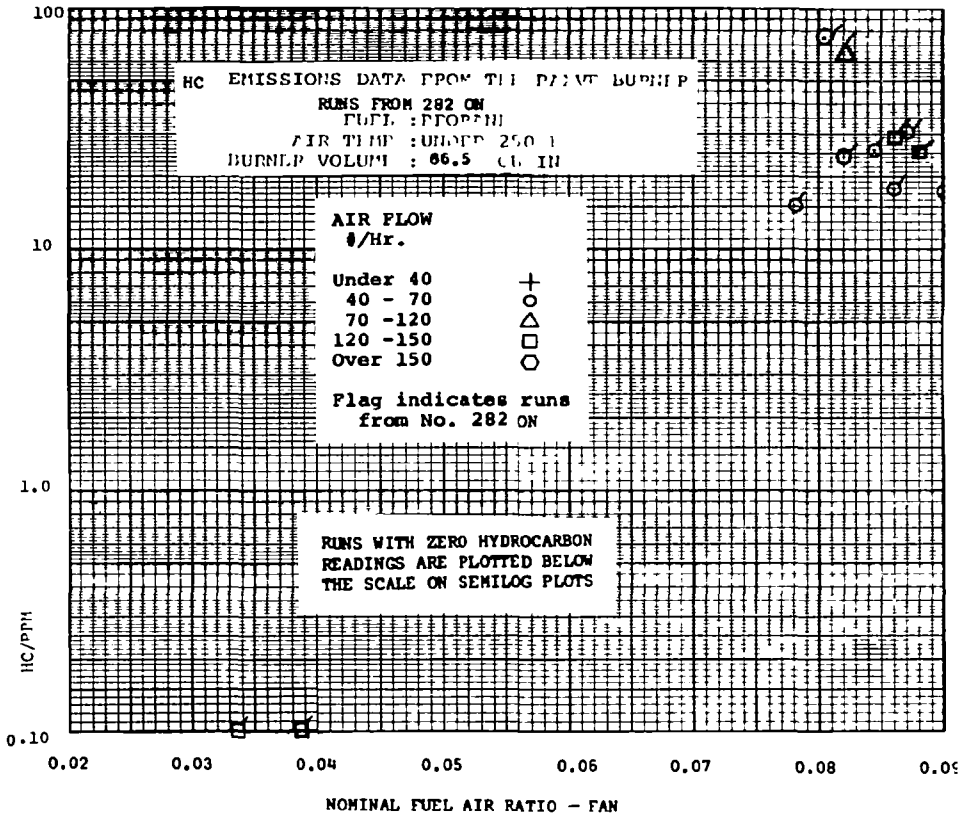

Figure
VI-50

HC EMISSIONS DATA FROM THE PAVT BURNER
FUEL :PROPANE
AIR TEMP :OVER 250 F
BURNER VOLUME : 52.3 CU IN

VAPOR GENERATOR EXHAUST DATA

RUNS FROM Nº 282 ON

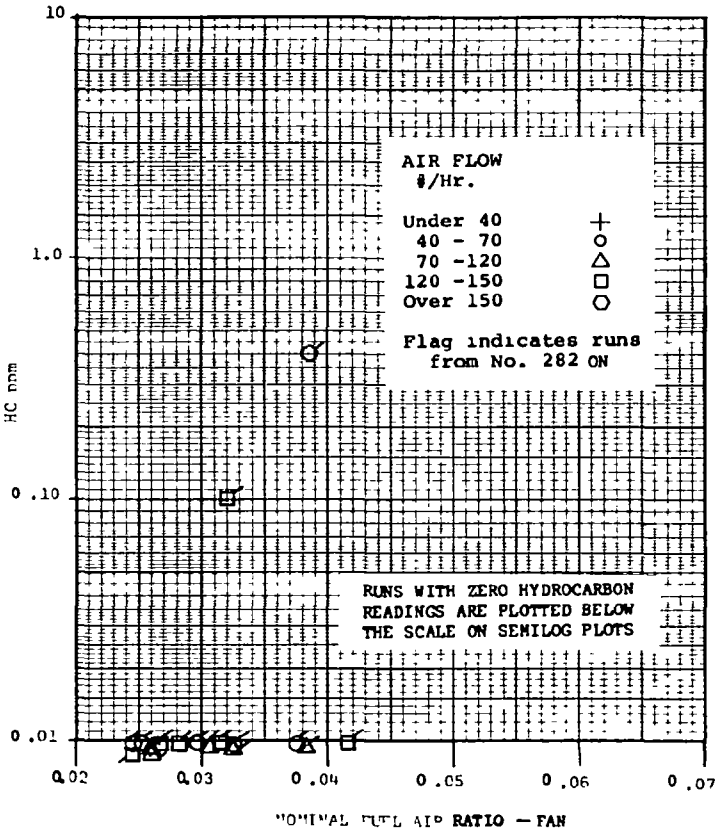

HC EMISSIONS DATA FROM THE PAXVE BURNER
FUEL :KEROSENE
AIR TEMP :UNDER 250 F
BURNER VOLUME : 52.3 CU IN

BURNER DATA
RUNS AFTER N^{o} 282

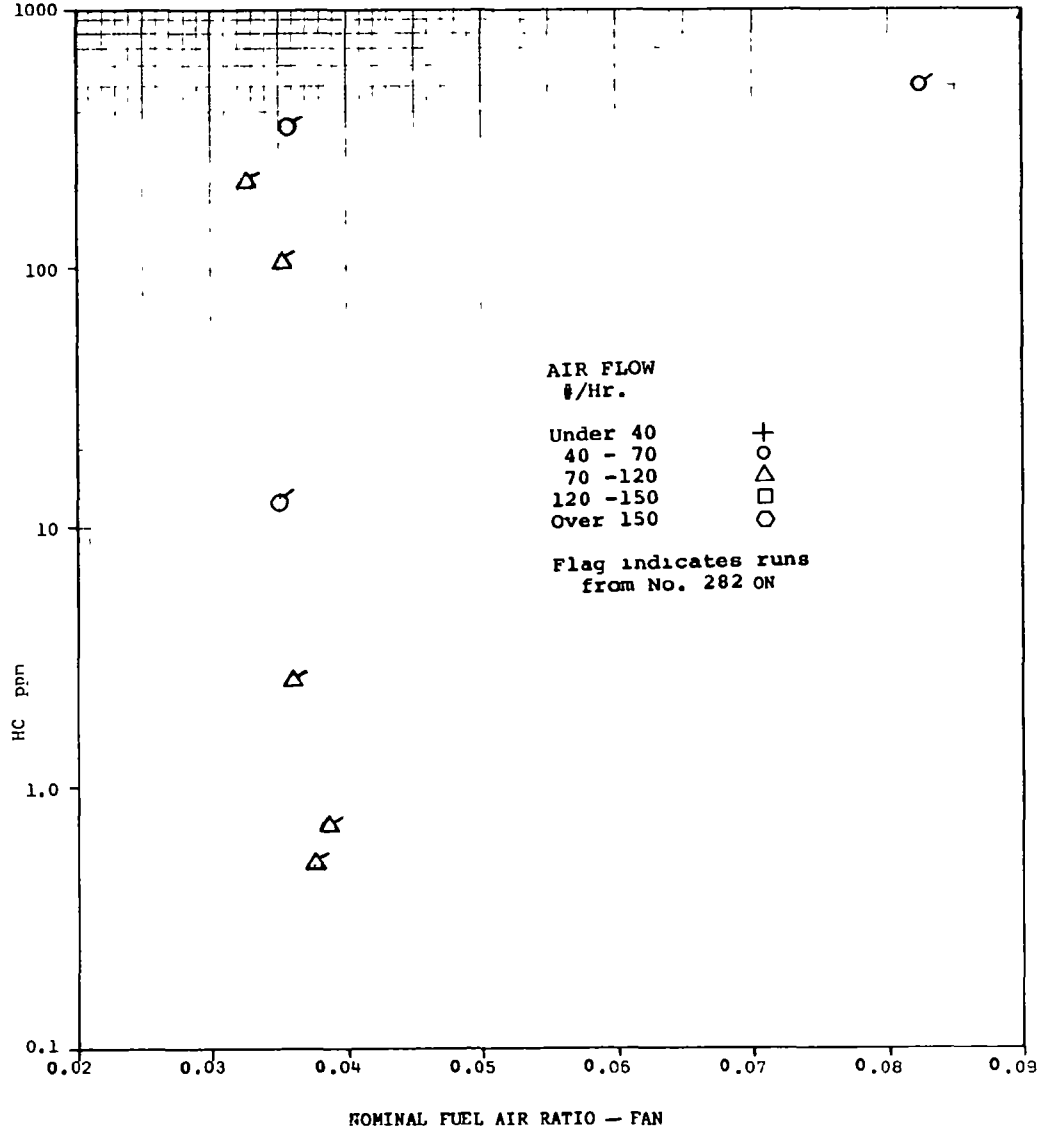

VI
Fig.52

HC EMISSIONS DATA FROM THE PAXVE BURNER
FUEL :KEROSENE
AIR TEMP :OVER 250 F
BURNER VOLUME : 52.3 CU IN

BURNER DATA
RUNS AFTER N^{o} 282

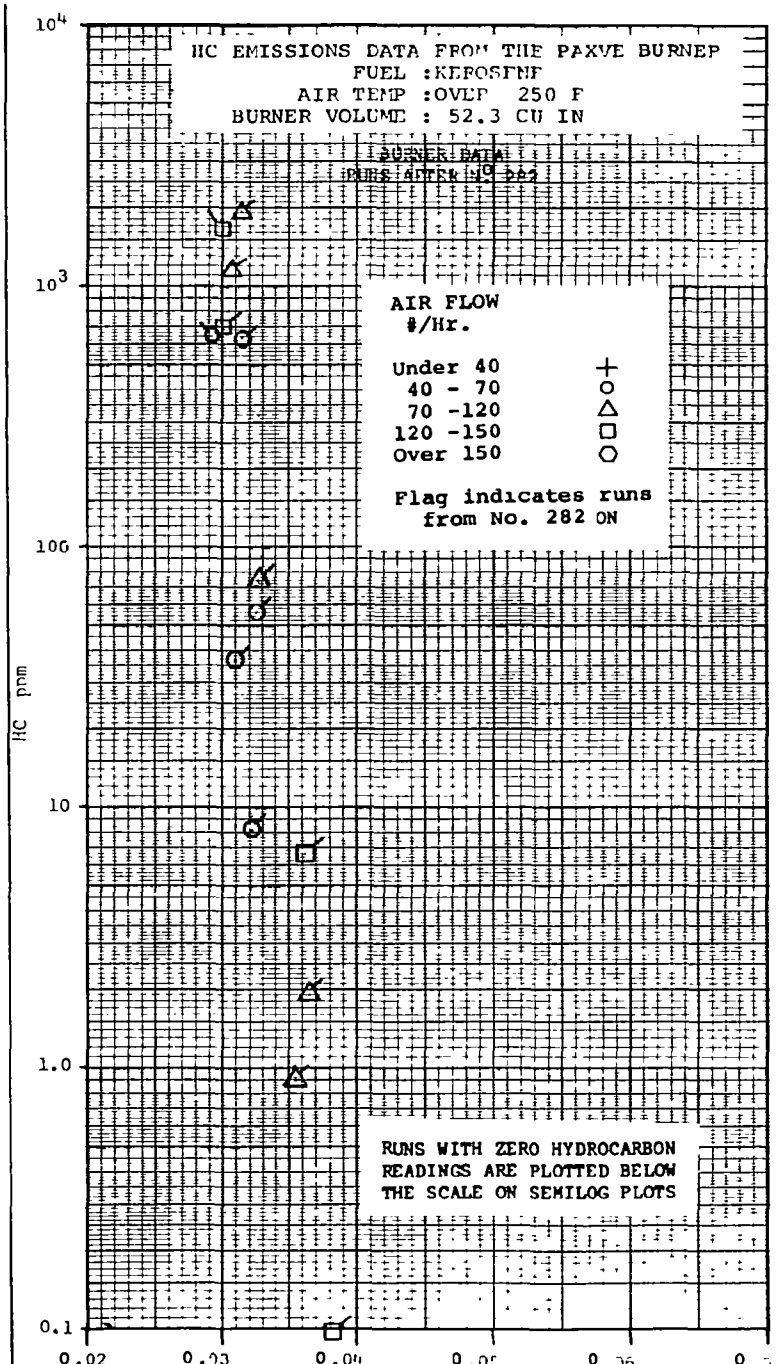

VI
Fig.53

HC EMISSIONS DATA FROM THE PAXVE BURNER
FUEL :KEROSENE
AIR TEMP :UNDER 250 F
BURNER VOLUME : 52.3 CU IN

VAPOR GENERATOR EXHAUST DATA
RUNS AFTER NO. 282

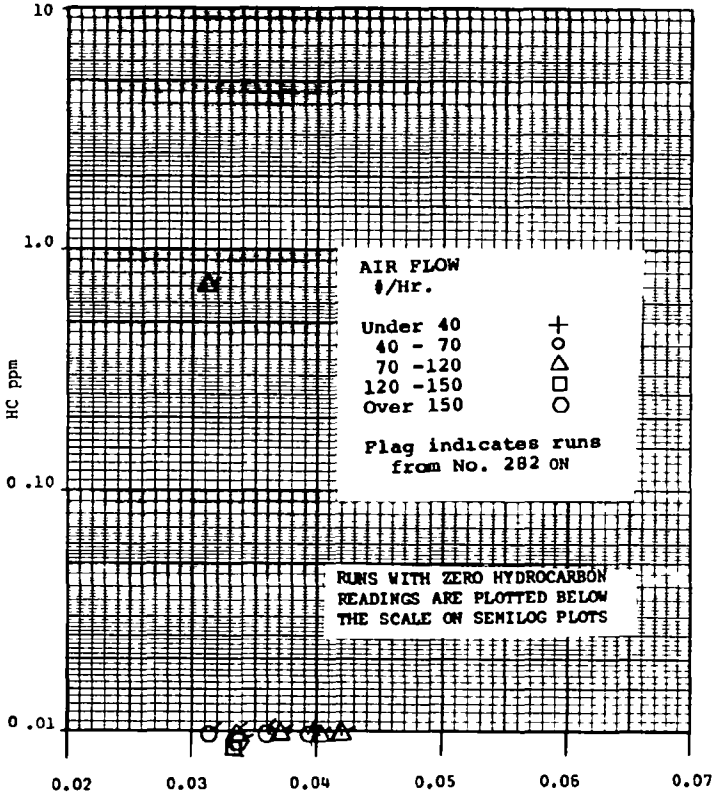

HC EMISSIONS DATA FROM THE PAXVE BURNER
FUEL :KEROSENE
AIR TEMP :OVER 250 F
BURNER VOLUME : 52.3 CU IN

LOOP DATA
RUNS AFTER NO. 282

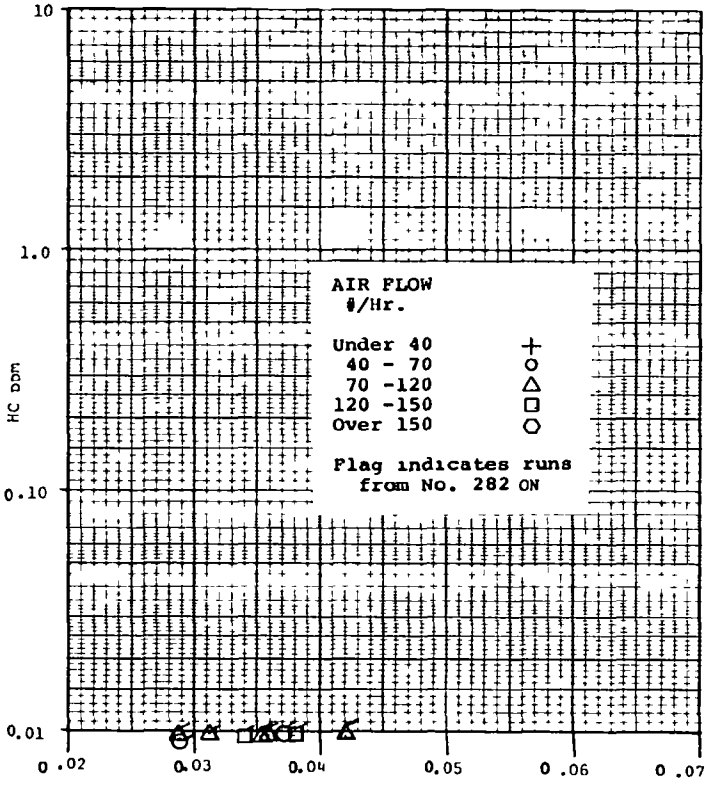

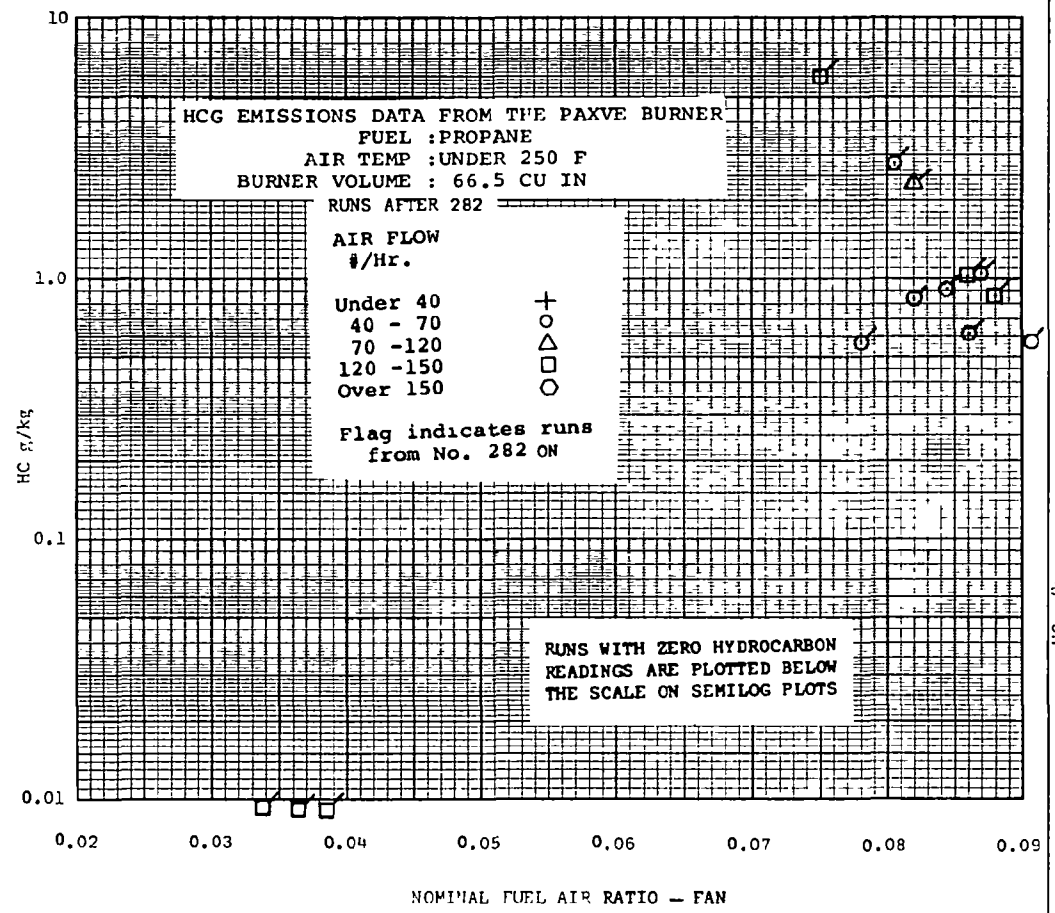
HCG EMISSIONS DATA FROM THE PAXVE BURNER
FUEL :PROPANE
AIR TEMP :UNDER 250 F
BURNER VOLUME : 66.5 CU IN
RUNS AFTER 282
AIR FLOW #/Hr.
Under 40
40 - 70
70 -120
120 -150
Over 150
Flag indicates runs from No. 282 ON
RUNS WITH ZERO HYDROCARBON READINGS ARE PLOTTED BELOW THE SCALE ON SEMILOG PLOTS
HC g/kg
10
1.0
0.1
0.01
0.02
0.03
0.04
0.05
0.06
0.07
0.08
0.09
NOMINAL FUEL AIR RATIO — FAN

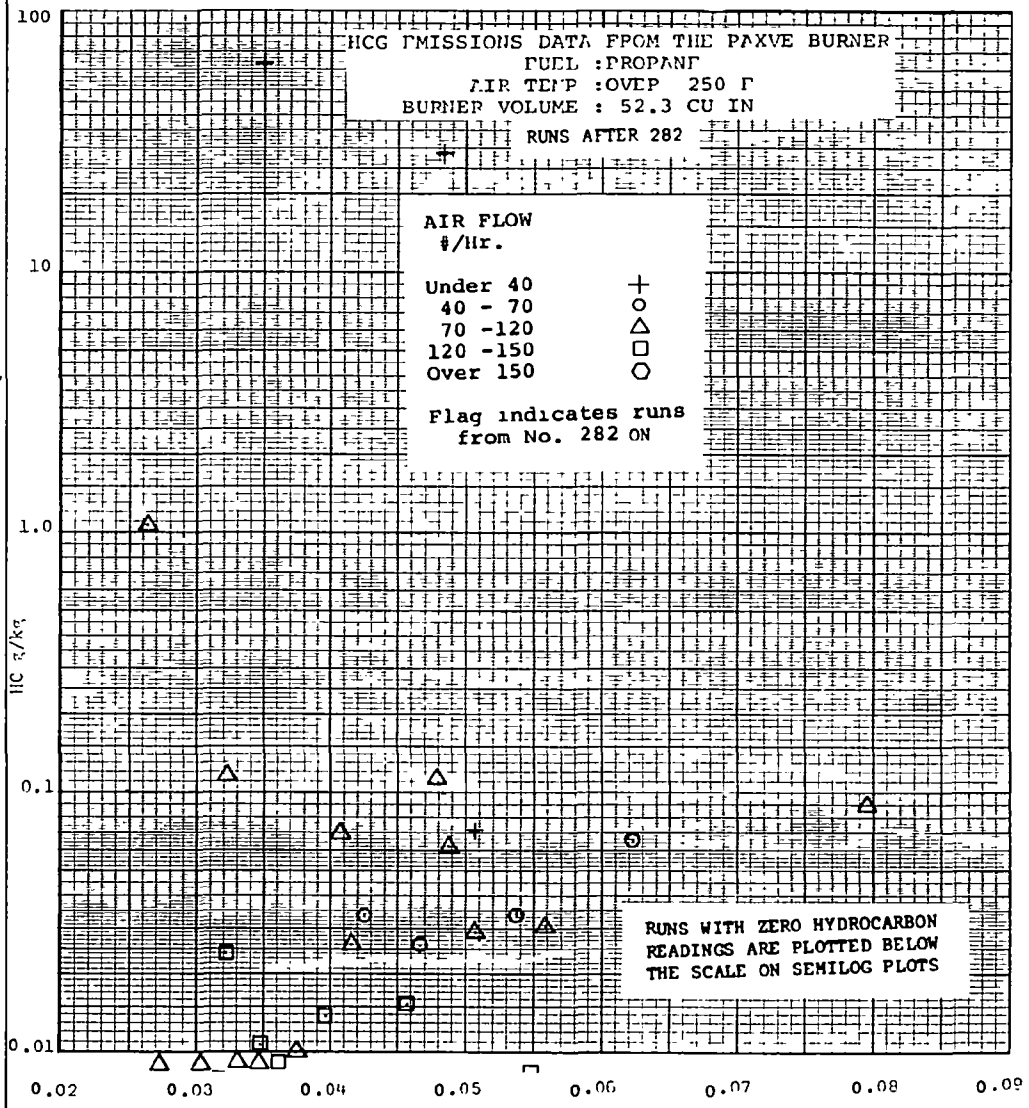
HCG EMISSIONS DATA FROM THE PAXVE BURNER
FUEL :PROPANE
AIR TEMP :OVER 250 F
BURNER VOLUME : 52.3 CU IN
RUNS AFTER 282
AIR FLOW #/Hr.
Under 40
40 - 70
70 -120
120 -150
Over 150
Flag indicates runs from No. 282 ON
RUNS WITH ZERO HYDROCARBON READINGS ARE PLOTTED BELOW THE SCALE ON SEMILOG PLOTS
HC g/kg
100
10
1.0
0.1
0.01
0.02
0.03
0.04
0.05
0.06
0.07
0.08
0.09
NOMINAL FUEL AIR RATIO — FAN

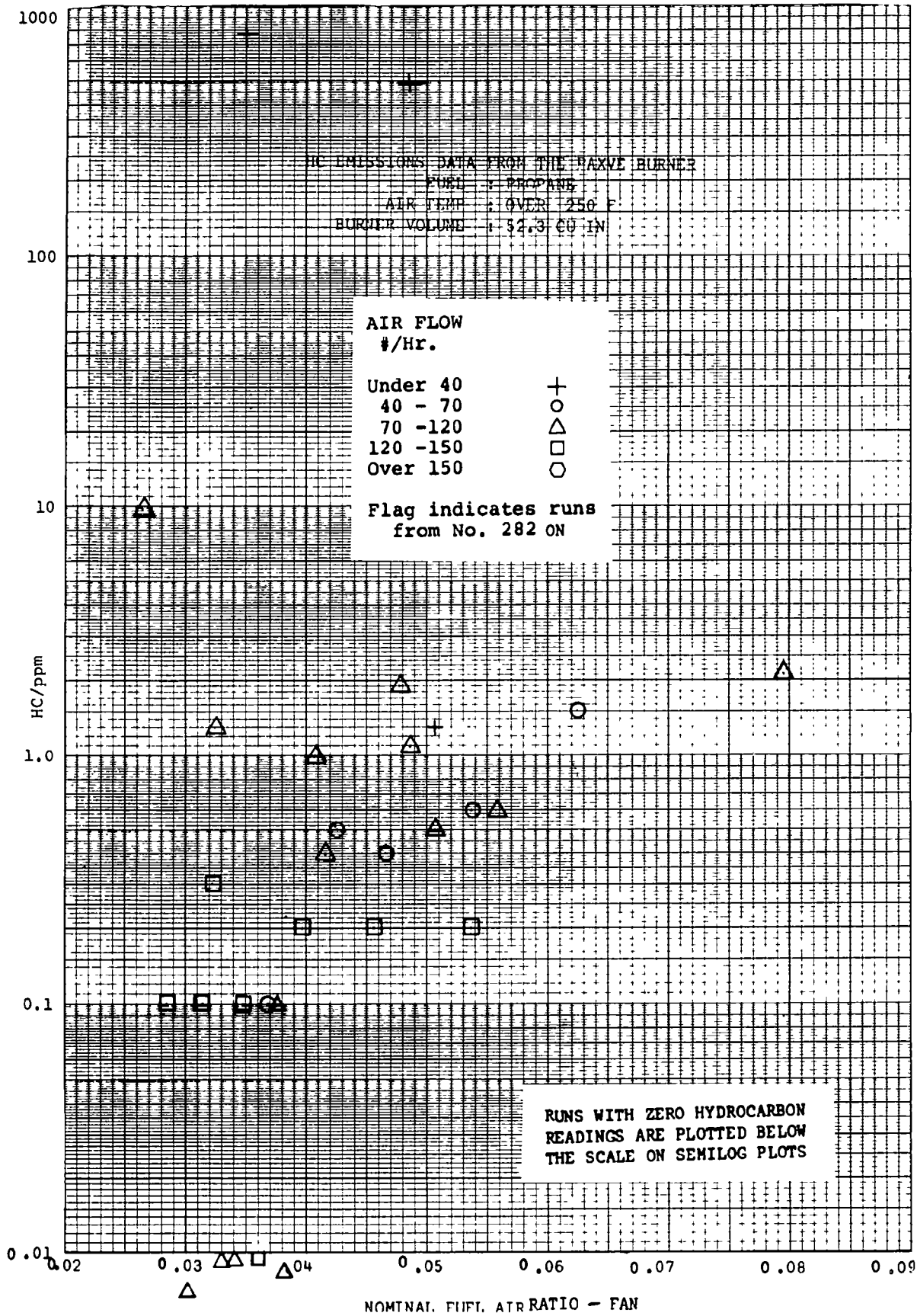
HC EMISSIONS DATA FROM THE DAXVE BURNER
FUEL : PROPANE
AIR TEMP : OVER 250 F
BURNER VOLUME : 52.3 CU IN
AIR FLOW #/Hr.
Under 40
40 - 70
70 -120
120 -150
Over 150
Flag indicates runs from No. 282 ON
RUNS WITH ZERO HYDROCARBON READINGS ARE PLOTTED BELOW THE SCALE ON SEMILOG PLOTS
HC/ppm
1000
100
10
1.0
0.1
0.01
0.02
0.03
0.04
0.05
0.06
0.07
0.08
0.09
NOMINAL FUEL AIR RATIO - FAN

VI
Fig.58

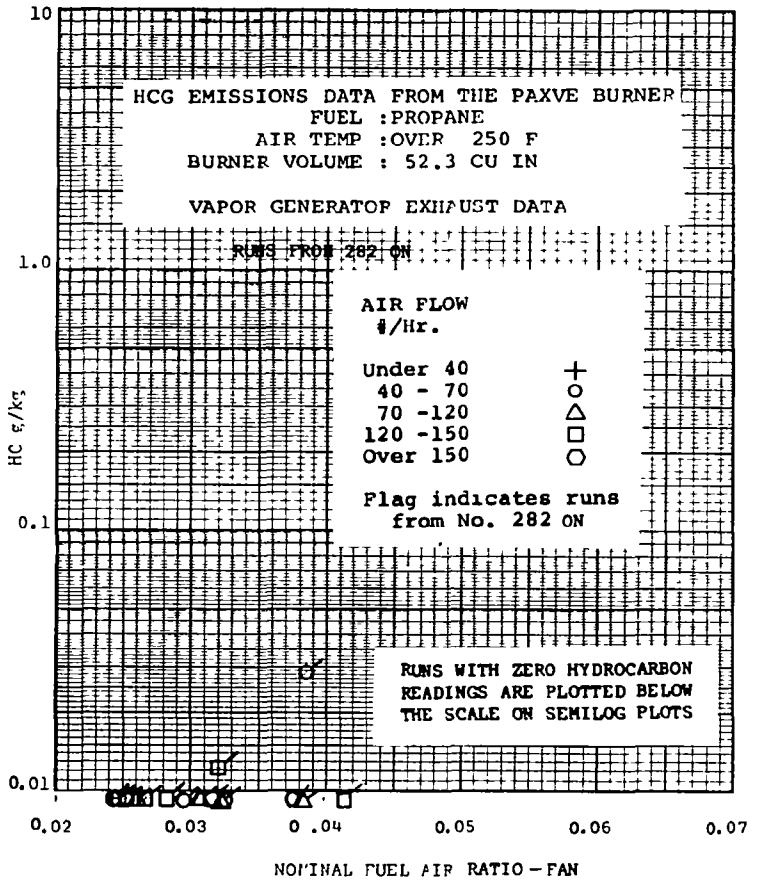

HCG EMISSIONS DATA FROM THE PAXVE BURNER
FUEL :PROPANE
AIR TEMP :UNDER 250 F
BURNER VOLUME : 52.3 CU IN

VAPOR GENERATOR EXHAUST DATA

RUNS FROM 282 ON

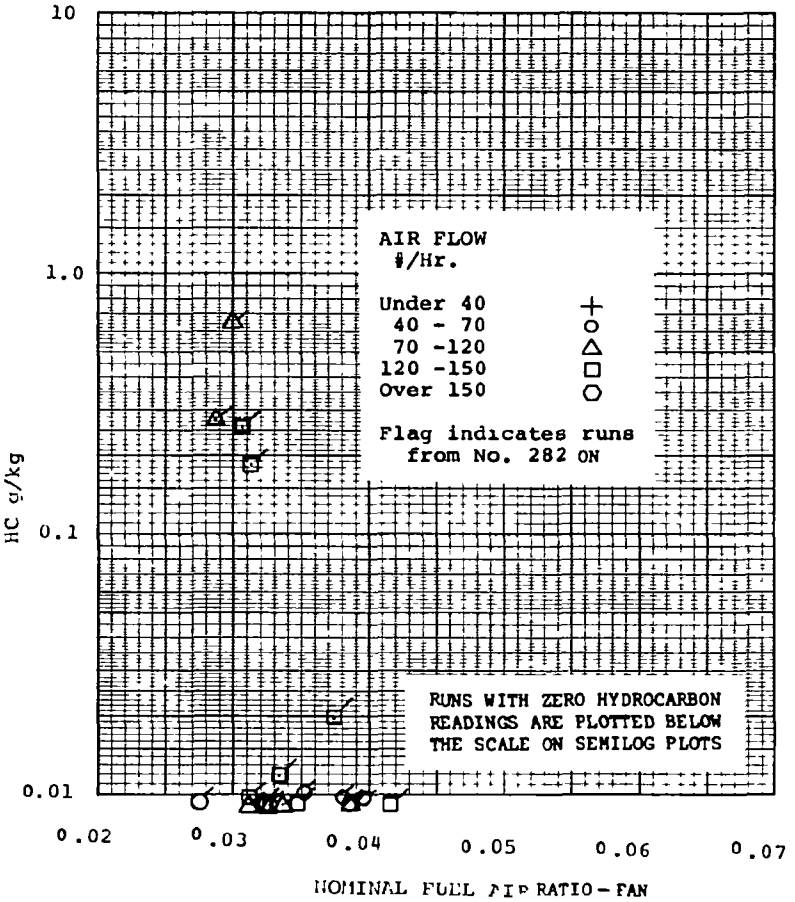

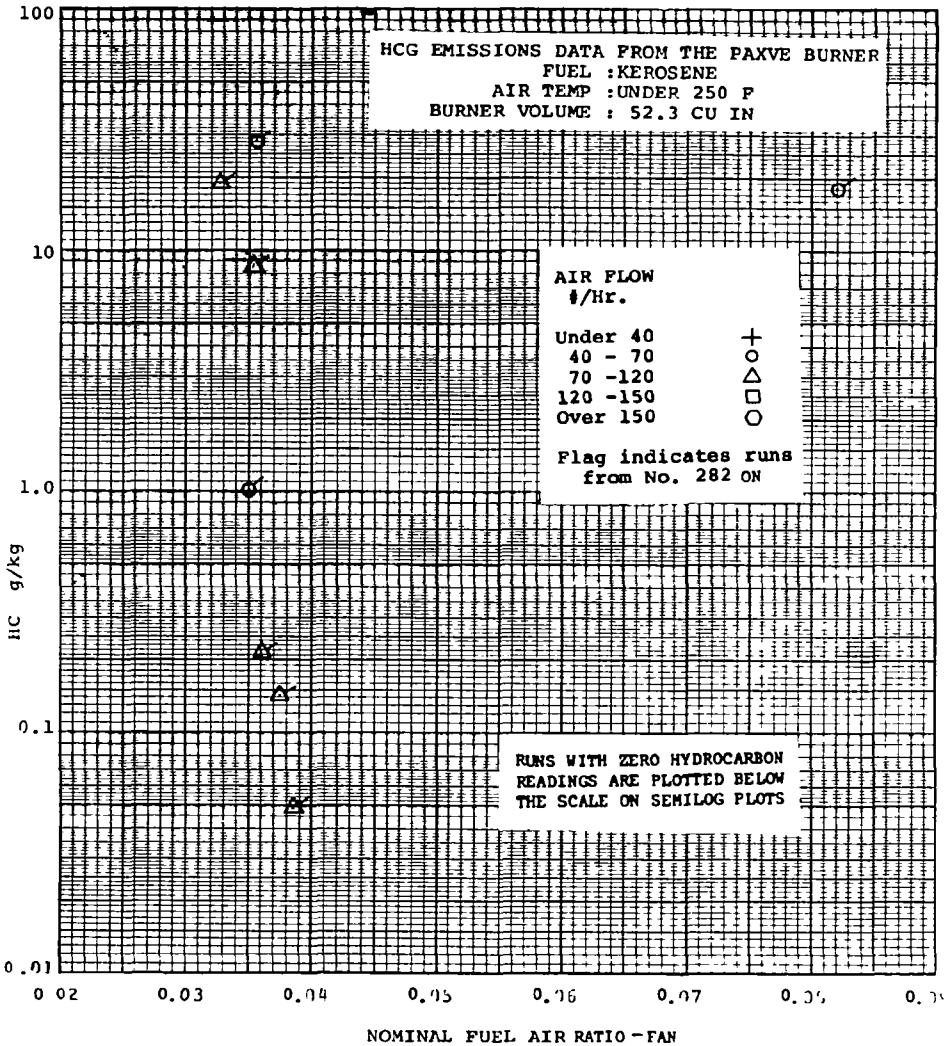
HCG EMISSIONS DATA FROM THE PAXVE BURNER
FUEL :KEROSENE
AIR TEMP :UNDER 250 F
BURNER VOLUME : 52.3 CU IN
AIR FLOW
#/Hr.
Under 40
40 - 70
70 -120
120 -150
Over 150
Flag indicates runs
from No. 282 ON
RUNS WITH ZERO HYDROCARBON
READINGS ARE PLOTTED BELOW
THE SCALE ON SEMILOG PLOTS
HC g/kg
100
10
1.0
0.1
0.01
0 02
0.03
0.04
0.05
0.06
0.07
NOMINAL FUEL AIR RATIO — FAN

VI
Fig.61

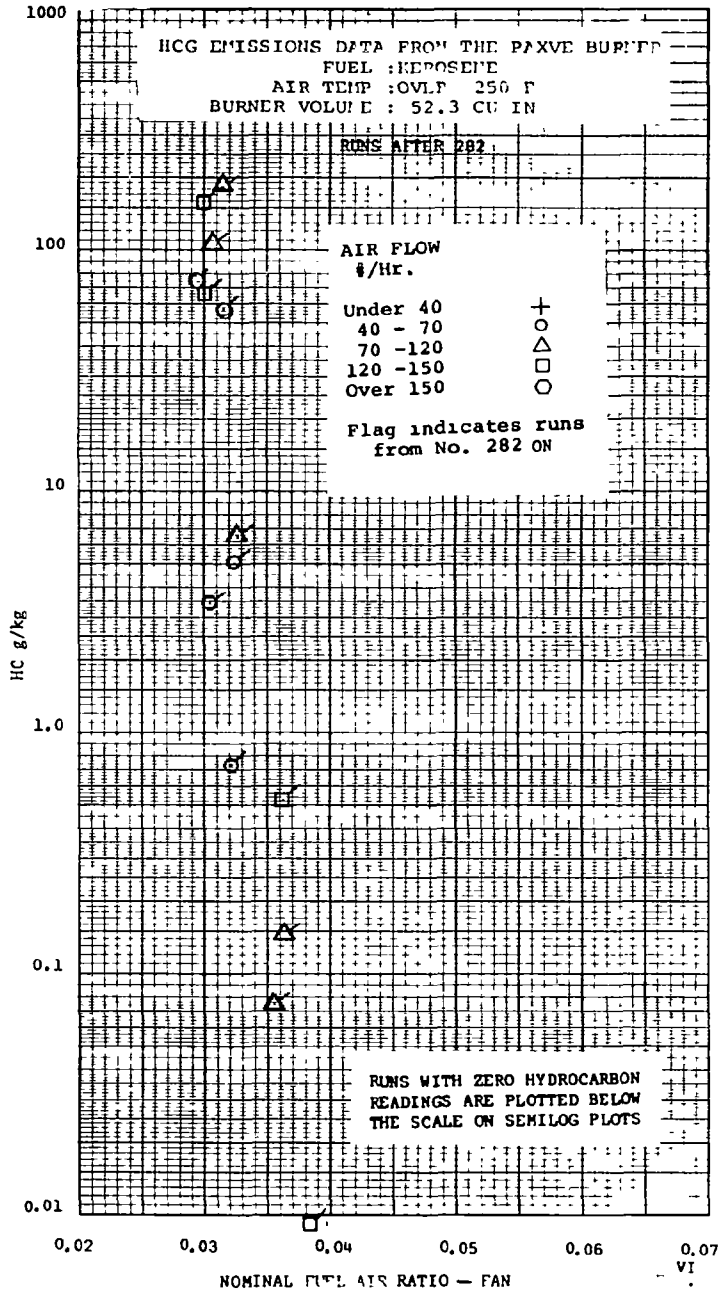
HCG EMISSIONS DATA FROM THE PAXVE BURNER
FUEL :KEROSENE
AIR TEMP :OVER 250 F
BURNER VOLUME : 52.3 CU IN
RUNS AFTER 282
AIR FLOW
#/Hr.
Under 40
40 - 70
70 -120
120 -150
Over 150
Flag indicates runs
from No. 282 ON
RUNS WITH ZERO HYDROCARBON
READINGS ARE PLOTTED BELOW
THE SCALE ON SEMILOG PLOTS
HC g/kg
1000
100
10
1.0
0.1
0.01
0.02
0.03
0.04
0.05
0.06
0.07
NOMINAL FUEL AIR RATIO — FAN

VI

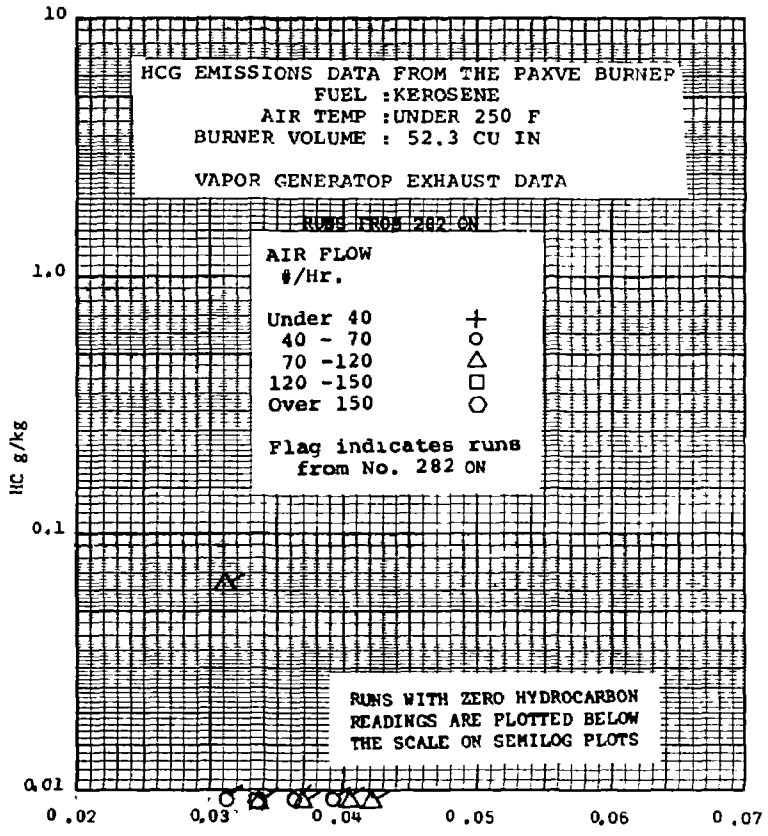
HCG EMISSIONS DATA FROM THE PAXVE BURNER
FUEL :KEROSENE
AIR TEMP :UNDER 250 F
BURNER VOLUME : 52.3 CU IN
VAPOR GENERATOP EXHAUST DATA
RUNS FROM 282 ON
AIR FLOW #/Hr.
Under 40 +
40 - 70 ○
70 -120 △
120 -150 □
Over 150 ⬡
Flag indicates runs from No. 282 ON
RUNS WITH ZERO HYDROCARBON READINGS ARE PLOTTED BELOW THE SCALE ON SEMILOG PLOTS
HC g/kg
10
1.0
0.1
0.01
0 .02
0.03
0 .04
0 .05
0.06
0 .07
NOMINAL FUEL AIR RATIO - FAN

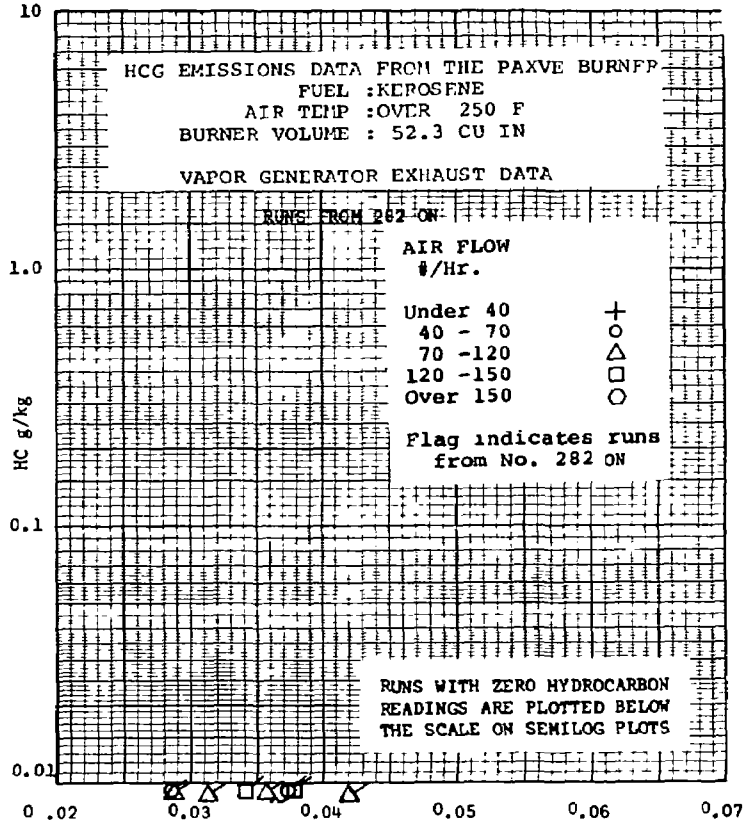
HCG EMISSIONS DATA FROM THE PAXVE BURNER
FUEL :KEROSENE
AIR TEMP :OVER 250 F
BURNER VOLUME : 52.3 CU IN
VAPOR GENERATOR EXHAUST DATA
RUNS FROM 282 ON
AIR FLOW #/Hr.
Under 40 +
40 - 70 ○
70 -120 △
120 -150 □
Over 150 ⬡
Flag indicates runs from No. 282 ON
RUNS WITH ZERO HYDROCARBON READINGS ARE PLOTTED BELOW THE SCALE ON SEMILOG PLOTS
HC g/kg
10
1.0
0.1
0.01
0 .02
0.03
0.04
0.05
0.06
0.07
NOMINAL FUEL AIR RATIO — FAN

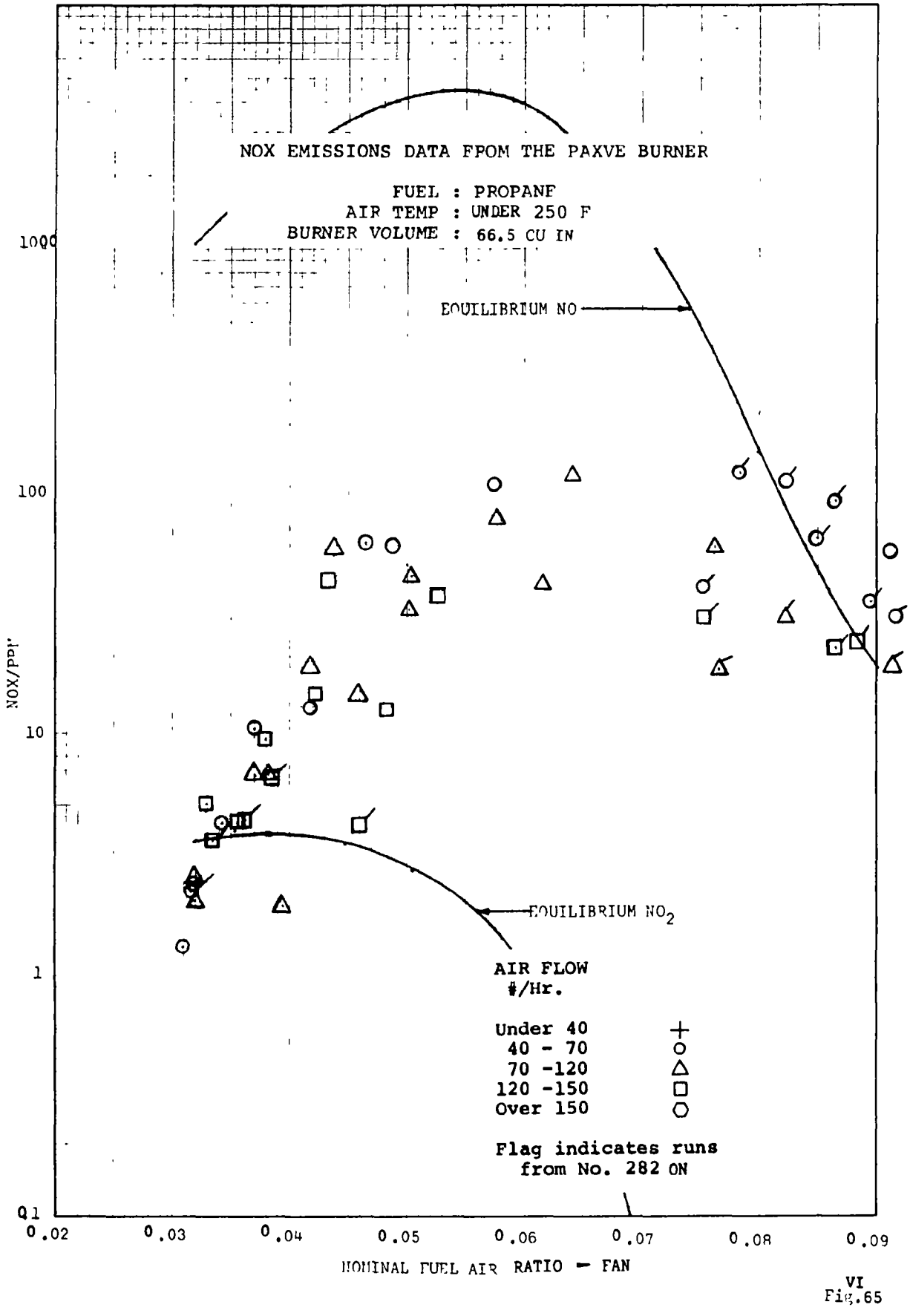
NOX EMISSIONS DATA FPOM THE PAXVE BURNER
FUEL : PROPANF
AIR TEMP : UNDER 250 F
BURNER VOLUME : 66.5 CU IN
EQUILIBRIUM NO
EQUILIBRIUM NO2
AIR FLOW #/Hr.
Under 40
40 - 70
70 -120
120 -150
Over 150
Flag indicates runs from No. 282 ON
NOX/PPM
1000
100
10
1
0.1
0.02
0.03
0.04
0.05
0.06
0.07
0.08
0.09
NOMINAL FUEL AIR RATIO - FAN

VI
Fig.65

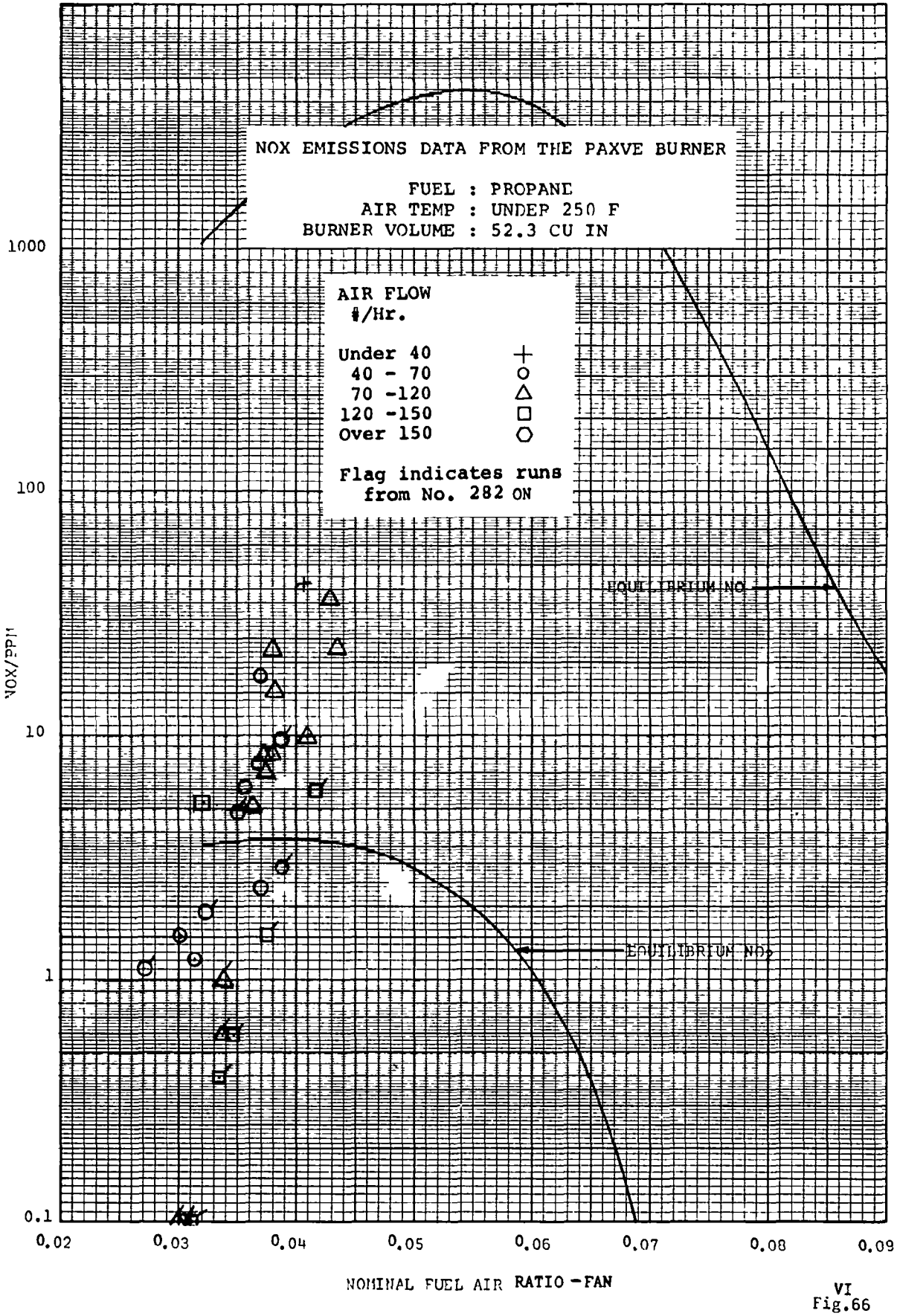
NOX EMISSIONS DATA FROM THE PAXVE BURNER
FUEL : PROPANE
AIR TEMP : UNDER 250 F
BURNER VOLUME : 52.3 CU IN
AIR FLOW #/Hr.
Under 40
40 - 70
70 -120
120 -150
Over 150
Flag indicates runs from No. 282 ON
EQUILIBRIUM NO
EQUILIBRIUM NO2
NOX/PPM
1000
100
10
1
0.1
0.02
0.03
0.04
0.05
0.06
0.07
0.08
0.09
NOMINAL FUEL AIR RATIO - FAN

VI
Fig.66

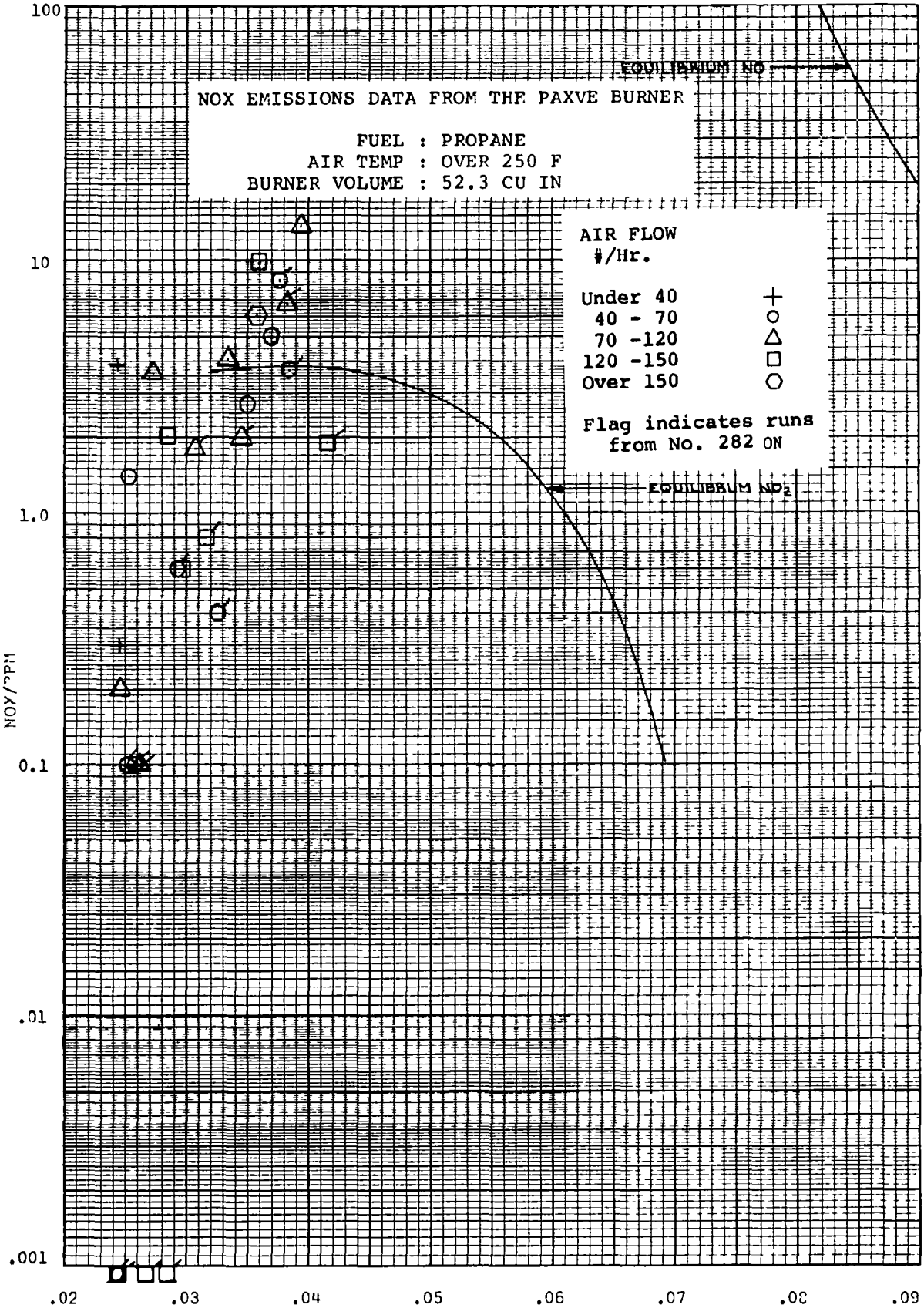
NOX EMISSIONS DATA FROM THE PAXVE BURNER
FUEL : PROPANE
AIR TEMP : OVER 250 F
BURNER VOLUME : 52.3 CU IN
AIR FLOW #/Hr.
Under 40
40 - 70
70 -120
120 -150
Over 150
Flag indicates runs from No. 282 ON
EQUILIBRIUM NO
EQUILIBRIUM NO2
NOX/PPM
100
10
1.0
0.1
.01
.001
.02
.03
.04
.05
.06
.07
.08
.09
NOMINAL FUEL AIR

VI
Fig.67

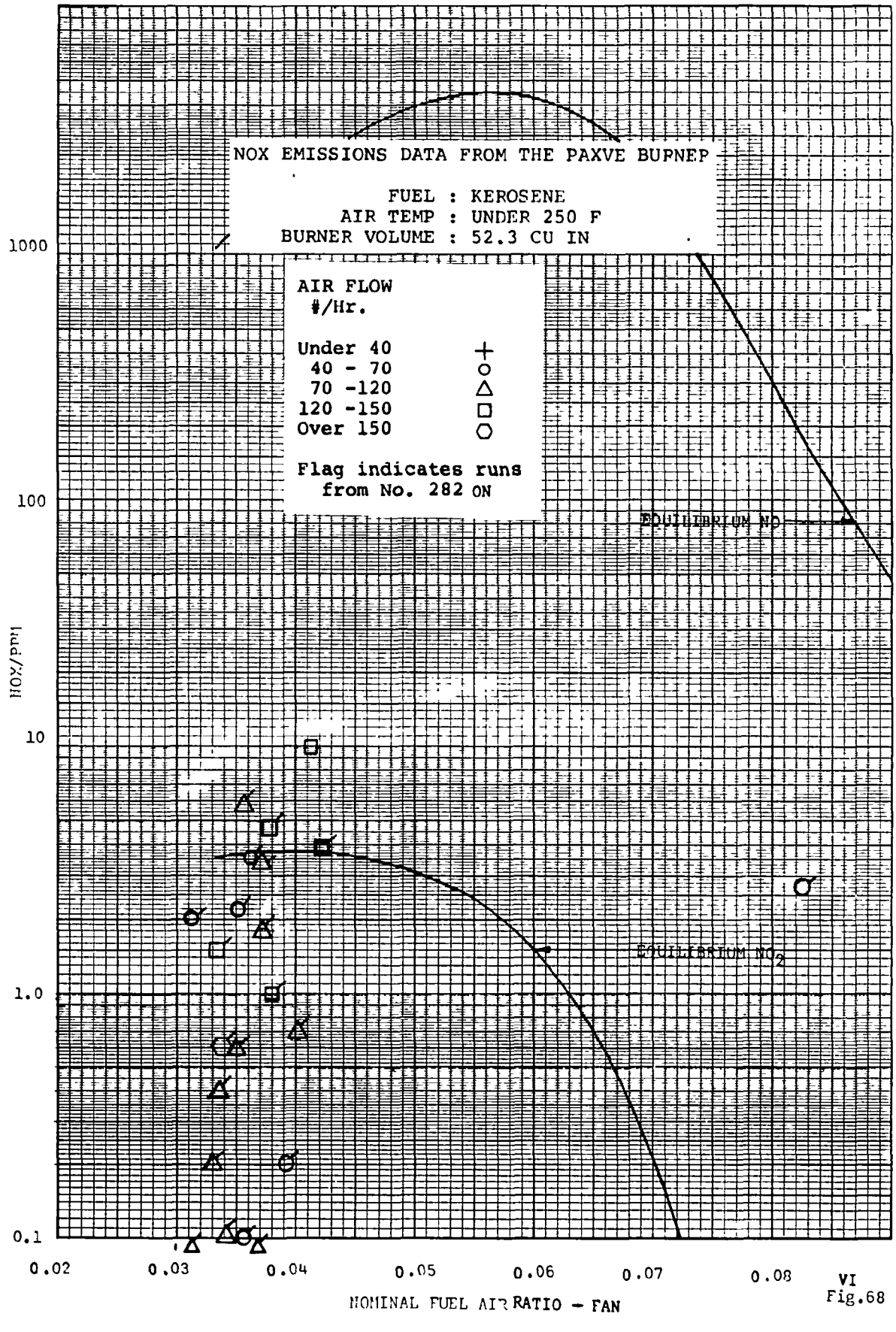
NOX EMISSIONS DATA FROM THE PAXVE BURNEP
FUEL : KEROSENE
AIR TEMP : UNDER 250 F
BURNER VOLUME : 52.3 CU IN
AIR FLOW #/Hr.
Under 40
40 - 70
70 -120
120 -150
Over 150
Flag indicates runs from No. 282 ON
EQUILIBRIUM NO
EQUILIBRIUM NO2
1000
100
10
1.0
0.1
NOX/ppm
0.02
0.03
0.04
0.05
0.06
0.07
0.08
NOMINAL FUEL AIR RATIO - FAN

VI
Fig.68

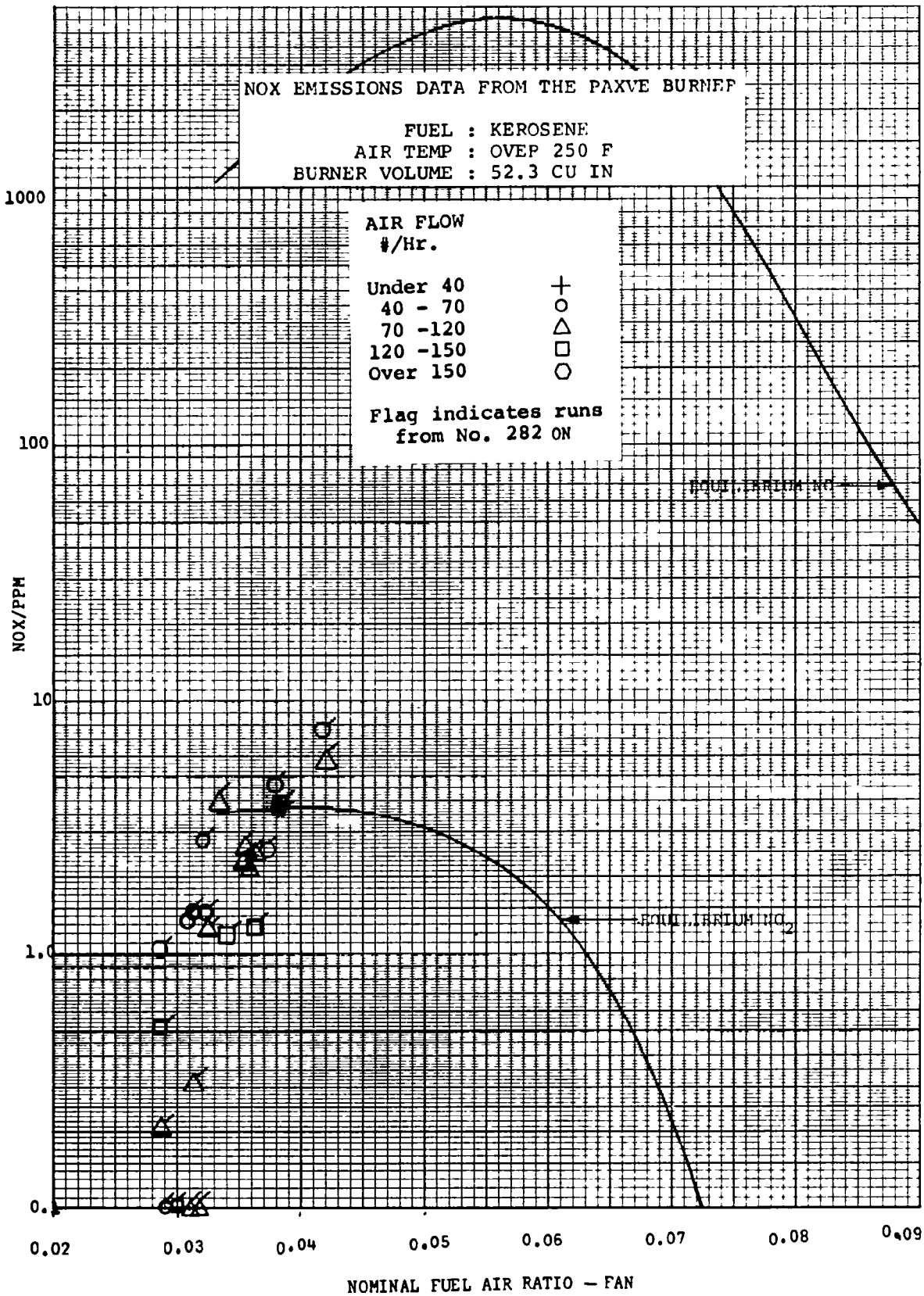
NOX EMISSIONS DATA FROM THE PAXVE BURNER
FUEL : KEROSENE
AIR TEMP : OVER 250 F
BURNER VOLUME : 52.3 CU IN
AIR FLOW #/Hr.
Under 40
40 - 70
70 -120
120 -150
Over 150
Flag indicates runs from No. 282 ON
EQUILIBRIUM NO
EQUILIBRIUM NO2
NOX/PPM
1000
100
10
1.0
0.1
0.02
0.03
0.04
0.05
0.06
0.07
0.08
0.09
NOMINAL FUEL AIR RATIO — FAN

VI
Fig. 69

NOx EMISSIONS DATA FROM THE PAXVE BURNER

FUEL : PROPANE
AIR TEMP : UNDER 250°F
BURNER VOLUME : 66.5 CU IN

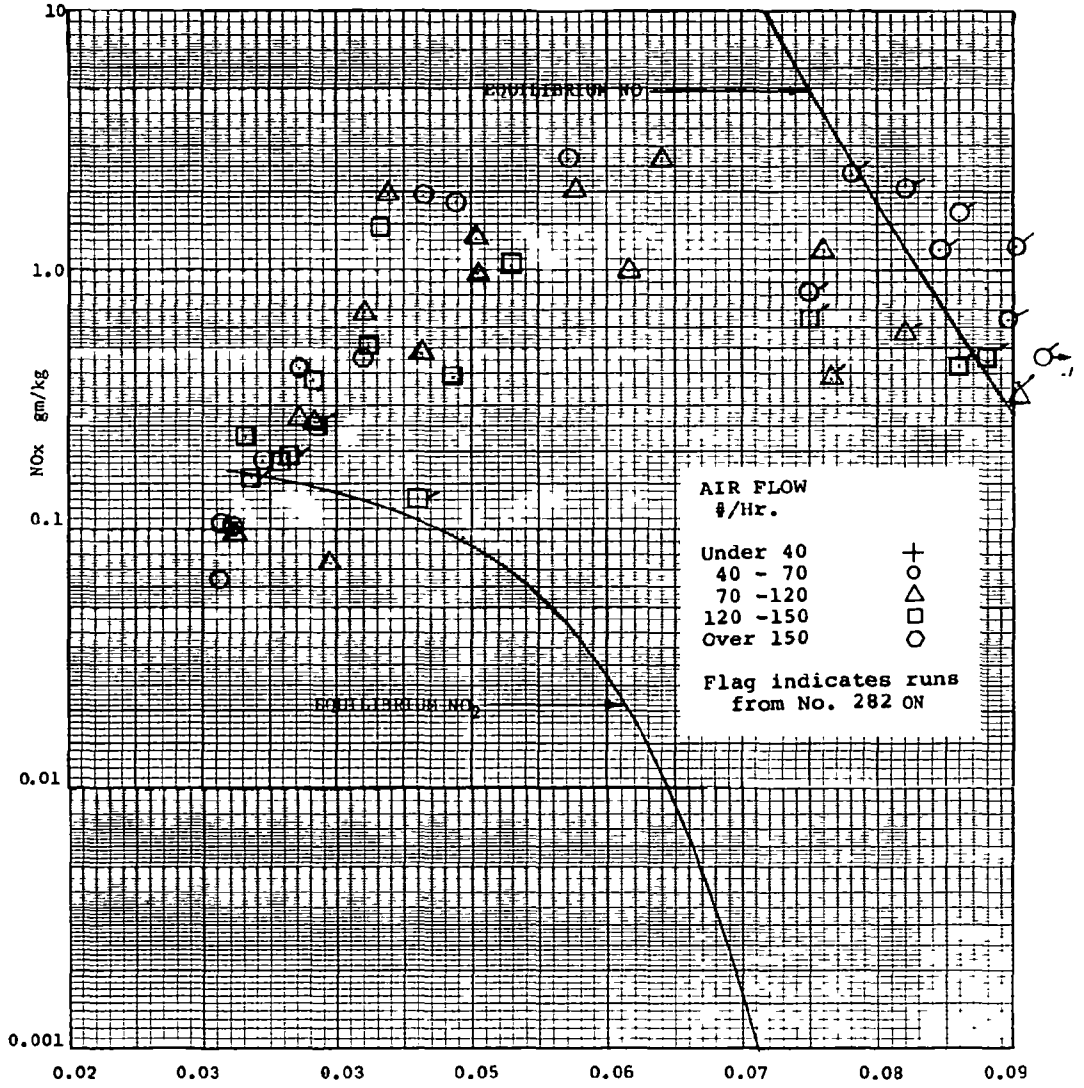

VI
Fig.70

NOx EMISSIONS DATA FROM THE PAXVE BURNER

FUEL :PROPANE
AIR TEMP :UNDER 250 F
BURNER VOLUME : 52.3 CU IN

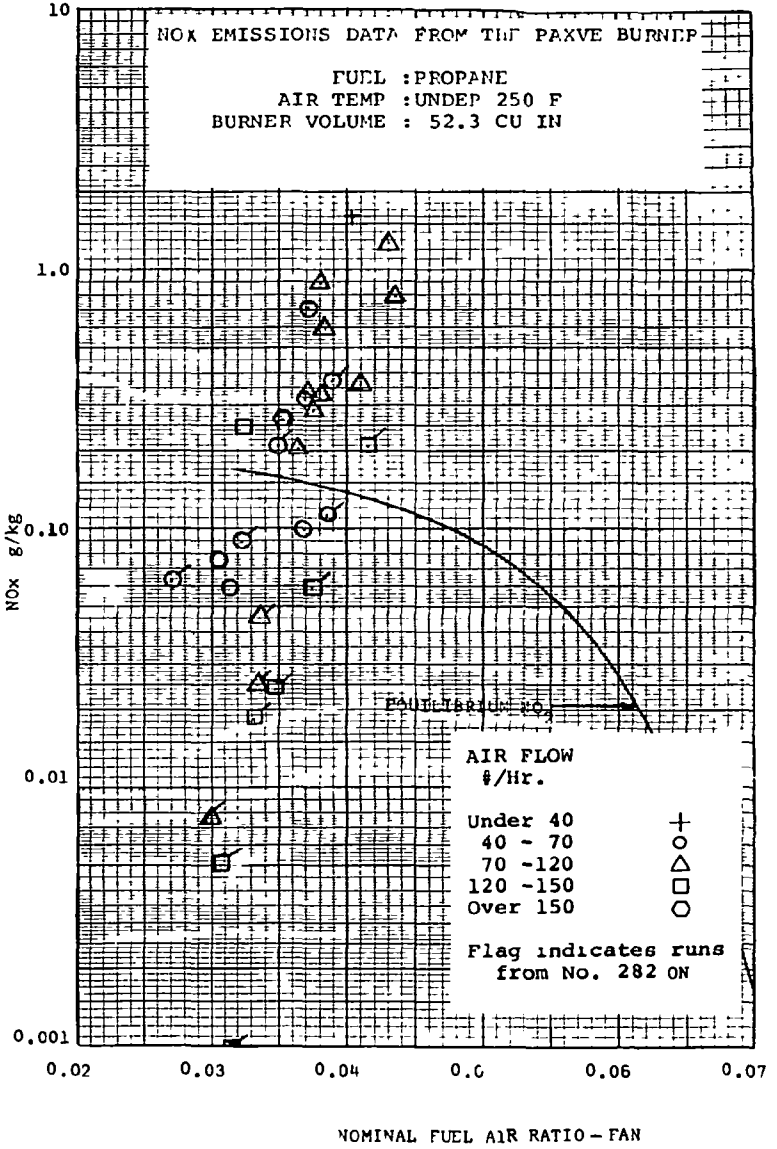

VI
Fig.71

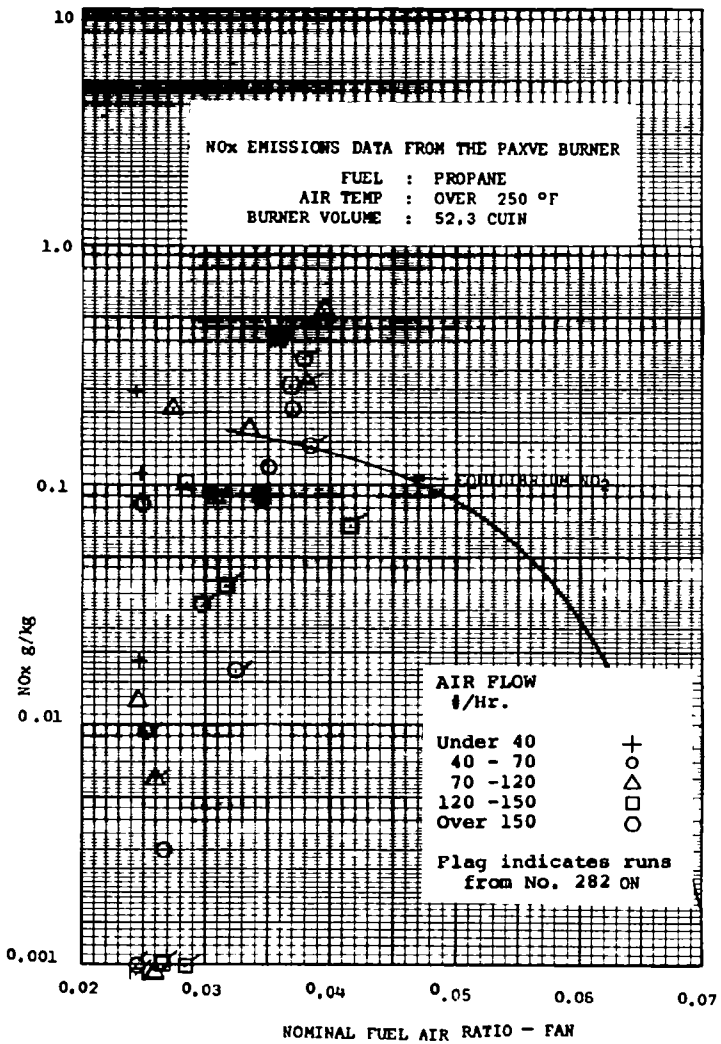

VI
Fig.72

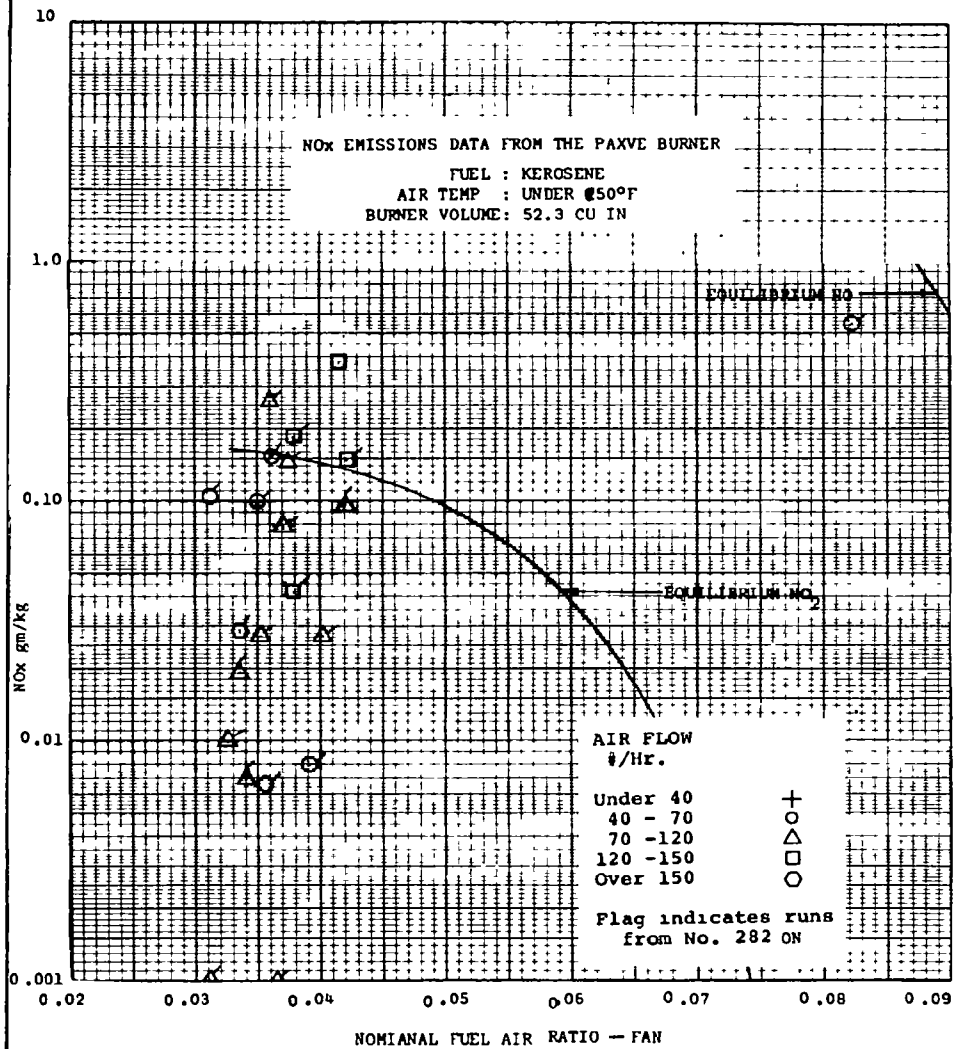

VI
Fig.73

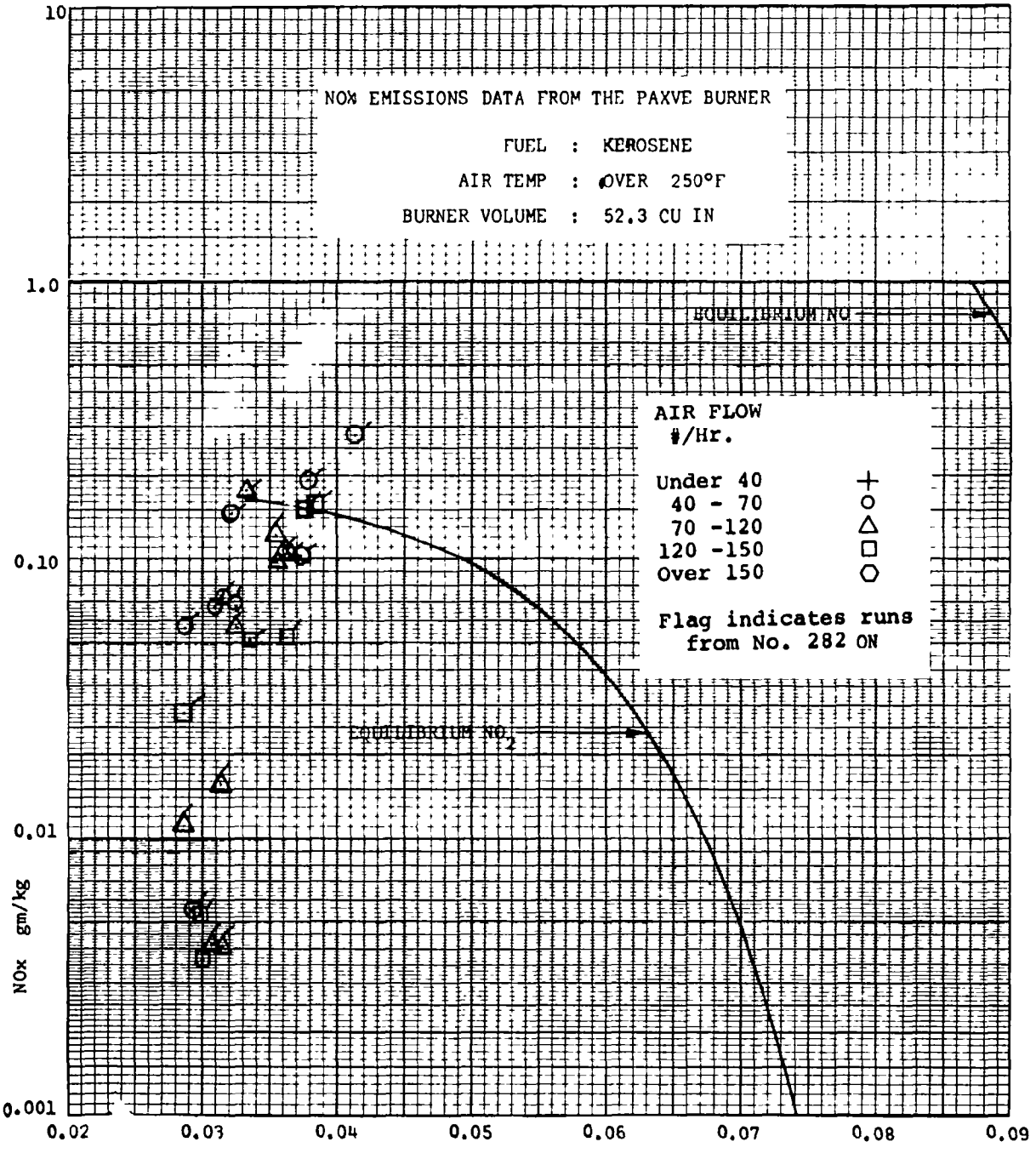
NOx EMISSIONS DATA FROM THE PAXVE BURNER
FUEL : KEROSENE
AIR TEMP : OVER 250°F
BURNER VOLUME : 52.3 CU IN
AIR FLOW #/Hr.
Under 40
40 - 70
70 -120
120 -150
Over 150
Flag indicates runs from No. 282 ON
EQUILIBRIUM NO
EQUILIBRIUM NO2
NOx gm/kg
10
1.0
0.10
0.01
0.001
0.02
0.03
0.04
0.05
0.06
0.07
0.08
0.09
NOMINAL FUEL AIR RATIO - FAN

VI
Fig.74

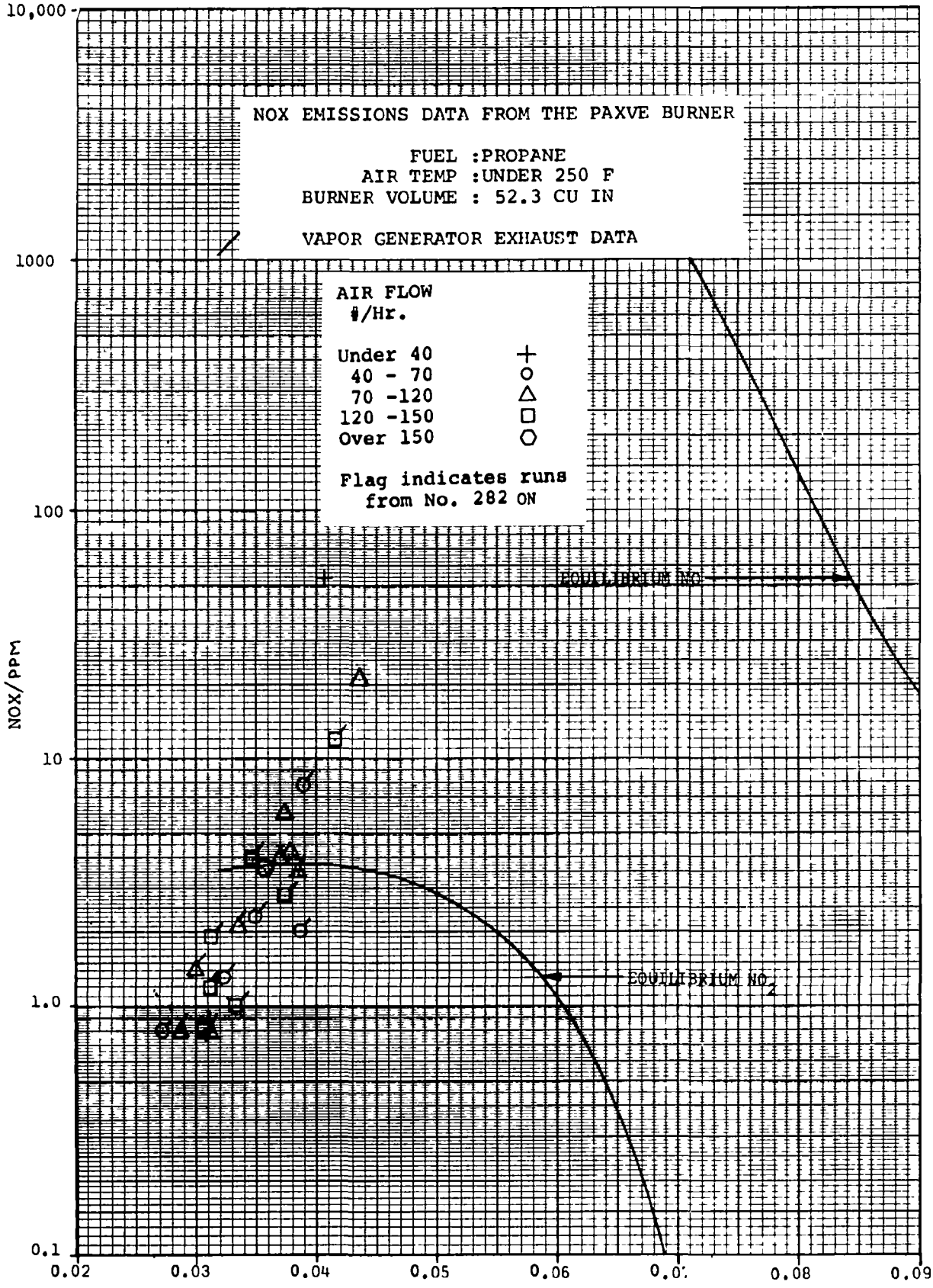
NOX EMISSIONS DATA FROM THE PAXVE BURNER
FUEL :PROPANE
AIR TEMP :UNDER 250 F
BURNER VOLUME : 52.3 CU IN
VAPOR GENERATOR EXHAUST DATA
AIR FLOW #/Hr.
Under 40
40 - 70
70 -120
120 -150
Over 150
Flag indicates runs from No. 282 ON
EQUILIBRIUM NO
EQUILIBRIUM NO2
NOX/PPM
10,000
1000
100
10
1.0
0.1
0.02
0.03
0.04
0.05
0.06
0.07
0.08
0.09
NOMINAL FUEL AIR RATIO — FAN

VI
Fig.75

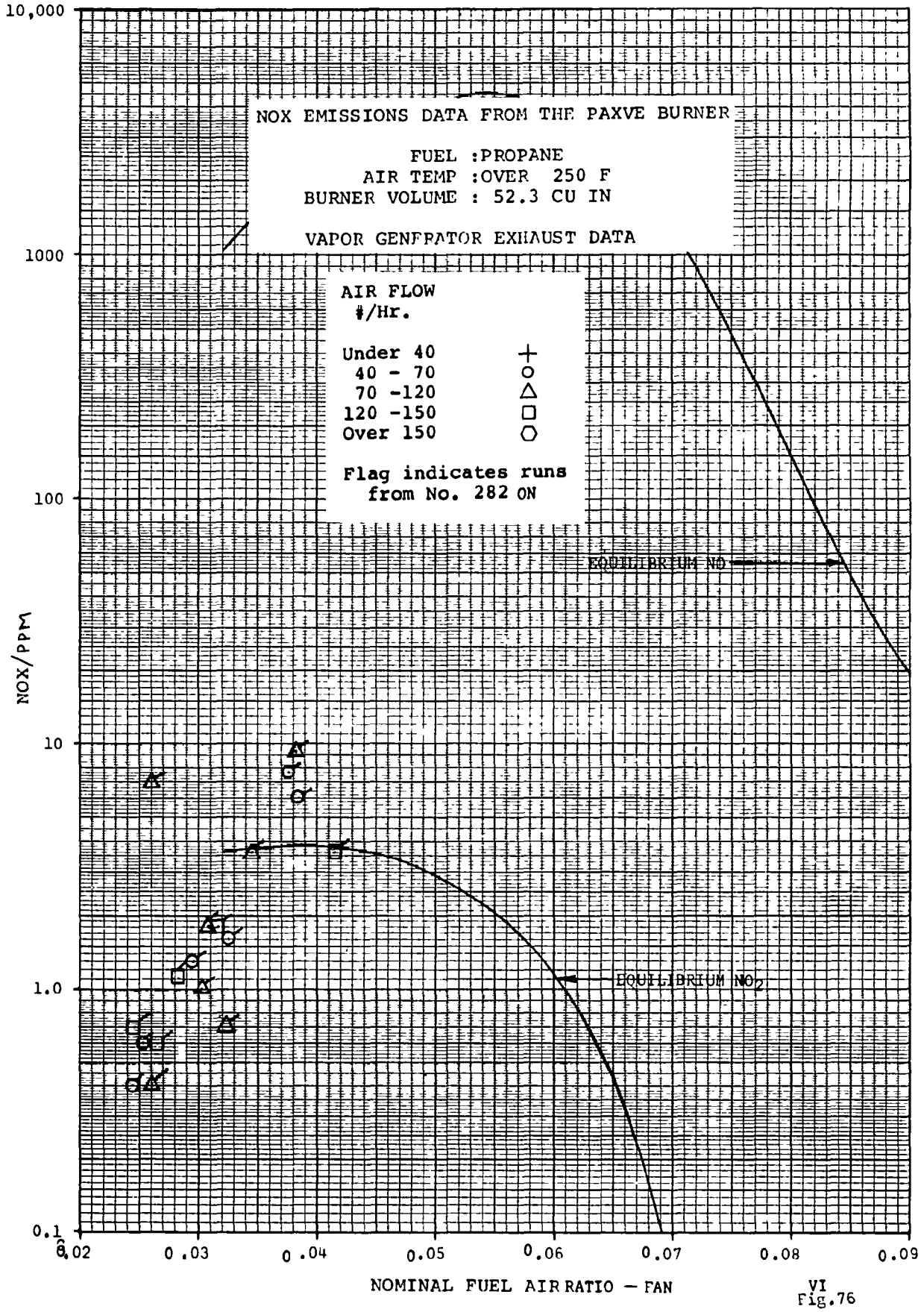
NOX EMISSIONS DATA FROM THE PAXVE BURNER
FUEL :PROPANE
AIR TEMP :OVER 250 F
BURNER VOLUME : 52.3 CU IN
VAPOR GENERATOR EXHAUST DATA
AIR FLOW #/Hr.
Under 40 +
40 - 70 ○
70 -120 △
120 -150 □
Over 150 ⬡
Flag indicates runs from No. 282 ON
EQUILIBRIUM NO
EQUILIBRIUM NO2
NOX/PPM
10,000
1000
100
10
1.0
0.1
0.02
0.03
0.04
0.05
0.06
0.07
0.08
0.09
NOMINAL FUEL AIR RATIO — FAN

VI
Fig.76

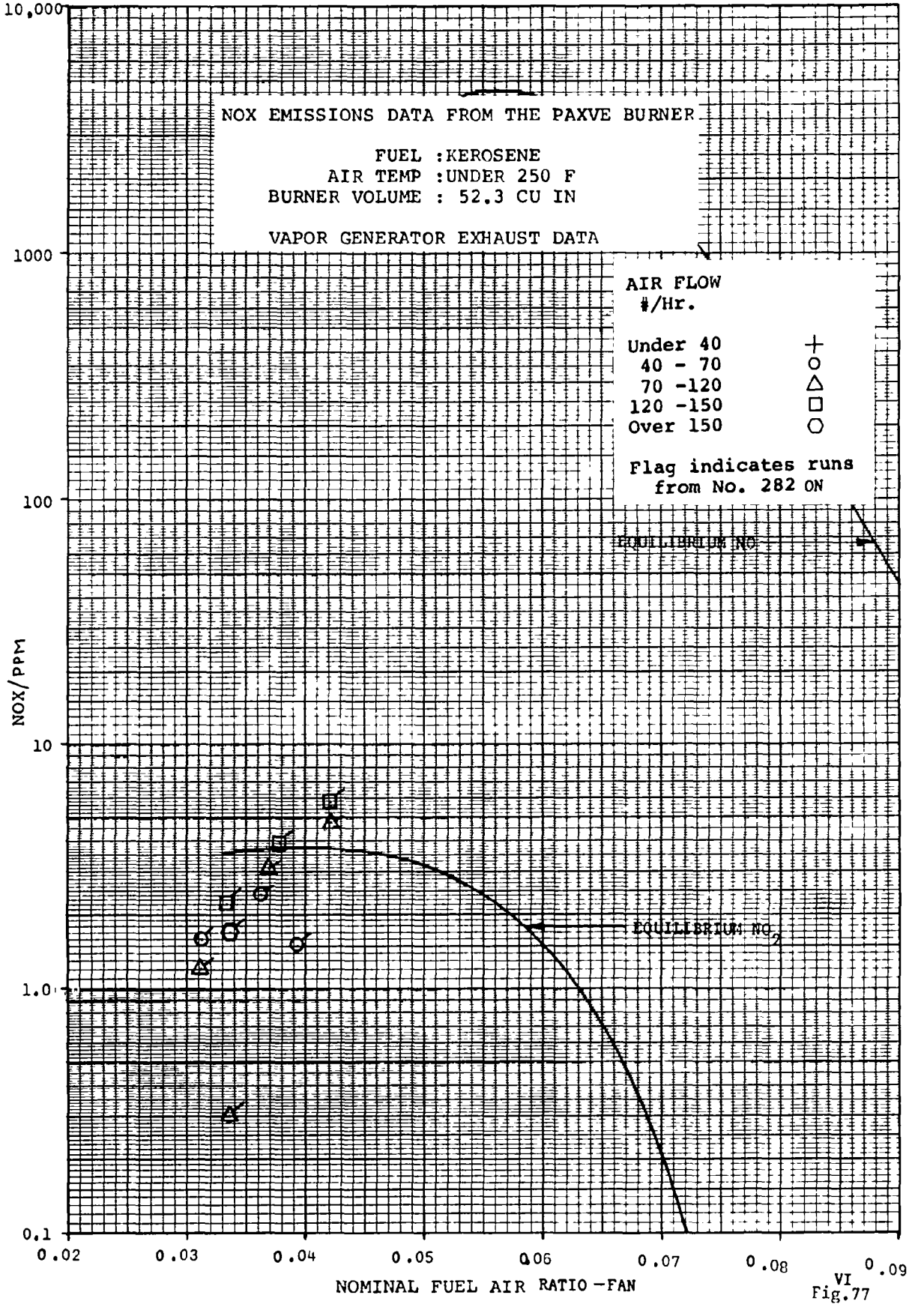
NOX EMISSIONS DATA FROM THE PAXVE BURNER
FUEL :KEROSENE
AIR TEMP :UNDER 250 F
BURNER VOLUME : 52.3 CU IN
VAPOR GENERATOR EXHAUST DATA
AIR FLOW #/Hr.
Under 40
40 - 70
70 -120
120 -150
Over 150
Flag indicates runs from No. 282 ON
EQUILIBRIUM NO
EQUILIBRIUM NO2
NOX/PPM
10,000
1000
100
10
1.0
0.1
0.02
0.03
0.04
0.05
0.06
0.07
0.08
0.09
NOMINAL FUEL AIR RATIO -FAN

VI
Fig.77

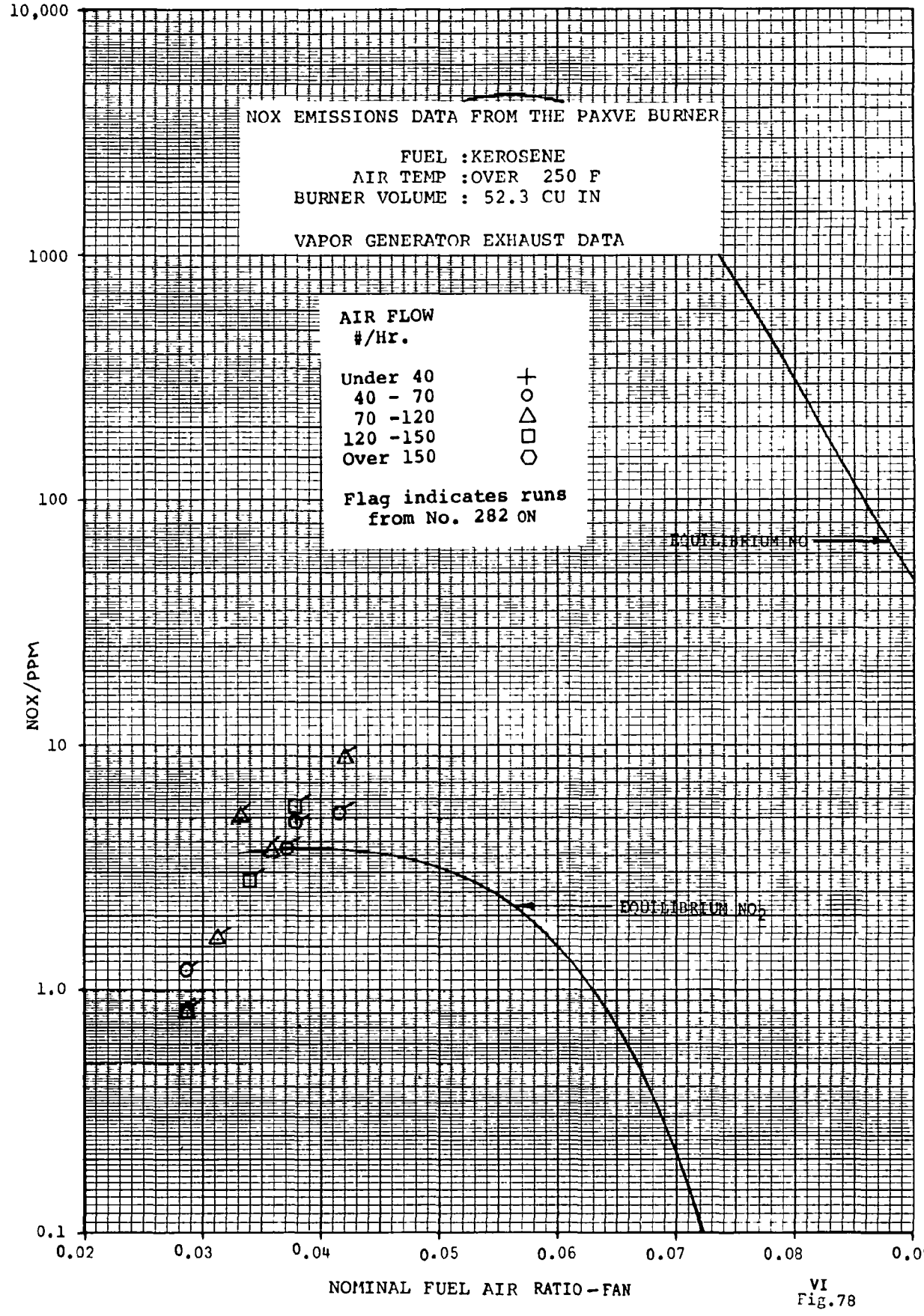
NOX EMISSIONS DATA FROM THE PAXVE BURNER
FUEL :KEROSENE
AIR TEMP :OVER 250 F
BURNER VOLUME : 52.3 CU IN
VAPOR GENERATOR EXHAUST DATA
AIR FLOW #/Hr.
Under 40
40 - 70
70 -120
120 -150
Over 150
Flag indicates runs from No. 282 ON
EQUILIBRIUM NO
EQUILIBRIUM NO2
NOX/PPM
10,000
1000
100
10
1.0
0.1
0.02
0.03
0.04
0.05
0.06
0.07
0.08
NOMINAL FUEL AIR RATIO-FAN

VI
Fig.78

NOX EMISSIONS DATA FROM THE PAXVE BURNER

FUEL :PROPANE
AIR TEMP :UNDER 250 F
BURNER VOLUME : 52.3 CU IN

VAPOR GENERATOR EXHAUST DATA

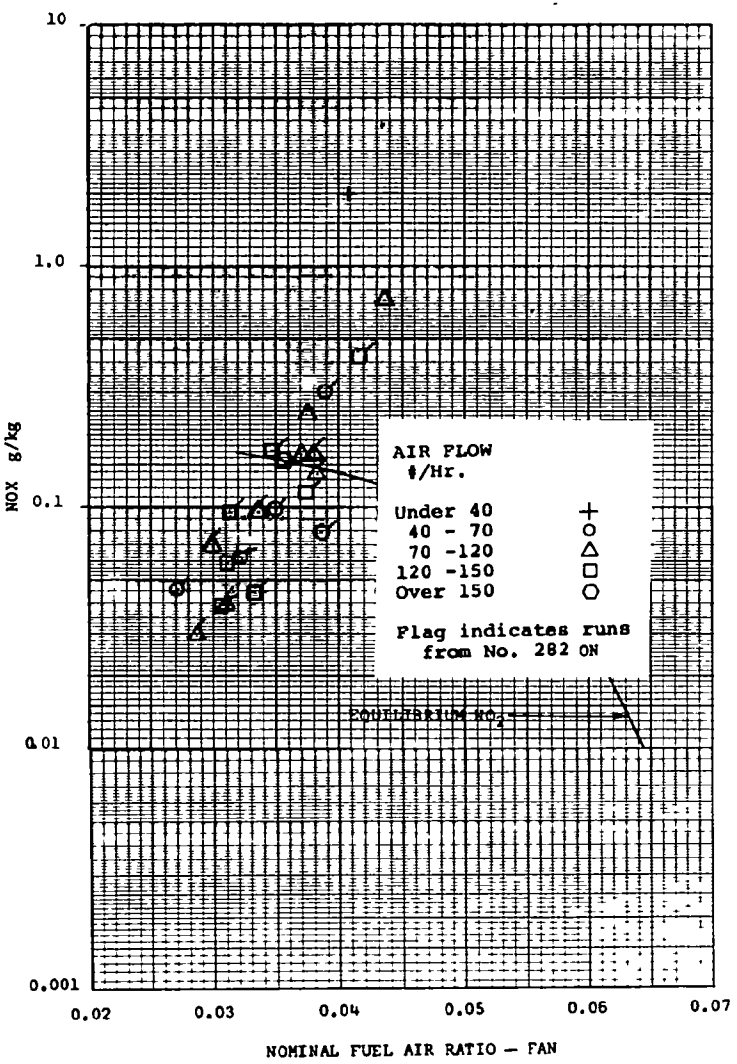

VI
Fig.79

NOX EMISSIONS DATA FROM THE PAXVE BURNER

FUEL :PROPANE
AIR TEMP :OVER 250 F
BURNER VOLUME : 52.3 CU IN

VAPOR GENERATOR EXHAUST DATA

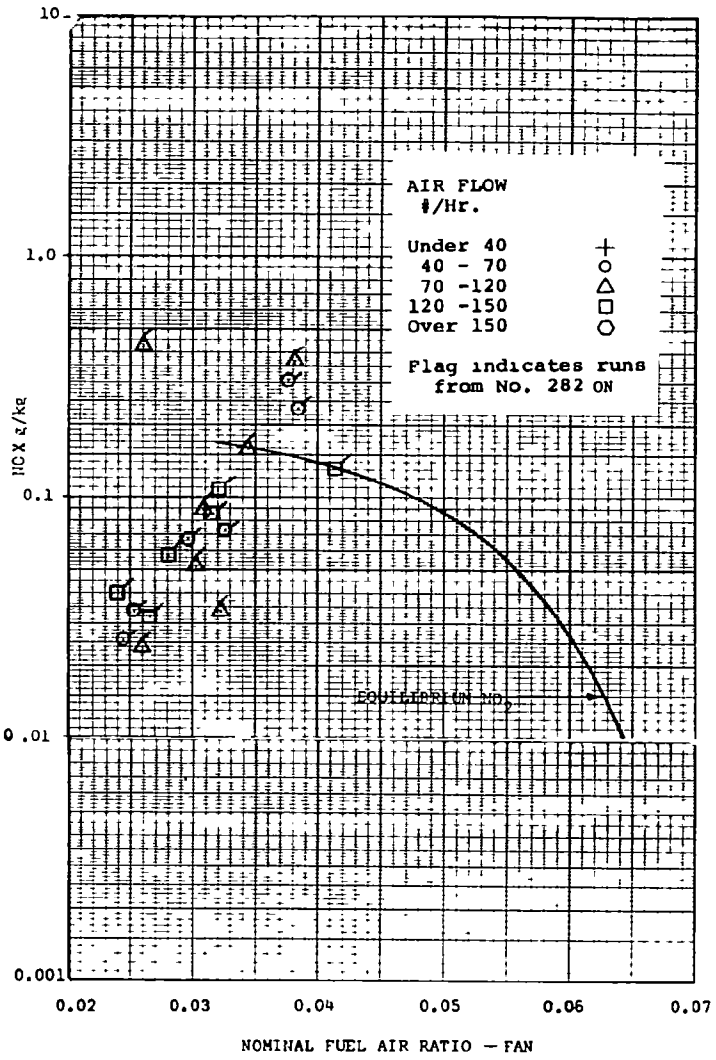

VI
Fig.80

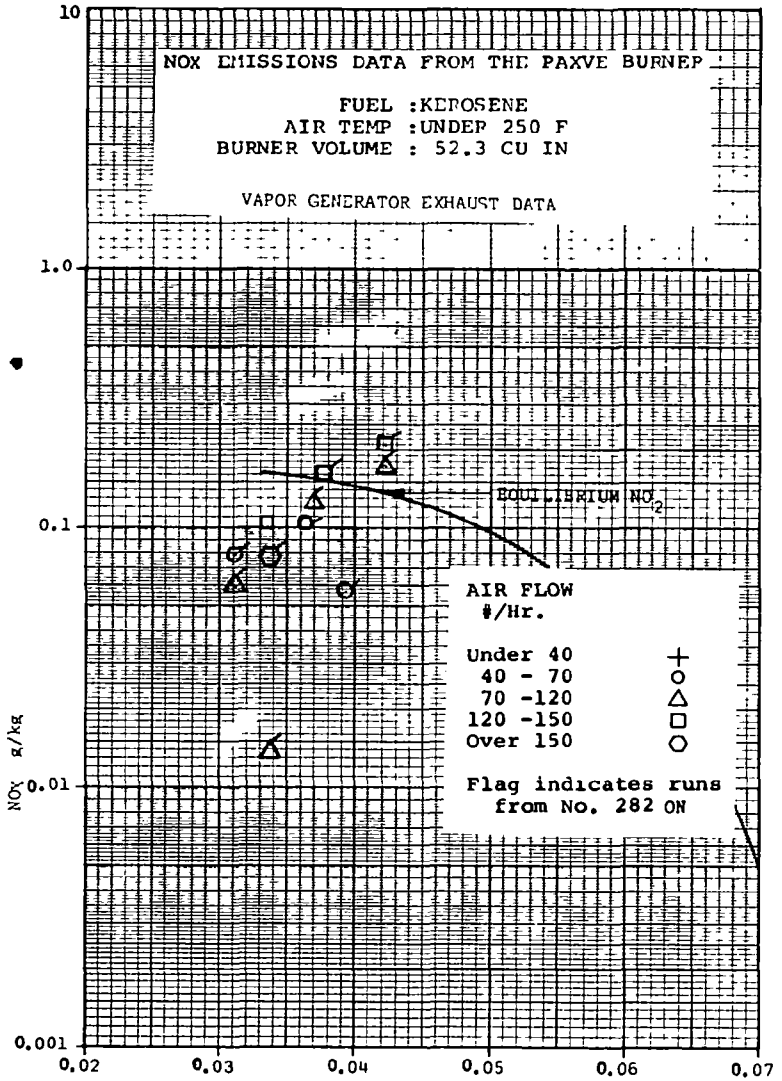
NOX EMISSIONS DATA FROM THE PAXVE BURNER
FUEL :KEROSENE
AIR TEMP :UNDER 250 F
BURNER VOLUME : 52.3 CU IN
VAPOR GENERATOR EXHAUST DATA
EQUILIBRIUM NO_2
AIR FLOW #/Hr.
Under 40
40 - 70
70 -120
120 -150
Over 150
Flag indicates runs from No. 282 ON
NOx g/kg
10
1.0
0.1
0.01
0.001
0.02
0.03
0.04
0.05
0.06
0.07
NOMINAL FUEL AIR RATIO — FAN

Fig.81

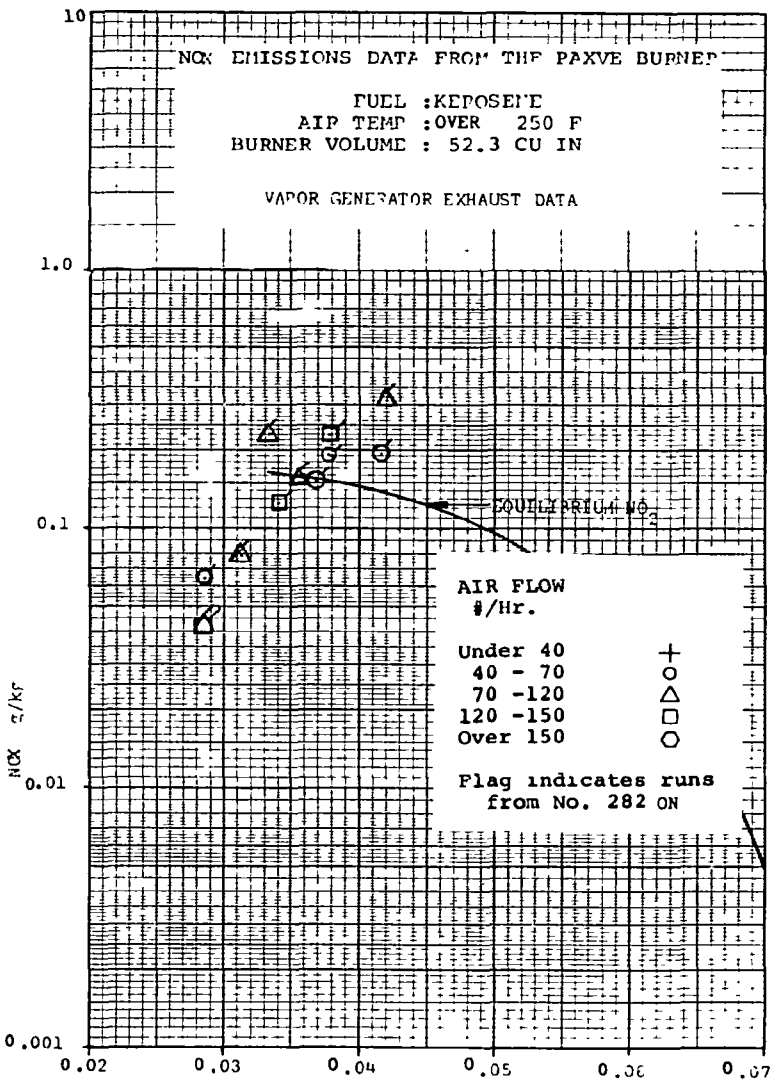
NOX EMISSIONS DATA FROM THE PAXVE BURNER
FUEL :KEROSENE
AIR TEMP :OVER 250 F
BURNER VOLUME : 52.3 CU IN
VAPOR GENERATOR EXHAUST DATA
EQUILIBRIUM NO_2
AIR FLOW #/Hr.
Under 40
40 - 70
70 -120
120 -150
Over 150
Flag indicates runs from No. 282 ON
NOx g/kg
10
1.0
0.1
0.01
0.001
0.02
0.03
0.04
0.05
0.06
0.07
NOMINAL FUEL AIR RATIO — FAN

Fig.82

VII. ANALYTICAL INVESTIGATION

During the course of the program Paxve conducted several analytical studies related to burner operation. The purpose of these studies was to model the performance of a burner to determine which parameters affect the stability limits, the completeness of combustion, and the burner emissions. It was found that a simplified well stirred reactor model could be used to correlate some of the experimental data. The background for that analytical study is presented in Section A below. The analysis itself is presented in Sections B and C.

A. Literature Survey

Combustion theory has been the subject of a wide variety of analytical and experimental investigations for the last several decades. Analyses have included ignition theory, flame stability theory for flame holders and enclosed burners, and analysis of operation and stabilization in recirculating burners.

1. Ignition Theory

Quoting Frank-Kamenetski (Reference 1), "The basic idea of the theory of thermal ignition is due to Van't Hoff (Reference 2). According to it, a condition of thermal ignition consists in the impossibility of a thermal equilibrium between the reacting system and the surrounding medium. The qualitative formulation of this condition as contact between the curve of heat supply and the straight line of heat removal was first given by Le Chatelier (Reference 3). The mathematical formulation was given by Semenov (Reference 4) who obtained an expression for the relation between the explosion parameters (temperature and pressure at the explosion limit) which was later confirmed by Zagulin and a number of other investigators."

The essence of the thermal ignition theory is illustrated in Figure 1 which shows the heat release and heat loss from a vessel in which a combustible mixture has been placed. The walls of the vessel are heated to a temperature T_W and the combustible material inside the vessel undergoes chemical reaction governed by an Arrhenius type equation of the form

$$Q_I = \text{B} \, e^{-E_A/RT}$$

where

Q_I = rate of heat release in the gas

B = a constant which takes into account the concetration of the fuel and oxidizer within the vessel and other parameters significant to the rate of the chemical reaction.

E_A = the activation energy of the combustion reaction

T = the gas temperature

R = the universal gas constant

The gas mixture in the vessel loses heat to the walls in accordance with an equation such as

$$Q_{II} = hA(T-T_W)$$

where

Q_{II} = rate of heat loss from the gas to the wall

h = heat transfer coefficient from gas to wall

A = wall surface area

T_W = wall temperature

Semenov examined these two curves, Q_I the heat production curve, and Q_{II} the heat loss curve. When the two curves intersect (line 3 in figure 1) the gas exists at a temperature slightly higher than the temperature of the wall (T_{W3}) with heat production in the gas being carried to the wall as a result of the minor temperature difference. For a higher wall temperature, T_{W2}, the two curves are tangent, and (case 2) the temperature of the gas rises, but there is still a point, T_A, at which the rate of heat production and the rate of heat loss to the wall are equal. Hence a stable system can exist.

At still higher wall temperature, T_{W1}, there is no point of intersection (case 1). The rate of heat production in the gas is now always greater than the rate in which heat can be lost to the wall. Thus in case 1, if the gas starts out initially at the wall temperature T_{W1}, the temperature of the gas will increase and although the rate of heat loss will also increase the heat production will always exceed the heat loss rate. Once the point T_A has been reached, the rate of heat production will accelerate and the temperature of the gas will increase at an exponential rate.

Semenov termed the value of T_{W2}, for which the tangent point case occurs, the adiabatic explosion temperature. The adiabatic explosion temperature depends not only on the factors influencing rate of heat liberation, but also on the surface area of the vessel. The time required for the gas to reach the exponential temperature rise situation is called the induction period. Semenov examined these factors mathematically in some detail.

2. Stability Theory for Combustion Chambers

Vulis (Ref. 5) performed an extensive analysis of the problems of furnance combustion using Semonov's thermal

ignition theory as a starting point. Vulis argued that, just as the rate of heat production and the rate of heat loss could be used to compute the ignition temperature, one could also compare the rate of heat production with the heat required in a flowing system to analyze the combustion process. The heat required is that needed to heat the inflowing gases to the chamber condition and to make up heat losses from the burner. Vulis analysis is very extensive and covers a great many of the cases of interest to us, and goes beyond those cases to consider in some detail the influence of heat loss by radiation and convection. He only considered first order reactions, however, which limits but greatly simplified the analysis. Vulis also considered the flow case in which heat is transferred back to the incoming gases by radiation and mixing.

Vulis' analysis for burner stability follows substantially the same lines as the analysis presented in Section VII B of this report. It differs from our analysis in two respects. First, Vulis considered only first order combustion kinetics. This greatly simplifies the analysis, but at the same time it restricts the validity of the results. In particular, the influence of pressure on stability tends to be lost with this approach. The other difference between Vulis' analysis and that presented below lies in the grouping of parameters used in the solution. Vulis defined a considerable number of non-dimensional parameters whose arrangement was convenient for his analytical work. Vulis' parameters, however, tend to obscure the heat release and the sensible heat requirements of the analysis. In our analytical work we have used parameter groupings of a more conventional type. Our analysis in this regard follows more closely the work of Longwell and Weiss.

Vulis' analysis, in common with Semenov, assumes that the rate of the combustion reaction is given by an Arrhenious equation. Vulis writes

$$Q_I = ko\ c\ q\ e^{-E_A/RT}$$

where

Q_I = heat release rate

ko = a constant

c = concentration of reacting material

q = heat release of the reaction

E_A, R, T = as before

This heat release is assumed to take place within a chamber as shown in Figure 2. Here combustible material enters the chamber from the left while burned material leaves the chamber on the right. It is assumed in the analysis that mixing of the unreacted material with the burning material in the chamber takes place instantaneously and continuously with zero mixing time and distance. It is also assumed that the concentration of reacting material varies

linearly with the temperature. In other words, as C goes from its initial value C_o to zero, the temperature increases from the inlet to the theoretical flame temperature.

The heat supply required to raise the incoming material to the temperature at which it leaves the chamber can be expressed in terms of the sensible heat of the reacting material

$$Q_{II} = W\ Cp\ (T-T_o)$$

where

Q_{II} = sensible heat increase in the exhaust products

W = flow rate of reacting material into the chamber

Cp = specific heat of the exhaust products

T = temperature in the chamber which is the same as the exhaust temperature

T_o = inlet temperature

Figure 3 shows the heat release (Q_I) and sensible heat (Q_{II}) curves as a function of the temperature in the combustion chamber. These curves are similar to those drawn by Semenov in his ignition theory analysis. There are two differences, however; in Semenov's analysis, only the lower portion of the heat release curve was considered. Vulis, on the other hand, considers the entire heat release curve from below the inlet temperature up to the theoretical flame temperature. The other difference is that the straight line in Semenov's theory represented heat loss to the wall. In Vulis' theory, the straight lines represent the sensible heat of the exit flow.

A stable situation for both Vulis' and Semenov's analyses is represented by an intersection of the two curves for which the heat requirement curve, Q_{II}, increases more rapidly to the right of the intersection than the heat supply, Q_I. An intersection for which Q_I increases faster than Q_{II} is an unstable point which cannot correspond to a steady state solution. This matter is discussed more fully under Section VII B below.

Vulis considered a number of concepts important in burner operation which can be understood by reference to the balance between the heat release rate and the sensible heat required. Figure 4 shows the influence of changing the inlet temperature. The effect here is very similar to that discussed by Semenov when he discussed the influence of changing wall temperature. At some sufficiently high inlet temperature, T_{I1}, there is only one intersection and hence only one operating point for the system. That intersection corresponds to stable combustion taking place within the chamber. This inlet temperature represents and gives rise to the situation in which spontaneous ignition occurs as the gas flows into the chamber.

If we lower the inlet temperature to the value labeled T_{I2}, spontaneous ignition no longer takes place. If there is no combustion occuring in the chamber, the gas will flow through the chamber and the stable intersection to the left of the figure which represents only a small temperature rise, will pertain. If on the other hand, combustion has already been initiated, then the stable intersection to the right will pertain, and the system will continue to burn even though we no longer have a temperature above the ignition temperature at the inlet.

If we further reduce the inlet temperature sufficiently, we can in principle cause the burner to go out. The incipient extinction condition corresponds to T_{I3} in Figure 4. Here, there is only a single point of tangency between the heat release curve and the heat required curve that corresponds to combustion within the chamber. A further reduction in inlet temperature will eliminate this solution which permits combustion to continue, and the burner will go out.

In a similar fashion, Vulis observed that air flow could be varied in such a fashion as to allow ignition or extinction of the chamber. Figure 5 illustrates the influence of varying the flow rate. Here the lower straight line labeled W_1 corresponds to the flow through the chamber for which spontaneous ignition will take place. The flow line W_2 allows for stable combustion to continue, provided it has somehow been initiated. The flow rate corresponding to W_2 will not, however allow the burner to spontaneously ignite. A further increase in flow to W_3 corresponds to incipient blow-out. Any further increase in flow will result in a situation in the burner for which no stable combustion solution exists, and the burner will be extinguished.

Another feature of combustion chambers which was noted by Vulis, is that for a sufficiently high inlet temperature, the critical phenomena of ignition and extinction do not occur. Such a situation is illustrated in Figure 6. We see that for a continuous variation flow rate from a very low value to a very high value, no tangent points exist between the straight line family of curves (Q_{II}) and the heat releases curves (Q_I). At this inlet temperature, only combustion solutions are possible since there is only one intersection between Q_{II} line and the Q_I curve. The combustion becomes increasingly efficient as the flow rate is reduced, but even at high flow rates some combustion takes place.

Vulis considered not only variations in flow and inlet temperature, but also variations in other significant parameters such as the heat of reaction (q). Additionally, he considered the influence of factors such as heat loss and flow recirculation on performance of combustion systems. By restricting himself to first order reaction kinetics he was able to handle the mathematical details of his analysis and provide generalized curves which are of great interest.

3. Gutter Burner and Can Burner Stability

Dezubay (Reference 6), Scurlock (Reference 7) and others have conducted experiments on flame stablization on bluff bodies. They were able to show that the flame holding action of a bluff body such as a disc or V shaped gutter can be correlated in terms of the flow velocity by the flame holder, the dimensions of the flame holder, the pressure level in the burner, and the fuel/air mixture ratio. Dezubay's empirical correlations were of the form shown in Figure 7. The ordinate in Figure 7 is the fuel/air ratio at the flame holder. The abcissa in Figure 7 is a combination of burner parameters given approximately by V/PD.

Longwell and Weiss (Reference 8) conducted experiments similar to those Dezubay except that their flame stabilization testing was done for a can type burner. Burner stability correlations for can burners are generally similar to those for gutter type burners. Figure 8 shows a typical can burner flame stabilization curve. The ordinate again is fuel/air ratio. The abcissa in this case is the burner intensity parameter $I = W_A/\text{Vol}\ p^2$.

Longwell and Weiss also conducted analyses similar to those of Vulis. They considered second order combustion reactions. Longwell is generally considered the author of the phrase "well stirred reactor theory" which covers the case which Vulis called the "zero dimensional case" in which rapid mixing of the inlet flow with the burning material in the chamber is assumed to take place.

Because we will use "well stirred reactor" theory in Section VII B, we will not deal extensively with the details of this type of analysis here. It is interesting to note however, that Dezubay's correlation parameter and the combustion intensity parameter of Longwell and Weiss are closely related. Figure 9 shows how each of these resembles the well stirred chamber considered by Vulis. On the left hand side of Figure 9 we have a sketch of the front portion of a can burner, the air flow W_A enters first row of holes and circulates within the pilot region of the burner, mixing with the burning gases which are contained therein. The volume of the pilot zone and its pressure level are the other parameters of significance in the intensity parameter. On the right hand side of Figure 9, we see a sketch of the recirculation region behind a gutter burner or disc type flame holder. As illustrated here a separated region exists downstream of the flame holder within which the material flowing past the obstruction is recirculated and mixed with burning material which has been stabilized on the baffle. The length of the separated recirculation wake will be proportional to the characteristic dimension of the flame holder, D. If we now consider the rate of air flow into the recirculation volume we can write

$$W_A \propto PVD^2$$

Similarly, the size of the recirculation volume should be given by

$$\text{Vol} \propto D^3$$

Thus, if we form the ratio for the combustion intensity parameter with regard to the separated wake on the baffle type flame holder, we see that

$$\frac{W_A}{\text{Vol } p^2} \propto \frac{PVD^2}{p^2 D^3} = \frac{V}{PD}$$

and therefore the two combustion parameter expressions are equivalent.

4. Comments on Well Stirred Reactor Analysis

Analyses of the well stirred reactor concept have been carried out by many investigators. References 9, 10, 11, and 12 as well as many others deal in various degrees of sophistication and elaboration on the concepts set forth in the works of Vulis and Longwell. It is interesting that this type of analysis is applicable to virtually any type of chemical reaction process in which heat release and a thermally controlled reaction rate are significant. Zwick and Bjerklie conducted analyses on the thermal decomposition of a monopropellant in a gas generator. Their analyses included a well stirred reactor approach as well as one dimensional kinetics approach. The well stirred reactor type of analysis was shown to give a means of correlating experimental data which agreed very well with the experimentally observed behavior of the monopropellant gas generator.

Well stirred reactor theory is quite useful in that it provides a means of correlating experimental data and predicting the influence of various parameters on burner operation. It is not in general an accurate description, however, of the actual situation existing within the chamber. In a well stirred reactor analysis, we assume that the temperature, pressure and compositon everywhere within the region being analyzed are uniform. In practice, of course this is not, and in fact cannot be true. It is not surprising therefore that real chambers show deviations from the predictions made by well stirred reactor analysis and that the variations depend on the extent to which the processes in the chamber lead to inhomogeneity and non-uniformity.

Longwell and Weiss fabricated a reactor which was designed to be as close a physcial embodiment of thorough mixing as they could acheive. Their analysis proved capable of correlating their experimental data quite closely, which is not too surprising since they had attempted to physically simulate the mathematical model. More recently however, Reference 13, has shown that even in an experimental well stirred reactor comparable to that used by Longwell and Weiss, details such as the size and location of the injection ports and the magnitude of the injection velocity influence the behavior of the system. This is of course what one might expect as a result of non-uniformity within the chamber itself.

We must expect therefore that well stirred reactor theory

will provide insight, but not complete detailed information on burner performance. In this regard it was inevitable that the simple "well stirred reactor" theory developed by Vulis and Longwell would lead to more elaborate treatments of burner behavior based on the same basic concepts. Several of the references cited above attempt to refine the analysis by examining in more detail the internal flow pattern, the chemical reactions, or the character of the combusiton products leaving the burner under conditons of incomplete combustion. While the merit of these refinements can be argued, it was our purpose in the present program to use this analytical method as means of understanding and interpreting the experimental behavior of a real burner. With this aim in mind, we decided to use the simplest model and analytical method which would involve the parameters of significance in our experimental program. The analysis itself is presented later in this section of the report. The numerical constants required for the chemical reaction rate expressions were obtained from Reference 14 which gives a review of the various analytical procedures devised by other investigators and also presents equations and constants which give the best fit to available experimental data.

5. Recirculating Flame Stabilization Analysis

In addition to well stirred reactor theory, there is another simple model of burner performance which also provides some interesting insight into burner operation and yet is relatively simple in basic concept. In the analysis by Zwick and Bjerklie (Reference 9) this type of process was defined as recirculation theory.

Vulis distinguishes between the well stirred reactor and the recirculation cases by identifying one of them as the zero dimensional case and the other as the one dimensional case.

The mode of analysis is illustrated in Figure 10. Here we assume instantaneous mixing of the recirculated portion of the exhaust products with the incoming stream of combustibles. After the mixing takes place, we follow the combustion process in the mixture as a funcion of time. The material which finally emerges from the chamber differs from the material present at the initial mixing point because of the reaction which takes place during passage through the chamber. This material now represents both the effluent from the chamber, and input to the recirculation pattern.

Recirculation theory leads to predictions of chamber performance which are similar to those of well stirred reactor theory. They include, however, an additional parameter, the degree of recirculation. When the degree of recirculation approaches infinity the two analytical procedures yield the same result.

Recirculation theory has an advantage over well stirred reactor theory in that it allows one to consider a wider variety of cases. Staged combustion which is common in many types of

gas turbine engine burners and two stage and multi-stage combustion industrial and public utility boilers are burners for which recirculation theory provides additional insight while still allowing for a simple and straight forward analytical procedure.

The true picture of what goes on within a combustion chamber is of course quite complex. Multi-dimensional analysis involving both space and time are required for an accurate model of any real system. Unfortunately such analytical procedures are extremely complex and further handicapped by the fact that the flow patterns and mixing patterns which actually exist in a real apparatus are sometimes unknown and almost beyond reach of any reasonable analysis.

B. Burner Analysis

1. General

For the work conducted here it was decided to perform a well stirred reactor type of analysis rather than to engage in a more sophisticated recirculation type of study. The Paxve burner has considerable internal mixing and hence should be fairly well modeled by well stirred reactor theory.

The purpose of this analysis was two fold. First, we wished to investigate the influence of various parameters such as fuel/air (mixture) ratio and inlet temperature on the stability of the burner. Early observations led us to believe that the Paxve burner was stable over a wider range of operating conditions than other burners with which we were familiar. The possibility of exploring this analytically was therefore desired. Secondly, we hoped that the analysis would shed some light on the relationship between burner operating conditons and the production of air pollution type emissions. In particular, the degree of completness of reaction was to be determined to see if this concept could serve as a means of correlating the experimental data.

The model for the burner analysis is illustrated in Figure 11. Here the burner is represented by a chamber into which the combustible mixture flows and from which the combustion gases exhaust. Within the burner a homogeneous mixture is undergoing chemical reaction. The rate of that reaction is assumed to be given by an Arrhenius type equation. Because we were principally interested in lean combustion we restricted our analyses to mixtures which were leaner than stoichiometric.

The heat which is being generated by chemical reaction within the chamber serves three purposes. First it raises the incoming gas to the temperature within the reaction chamber. Secondly, it sustains the reaction at a rate which is dependent on that temperature. Thirdly, it supplies the heat which leaves the chamber both in the form of hot gases in the exhaust and also in the form of heat loss to the surroundings.

Chamber heat loss is potentially an important parameter

in the analysis. If the walls of the chamber are radiating to the outside there will be heat loss which must be supplied to those walls by convection and radiation from the combustion gases. The chamber can also lose heat to the outside by conduction through the chamber walls. This heat loss must be made up by extraction of heat from the combustion process. Because the stability and efficiency of the burner are very sensitive to the combustion temperature, any heat loss will be significant. The Paxve burner is a relatively well insulated chamber. To a first approximation, therefore, we have ignored heat loss from the burner.

2. Basic Flame Stabilization Analysis

The fundamental concepts involved in combustion within an enclosed space such as the burner of a gas turbine engine can be understood by reference to Figure 11. Here we see a volumne with a fuel air mixture entering from the left at a given set of initial conditions and combustion products leaving on the right. The simplest method of analysis for such a system involves the so called well-stirred reactor concept. The idea is that as the material on the left enters the reactor, it mixes instantaneously and uniformly with the material contained in the volume where the combustion process is taking place. The material which leaves the combustion chamber is assumed to have exactly the same properties as the material contained within the chamber, and the exit flow rate is assumed to be equal to the inlet flow rate.

The analytical method involves equating the rate of heat release in the chamber, determined by chemical kinetic considerations, to the rate of heat release required to raise the gaseous exhaust products to their final temperature. In performing this heat balance we make use of a concept which runs through the entire analytical scheme; that one can consider the reaction as only being partially complete. We use the Greek letter ε to symoblize the "reactedness" of the material passing through the combustion chamber. It corresponds roughly to a combustion efficiency. For a reactedness of 1.0, all of the material which enters the chamber from the left leaves in the form of theoretical combustion products and temperature in the chamber is the theoretical flame temperature diminished by any heat transfer which occurs from the combustion gases to the outside through the chamber walls. If ε, is less than 1.0, a portion of the exhaust products is unburned material and the combustion temperature is correspondingly less.

The analysis is subject to various degrees of sophistication depending on how one treats the unreacted or partially reacted material which leaves a chamber. The simpliest treatment, and the one which will be followed here, is to assume that it leaves as vaporized fuel. A more sophisticated approach which more nearly fits the facts for lean mixtures of hydrocarbon fuels with air, is to assume that the unreacted material leaves as the partial reaction products which are water and carbon monoxide. The degree of unreactedness is then represented by the failure of the carbon monoxide formed to convert to carbon dioxide before leaving the

chamber. While this more sophisticated approach is in closer agreement with reality, it introduces some difficulties in the analysis which do not help to clarify the points which we wish to make in this report. We will adopt the simpler approach here.

3. Mass Balance

Entering the burner are a flow of air, $\dot{W}_A$, and a flow of fuel, $\dot{W}_f$. Flowing out is a mixture of combustion products, $\dot{W}_B$, together with the unburned material, $\dot{W}_U$. The chemical reaction involved (at stoichiometric mixture) is

$$A + F \rightarrow B + \Delta H_B$$

The unburned material exists in a state which may be different from the original, perhaps involving only vaporization of liquid, or possibly involving partial reaction.

Let

θ = stoichiometric f/a

$\phi = (f/a) \cdot \theta$

ε = fraction reacted

Then for lean operation, the air which can burn with W_F is

$$\dot{W}_{AB} = \frac{\dot{W}_F}{\theta}$$

leaving

$$\dot{W}_{AX} = \dot{W}_A - \frac{\dot{W}_F}{\theta}$$

which is excess air.

The fraction of the combustible mixture which burns produces exhaust flow

$$\dot{W}_B = \varepsilon \left(\dot{W}_F + \frac{\dot{W}_F}{\theta} \right)$$

The excess air fraction together with the unburned portion of the combustible mixture yields

$$\dot{W}_U = \left(\dot{W}_A - \frac{\dot{W}_F}{\theta} \right) + \left(\dot{W}_F + \frac{\dot{W}_F}{\theta} \right) \left(1 - \varepsilon \right)$$

If we divide the above expressions by the air flow, $\dot{W}_A$, and substitute and simplify we obtain

$$\frac{\dot{W}_B}{\dot{W}_A} = \varepsilon\phi(1+\theta)$$

$$\frac{\dot{W}_U}{\dot{W}_A} = (1-\phi) + \phi(1+\theta)(1-\varepsilon)$$

The unburned material may be thought of as unburned air, $\dot{W}_{AU}$, plus unburned fuel, $\dot{W}_{FU}$,

then

$$\dot{W}_{AU} = \dot{W}_A(1-\phi) + \dot{W}_A\phi(1-\varepsilon)$$
$$= \dot{W}_A(1-\varepsilon\phi)$$

and

$$\dot{W}_{F_U} = \dot{W}_F(1-\varepsilon)$$
$$= \dot{W}_A\,\phi\theta(1-\varepsilon)$$

4. Heat Balance

The heat release will be assumed to be given by

$$\dot{Q}_I = \dot{W}_B\Delta H_B$$
$$= \dot{W}_A\Delta H_B\varepsilon\phi(1+\theta)$$

For no heat loss from the system, the heat balance in terms of mean specific heats is

$$\dot{Q}_{II} = \dot{W}_B\Delta H_B = (\dot{W}_B C_{P_B} + \dot{W}_{AU}\,C_{P_A} + \dot{W}_{FU}\,C_{P_F})\,\Delta T + \dot{W}_{FU}\,\Delta H_V$$
$$= \dot{W}_A\,[(\varepsilon\phi(1+\theta)\,C_{P_B} + (1-\varepsilon\phi)\,C_{P_A} + (1-\varepsilon)\phi\theta C_{P_F})\Delta T + (1-\varepsilon)\phi\theta\Delta H_V]$$

where

ΔH_V = latent heat of vaporization of fuel

W_{FU}, W_{AU} = total unburned fuel and air in exhaust

C_{P_B}, C_{P_A}, C_{P_F} = mean specific heats of combustion products, air and fuel

This yields a combustion temperature of

$$T_B = T_1 + \frac{\varepsilon\phi(1+\theta)\Delta H_B - (1-\varepsilon)\theta\phi\Delta H_V}{C_{P_B}\,\varepsilon\phi(1+\theta) + C_{P_A}\,(1-\varepsilon\theta) + C_{P_F}\,(1-\varepsilon)\phi\theta}$$

5. Reaction Rate

The reaction rate for the combustion reaction in the volume is given by

$$\dot{W}_B = K\,[F]^x\,[a]^{n-y}\left(\frac{P}{RT_B}\right)^n \text{Vol}\; e^{-E/RT_B}$$

where

$K = K(T)$ = collision factor

$[F]$, $[a]$ = concentration of reactants in mole fraction

x = fractional order $\simeq 1$

n = order of reaction $\simeq 2$

vol = volume of chamber

E = activation energy of the combustion reaction

We can easily show that

$$[F] = \left[\frac{W_F/M_F}{W_B/M_B + W_{AV}/M_A + W_F/M_F}\right]$$

$$= \frac{(1-\varepsilon)\phi\theta}{(1-\varepsilon)\phi\theta + (1-\varepsilon\phi)\frac{M_F}{M_A} + \varepsilon\phi(1+\theta)\frac{M_F}{M_B}}$$

and

$$[a] = \frac{(1-\varepsilon\phi)\frac{M_F}{M_A}}{(1-\varepsilon)\phi\theta + (1-\varepsilon\phi)\frac{M_F}{M_A} + \varepsilon\phi(1+\theta)\frac{M_F}{M_B}}$$

where

M_A, M_B, M_F - Molecular weights of air, combustion gases, and fuel vapor

This gives us

$$\dot{W}_B = \frac{K(1-\varepsilon)^x (1-\varepsilon\phi)^{n-x} \theta\phi \frac{M_F}{M_A}\left(\frac{P}{RT}\right)^n \text{Vol}\, e^{-E/RT_B}}{\left[(1-\varepsilon)\phi\theta + (1-\varepsilon\phi)\frac{M_F}{M_A} + \varepsilon\phi(H\theta)\frac{M_F}{M_B}\right]^2}$$

6. Stability Requirement

Stable operation will take place if the rate of heat release is equal to the heat production necessary to heat the exhaust products. There are several ways to approach this last equation. Perhaps the clearest is the one which involves plotting the heat release rate and the heat production rate required against temperature in the burner. The result is two curves of the sort shown in Figure 12.

In Figure 12 there are two lines, one labeled Q_{II} and the other Q_I. Q_I is the rate of heat release based on the reaction

rate equation while Q_{II} is the heat flux necessary to achieve the indicated temperature. In general these curves will have 3 points of intersection, one close to the origin and the other two as noted in Figure 12 and marked a and b.

The intersection at point b represents a stable operating point for the burner. For temperatures higher than T_b, the heat flux necessary to achieve the indicated temperature is higher than the rate of heat generation available in the burner. As a result, if the burner is initially at a temperature slightly higher than T_b, it will come back to the operating point indicated by b. On the other hand, if the temperature is slightly less than the temperature corresponding to intersection b, the rate of heat flux in the system is greater than that necessary to heat the products to the indicated temperature and hence the temperature in the combustion volume will increase until the stable operating point b is reached.

Point a is an unstable point. If the temperature is slightly less than that indicated by the intersection at a, the rate of heat production is less than the heat necessary to achieve the indicated operating temperature. The temperature of the combustion gases will fall towards zero and the burner will go out. If the termperature of the gas in the burner is slightly higher than T_a, the rate of heat production will exceed the rate of heat required for the temperature in question and the temperature of the gases in the burner will increase until stable point b is again reached.

It is interesting that in practical combustion devices the phenomena discussed above can be observed, sometimes with unusual results. For example a small gas generator with which we have had operating experience, could be inadvertantly placed into operation at this partial reaction point for a matter of many minutes before it would either jump up to point b and operate stable and efficiently, or else quench and go out.

The heat release rate indicated by the curve Q_I depends on the volume of the system, its pressure and temperature, but does not depend directly on the flow rate through the burner. The curve labeled Q_{Bal}, on the other hand, is directly proportional to the flow rate through the burner. If we increase the flow rate, new points of intersection between the two curves will be achieved. Figure 13 shows the limiting case where the two curves are tangent at only one point which in this case is labeled c. Point c is the incipient blowout limit of the burner. The burner may operate at this point for an extended period of time, but it has no stability margin. Any minor shift in conditions in an unfavorable direction will cause the reaction to die away.

It should be noted that there are two ways in which one can reach a point of incipient blowout in a given burner. We can change the conditions of the line affecting Q_{II} by increasing the air flow, or we can change the factors affecting Q_I. The principal factor influencing Q React in an otherwise stable situation is the equivalence ratio ϕ. One might also, however,

change the reaction rate as a result in change of pressure. In the experiments conducted by Paxve on the Paxve Burner for APCO, we have determined incipient blowout by reducing the fuel/air ratio until the lean limit was reached.

A factor which was not introduced in the above equation, but which is significiant in a real burner, is heat transfer from the gases. Heat transfer has the effect of reducing the heat release indicated by the curve Q_I by an amount which depends on the temperature of the surroundings and the mode of heat transfer involved. In particular, heat transfer to the wall of the burner has a dramatic affect on the stability of the burner. A burner of the type utilized by Paxve has very little heat transfer to the walls under steady state operating conditions. During startup and shutdown, and when changing operating conditions, heat exchange between the gases and the wall plays a significant role. As incipient blowout is reached, the burner will remain lit for a matter of 10 to 20 minutes even though the equivalence ratio has been reduced below blowout limit. The difference between the heat required and the heat available in these conditions is quite small, and the warm walls of the burner provide the necessary difference during the time the burner takes to go out.

If we equate the heat production required to achieve a given temperature with the heat production available as a function of reaction rate, we obtain the following equation.

$$I = \frac{W_A}{P^2\ Vol} = \frac{k(1-\varepsilon)(1-\varepsilon\phi)\,\theta\,\frac{M_F}{M_A}\,e^{-E_B/RT_B}}{\varepsilon(1+\theta)\left[\phi(1+\theta)\varepsilon\,\frac{M_F}{M_B} + (1-\varepsilon\phi)\,\frac{M_F}{M_A} + (1-\varepsilon)\varepsilon\phi\right]^2 T_B^{\,1.5}}$$

The reaction rate constant K here has been related to temperature by

$$K = k\ T^{0.5}$$

and x = 1 and n = 2 are assumed.

The equation for I can be solved if we have values for all of the parameters and TB. The equation for TB requires that we have values for the average specific heats of the air, the fuel and combustion products. For the present analysis, equations were generated for these specific heat values using data from reference 15.

The specific heat data (in metric units) and the averaging equations (in English units) were:

Air

$$\tilde{c}_p = 6.557 + 1.477 \times 10^{-3}\ T - 2.148 \times 10^{-6}\ T^2 \quad \text{cal/Mole °K}$$

$$CA_{avg} = 0.22618 + 1.4147 \times 10^{-5}(T+T_o) - 7.8229 \times 10^{-10}\,(T^3 - T_o^{\,3}) / (T-T_o) \quad \text{BTU/lb°R}$$

Fuel

$$c_p = 0.02 + 1.51 \times 10^{-3}T - 7.7 \times 10^{-7}T^2 + 1.5 \times 10^{-10}T^3 \text{ Cal/gm°K}$$

$$C_{F_{avg}} = 0.02 + 4.194 \times 10^{-4}(T+To) - 7.9218 \times 10^{-8}(T^3-To^3)/(T-To) + 6.43 \times 10^{-12}(T^4-To^4)/(T-To) \quad \text{BTU/lb°R}$$

CO_2

$$\tilde{c}_p = 18.036 - 4.474 \times 10^{-5}\ T - 158.08\ /\sqrt{T} \quad \text{Cal/mole°K}$$

$$C_{CO2avg} = 0.40991 - 2.8245 \times 10^{-7}(T+To) - 9.6403\ (\sqrt{T} - \sqrt{To})/(T-To) \text{ BTU/lb°R}$$

H_2O

$$\tilde{c}_p = 6.970 + 3.464 \times 10^{-3}\ T - 4.833 \times 10^{-7}\ T^2 \quad \text{Cal/mol°K}$$

$$C_{H_2O_{avg}} = 0.38722 + 5.3457 \times 10^{-5}\ (T+To) - 2.7623 \times 10^{-9}(T^3-To^3)/(T-To) \quad \text{BTU/lb°R}$$

N_2

$$\tilde{c}_p = 6.529 + 1.488 \times 10^{-3}\ T - 2.271 \times 10^{-7}\ T^2 \quad \text{Cal/mole °K}$$

$$C_{N_{2avg}} = 0.23318 + 1.4762 \times 10^{-5}(T+To) - 8.3444 \times 10^{-10}(T^3-To^3)/(T-To) \quad \text{BTU/lb°R}$$

For purposes of the analysis, the reaction taking place was assumed to be that of octane with air. The reaction was given by

$$C_8 H_{18} + \frac{25}{2}(O_2 + 3.77\ N_2) \rightarrow 8CO_2 + 9H_2O + 47.125\ N_2$$

This gives an exhaust gas composition of

N_2 - 73.489 Mole% - 71.966 Wt%

CO_2 - 12.476 Mole% - 19.198 Wt%

H_2O - 14.035 Mole% - 8.8356 Wt%

The average specific heat of the combustion products is therefore:

$$C_{B_{avg}} = 0.28072 + 1.5293 \times 10^{-5}(T+To) - 8.4458 \times 10^{-10}(T^3-To^3)/(T-To) - 1.8508\ (\sqrt{T} - \sqrt{To})/(T-To) \quad \text{BTU/lb°R}$$

7. Limitations on the Analysis

The theoretical analysis performed here was limited in two major aspects. First the influence of heat loss on the stability and performance of the burner was not investigated. Secondly, the performance and stability of the burner for fuel rich operation were not investigated. The failure to investigate heat loss effects was the result of a lack of available funds on the program rather than a lack of interest in the

subject. Failure to investigate fuel rich operation was due primarily to a combination of lack of interest and the factors sighted above.

The influence of heat loss on burner performance and stability is a subject which should be studied closely. It may be that the outstanding performance of the Paxve burner is in some measure attributable to the low heat loss characteristics of this device. Fuel rich operation is of some interest for burner applications to systems in which two stage combustion would be a desirable feature. Fuel rich operation of the Paxve burner is not contemplated for automotive Rankine cycle or automotive gas turbine applications.

C. Computer Analysis

The theoretical burner analysis equations presented above were programmed for analysis on a digital computer. The programs were written in APL, a new programming language devised by IBM and made available on a time sharing basis through Proprietary Computer Services, Inc., of Van Nuys. A number of programs and sub-routines were written. The purpose of each program and the results of the analyses are discussed below.

1. Program CAL

Program CAL, shown in Table 1, is the basic computation program used in the burner analysis. This program was used as a subroutine in a number of the other programs. For given input values of air inlet temperatures, (TI - degrees Rankine) and equivalence ratio (PH), CAL computes the combustion temperature (TB) and the combustion intensity parameter (INT).

CAL includes a correction to the heat of combustion which allows for the heat required to warm the fuel up to the initial temperature, and an iteration procedure for the specific heats of the air/fuel and combustion products. Initial values for these three specific heats are assumed in order to make an initial estimate of the combustion temperature. The specific heats are then corrected for the average value between the inlet temperature and the combustion temperature and the process iterated until the computed combustion temperature agrees with the previous value to within one degree.

CAL returns values of TB (the combustion temperature), and INT (the combustion intensity parameter) to the other programs.

2. Program HOT

Program HOT, shown in Table 2 was used to compute tables of TB and INT for sets of inlet temperature, equivalence ratio, and combustion efficiency values. HOT calls CAL as a subroutine. HOT was used to generate the results presented in Tables 3 through 8.

During the course of the contract, we frequently found

it desirable to be able to compare the predicted efficiency of the burner with the experimentally measured values of carbon monoxide and unburned hydrocarbons. In this regard, curves were made of the so-called "unreactedness" which is defined as

$$\delta = 1 - E$$

where

E = Burner Efficiency

Figures 14 thru 19 show the unreactedness plotted against the intensity parameter I for various values of inlet temperature. The parameter in the curves is the equivalence ratio PHI.

3. Programs BURN and STABILITY

BURN is the computer program which was used to compute the stability of the burner. BURN accepts an inlet temperature TI as its input. It then examines the value of the combustion intensity parameter, INT, over the range of burner efficiencies from 0.3 up to 1.0. It uses the subroutine CAL to perform this calculation. BURN then selects the maximum value of INT, and calculates 10 new values, five on either side of the maximum. It returns this value of INT together with the corresponding value of burner temp. (TB) and combustion efficiency (E).

STABILITY is a small program shown in Table 9 which was used to vary the imput temperature and accumulate the output for the combustion stability calculations. It used BURN as a subroutine for the stability calculation.

Tables 10 and 11 show the results of the stability calculations made using STABILITY and BURN. The output columns give the equivalence ratio, the efficiency at the stability limit, the predicted combustion temperature at the stability limit allowing for the inefficiency, and the combustion intensity parameter at the stability limit.

Figure 20 shows a plot of the combustion stability data. In this figure, the limiting value of the combustion intensity parameter is the abscissa and the equivalence ratio is the ordinate. The parameter for the curves is the burner air inlet temperature.

4. Program INTPLOT

In performing the combustion stability analysis with Program BURN, we assumed that the intensity parameter would show a local maximum with varying efficiency. This is not always the case, as was pointed out in the earlier discussion of combustion theory. When the inlet temperature is raised to a sufficiently high value we find that the critical conditions which normally characterize burner operation are no longer

present.

The normal phenomena in a burner involves both ignition and extinction limits. For a given value of an inlet temperature and equivalence ratio there are normally two air flow rates (combustion intensity parameter conditions) which correspond to these two critical values. At a sufficiently low value of air flow rate, an adiabatic burner will spontaneously ignite. At some higher value of air flow rate the burner is unable to sustain combustion and the burner blows out.

This form of ignition only occurs in practice at high inlet temperatures. It is not the one which is used in most conventional burners. It is nevertheless a concept which is readily apparent from the combustion analysis. High flow rate flame-out is, however, a common occurence in any burner system.

In order to examine this question further, the values of combustion intensity parameter corresponding to various values of combustion efficiency and equivalence ratio were computed using computer program INTPLOT, shown in Table 12. It uses CAL as a subroutine for computing temperature and intensity parameter. The results from INTPLOT are shown in Table 13. This same information is plotted in Figure 21. The ordinate of the figure is the fraction burned or as it is more generally termed, the combustion efficiency. The abscissa is the intensity parameter.

Examination of the curves in Figure 21 reveal clearly the nature of the critical conditions which normally exist within a burner, and how, for some values of burner operating conditions, these critical phenomena no longer occur. Referring to the curve for equivalence ratio 1.0, we see that the ignition condition corresponds approximately to INT = 371 which occurs at about 10% combustion efficiency. This means that for an inlet temperature of 2000°F, with a stoichiometric mixture, we will achieve spontaneous ignition in the burner if we reduce the air flow level to the point where the itensity parameter is below the value 371 which corresponds to the ignition critical point.

The blow out condition, on the other hand, can be seen from Figure 21 to occur at I = 982, at an equivalence ratio of 0.5. This means that once we have ignited the burner, we can then increase the flow rate through the burner to approximately 2.5 times the flow rate at ignition before the burner will blow out.

Examination of the other curves in Figure 21 show that these two critical conditions, which correspond to the vertical tangents of the constant equivalence ratio curves, exist for those curves for which the equivalence ratio is 0.3 or higher. For $\phi < 0.3$, the curve has no vertical intercept. The curve for an equivalence ratio of 0.1 does not even approach a vertical slope. For this set of burner operating conditions, therefore, we cannot speak of an ignition or a blow out condition. Some reaction will take place within the burner at any value of flow rate. In a manner of speaking, the burner is always ignited and cannot be blown out. This is a particularly interesting phenomena

in view of the fact that the combination of high inlet temperatures and low equivalence ratios which lead to this situation may arise in burners for regenerative gas turbines.

It should be appreciated that the stability analysis which was conducted using program BURN was not able to evaluate stability limits when in fact none existed. To prevent the computer from encountering this situation two safeguards were put into program BURN. First, no efficiency values less than 0.3 were examined by the computer. Secondly, if the maximum value of the intensity parmeter within the region of the analysis was corresponded to the first point analyzed (E=0.35), the computer skipped the remainder of the calculation and went on to the next point in the table of values that it was computing. The conditions in Table 11 for which no critical phenomena occur are indicated by *****.

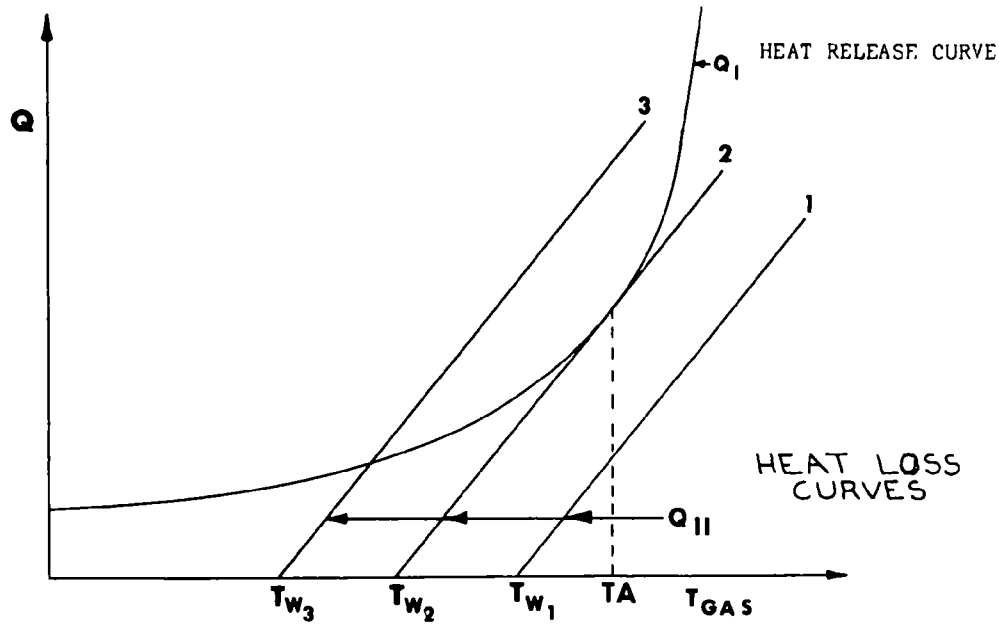

SEMENOV'S THERMAL IGNITION THEORY

Figure VII-1

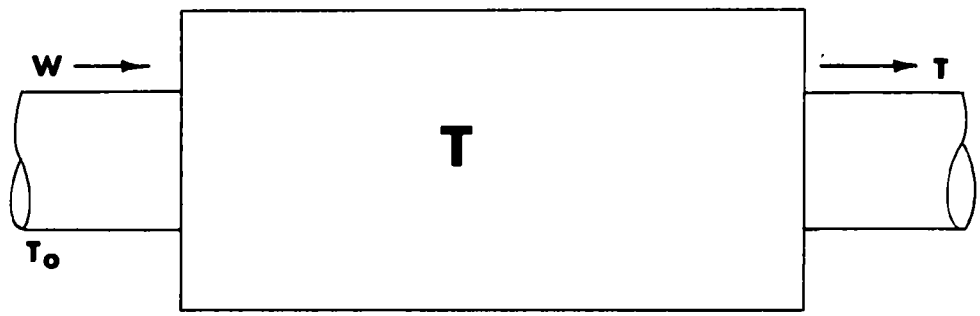

SIMPLIFIED COMBUSTION MODEL

Figure VII-2

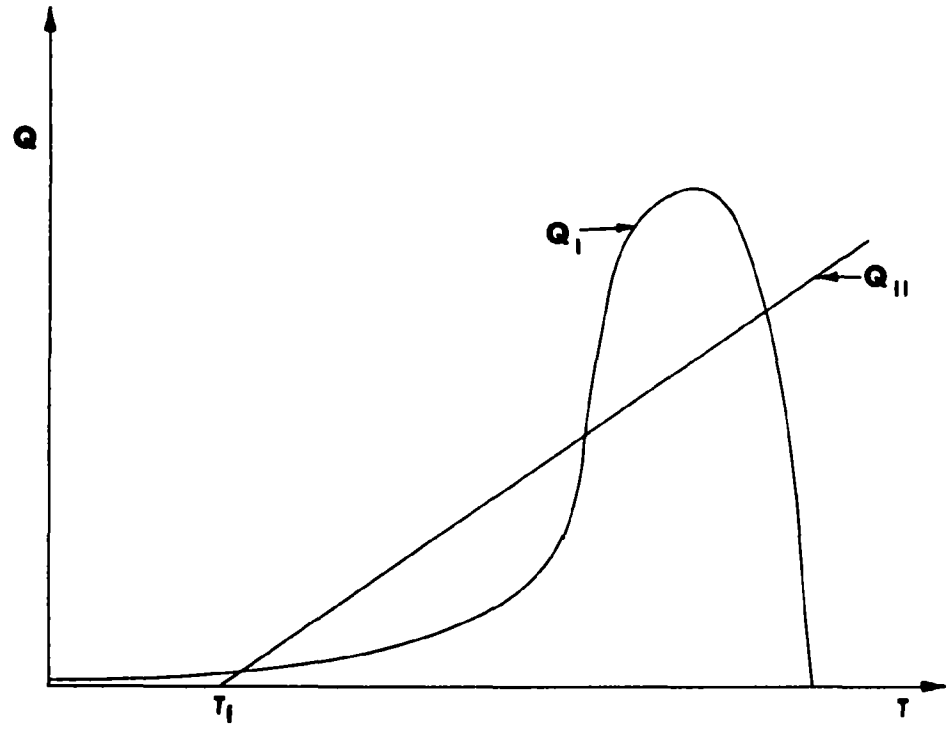

VULIS' COMBUSTION THEORY

Figure VII-3

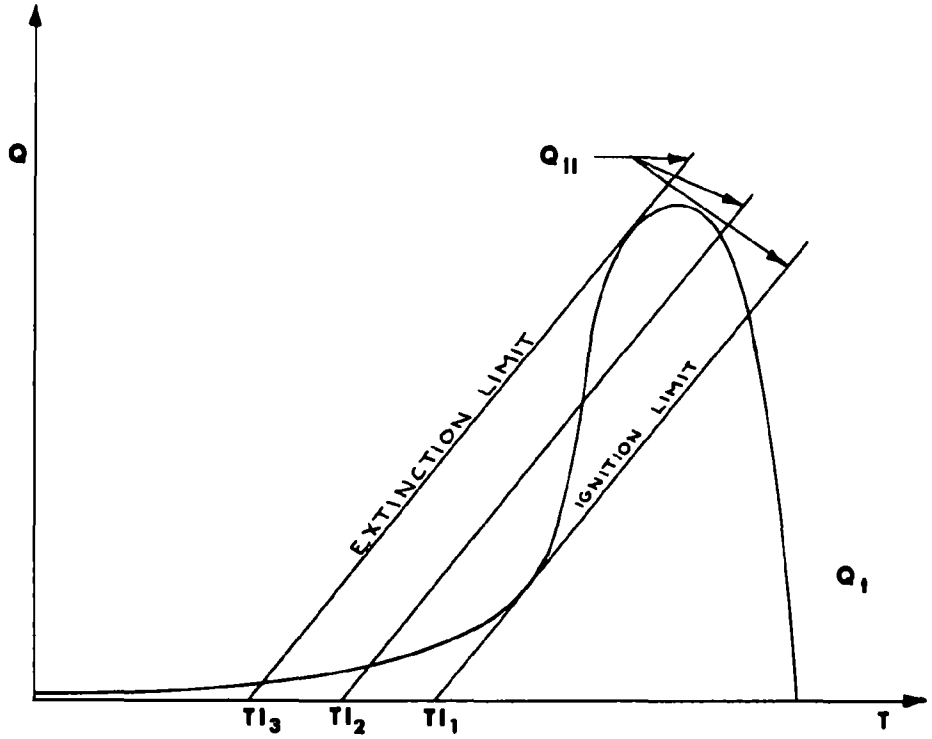

EFFECT OF INLET TEMPERATURE
ON CRITICAL PHENOMENON

Figure VII-4

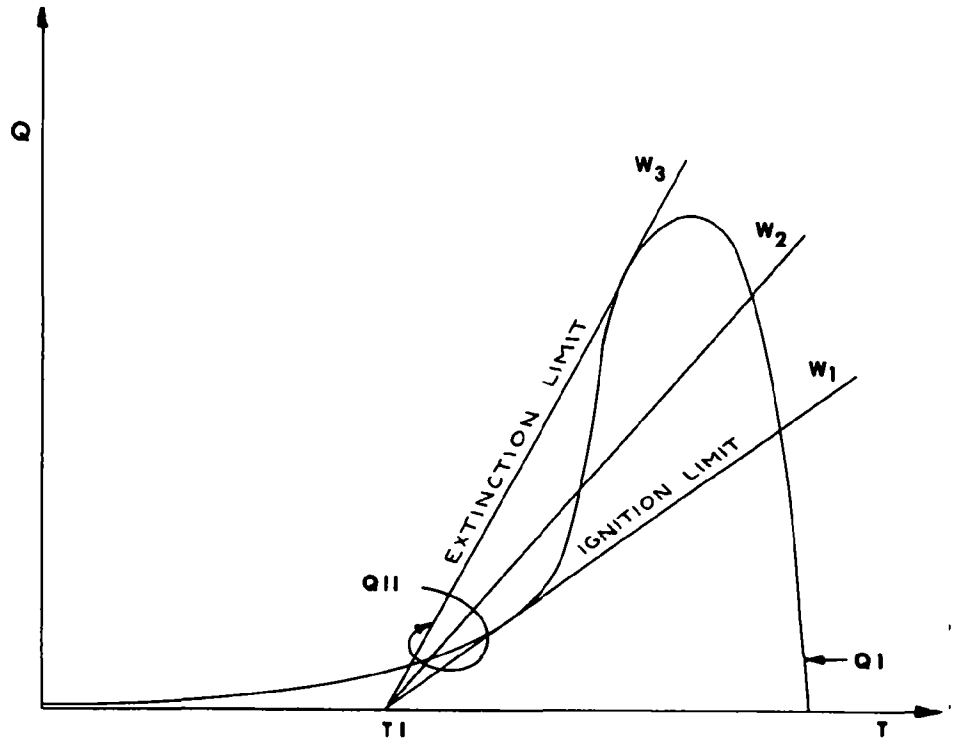

EFFECT OF FLOW RATE ON CRITICAL PHENOMENON Figure VII-5

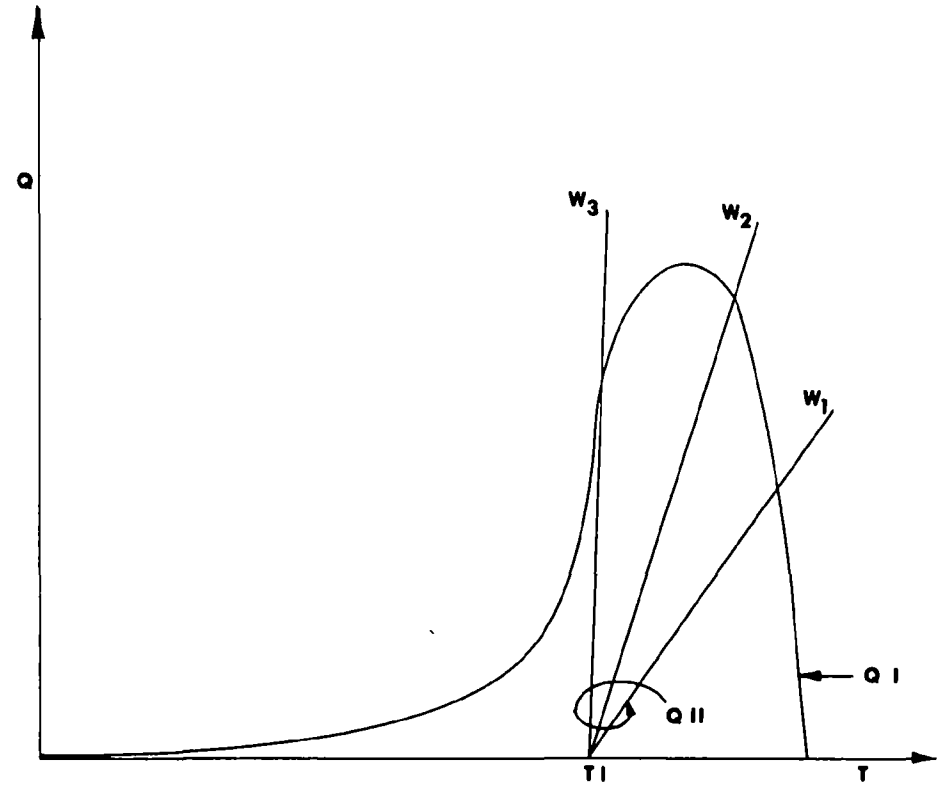

COMBUSTION SYSTEM

WITHOUT CRITICAL (IGNITION AND EXTINCTION) PHENOMENON Figure VII-6

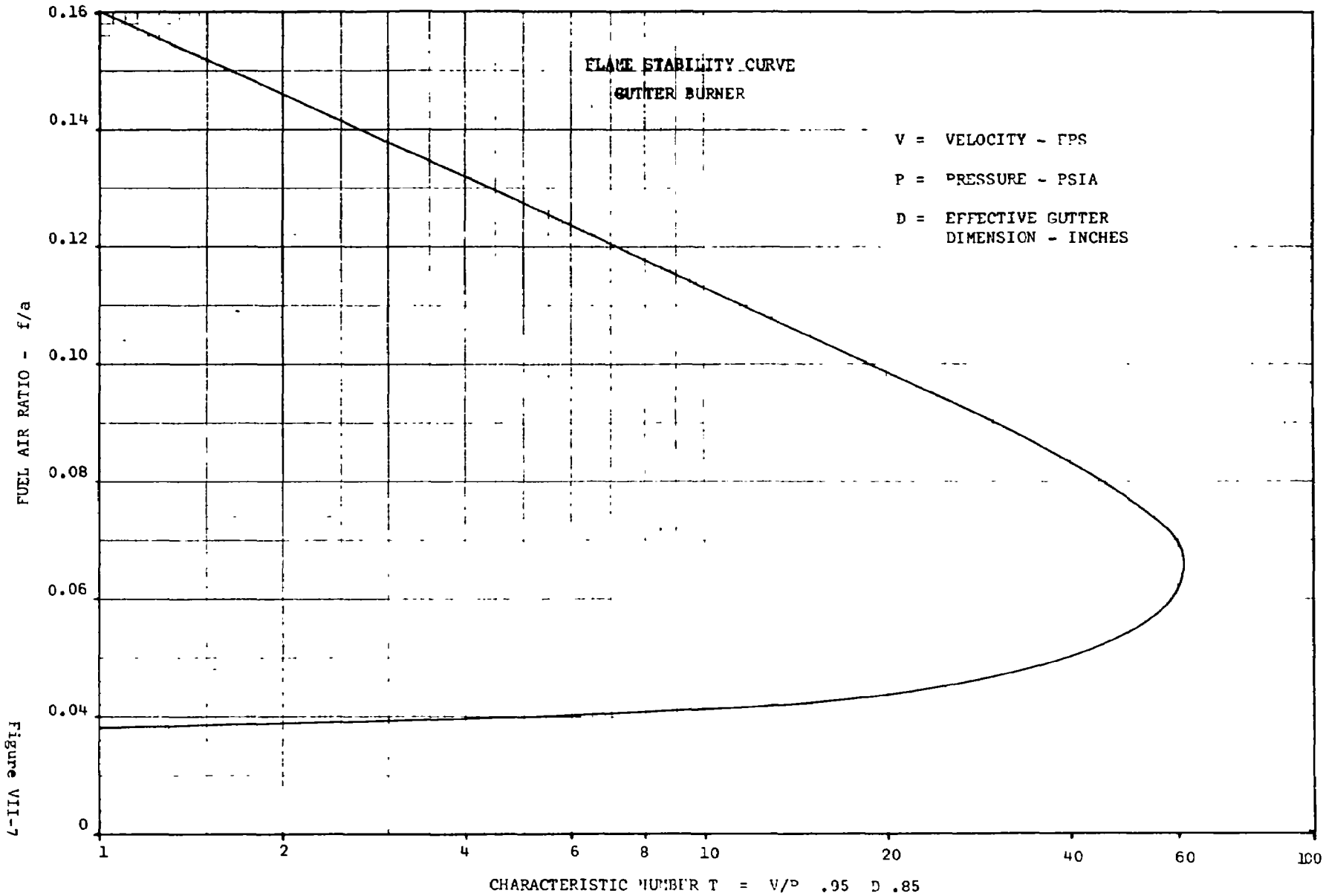
FLAME STABILITY CURVE
GUTTER BURNER
V = VELOCITY - FPS
P = PRESSURE - PSIA
D = EFFECTIVE GUTTER DIMENSION - INCHES
FUEL AIR RATIO - f/a
0.16
0.14
0.12
0.10
0.08
0.06
0.04
0
1
2
4
6
8
10
20
40
60
100
CHARACTERISTIC NUMBER T = V/P .95 D .85

Figure VII-7

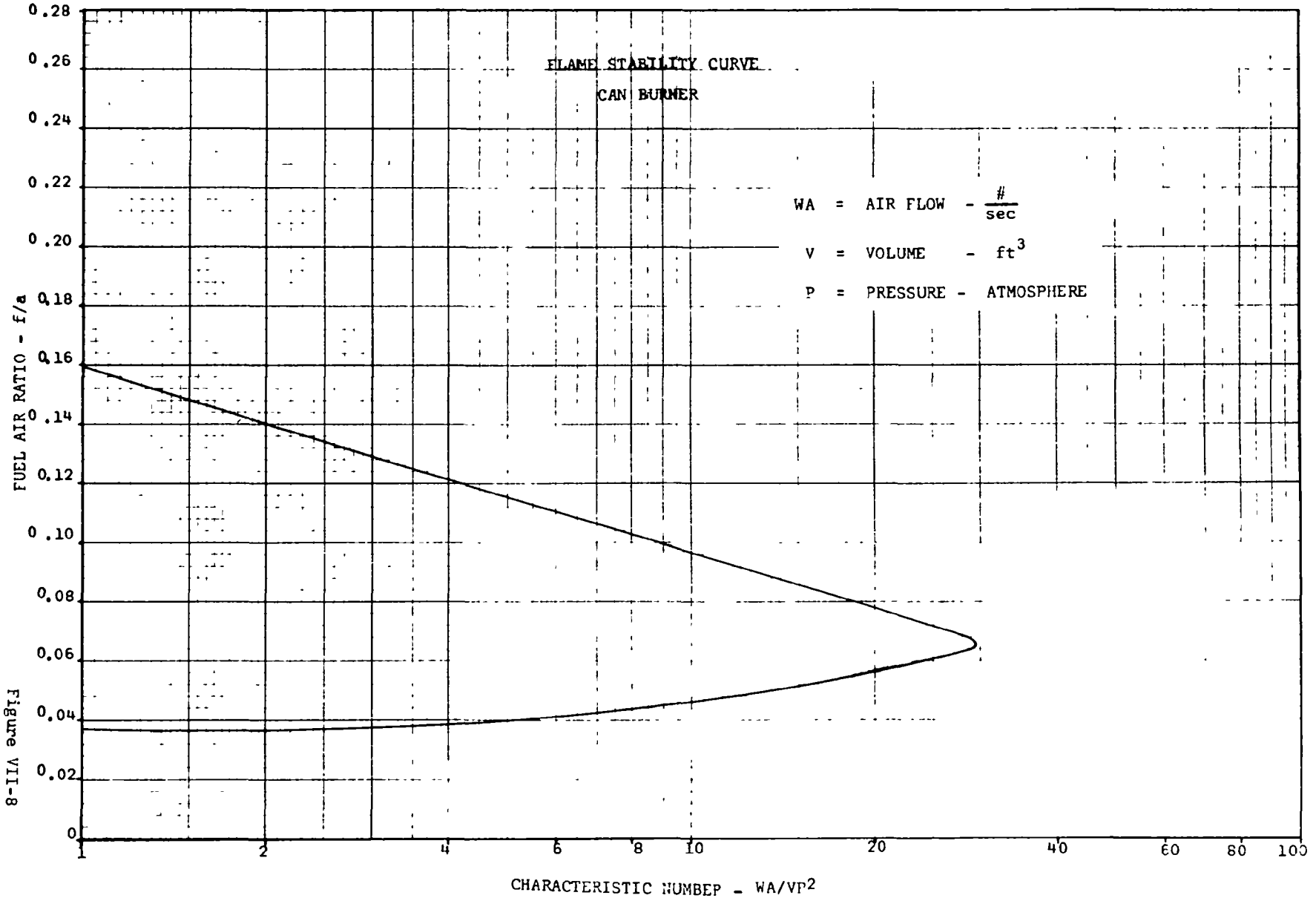
FLAME STABILITY CURVE
CAN BURNER
WA = AIR FLOW - #/sec
V = VOLUME - ft3
P = PRESSURE - ATMOSPHERE
FUEL AIR RATIO - f/a
0.28
0.26
0.24
0.22
0.20
0.18
0.16
0.14
0.12
0.10
0.08
0.06
0.04
0.02
0
1
2
4
6
8
10
20
40
60
80
100
CHARACTERISTIC NUMBER - WA/VP2

Figure VII-8

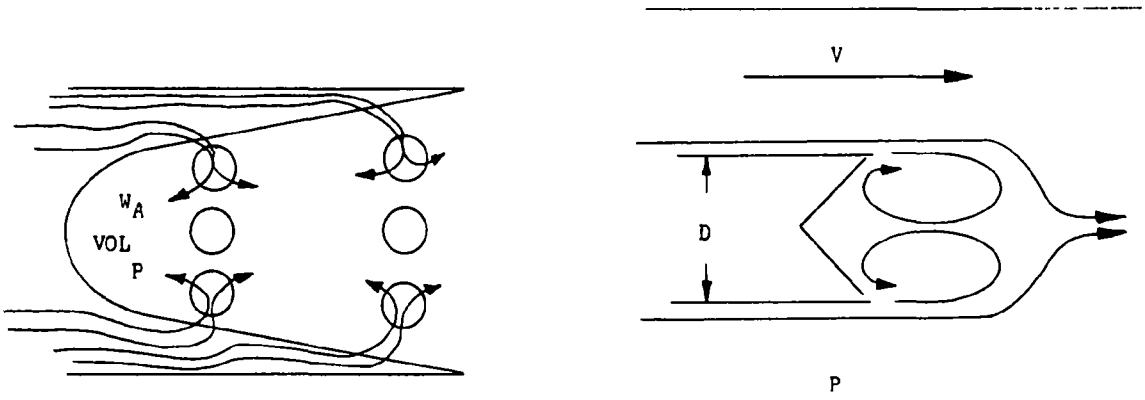

CAN BURNER AND GUTTER BURNER CONCEPTS

Figure VII-9

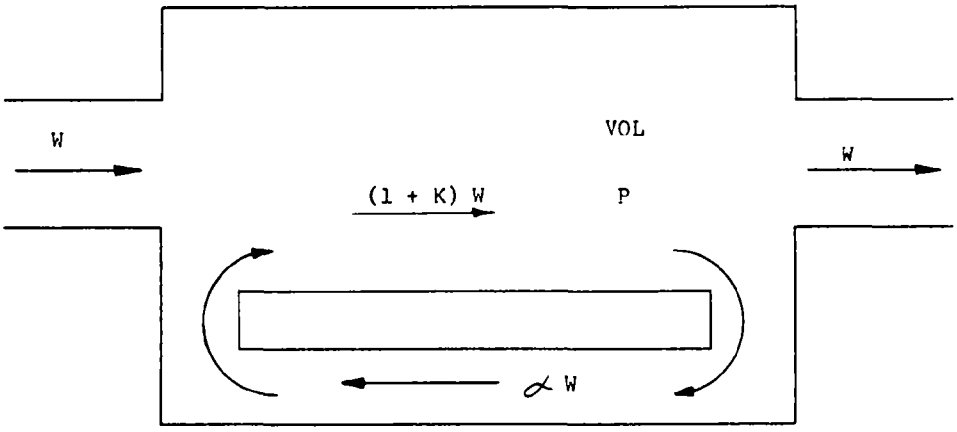

RECIRCULATION MODEL

Figure VII-10

BURNER ANALYSIS TECHNOLOGY

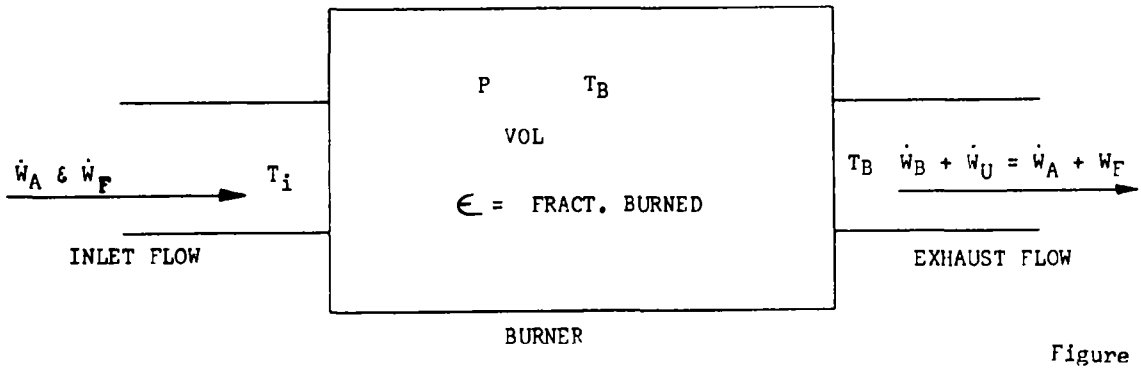

Figure VII-11

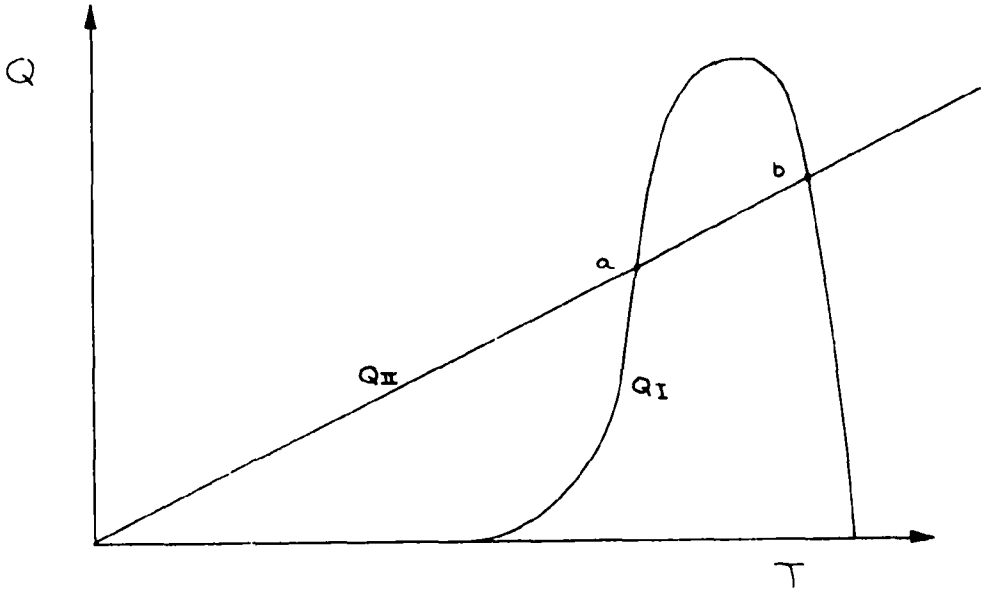

STABLE OPERATING HEAT BALANCE

Figure VII-12

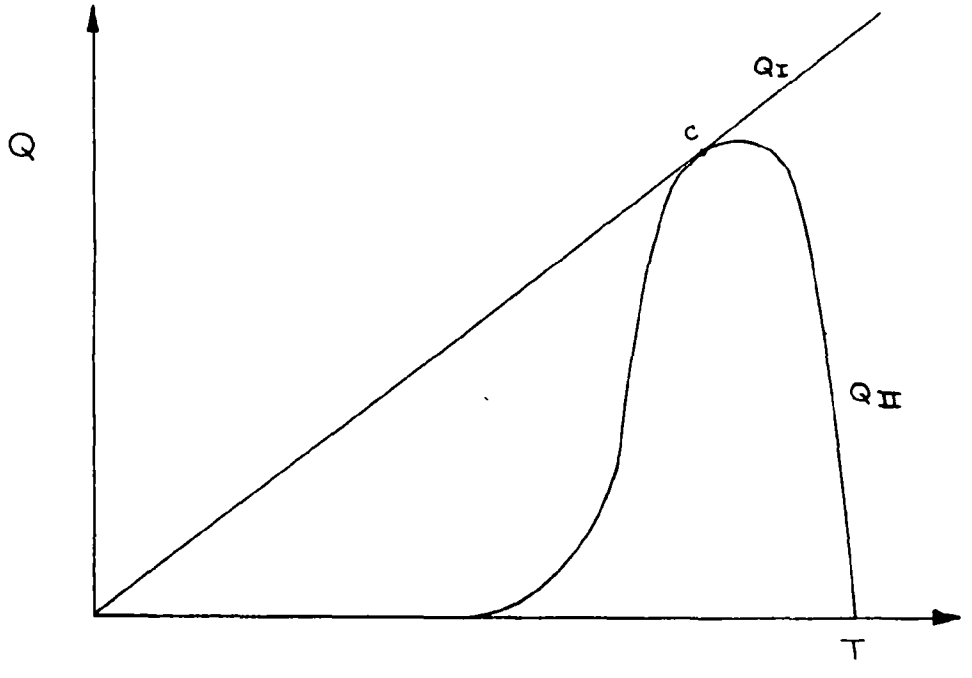

INCIPIENT BLOWOUT HEAT BALANCE

Figure VII-13

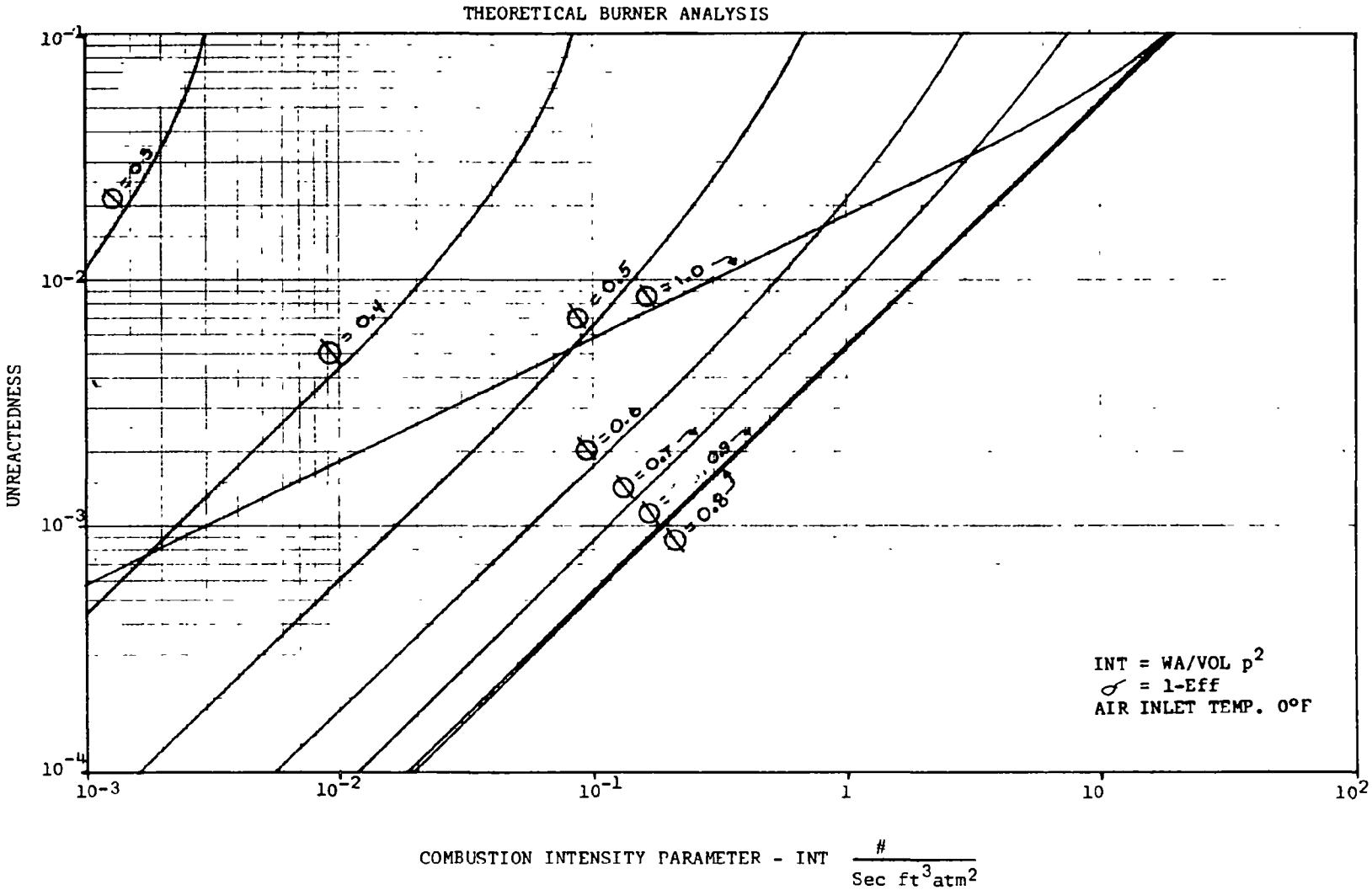

Figure VII - 14

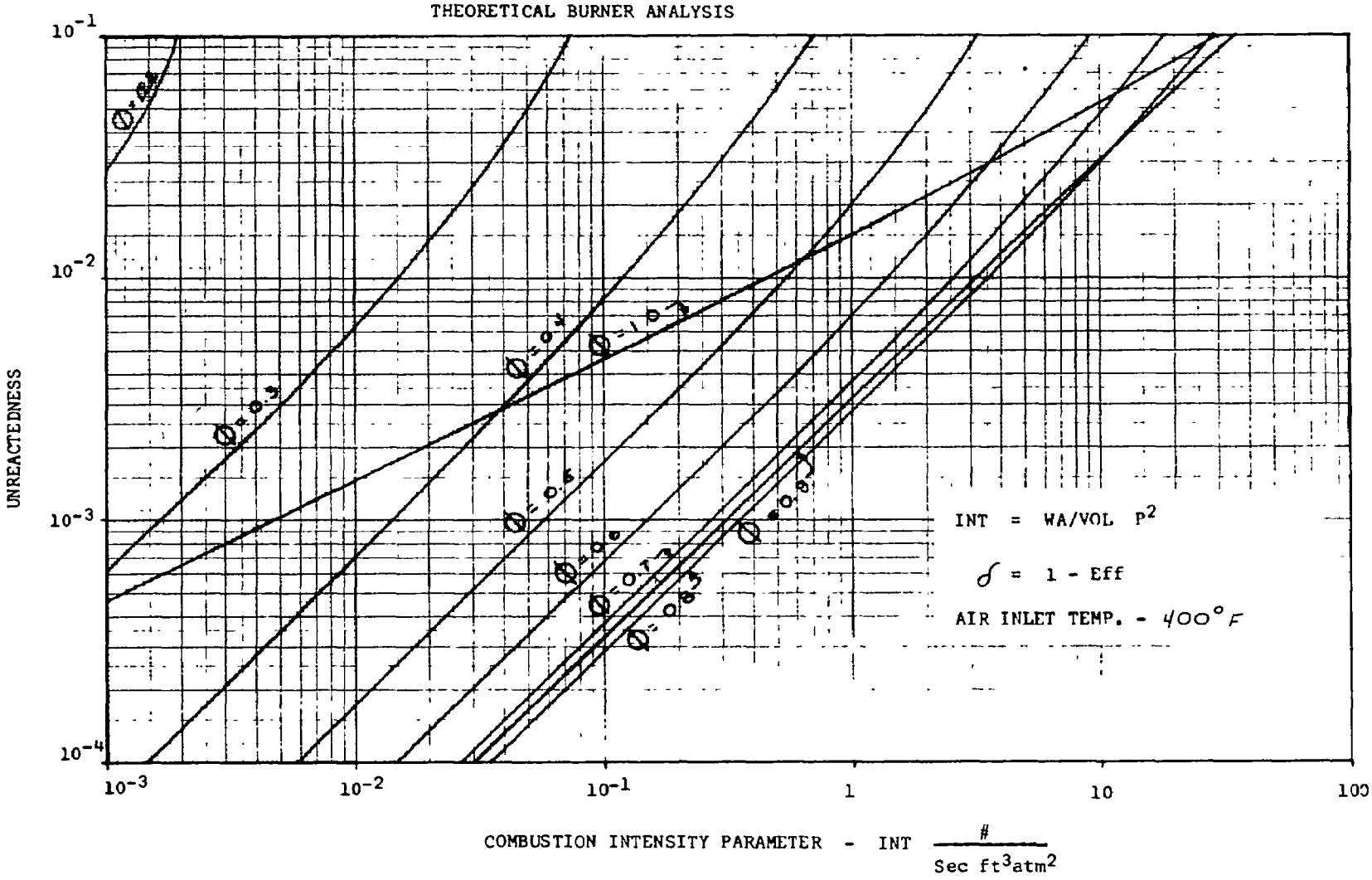

Figure VII - 15

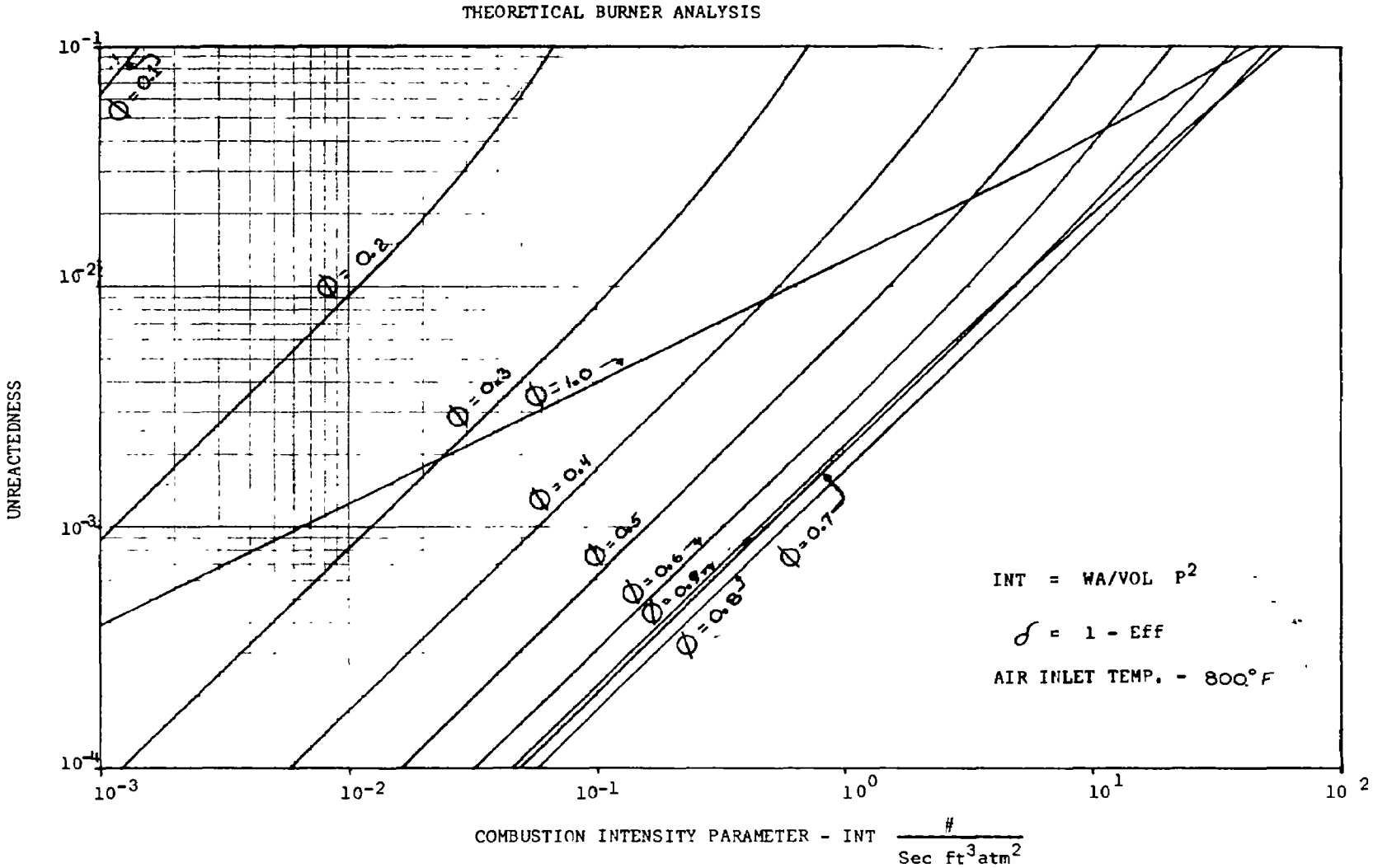

Figure VII - 16

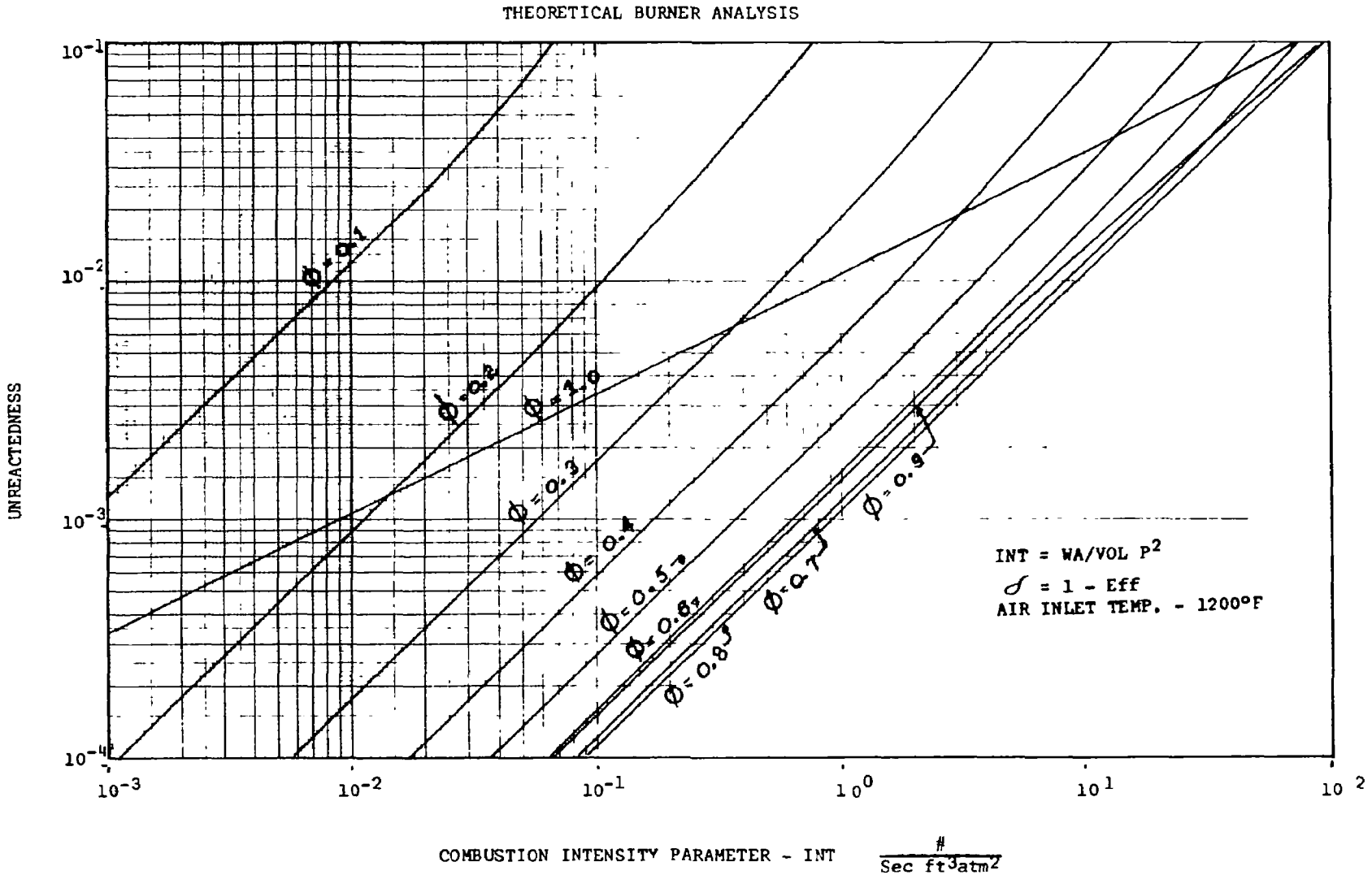

Figure VII - 17

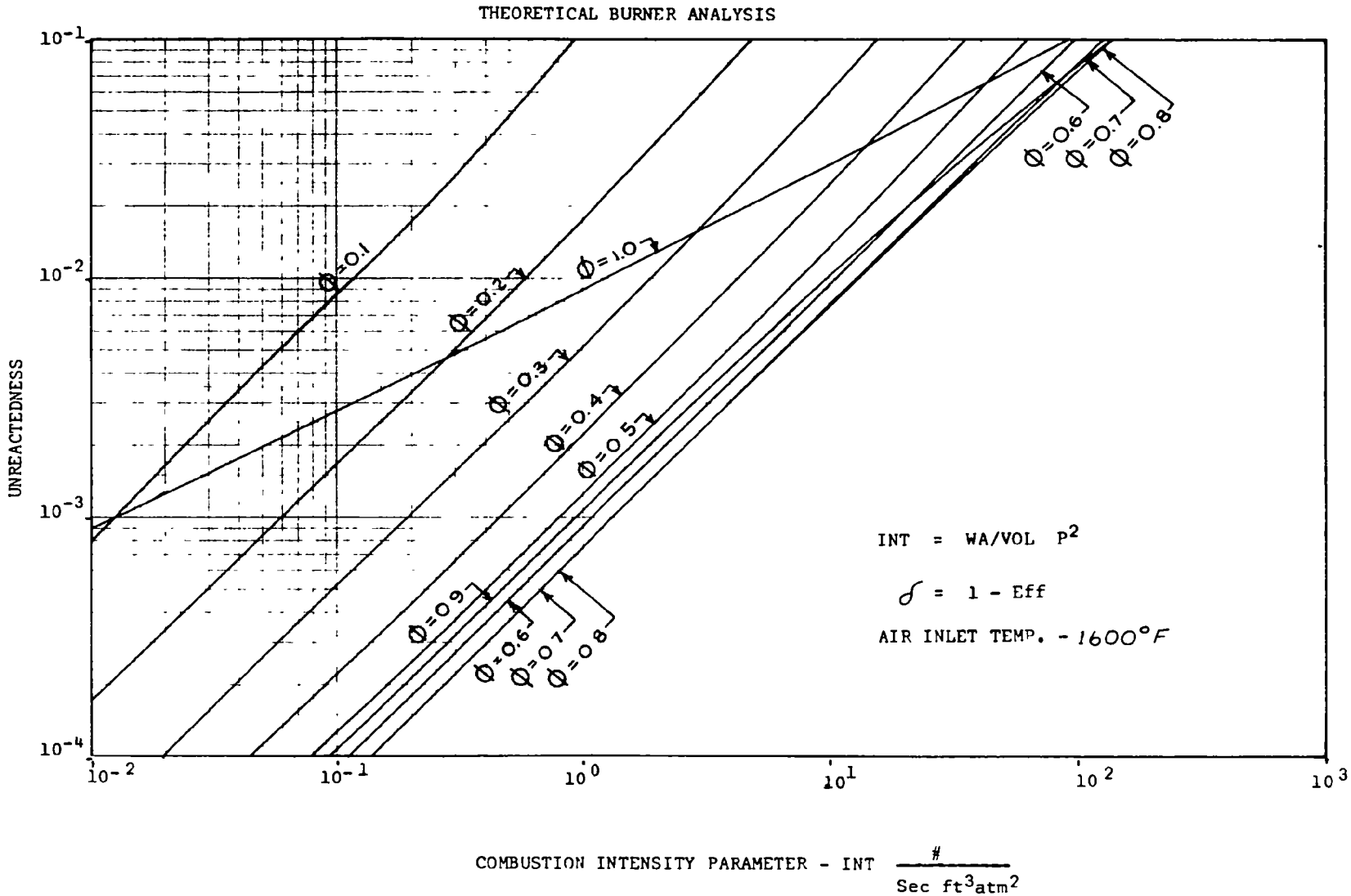

Figure VII - 18

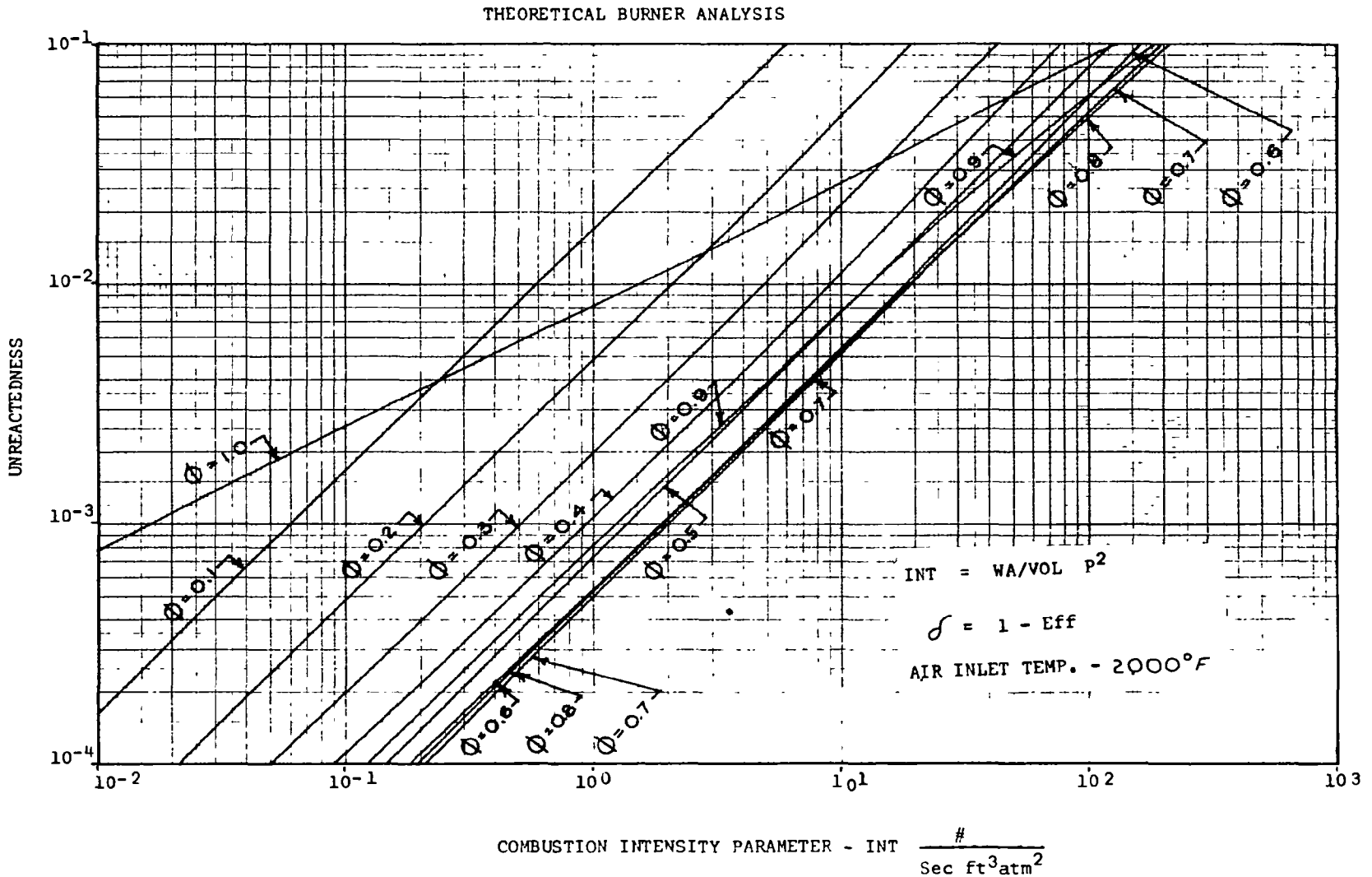

Figure VII - 19

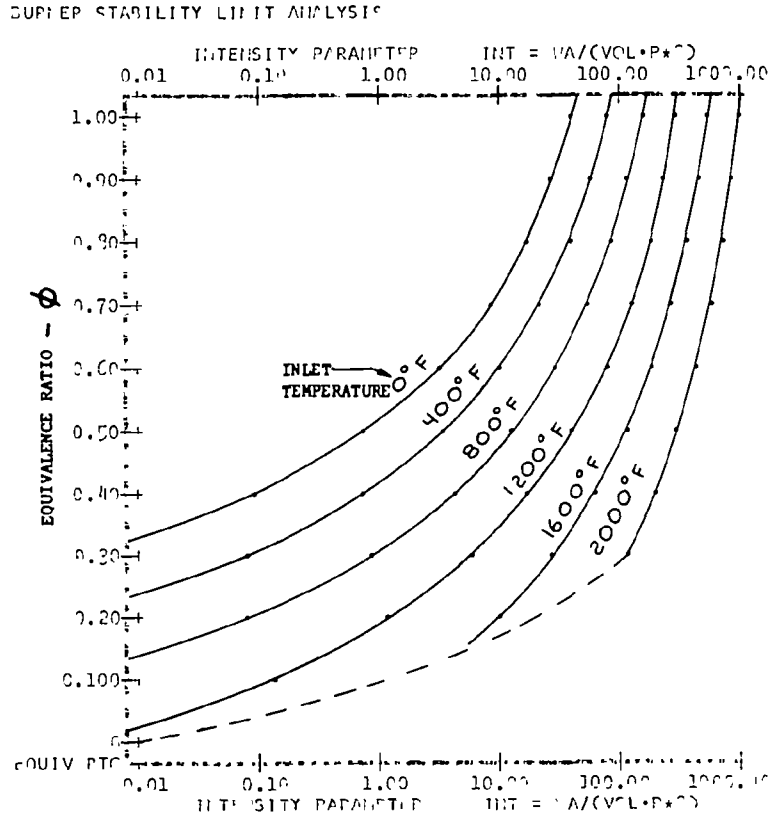

Figure VII-20

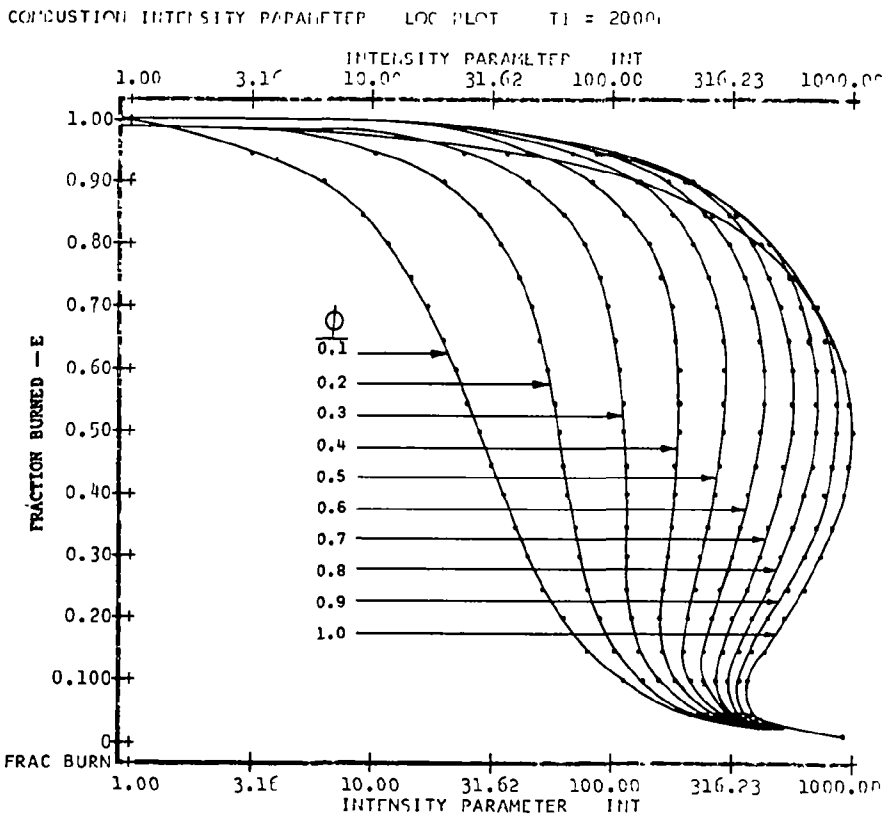

Figure VII-21

```
      ∇CAL[□]
    ∇ CAL
[1]   CA←0.27
[2]   CF←0.7
[3]   CB←0.32
[4]   TBI←TI
[5]   HF←(0.02×TI-537)+(0.0004194×((TI*2)-537*2))+(¯7.9218E¯8×((TI*3)-537*3))+6.43E¯12×(TI*4)-537*4
[6]   HB←HBO-(0.81÷0.633)×HF×TH÷1+TH
[7]  TEMP:TI←TI
[8]   TB←TI+((HB×PH×(1+TH)×E)-(PH×TH×HV×1-E))÷((CB×PH×(1+TH)×E)+(CA×(1-E×PH))+CF×PH×TH×1-E)
[9]   →((|TB-TBI)≤1)/CONT
[10]  TBI←TB
[11]  CA←(0.22618)+(1.4147E¯5×TB+TI)+¯7.8229E¯10×(TB*2)+(TB×TI)+TI*2
[12]  CF←(0.02)+(0.0004194×TB+TI)+(¯7.9218E¯8×(TB*2)+(TB×TI)+TI*2)+6.43E¯12×((TB*4)-(TI*4))÷TB-TI
[13]  CB←(0.28072)+(1.5293E¯5×TB+TI)+(¯8.4458E¯10×(TB*2)+(TB×TI)+(TI*2))
[14]  CB←CB+(¯1.8508×((TB*0.5)-(TI*0.5))÷TB-TI)-88.356÷TB-TI
[15]  →TEMP
[16] CONT:TBI←TB
[17]  INT←K×(1-E)×TH×(1-E×PH)×(MF÷MA)×(*-EA÷R×TB)÷(1+TH)×E×((PH×TH×1-E)+((1-E×PH)×MF÷MA)+PH×E×(1+TH)×MF÷MB)*2
[18]  INT←INT×(TB*0.5)×(29×2116÷1545×TB)*2
    ∇
[19]
```

Table VII - 1

```
      ∇HOT[⎕]∇
    ∇ HOT;J;I
[1]   PHA←0.1×⍳10
[2]   TIA←460+ 0 400 800 1200 1600 2000
[3]   E← 0.9 0.99 0.999 0.9999
[4]   ALF←((ρTIA),(ρPHA),(ρE),5)ρ0
[5]   I←1
[6]  IUP:TI←TIA[I]
[7]   J←1
[8]  JUP:PH←PHA[J]
[9]   CAL
[10]  ALF[I;J;;]←⍉(5,(ρE))ρ((ρE)ρTI-460),((ρE)ρPH),V,(TI-460),E
[11]  J←J+1
[12]  →(J≤ρPHA)/JUP
[13]  I←I+1
[14]  →(I≤ρTIA)/IUP
    ∇
```

Table VII-2

THEORETICAL BURNER ANALYSIS

Effect Of Equivalence Ratio and Efficiency On
Temperature and Intensity Parameter
Air Temp. = 0°F

TA	PHI	ETA	TB	INT
0.0000E0	1.0000E-1	9.0000E-1	4.0975E2	2.9619E-11
0.0000E0	1.0000E-1	9.9000E-1	4.1543E2	2.1999E-11
0.0000E0	1.0000E-1	9.9900E-1	4.2097E2	2.0311E-12
0.0000E0	1.0000E-1	9.9990E-1	4.2645E2	2.0240E-13
0.0000E0	2.0000E-1	9.0000E-1	8.4275E2	8.0158E-6
0.0000E0	2.0000E-1	9.9000E-1	8.5708E2	3.0846E-6
0.0000E0	2.0000E-1	9.9900E-1	8.7067E2	8.2156E-7
0.0000E0	2.0000E-1	9.9990E-1	8.8313E2	4.2703E-8
0.0000E0	3.0000E-1	9.0000E-1	1.3041E3	2.9197E-3
0.0000E0	3.0000E-1	9.9000E-1	1.4367E3	9.5409E-4
0.0000E0	3.0000E-1	9.9900E-1	1.4630E3	1.0618E-4
0.0000E0	3.0000E-1	9.9990E-1	1.4882E3	1.0731E-5
0.0000E0	4.0000E-1	9.0000E-1	1.6780E3	8.4262E-2
0.0000E0	4.0000E-1	9.9000E-1	1.7341E3	2.1775E-2
0.0000E0	4.0000E-1	9.9900E-1	1.8490E3	2.3733E-3
0.0000E0	4.0000E-1	9.9990E-1	1.8511E3	2.3936E-4
0.0000E0	5.0000E-1	9.0000E-1	2.0273E3	5.9944E-1
0.0000E0	5.0000E-1	9.9000E-1	2.2149E3	1.5211E-1
0.0000E0	5.0000E-1	9.9900E-1	2.2335E3	1.6307E-2
0.0000E0	5.0000E-1	9.9990E-1	2.2354E3	1.6413E-3
0.0000E0	6.0000E-1	9.0000E-1	2.3569E3	2.8734E0
0.0000E0	6.0000E-1	9.9000E-1	2.5729E3	5.3829E-1
0.0000E0	6.0000E-1	9.9900E-1	2.5944E3	5.5867E-2
0.0000E0	6.0000E-1	9.9990E-1	2.5966E3	5.7176E-3
0.0000E0	7.0000E-1	9.0000E-1	2.6673E3	7.4900E0
0.0000E0	7.0000E-1	9.9000E-1	2.9168E3	1.2110E0
0.0000E0	7.0000E-1	9.9900E-1	2.9351E3	1.2600E-1
0.0000E0	7.0000E-1	9.9990E-1	2.9375E3	1.2649E-2
0.0000E0	8.0000E-1	9.0000E-1	2.9611E3	1.3971E1
0.0000E0	8.0000E-1	9.9000E-1	3.2309E3	1.8889E0
0.0000E0	8.0000E-1	9.9900E-1	3.2577E3	1.9249E-1
0.0000E0	8.0000E-1	9.9990E-1	3.2604E3	1.9283E-2
0.0000E0	9.0000E-1	9.0000E-1	3.2401E3	1.9334E1
0.0000E0	9.0000E-1	9.9000E-1	3.5349E3	1.9094E0
0.0000E0	9.0000E-1	9.9900E-1	3.5643E3	1.8562E-1
0.0000E0	9.0000E-1	9.9990E-1	3.5672E3	1.8503E-2
0.0000E0	1.0000E0	9.0000E-1	3.5055E3	1.8103E1
0.0000E0	1.0000E0	9.9000E-1	3.8246E3	2.0759E-1
0.0000E0	1.0000E0	9.9900E-1	3.8564E3	3.1121E-3
0.0000E0	1.0000E0	9.9990E-1	3.8596E3	3.1259E-5

TA - Air Inlet Temperature °F
PHI - Equivalence Ratio
ETA - Efficiency
TB - Combustion Temperature °F
INT - Burner Intensity Parameter

THEORETICAL BURNER ANALYSIS

Effect of Equivalence Ratio and Efficiency On
Temperature and Intensity Parameter
Air Temp. = 400°F

TA	PHI	ETA	TB	INT
4.0000E2	1.0000E-1	9.0000E-1	9.4524E2	3.0059E-6
4.0000E2	1.0000E-1	9.9000E-1	8.8509E2	6.6389E-7
4.0000E2	1.0000E-1	9.9900E-1	8.9340E2	7.1649E-8
4.0000E2	1.0000E-1	9.9990E-1	8.9390E2	7.2195E-9
4.0000E2	2.0000E-1	9.0000E-1	1.2579E3	1.9884E-3
4.0000E2	2.0000E-1	9.9000E-1	1.3402E3	4.8761E-4
4.0000E2	2.0000E-1	9.9900E-1	1.3486E3	4.9497E-5
4.0000E2	2.0000E-1	9.9990E-1	1.3494E3	4.8788E-6
4.0000E2	3.0000E-1	9.0000E-1	1.6405E3	7.2645E-2
4.0000E2	3.0000E-1	9.9000E-1	1.7534E3	1.5385E-2
4.0000E2	3.0000E-1	9.9900E-1	1.7712E3	1.6496E-3
4.0000E2	3.0000E-1	9.9990E-1	1.7724E3	1.6610E-4
4.0000E2	4.0000E-1	9.0000E-1	1.9993E3	8.9925E-1
4.0000E2	4.0000E-1	9.9000E-1	2.1567E3	1.3421E-1
4.0000E2	4.0000E-1	9.9900E-1	2.1638E3	1.4248E-2
4.0000E2	4.0000E-1	9.9990E-1	2.1673E3	1.4339E-3
4.0000E2	5.0000E-1	9.0000E-1	2.3351E3	3.1673E0
4.0000E2	5.0000E-1	9.9000E-1	2.5179E3	5.5094E-1
4.0000E2	5.0000E-1	9.9900E-1	2.5361E3	5.7913E-2
4.0000E2	5.0000E-1	9.9990E-1	2.5379E3	5.8203E-3
4.0000E2	6.0000E-1	9.0000E-1	2.6534E3	8.9556E0
4.0000E2	6.0000E-1	9.9000E-1	2.8043E3	1.4092E0
4.0000E2	6.0000E-1	9.9900E-1	2.8853E3	1.4661E-1
4.0000E2	6.0000E-1	9.9990E-1	2.8874E3	1.4719E-2
4.0000E2	7.0000E-1	9.0000E-1	2.9534E3	1.8222E1
4.0000E2	7.0000E-1	9.9000E-1	3.1917E3	2.5601E0
4.0000E2	7.0000E-1	9.9900E-1	3.2155E3	2.6312E-1
4.0000E2	7.0000E-1	9.9990E-1	3.2179E3	2.6382E-2
4.0000E2	8.0000E-1	9.0000E-1	3.2380E3	2.8599E1
4.0000E2	8.0000E-1	9.9000E-1	3.5025E3	3.4434E0
4.0000E2	8.0000E-1	9.9900E-1	3.5288E3	3.4737E-1
4.0000E2	8.0000E-1	9.9990E-1	3.5315E3	3.4764E-2
4.0000E2	9.0000E-1	9.0000E-1	3.5086E3	3.4912E1
4.0000E2	9.0000E-1	9.9000E-1	3.7982E3	3.1274E0
4.0000E2	9.0000E-1	9.9900E-1	3.8271E3	3.0147E-1
4.0000E2	9.0000E-1	9.9990E-1	3.8300E3	3.0025E-2
4.0000E2	1.0000E0	9.0000E-1	3.7664E3	2.3755E1
4.0000E2	1.0000E0	9.9000E-1	4.0803E3	4.4999E-1
4.0000E2	1.0000E0	9.9900E-1	4.1117E3	4.6720E-3
4.0000E2	1.0000E0	9.9990E-1	4.1148E3	4.6894E-5

TA - Inlet Temperature °F
PHI - Equivalence Ratio
ETA - Efficiency
TB - Combustion Temperature °F
INT - Burner Intensity Parameter

THEORETICAL BURNER ANALYSIS

Effect of Equivalence Ratio and Efficiency On
Temperature and Intensity Parameter
Air Temp. = 800°F

TA	PHI	ETA	TB	INT
8.0000E2	1.0000E-1	9.0000E-1	1.2291E3	1.4138E-3
8.0000E2	1.0000E-1	9.9000E-1	1.2639E3	2.1215E-4
8.0000E2	1.0000E-1	9.9900E-1	1.2681E3	2.2071E-5
8.0000E2	1.0000E-1	9.9990E-1	1.2685E3	2.2150E-6
8.0000E2	2.0000E-1	9.0000E-1	1.6143E3	6.2564E-2
8.0000E2	2.0000E-1	9.9000E-1	1.6939E3	1.1000E-2
8.0000E2	2.0000E-1	9.9900E-1	1.7019E3	1.1532E-3
8.0000E2	2.0000E-1	9.9990E-1	1.7026E3	1.1585E-4
8.0000E2	3.0000E-1	9.0000E-1	1.9807E3	7.2310E-1
8.0000E2	3.0000E-1	9.9000E-1	2.0948E3	1.1042E-1
8.0000E2	3.0000E-1	9.9900E-1	2.1062E3	1.2404E-2
8.0000E2	3.0000E-1	9.9990E-1	2.1074E3	1.2461E-3
8.0000E2	4.0000E-1	9.0000E-1	2.3243E3	3.5343E0
8.0000E2	4.0000E-1	9.9000E-1	2.4706E3	5.5422E-1
8.0000E2	4.0000E-1	9.9900E-1	2.4850E3	5.7774E-2
8.0000E2	4.0000E-1	9.9990E-1	2.4866E3	5.8013E-3
8.0000E2	5.0000E-1	9.0000E-1	2.6478E3	1.0596E1
8.0000E2	5.0000E-1	9.9000E-1	2.8242E3	1.5071E0
8.0000E2	5.0000E-1	9.9900E-1	2.8418E3	1.6235E-1
8.0000E2	5.0000E-1	9.9990E-1	2.8436E3	1.6292E-2
8.0000E2	6.0000E-1	9.0000E-1	3.0535E3	2.2855E1
8.0000E2	6.0000E-1	9.9000E-1	3.1584E3	3.1475E0
8.0000E2	6.0000E-1	9.9900E-1	3.1738E3	3.2363E-1
8.0000E2	6.0000E-1	9.9990E-1	3.1754E3	3.2451E-2
8.0000E2	7.0000E-1	9.0000E-1	3.2431E3	3.8382E1
8.0000E2	7.0000E-1	9.9000E-1	3.4751E3	4.8487E0
8.0000E2	7.0000E-1	9.9900E-1	3.4983E3	4.9945E-1
8.0000E2	7.0000E-1	9.9990E-1	3.5006E3	4.9429E-2
8.0000E2	8.0000E-1	9.0000E-1	3.5182E3	5.2922E1
8.0000E2	8.0000E-1	9.9000E-1	3.7763E3	5.7959E0
8.0000E2	8.0000E-1	9.9900E-1	3.8020E3	5.7984E-1
8.0000E2	8.0000E-1	9.9990E-1	3.8046E3	5.7981E-2
8.0000E2	9.0000E-1	9.0000E-1	3.7801E3	5.8432E1
8.0000E2	9.0000E-1	9.9000E-1	4.0633E3	4.8237E0
8.0000E2	9.0000E-1	9.9900E-1	4.0916E3	4.6167E-1
8.0000E2	9.0000E-1	9.9990E-1	4.0944E3	4.5948E-2
8.0000E2	1.0000E0	9.0000E-1	4.0300E3	4.6110E1
8.0000E2	1.0000E0	9.9000E-1	4.3375E3	6.4936E-1
8.0000E2	1.0000E0	9.9900E-1	4.3683E3	6.7003E-3
8.0000E2	1.0000E0	9.9990E-1	4.3713E3	6.7211E-5

TA - Inlet Temperature °F
PHI - Equivalence Ratio
ETA - Efficiency
TB - Combustion Temperature °F
INT - Burner Intensity Parameter

THEORETICAL BURNER ANALYSIS

Effect of Equivalence Ratio and Efficiency On
Temperature and Intensity Parameter
Air Temp. = 1200°F

TA	PHI	ETA	TB	INT
1.2000E3	1.0000E-1	9.0000E-1	1.6001E3	[illegible]
1.2000E3	1.0000E-1	9.9000E-1	1.6339E3	8.2493E-3
1.2000E3	1.0000E-1	9.9900E-1	1.6439E3	8.4063E-4
1.2000E3	1.0000E-1	9.9990E-1	1.6443E3	8.4242E-5
1.2000E3	2.0000E-1	9.0000E-1	1.9735E3	7.8585E-1
1.2000E3	2.0000E-1	9.9000E-1	2.0495E3	1.0707E-1
1.2000E3	2.0000E-1	9.9900E-1	2.0571E3	1.1031E-2
1.2000E3	2.0000E-1	9.9990E-1	2.0579E3	1.1063E-3
1.2000E3	3.0000E-1	9.0000E-1	2.3231E3	4.0466E0
1.2000E3	3.0000E-1	9.9000E-1	2.4328E3	5.6029E-1
1.2000E3	3.0000E-1	9.9900E-1	2.4437E3	5.7781E-2
1.2000E3	3.0000E-1	9.9990E-1	2.4448E3	5.7958E-3
1.2000E3	4.0000E-1	9.0000E-1	2.6521E3	1.2627E1
1.2000E3	4.0000E-1	9.9000E-1	2.7931E3	1.7176E0
1.2000E3	4.0000E-1	9.9900E-1	2.8071E3	1.7674E-1
1.2000E3	4.0000E-1	9.9990E-1	2.8085E3	1.7725E-2
1.2000E3	5.0000E-1	9.0000E-1	2.9627E3	2.8295E1
1.2000E3	5.0000E-1	9.9000E-1	3.1331E3	3.7092E0
1.2000E3	5.0000E-1	9.9900E-1	3.1501E3	3.8012E-1
1.2000E3	5.0000E-1	9.9990E-1	3.1518E3	3.8104E-2
1.2000E3	6.0000E-1	9.0000E-1	3.2567E3	4.9972E1
1.2000E3	6.0000E-1	9.9000E-1	3.4552E3	6.2081E0
1.2000E3	6.0000E-1	9.9900E-1	3.4750E3	6.3242E-1
1.2000E3	6.0000E-1	9.9990E-1	3.4770E3	6.3358E-2
1.2000E3	7.0000E-1	9.0000E-1	3.5358E3	7.3095E1
1.2000E3	7.0000E-1	9.9000E-1	3.7610E3	8.4038E0
1.2000E3	7.0000E-1	9.9900E-1	3.7835E3	8.4847E-1
1.2000E3	7.0000E-1	9.9990E-1	3.7858E3	8.4925E-2
1.2000E3	8.0000E-1	9.0000E-1	3.8013E3	9.0145E1
1.2000E3	8.0000E-1	9.9000E-1	4.0523E3	9.1346E0
1.2000E3	8.0000E-1	9.9900E-1	4.0774E3	9.0758E-1
1.2000E3	8.0000E-1	9.9990E-1	4.0799E3	9.0691E-2
1.2000E3	9.0000E-1	9.0000E-1	4.0544E3	9.1763E1
1.2000E3	9.0000E-1	9.9000E-1	4.3302E3	7.0746E0
1.2000E3	9.0000E-1	9.9900E-1	4.3579E3	6.7302E-1
1.2000E3	9.0000E-1	9.9990E-1	4.3606E3	6.6943E-2
1.2000E3	1.0000E0	9.0000E-1	4.2959E3	6.7954E1
1.2000E3	1.0000E0	9.9000E-1	4.5961E3	9.0065E-1
1.2000E3	1.0000E0	9.9900E-1	4.6262E3	9.2436E-3
1.2000E3	1.0000E0	9.9990E-1	4.6292E3	9.2675E-5

TA - Inlet Temperature °F **PHI - Equivalence Ratio**
ETA - Efficiency **TB - Combustion Temperature °F**
INT - Burner Intensity Parameter

THEORETICAL BURNER ANALYSIS

Effect of Equivalence Ratio and Efficiency On
Temperature and Intensity Parameter
Air Temp. = 1600°F

TA	PHI	ETA	TB	INT
1.6000E3	1.0000E-1	9.0000E-1	1.[illegible]E3	9.1061E-1
1.6000E3	1.0000E-1	9.9000E-1	2.0172E3	1.0159E-1
1.6000E3	1.0000E-1	9.9900E-1	2.[illegible]E3	1.0271E-2
1.6000E3	1.0000E-1	9.9990E-1	2.0214E3	1.0283E-3
1.6000E3	2.0000E-1	9.0000E-1	2.3348E3	4.8200E0
1.6000E3	2.0000E-1	9.9000E-1	2.4077E3	5.8167E-1
1.6000E3	2.0000E-1	9.9900E-1	2.4145E3	5.9241E-2
1.6000E3	2.0000E-1	9.9990E-1	2.4152E3	5.9349E-3
1.6000E3	3.0000E-1	9.0000E-1	2.6634E3	1.5362E1
1.6000E3	3.0000E-1	9.9000E-1	2.7735E3	1.8970E0
1.6000E3	3.0000E-1	9.9900E-1	2.7840E3	1.9355E-1
1.6000E3	3.0000E-1	9.9990E-1	2.7850E3	1.9394E-2
1.6000E3	4.0000E-1	9.0000E-1	2.9836E3	3.5174E1
1.6000E3	4.0000E-1	9.9000E-1	3.1187E3	4.3171E0
1.6000E3	4.0000E-1	9.9900E-1	3.1322E3	4.4004E-1
1.6000E3	4.0000E-1	9.9990E-1	3.1336E3	4.4087E-2
1.6000E3	5.0000E-1	9.0000E-1	3.2805E3	6.3775E1
1.6000E3	5.0000E-1	9.9000E-1	3.4452E3	7.6323E0
1.6000E3	5.0000E-1	9.9900E-1	3.4616E3	7.7566E-1
1.6000E3	5.0000E-1	9.9990E-1	3.4632E3	7.7690E-2
1.6000E3	6.0000E-1	9.0000E-1	3.5634E3	9.6847E1
1.6000E3	6.0000E-1	9.9000E-1	3.7551E3	1.1100E1
1.6000E3	6.0000E-1	9.9900E-1	3.7742E3	1.1225E0
1.6000E3	6.0000E-1	9.9990E-1	3.7761E3	1.1237E-1
1.6000E3	7.0000E-1	9.0000E-1	3.8319E3	1.2669E2
1.6000E3	7.0000E-1	9.9000E-1	4.0499E3	1.3559E1
1.6000E3	7.0000E-1	9.9900E-1	4.0717E3	1.3602E0
1.6000E3	7.0000E-1	9.9990E-1	4.0739E3	1.3606E-1
1.6000E3	8.0000E-1	9.0000E-1	4.0877E3	1.4350E2
1.6000E3	8.0000E-1	9.9000E-1	4.3311E3	1.3641E1
1.6000E3	8.0000E-1	9.9900E-1	4.3555E3	1.3476E0
1.6000E3	8.0000E-1	9.9990E-1	4.3579E3	1.3459E-1
1.6000E3	9.0000E-1	9.0000E-1	4.3316E3	1.3669E2
1.6000E3	9.0000E-1	9.9000E-1	4.5998E3	9.9520E0
1.6000E3	9.0000E-1	9.9900E-1	4.6267E3	9.4195E-1
1.6000E3	9.0000E-1	9.9990E-1	4.6294E3	9.3645E-2
1.6000E3	1.0000E0	9.0000E-1	4.5648E3	9.6031E1
1.6000E3	1.0000E0	9.9000E-1	4.8573E3	1.2088E0
1.6000E3	1.0000E0	9.9900E-1	4.8807E3	1.2350E-2
1.6000E3	1.0000E0	9.9990E-1	4.8897E3	1.2376E-4

TA - Air Inlet Temperature °F
PHI - Equivalence Ratio
ETA - Efficiency
TB - Combustion Temperature °F
INT - Burner Intensity Parameter

THEORETICAL BURNER ANALYSIS

Effect of Equivalence Ratio and Efficiency On
Temperature and Intensity Parameter
Air Temp. = 2000°F

TA	PHI	ETA	TB	INT
2.0000E3	1.0000E-1	9.0000E-1	2.3599E3	6.0166E0
2.0000E3	1.0000E-1	9.9000E-1	2.3959E3	6.2951E-1
2.0000E3	1.0000E-1	9.9900E-1	2.3995E3	6.3251E-2
2.0000E3	1.0000E-1	9.9990E-1	2.3998E3	6.3282E-3
2.0000E3	2.0000E-1	9.0000E-1	2.6978E3	1.9203E1
2.0000E3	2.0000E-1	9.9000E-1	2.7672E3	2.1416E0
2.0000E3	2.0000E-1	9.9900E-1	2.7741E3	2.1645E-1
2.0000E3	2.0000E-1	9.9990E-1	2.7748E3	2.1668E-2
2.0000E3	3.0000E-1	9.0000E-1	3.0163E3	4.4326E1
2.0000E3	3.0000E-1	9.9000E-1	3.1163E3	5.0493E0
2.0000E3	3.0000E-1	9.9900E-1	3.1270E3	5.1129E-1
2.0000E3	3.0000E-1	9.9990E-1	3.1280E3	5.1191E-2
2.0000E3	4.0000E-1	9.0000E-1	3.3174E3	8.1307E1
2.0000E3	4.0000E-1	9.9000E-1	3.4475E3	9.2595E0
2.0000E3	4.0000E-1	9.9900E-1	3.4604E3	9.3715E-1
2.0000E3	4.0000E-1	9.9990E-1	3.4617E3	9.3827E-2
2.0000E3	5.0000E-1	9.0000E-1	3.6027E3	1.2616E2
2.0000E3	5.0000E-1	9.9000E-1	3.7608E3	1.4090E1
2.0000E3	5.0000E-1	9.9900E-1	3.7766E3	1.4217E0
2.0000E3	5.0000E-1	9.9990E-1	3.7782E3	1.4231E-1
2.0000E3	6.0000E-1	9.0000E-1	3.8738E3	1.7059E2
2.0000E3	6.0000E-1	9.9000E-1	4.0587E3	1.9347E1
2.0000E3	6.0000E-1	9.9900E-1	4.0772E3	1.8446E0
2.0000E3	6.0000E-1	9.9990E-1	4.0791E3	1.8455E-1
2.0000E3	7.0000E-1	9.0000E-1	4.1318E3	2.0431E2
2.0000E3	7.0000E-1	9.9000E-1	4.3426E3	2.0638E1
2.0000E3	7.0000E-1	9.9900E-1	4.3637E3	2.0595E0
2.0000E3	7.0000E-1	9.9990E-1	4.3658E3	2.0590E-1
2.0000E3	8.0000E-1	9.0000E-1	4.3777E3	2.1604E2
2.0000E3	8.0000E-1	9.9000E-1	4.6137E3	1.9486E1
2.0000E3	8.0000E-1	9.9900E-1	4.6374E3	1.9159E0
2.0000E3	8.0000E-1	9.9990E-1	4.6398E3	1.9125E-1
2.0000E3	9.0000E-1	9.0000E-1	4.6124E3	1.9481E2
2.0000E3	9.0000E-1	9.9000E-1	4.8727E3	1.3517E1
2.0000E3	9.0000E-1	9.9900E-1	4.8989E3	1.2738E0
2.0000E3	9.0000E-1	9.9990E-1	4.9015E3	1.2659E-1
2.0000E3	1.0000E0	9.0000E-1	4.8369E3	1.3093E2
2.0000E3	1.0000E0	9.9000E-1	5.1241E3	1.5813E0
2.0000E3	1.0000E0	9.9900E-1	5.1531E3	1.6097E-2
2.0000E3	1.0000E0	9.9990E-1	5.1560E3	1.6125E-4

TA - Air Inlet Temperature °F
PHI - Equivalence Ratio
ETA - Efficiency
TB - Combustion Temperature °F
INT - Burner Intensity Parameter

```
      ∇STABILITY[⎕]∇
    ∇ STABILITY;I
[1]   TIL←460+ 0 400 800 1200 1600 2000
[2]   ANSR←0⍴0
[3]   I←1
[4]   TI←TIL[I]
[5]   BURN
[6]   ANSR←ANSR,(,ANS)
[7]   ' '
[8]   I←I+1
[9]   →(I≤⍴TIL)/4
    ∇

      ∇BURN[⎕]∇
    ∇ BURN;I;J
[1]   ANS← 12 5 ⍴0
[2]   →(PRINT=0)/SKIP
[3]   '                    TI = ';(TI-460);' OF'
[4]   '         PHI         ETA         TB            INT      '
[5]  SKIP:PHA←0.1×⍳10
[6]   J←1
[7]  JUP:PH←PHA[J]
[8]   COUNT←0
[9]   E←0.3+0.05×⍳14
[10] ITT:COUNT←COUNT+1
[11]  CAL
[12]  INTM←⌈/INT
[13]  I←INT⍳INTM
[14]  →(I=1)/OUT
[15]  →(COUNT=3)/OUT
[16]  E←E[I-1]+(0.1*COUNT+1)×⍳10
[17]  →ITT
[18] OUT:→(PRINT=0)/STOR
[19]  12 3 12 4 12 1 12 6 DFT PH,E[I],(TB[I]-460),INT[I]
[20] STOR:ANS[J;]←((TI-460),PH,E[I],(TB[I]-460),INT[I])×I≠1
[21]  J←J+1
[22]  →(J≤10)/JUP
    ∇
```

Table VII-9

THEORETICAL BURNER ANALYSIS

Stability Limits

TI = 0 °F

PHI	ETA	TB	INT
0.100	0.9480	494.1	0.000000
0.200	0.9390	940.2	0.000010
0.300	0.9250	1338.3	0.003139
0.400	0.9100	1695.4	0.084935
0.500	0.8960	2019.6	0.700102
0.600	0.8790	2306.2	2.936463
0.700	0.8590	2555.6	8.030965
0.800	0.8390	2742.7	16.408577
0.900	0.8000	2809.8	27.083865
1.000	0.7600	3004.9	38.156782

TI = 400 °F

PHI	ETA	TB	INT
0.100	0.8900	840.4	0.000003
0.200	0.8980	1255.5	0.001949
0.300	0.8900	1627.6	0.073046
0.400	0.8770	1960.5	0.715631
0.500	0.8600	2254.6	3.347339
0.600	0.8450	2523.7	9.950050
0.700	0.8200	2740.1	21.800524
0.800	0.7990	2939.1	38.516837
0.900	0.7760	3074.3	57.941062
1.000	0.7280	3162.3	77.320775

TI = 800 °F

PHI	ETA	TB	INT
0.100	0.7900	1170.8	0.001762
0.200	0.8380	1559.3	0.074312
0.300	0.8400	1904.2	0.805498
0.400	0.8300	2209.8	4.038581
0.500	0.8200	2490.0	12.647128
0.600	0.8000	2724.2	29.034448
0.700	0.7800	2931.6	53.657546
0.800	0.7550	3099.8	84.558451
0.900	0.7200	3210.6	118.108823
1.000	0.6870	3299.2	150.905892

TI - **Air Inlet Temperature °F**
PHI - **Equivalence Ratio**
ETA - **Burner Efficiency**
TB - **Combustion Temperature °F**
INT - **Combustion Intensity Parameter**
********* - **No Critical Conditions Arise**

THEORETICAL BURNER ANALYSIS

Stability Limits

TI = 1000 °F

PHI	ETA	TB	INT
0.100	0.5900	1402.3	0.126897
0.200	0.7480	1844.3	1.118179
0.300	0.7700	2184.0	5.476256
0.400	0.7700	2447.3	17.233346
0.500	0.7700	2695.8	40.177244
0.600	0.7480	2919.4	75.838458
0.700	0.7280	3102.9	122.015197
0.800	0.7090	3240.3	176.558030
0.900	0.6700	3347.2	232.570049
1.000	0.6300	3425.2	286.239136

TI = 1600 °F

PHI	ETA	TB	INT
0.100	*****	*****	*****
0.200	0.5800	2074.2	9.724018
0.300	0.6670	2394.4	27.133038
0.400	0.6870	2660.3	60.721746
0.500	0.6860	2887.9	113.124843
0.600	0.6760	3083.6	183.183256
0.700	0.6590	3245.6	266.406383
0.800	0.6360	3372.0	356.503031
0.900	0.6090	3465.3	447.141329
1.000	0.5800	3530.4	533.266681

TI = 2000 °F

PHI	ETA	TB	INT
0.100	*****	*****	*****
0.200	*****	*****	*****
0.300	0.4060	2458.5	113.805829
0.400	0.5400	2801.9	190.508831
0.500	0.5700	3019.4	295.597717
0.600	0.5700	3192.6	422.142911
0.700	0.5650	3345.7	562.614364
0.800	0.5480	3459.8	708.456281
0.900	0.5270	3540.1	851.956971
1.000	0.5000	3587.8	988.108951

TI - Air Inlet Temperature °F
PHI - Equivalence Ratio
ETA - Burner Efficiency
TB - Combustion Temperature °F
INT - Combustion Intensity Parameter
***** - No Critical Conditions Arise

```
      ∇INTPLOT[□]∇
    ∇ INTPLOT
[1]   NO←1
[2]   PINT←0ρ0
[3]   PE←0ρ0
[4]   PHN←0.1×⍳10
[5]   E← 0.01 0.025 ,0.05×⍳20
[6]  ITT:PH←PHN[NO]
[7]   CAL
[8]   PINT←PINT,INT
[9]   PE←PE,E
[10]  NO←NO+1
[11]  →(NO≤10)/ITT
    ∇
```

THEORETICAL BURNER ANALYSIS

COMBUSTION INTENSITY PARAMETER INT(TI,E,PH)
TI = 2000 F

E↓ PH→	0.1	0.2	0.3	0.4	0.5	0.6	0.7	0.8	0.9	1.0
0.011	921.08	922.4[illegible]	923.7	924.79	925.74	926.56	927.26	927.83	928.29	928.65
0.025	412.92	426.55	433.75	452.53	464.89	476.85	488.39	499.53	510.26	520.65
0.05	212.45	230.63	249.19	267.92	286.76	305.66	324.63	343.64	362.34	380.83
0.10	112.07	134	156.01	184.08	211.89	241.33	272.48	305.59	337.8	371.02
0.15	78.423	102.72	131.25	163.92	200.64	241.27	285.69	333.06	383.34	436.13
0.20	61.401	87.646	120.43	159.92	206.19	259.11	318.16	383.14	452.87	526.91
0.25	50.978	78.924	115.85	162.32	218.64	284.71	360.11	443.33	533.66	629.75
0.30	43.809	73.227	114.13	167.5	234.15	313.69	405.42	507.17	617.51	734.15
0.35	38.454	69.1	113.73	173.95	250.53	343.17	450.49	569.31	697.11	830.28
0.40	34.192	65.783	113.75	180.25	266.15	370.76	491.83	624.75	765.53	908.85
0.45	30.616	62.824	113.6	185.6	279.6	394.27	526.15	668.82	816.45	961.71
0.50	27.48	59.924	112.83	189.21	289.59	411.64	550.46	697.4	844.59	982.46
0.55	24.624	56.866	111.09	190.39	294.89	421.01	562.12	707.14	846.05	967.07
0.60	21.938	53.479	107.91	188.47	294.42	420.75	559.02	695.71	818.72	914.33
0.65	19.343	49.62	103.11	183.85	287.17	409.52	539.71	661.98	762.49	826.95
0.70	16.78	45.165	96.286	172.04	272.29	386.35	503.16	606.14	679.4	707.22
0.75	**14.204**	**39.999**	**87.337**	**158.25**	**249.1**	**350.69**	**450.41**	529.85	573.69	565.9
0.80	11.576	34.018	75.819	138.32	217.13	302.46	381.54	436.01	451.72	413.13
0.85	8.8667	27.12	61.548	112.78	176.12	242.08	298.78	330.72	328.09	268.71
0.90	6.0492	19.212	44.293	81.322	126.96	175.48	204.96	216.47	195.09	130.93
0.95	3.1005	10.291	23.89	43.763	67.152	89.122	103.82	103.69	83.023	36.445
1.00	0	0	0	0	0	0	0	0	0	0

TI - AIR INLET TEMPERATURE °F
INT - COMBUSTION INTENSITY PARAMETER
PH - EQUIVALENCE RATIO
E - COMBUSTION EFFICIENCY

VIII. CORRELATION OF THE EXPERIMENTAL DATA WITH A THEORETICAL MODEL

The experimental data obtained in this program would be of value by itself without additional theoretical analysis, since it shows the remarkably low emissions which can be obtained by proper operation of the Paxve burner. The value of this data, however is immeasureably increased by our ability to interpret it in the light of the theoretical burner analysis presented in Secion VII of this report. We have been able to use this analytical background as the basis for data correlations. With those correlations, we can predict performance of burners having widely different sizes and operating conditions. Such correlations and the theoretical understanding of burner operation are of particular value when new operating conditions are of interest.

The Paxve burner tested here had a maximum air flow rate of 180 lbs/hr. The highest flow rate normally tested was approximately 140 lbs/hr. At the nominal operating condition for the burner (f/a = 0.038) this yields approximately 100,000 BTU/hr of heat release. The volume of the burner was on the order of 0.03 ft^3 and hence the nominal heat release rate was approximately 3×10^6 BTU/hr. ft^3.

The main thrust of the EPA program, of which this research work was a part, deals with burners of considerably larger heat release; on the order of 2,500,000 BTU/hr. The first task of data correlation, therefore is to be able to predict the influence of increasing the scale of the burner by at least a factor of 25. There is also a great deal of interest at the present time in low emission burners for application to gas turbine engines. Gas turbine burners operate at higher inlet pressures and temperatures than the burner under test here. It is therefore desirable to have a means for designing a burner which will have low emissions at elevated pressures and temperatures and to be able to predict the influence of these parameters as well as scale size on both burner stability and emission characteristics.

In order to accomplish the goals outlined above, several types of experimental data correlations were investigated. The stability data was correlated with the theoretical prediction of the burner theory outlined in Section VII. The correlation is presented herein. The carbon monoxide and hydrocarbon emissions from the burner were correlated in terms of the efficiency predictions of the burner theory outlined in Section VII above. Correlation of the oxides of nitrogen data is discussed herein. The combustion temperatures used in that correlation are those predicted by the combustion theory.

A. Correlation of the Experimental Stability Data

Figure 20 of Section VI, shows the experimental blowout data from the Paxve burner plotted against air flow; this data can be compared directly with the predictions of the burner theory

discussed in Section VII. In order to accomplish such a comparison, a computer program, PREDICT, was written which examines all of the lean burning experimental runs in terms of the burner theory outlined previously.

1. Program PREDICT

Program PREDICT is shown in Table 1. An examination of this program will be helpful in discussing the experimental data correlations which are to follow. Because of the limitations of the analysis, only equivalence ratios of 1 or less were considered. For each of the lean runs, a value of the combustion intensity parameter, INTD, at which the burner was tested was computed. Using the burner air inlet temperature and equivalance ratio, a subroutine, Program LIMIT was called.

Program LIMIT, shown in Table 2, finds the limiting value of the intensity parameter INTL corresponding to the stability limit of the burner. Program LIMIT in turn called CAL, discussed previously, which finds values of combustion temperature and combustion intensity parameter as a function of the burner efficiency. Program LIMIT performs essentially the same calculation as that performed by Program BURN described previously. Program LIMIT returns values of the limiting intensity parameter, INTL and the efficiency and burner temperature which exist at the blowout limit, EL and TBL.

Program PREDICT now compares the intensity parameter at which the burner was operating with the value of the intensity parameter at the stability limit. A stability prediction parameter is formed given by

$$INTR = \frac{INTD}{INTL}$$

INTR greater than 1.0 implies that the burner will not stay lit. The air flow rate and hence INTD exceeds the limiting value for stable operation. INTR less than or equal to 1.0 implies that stable burner operation should occur.

We must now compute the operating efficiency and burner temperature. To accomplish this Program PREDICT uses, EL, INTL, and INTD to make an estimate of the operating efficiency of the burner. It then calls Program CAL and uses this estimated efficiency to compute new values for burner intensity parameter and operating temperature. The new value of intensity parameter, INT, is compared with INTD and the estimate of efficiency revised. The process is iterated until the value of INT agrees to within 1% with INTD. The efficiency EFF and operating temperature TP of the burner are now stored for this run and the next set of operating data is examined. The process is repeated until all of the data has been exhausted.

The results of Program PREDICT are seen to be of several types. First, we obtain a value of INTR for every lean run, and

hence a prediction of whether or not the burner will be stable. Secondly, for those conditions where the burner will be stable, we obtain values of EFF and TP: the predicted efficiency and operating temperature of the burner. Finally, for all runs including both stable and unstable runs, we obtain values of the efficiency and combustion temperature at the stability limit.

The use of Program PREDICT for comparison of burner stability limits with theory requires some ingenuity as to how one should present the data. In this regard it was decided that a plot of the experimental observations of burner operating condition versus INTR would be of some interest. A variable named BURN was devised to assist in making this comparison. For those runs in which the burner was considered to be operating normally, a value of 2 was assigned to BURN. For those runs for which the burner was definitely going out in a reasonable period of time (less than five minutes), a value of 0 was assigned to BURN. Those runs for which the burner was operating in an erratic fashion, or for which the burner eventually went out after a long period of time, were assigned a value of BURN equal to 1.

Figure 1 shows a plot of BURN versus INTR. The upper line represents conditions for which the burner was stable. The middle line represents stability limit operation. The bottom line represents test runs for which the burner was going out. Clearly the assignment of a value to BURN is a matter of judgment, and hence it is not surprising that there is some scatter in the data.

Figure 1 shows a surprisingly good correlation for the predictions from the values of INTR and the BURN = 0 and BURN = 2 lines. Virtually all of the BURN = 2 values lie below INTR = 1.0. Of the runs for which BURN = 2, only 12 of these have values on INTR greater than 1. The highest is run No. 223 for which INTR = 1.96. Similarly, of the runs for which BURN = 0 was assigned, only one run, No. 391 had a value of INTR below 1.0. For run No. 391, INTR = 0.84.

The runs for which BURN = 1 was assigned do not show quite such good correlation. Here there are lean limit runs for which INTR = 0.25 and other lean limit runs for which INTR = 2.5. Most of these lean limit discrepancies appear to be a result of the difficulty associated with obtaining accurate fuel/air ratio data. While the volumetric gas analysis equipment is quite accurate for normal burning runs, it becomes less valuable near a blowout condition. When the burner is near blowout, the efficiency of the burner may drop to as low as 90%. Under these conditions, the fuel/air ratios based on the volumetric data should be in error by about 10%. While this may seem like a small error, a change of burner temperature of 200°F has a pronounced effect on the computed value of INTR.

2. Stability Tests From Program PREDICT

The stability predictions obtained from

Program PREDICT are tabulated in Tables 3 through 18. The first column in each of these tables shows the run number. Next we see volume of the burner under test, then the inlet temperature and the air flow rate. In Column 5, the equivalence ratio at which the burner was operated is shown. This is based on the nominal fuel/air ratio discussed previously. Column 6 shows the burner intensity parameter based on the flow rate and volume of the burner. Column 7 shows the limiting value of intensity parameter at lean blowout as computed from the equivalence ratio and air inlet temperature. From these the stability parameter INTR in Column 8 is computed. Column 9, labeled BURN, shows the estimate of burner stability provided by the burner operator or the data in the burner notebook. As explained above, 2 represents stable operation of the burner, 1 represents lean limit operation and 0 corresponds to operating conditions for which the burner will go out.

Examination of Table 3 through 18 provides additional insight into the validity of the burner stability theory. We see that in many instances where it was difficult to judge how close we were to the stability limit, the value of INTR is in fact close to 1.

Another interesting observation from the Table deals with those values for which the burner was at or near lean limit operation while the value of INTR is low. Here, the computer program predicts that the burner will have some considerable margin of stable operation, while in fact it was near or at its blowout limit. These were usually runs at low air flow rates in test Stand 2. This burner is more subject to heat loss than the other burners tested. The influence of heat loss on the stability of the burner can be significant, particularly at low air flow rates. Since the burner stability analysis program did not take this heat loss into account, it is not surprising that there are some differences between the prediction and the experiment at the low flow rates.

3. Correlation of Stability Data with Theoretical Stability Curves

In addition to the information obtained from Program PREDICT, the stability limit data previously obtained from Programs STABILITY and BURN can be used to correlate burner blowout data.

Figures 20, 21, 22, 24 and 25 in Section VI show blowout data for the Paxve Burner. Superimposed on these figures are theoretical stability limit curves based on the analyses of Section VII. It is clear that the theoretical limit curves agree well with the experimental data. The propane curves are more complete than the kerosene curves because it was easier to run the propane tests. Figure VI 20 is for propane at ambient temperature in a 33 cu. in. burner. This figure shows that all of the blowout points (squares) lie to the left of the theoretical limit line, while all but two of the stable burning points (circles) lie to the right of the line. The lean limit points showing marginal stability (triangles) are scattered around the theoretical limit

line.

Another way of showing the same information is to plot the data on a curve of equivalence ratio versus burner intensity parameter. Figure 2 shows such a plot for the ambient temperature data. Superimposed on the data is the theoretical limit line for 75°F inlet temperature; we again see that the data and the theory are in substantial agreement.

4. Final Comments on Burner Stability Correlation

The experimental stability data from the Paxve burner agrees quite well with the predictions obtained from the burner theory, particularly at high flow rates. There are several matters which bear further investigation.

a. The stability of the burner is particularly sensitive to extraneous heat loss. Incorporation of a heat loss term in the stability analysis should improve the correlation between the experimental and theoretical predictions, particularly at low flow rates. The interpretation of such a burner heat loss parameter in terms of burner construction considerations would be of great value in the improvement of burner design.

b. The burner stability prediction program assumed that the fuel entering the burner was at ambient temperature. A correction was made for the heat input necessary to raise the fuel to the air inlet temperature. During many of the runs, particularly those with kerosene, the fuel was at an elevated temperature. This seems to increase the burner stability. The burner stability prediction program could be readily modified to take into account the fuel inlet temperature.

c. The burner analysis was limited to lean operation. This was primarily a result of the limited funding available for this effort and a corresponding limited interest in this area of burner operation for automotive application. Some industrial processes utilize staged combustion with rich mixtures in the first stage. An extension of the present work to investigate rich operation may reveal procedures that would assist in reducing the level of pollutants emitted from these sources.

d. The stability of the burner as well as its emission characteristics are influenced by the uniformity of the fuel/air distribution within the burner. Burners which have highly homogenous fuel/air mixtures at the inlet are generally somewhat less stable than burners which have non-uniform fuel/air distributions. This is due to the fact that the flame can stabilize in a locally rich portion of the flow and then spread through the rest of the stream.

Non-uniform fuel/air distribution is also a factor in burner emissions. The problems of hydrocarbon emissions from the top of the vapor generator stack, which caused so much trouble during

the course of this program, was finally traced to a badly distorted fuel/air profile in the air/fuel mixture ahead of the burner inlet. Once this non-uniform fuel/air condition had been corrected, the hydrocarbon emission problem was immediately cleared up. Unfortunately it is not possible at this time to go back and establish a uniformity of the fuel/air mixture during the early stability tests.

If the indicated improvements in the burner theory were made, it seems clear that the theoretical analysis will be more than adequate to serve as a basic tool in burner design and development. The burner stability theory predicts the influence not only of flow rate and burner volume, but also air inlet temperature and pressure. Verification of the validity of this analysis at high inlet pressure and temperature is a task of great importance. That work was beyond the scope of this program.

B. Correlation of the Oxides of Nitrogen Data

It is clear from an examination of the experimental data that the oxides of nitrogen emissions from the Paxve burner exhaust are a strong function of fuel/air ratio and not strongly dependent on air flow rate through the burner. An examination of comparable data from cold air and hot air runs shows somewhat higher NOx levels at the elevated inlet temperatures. Although the data scatter makes an exact comparison difficult, it appears that the influence of inlet temperature is what one would expect if the NOx were a function of combustion temperature only. Figure VI-19 shows all of the NOx data from the burner plotted against burner temperature. Despite the scatter it is clear that a correlation between these two variables exist.

It seems reasonable to presume that the oxides of nitrogen in the burner exhaust are formed in the burner by a chemical reaction whose rate is given by an Arrhenius type equation

$$\frac{d}{dt}(NO) = K[O_2]^a \quad Vol \; e^{-E/RT}$$

where: NO = Wt of NO formed

Vol = burner volume

E = activation energy of the over-all reaction

Since the NOx concentration in ppm is the ratio of the NOx weight flow to the air weight flow, we might expect that the NOx in parts per million would be given by an equation of the form

$$[NO] = \frac{K[O_2]^a \; e^{-E/RT}}{W_A/Vol}$$

Examination of the data, however, shows that the predicted inverse dependence of NOx with air flow rate either does not exist,

or else is suppressed by the data scatter. The predicted dependence on temperature however, is clearly evident, and can be further characterized by plotting the NOx concentration against reciprocal combustion temperature.

Figure 3 shows such a plot for all of the data. Figure 4 shows a similar plot for the small sample of the data in which the fuel type and general operating conditions were relatively fixed. In both cases, we can draw a straight line through the data and obtain an empirical correlation.

Paxve has examined several approaches to the correlation of the NOx data obtained during this program. The possibility in involving the air flow, and the oxygen concentration in the result was investigated. We found that a better correlation could be obtained by using the combustion temperature alone than could be obtained by including these other factors. The ambient temperature data appears to be well fitted by an equation of the form

$$NOx = 4.38 \times 10^5 \times e^{-E/RT}$$

with

$$E = 36.7 \text{ K cal/mole}$$

Figure 5 shows this equation superimposed on the summary NOx curve, using the theoretical flame temperatures for 70°F and 400°F inlet temperatures. It is clear that the curves give a reasonable fit to the data, although the 400°F curve is somewhat conservative as compared to the bulk of the high temperature data.

C. Correlation of the CO Emissions Data

The theoretical burner analysis described in Section VII of this report provides a basis for correlating the CO emissions from the burner. The theory yields values for the burner efficiency as a function of the inlet temperature and the burner intensity parameter. If we substract the efficiency, from 1.0, we obtain the unreactedness, δ, which should be proportional to the emissions of unburned or partially burned material in the burner exhaust. Program PREDICT gave an evaluation of each lean test point. Tables showing the predicted burner efficiency, the predicted emissions, and the acutal values of the CO, HC, and NOx emissions, are presented in Tables 19 through 31. Examination of the data in those tables show that the CO emissions are generally less than the predicted values.

In order to examine this further we have taken some typical sets of CO gm/Kg emissions data and superimposed the predicted emission levels based on the analysis. Figure 6 shows the CO emissions from the burner for the small burner (33 CU. IN.) on test stand 1 with ambient air and propane. The CO emissions are obviously strongly influenced by the air flow rate. Curves

through the data for air flow rates of 25 lb/hr, 50 lb/hr, and 100 lb/hr have been drawn on the figure as solid lines. Predictions based on the theoretical burner analysis are shown on the figure as dotted lines. Two of these theoretical prediction lines are shown, one for 25 lb/hr, the other for 100 lb/hr.

Figure 7 shows a similar set of data for later runs in test stand 2 burning kerosene with elevated inlet temperatures. Once again, the predicted values are substantially higher than the experimentally determined CO emission levels.

We do not have a simple explanation for the low levels of CO emissions observed. We suspect, however, that this is a consequence of the oversimplification involved in arriving at the predicted values. The theoretical analysis was based on the assumption that the unreactedness (the combustion inefficiency) was represented by vaporized but unburned raw fuel. The predicted heat release was therefore reduced directly with the unreactedness. Experimentally, however, the unburned material which is most significant in the combustion chamber under lean operating conditions is not raw fuel, but rather carbon monoxide. In order to correlate the CO data, we therefore assumed that the CO levels would be equal to the predicted unreactedness. This is clearly inconsistent. If we had refined our analysis to allow for partially reacted material leaving the chamber (the fuel converting into water vapor and carbon monoxide), then the heat release used in the analysis at low efficiency points would have been greater and the predicted emissions would have been less as the blow out limits were approached. A revision of the analysis to account for this partial reaction process would be desirable, but it was not feasible within the financial limitations of the present contract. In any case, it seems clear that the CO emissions to be expected from the Paxve burner will be less than those predicted by the present theory. This gives us a method for obtaining CO emission estimates which will be conservative for burner application studies.

Figure 6 also shows the dramatic reduction in CO emissions which occur as the exhaust gases pass through the vapor generator stack. This is undoubtedly a result of the continued oxidation of the CO to CO_2 which occurs as the gases cool off during their passage through the heat exchanger. The rate of the CO oxidation reaction is still substantial at temperatures over 2000°F. As the gases cool, there is time for the combustion reaction to come closer to completion. There is also time for CO which arises from the high temperature equilibrium dissociation reaction to recombine as the equilibrium shifts during cooling. The theoretical predictions are thus even more conservative for a burner coupled to a heat exchanger.

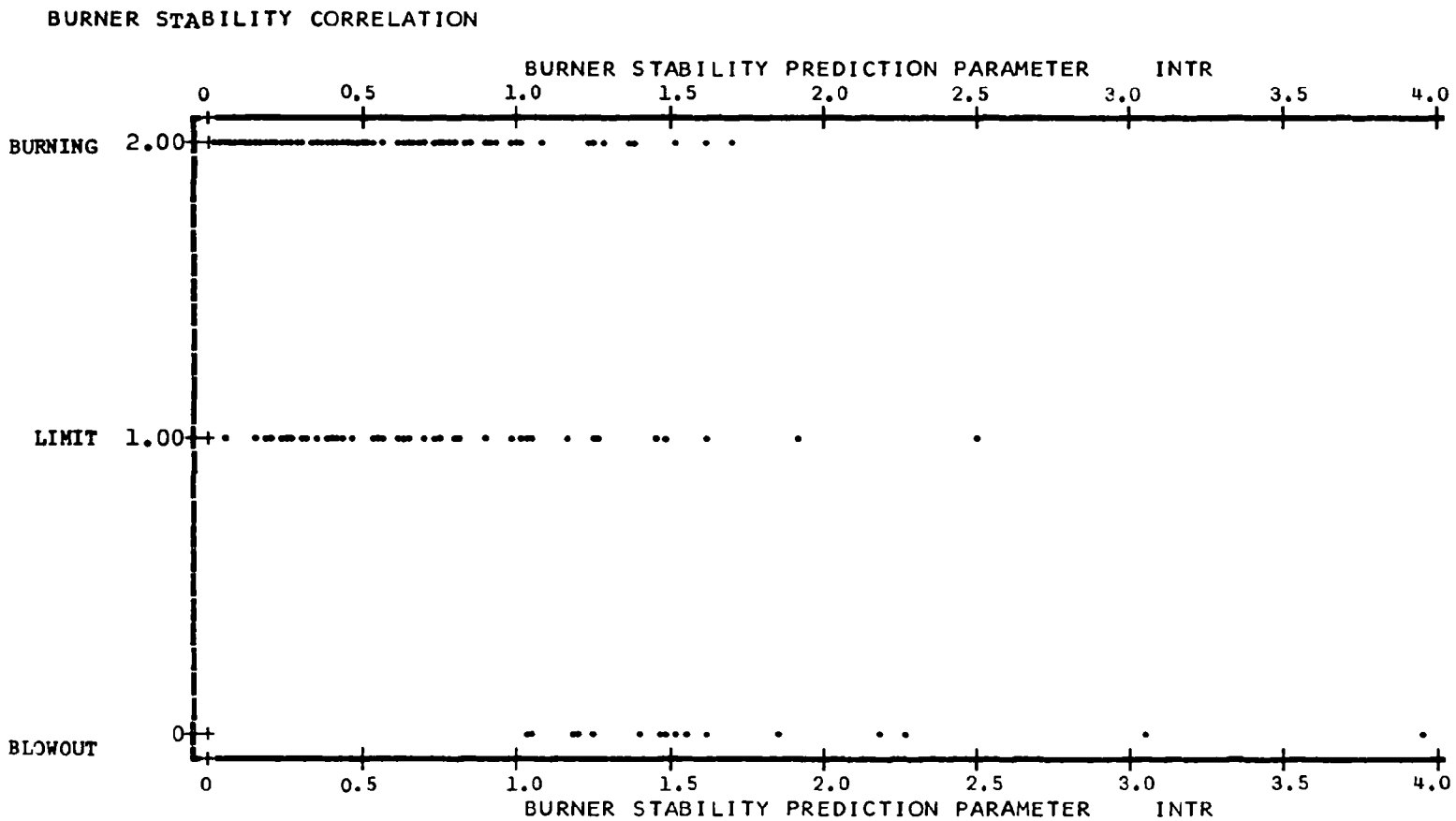
BURNER STABILITY CORRELATION
BURNER STABILITY PREDICTION PARAMETER INTR
0
0.5
1.0
1.5
2.0
2.5
3.0
3.5
4.0
BURNING
2.00
LIMIT
1.00
BLOWOUT
0
BURNER STABILITY PREDICTION PARAMETER INTR

Fig VIII-1

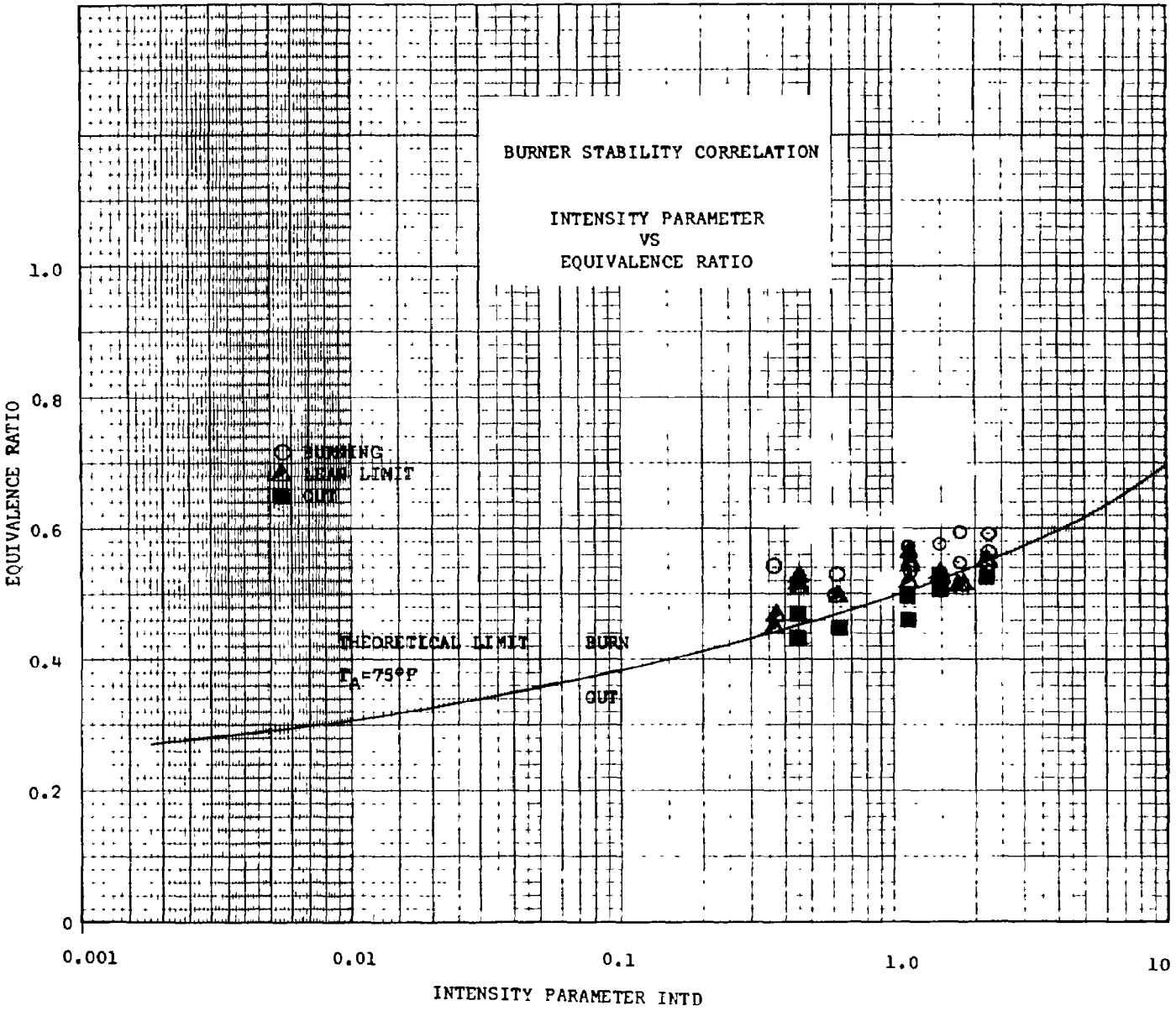
BURNER STABILITY CORRELATION
INTENSITY PARAMETER
VS
EQUIVALENCE RATIO
EQUIVALENCE RATIO
1.0
0.8
0.6
0.4
0.2
0
BLOWING
LEAN LIMIT
OUT
THEORETICAL LIMIT
T_A=75°F
BURN
OUT
0.001
0.01
0.1
1.0
10
INTENSITY PARAMETER INTD

FIG. VIII 2

CORRELATION OF OXIDES OF NITROGEN DATA

WITH RECIPROCAL COMBUSTION TEMPERATURE

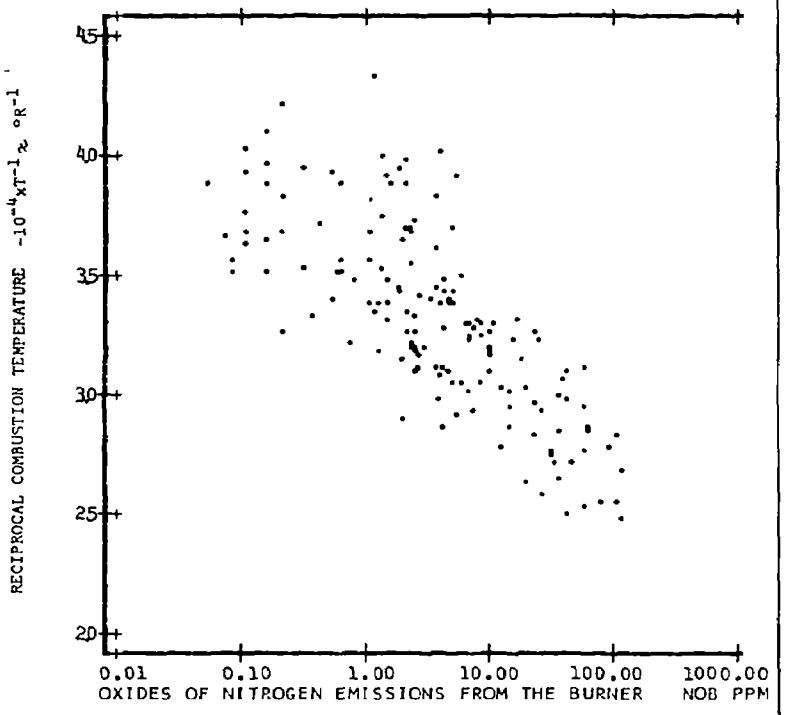

Fig.
VIII-3

CORPELATION OF OXIDES OF NITPOGEN DATA

KFROSENF——HOT——BUPNER DATA

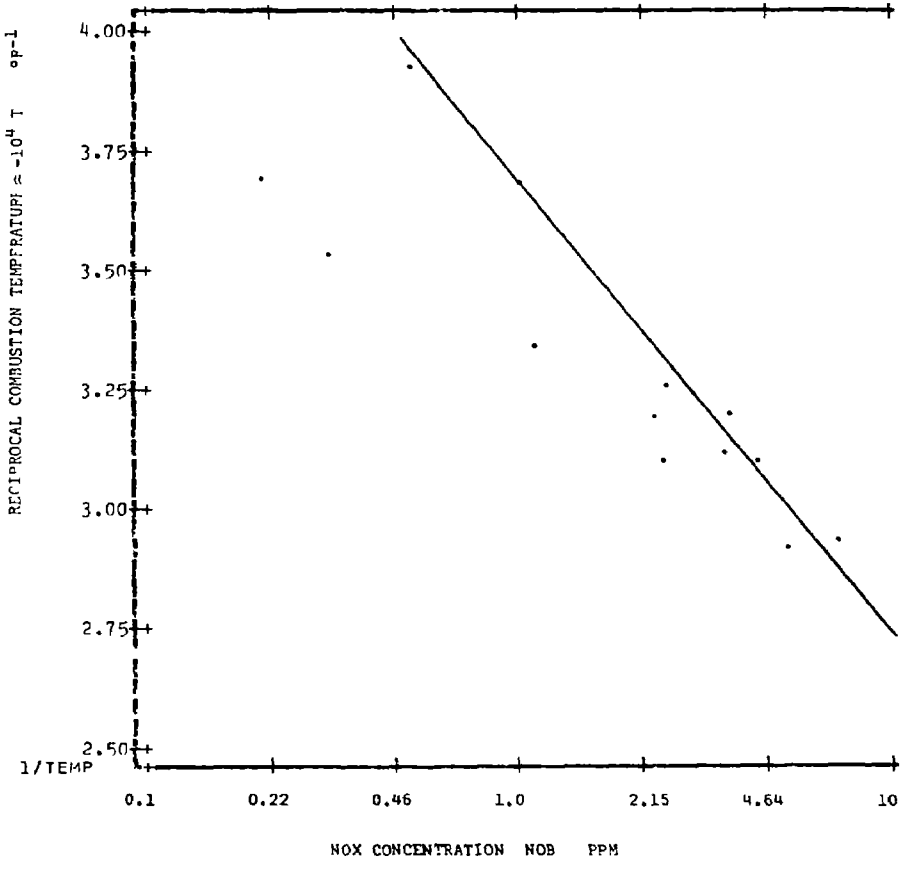

Fig.
VIII-4

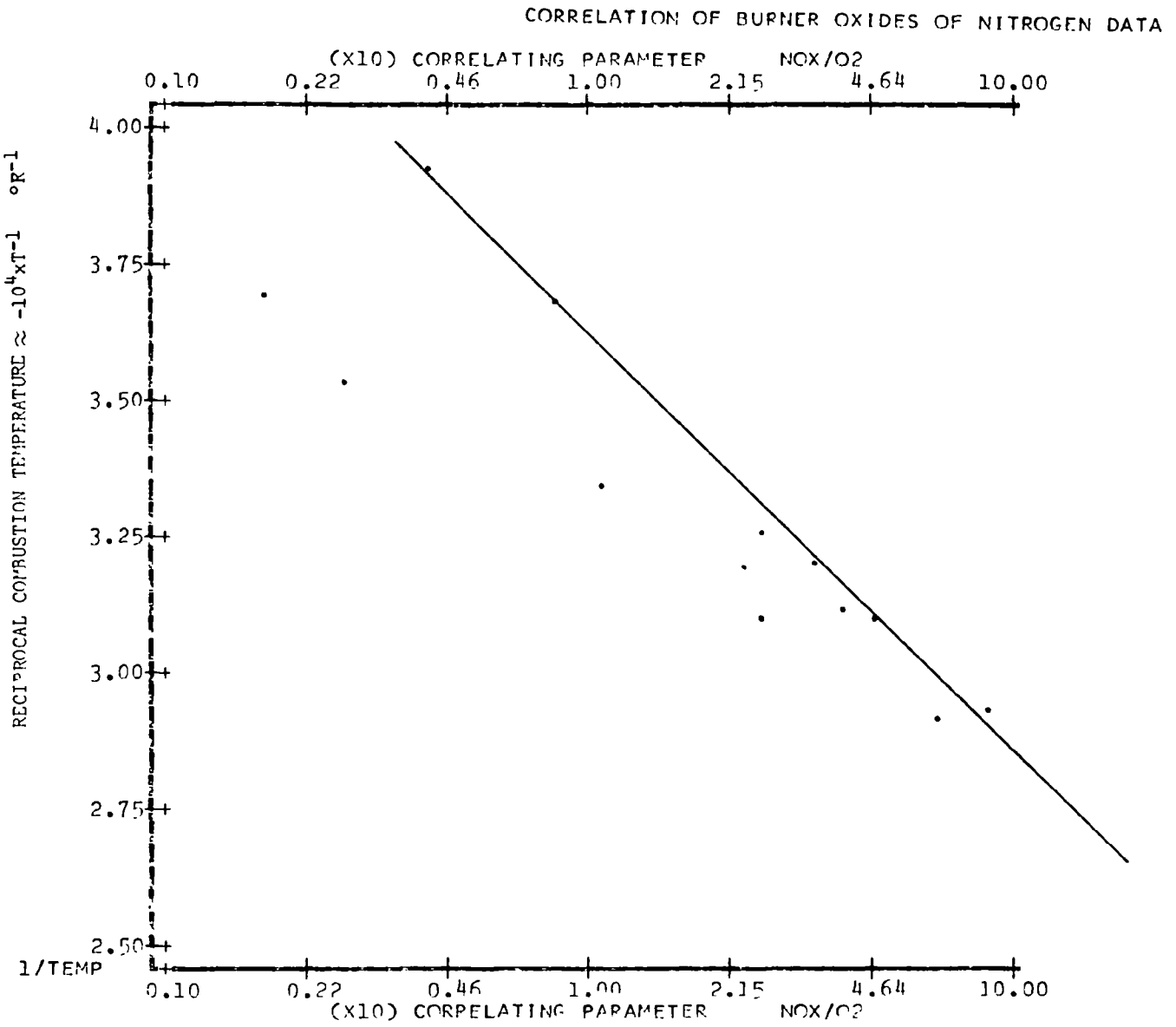
CORRELATION OF BURNER OXIDES OF NITROGEN DATA
(X10) CORRELATING PARAMETER NOX/O2
0.10
0.22
0.46
1.00
2.15
4.64
10.00
4.00
3.75
3.50
3.25
3.00
2.75
2.50
RECIPROCAL COMBUSTION TEMPERATURE ≈ -10⁴xT⁻¹ °R⁻¹
1/TEMP
(X10) CORPELATING PARAMETER NOX/O2

Fig. VIII-5

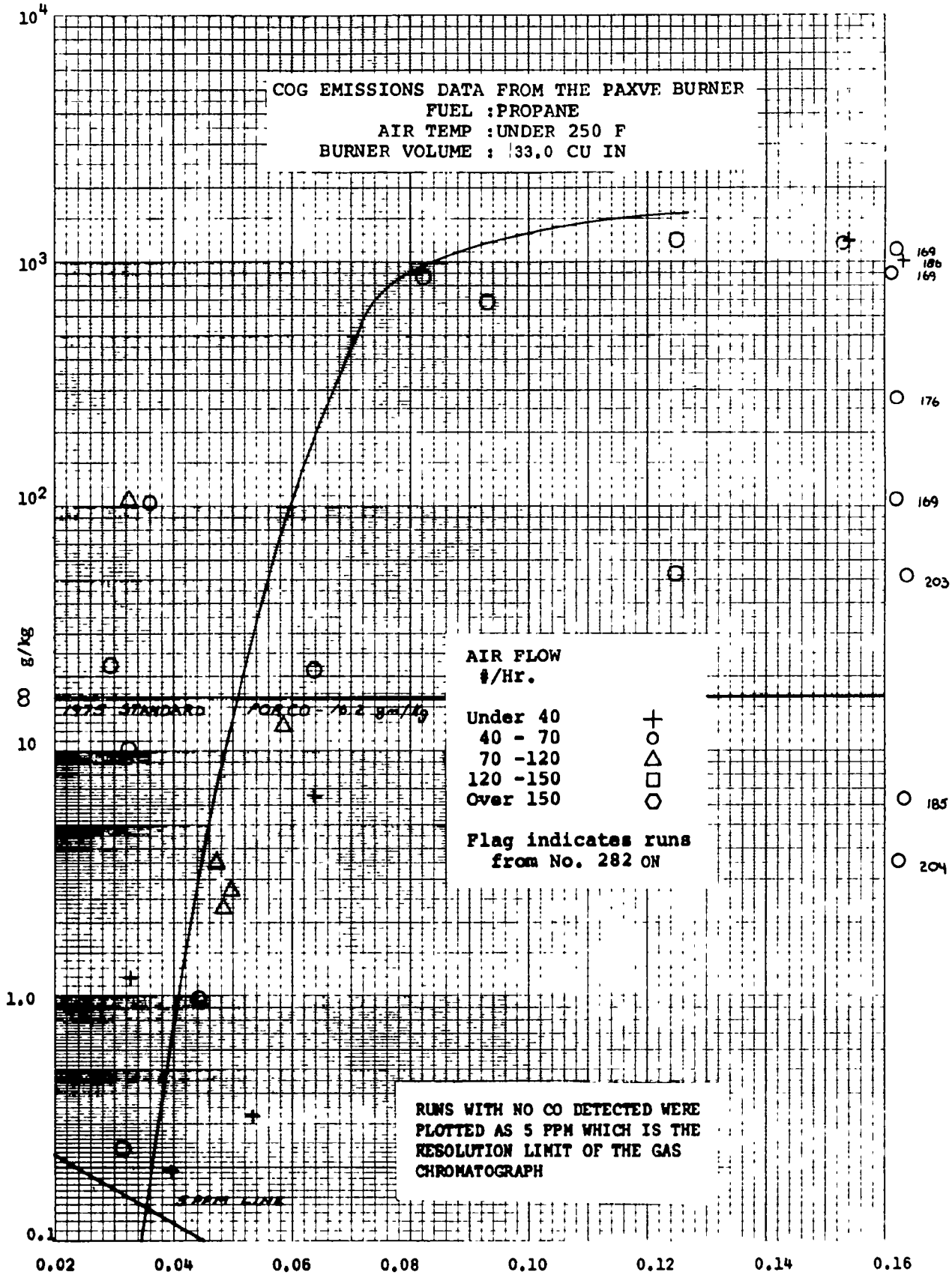
COG EMISSIONS DATA FROM THE PAXVE BURNER
FUEL :PROPANE
AIR TEMP :UNDER 250 F
BURNER VOLUME : 33.0 CU IN
AIR FLOW
#/Hr.
Under 40
40 - 70
70 -120
120 -150
Over 150
Flag indicates runs from No. 282 ON
RUNS WITH NO CO DETECTED WERE PLOTTED AS 5 PPM WHICH IS THE RESOLUTION LIMIT OF THE GAS CHROMATOGRAPH
1975 STANDARD
SMOKE LINE
g/kg
NOMINAL FUEL AIR RATIO FAN
169
186
169
176
169
203
185
204

Fig. VIII-6

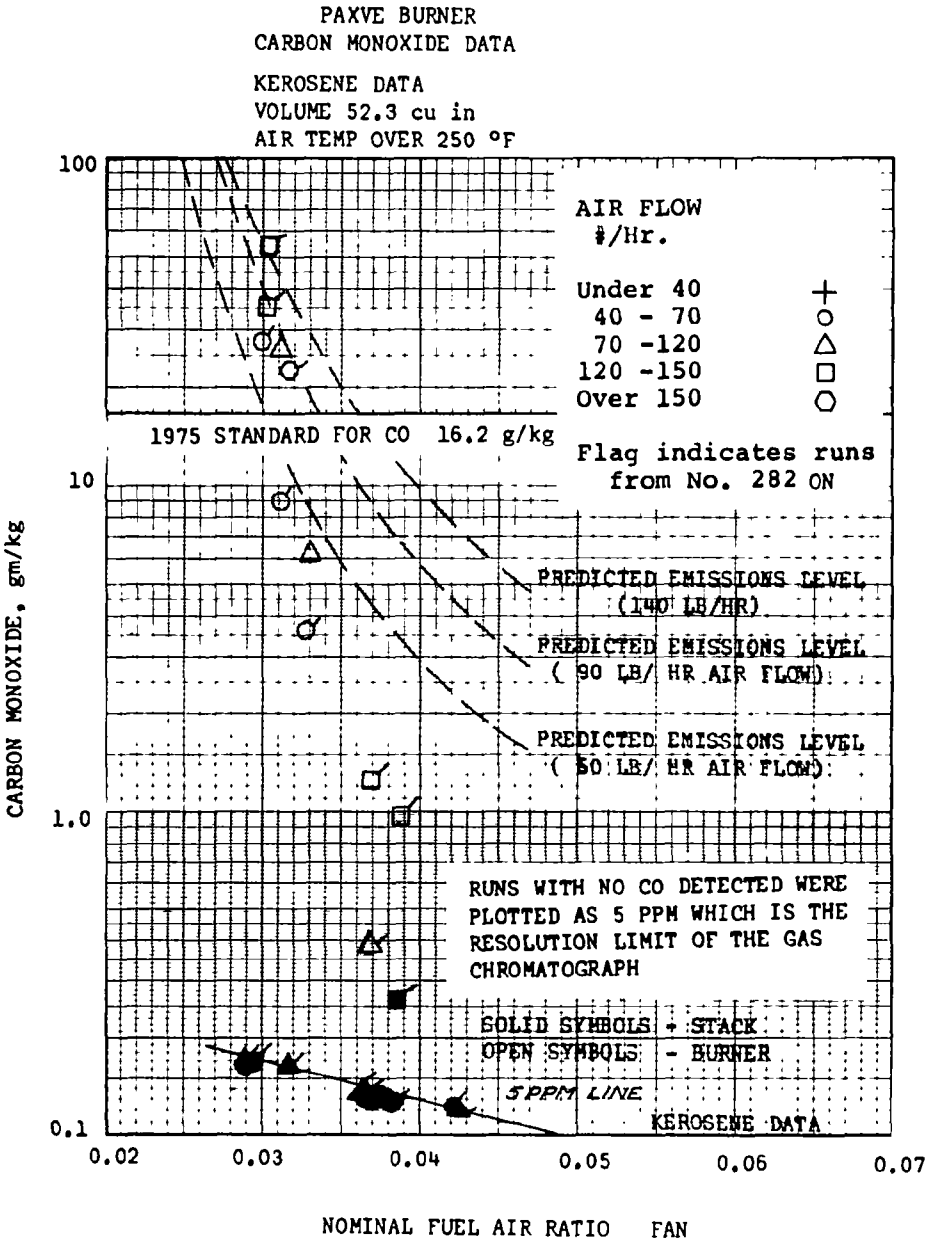
PAXVE BURNER
CARBON MONOXIDE DATA
KEROSENE DATA
VOLUME 52.3 cu in
AIR TEMP OVER 250 °F
AIR FLOW
#/Hr.
Under 40
40 - 70
70 -120
120 -150
Over 150
1975 STANDARD FOR CO 16.2 g/kg
Flag indicates runs from No. 282 ON
PREDICTED EMISSIONS LEVEL (140 LB/HR)
PREDICTED EMISSIONS LEVEL (90 LB/ HR AIR FLOW)
PREDICTED EMISSIONS LEVEL (50 LB/ HR AIR FLOW)
RUNS WITH NO CO DETECTED WERE PLOTTED AS 5 PPM WHICH IS THE RESOLUTION LIMIT OF THE GAS CHROMATOGRAPH
SOLID SYMBOLS - STACK
OPEN SYMBOLS - BURNER
5PPM LINE
KEROSENE DATA
CARBON MONOXIDE, gm/kg
100
10
1.0
0.1
0.02
0.03
0.04
0.05
0.06
0.07
NOMINAL FUEL AIR RATIO FAN

Fig.
VIII-7

PROGRAM PREDICT

```
    ∇ PREDICT;I;PH;TI;INTD;LIT;CA;CF;CP;TEST
[1]   NL←⍴PHIG
[2]   I←1
[3]   INTD1←INTL←INTR←TBL1←EL←EFF←TP←(⍴PHIG)⍴0
[4]  GO:PH←PHIG[I]
[5]   TI←TAG[I]
[6]   WAD←WAG[I]
[7]   INTD1[I]←INTD←WAD×CONST[I]
[8]   LIMIT
[9]   INTR[I]←INTD+INT
[10]  INTL[I]←INT
[11]  TBL1[I]←TB
[12]  EL[I]←E
[13]  LIT←INTD≤INT
[14]  →(LIT=0)/OUT
[15] BRN:E←1-(1-E)×(INTD÷INT)*1-(PH=1)÷2
[16]  CAL
[17]  TEST←(1-INTD÷INT)
[18]  →((|TEST)>0.01)/BRN
[19] OUT:EFF[I]←LIT×E
[20]  TP[I]←(TB×LIT)+(1-LIT)×TI-460
[21]  I
[22]  I←I+1
[23]  →(I≤NL)/GO
    ∇
```

Table VIII-1

PROGRAM LIMIT

```
    ∇ LIMIT;I;COUNT;INTM
[1]   COUNT←0
[2]   E←0.3+0.05×⍳14
[3]  ITT:COUNT←COUNT+1
[4]   CAL
[5]   INTM←⌈/INT
[6]   I←INT⍳INTM
[7]   →(I=1)/OUT
[8]   →(COUNT=3)/OUT
[9]   E←E[I-1]+(0.1*COUNT+1)×⍳10
[10]  →ITT
[11] OUT:E←E[I]
[12]  INT←INT[I]
[13]  TB←TB[I]
    ∇
```

Table VIII-2

COMPARISON OF PREDICTED AND EXPERIMENTAL BURNER STABILITY DATA PAGE 1

RUN NO.	VOL IN*3	AIR TEMP oF	AIR FLOW LBS/HR	EQUIV RATIO	INT DATA W/VP*2	INT LIM W/VP*2	INT RAT ID/IL	BURN
1	33.0	75	22.3	0.4678	0.3244	0.5487	0.5906	-1
2	33.0	80	22.2	0.5309	0.3229	1.5621	0.2065	-1
3	33.0	85	45.3	0.4822	0.6585	0.7412	0.8875	-1
4	33.0	85	45.3	0.4524	0.6585	0.4299	1.5303	-1
5	33.0	85	47.0	0.4650	0.6830	0.5447	1.2526	-1
6	33.0	88	61.8	0.4501	0.8991	0.4176	2.1505	-1
7	33.0	90	61.7	0.4948	0.8974	0.9350	0.9588	-1
8	33.0	90	61.7	0.6326	0.8974	5.4903	0.1633	2
9	33.0	90	61.7	0.5073	0.8974	1.1420	0.7850	1
10	33.0	90	61.7	0.4697	0.8974	0.6079	1.4747	0
11	33.0	90	61.7	0.5230	0.8974	1.4478	0.6192	1
12	33.0	90	61.7	0.4322	0.8974	0.2935	3.0539	0
13	33.0	90	61.7	0.5386	0.8974	1.8107	0.4951	-1
14	33.0	90	61.7	0.5073	0.8974	1.1420	0.7850	1
15	33.0	90	61.7	0.5089	0.8974	1.1695	0.7666	2
16	33.0	90	78.1	0.5689	1.1362	2.6981	0.4207	2
17	33.0	90	78.1	0.5417	1.1362	1.8890	0.6009	1
18	33.0	90	78.1	0.5541	1.1362	2.2311	0.5087	2
19	33.0	91	78.0	0.6115	1.1352	4.4320	0.2559	2
20	33.0	92	78.0	0.5377	1.1341	1.8009	0.6291	2
21	33.0	92	78.0	0.4609	1.1341	0.5216	2.1721	0
22	33.0	93	77.9	0.4960	1.1331	0.9661	1.1716	0
23	33.0	93	77.9	0.5209	1.1331	1.4192	0.7976	1
24	33.0	93	77.9	0.5382	1.1331	1.8199	0.6220	1
25	33.0	93	77.9	0.5631	1.1331	2.5330	0.4469	1

BURN = 2 --- STABLE OPERATION
BURN = 1 --- STABILITY LIMIT
BURN = 0 --- BURNER GOES OUT

UNITS OF INT ARE LBS/SEC FT*3 ATM*2

Table VIII-3

COMPARISON OF PREDICTED AND EXPERIMENTAL BURNER STABILITY DATA PAGE 2

RUN NO.	VOL IN*3	AIR TEMP OF	AIR FLOW LBS/HR	EQUIV RATIO	INT DATA W/VP*2	INT LIM W/VP*2	INT RAT ID/IL	BURN
26	33.0	90	103.3	0.6937	1.5030	9.5186	0.1578	2
27	33.0	93	103.1	0.5794	1.4989	3.0973	0.4835	2
28	33.0	96	102.8	0.5227	1.4949	1.4727	1.0140	0
29	33.0	97	102.7	0.5118	1.4935	1.2588	1.1852	0
30	33.0	97	102.7	0.5231	1.4935	1.4887	1.0022	1
31	33.0	102	120.9	0.5930	1.7583	3.7383	0.4699	2
32	33.0	105	120.6	0.5465	1.7537	2.1285	0.8231	2
33	33.0	108	120.2	0.5158	1.7490	1.3937	1.2537	1
34	33.0	95	121.6	0.5099	1.7694	1.2117	1.4587	0
35	33.0	102	120.9	0.5190	1.7583	1.4273	1.2307	1
36	33.0	112	153.8	0.5878	2.2377	3.6370	0.6147	2
37	33.0	117	153.2	0.5613	2.2280	2.6910	0.8272	2
38	33.0	120	152.8	0.5451	2.2222	2.2041	1.0073	2
39	33.0	120	152.8	0.5299	2.2222	1.7910	1.2396	0
40	33.0	120	152.8	0.5135	2.2222	1.4105	1.5739	1
41	33.0	124	152.3	0.5470	2.2146	2.2941	0.9654	1
42	33.0	91	103.2	0.7565	1.5016	15.0328	0.0998	2
43	33.0	93	103.1	0.5222	1.4989	1.4474	1.0345	1
44	33.0	87	41.8	0.7529	0.6085	14.5467	0.0418	2
45	33.0	85	41.9	0.6916	0.6096	9.2316	0.0660	2
46	33.0	84	41.9	0.6132	0.6096	4.4163	0.1379	2
47	33.0	82	42.0	0.5333	0.6113	1.6303	0.3745	2
48	33.0	82	42.1	0.4910	0.6124	0.8497	0.7199	2
49	33.0	80	42.1	0.4497	0.6124	0.3988	1.5337	0
50	33.0	80	42.1	0.4997	0.6124	0.9710	0.6300	1

BURN = 2 --- STABLE OPERATION
BURN = 1 --- STABILITY LIMIT
BURN = 0 --- BURNER GOES OUT

UNITS OF INT ARE LBS/SEC FT*3 ATM*2

Table VIII-4

RUN NO.	VOL IN*3	AIR TEMP oF	AIR FLOW LBS/HR	EQUIV RATIO	INT DATA W/VP*2	INT LIM W/VP*2	INT RAT ID/IL	BURN
51	33.0	83	25.4	0.6097	0.3688	4.2404	0.0869	2
52	33.0	82	25.4	0.5406	0.3691	1.8068	0.2041	2
53	33.0	82	25.4	0.4645	0.3691	0.5329	0.6919	1
54	33.0	83	25.4	0.4510	0.3688	0.4144	0.8888	1
55	-1.0	83	42.0	3.1753	-1.0000	-1.0000	-1.0000	-1
56	-1.0	81	42.1	2.6412	-1.0000	-1.0000	-1.0000	-1
57	-1.0	82	42.0	2.8966	-1.0000	-1.0000	-1.0000	-1
58	-1.0	85	41.9	2.6510	-1.0000	-1.0000	-1.0000	-1
59	-1.0	85	41.9	3.1812	-1.0000	-1.0000	-1.0000	-1
60	-1.0	90	41.7	1.9452	-1.0000	-1.0000	-1.0000	-1
61	-1.0	90	41.7	1.9452	-1.0000	-1.0000	-1.0000	-1
62	-1.0	85	41.9	2.6510	-1.0000	-1.0000	-1.0000	-1
63	-1.0	87	41.8	3.1870	-1.0000	-1.0000	-1.0000	-1
64	-1.0	85	41.9	2.6510	-1.0000	-1.0000	-1.0000	-1
65	-1.0	88	41.8	2.7692	-1.0000	-1.0000	-1.0000	-1
66	-1.0	85	41.9	2.8585	-1.0000	-1.0000	-1.0000	-1
67	-1.0	85	41.9	2.7616	-1.0000	-1.0000	-1.0000	-1
68	-1.0	78	25.5	2.5262	-1.0000	-1.0000	-1.0000	-1
69	-1.0	82	24.7	2.3985	-1.0000	-1.0000	-1.0000	-1
70	-1.0	85	25.3	2.9167	-1.0000	-1.0000	-1.0000	-1
71	-1.0	86	25.3	3.0646	-1.0000	-1.0000	-1.0000	-1
72	-1.0	90	61.7	2.3863	-1.0000	-1.0000	-1.0000	-1
73	-1.0	93	61.5	2.4493	-1.0000	-1.0000	-1.0000	-1
74	33.0	86	25.3	0.5044	0.3677	1.0731	0.3423	1
75	33.0	85	25.3	0.6219	0.3681	4.8599	0.0757	2

BURN = 2 --- STABLE OPERATION
BURN = 1 --- STABILITY LIMIT
BURN = 0 --- BURNER GOES OUT

UNITS OF INT ARE LBS/SEC FT*3 ATM*2

Table VIII-5

COMPARISON OF PREDICTED AND EXPERIMENTAL BURNER STABILITY DATA PAGE 4

RUN NO.	VOL IN*3	AIR TEMP oF	AIR FLOW LBS/HR	EQUIV RATIO	INT DATA W/VP*2	INT LIM W/VP*2	INT RAT ID/IL	BURN
76	33.0	85	25.3	0.8339	0.3681	22.9747	0.0160	2
77	33.0	85	25.3	0.9960	0.3681	41.5938	0.0088	2
78	33.0	90	61.7	0.5574	0.8974	2.3338	0.3845	1
79	33.0	92	61.6	0.6869	0.8958	9.0511	0.0989	2
80	33.0	90	61.7	0.9927	0.8974	41.6033	0.0216	2
81	1.0	92	61.6	1.4432	1.0000	1.0000	1.0000	1
82	33.0	103	102.1	0.5050	1.4855	1.1611	1.2781	2
83	33.0	105	101.9	0.7666	1.4829	16.5407	0.0896	2
84	33.0	100	102.4	0.7464	1.4895	14.3647	0.1036	2
85	33.0	103	102.1	0.9178	1.4855	33.8123	0.0439	2
86	1.0	105	101.9	1.2812	1.0000	1.0000	1.0000	1
87	33.0	300	59.3	0.5391	0.8628	3.8187	0.2259	2
88	33.0	300	59.3	0.6869	0.8628	15.3308	0.0563	2
89	1.0	300	59.3	1.1075	1.0000	1.0000	1.0000	1
90	33.0	300	59.6	0.5770	0.8665	5.8483	0.1482	2
91	33.0	310	59.3	0.8222	0.8628	34.3220	0.0251	2
92	1.0	300	59.3	1.1075	1.0000	1.0000	1.0000	1
93	52.3	250	165.3	0.4863	1.5174	1.5676	0.9680	2
94	52.3	250	165.3	0.6478	1.5174	9.9126	0.1531	2
95	52.3	250	165.3	0.8299	1.5174	31.5282	0.0481	2
96	52.3	250	132.9	0.9865	1.2193	54.2496	0.0225	2
97	52.3	95	55.9	0.4881	0.5126	0.8554	0.5986	2
98	52.3	95	55.9	0.6175	0.5126	4.7821	0.1071	2
99	52.3	95	55.9	0.8087	0.5126	20.6232	0.0248	2
100	52.3	100	55.6	0.9984	0.5103	42.9648	0.0119	2

BURN = 2 --- STABLE OPERATION
BURN = 1 --- STABILITY LIMIT
BURN = 0 --- BURNER GOES OUT

UNITS OF INT ARE LBS/SEC FT*3 ATM*2

Table VIII-6

RUN NO.	VOL IN*3	AIR TEMP oF	AIR FLOW LBS/HR	EQUIV RATIO	INT DATA W/VP*2	INT LIM W/VP*2	INT RAT ID/IL	BURN
101	-1.0	102	55.5	1.1925	0.0000	0.0000	0.0000	-1
102	52.3	102	89.0	0.7520	0.8165	14.9787	0.0545	2
103	52.3	400	50.0	0.8359	0.4593	43.4487	0.0106	2
104	52.3	400	50.0	0.5406	0.4593	5.4104	0.0849	2
105	52.3	84	49.9	0.9250	0.4581	33.4897	0.0137	2
106	52.3	85	49.9	0.4888	0.4581	0.8290	0.5519	1
107	52.3	85	49.9	0.3925	0.4581	0.1159	3.9481	0
108	52.3	85	49.9	0.4448	0.4576	0.3703	1.2345	2
109	52.3	85	49.9	0.5563	0.4576	2.2581	0.2027	2
110	52.3	400	50.0	0.4039	0.4593	0.7676	0.5984	2
111	52.3	400	50.0	0.3915	0.4593	0.6090	0.7543	2
112	52.3	400	33.2	0.4688	0.3048	2.1848	0.1395	2
113	52.3	400	33.2	0.3891	0.3048	0.5814	0.5243	2
114	52.3	400	33.2	0.3805	0.3043	0.4912	0.6194	2
115	52.3	400	33.1	0.3883	0.3040	0.5727	0.5309	1
116	52.3	400	82.7	0.5375	0.7587	5.2248	0.1452	2
117	52.3	400	82.8	0.4312	0.7601	1.2303	0.6178	2
118	52.3	400	82.8	0.3861	0.7601	0.5487	1.3851	0
119	52.3	400	126.8	0.4672	1.1634	2.1364	0.5446	2
120	52.3	400	127.0	0.4279	1.1654	1.1641	1.0012	2
121	52.3	400	126.8	0.4469	1.1634	1.5783	0.7371	2
122	52.3	400	126.8	0.4010	1.1634	0.7272	1.5998	0
123	52.3	74	50.5	0.7951	0.4634	18.2890	0.0253	2
124	52.3	80	49.5	0.4743	0.4542	0.6308	0.7192	1
125	52.3	85	47.6	0.4930	0.4369	0.8895	0.4906	-1

BURN = 2 --- STABLE OPERATION
BURN = 1 --- STABILITY LIMIT
BURN = 0 --- BURNER GOES OUT

*UNITS OF INT ARE LBS/SEC FT*3 ATM*2*

Table VIII-7

COMPARISON OF PREDICTED AND EXPERIMENTAL BURNER STABILITY DATA PAGE 6

RUN NO.	VOL IN*3	AIR TEMP oF	AIR FLOW LBS/HR	EQUIV RATIO	INT DATA W/VP*2	INT LIM W/VP*2	INT RAT ID/IL	BURN
126	52.3	95	127.3	0.5049	1.1684	1.1230	1.0404	0
127	52.3	95	119.6	0.5687	1.0976	2.7371	0.4006	1
128	52.3	90	67.8	0.5411	0.6226	1.8745	0.3318	2
129	52.3	80	86.2	0.5061	0.7910	1.0758	0.7344	2
130	52.3	80	82.8	0.5822	0.7604	3.0707	0.2474	2
131	52.3	80	66.7	0.6869	0.6124	8.7686	0.0698	2
132	-1.0	80	44.5	1.0553	0.0000	0.0000	0.0000	-1
133	52.3	80	83.4	0.5628	0.7655	2.4145	0.3167	2
134	52.3	80	66.7	0.7036	0.6124	10.0334	0.0610	2
135	52.3	80	72.3	0.4347	0.6634	0.2940	2.2538	0
136	52.3	88	72.3	0.5318	0.6634	1.6320	0.4061	2
137	52.3	90	66.7	0.7036	0.6124	10.2913	0.0594	2
138	52.3	95	96.6	0.6404	0.8867	6.0209	0.1471	2
139	52.3	95	95.0	0.7260	0.8715	12.3178	0.0707	2
140	-1.0	95	91.1	1.0266	0.0000	0.0000	0.0000	-1
141	-1.0	95	77.3	1.2099	0.0000	0.0000	0.0000	-1
142	52.3	95	77.8	0.5389	0.7145	1.8518	0.3854	2
143	-1.0	95	77.8	1.2013	0.0000	0.0000	0.0000	-1
144	-1.0	95	91.1	1.0266	0.0000	0.0000	0.0000	-1
145	52.3	95	94.4	0.7302	0.8665	12.6988	0.0682	2
146	52.3	95	96.6	0.5433	0.8867	1.9654	0.4507	2
147	52.3	95	98.3	0.4702	0.9019	0.6264	1.4383	1
148	52.3	95	90.5	0.7614	0.8310	15.6459	0.0531	2
149	-1.0	95	53.6	1.2873	0.0000	0.0000	0.0000	-1
150	52.3	95	56.9	0.4388	0.5219	0.3447	1.5126	2

BURN = 2 --- STABLE OPERATION
BURN = 1 --- STABILITY LIMIT
BURN = 0 --- BURNER GOES OUT

UNITS OF INT ARE LBS/SEC FT*3 ATM*2

Table VIII-8

COMPARISON OF PREDICTED AND EXPERIMENTAL BURNER STABILITY DATA PAGE 7

RUN NO.	VOL IN*3	AIR TEMP oF	AIR FLOW LBS/HR	EQUIV RATIO	INT DATA W/VP*2	INT LIM W/VP*2	INT RAT ID/IL	BURN
151	52.3	400	84.0	0.7066	0.7706	22.2613	0.0346	2
152	52.3	400	79.5	0.7461	0.7297	28.1965	0.0259	2
153	52.3	360	111.2	0.4703	1.0206	1.9112	0.5341	1
154	52.3	355	55.6	0.7013	0.5103	19.3644	0.0263	2
155	52.3	270	98.9	0.5043	0.9081	2.1939	0.4136	2
156	52.3	260	103.3	0.4292	0.9484	0.6331	1.4983	0
157	52.3	260	100.0	0.5856	0.9182	5.6586	0.1622	1
158	52.3	260	100.6	0.6375	0.9232	9.3190	0.0990	2
159	52.3	265	97.3	0.7598	0.8929	22.6992	0.0393	2
160	-1.0	270	90.7	1.2226	0.0000	0.0000	0.0000	-1
161	-1.0	275	89.6	1.2418	0.0000	0.0000	0.0000	-1
162	-1.0	275	87.9	1.5592	0.0000	0.0000	0.0000	-1
163	52.3	360	22.0	0.5464	0.2018	5.0677	0.0398	1
164	52.3	370	22.0	0.7565	0.2018	27.9911	0.0072	2
165	52.3	375	30.8	0.7925	0.2825	34.0641	0.0083	2
166	52.3	365	44.5	0.6641	0.4086	15.2380	0.0268	2
167	52.3	370	44.0	0.8406	0.4036	41.7926	0.0097	2
168	52.3	370	41.2	0.9728	0.3784	64.4761	0.0059	2
169	52.3	345	55.0	0.7296	0.5045	22.6681	0.0222	2
170	52.3	325	69.8	0.5771	0.6407	6.3214	0.1013	2
171	52.3	305	78.1	0.5162	0.7164	2.9222	0.2450	2
172	52.3	275	97.8	0.4118	0.8980	0.4885	1.8383	0
173	-1.0	-1	-1.0	-1.0000	0.0000	0.0000	0.0000	-1
174	52.3	400	96.6	0.6507	0.8864	15.0295	0.0589	2
175	52.3	405	93.3	0.7925	0.8561	36.1910	0.0236	2

BURN = 2 --- STABLE OPERATION
BURN = 1 --- STABILITY LIMIT
BURN = 0 --- BURNER GOES OUT

UNITS OF INT ARE LBS/SEC FT*3 ATM*2

Table VIII-9

COMPARISON OF PREDICTED AND EXPERIMENTAL BURNER STABILITY DATA PAGE 8

RUN NO.	VOL IN*3	AIR TEMP oF	AIR FLOW LBS/HR	EQUIV RATIO	INT DATA W/VP*2	INT LIM W/VP*2	INT RAT ID/IL	BURN
176	52.3	405	93.1	0.8733	0.8547	50.6320	0.0169	2
177	52.3	405	98.6	0.4239	0.9049	1.1124	0.8135	2
178	52.3	405	95.9	0.5413	0.8806	5.5355	0.1591	2
179	52.3	350	133.7	0.8388	1.2275	39.9028	0.0307	2
180	52.3	345	134.6	0.7140	1.2354	20.5484	0.0601	2
181	52.3	340	136.1	0.6205	1.2493	9.9945	0.1249	2
182	52.3	340	138.8	0.5458	1.2743	4.7161	0.2700	2
183	52.3	335	139.0	0.4894	1.2754	2.2792	0.5596	2
184	52.3	334	141.7	0.4435	1.3004	1.1318	1.1491	1
185	52.3	335	139.0	0.5014	1.2754	2.6829	0.4754	2
186	52.3	335	139.0	0.5631	1.2754	5.6213	0.2269	2
187	-1.0	-1	-1.0	-1.0000	0.0000	0.0000	0.0000	-1
188	52.3	430	77.9	0.6830	0.7145	20.4438	0.0349	2
189	52.3	430	79.0	0.5532	0.7252	6.8132	0.1065	2
190	52.3	430	79.0	0.4885	0.7252	3.2004	0.2266	1
191	52.3	400	66.9	0.5766	0.6144	7.8786	0.0780	2
192	52.3	405	56.0	0.6896	0.5137	20.1414	0.0255	2
193	-1.0	410	51.6	1.2578	0.0000	0.0000	0.0000	-1
194	52.3	410	113.0	0.5463	1.0374	5.9429	0.1746	-1
195	52.3	410	113.6	0.4858	1.0425	2.8719	0.3630	-1
196	52.3	410	115.2	0.4920	1.0576	3.1155	0.3395	-1
197	52.3	430	101.4	0.5304	0.9309	5.3194	0.1750	-1
198	52.3	360	41.2	0.6579	0.3780	14.3547	0.0263	-1
199	52.3	340	38.5	0.9818	0.3531	62.6358	0.0056	-1
200	52.3	410	38.5	0.6616	0.3531	16.7434	0.0211	-1

BURN = 2 --- STABLE OPERATION
BURN = 1 --- STABILITY LIMIT
BURN = 0 --- BURNER GOES OUT

*UNITS OF INT ARE LBS/SEC FT*3 ATM*2*

Table VIII-10

RUN NO.	VOL IN*3	AIR TEMP oF	AIR FLOW LBS/HR	EQUIV RATIO	INT DATA W/VP*2	INT LIM W/VP*2	INT RAT ID/IL	BURN
201	52.3	86	83.2	0.8221	0.7634	21.7050	0.0351	2
202	52.3	82	102.9	0.7187	0.9441	11.3179	0.0833	2
203	52.3	110	148.0	0.6216	1.3581	5.2160	0.2601	2
204	-1.0	-1	-1.0	-1.0000	0.0000	0.0000	0.0000	-1
205	52.3	313	76.8	0.6978	0.7049	17.1035	0.0412	2
206	52.3	253	167.8	0.6498	1.5402	10.1619	0.1515	2
207	52.3	245	181.5	0.5601	1.6655	4.0754	0.4084	2
208	66.5	70	51.5	0.8177	0.3718	20.5144	0.0181	-1
209	66.5	70	49.9	0.9883	0.3598	39.6679	0.0091	-1
210	66.5	70	49.9	0.6666	0.3598	7.1656	0.0502	-1
211	-1.0	70	49.9	1.0852	0.0000	0.0000	0.0000	-1
212	66.5	70	102.9	0.6368	0.7425	5.4032	0.1373	-1
213	66.5	70	99.7	0.7865	0.7199	17.2529	0.0417	-1
214	-1.0	70	96.6	1.0999	0.0000	0.0000	0.0000	-1
215	66.5	70	49.9	0.4845	0.3598	0.7215	0.4981	-1
216	66.5	70	48.2	0.6615	0.3479	6.8425	0.0508	-1
217	52.3	80	83.8	0.6044	0.7689	3.9655	0.1937	2
218	66.5	100	91.5	0.6187	0.6606	4.9179	0.1343	2
219	66.5	110	95.3	0.7845	0.6881	18.6383	0.0369	2
220	52.3	100	86.2	0.5854	0.7910	3.4036	0.2322	2
221	52.3	100	116.8	0.5761	1.0717	3.0495	0.3511	2
222	52.3	100	131.8	0.5105	1.2094	1.2482	0.9679	2
223	52.3	100	108.4	0.6205	0.9951	5.0047	0.1986	2
224	52.3	100	168.5	0.5562	1.5462	2.3779	0.6503	2
225	52.3	100	151.8	0.6173	1.3932	4.8472	0.2874	2

BURN = 2 --- STABLE OPERATION
BURN = 1 --- STABILITY LIMIT
BURN = 0 --- BURNER GOES OUT

*UNITS OF INT ARE LBS/SEC FT*3 ATM*2*

Table VIII-11

COMPARISON OF PREDICTED AND EXPERIMENTAL BURNER STABILITY DATA PAGE 10

RUN NO.	VOL IN*3	AIR TEMP oF	AIR FLOW LBS/HR	EQUIV RATIO	INT DATA W/VP*2	INT LIM W/VP*2	INT RAT ID/IL	BURN
226	52.3	100	177.9	0.5266	1.6330	1.5866	1.0293	1
227	52.3	76	55.8	0.5796	0.5121	2.9354	0.1743	2
228	52.3	82	58.4	0.5761	0.5358	2.8714	0.1864	2
229	52.3	85	57.6	0.5773	0.5288	2.9431	0.1795	2
230	52.3	433	57.6	0.5779	0.5284	8.7961	0.0601	2
231	52.3	420	60.8	0.5473	0.5579	6.2023	0.0900	2
232	52.3	410	90.9	0.5203	0.8346	4.4305	0.1884	2
233	52.3	407	90.2	0.6172	0.8281	11.6716	0.0709	2
234	52.3	90	76.9	0.6725	0.7062	7.9725	0.0885	2
235	52.3	92	77.3	0.5930	0.7094	3.6204	0.1957	2
236	52.3	89	77.7	0.6003	0.7132	3.8997	0.1829	2
237	52.3	82	38.4	0.6353	0.3524	5.5154	0.0638	2
238	66.5	79	49.1	0.4880	0.3544	0.7973	0.4445	2
239	66.5	80	48.9	0.5391	0.3531	1.7569	0.2010	2
240	66.5	82	48.9	0.6563	0.3528	6.7467	0.0523	2
241	66.5	82	48.8	0.7266	0.3522	11.9947	0.0294	2
242	66.5	78	49.2	0.7617	0.3554	15.0894	0.0236	2
243	66.5	80	48.8	0.8945	0.3522	29.7059	0.0119	2
244	66.5	79	98.1	0.5043	0.7082	1.0409	0.6796	2
245	66.5	80	97.6	0.5994	0.7043	3.7461	0.1878	2
246	66.5	80	60.5	0.6393	0.4364	5.7049	0.0765	-1
247	-1.0	75	-1.0	0.4609	0.0000	0.0000	0.0000	-1
248	66.5	85	47.2	0.5625	0.3404	2.4459	0.1390	-1
249	66.5	75	49.2	0.8476	0.3554	24.0592	0.0148	-1
250	66.5	85	48.8	0.8555	0.3522	25.4455	0.0138	-1

BURN = 2 --- STABLE OPERATION
BURN = 1 --- STABILITY LIMIT
BURN = 0 --- BURNER GOES OUT

UNITS OF INT ARE LBS/SEC FT*3 ATM*2

Table VIII-12

RUN NO.	VOL IN*3	AIR TEMP oF	AIR FLOW LBS/HR	EQUIV RATIO	INT DATA W/VP*2	INT LIM W/VP*2	INT RAT ID/IL	BURN
251	66.5	85	100.8	0.4983	0.7278	0.9702	0.7502	-1
252	66.5	90	100.4	0.5006	0.7245	1.0273	0.7052	-1
253	66.5	92	97.0	0.5772	0.6998	3.0094	0.2326	-1
254	66.5	93	100.1	0.6412	0.7225	6.0290	0.1197	-1
255	52.3	93	90.0	0.6063	0.8260	4.2127	0.1959	2
256	66.5	85	97.6	0.7188	0.7043	11.4080	0.0617	2
257	66.5	85	97.6	0.7852	0.7043	17.6921	0.0398	2
258	66.5	85	97.5	0.9004	0.7037	30.6648	0.0229	2
259	66.5	85	97.4	1.0000	0.7030	42.0062	0.0167	2
260	66.5	85	97.3	0.9609	0.7024	37.6931	0.0186	2
261	-1.0	89	97.2	1.1875	0.0000	0.0000	0.0000	-1
262	66.5	90	144.4	0.5167	1.0421	1.3178	0.7900	2
263	66.5	97	143.5	0.5957	1.0355	3.7940	0.2727	2
264	66.5	85	48.8	0.4951	0.3522	0.9199	0.3824	2
265	66.5	85	48.8	0.5820	0.3522	3.1141	0.1130	2
266	66.5	96	143.0	0.5677	1.0319	2.7115	0.3802	2
267	66.5	96	97.8	0.5045	0.7063	1.1193	0.6304	2
268	66.5	96	97.2	0.5817	0.7018	3.2131	0.2182	2
269	66.5	96	97.2	0.6582	0.7018	7.1329	0.0983	2
270	66.5	96	97.1	0.6860	0.7011	9.0735	0.0772	2
271	66.5	100	144.1	0.5576	1.0402	2.4183	0.4297	2
272	66.5	100	141.7	0.6618	1.0231	7.4548	0.1371	2
273	66.5	100	143.1	0.6745	1.0328	8.3279	0.1239	2
274	66.5	100	143.5	0.7565	1.0355	15.3389	0.0675	2
275	66.5	95	143.7	0.8254	1.0374	22.4802	0.0461	2

BURN = 2 --- STABLE OPERATION
BURN = 1 --- STABILITY LIMIT
BURN = 0 --- BURNER GOES OUT

*UNITS OF INT ARE LBS/SEC FT*3 ATM*2*

Table VIII-13

COMPARISON OF PREDICTED AND EXPERIMENTAL BURNER STABILITY DATA PAGE 12

RUN NO.	VOL IN*3	AIR TEMP oF	AIR FLOW LBS/HR	EQUIV RATIO	INT DATA W/VP*2	INT LIM W/VP*2	INT RAT ID/IL	BURN
276	-1.0	-1	130.0	-1.0000	0.0000	0.0000	0.0000	-1
277	-1.0	-1	140.0	-1.0000	0.0000	0.0000	0.0000	-1
278	-1.0	-1	-1.0	-1.0000	0.0000	0.0000	0.0000	-1
279	52.3	109	91.0	0.5791	0.8353	3.2549	0.2564	2
280	52.3	110	90.9	0.6808	0.8346	9.0216	0.0924	2
281	52.3	110	111.3	0.5932	1.0217	3.8430	0.2656	2
282	52.3	94	46.4	0.6072	0.4258	4.2688	0.0997	2
283	52.3	100	47.3	0.6024	0.4338	4.1303	0.1050	2
284	52.3	105	46.5	0.4239	0.4268	0.2659	1.6031	2
285	52.3	116	136.5	0.4873	1.2529	0.9210	1.3590	2
286	66.5	82	58.8	0.5010	0.4246	1.0009	0.4237	2
287	66.5	92	144.0	0.5260	1.0394	1.5258	0.6812	2
288	66.5	90	144.3	0.5654	1.0413	2.5809	0.4030	2
289	66.5	95	143.6	0.6016	1.0366	4.0261	0.2572	2
290	66.5	99	142.9	0.7193	1.0318	11.8468	0.0870	2
291	-1.0	73	66.0	1.3984	0.0000	0.0000	0.0000	-1
292	-1.0	75	49.1	1.5625	0.0000	0.0000	0.0000	-1
293	-1.0	82	47.1	1.3594	0.0000	0.0000	0.0000	-1
294	-1.0	90	51.1	1.2578	0.0000	0.0000	0.0000	-1
295	-1.0	72	49.2	1.3203	0.0000	0.0000	0.0000	-1
296	-1.0	86	48.6	1.3438	0.0000	0.0000	0.0000	-1
297	-1.0	92	48.3	1.4141	0.0000	0.0000	0.0000	-1
298	-1.0	95	48.2	1.2813	0.0000	0.0000	0.0000	-1
299	-1.0	96	87.2	1.3750	0.0000	0.0000	0.0000	-1
300	-1.0	85	49.3	1.1719	0.0000	0.0000	0.0000	-1

BURN = 2 --- STABLE OPERATION
BURN = 1 --- STABILITY LIMIT
BURN = 0 --- BURNER GOES OUT

UNITS OF INT ARE LBS/SEC FT*3 ATM*2

Table VIII-14

RUN NO.	VOL IN*3	AIR TEMP oF	AIR FLOW LBS/HR	EQUIV RATIO	INT DATA W/VP*2	INT LIM W/VP*2	INT RAT ID/IL	BURN
301	-1.0	88	48.5	1.2188	0.0000	0.0000	0.0000	-1
302	-1.0	92	96.9	1.4219	0.0000	0.0000	0.0000	-1
303	-1.0	74	98.5	1.2813	0.0000	0.0000	0.0000	-1
304	-1.0	87	141.5	1.3438	0.0000	0.0000	0.0000	-1
305	-1.0	100	124.2	1.3750	0.0000	0.0000	0.0000	-1
306	-1.0	100	139.8	1.1719	0.0000	0.0000	0.0000	-1
307	-1.0	104	94.3	1.1953	0.0000	0.0000	0.0000	-1
308	52.3	90	46.6	0.5469	0.4279	2.0293	0.2109	2
309	52.3	98	47.5	0.5052	0.4362	1.1405	0.3820	2
310	52.3	94	48.4	0.3436	0.4443	0.0318	13.9791	-1
311	52.3	385	49.4	0.5886	0.4533	8.4696	0.0535	2
312	52.3	388	48.3	0.5098	0.4432	3.6137	0.1226	2
313	52.3	395	47.2	0.3945	0.4331	0.6289	0.6887	2
314	52.3	340	88.2	0.5392	0.8094	4.3720	0.1851	2
315	52.3	364	93.1	0.4726	0.8547	2.0056	0.4261	2
316	52.3	400	90.5	0.5043	0.8310	3.5181	0.2362	2
317	52.3	435	90.0	0.4059	0.8259	0.9363	0.8821	2
318	52.3	350	137.1	0.4935	1.2582	2.5485	0.4937	2
319	52.3	350	137.2	0.4150	1.2589	0.7428	1.6949	2
320	52.3	351	134.5	0.6484	1.2340	13.0187	0.0948	2
321	52.3	140	89.8	0.5978	0.8238	4.4449	0.1852	2
322	52.3	115	90.0	0.4857	0.8259	0.8930	0.9240	2
323	52.3	105	90.0	0.4477	0.8259	0.4324	1.9101	1
324	52.3	95	135.5	0.5847	1.2436	3.3180	0.3744	2
325	52.3	105	137.3	0.5181	1.2604	1.4278	0.8827	2

BURN = 2 --- STABLE OPERATION
BURN = 1 --- STABILITY LIMIT
BURN = 0 --- BURNER GOES OUT

*UNITS OF INT ARE LBS/SEC FT*3 ATM*2*

Table VIII-1s

COMPARISON OF PREDICTED AND EXPERIMENTAL BURNER STABILITY DATA PAGE 14

RUN NO.	VOL IN*3	AIR TEMP OF	AIR FLOW LBS/HR	EQUIV RATIO	INT DATA W/VP*2	INT LIM W/VP*2	INT RAT ID/IL	BURN
326	52.3	110	138.7	0.4796	1.2732	0.7905	1.6107	1
327	52.3	412	48.2	0.6017	0.4420	10.3270	0.0428	2
328	52.3	395	47.3	0.4641	0.4338	2.0023	0.2166	2
329	52.3	390	47.1	0.3821	0.4318	0.4819	0.8961	2
330	52.3	407	90.3	0.5955	0.8288	9.6208	0.0862	2
331	52.3	400	92.7	0.4834	0.8511	2.6750	0.3182	2
332	52.3	435	89.7	0.4059	0.8231	0.9363	0.8791	1
333	52.3	392	135.2	0.4401	1.2411	1.3715	0.9050	2
334	52.3	395	140.3	0.3843	1.2877	0.5173	2.4893	1
335	52.3	92	91.3	0.5556	0.8383	2.2910	0.3655	2
336	52.3	90	92.6	0.4667	0.8498	0.5751	1.4759	1
337	52.3	90	48.5	0.5434	0.4447	1.9337	0.2297	2
338	52.3	90	49.6	0.5899	0.4548	3.4713	0.1309	2
339	52.3	100	136.7	0.5685	1.2547	2.7770	0.4514	2
340	52.3	395	138.3	0.4997	1.2691	3.2593	0.3894	2
341	52.3	150	92.4	0.5245	0.8483	1.8563	0.4566	2
342	52.3	90	93.3	0.5472	0.8563	2.0349	0.4204	2
343	52.3	102	91.3	0.5273	0.8381	1.6153	0.5189	2
344	52.3	100	91.9	0.4688	0.8439	0.6253	1.3496	2
345	52.3	102	135.3	0.5445	1.2414	2.0530	0.6047	2
346	52.3	105	138.2	0.4898	1.2682	0.9186	1.3806	2
347	52.3	105	134.5	0.6523	1.2343	6.9392	0.1779	2
348	52.3	107	90.1	0.6022	0.8274	4.2116	0.1963	2
349	52.3	100	91.9	0.5137	0.8431	1.3105	0.6427	2
350	52.3	101	136.4	0.5697	1.2514	2.8268	0.4423	2

BURN = 2 --- STABLE OPERATION
BURN = 1 --- STABILITY LIMIT
BURN = 0 --- BURNER GOES OUT

UNITS OF INT ARE LBS/SEC FT*3 ATM*2

Table VIII-16

COMPARISON OF PREDICTED AND EXPERIMENTAL BURNER STABILITY DATA

RUN NO.	VOL IN*3	AIR TEMP OF	AIR FLOW LBS/HR	EQUIV RATIO	INT DATA W/VP*2	INT LIM W/VP*2	INT RAT ID/IL	BURN
351	52.3	105	92.4	0.6311	0.8484	5.6528	0.1500	2
352	52.3	110	93.1	0.5036	0.8548	1.1679	0.7312	1
353	52.3	120	137.7	0.6311	1.2636	5.9076	0.2137	2
354	52.3	430	81.4	0.5379	0.7471	5.7838	0.1292	2
355	52.3	438	82.0	0.4309	0.7528	1.4414	0.5223	2
356	52.3	450	43.8	0.5570	0.4018	7.5311	0.0534	2
357	52.3	140	180.5	0.5053	1.6565	1.3504	1.2255	2
358	52.3	110	46.8	0.4673	0.4299	0.6363	0.6750	2
359	52.3	120	138.2	0.5022	1.2686	1.1888	1.0661	2
360	52.3	380	92.6	0.5322	0.8498	4.6028	0.1846	2
361	52.3	400	90.9	0.4673	0.8339	2.1392	0.3898	2
362	52.3	405	89.8	0.6305	0.8245	12.9777	0.0635	2
363	52.3	405	90.8	0.4984	0.8332	3.3250	0.2506	2
364	52.3	405	48.7	0.5691	0.4471	7.4243	0.0602	2
365	52.3	405	48.0	0.6244	0.4404	12.3431	0.0357	2
366	52.3	410	47.9	0.4309	0.4393	1.2784	0.3436	2
367	52.3	405	137.0	0.5100	1.2571	3.8435	0.3271	2
368	52.3	410	137.1	0.4309	1.2578	1.2784	0.9839	2
369	52.3	400	136.3	0.5691	1.2507	7.3129	0.1710	2
370	52.3	403	90.9	0.5475	0.8339	5.8881	0.1416	2
371	52.3	426	137.1	0.5738	1.2582	8.2811	0.1519	2
372	52.3	425	138.7	0.5438	1.2732	6.0652	0.2099	1
373	52.3	425	90.9	0.5325	0.8346	5.3562	0.1558	2
374	52.3	430	90.3	0.4913	0.8288	3.3181	0.2498	1
375	52.3	400	91.4	0.4618	0.8388	1.9765	0.4244	1

BURN = 2 --- STABLE OPERATION
BURN = 1 --- STABILITY LIMIT
BURN = 0 --- BURNER GOES OUT

UNITS OF INT ARE . LBS/SEC FT*3 ATM*2

Table VIII-17

COMPARISON OF PREDICTED AND EXPERIMENTAL BURNER STABILITY DATA

RUN NO.	VOL IN*3	AIR TEMP OF	AIR FLOW LBS/HR	EQUIV RATIO	INT DATA W/VP*2	INT LIM W/VP*2	INT RAT ID/IL	BURN
376	52.3	400	90.3	0.4711	0.8288	2.2577	0.3671	1
377	52.3	405	48.3	0.4838	0.4432	2.7404	0.1617	2
378	52.3	428	45.5	0.4875	0.4173	3.1372	0.1330	1
379	52.3	375	47.0	0.4650	0.4311	1.8754	0.2299	1
380	52.3	412	45.7	0.4395	0.4198	1.4789	0.2839	1
381	52.3	411	138.5	0.4507	1.2710	1.7498	0.7264	1
382	52.3	411	138.7	0.4501	1.2728	1.7336	0.7342	1
383	52.3	403	47.1	0.4725	0.4320	2.3309	0.1853	1
384	52.3	76	91.4	0.5775	0.8390	2.8643	0.2929	1
385	52.3	90	91.6	0.5625	0.8410	2.4911	0.3376	2
386	52.3	91	89.8	0.5284	0.8245	1.5705	0.5244	1
387	52.3	80	47.8	0.5255	0.4389	1.4450	0.3034	1
388	52.3	81	45.5	0.5337	0.4180	1.6331	0.2557	1
389	-1.0	85	48.2	1.2334	0.0000	0.0000	0.0000	-1
390	52.3	90	80.9	0.5400	0.7428	1.8470	0.4021	1
391	52.3	93	80.5	0.4900	0.7384	0.8741	0.8439	2

BURN = 2 --- STABLE OPERATION
BURN = 1 --- STABILITY LIMIT
BURN = 0 --- BURNER GOES OUT

UNITS OF INT ARE LBS/SEC FT*3 ATM*2

Table VIII-18

COMPARISON OF PREDICTED BURNER INEFFICIENCY AND EXPERIMENTAL EMISSIONS DATA

RUN NO.	BURN	AIR TEMP °F	FUEL TEMP °F	AIR FLOW LBS/HR	EQUIV RATIO	COMB TEMP °F	PRED EFFY	PRED EMM G/KG	COG EMM G/KG	HCG EMM G/KG	NOBG EMM G/KG	NOTG EMM G/KG
1	-1	75	71	22.3	0.4678	2107	0.9671	32.8552	-1.0000	-1.0000	-1.0000	-1.0000
2	-1	80	71	22.2	0.5309	2384	0.9893	10.7091	-1.0000	-1.0000	-1.0000	-1.0000
3	-1	85	72	45.3	0.4822	2098	0.9325	67.5205	-1.0000	-1.0000	-1.0000	-1.0000
4	-1	85	73	45.3	0.4524	1924	0.8970	103.0000	-1.0000	-1.0000	-1.0000	-1.0000
5	-1	85	73	47.0	0.4650	1954	0.8900	110.0000	-1.0000	-1.0000	-1.0000	-1.0000
6	-1	88	74	61.8	0.4501	1919	0.8970	103.0000	-1.0000	-1.0000	-1.0000	-1.0000
7	-1	90	75	61.7	0.4948	2108	0.9141	85.8886	-1.0000	-1.0000	-1.0000	-1.0000
8	2	90	73	61.7	0.6326	2742	0.9898	10.1917	-1.0000	-1.0000	-1.0000	-1.0000
9	1	90	74	61.7	0.5073	2215	0.9451	54.9107	-1.0000	-1.0000	-1.0000	-1.0000
10	0	90	74	61.7	0.4697	1974	0.8900	110.0000	-1.0000	-1.0000	-1.0000	-1.0000
11	1	90	74	61.7	0.5230	2303	0.9611	38.9454	-1.0000	-1.0000	-1.0000	-1.0000
12	0	90	74	61.7	0.4322	1864	0.9000	100.0000	-1.0000	-1.0000	-1.0000	-1.0000
13	-1	90	74	61.7	0.5386	2378	0.9701	29.8793	-1.0000	-1.0000	-1.0000	-1.0000
14	1	90	75	61.7	0.5073	2215	0.9451	54.9107	-1.0000	-1.0000	-1.0000	-1.0000
15	2	90	74	61.7	0.5089	2225	0.9473	52.7360	-1.0000	-1.0000	-1.0000	-1.0000
16	2	90	75	78.1	0.5689	2491	0.9743	25.7034	-1.0000	-1.0000	-1.0000	-1.0000
17	1	90	75	78.1	0.5417	2369	0.9615	38.5179	-1.0000	-1.0000	-1.0000	-1.0000
18	2	90	73	78.1	0.5541	2427	0.9682	31.7835	-1.0000	-1.0000	-1.0000	-1.0000
19	2	91	73	78.0	0.6115	2659	0.9841	15.9106	-1.0000	-1.0000	-1.0000	-1.0000
20	2	92	74	78.0	0.5377	2352	0.9591	40.8980	-1.0000	-1.0000	-1.0000	-1.0000
21	0	92	74	78.0	0.4609	1946	0.8900	110.0000	-1.0000	-1.0000	-1.0000	-1.0000
22	0	93	72	77.9	0.4960	2063	0.8890	111.0000	-1.0000	-1.0000	-1.0000	-1.0000
23	1	93	72	77.9	0.5209	2258	0.9421	57.9394	-1.0000	-1.0000	-1.0000	-1.0000
24	1	93	74	77.9	0.5382	2356	0.9597	40.2943	-1.0000	-1.0000	-1.0000	-1.0000
25	1	93	75	77.9	0.5631	2470	0.9726	27.4482	-1.0000	-1.0000	-1.0000	-1.0000
26	2	90	72	103.3	0.6937	2934	0.9887	11.3444	-1.0000	-1.0000	-1.0000	-1.0000
27	2	93	73	103.1	0.5794	2517	0.9688	31.1919	-1.0000	-1.0000	-1.0000	-1.0000
28	0	96	73	102.8	0.5227	2133	0.8800	120.0000	-1.0000	-1.0000	-1.0000	-1.0000
29	0	97	73	102.7	0.5118	2114	0.8870	113.0000	-1.0000	-1.0000	-1.0000	-1.0000
30	1	97	74	102.7	0.5231	2136	0.8800	120.0000	-1.0000	-1.0000	-1.0000	-1.0000

BURN=2---STABLE
BURN=1---LIMIT
BURN=0---GOING OUT

PRED EMM = 1000×(1-EFFY)
PRED EFFY FROM THEORY

NOB - BURNER DATA FOR NOX
NOT - NOX FROM VAPOR GENERATOR EXH.

RUN NO.	*BURN*	*AIR TEMP oF*	*FUEL TEMP oF*	*AIR FLOW LBS/HR*	*EQUIV RATIO*	*COMB TEMP oF*	*PRED EFFY*	*PRED EMM G/KG*	*COG EMM G/KG*	*HCG EMM G/KG*	*NOBG EMM G/KG*	*NOTG EMM G/KG*
31	2	102	75	120.9	0.5930	2569	0.9690	31.0396	-1.0000	-1.0000	-1.0000	-1.0000
32	2	105	75	120.6	0.5465	2339	0.9353	64.7047	-1.0000	-1.0000	-1.0000	-1.0000
33	1	108	77	120.2	0.5158	2120	0.8800	120.0000	-1.0000	-1.0000	-1.0000	-1.0000
34	0	95	75	121.6	0.5099	2106	0.8870	113.0000	-1.0000	-1.0000	-1.0000	-1.0000
35	1	102	73	120.9	0.5190	2126	0.8800	120.0000	-1.0000	-1.0000	-1.0000	-1.0000
36	2	112	74	153.8	0.5878	2530	0.9563	43.7293	-1.0000	-1.0000	-1.0000	-1.0000
37	2	117	74	153.2	0.5613	2392	0.9325	67.4910	-1.0000	-1.0000	-1.0000	-1.0000
38	2	120	74	152.8	0.5451	2221	0.8790	121.0000	-1.0000	-1.0000	-1.0000	-1.0000
39	0	120	75	152.8	0.5299	2175	0.8800	120.0000	-1.0000	-1.0000	-1.0000	-1.0000
40	1	120	75	152.8	0.5135	2122	0.8800	120.0000	-1.0000	-1.0000	-1.0000	-1.0000
41	1	124	75	152.3	0.5470	2282	0.9021	97.9472	-1.0000	-1.0000	-1.0000	-1.0000
42	2	91	75	103.2	0.7565	3127	0.9915	8.5202	2.3336	-1.0000	-1.0000	-1.0000
43	1	93	75	103.1	0.5222	2140	0.8850	115.0000	-1.0000	-1.0000	-1.0000	-1.0000
44	2	87	73	41.8	0.7529	3127	0.9965	3.4990	-1.0000	-1.0000	-1.0000	-1.0000
45	2	85	75	41.9	0.6916	2941	0.9954	4.5711	-1.0000	-1.0000	-1.0000	-1.0000
46	2	84	75	41.9	0.6132	2678	0.9918	8.1577	-1.0000	-1.0000	-1.0000	-1.0000
47	2	82	75	42.0	0.5333	2373	0.9791	20.8626	-1.0000	-1.0000	-1.0000	-1.0000
48	2	82	74	42.1	0.4910	2170	0.9542	45.8251	0.2371	-1.0000	-1.0000	-1.0000
49	0	80	72	42.1	0.4497	1913	0.8980	102.0000	22.3454	-1.0000	-1.0000	-1.0000
50	1	80	73	42.1	0.4997	2215	0.9619	38.1283	10.1863	-1.0000	-1.0000	-1.0000
51	2	83	73	25.4	0.6097	2673	0.9950	5.0074	-1.0000	-1.0000	-1.0000	-1.0000
52	2	82	73	25.4	0.5406	2420	0.9892	10.7788	-1.0000	-1.0000	-1.0000	-1.0000
53	1	82	73	25.4	0.4645	2083	0.9584	41.5690	-1.0000	-1.0000	-1.0000	-1.0000
54	1	83	73	25.4	0.4510	1992	0.9356	64.3729	-1.0000	-1.0000	-1.0000	-1.0000
55	-1	83	73	42.0	3.1753	1492	0.0000	0.0000	-1.0000	-1.0000	-1.0000	-1.0000
56	-1	81	73	42.1	2.6412	1798	0.0000	0.0000	-1.0000	-1.0000	-1.0000	-1.0000
57	-1	82	73	42.0	2.8966	1639	0.0000	0.0000	6.4517	-1.0000	-1.0000	-1.0000
58	-1	85	75	41.9	2.6510	1794	0.0000	0.0000	109.9697	-1.0000	-1.0000	-1.0000
59	-1	85	75	41.9	3.1812	1490	0.0000	0.0000	50.9444	-1.0000	-1.0000	-1.0000
60	-1	90	75	41.7	1.9452	2447	0.0000	0.0000	53.2602	-1.0000	-1.0000	-1.0000

BURN=2---STABLE
BURN=1---LIMIT
BURN=0---GOING OUT

PRED EMM = 1000×(1-EFFY)
PRED EFFY FROM THEORY

NOB - BURNER DATA FOR NOX
NOT - NOX FROM VAPOR GENERATOR EXH.

RUN NO.	BURN	AIR TEMP oF	FUEL TEMP oF	AIR FLOW LBS/HR	EQUIV RATIO	COMB TEMP oF	PRED EFFY	PRED EMM G/KG	COG EMM G/KG	HCG EMM G/KG	NOBG EMM G/KG	NOTG EMM G/KG
61	-1	90	75	41.7	1.9452	2447	0.0000	0.0000	1254.8720	-1.0000	-1.0000	-1.0000
62	-1	85	72	41.9	2.6510	1794	0.0000	0.0000	1135.7524	-1.0000	0.0013	-1.0000
63	-1	87	72	41.8	3.1870	1488	0.0000	0.0000	3.5209	-1.0000	0.0023	-1.0000
64	-1	85	72	41.9	2.6510	1794	0.0000	0.0000	910.4047	-1.0000	0.0004	-1.0000
65	-1	88	75	41.8	2.7692	1717	0.0000	0.0000	-1.0000	-1.0000	-1.0000	-1.0000
66	-1	85	75	41.9	2.8585	1661	0.0000	0.0000	-1.0000	-1.0000	-1.0000	-1.0000
67	-1	85	75	41.9	2.7616	1720	0.0000	0.0000	284.0345	-1.0000	0.0013	-1.0000
68	-1	78	75	25.5	2.5262	1875	0.0000	0.0000	-1.0000	-1.0000	-1.0000	-1.0000
69	-1	82	75	24.7	2.3985	1978	0.0000	0.0000	1272.6096	122.4420	0.0016	-1.0000
70	-1	85	78	25.3	2.9167	1629	0.0000	0.0000	1041.4344	472.0485	0.0007	-1.0000
71	-1	86	78	25.3	3.0646	1549	0.0000	0.0000	-1.0000	-1.0000	-1.0000	-1.0000
72	-1	90	78	61.7	2.3863	1993	0.0000	0.0000	1200.7858	151.4368	0.0006	-1.0000
73	-1	93	78	61.5	2.4493	1942	0.0000	0.0000	-1.0000	-1.0000	-1.0000	-1.0000
74	1	86	73	25.3	0.5044	2278	0.9821	17.9200	1.2104	9.5854	0.0014	-1.0000
75	2	85	73	25.3	0.6219	2717	0.9955	4.4678	0.1944	-1.0000	0.1023	-1.0000
76	2	85	75	25.3	0.8339	3339	0.9981	1.9035	0.3193	4.9987	0.4057	-1.0000
77	2	85	75	25.3	0.9960	3558	0.9877	12.3041	6.6866	2.3294	0.3974	-1.0000
78	1	90	75	61.7	0.5574	2459	0.9774	22.6080	101.7531	57.3660	0.0119	-1.0000
79	2	92	79	61.6	0.6869	2926	0.9931	6.8677	0.9586	1.4905	0.2489	-1.0000
80	2	90	79	61.7	0.9927	3555	0.9812	18.7995	21.5030	-1.0000	0.3622	-1.0000
81	-1	92	80	61.6	1.4432	3143	0.0000	0.0000	688.0142	-1.0000	0.0000	-1.0000
82	2	103	75	102.1	0.5050	2096	0.8870	113.0000	105.3359	7.7417	0.0000	-1.0000
83	2	105	78	101.9	0.7666	3165	0.9920	7.9883	2.7654	3.4637	0.3348	-1.0000
84	2	100	72	102.4	0.7464	3104	0.9914	8.6103	3.5505	3.9463	0.4516	-1.0000
85	2	103	77	102.1	0.9178	3493	0.9899	10.1368	12.6460	1.3655	0.4084	-1.0000
86	-1	105	77	101.9	1.2812	3502	0.0000	0.0000	866.5566	0.9724	0.0264	-1.0000
87	2	300	600	59.3	0.5391	2569	0.9859	14.0724	0.1344	1.5420	0.0411	-1.0000
88	2	300	600	59.3	0.6869	3071	0.9955	4.4707	1.2088	0.2238	0.3218	-1.0000
89	-1	300	600	59.3	1.1075	3658	0.0000	0.0000	476.8417	0.8592	0.0356	-1.0000
90	2	300	720	59.6	0.5770	2708	0.9904	9.5539	0.4080	0.5712	0.2221	-1.0000

BURN=2---STABLE
BURN=1---LIMIT
BURN=0---GOING OUT

PRED EMM = 1000×(1-EFFY)
PRED EFFY FROM THEORY

NOB - BURNER DATA FOR NOX
NOT - NOX FROM VAPOR GENERATOR EXH.

Table
VIII-21

RUN NO.	BURN	AIR TEMP °F	FUEL TEMP °F	AIR FLOW LBS/HR	EQUIV RATIO	COMB TEMP °F	PRED EFFY	PRED EMM G/KG	COG EMM G/KG	HCG EMM G/KG	NOBG EMM G/KG	NOTG EMM G/KG
91	2	310	720	59.3	0.8222	3440	0.9967	3.3125	1.7928	0.0851	0.3795	-1.0000
92	1	300	720	59.3	1.1075	3658	0.0000	0.0000	699.7134	0.1234	0.0915	-1.0000
93	2	250	440	165.3	0.4863	2176	0.9011	98.8889	51.3433	-1.0000	0.0128	-1.0000
94	2	250	485	165.3	0.6478	2900	0.9890	11.0026	4.0006	-1.0000	0.1154	-1.0000
95	2	250	510	165.3	0.8299	3416	0.9937	6.2930	9.3111	-1.0000	0.5037	-1.0000
96	2	250	520	132.9	0.9865	3636	0.9817	18.2715	207.8635	-1.0000	0.4010	-1.0000
97	2	95	77	55.9	0.4881	2192	0.9648	35.1657	-1.0000	-1.0000	0.3787	-1.0000
98	2	95	77	55.9	0.6175	2705	0.9936	6.3709	-1.0000	-1.0000	0.4642	-1.0000
99	2	95	77	55.9	0.8087	3283	0.9974	2.6068	-1.0000	-1.0000	0.4747	-1.0000
100	2	100	77	55.6	0.9984	3565	0.9841	15.8934	-1.0000	-1.0000	0.3623	-1.0000
101	1	102	77	55.5	1.1925	3485	0.0000	0.0000	-1.0000	-1.0000	0.3553	-1.0000
102	2	102	77	89.0	0.7520	3132	0.9954	4.5716	-1.0000	-1.0000	0.4443	-1.0000
103	2	400	770	50.0	0.8359	3525	0.9984	1.6190	-1.0000	-1.0000	-1.0000	-1.0000
104	2	400	800	50.0	0.5406	2666	0.9946	5.4009	-1.0000	-1.0000	-1.0000	-1.0000
105	2	84	88	49.9	0.9250	3503	0.9964	3.6101	-1.0000	-1.0000	-1.0000	-1.0000
106	1	85	95	49.9	0.4888	2194	0.9687	31.2602	3.9308	-1.0000	0.0049	-1.0000
107	0	85	89	49.9	0.3925	1729	0.9060	94.0000	-1.0000	-1.0000	-1.0000	-1.0000
108	2	85	92	49.9	0.4448	1900	0.8980	102.0000	-1.0000	-1.0000	-1.0000	-1.0000
109	2	85	98	49.9	0.5563	2477	0.9890	11.0324	-1.0000	-1.0000	-1.0000	-1.0000
110	2	400	730	50.0	0.4039	2115	0.9606	39.3993	16.3425	-1.0000	0.0030	-1.0000
111	2	400	730	50.0	0.3915	2044	0.9450	55.0286	47.2658	-1.0000	0.0832	-1.0000
112	2	400	720	33.2	0.4688	2407	0.9919	8.0925	0.1555	-1.0000	0.7380	-1.0000
113	2	400	725	33.2	0.3891	2072	0.9677	32.3190	17.5557	-1.0000	0.1116	-1.0000
114	2	400	730	33.2	0.3805	2027	0.9598	40.1876	11.5914	-1.0000	0.2476	-1.0000
115	1	400	720	33.1	0.3883	2068	0.9672	32.8187	-1.0000	-1.0000	0.0186	-1.0000
116	2	400	710	82.7	0.5375	2647	0.9906	9.3964	-1.0000	-1.0000	-1.0000	-1.0000
117	2	400	710	82.8	0.4312	2209	0.9573	42.7243	-1.0000	-1.0000	-1.0000	-1.0000
118	0	400	730	82.8	0.3861	1916	0.8790	121.0000	68.5008	-1.0000	0.0125	-1.0000
119	2	400	720	126.8	0.4672	2346	0.9623	37.7045	-1.0000	-1.0000	0.0308	-1.0000
120	2	400	475	127.0	0.4279	2041	0.8700	130.0000	-1.0000	-1.0000	-1.0000	-1.0000

BURN=2---STABLE *PRED EMM = 1000×(1-EFFY)* *NOB - BURNER DATA FOR NOX*
BURN=1---LIMIT *PRED EFFY FROM THEORY* *NOT - NOX FROM VAPOR GENERATOR EXH.*
BURN=0---GOING OUT

RUN NO.	BURN	AIR TEMP °F	FUEL TEMP °F	AIR FLOW LBS/HR	EQUIV RATIO	COMB TEMP °F	PRED EFFY	PRED EMM G/KG	COG EMM G/KG	HCG EMM G/KG	NOBG EMM G/KG	NOTG EMM G/KG
121	2	400	450	126.8	0.4469	2239	0.9432	56.7651	-1.0000	-1.0000	-1.0000	-1.0000
122	0	400	450	126.8	0.4010	1963	0.8770	123.0000	-1.0000	-1.0000	-1.0000	-1.0000
123	2	74	70	50.5	0.7951	3236	0.9975	2.4595	0.3215	-1.0000	0.4284	-1.0000
124	-1	80	78	49.5	0.4743	2112	0.9556	44.4243	13.8280	-1.0000	0.0757	-1.0000
125	-1	85	78	47.6	0.4930	2218	0.9728	27.2300	17.2647	-1.0000	0.0582	-1.0000
126	0	95	78	127.3	0.5049	2092	0.8880	112.0000	12.3792	-1.0000	0.2459	-1.0000
127	1	95	78	119.6	0.5687	2498	0.9757	24.3086	16.0140	-1.0000	0.2088	-1.0000
128	2	90	100	67.8	0.5411	2411	0.9815	18.4842	-1.0000	-1.0000	-1.0000	-1.0000
129	2	80	80	86.2	0.5061	2217	0.9515	48.4529	-1.0000	-1.0000	-1.0000	-1.0000
130	2	80	80	82.8	0.5822	2556	0.9856	14.3664	-1.0000	-1.0000	-1.0000	-1.0000
131	2	80	80	66.7	0.6869	2923	0.9952	4.7632	-1.0000	-1.0000	-1.0000	-1.0000
132	-1	80	80	44.5	1.0553	3562	0.0000	0.0000	-1.0000	-1.0000	-1.0000	-1.0000
133	2	80	80	83.4	0.5628	2480	0.9819	18.0994	-1.0000	-1.0000	-1.0000	-1.0000
134	2	80	80	66.7	0.7036	2975	0.9957	4.3442	-1.0000	-1.0000	-1.0000	-1.0000
135	0	80	80	72.3	0.4347	1864	0.9000	100.0000	-1.0000	38.1951	-1.0000	-1.0000
136	2	88	90	72.3	0.5318	2367	0.9770	23.0175	-1.0000	95.3023	-1.0000	-1.0000
137	2	90	90	66.7	0.7036	2982	0.9957	4.2635	-1.0000	0.9204	-1.0000	-1.0000
138	2	95	95	96.6	0.6404	2773	0.9907	9.3221	-1.0000	-1.0000	0.3612	-1.0000
139	2	95	100	95.0	0.7260	3050	0.9946	5.4436	-1.0000	-1.0000	-1.0000	-1.0000
140	-1	95	100	91.1	1.0266	3569	0.0000	0.0000	-1.0000	-1.0000	-1.0000	-1.0000
141	-1	95	100	77.3	1.2099	3460	0.0000	0.0000	-1.0000	-1.0000	-1.0000	-1.0000
142	2	95	100	77.8	0.5389	2399	0.9780	22.0132	-1.0000	-1.0000	-1.0000	-1.0000
143	-1	95	100	77.8	1.2013	3472	0.0000	0.0000	-1.0000	-1.0000	-1.0000	-1.0000
144	-1	95	100	91.1	1.0266	3569	0.0000	0.0000	-1.0000	-1.0000	-1.0000	-1.0000
145	2	95	100	94.4	0.7302	3062	0.9947	5.3162	-1.0000	-1.0000	-1.0000	-1.0000
146	2	95	100	96.6	0.5433	2404	0.9732	26.8288	-1.0000	-1.0000	-1.0000	-1.0000
147	1	95	100	98.3	0.4702	1979	0.8900	110.0000	-1.0000	-1.0000	-1.0000	-1.0000
148	2	95	100	90.5	0.7614	3153	0.9954	4.6212	-1.0000	-1.0000	-1.0000	-1.0000
149	-1	95	100	53.6	1.2873	3356	0.0000	0.0000	-1.0000	-1.0000	0.0000	-1.0000
150	2	95	100	56.9	0.4388	1887	0.8980	102.0000	-1.0000	-1.0000	-1.0000	-1.0000

BURN=2---STABLE
BURN=1---LIMIT
BURN=0---GOING OUT

PRED EMM = 1000×(1-EFFY)
PRED EFFY FROM THEORY

NOB - BURNER DATA FOR NOX
NOT - NOX FROM VAPOR GENERATOR EXH.

Table
VIII-23

RUN NO.	BURN	AIR TEMP oF	FUEL TEMP oF	AIR FLOW LBS/HR	EQUIV RATIO	COMB TEMP oF	PRED EFFY	PRED EMM G/KG	COG EMM G/KG	HCG EMM G/KG	NOBG EMM G/KG	NOTG EMM G/KG
151	2	400	160	84.0	0.7066	3197	0.9969	3.1313	-1.0000	-1.0000	-1.0000	-1.0000
152	2	400	330	79.5	0.7461	3308	0.9974	2.6398	-1.0000	0.1098	-1.0000	-1.0000
153	1	360	300	111.2	0.4703	2329	0.9642	35.8068	-1.0000	0.0000	-1.0000	-1.0000
154	2	355	200	55.6	0.7013	3155	0.9977	2.2649	-1.0000	-1.0000	-1.0000	-1.0000
155	2	270	275	98.9	0.5043	2401	0.9743	25.7017	-1.0000	0.1179	-1.0000	-1.0000
156	0	260	255	103.3	0.4292	1963	0.8860	114.0000	-1.0000	-1.0000	-1.0000	-1.0000
157	1	260	290	100.0	0.5856	2706	0.9896	10.3856	-1.0000	0.0099	-1.0000	-1.0000
158	2	260	317	100.6	0.6375	2884	0.9931	6.8859	-1.0000	0.0700	-1.0000	-1.0000
159	2	265	350	97.3	0.7598	3257	0.9962	3.8282	-1.0000	0.0621	-1.0000	-1.0000
160	-1	270	410	90.7	1.2226	3546	0.0000	0.0000	-1.0000	-1.0000	-1.0000	-1.0000
161	-1	275	392	89.6	1.2418	3525	0.0000	0.0000	-1.0000	0.0789	-1.0000	-1.0000
162	-1	275	480	87.9	1.5592	3096	0.0000	0.0000	-1.0000	6.4648	-1.0000	-1.0000
163	1	360	110	22.0	0.5464	2663	0.9976	2.4453	-1.0000	63.1902	-1.0000	-1.0000
164	2	370	120	22.0	0.7565	3321	0.9993	0.7427	-1.0000	28.6829	-1.0000	-1.0000
165	2	375	120	30.8	0.7925	3415	0.9990	0.9942	-1.0000	0.0721	-1.0000	-1.0000
166	2	365	140	44.5	0.6641	3051	0.9979	2.1090	-1.0000	0.0337	-1.0000	-1.0000
167	2	370	150	44.0	0.8406	3518	0.9985	1.4867	-1.0000	0.0336	-1.0000	-1.0000
168	2	370	170	41.2	0.9728	3701	0.9950	4.9734	-1.0000	0.0649	-1.0000	-1.0000
169	2	345	180	55.0	0.7296	3230	0.9979	2.0617	-1.0000	0.0260	-1.0000	-1.0000
170	2	325	190	69.8	0.5771	2733	0.9935	6.5443	-1.0000	0.0051	-1.0000	-1.0000
171	2	305	195	78.1	0.5162	2491	0.9851	14.8941	-1.0000	0.0000	-1.0000	-1.0000
172	0	275	195	97.8	0.4118	1917	0.8870	113.0000	-1.0000	1.0630	-1.0000	-1.0000
173	-1	-1	-1	-1.0	-1.0000	-1	0.0000	0.0000	-1.0000	-1.0000	-1.0000	-1.0000
174	2	400	250	96.6	0.6507	3027	0.9954	4.6110	-1.0000	0.0261	-1.0000	-1.0000
175	2	405	275	93.3	0.7925	3428	0.9971	2.9001	-1.0000	0.0291	-1.0000	-1.0000
176	2	405	280	93.1	0.8733	3597	0.9967	3.3376	-1.0000	0.0308	-1.0000	-1.0000
177	2	405	200	98.6	0.4239	2145	0.9338	66.1992	-1.0000	0.0000	0.2043	-1.0000
178	2	405	195	95.9	0.5413	2661	0.9896	10.4432	-1.0000	0.0000	-1.0000	-1.0000
179	2	350	300	133.7	0.8388	3497	0.9954	4.5738	-1.0000	0.0088	-1.0000	-1.0000
180	2	345	310	134.6	0.7140	3178	0.9947	5.3268	-1.0000	0.0151	-1.0000	-1.0000

BURN=2---STABLE
BURN=1---LIMIT
BURN=0---GOING OUT

PRED EMM = 1000×(1-EFFY)
PRED EFFY FROM THEORY

NOB - BURNER DATA FOR NOX
NOT - NOX FROM VAPOR GENERATOR EXH.

Table
VIII-24

RUN NO.	BURN	AIR TEMP oF	FUEL TEMP oF	AIR FLOW LBS/HR	EQUIV RATIO	COMB TEMP oF	PRED EFFY	PRED EMM G/KG	COG EMM G/KG	HCG EMM G/KG	NOBG EMM G/KG	NOTG EMM G/KG
181	2	340	305	136.1	0.6205	2880	0.9911	8.9491	-1.0000	0.0137	-1.0000	-1.0000
182	2	340	303	138.8	0.5458	2613	0.9821	17.8870	-1.0000	0.0108	-1.0000	-1.0000
183	2	335	295	139.0	0.4894	2372	0.9616	38.3977	-1.0000	0.0062	-1.0000	-1.0000
184	1	334	280	141.7	0.4435	2053	0.8770	123.0000	-1.0000	0.0069	0.1083	-1.0000
185	2	335	320	139.0	0.5014	2427	0.9681	31.8877	-1.0000	0.0240	-1.0000	-1.0000
186	2	335	340	139.0	0.5631	2674	0.9849	15.1181	-1.0000	0.0000	0.4135	-1.0000
187	-1	-1	-1	-1.0	-1.0000	-1	0.0000	0.0000	-1.0000	-1.0000	-1.0000	-1.0000
188	2	430	340	77.9	0.6830	3149	0.9970	3.0325	-1.0000	0.0077	-1.0000	-1.0000
189	2	430	320	79.0	0.5532	2727	0.9929	7.1253	-1.0000	0.0000	-1.0000	-1.0000
190	1	430	300	79.0	0.4885	2488	0.9856	14.3782	-1.0000	0.0000	-1.0000	-1.0000
191	2	400	295	66.9	0.5766	2788	0.9947	5.2707	-1.0000	0.0148	-1.0000	-1.0000
192	2	405	295	56.0	0.6896	3153	0.9978	2.2005	-1.0000	0.0039	-1.0000	-1.0000
193	-1	410	360	51.6	1.2578	3587	0.0000	0.0000	-1.0000	23.7001	-1.0000	-1.0000
194	-1	410	420	113.0	0.5463	2679	0.9883	11.6743	-1.0000	0.0314	-1.0000	-1.0000
195	-1	410	410	113.6	0.4858	2446	0.9762	23.7640	-1.0000	0.0353	-1.0000	-1.0000
196	-1	410	390	115.2	0.4920	2470	0.9778	22.1823	-1.0000	8.9366	-1.0000	-1.0000
197	-1	430	340	101.4	0.5304	2640	0.9884	11.5726	-1.0000	0.9200	-1.0000	-1.0000
198	-1	360	260	41.2	0.6579	3028	0.9980	2.0329	-1.0000	0.0084	-1.0000	-1.0000
199	-1	340	320	38.5	0.9818	3690	0.9938	6.1932	-1.0000	0.0380	-1.0000	-1.0000
200	-1	410	270	38.5	0.6616	3074	0.9983	1.6980	-1.0000	0.5087	-1.0000	-1.0000
201	2	86	82	83.2	0.8221	3307	0.9961	3.9168	-1.0000	-1.0000	-1.0000	-1.0000
202	2	82	82	102.9	0.7187	3017	0.9938	6.2446	-1.0000	-1.0000	-1.0000	-1.0000
203	2	110	100	148.0	0.6216	2704	0.9832	16.7514	1.8195	0.0278	0.3728	-1.0000
204	-1	-1	-1	-1.0	-1.0000	-1	0.0000	0.0000	-1.0000	-1.0000	-1.0000	-1.0000
205	2	313	77	76.8	0.6978	3114	0.9966	3.3925	-1.0000	-1.0000	-1.0000	-1.0000
206	2	253	77	167.8	0.6498	2909	0.9890	10.9588	-1.0000	-1.0000	-1.0000	-1.0000
207	2	245	77	181.5	0.5601	2572	0.9728	27.2419	-1.0000	-1.0000	0.2588	0.1527
208	-1	70	-1	51.5	0.8177	3292	0.9980	1.9506	-1.0000	-1.0000	-1.0000	-1.0000
209	-1	70	-1	49.9	0.9883	3549	0.9904	9.5711	-1.0000	-1.0000	-1.0000	-1.0000
210	-1	70	-1	49.9	0.6666	2856	0.9968	3.2151	-1.0000	-1.0000	-1.0000	-1.0000

BURN=2---STABLE
BURN=1---LIMIT
BURN=0---GOING OUT

PRED EMM = 1000×(1-EFFY)
PPED EFFY FROM THEORY

NOB - BURNER DATA FOR NOX
NOT - NOX FROM VAPOR GENERATOR EXH.

RUN NO.	BURN	AIR TEMP oF	FUEL TEMP oF	AIR FLOW LBS/HR	EQUIV RATIO	COMB TEMP oF	PRED EFFY	PRED EMM G/KG	COG EMM G/KG	HCG EMM G/KG	NOBG EMM G/KG	NOTG EMM G/KG
211	-1	70	-1	49.9	1.0852	3544	0.0000	0.0000	-1.0000	-1.0000	-1.0000	-1.0000
212	-1	70	-1	102.9	0.6368	2746	0.9915	8.4514	-1.0000	-1.0000	-1.0000	-1.0000
213	-1	70	-1	99.7	0.7865	3208	0.9961	3.9081	-1.0000	-1.0000	-1.0000	-1.0000
214	-1	70	-1	96.6	1.0999	3537	0.0000	0.0000	-1.0000	-1.0000	-1.0000	-1.0000
215	-1	70	-1	49.9	0.4845	2175	0.9729	27.0681	-1.0000	-1.0000	-1.0000	-1.0000
216	-1	70	-1	48.2	0.6615	2839	0.9968	3.2156	-1.0000	-1.0000	-1.0000	-1.0000
217	2	80	-1	83.8	0.6044	2638	0.9885	11.4746	-1.0000	-1.0000	-1.0000	-1.0000
218	2	100	70	91.5	0.6187	2708	0.9919	8.1171	0.1629	-1.0000	0.0726	-1.0000
219	2	110	70	95.3	0.7845	3228	0.9965	3.5301	5.5606	-1.0000	0.9701	-1.0000
220	2	100	100	86.2	0.5854	2583	0.9863	13.6626	-1.0000	0.3391	0.2876	0.2431
221	2	100	100	116.8	0.5761	2534	0.9788	21.1727	-1.0000	0.3523	-1.0000	-1.0000
222	2	100	100	131.8	0.5105	2156	0.9078	92.1901	-1.0000	2.0954	-1.0000	-1.0000
223	2	100	100	108.4	0.6205	2704	0.9877	12.3488	-1.0000	0.5651	-1.0000	-1.0000
224	2	100	100	168.5	0.5562	2413	0.9555	44.5324	-1.0000	0.3447	-1.0000	-1.0000
225	2	100	100	151.8	0.6173	2679	0.9817	18.2645	-1.0000	0.9205	-1.0000	-1.0000
226	1	100	100	177.9	0.5266	2149	0.8800	120.0000	-1.0000	-1.0000	-1.0000	-1.0000
227	2	76	82	55.8	0.5796	2554	0.9903	9.7308	0.1744	0.9677	0.7041	-1.0000
228	2	82	90	58.4	0.5761	2545	0.9896	10.4349	0.1755	0.4170	0.0989	-1.0000
229	2	85	95	57.6	0.5773	2552	0.9899	10.0640	0.1751	0.6529	0.3103	-1.0000
230	2	433	98	57.6	0.5779	2818	0.9959	4.1452	-1.0000	0.4560	0.2053	-1.0000
231	2	420	100	60.8	0.5473	2702	0.9941	5.8817	-1.0000	0.3310	0.1174	-1.0000
232	2	410	100	90.9	0.5203	2589	0.9878	12.1522	-1.0000	0.2877	0.1879	-1.0000
233	2	407	100	90.2	0.6172	2925	0.9948	5.2052	-1.0000	0.4614	0.5288	-1.0000
234	2	90	82	76.9	0.6725	2881	0.9941	5.9028	-1.0000	1.5728	1.2813	-1.0000
235	2	92	89	77.3	0.5930	2608	0.9886	11.4415	-1.0000	2.6491	0.8953	-1.0000
236	2	89	89	77.7	0.6003	2632	0.9892	10.7661	-1.0000	2.9769	0.5918	-1.0000
237	2	82	82	38.4	0.6353	2760	0.9961	3.8535	-1.0000	2.9425	1.5835	1.9999
238	2	79	70	49.1	0.4880	2202	0.9763	23.7091	-1.0000	-1.0000	0.0637	-1.0000
239	2	80	71	48.9	0.5391	2414	0.9894	10.5573	-1.0000	-1.0000	0.1855	-1.0000
240	2	82	71	48.9	0.6563	2830	0.9967	3.2991	-1.0000	-1.0000	0.4526	-1.0000

BURN=2---STABLE *PRED EMM = 1000×(1-EFFY)* *NOB - BURNER DATA FOR NOX*
BURN=1---LIMIT *PRED EFFY FROM THEORY* *NOT - NOX FROM VAPOR GENERATOR EXH.*
BURN=0---GOING OUT

Table
VIII-26

RUN NO.	BURN	AIR TEMP oF	FUEL TEMP oF	AIR FLOW LBS/HR	EQUIV RATIO	COMB TEMP oF	PRED EFFY	PRED EMM G/KG	COG EMM G/KG	HCG EMM G/KG	NOBG EMM G/KG	NOTG EMM G/KG
241	2	82	72	48.8	0.7266	3051	0.9978	2.2394	-1.0000	-1.0000	1.9359	-1.0000
242	2	78	68	49.2	0.7617	3150	0.9980	2.0079	-1.0000	-1.0000	1.8018	-1.0000
243	2	80	72	48.8	0.8945	3457	0.9978	2.2083	-1.0000	-1.0000	2.6989	-1.0000
244	2	79	68	98.1	0.5043	2221	0.9570	43.0363	-1.0000	-1.0000	0.1184	-1.0000
245	2	80	70	97.6	0.5994	2622	0.9890	10.9873	-1.0000	-1.0000	0.2608	-1.0000
246	-1	80	70	60.5	0.6393	2770	0.9953	4.6675	-1.0000	-1.0000	-1.0000	-1.0000
247	-1	75	70	-1.0	0.4609	2131	0.0000	0.0000	-1.0000	-1.0000	-1.0000	-1.0000
248	-1	85	70	47.2	0.5625	2507	0.9925	7.4574	-1.0000	-1.0000	-1.0000	-1.0000
249	-1	75	70	49.2	0.8476	3363	0.9981	1.8957	-1.0000	-1.0000	0.1125	-1.0000
250	-1	85	70	48.8	0.8555	3386	0.9981	1.8842	-1.0000	-1.0000	1.2634	-1.0000
251	-1	85	70	100.8	0.4983	2190	0.9502	49.7573	-1.0000	-1.0000	0.0767	-1.0000
252	-1	90	70	100.4	0.5006	2210	0.9543	45.7280	-1.0000	-1.0000	0.0501	-1.0000
253	-1	92	70	97.0	0.5772	2549	0.9866	13.4016	-1.0000	-1.0000	0.1275	-1.0000
254	-1	93	70	100.1	0.6412	2779	0.9925	7.5138	-1.0000	-1.0000	0.2430	-1.0000
255	2	93	70	90.0	0.6063	2653	0.9882	11.7618	-1.0000	-1.0000	-1.0000	-1.0000
256	2	85	70	97.6	0.7188	3024	0.9954	4.6069	-1.0000	-1.0000	0.4797	-1.0000
257	2	85	70	97.6	0.7852	3214	0.9963	3.7465	-1.0000	-1.0000	1.3082	-1.0000
258	2	85	70	97.5	0.9004	3466	0.9955	4.4843	-1.0000	-1.0000	2.0235	-1.0000
259	2	85	70	97.4	1.0000	3556	0.9804	19.6038	-1.0000	-1.0000	2.6256	-1.0000
260	2	85	70	97.3	0.9609	3538	0.9915	8.5162	-1.0000	-1.0000	0.9896	-1.0000
261	-1	89	70	97.2	1.1875	3482	0.0000	0.0000	-1.0000	-1.0000	1.1944	-1.0000
262	2	90	70	144.4	0.5167	2244	0.9436	56.4055	-1.0000	-1.0000	0.2285	-1.0000
263	2	97	70	143.5	0.5957	2609	0.9835	16.4723	-1.0000	-1.0000	0.3739	-1.0000
264	2	85	73	48.8	0.4951	2240	0.9799	20.0719	0.1469	-1.0000	0.1062	-1.0000
265	2	85	73	48.8	0.5820	2577	0.9938	6.2279	0.1737	-1.0000	0.4157	-1.0000
266	2	96	70	143.0	0.5677	2498	0.9772	22.8177	0.2547	-1.0000	-1.0000	-1.0000
267	2	96	70	97.8	0.5045	2243	0.9611	38.9211	-1.0000	-1.0000	0.0970	-1.0000
268	2	96	70	97.2	0.5817	2569	0.9874	12.6322	-1.0000	-1.0000	0.2692	-1.0000
269	2	96	72	97.2	0.6582	2838	0.9936	6.3814	-1.0000	-1.0000	0.6805	-1.0000
270	2	96	72	97.1	0.6860	2929	0.9947	5.3297	-1.0000	-1.0000	1.9372	-1.0000

BURN=2---STABLE
BURN=1---LIMIT
BURN=0---GOING OUT

PRED EMM = 1000×(1-EFFY)
PRED EFFY FROM THEORY

NOB - BURNER DATA FOR NOX
NOT - NOX FROM VAPOR GENERATOR EXH.

Table VIII-27

RUN NO.	BURN	AIR TEMP °F	FUEL TEMP °F	AIR FLOW LBS/HR	EQUIV RATIO	COMB TEMP °F	PRED EFFY	PRED EMM G/KG	COG EMM G/KG	HCG EMM G/KG	NOBG EMM G/KG	NOTG EMM G/KG
271	2	100	75	144.1	0.5576	2459	0.9740	26.0316	-1.0000	-1.0000	0.1791	-1.0000
272	2	100	71	141.7	0.6618	2846	0.9909	9.1203	-1.0000	-1.0000	0.5020	-1.0000
273	2	100	70	143.1	0.6745	2888	0.9915	8.4565	-1.0000	-1.0000	1.4659	-1.0000
274	2	100	70	143.5	0.7565	3140	0.9942	5.7548	0.4611	0.0000	0.3865	-1.0000
275	2	95	70	143.7	0.8254	3317	0.9947	5.2594	0.7331	-1.0000	1.0296	-1.0000
276	-1	-1	-1	130.0	-1.0000	-1	0.0000	0.0000	-1.0000	-1.0000	-1.0000	-1.0000
277	-1	-1	-1	140.0	-1.0000	-1	0.0000	0.0000	-1.0000	-1.0000	-1.0000	-1.0000
278	-1	-1	-1	-1.0	-1.0000	-1	0.0000	0.0000	-1.0000	-1.0000	-1.0000	-1.0000
279	2	109	70	91.0	0.5791	2564	0.9848	15.1737	0.1247	0.1994	0.3360	0.1639
280	2	110	70	90.9	0.6808	2920	0.9936	6.3889	0.2104	0.9399	0.7810	0.7188
281	2	110	70	111.3	0.5932	2610	0.9838	16.2248	0.1216	0.0485	0.3316	0.1638
282	2	94	70	46.4	0.6072	2670	0.9942	5.7850	0.1187	0.0000	0.3665	0.3002
283	2	100	70	47.3	0.6024	2658	0.9939	6.0739	0.1196	0.0000	0.1101	0.0786
284	2	105	70	46.5	0.4239	1846	0.9000	100.0000	0.1727	0.0000	0.0624	0.0454
285	2	116	70	136.5	0.4873	2051	0.8890	111.0000	0.2450	0.0000	-1.0000	0.0589
286	2	82	75	58.8	0.5010	2253	0.9771	22.8988	-1.0000	-1.0000	0.1097	-1.0000
287	2	92	70	144.0	0.5260	2302	0.9548	45.1854	2.6202	0.0000	0.1586	-1.0000
288	2	90	69	144.3	0.5654	2483	0.9757	24.2540	-1.0000	0.0000	0.1849	-1.0000
289	2	95	69	143.6	0.6016	2629	0.9843	15.7393	-1.0000	0.0000	0.2559	-1.0000
290	2	99	60	142.9	0.7193	3029	0.9934	6.6129	0.8138	0.3568	0.1304	-1.0000
291	-1	73	68	66.0	1.3984	3192	0.0000	0.0000	-1.0000	-1.0000	0.6409	-1.0000
292	-1	75	70	49.1	1.5625	2965	0.0000	0.0000	0.1314	161.4518	0.4629	-1.0000
293	-1	82	70	47.1	1.3594	3251	0.0000	0.0000	1109.9767	1.0542	-1.0000	-1.0000
294	-1	90	70	51.1	1.2578	3393	0.0000	0.0000	764.7702	2.7660	-1.0000	-1.0000
295	-1	72	70	49.2	1.3203	3297	0.0000	0.0000	961.8264	0.9149	1.1960	-1.0000
296	-1	86	73	48.6	1.3438	3274	0.0000	0.0000	944.0615	0.6170	1.6858	-1.0000
297	-1	92	71	48.3	1.4141	3183	0.0000	0.0000	1152.1380	0.5784	1.0119	-1.0000
298	-1	95	71	48.2	1.2813	3364	0.0000	0.0000	879.4185	0.8733	2.1113	-1.0000
299	-1	96	71	87.2	1.3750	3238	0.0000	0.0000	984.6333	0.9159	-1.0000	-1.0000
300	-1	85	69	49.3	1.1719	3494	0.0000	0.0000	1013.6513	1.0314	0.8173	-1.0000

BURN=2---STABLE
BURN=1---LIMIT
BURN=0---GOING OUT

PRED EMM = 1000×(1-EFFY)
PRED EFFY FROM THEORY

NOB - BURNER DATA FOR NOX
NOT - NOX FROM VAPOR GENERATOR EXH.

Table VIII-28

RUN NO.	BURN	AIR TEMP OF	FUEL TEMP OF	AIR FLOW LBS/HR	EQUIV RATIO	COMB TEMP OF	PRED EFFY	PRED EMM G/KG	COG EMM G/KG	HCG EMM G/KG	NOBG EMM G/KG	NOTG EMM G/KG
301	-1	88	69	48.5	1.2188	3444	0.0000	0.0000	629.4393	-0.5725	2.3267	-1.0000
302	-1	92	70	96.9	1.4219	3172	0.0000	0.0000	1104.4730	-1.0000	0.3230	-1.0000
303	-1	74	68	98.5	1.2813	3352	0.0000	0.0000	424.4660	2.3409	0.5779	-1.0000
304	-1	87	70	141.5	1.3438	3275	0.0000	0.0000	950.9025	1.0133	0.4252	-1.0000
305	-1	100	67	124.2	1.3750	3241	0.0000	0.0000	1030.7704	0.8641	0.4437	-1.0000
306	-1	100	68	139.8	1.1719	3503	0.0000	0.0000	570.8785	6.0176	0.6130	-1.0000
307	-1	104	69	94.3	1.1953	3483	0.0000	0.0000	558.1266	-1.0000	0.3789	-1.0000
308	2	90	320	46.6	0.5469	2447	0.9886	11.3665	1.9862	-1.0000	0.2088	0.0979
309	2	98	350	47.5	0.5052	2285	0.9794	20.5938	2.1579	0.0000	0.0898	0.0614
310	-1	94	310	48.4	0.3436	1562	0.9100	90.0000	0.5925	0.1868	0.0529	0.0529
311	2	385	350	49.4	0.5886	2820	0.9964	3.6314	1.8390	0.0000	0.3384	0.3061
312	2	388	348	48.3	0.5098	2546	0.9925	7.4545	0.1425	0.0000	0.0164	0.0726
313	2	395	340	47.2	0.3945	2063	0.9522	47.8285	0.1861	0.0000	0.0092	0.0336
314	2	340	450	88.2	0.5392	2603	0.9883	11.6792	-1.0000	-1.0000	0.0883	0.1590
315	2	364	450	93.1	0.4726	2357	0.9727	27.2698	-1.0000	-1.0000	-1.0000	0.0507
316	2	400	460	90.5	0.5043	2520	0.9849	15.0668	0.1441	0.0000	-1.0000	0.0332
317	2	435	460	90.0	0.4059	2085	0.9216	78.3522	0.1806	0.0000	0.0059	0.0237
318	2	350	638	137.1	0.4935	2408	0.9665	33.4715	0.1474	0.0000	0.0378	0.0848
319	2	350	620	137.2	0.4150	1976	0.8800	120.0000	0.3249	0.0000	0.0000	0.0319
320	2	351	600	134.5	0.6484	2981	0.9928	7.1961	0.1838	0.0000	0.0673	0.1328
321	2	140	540	89.8	0.5978	2659	0.9887	11.2516	0.3619	0.0000	0.0951	0.1367
322	2	115	490	90.0	0.4857	2115	0.9234	76.5982	0.5007	0.0000	0.0074	0.0394
323	1	105	530	90.0	0.4477	1922	0.8960	104.0000	5.1723	0.2758	-1.0000	0.0295
324	2	95	585	135.5	0.5847	2555	0.9769	23.0948	0.1235	0.0198	0.0588	0.1144
325	2	105	550	137.3	0.5181	2229	0.9286	71.4471	0.9387	0.0117	0.0184	0.0437
326	1	110	610	138.7	0.4796	2023	0.8900	110.0000	4.5562	0.2561	0.0050	0.0399
327	2	412	77	48.2	0.6017	2884	0.9970	3.0281	0.4025	0.0286	0.1456	0.2342
328	2	395	90	47.3	0.4641	2378	0.9871	12.8502	0.4998	0.0000	0.0320	0.0671
329	2	390	95	47.1	0.3821	1968	0.9244	75.6240	3.1701	0.0000	0.0000	0.0253
330	2	407	97	90.3	0.5955	2853	0.9939	6.0797	0.1211	0.0000	0.2646	0.3661

BURN=2---STABLE *PRED EMM = 1000×(1-EFFY)* *NOB - BURNER DATA FOR NOX*
BURN=1---LIMIT *PRED EFFY FROM THEORY* *NOT - NOX FROM VAPOR GENERATOR EXH.*
BURN=0---GOING OUT

Table
VIII-29

RUN NO.	BURN	AIR TEMP °F	FUEL TEMP °F	AIR FLOW LBS/HR	EQUIV RATIO	COMB TEMP °F	PRED EFFY	PRED EMM G/KG	COG EMM G/KG	HCG EMM G/KG	NOBG EMM G/KG	NOTG EMM G/KG
331	2	400	100	92.7	0.4834	2436	0.9798	20.1670	0.1506	0.0000	0.0891	0.0891
332	1	435	92	89.7	0.4059	2086	0.9223	77.6826	358.7488	0.0000	0.0000	0.4155
333	2	392	95	135.2	0.4401	2160	0.9166	83.4309	4.7839	0.0000	0.0000	0.0573
334	1	395	100	140.3	0.3843	1908	0.8800	120.0000	-1.0000	0.0000	0.0000	0.0408
335	2	92	590	91.3	0.5556	2457	0.9787	21.2564	0.1263	0.0000	0.0770	0.1287
336	1	90	630	92.6	0.4667	1964	0.8900	110.0000	9.0811	0.0631	0.0000	0.0597
337	2	90	610	48.5	0.5434	2432	0.9876	12.4134	0.1292	0.0000	0.1511	0.1019
338	2	90	660	49.6	0.5899	2605	0.9926	7.4003	0.1186	0.0000	0.0080	0.0565
339	2	100	660	136.7	0.5685	2492	0.9718	28.1970	-1.0000	0.1976	0.1838	0.1580
340	2	395	90	138.3	0.4997	2478	0.9739	26.0525	0.1455	0.0121	0.0239	0.1076
341	2	150	100	92.4	0.5245	2378	0.9725	27.4705	0.1383	0.0000	0.0250	0.0955
342	2	90	85	93.3	0.5472	2419	0.9753	24.7073	0.1283	-1.0000	0.0000	0.8349
343	2	102	100	91.3	0.5273	2344	0.9686	31.4349	0.1375	0.0000	0.0452	0.0949
344	2	100	100	91.9	0.4688	1979	0.8900	110.0000	0.1555	0.6505	0.0077	0.0690
345	2	102	95	135.3	0.5445	2386	0.9606	39.3849	0.1330	0.0000	0.0240	0.1704
346	2	105	95	138.2	0.4898	2051	0.8890	111.0000	-1.0000	0.1853	0.0000	0.0952
347	2	105	97	134.5	0.6523	2813	0.9882	11.7854	-1.0000	0.0000	0.2097	0.4230
348	2	107	95	90.1	0.6022	2649	0.9882	11.8085	0.9708	0.0000	0.0275	0.5474
349	2	100	100	91.9	0.5137	2274	0.9592	40.7793	128.2549	2.5352	0.0070	0.1373
350	2	101	105	136.4	0.5697	2498	0.9724	27.5751	13.6585	0.0998	0.0417	0.3315
351	2	105	810	92.4	0.6311	2749	0.9906	9.3830	0.1105	0.0000	0.0973	0.1707
352	1	110	815	93.1	0.5036	2230	0.9510	48.9656	0.1399	0.0000	0.0190	0.0138
353	2	120	790	137.7	0.6311	2749	0.9861	13.8546	0.1105	1.3118	0.1497	0.2070
354	2	430	630	81.4	0.5379	2672	0.9915	8.4997	0.1306	0.0000	0.1018	0.1588
355	2	438	610	82.0	0.4309	2251	0.9646	35.3630	0.1643	0.0000	0.0112	0.0432
356	2	450	625	43.8	0.5570	2762	0.9964	3.5851	0.1260	0.0000	0.1024	0.1531
357	2	140	690	180.5	0.5053	2111	0.8800	120.0000	0.1394	0.0000	0.0284	0.0779
358	2	110	690	46.8	0.4673	2116	0.9590	41.0407	0.1512	0.0000	0.1025	0.0795
359	2	120	730	138.2	0.5022	2097	0.8860	114.0000	0.1403	0.0000	0.0666	0.1014
360	2	380	570	92.6	0.5322	2608	0.9881	11.8535	0.1321	0.0000	0.1119	0.1649

BURN=2---STABLE *PRED EMM = 1000×(1-EFFY)* *NOB - BURNER DATA FOR NOX*
BURN=1---LIMIT *PRED EFFY FROM THEORY* *NOT - NOX FROM VAPOR GENERATOR EXH.*
BURN=0---GOING OUT

Table
VIII-30

RUN NO.	BURN	AIR TEMP oF	FUEL TEMP oF	AIR FLOW LBS/HR	EQUIV RATIO	COMB TEMP oF	PRED EFFY	PRED EMM G/KG	COG EMM G/KG	HCG EMM G/KG	NOBG EMM G/KG	NOTG EMM G/KG
361	2	400	620	90.9	0.4673	2370	0.9750	24.9818	0.1512	0.0000	0.0154	0.0795
362	2	405	670	89.8	0.6305	2967	0.9952	4.7757	0.1106	0.0000	0.1986	0.3236
363	2	405	645	90.8	0.4984	2501	0.9840	16.0114	0.1414	0.0586	0.1774	0.2323
364	2	405	670	48.7	0.5691	2769	0.9960	4.0079	0.1232	0.4965	0.1836	0.1943
365	2	405	670	48.0	0.6244	2953	0.9974	2.6264	0.1118	0.0616	0.2725	0.1910
366	2	410	660	47.9	0.4309	2255	0.9794	20.6335	0.1643	0.0000	0.0558	0.0648
367	2	405	670	137.0	0.5100	2530	0.9782	21.7602	1.0000	0.0000	0.0515	0.1270
368	2	410	690	137.1	0.4309	2087	0.8855	114.4709	0.1643	1.0000	0.0279	0.0432
369	2	400	690	136.3	0.5691	2748	0.9882	11.7979	0.2464	0.0000	0.1502	0.2267
370	2	403	710	90.9	0.5475	2683	0.9907	9.3231	0.3745	0.1464	0.1043	1.0000
371	2	426	720	137.1	0.5738	2785	0.9893	10.6911	0.9111	0.0000	0.1572	1.0000
372	1	425	700	138.7	0.5438	2676	0.9856	14.3504	1.1935	0.5236	0.0525	1.0000
373	2	425	720	90.9	0.5325	2646	0.9898	10.2252	0.1320	0.0757	0.0984	1.0000
374	1	430	700	90.3	0.4913	2495	0.9839	16.0845	5.8846	6.5336	0.0584	1.0000
375	1	400	710	91.4	0.4618	2346	0.9725	27.4727	25.2456	108.5867	0.0042	1.0000
376	1	400	710	90.3	0.4711	2387	0.9766	23.3936	85.4441	180.1626	0.0041	1.0000
377	2	405	705	48.3	0.4838	2462	0.9903	9.7117	1.0000	0.7287	0.1335	1.0000
378	1	428	730	45.5	0.4875	2496	0.9919	8.0865	3.3900	5.0370	0.0687	1.0000
379	1	375	720	47.0	0.4650	2364	0.9865	13.5247	8.5400	3.4403	0.0670	1.0000
380	1	412	715	45.7	0.4395	2294	0.9832	16.8192	27.7000	75.2300	0.0055	1.0000
381	1	411	728	138.5	0.4507	2262	0.9438	56.1542	32.1684	66.5627	0.0037	1.0000
382	1	411	721	138.7	0.4501	2258	0.9429	57.1028	49.3421	156.2723	0.0053	1.0000
383	1	403	700	47.1	0.4725	2418	0.9890	11.0430	20.7706	57.4081	0.0710	1.0000
384	1	76	710	91.4	0.5775	2531	0.9830	16.9827	0.4440	0.0488	0.0822	1.0000
385	2	90	430	91.6	0.5625	2483	0.9804	19.6011	1.0000	0.0402	0.1436	1.0000
386	1	91	470	89.8	0.5284	2339	0.9686	31.3526	32.2044	8.5927	0.0271	1.0000
387	1	80	740	47.8	0.5255	2353	0.9839	16.1210	4.0152	1.0001	0.0998	1.0000
388	1	81	740	45.5	0.5337	2389	0.9865	13.5103	53.5975	28.3174	0.0067	1.0000
389	1	85	390	48.2	1.2334	3423	0.0000	0.0000	1194.6713	18.0370	0.5425	1.0000
390	1	90	515	80.9	0.5400	2397	0.9769	23.1205	0.1301	0.2117	0.2557	1.0000
391	2	93	550	80.5	0.4900	2144	0.9388	61.1581	77.7172	19.0275	0.0098	1.0000

BURN=2---STABLE PRED EMM = 1000×(1-EFFY) NOB - BURNER DATA FOR NOX
BURN=1---LIMIT PRED EFFY FROM THEORY NOT - NOX FROM VAPOR GENERATOR EXH.
BURN=0---GOING OUT

Table
VIII-31

APPENDICES

REFERENCES

1. Frank-Kamenetskii, D.A., "Diffusion and Heat Exchange in Chemical Kinetics", Quoted by Frank-Kamenetskii, Princeton University Press, 1955.

2. Van't Hoff, "Etudes de Dynamique Chimique", Amsterdam, 1884.

3. LeChatelier, Quoted by Frank-Kamenetskii after Jouget, "Mechanique des Explosifs", Paris 1937.

4. Semenov, N.N., quoted by Frank-Kamenetskii, Z. Tnysik, Chem. 48, 571, 1928.

5. Vulis, L.A., "Thermal Regimes of Combustion", McGraw Hill, 1961.

6. Dezubay, E.A., "Characteristics of Disc-Controlled Flame", Aero Digest, July 1950.

7. Scurlock, A.C., "Flame Stabilization and Propagation High Velocity Gas Streams", Third Symposium on Combustion Flame and Explosion Phenomena page 21, Williams and Wilkins, 1949.

8. Longwell, J.P., and Weiss, M.A., "Flame Stability in Bluff Body Recirculation Zones", pp 98, Ind. Eng. Chem, 5,1629, 1953 8th Symposium on Combustion.

9. Zwick, E.B., & Bjerklie, J.W., "The Mechanism of Combustion Stabilization in Monopropellant Reaction Chambers", Sundstrand-Turbo, Pacoima, 1958.

10. Clarke, A.E., Harrison, A.J., Odgers, J., "Combustion Stability in a Spherical Combustor", pp 664, 7th Symposium on Combustion, Buttorworths, 1959.

11. Jeffs, R.A., "The Flame Stability and Heat Release Rates of Some Can-Type Combustion Chambers", 8th Symposium on Combustion pp 1014, Williams & Wilkins, 1960.

12. Williams,et al, "The Combustion of Methane in a Jet-Mixed Reactor", 12th Symposium on Combustion, pp 913, 1969.

13. Clarke, A.E., "Further Studies of Combustion Phenomena in a Spherical Combustor", 8th Symposium on Combustion, pp 982, Williams & Wilkins, 1960

14. Herbert, M.V., "A Theoretical Analysis of Reaction Rate Controlled Systems Part II", 8th Symposium on Combustion, pp 970-981, Williams Wilkins, 1960.

15. Hougen, O., Watson, K., Ragatz, "Chemical Process Principles", J. Wiley & Sons, 1947.

Colorimetric Microdetermination of Nitrogen Dioxide in the Atmosphere

BERNARD E. SALTZMAN

Division of Special Health Service, U. S. Department of Health, Education, and Welfare, Cincinnati, Ohio

The determination of nitrogen dioxide in the atmosphere has heretofore been hampered by difficulties in sample absorption and lack of specificity. A new specific reagent has been developed and demonstrated to absorb efficiently in a midget fritted bubbler at levels below 1 p.p.m. The reagent is a mixture of sulfanilic acid, *N*-(1-naphthyl)-ethylenediamine dihydrochloride, and acetic acid. A stable direct color is produced with a sensitivity of a few parts per billion for a 10-minute sample at 0.4 liter per minute. Ozone in five-fold excess and other gases in ten-fold excess produce only slight interfering effects; these may be reduced further by means which are described.

TOXIC oxides of nitrogen, liberated during the use of explosives, in welding operations, in the exhaust of internal combustion engines, and in chemical processes involving nitration by the use of nitric acid, are well known health hazards. In recent years new interest has been directed toward concentrations of a few tenths of a part per million of nitrogen dioxide, which are believed to play a vital role in the creation of irritating smog (*4, 10*). Toxicologic studies (*8, 9, 15, 22, 24*) call attention to the fact that nitrogen dioxide is the most toxic of the various nitrogen oxides by a large factor, and that confusion in the evaluation of the health hazards has resulted from analytical methods which fail to differentiate this oxide from the others in a mixture. In terms of nitrogen dioxide, a figure of 5 p.p.m. is the maximum safe allowable concentration proposed (*8, 9*). All these considerations require its determination in air at much lower levels than previously thought necessary.

The major problem of past analytical methods has been the difficulty in absorbing the gas from a sufficiently large sample. Results have been uncertain for levels below 5 p.p.m. Samples must be collected in large bottles for the well known phenolsulfonic acid method (*3, 6*), and days are required for complete absorption, low results have been reported (*16*) and confirmed in the present study. Similar difficulties occur with the *m*-xylenol methods (*11, 25*). Both determine all nitrogen oxides in the form of nitrate, rather than nitrogen dioxide specifically.

Attempts have been made to use reagents for nitrite ion, which would be specific for nitrogen dioxide, but an absorption efficiency of only about 5% was reported (*16*) when a midget impinger was used. However, these reagents were found to be very convenient for higher levels using a glass syringe for collecting the sample (*1, 12, 16*), low levels have been determined using a laboratory [illegible]. Continuous samples have been collected by using low temperatures (*7*) or alkali bubblers (*21*), neither being of unknown efficiency.

The present report deals with the development and demonstration of a reagent which is specific for nitrogen dioxide and is suited for continuous sampling with a high efficiency. The problem of determining absorption efficiency was reduced to the construction of an apparatus capable of generating known concentrations of nitrogen dioxide of a few tenths of a part per million with a variation of less than 1%. The reagent which was finally developed conveniently produces a stable dye for which can be measured visually or spectrophotometrically. Both 10 ml. are used in a midget fritted bubbler and air is sampled at a rate of 0.4 liter per minute, a sensitivity of a few parts per billion is attained with a 10-minute sample. The effect of various interfering gases was found to be slight.

APPARATUS

Spectrophotometer, Beckman Model DU. A set of matched test tubes, 22 × 175 mm., giving an optical light path of 2.02 cm. was used in a special holder fitted to the spectrophotometer.

Midget Fritted Bubblers, all-glass, capacity 60 ml., with upward-facing, 8-mm. diameter fritted disks. When used with 10 ml. of the absorbing reagent, drawing air through at the rate of 0.4 liter per minute should produce 20 to 30 ml. of fine froth above the solution.

Grab-Sample Bottles, having standard-taper ground-joint connection to stopcocks for evacuation, with calibrated volumes varying from 30 to 250 ml. Ordinary glass-stoppered borosilicate glass bottles are suitable. Fifty-milliliter glass syringes are convenient for moderately high concentrations.

REAGENTS

All reagents are made from analytical grade chemicals in nitrite-free water prepared by redistilling distilled water in an all-glass still after adding a crystal each of potassium permanganate and of barium hydroxide. They are stable for several months if kept well stoppered in brown bottles in the refrigerator.

***N*-(1-Naphthyl)-ethylenediamine Dihydrochloride,** 0.1%. Dissolve 0.1 gram of the reagent in 100 ml. of water. Stock solution.

Absorbing Reagent. Dissolve 5 grams of sulfanilic acid in almost a liter of water containing 140 ml. of glacial acetic acid, add 20 ml. of the 0.1% stock solution of *N*-(1-naphthyl)-ethylenediamine dihydrochloride, and dilute to 1 liter.

Standard Sodium Nitrite Solution, 0.0203 gram per liter. One milliliter of this working solution produces a color equivalent to that of 10 µl. of nitrogen dioxide (10 p.p.m. in 1 liter of air at 760 mm. of mercury and 25° C.). Prepare fresh by dilution from a stronger stock solution. The latter may be prepared from Merck reagent grade granular solid, which has been shown (*17*) to assay 99.4%, in another study (*5*) it was found to assay 100.4%, drying was said to be unnecessary, and a stock solution of 8 grams per liter was found to be stable for 90 days.

PROCEDURE

Sampling for Levels of 1 P.P.M. and Below. Place 10 ml. of absorbing reagent in a midget fritted bubbler and draw a sample through it at the rate of 0.4 liter per minute until sufficient color has developed (about 10 minutes). Note the total air volume sampled. Pure gum rubber surgical tubing may be used for connections without losses if lengths are kept minimal.

Sampling for Levels above 1 P.P.M. Sample in an evacuated bottle of appropriate size (30 ml. for up to 100 p.p.m., to 250 ml. for down to 1 p.p.m.) containing 10 ml. of absorbing reagent. If a good source of vacuum is available at the place of sampling, it is best to evacuate just before sampling to eliminate any uncertainty about loss of vacuum. A three-way T stopcock connection to the vacuum pump is convenient. In the first position the bottle is evacuated to the vapor pressure of the absorbing reagent and the actual vacuum is read. In the second position the sampling bottle is closed and the vacuum pump draws air through the sampling line to thoroughly flush it. In the third position the sampling line is connected to the evacuated bottle and the sample is collected. For calculation of the sample volume the pressure is recorded as the difference between the filled and evacuated conditions, and the volume is that of the bottle plus that of the connection up to the stopcock minus the volume of absorbing reagent. Allow 15 minutes with occasional shaking for complete absorption and color development.

Another more convenient but less accurate field method for moderately high levels is to use 50-ml. glass syringes. Ten milliliters of absorbing reagent may be kept in the capped syringes, and 40 ml. of air may be drawn in at the time of sampling. If insufficient color is expected, the absorption may be completed by shaking vigorously for 1 to 2 minutes after which the air may be expelled and additional air drawn in.

Determination. After collection or absorption of the sample, a discrete violet color appears. Color development is complete within 15 minutes at ordinary temperatures. Color may be

with standards visually or read in a spectrophotometer at 550 mμ, using unexposed reagent as a reference. Colors may be preserved, if well stoppered, with only 3 to 4% loss in absorption per day; however, if strong oxidising or reducing gases are present in the sample in concentrations considerably exceeding that of the nitrogen dioxide, the colors should be determined as soon as possible to minimize any loss

Standardization. Add graduated amounts of standard sodium nitrite solution up to 1 ml. to a series of 25-ml. volumetric flasks, and dilute to marks with absorbing reagent. Mix, allow 15 minutes for complete color development, and read the colors. The 1-ml. standard is equivalent to 1 μl. of nitrogen dioxide per 10 ml. of absorbing reagent.

Calculations. For convenience, standard conditions are taken as 760 mm. of mercury and 25° C., thus only slight correction is ordinarily required to get V, the standard volume in liters of the air sample. Quantities of nitrogen dioxide may be expressed as microliters, μl., defined as V times the parts per million of nitrogen dioxide. It has been determined empirically that 0.72 mole of sodium nitrite produces the same color as 1 mole of nitrogen dioxide, hence 2.03 γ of sodium nitrite is equivalent to 1 μl. of nitrogen dioxide.

Plot the absorbances of the standard colors, corrected for the blank, against the milliliters of standard solution. Beer's law is followed. Draw the straight line giving the best fit, and determine the value of milliliters of sodium nitrite intercepted at absorbance of exactly 1. This value multiplied by 4 gives the standardization factor, M, defined as the number of microliters of nitrogen dioxide required by 10 ml. of absorbing reagent to give an absorbance of 1. For 2-cm. cells the value was 3.65. Then:

$$\text{P.p.m. of nitrogen dioxide} = \text{corrected absorbance} \times M/V$$

If the volume of the air sample, V, is a simple multiple of M, calculations are simplified. Thus, for the M value of 3.65 previously cited, if exactly 3.65 liters of air are sampled through a bubbler, the corrected absorbance is also parts per million directly. If other volumes of absorbing reagent are used, V is taken as the volume of air sample per 10 ml. of reagent.

EXPERIMENTAL

Preparation of Known Low Concentrations of Nitrogen Dioxide. The first step in the study was the development of a suitable reagent which would give a high absorption efficiency with continuous sampling, so that the low levels (below 1 p.p.m.) could be determined. These nitrogen dioxide concentrations were prepared in the apparatus shown in Figure 1.

The source of the nitrogen dioxide was a standardized air mixture contained in a 46-liter carboy and available through an all-glass system of 1-mm. bore tubing and ground joints lightly greased with silicone grease. The mixture was made by introducing a few milliliters of nitric oxide, generated in a nitrometer, into the partially evacuated carboy, and flushing it in with air until normal pressure was attained. A few days were allowed for air oxidation of the nitric oxide to nitrogen dioxide and equilibration with the apparatus. The resulting concentration of nitrogen dioxide was 20 p.p.m., which was well within the range of accurate analysis by existing methods, and could be determined by collecting a sample in a 60-ml. evacuated bottle through stopcocks B and C. The composition of the air in the carboy was found to remain remarkably constant. During a period of 4 months it dropped to 15 p.p.m. Most of this loss could be accounted for by the more than 100 portions which were withdrawn, each amounting to about 1/1000th of the contents of the carboy. The vacuum that developed in the carboy was measured and relieved by admitting outside air periodically, through operation of stopcock D, which was ordinarily kept in the closed position.

Known low concentrations of nitrogen dioxide were prepared by accurate dilution of this standardized carboy air mixture in the following manner. A 50-ml. portion was withdrawn into a glass syringe through stopcock A, and then slowly injected into a 1-liter-per-minute air stream by means of a motor-driven slide. A dilution of 1 to 147 was usually used, the value could be varied by moving the belt on the stepped pulleys of the synchronous motor. (The second syringe driven by the same slide, shown in Figure 1, was used in later tests to inject an interfering gas into the air stream by similar manipulation of stopcock A.)

The air stream used for dilution of the nitrogen dioxide was taken in through a universal type gas-mask canister; this reduced the normal nitrogen dioxide concentration in the laboratory air, which at times reached 0.1 p.p.m., to considerably less than 0.01 p.p.m. (A U-tube containing Ascarite was found almost equally efficacious.) A mixing chamber was provided for the stream below each point of gas injection. Flow was controlled by a critical orifice in the suction line to an aspirator in the hood, preceded by a trap with a mercury manometer connection.

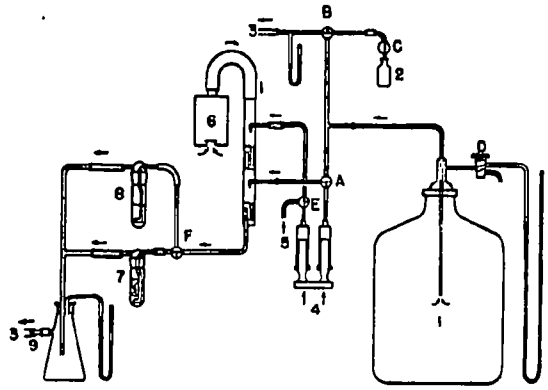

Figure 1. Apparatus for Preparing Known Low Concentrations of Nitrogen Dioxide

1. 46-Liter carboy containing 20 p.p.m. of nitrogen dioxide air mixture
2. 60-Ml. sampling bottle
3. Vacuum connection to aspirator in hood
4. 50-Ml. glass syringes and motor-driven slide
5. Intake for second gas
6. Universal gas mask canister
7. Sampling device
8. Bypass device
9. Critical orifice

Precise measurement of the amount of nitrogen dioxide injected was made by reading a counter on the motor drive. The apparatus was started and flushed with stopcock F in position to divert the air stream through a bypass of the same resistance as the sampling device. At the moment when a predetermined reading was obtained, F was turned to direct the air through the sampler. When the syringe was fully discharged, a limit switch stopped the motor, and F was again turned at that instant to the bypass position again. The volume of carboy air mixture which had passed through the sampling device could be calculated from the difference in counter readings and from micrometer measurements of the syringe plunger diameter.

A modified Shaw scrubber (*14*) was used as the sampling device for the screening tests of various reagents, although a midget fritted bubbler was later found more efficient. In the Shaw scrubber the air stream entered a lift pump raising absorbing reagent to the top of a column, which had a 10-mm. diameter and was 90 mm. high, packed with glass helices. The sample was absorbed on the wetted surfaces of these helices as the gas and liquid both flowed downward, the air then flowed to the vacuum source while the absorbing liquid drained back to the pump. Twenty milliliters of absorbing reagent were required.

The absorption efficiency that could be obtained in the scrubber at low concentrations of nitrogen dioxide was the critical factor in the tests. This efficiency was calculated as follows:

$$\text{Absorption efficiency} = \frac{A_s R_s V_b}{A_b R_b V_s}$$

where A_s is the absorbance of the color obtained from the scrubber

reagent (corrected for the value obtained in a blank run with no nitrogen dioxide addition), A_b is the absorbance of the color obtained using the same reagent in the evacuated bottle and sampling directly from the carboy (corrected for the blank value of unexposed reagent), R_s and R_b are the volumes of the reagent used in the scrubber and evacuated bottle, and V_s and V_b are the corresponding volumes of carboy air mixture which these colors represent. The colors obtained from the evacuated bottle were known or expected to be true values with the types of reagent tested.

Tests of Various Absorbing Reagents. Only reagents for nitrite were tested because it was expected that they would not only be specific for nitrogen dioxide but also possess the required sensitivity. Studies were made of various combinations of chemicals and their resultant absorption efficiencies, color stabilities and sensitivities, of the optimal methods of color development, of the optimum concentrations and acidities for these chemicals, and of the effect of various metals added as catalysts. Table I presents the data which were obtained. The reagent finally adopted, listed as No. 23, showed the highest efficiency (77%) and excellent color stability and sensitivity, the maximal absorption of the red-violet color being at 550 mμ.

Four combinations of chemicals were tried:

The combination of sulfanilic acid and 1-naphthylamine (Reagents 1 to 6) was finally rejected because of poor color stability and occasional false color production after aeration. Reagent 4 is similar to but somewhat stronger than one previously found by Patty (*16*) to give 5% efficiency in a midget impinger but successfully used in a 50-ml glass syringe.

More stable and intense colors were obtained with sulfanilamide and *N*-(1-naphthyl)-ethylenediamine dihydrochloride (Reagents 7 to 17), with an efficiency as high as 84% (Reagent 12). These chemicals were used in powder form with tartaric acid by Jacobs (*12*) and found to be stored conveniently and satisfactorily used in a 50-ml glass syringe after dissolving in water.

A higher efficiency was obtained by substituting anthranilic acid for the sulfanilamide (Reagent 18), since this was known to have a very rapid diazotization rate, but poor color intensity and very slow color development were found.

Best results were obtained with the previously unreported combination of sulfanilic acid and *N*-(1-naphthyl)-ethylenediamine dihydrochloride (Reagents 19 to 32), which was the one finally adopted.

Two methods of color development were investigated.

STEPWISE METHOD, in which sample absorption in the diazotizing reagent is carried out under the optimal strongly acid conditions, after which the pH is increased with a buffer and the coupling reagent is added for optimal color development. The method, which is in accordance with studies of procedures for nitrite (*8, 18, 19*), was used for Reagents 1 to 3 and 7 to 10 (Table I), as well as in other tests not shown with sulfanilic acid and sulfuric or hydrochloric acid, followed by various buffers and 1-naphthylamine. This method is subject to losses due to decomposition of the unstable diazo intermediate during the intense aeration of sampling.

DIRECT COLOR METHOD, in which the reagent contains all ingredients and after absorption produces the color with no further operations. This method is subject to losses because of side reactions between nitrite and the coupling reagent, and because of not having optimal pH for diazotization and coupling. This method, which was used for the remainder of the reagents listed in Table I, was found to produce more color in the scrubber, even though it produced less with a standard bottle sample or nitrite portion. The direct color type of reagent, containing all ingredients, was therefore adopted because of greater convenience and a higher absorption efficiency.

Optimum concentrations and acidities for each combination of chemicals were determined in order to obtain a true evaluation of their worth. The results in Table I showed that the highest

Table I. Screening Tests for Reagents to Obtain High Absorption Efficiency

No.	Absorbing Reagent[a]	Procedure for Color Development and Remarks[a]	Absorption Efficiency, %[b]	Absorbance: Std. air sample[c]	Absorbance: Std. nitrite portion[d]
	D = Sulfanilic acid, C = 1-Naphthylamine, 520 mμ				
1	0.01 *N* NaOH	Add 10% AcOH, 0.05% D, after 20 min. add 0.03% C	30		
2	0.05% D	After 10 min. add 0.03% C	27	0.188	0.142
3	0.05% D, 15% AcOH	After 10 min. add 0.03% C	40		
4	0.05% D, 0.03% C, 14% AcOH	Direct color	52–60	0.183	0.134
5	0.12% D, 0.075% C, 14% AcOH	Direct color	66		
6	0.5% D, 0.03% C, 14% AcOH	Direct color	55		
	D = Sulfanilamide, C = *N*-(1-naphthyl)-ethylenediamine dihydrochloride, 544 mμ				
7	0.02% D, 1% HCl	After 6 min. add 0.002% C	56	0.190	
8	0.02% D, 10% AcOH	After 15 min. add 0.002% C	40		
9	0.02% D, 10% AcOH, 2.5% H_3BO_3	After 15 min. add 0.002% C. Very slow color development	40		
10	0.5% D, 1% HCl	After 15 min. add 0.002% C	52		
11	0.02% D, 0.002% C, 1% HCl	Direct color	48	0.184	
12	0.5% D, 0.002% C, 1% HCl	Direct color	64	0.329	
13	4.0% D, 0.003% C, 1% HCl, 40% Ethylene glycol	Direct color. Ethylene glycol added to increase solubility of D		0.080	
14	4.0% D, 0.004% C, 1% HCl, 10% AcOH, 8% Ethylene glycol	Direct color. Ethylene glycol and AcOH added to increase solubility of D		0.195	
15	Same as 12 + 0.0025% Cu(II)	Direct color. Test of catalytic effect	48		
16	Same as 12 + 0.05% Fe(II)	Direct color. Test of catalytic effect	57		
17	0.5% D, 0.002% C, 2.5% H_3PO_4, + 0.05% Fe(II)	Direct color. Test of catalytic effect	62		
	D = Anthranilic acid, C = *N*-(1-naphthyl) ethylenediamine dihydrochloride, 500 mμ				
18	0.05% D, 0.002% C, 0.1% HCl	Direct color. Very slow color development	82	0.140	
	D = Sulfanilic acid, C = *N*-(1-naphthyl)-ethylenediamine dihydrochloride, 550 mμ				
19	0.05% D, 0.002% C, 14% AcOH	Direct color	53		
20	0.5% D, 0.002% C, 5% HCl	Direct color. Slow coupling		0.239	
21	0.5% D, 0.002% C, 2% tartaric acid	Direct color	68		
22	0.4% D, 0.025% C, 14% AcOH	Direct color	65		
23	0.5% D, 0.002% C, 14% AcOH	Direct color. Final reagent	77	0.270	0.191
24	Same as 23 + 0.005% Zn(II)	Direct color. Test of catalytic effect	75		
25	Same as 23 + 0.125% Zn(II)	Direct color. Test of catalytic effect	75		
26	Same as 23 + 0.005% Fe(II)	Direct color. Test of catalytic effect	78		
27	Same as 23 + 0.05% Fe(II)	Direct color. Test of catalytic effect. Unstable colors obtained	71–82	0.294	
28	Same as 23 + 2.5% Fe(II)	Direct color. Test of catalytic effect. Unstable colors obtained	78		
29	Same as 23 + 0.01% Fe(III)	Turbid brown color developed			
30	Same as 23 + 0.005% V(V)	No color developed. C destroyed			
31	Same as 23 + 0.005% Co(II)	Direct color. Test of catalytic effect	72		
32	Same as 23 + 0.09% As(III)	Direct color. Test of catalytic effect	65		

[a] % refers to final concentration in mixture. w/v for solids and v/v for liquids. D = diazotizing reagent. C = coupling reagent for color development. AcOH = glacial acetic acid.
[b] Modified Shaw scrubber used at 1 liter per minute (0.11 p.p.m. of nitrogen dioxide).
[c] Calculated for a standard sample of 1 μl. of nitrogen dioxide (or 60 ml. at 20 p.p.m.) absorbed in 10 ml. of reagent in an evacuated bottle.
[d] Calculated for 1.74 γ of potassium nitrite (would be equivalent to 1 microliter of nitrogen dioxide if 0.5 mole of potassium nitrite were equivalent to 1 mole of nitrogen dioxide) in 10 ml. of reagent.

possible concentration of diazotizing reagent was desirable, not only was the absorption efficiency increased, but even the color obtained in a bottle with a standard air sample (Reagents 11 and 12) Too high a concentration of the coupling reagent, on the other hand, reduced the color produced (Reagents 22 and 23), probably because of increased side reaction directly between this reagent and the nitrite. A high acidity (Reagent 20) greatly slowed the coupling step for the finally adopted combination of chemicals Acetic acid was best because it provided the best compromise pH and also had surface tension properties which provided a fine froth in the sampling device Reagent 23, based on these principles, was found to give the highest absorption efficiency.

The effect of various metals added as catalysts was slight (Reagents 15 to 17, 24 to 32). The most effective metal was 0 05% iron(II) (Reagent 27), which improved absorption and color intensity, but was considered undesirable because of color instability which would result if oxidation to the iron(III) form occurred (Reagent 29)

Table II. Influence of Reagent Composition on the Nitrite Equivalent of Nitrogen Dioxide

No	Absorbing Reagent[a]	Procedure for Color Development and Remarks[a]	Absorbance: Std air sample[b]	Absorbance: Std nitrite portion[c]	Moles of Nitrite Equivalent to 1 Mole of NO_2[d]
	D = Sulfanilic acid, C = *N*-(1-naphthyl)-ethylenediamine dihydrochloride, 550 mμ				
33	14% AcOH	Absorb 20 min., add 0 02% D, after 15 min., add 0 002% C	0 183	0 189	0 48
34	0 02% D, 14% AcOH	Absorb 20 min., add 0 002% C	0 106	0 186	0 73
35	0 5% D, 14% AcOH	Absorb 20 min., add 0 002% C	0 250	0 191	0 95
36	0 5% D, 0 002% C	Absorb 20 min Direct color	0 245	0 170	0 72
23	0.5% D, 0 002% C, 14% AcOH	Absorb 20 min Direct color, Final reagent	0 276	0 191	0 72
37	0 5% D, 0 002% C, 50% AcOH	Absorb 20 min Direct color	0 231	0 182	0 94

[a] % refers to final concentration in mixture w/v for solids and v./v for liquids D = diazotizing reagent, C = coupling reagent for color development AcOH = glacial acetic acid
[b] Calculated for a standard sample of 1 μl of nitrogen dioxide (or 50 ml at 20 p p m) absorbed in 10 ml of reagent in an evacuated bottle
[c] Calculated for 1.74 γ of potassium nitrite (would be equivalent to 1 microliter of nitrogen dioxide if 0 5 mole of potassium nitrite were equivalent to 1 mole of nitrogen dioxide) in 10 ml of reagent
[d] Obtained by dividing absorbance of standard air sample by twice the absorbance of standard nitrite portion

Table III. Absorption Efficiency with Various Sampling Devices

Device	Vol of Reagent, Ml	Sampling Rate, Liter/Min	Head Loss, Mm of Hg	Test P P M. of NO_2	Absorption Efficiency, %
Standard midget impinger	10	1	1	0 14	32
Standard midget impinger	10	0 5	1	0 8	31
Modified Shaw scrubber used for screening tests, 110 ml of glass helices	20	1	0 7	0 14	77
Midget impinger with fritted tube end	10	0 5	2	0 28	75-92
Midget bubbler with 8-mm fritted disk	10	0 4	54	0 3	99
Midget bubbler with 8-mm fritted disk	10	0 4	36	0 3	94
Midget bubbler with 8-mm fritted disk	10	0 4	34	0 4	95

Nitrite Equivalent of Nitrogen Dioxide. Practically, standardization of the reagent is best achieved with standard nitrite solution, rather than with difficultly prepared standard gas samples The initial presumption was that 0 5 mole of nitrite would be equivalent to 1 mole of nitrogen dioxide, by dissolution in water of the latter to give equal quantities of nitric and nitrous acids (Equation 1 below) The last two columns of Table I, giving the absorbances obtained with 1 μl of nitrogen dioxide in an air sample, and with the equivalent amount of nitrite on the above basis, showed that this presumption was not correct, dividing the first figure by twice the second gives the actual molar equivalent obtained The previously mentioned study by Patty (*16*) found a relationship of 0 57, although a satisfactory explanation of the difference from 0 5 was not presented In an effort to find the cause of disagreement, a more complete investigation was undertaken of the relationship between the color obtained in an evacuated bottle with a standardized air sample, and the color obtained in solution with standard nitrite reagent

The effect on the color intensity, which could be produced by varying the concentrations and combinations of the ingredients of the final reagent, is shown in Table II All solutions gave about the same color intensity with a standard nitrite portion, but the color intensity with a standard air sample varied more widely Values close to 0 5*M* equivalence were obtained when the air sample was absorbed in acetic acid alone (Reagent 33) or in a dilute sulfanilic-acetic acid reagent (Reagent 34) A value of 0 51*M* equivalence was obtained with Reagent 23 (the finally adopted reagent) in another test not shown in which the air sample was increased to 500 μl (of nitrogen dioxide) In this case the range of the reagent was exceeded and only a weak orange-red color was obtained, but upon dilution 100 times with additional reagent the characteristic color was obtained However, higher values were obtained with stronger sulfanilic acid (Reagent 35), and these were even higher when the coupling reagent was also present (Reagents 36, 23, and 37)

These results may be explained by hypothesizing that the nitrogen dioxide may react either as in Equation 1, with water alone to produce equimolar quantities of nitrite and nitrate (50% equivalence), or as in Equation 2, directly with sulfanilic acid and water as a peroxide to yield 100% equivalence, and that the presence of high concentrations of sulfanilic acid, as well as of a small amount of coupling reagent, permits the latter reaction to occur with equal frequency In the formulas presented below, nitrogen dioxide is written as the peroxide form of the dimer, nitrogen tetroxide, to simplify structural relationships:

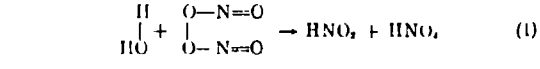

(1)

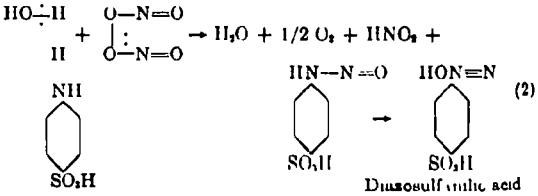

(2)

Sulfanilic acid

Diazosulfanilic acid

In either reaction the nitrous acid formed produces another molecule of diazosulfanilic acid. In Equation 2 either oxygen or hydrogen peroxide may be produced It was found experimentally that small amounts of hydrogen peroxide did not prevent color development or bleach the color. Equation 2 may also be written to show two molecules of sulfanilic acid combining with the nitrogen tetroxide, with the same end result

Absorption Efficiency with Various Sampling Devices. After the most suitable reagent had been developed in conjunction with the modified Shaw scrubber, it was found that much better efficiency could be obtained using midget fritted bubblers The acetic acid content of the reagent made possible a fine and stable foam of 20- to 30-ml volume above 10 ml of reagent and

(9) Gray, E LeB, MacNamee, J K, and Goldberg, S B, *Arch. Ind Hyg and Occupational Med*, 6, 20 (1952)
(10) Haagen-Smit, A J, *Ind Eng Chem*, 44, 1342 (1952)
(11) Holler, A C, and Huch, R V, ANAL CHEM, 21, 1385 (1949)
(12) Jacobs, M B, "The Analytical Chemistry of Industrial Poisons, Hazards, and Solvents," 2nd ed, p 358, New York, Interscience Publishers, 1949
(13) Johnston, H S, and Yost, D M., *J Chem Phys*, 17, 386 (1949).
(14) Kieselbach, R, IND ENG CHEM, ANAL ED, 16, 766 (1944)
(15) LaTowsky, L W, *et al*, *J Ind Hyg Toxicol*, 23, 129–47 (1941)
(16) Patty, F A and Petty, G M, *Ibid*, 25, 361 (1914)
(17) Reindollar, W I IND ENG CHEM, ANAL ED, 12, 325 (1940).
(18) Rider, B F, with Mellon, M G, *Ibid*, 18, 96 (1946)
(19) Shum, M B, *Ibid*, 13, 33 (1941)
(20) Shreidman, L, and Yeaw, J S, *Am Gas Assoc. Proc*, 24 (1942), 277
(21) Stanford Research Institute, "Third Interim Report on the Smog Problem in Los Angeles County," 1950
(22) U S Public Health Service, *Public Health Bull*, No 272, 1941
(23) Usher, F L, and Rao, B S, *J Chem Soc*, 111, 709 (1917)
(24) Wade H A Elkins, H B, and Ruotolo B P W, *Arch Ind Hyg and Occupational Med*, 1, 81 (1950),
(25) Yagoda, H, and Goldman F H, *J Ind Hyg Toxicol*, 25, 440 (1943)

RECEIVED for review June 21, 1954 Accepted September 1, 1954

ovided a large surface area for good absorption. An upward-ing fritted disk was better than vertical or downward-facing ks because there was less coalescing of bubbles with conse-ent loss of surface area In Table III are shown the absorp-n efficiencies obtained for various sampling devices The three idget fritted bubblers tested showed 91 to 99% efficiency at 3 to 0 1 p.p m of nitrogen dioxide By using two in series necessary, practically 100% efficiency may be obtained, a test th such arrangement showed the second bubbler recovered 61% the few hundredths of a part per million which passed the t bubbler. The fritted bubbler with the highest pressure drop o showed the highest efficiency.

Standardization against Known Concentrations of Nitrogen oxide. In the work described above, the assumption was de that the final reagent gave true values when used in the a mixed bottle to sample undiluted carboy air mixture, and bsorption efficiencies were calculated on the basis of the relative lor obtained in this manner as compared to that obtained hen sampling diluted carboy air mixture It remained to demonstrate the accuracy of this presumption by sampling higher concentrations of nitrogen dioxide of known value. Three systems were used to prepare such concentrations in an absolute manner by direct measurement of pure nitrogen dioxide from a tank, and simultaneous samples were collected in evacuated bottles using both the present reagent and the phenoldisulfonic acid method (*3*).

In the first system a small evacuated pipet was used to measure nitrogen dioxide gas, and the contents were introduced into bottles or carboys. In a typical run in this group, 0 3 ml of gas was pipetted into a 4 6-liter bottle to give a theoretical concentration of 106 p p m after allowing for the deviation from ideal gas volume Analysis by the present procedure gave 60 2 and 61 5 p p m , by phenoldisulfonic acid 59 0, 57 9, and 59 0 p p m Thus while good analytical agreement was obtained, half of the nitrogen dioxide appeared to be lost on the glass or stopcocks and the system was unsuccessful in preparing known concentrations Similar losses previously had been noted when the observed value of 20 p p m in the carboy of Figure 1 was compared to the value expected from the amount of nitric oxide introduced from the nitrometer The following two systems, however, yielded good agreement between calculated and obtained values

In the second system, 0 4 gram of liquid nitrogen dioxide was accurately weighed in a sealed glass ampoule, which was then broken in a closed, stainless-steel, cubical chamber which measured 5 feet on edge An electric fan was used to mix the contents The theoretical concentration was computed at 66 4 p p m The following results were obtained:

Minutes after breaking	10	20	30	35	90	125	155
P P M , present method	66 7	66 6			62 8	63 1	61 7
P P M , phenoldisulfonic acid method			64 2	65 9			

The concentration dropped slowly, but the data indicate that the early samples were substantially identical This run was used as the absolute standard of the entire investigation The analyses showed good agreement, although samples of different size were taken

In the third system known concentrations of nitrogen dioxide were prepared by means of four flowmeters A special flowmeter was constructed to measure very small tank nitrogen dioxide flows below 10 ml per minute The principle of this flowmeter was that the gas was made to flow through a fine fritted-glass filter and a fine capillary tube, and the pressure drop was measured by a manometer containing fluorocarbon liquid, it was calibrated by passing the gas directly into weighing bottles containing Ascarite and noting the gain in weight, manometer readings, the flow time This flow was injected into a metered air stream, and a portion of the mixture was taken off through an all-glass rotometer into a second metered air stream. The final mixture flowed into a glass jar from which samples could be collected. It was necessary to scrub all the air with dilute dichromate-sulfuric acid to remove impurities such as ammonia which precipitated or consumed nitrogen dioxide.

The results of the analyses of simultaneous samples were as follows

	P P M			
Flow meter value	8 8	15 1	27 2	40 6
Analysis by present method	8 2	16 6	27 8	42 0
Analysis by phenoldisulfonic acid method	5 3	10 9	20 5	33 4

Good agreement was obtained with the present method even with sample sizes varying from 45 to 250 ml

The phenoldisulfonic acid procedure was systematically low, as has been reported for similar gas concentrations (*16*) Previous tests with this procedure had shown that absorption of lower concentrations in large bottles was very slow, although 3 days had been allowed, slightly higher results could be obtained with 1-week absorption These samples were collected in 2.5-liter acid bottles with 15 ml. of absorbing reagent, in the figures previously quoted for the stainless-steel chamber, 500-ml bottles were used because of the higher concentrations and 1 day of absorption in the refrigerator was adequate.

The result of these studies was the absolute standardization of the method and the establishment of the validity of the absorption efficiencies which were obtained with the apparatus shown in Figure 1

EFFECT OF INTERFERING GASES

The effect of various interfering gases was found to be unimportant unless the concentration was much higher than that of the nitrogen dioxide Because of the possibility of widely varying sample sizes and concentrations, all the results below are expressed in terms of microliters (corrected volume in liters times parts per million) per 10 ml of absorbing reagent For comparison, 2 or 3 μl of nitrogen dioxide are ordinarily required to develop a color of suitable intensity, the normal color was found to fade at the rate of 3 to 4% of absorbance per day

Ozone The effect of ozone is complicated by the fact that this gas reacts very rapidly with nitrogen dioxide producing nitrogen pentoxide and oxygen Calculations made on the basis of published kinetic data (*13*) indicated that, assuming the nitrogen dioxide concentration was much smaller than that of the ozone, and that the concentration of the latter therefore remained substantially constant as the reaction proceeded, the half life of the nitrogen dioxide was 4 5 minutes divided by the parts per million of ozone For 1 p p m of ozone the half life would be 4 5 minutes; for 10 p p m it would be 0 45 minute Thus, for appreciable amounts of ozone the system is actively changing, and evaluation of the interference is difficult

For test purposes the apparatus shown in Figure 1 was modified so that a stream of ozonized air, from a Westinghouse 794H ultraviolet lamp, could be mixed with the stream containing nitrogen dioxide just in front of the sampling device The age of the mixture could be varied by adding U-tubes to the train. Ozone was determined by absorption in alkaline iodide and spectrophotometric estimation of iodine liberated on acidification with sulfamic-phosphoric acid The sulfamic acid destroyed any interfering nitrite which might be present

Two microliters of ozone caused a slightly orange tint to an otherwise normal color Eleven microliters caused an increase in the absorbance equivalent to 1/5th of that amount of nitrogen dioxide, the maximal effect occurring in 3 hours Thirty microliters completely destroyed the coupling reagent and also the diazosulfanilic acid The reagent assumed a yellow-brown tint with an absorbance equivalent to about 2 μl of nitrogen dioxide.

The most convenient method found for removing ozone was to pass the sample over a specially prepared manganese dioxide catalyst at room temperature. The manganese dioxide completely destroyed the ozone, and no visible interference from 30 μl. occurred The catalyst, however, was found to accelerate the

oxidation of nitrogen dioxide by the ozone. The correction to the analysis for this effect was roughly computed as +10% for 1 p p m. of ozone, +21% for 2 p.p.m., and +60% for 5 p.p m , the log of the correction factor was proportional to the concentration of ozone This method was very convenient and satisfactory for less than 2 or 3 p p m of ozone; at higher values the correction became high and uncertain.

Ordinary, reagent-grade manganese dioxide was found unsatisfactory for this use because of its appreciable absorption of nitrogen dioxide. After attempting to purify various batches, success was attained in the following manner: A plug of glass wool, cleaned with dichromate cleaning solution and washed, was moistened with manganese(II) nitrate solution and dried in an oven at 200° C for 1 hour. The final plug used was 1 cm in diameter and 1 5 cm long and required about 0 5 ml of 75% manganese(II) nitrate hexahydrate Manganese dioxide was produced as the salt decomposed with loss of nitrogen dioxide The plug was placed in a U-tube and air was drawn through for an hour to sweep out the nitrogen dioxide and reduce the blank to about 0 01 p.p m ; an even lower value may be obtained by electrically heating the tube at temperatures up to 200° C during this aeration Better than 99% of 0 3 p p m of nitrogen dioxide passed through unabsorbed After long use the catalyst becomes exhausted and requires replacement

Sulfur Dioxide. Tests with this gas were made using the twin syringe of the apparatus shown in Figure 1 Sulfur dioxide alone produced no color with the reagent. Extremely large amounts slowly bleached the color formed with nitrogen dioxide Thus, 20 μl of sulfur dioxide produced no effect, 90 μl reduced the recovery 4% and required the color to be read within 45 minutes, the fading after 18 hours being 16%, 900 μl reduced the recovery by 11%, and all color was lost after 17 hours Numerous materials were tried as color stabilizers. It was found that the addition of 1% acetone to the reagent before use greatly retarded the fading by forming a temporary addition product with sulfur dioxide With 90 μl of sulfur dioxide, good results could be obtained by reading the color within 4 to 5 hours, instead of the 45 minutes required without the acetone Tests were also made with water solutions of sodium bisulfite equivalent to 125 μl of sulfur dioxide Color loss in 2 hours was 64% without acetone, and 15% with 1% acetone

Numerous experiments were made using a U-tube containing chromium trioxide on glass wool, as previously recommended (*23*), to destroy the sulfur dioxide It was found that 30 p p m. of this gas was completely removed so that perfectly stable colors were obtained The moisture content was found to be rather critical When the chromium trioxide was visibly wet (after sampling air of high humidity) only 70% of 0 3 p p m nitrogen dioxide was passed, when it was dried again 96% was passed However, a completely dry tube did not remove the sulfur dioxide. The losses of nitrogen dioxide appeared to be related more to the moisture content than to the amount of reduced chromium, since good performance was obtained from a tube which contained 20% of the chromium in reduced form A number of experiments were made using desiccants to control the humidity It was found that the best desiccants also removed the nitrogen dioxide; for 0 3 p p m at 0 5 liter per minute the losses were: magnesium perchlorate, 93%, Drierite, 80%, calcium chloride dihydrate, 21%, granular anhydrous calcium chloride, 20%, and phosphorus pentoxide, 10%

In summary, no interference from sulfur dioxide occurred from amounts up to 10 times that of nitrogen dioxide, interference from larger amounts may be reduced by using acetone if the color can be read without great delay, or a chromium trioxide U-tube The moisture content of the latter must be kept between visibly wet and bone dry The use of desiccants in the train is not permissible

Other Nitrogen Oxides. The interference from other nitrogen oxides is negligible

The evaluation of the interference of nitric oxide, NO, is complicated by the fact that this compound is slowly converted by air to nitrogen dioxide However it has been studied in the absence of air in the gas industry (*20*), using sulfanilic acid and 1-naphthylamine, and found not to produce any color unless converted to nitrogen dioxide by a special oxidizing scrubber. Since the present reagent produces a color by a similar reaction, it may safely be said that this gas does not interfere

Equilibrium calculations show that nitrous acid anhydride, N_2O_3, and nitrogen tetroxide, N_2O_4, do not exist at concentrations of 100 p p m and below Kinetic data show that their dissociation is practically instantaneous Hence these nitrogen oxides may be disregarded

Nitrogen pentoxide is rarely found, because it is readily hydrated to nitric acid vapor, and is also an unstable compound which is very sensitive to heat, the half life is 6 hours at 25° C., 86 minutes at 35° C , and only 5 seconds at 100° C. The decomposition products are nitrogen dioxide and oxygen This compound was prepared by mixing a stream of nitrogen dioxide with ozone in 0 5 p p m excess using the flowmeter apparatus previously referred to The stream contained 25 p p m of nitrogen pentoxide (equivalent to 50 p p.m as nitrogen dioxide), and gave a test for about 5 p p m. of nitrogen dioxide It is likely that this was due to impurity or decomposition of the nitrogen pentoxide

Nitric acid does not interfere with the determination When added in solution to the reagent it produced no color, nor did it affect the development of color with nitrite solution or nitrogen dioxide gas In the form of vapor, a 5000-p p m sample collected in an evacuated bottle gave a test for only 23 p p m. of nitrogen dioxide The sample was prepared by allowing a small amount of concentrated nitric acid to stand in a closed bottle, with the addition of a crystal of sulfamic acid to destroy nitrous acid impurities The small interference found may actually be nitrogen dioxide produced by decomposition in spite of this precaution

Other Interfering Gases. A number of other gases were investigated by adding them in the form of water solution to a reagent solution which contained a color equivalent to about 2 μl of nitrogen dioxide The amount added was equivalent to 125 μl of interfering material Hydrogen sulfide produced no effect Chlorine partially bleached the color instantly, causing a 45% loss and changing the tint to orange, the final color remained perfectly stable Hydrogen peroxide increased the color slightly (+4% in 2 hours), after 3 days the color had increased 16% and had a slightly different tint with less violet than the normal color Formaldehyde produced no appreciable effect in 2 hours, in 3 days a 15% greater than normal color loss occurred with production of an orange-yellow tint In the presence of 1% acetone (used for sulfur dioxide) the interferences of all these materials was the same, except for that of formaldehyde which still did not interfere within 2 hours, but caused almost complete loss of color in 3 days

ACKNOWLEDGMENT

The author is grateful to J T Mountain for many helpful suggestions, and to D H Byers and H E Stokinger, under whose direction the work was carried out, for their valuable review and criticism

LITERATURE CITED

(1) Averell, P R , Hart, W F , Woodbury, N T , and Bratley, W. R , ANAL CHEM , 19, 1010 (1947)
(2) Barnes, H , and Folkard, A R , *Analyst*, 76, 599 (1951).
(3) Beatty, R L , Berger, L B , and Schrenk, H H , U. S Bur Mines, *Rept Invest* 3687 (1943)
(4) Blacet, F E , *Ind Eng Chem* , 44, 1339 (1952).
(5) Brasted, R C , ANAL CHEM , 23, [illegible] (1951)
(6) Cholak, J , and McNary, R , *J Ind. Hyg Toxicol* , 25, 354 (1943)
(7) Edgar, J L., and Paneth, F A , *J Chem Soc* , 1941, 511, 519.
(8) Elkins, H B , *J Ind Hyg Toxicol* , 28, 37 (1946)

OXIDES OF NITROGEN
GRIESS-SALTZMAN METHOD
APCD 11-56

SCOPE

This method is used to determine small concentrations of nitrogen dioxide found in the atmosphere. The lower limit of the method is about 0.1 p.p.m. in a 500-ml. sample bottle. By altering the volume of the sample, nitrogen dioxide in specific sources can also be measured. However, the phenoldisulfenic acid method is generally employed by this laboratory for source testing. (N. B.)

METHOD SUMMARY

The samples are collected in evacuated bottles containing the absorbing solution. The absorbing solution consists of a mixture of sulfanilic acid, acetic acid, and N-(1-naphthyl)-ethylenediamine dihydrochloride. After shaking, the nitrogen dioxide diazotizes the sulfanilic acid which then couples with N-(1-naphthyl)-ethylenediamine forming a dye. The intensity of the color is measured with a colorimeter and the concentration of nitrogen dioxide read from a calibration curve.

SPECIAL APPARATUS

COLLECTION:

Chaney rotary sampler (Figure 1), 500-ml. bottles with narrow necks containing tabulated sidearms, 3-inch pieces of heavy-wall gum-rubber tubing, screw clamps, solid-glass plugs, and serological stoppers(Figure 2).

ANALYTICAL:

Spectrophotometer (Coleman Universal Model 14), microcuvettes (Coleman No. 14-315, minimum volume 2.5 ml.).

REAGENTS

COLLECTION:

0.1% N-(1-Naphthyl)-Ethylenediamine Dihydrochloride. Dissolve 0.1 gram of the solid  ·2HCl in 100 ml. of water.

Absorbing Reagent. Dissolve 5 grams of sulfanilic acid (HO_3S-  -$NH_2 \cdot H_2O$) in 800 ml. of water. Add 140 ml. of glacial acetic acid and 20 ml. of 0.1% N-(1-naphthyl)-ethylenediamine dihydrochloride solution. Dilute to 1 liter.

ANALYTICAL:

Standard Sodium Nitrite Solution. Accurately weigh 0.2755 gram of sodium

N. B.: This laboratory method has been superseded by the District since August 1956 for air monitoring purposes by an automatic recording instrument, Nitrogen Oxides Recorder, Model 3011, manufactured by Barman Engineering, Inc., North Hollywood, California, to District specifications and later modified by the Los Angeles County Air Pollution Control District.

nitrite ($NaNO_2$, 98% weight assay) and dissolve in water. Make up to volume in a 1-liter volumetric flask. Transfer 1 ml. of the solution, by means of a calibrated pipet, to a 50-ml. volumetric flask and make up to volume with water. One milliliter of the latter solution contains the equivalent of 5 μg. of nitrogen dioxide gas (based on the 0.72 factor from Saltzman) and will be referred to, hereafter, as the standard solution.

Transfer the following amounts of the standard solution to a series of 25-ml. volumetric flasks using a measuring pipet or 5-ml buret 0.1 ml. to the first, 0.2 ml. to the second, 0.3 ml. to the third, 0.4 ml. to the fourth, 0 5 ml. to the fifth, 0.6 ml. to the sixth, 0.7 ml. to the seventh, 0.8 ml. to the eighth, 0.9 ml. to the ninth, 1.0 ml. to the tenth, 1.1 ml to the eleventh, 1.2 ml. to the twelfth, 1.3 ml. to the thirteenth, and 1.4 ml. to the fourteenth Dilute each solution to volume with absorbing reagent. The flasks will then contain the equivalent of the following concentrations of nitrogen dioxide gas in micrograms per 10 ml. of absorbing reagent, respectivaly: 0.2, 0 4 0.6, 0.8, 1.0, 1.2, 1.4, 1.6, 1.8, 2.0, 2.2, 2 4, 2.6, and 2.8. Shake the solutions and allow to stand for 15 minutes for complete color development. Place the samples in the spectrophotometer cell and read the absorbance of the solutions at 550 mμ against a blank of water. Obtain a blank value by reading the absorbance of an unexposed sample of the same batch of absorbing solution. Subtract the blank value from the sample values. Plot the corrected absorbances vs. micrograms of nitrogen dioxide per 10 ml. of reagent on rectangular-coordinate graph paper.

1N (approximate) Sodium Hydroxide. Dissolve 4 grams of sodium hydroxide pellets in 100 ml. of water.

0.001N (approximate) Hydrochloric Acid. Dilute 1 ml. of concentrated hydrochloric acid to 100 ml. with water and then dilute 1 ml. of this solution to 1 liter with water.

COLLECTION OF THE SAMPLE

Soak the serological stoppers and the 3-inch lengths of rubber tubing in 1N sodium hydroxide overnight. Rinse with distilled water, then with 0.001N hydrochloric acid, and again with distilled water. Allow to dry.

Place a serological stopper on the neck of the collection bottle. Attach a piece of rubber tubing to the sidearm of the bottle and evacuate to a pressure of about 25 mm of mercury. Tighten the screw clamp on the rubber tubing and disconnect from the source of vacuum. Insert the solid-glass plug into the end of the rubber tubing. Add 10 ml. of absorbing solution to the bottle by poking the needle of a syringe (containing the absorbing solution) through the serological stopper. The vacuum of the bottle will draw the absorbing solution in. Remove the syringe. Number the bottle in any convenient manner. Load the bottle on the circular platform of the Chaney rotary sampler. The top of the bottle fits into a sleeve on a guide plate which has the time

of the sample marked on it, and which is on the same shaft as the platform. The circular platform rotates by means of a timing mechanism so that a new bottle is placed into position for sampling each hour. The sampler holds 8 bottles.

The sample is taken by means of a hypodermic needle connected to a piece of tubing leading to the atmosphere. When a bottle moves underneath the needle, the guide plate activates a microswitch mounted on the solenoid assembly. The solenoid is energized and the plunger of the solenoid moves the hypodermic needle down through the stopper on the bottle. After about 30 seconds, another microswitch on the solenoid assembly releases the solenoid. This procedure is repeated for each sample bottle. An electric interval timer turns the power to the sampler on and off at any preset time.

Upon arriving at the sampler location, turn the power switch and drive switch off. Remove the previous samples, and record the numbers of the bottles, times, and date. Place the next set of bottles in position on the platform and note the numbers of the bottles, times, and date. Check to see that the needle will hit the stopper, and not the guide plates, by turning the platform by hand slowly until the first microswitch clicks. Manually depress the lever arm holding the needle slowly to within about 1/4 inch of the stopper (do not puncture the stopper). The needle must be approximately in the center of the stopper. If it hits any of the metal parts, it must be adjusted or bent, so that it is in the correct position. This procedure is repeated for each bottle. Generally, if the needle is aligned for the first bottle, it will be correct for the others. Manually turn the platform to the correct time, check the timer for correctness, and turn the switches on.

If it is desired to take a sample manually, the sample bottle may be punctured with a needle, or the glass plug removed and the screw clamp opened for about 10 seconds. A 2-liter sample flask, similar to the ones used in the Phenoldisulfonic Acid Method for nitrogen oxides, may also be used. In this case, place 10 ml of absorbing solution in the flask and evacuate to the vapor pressure of the solution. Close the screw clamp, and insert the solid-glass plug in the rubber tubing. Take the sample by opening the flask for about 10 seconds. Replace the screw clamp, solid-glass plug, and return to the laboratory for analysis.

SAMPLE PREPARATION

Shake the bottle (or flask) containing the sample for 15 minutes on a mechanical shaker to allow for complete color development.

ANALYTICAL PROCEDURE

Transfer the sample from the bottle (or flask) directly to the spectrophotometer cell and read the absorbance at 550 mμ against water. Obtain a blank value by reading the absorbance of the original absorbing solution. Subtract the blank value from the sample value to obtain the corrected absorbance. Read the weight of nitrogen dioxide corresponding to the corrected absorbance from the calibration curve.

ADDITIONAL NOTES

When operating the Coleman spectrophotometer, check the setting for zero absorbance before each reading since the instrument drifts gradually. To simplify this process, one of the two microcuvettes in the holder is always kept filled with water and the zero checked against this cell before each reading. Since it is important that the portion of the cuvette in the light path be completely full, the analyst should realize that the cuvette is tilted slightly and should fill it so that the side arms are about half full.

If only a few samples are to be analyzed, the spectrophotometer may be zeroed against the blank. However, if a large number of samples are to be analyzed, it is better to zero the instrument with water and subtract the blank. This will avoid the possibility of low sample values due to the gradual absorption of nitrogen dioxide from the laboratory atmosphere by the blank.

REPORTING AND CALCULATIONS

Calculate the parts per million of nitrogen dioxide as follows.

$$\frac{0.532\,W}{v_c} \qquad (1)$$

where

W = micrograms of nitrogen dioxide per 10 ml. of absorbing solution

v_c = volume of air sampled, liters, at 760 mm. of mercury and 25°C. Generally pressure and temperature corrections are neglected, and the measured volume of the bottle or flask is used

To convert to grains per standard cubic foot (60°F. and 1 atmosphere), multiply the parts per million by 8.48×10^{-4}.

REFERENCES

Griess, P., Ber., 12, 427(1879).

Saltzman, Bernard, Anal Chem , 26, 1949-55(1954).